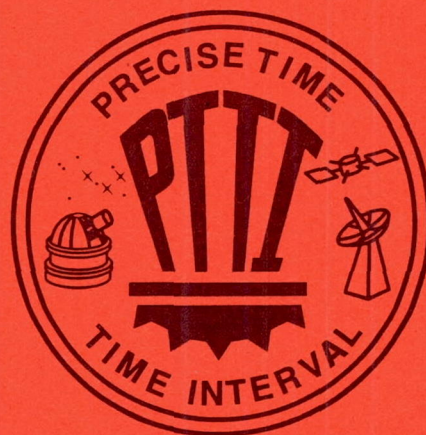


# **27th Annual Precise Time and Time Interval (PTTI) Applications and Planning Meeting**



*Proceedings of a meeting held at  
The Doubletree Hotel  
at Horton Plaza  
San Diego, California  
November 29 – December 1, 1995*





# **27th Annual Precise Time and Time Interval (PTTI) Applications and Planning Meeting**

*Editorial Committee Chairman*

Richard L. Sydnor

*Jet Propulsion Laboratory*

*California Institute of Technology*

Proceedings of a meeting sponsored by the  
U.S. Naval Observatory, the NASA Goddard  
Space Flight Center, the NASA Jet Propulsion  
Laboratory, the Space and Naval Warfare  
Systems Command, the U.S. Naval Research  
Laboratory, the U.S. Air Force Space Command,  
and the Air Force Office of Scientific Research  
and held at

The Doubletree Hotel

at Horton Plaza

San Diego, California

November 29 – December 1, 1995



National Aeronautics  
and Space Administration

**Goddard Space Flight Center**  
Greenbelt, Maryland 20771



This publication is available from the NASA Center for AeroSpace Information,  
800 Elkridge Landing Road, Linthicum Heights, MD 21090-2934, (301) 621-0390.



# PRECISE TIME AND TIME INTERVAL APPLICATIONS AND PLANNING MEETING

## ORDER FORM FOR THE PROCEEDINGS

	<u>Year</u>	<u>Cost</u>
1*	1969	N/C
2**	1970	\$25.00
3**	1971	\$25.00
4**	1972	\$25.00
5**	1973	\$25.00
6	1974	\$25.00
7	1975	\$25.00
8**	1976	\$25.00
9**	1977	\$25.00
10	1978	\$25.00
11	1979	\$25.00
12	1980	\$25.00
13	1981	\$25.00
14**	1982	\$25.00
15**	1983	\$25.00
16	1984	\$25.00
17	1985	\$25.00
18	1986	\$25.00
19	1987	\$25.00
20	1988	\$35.00
21	1989	\$65.00
22	1990	\$70.00
23	1991	\$85.00
24	1992	\$85.00
25	1993	\$85.00
26	1994	\$95.00
27	1995	\$115.00

Please circle copy(ies) requested and make the check payable to "Treasurer, PTTI". Do not add personal names or addresses to the pay to line on the check. We can bill, but accept only checks for payment.  
Please return payment and order form to:

PTTI Executive Committee  
U.S. Naval Observatory  
Time Service Department (TS)  
3450 Massachusetts Avenue, N.W.  
Washington, D.C. 20392-5420  
202/762-1481 or 1414  
Fax 202/762-1511

When you register for the PTTI Meeting or order the Proceedings, you name is added to the PTTI mailing list to automatically receive future meeting information.

\* An 8-page typed report is the result from the 1969 meeting.

\*\* Original copies of the Proceedings are no longer available. However, copies for purchase are made from the original Proceeding.



## **EXECUTIVE COMMITTEE**

**MRS. SHEILA FAULKNER, CHAIRMAN**  
U. S. Naval Observatory

**COMMANDER MARK ATKISSON**  
U.S. Naval Observatory

**MR. RONALD L. BEARD**  
Naval Research Laboratory

**LIEUTENANT COLONEL MICHAEL CIMA FONTE**  
U.S. Air Force Space Command

**MR. RAYMOND L. GRANATA**  
NASA Goddard Space Flight Center

**DR. HELMUT HELLWIG**  
Air Force Office of Scientific Research

**DR. WILLIAM J. KLEPCZYNSKI**  
U. S. Naval Observatory

**MR. PAUL F. KUHNLE**  
NASA Jet Propulsion Laboratory

**COMMANDER DAVID MARKHAM**  
Space and Naval Warfare Systems Command

**MR. JOHN J. RUSH**  
NASA Headquarters

**DR. RICHARD L. SYDNOR**  
NASA Jet Propulsion Laboratory

**MS. FRANCINE M. VANNICOLA**  
U.S. Naval Observatory

**DR. JOHN R. VIG**  
U.S. Army Research Laboratory

**DR. JOSEPH D. WHITE**  
Naval Research Laboratory

**MS. NICOLETTE JARDINE**  
Support Assistance  
U. S. Naval Observatory



## **OFFICERS**

*GENERAL CHAIRMAN*  
**MR. RONALD L. BEARD**  
Naval Research Laboratory

*TECHNICAL PROGRAM COMMITTEE CHAIRMAN*  
**DR. SAMUEL R. STEIN**  
Timing Solutions, Inc.

### *TECHNICAL PROGRAM COMMITTEE*

**DR. LEONARD S. CUTLER**  
Hewlett-Packard Company

**DR. HENRY F. FLIEGEL**  
The Aerospace Corporation

**MR. PAUL F. KUHNLE**  
Jet Propulsion Laboratory

**DR. RICHARD L. SYDNOR**  
Jet Propulsion Laboratory

**MR. S. CLARK WARDRIP**  
AlliedSignal Technical Services Corporation

### *EDITORIAL COMMITTEE CHAIRMAN*

**DR. RICHARD L. SYDNOR**  
Jet Propulsion Laboratory

*ASSISTANT EDITORIAL COMMITTEE CHAIRMAN*  
**DR. LEE A. BREAKIRON**  
U.S. Naval Observatory

*EXHIBITS AND PUBLICITY COMMITTEE CHAIRMAN*  
**MR. DONALD H. MITCHELL**  
TrueTime

*TECHNICAL ASSISTANCE*  
**MR. JEFFREY S. INGOLD**  
**MRS. BEA M. BELOVARICH**  
AlliedSignal Technical Services Corporation



## **PTTI AWARD COMMITTEE**

**DR. LEONARD S. CUTLER, CHAIRMAN**

Hewlett-Packard Company

**DR. RICHARD L. SYDNOR**

Jet Propulsion Laboratory

**DR. HENRY F. FLIEGEL**

The Aerospace Corporation

## **SESSION CHAIRMEN**

### **SESSION I**

**Dr. John R. Vig**

U.S. Army Research Laboratory

### **SESSION II**

**Mr. Al Gifford**

U.S. Naval Observatory

### **SESSION III**

**Ms. Francine M. Vannicola**

U.S. Naval Observatory

and

**Mr. Thomas R. Bartholomew**

The Analytical Sciences Corporation

### **SESSION IV**

**Dr. Malcolm D. Calhoun**

Jet Propulsion Laboratory

### **SESSION V**

**Mr. Franco Cordara**

Istituto Elettrotecnico Nazionale Galileo Ferraris

### **SESSION VI**

**Dr. Mark A. Weiss**

National Institute of Standards and Technology

### **SESSION VII**

**Dr. William J. Klepczynski**

U.S. Naval Observatory

### **TUTORIAL**

**Mr. Philip E. Talley, Jr.**

The Aerospace Corporation, Retired

### **SESSION VIII**

**Dr. Henry F. Fliegel**

The Aerospace Corporation

### **SESSION IX**

**Dr. Judah Levine**

National Institute of Standards and Technology

### **SESSION X**

**Mr. Paul F. Kuhnle**

Jet Propulsion Laboratory



## **ARRANGEMENTS**

Mrs. Sheila Faulkner  
Mr. Paul F. Kuhnle  
Dr. Richard L. Sydnor

## **FINANCE COMMITTEE**

Dr. William J. Klepczynski  
Mrs. Sheila Faulkner

## **RECEPTIONISTS**

The receptionists at the 27th Annual PTTI meeting were:

Ms. Nicolette Jardine, U.S. Naval Observatory  
Ms. Kathy Hibbard, Datum  
Mrs. Aline Kuhnle, Jet Propulsion Laboratory  
Mrs. Lyn McNabb, TRAK Microwave  
Mrs. Dot Smith, TRAK Microwave

## ADVISORY BOARD MEMBERS

Mr. S. Clark Wardrip, Chairman  
AlliedSignal Technical Services Corporation

Mr. David W. Allan  
Allan's TIME

Mr. Jerry Norton  
The Johns Hopkins University

Professor Carroll O. Alley  
University of Maryland

Mr. Allen W. Osborne, III  
Allen Osborne Associates

Dr. James A. Barnes  
Austron, Inc., Retired

Mr. Terry N. Osterdock  
Absolute Time

Mr. Martin B. Bloch  
Frequency Electronics, Inc.

Dr. Bradford W. Parkinson  
Stanford University

Mrs. Mary Chiu  
The Johns Hopkins University  
Applied Physics Laboratory

Mr. Harry E. Peters  
Sigma Tau Standards Corporation

Dr. Leonard S. Cutler  
Hewlett-Packard Company

Dr. Victor S. Reinhardt  
Hughes Aircraft

Dr. Henry F. Fliegel  
The Aerospace Corporation

Mr. William J. Riley  
EG&G, Inc.

Mr. Jeffrey S. Ingold  
AlliedSignal Technical Services  
Corporation

Dr. Harry Robinson  
Duke University

Mr. Robert H. Kern  
Kernco, Inc.

Mr. Ron Roloff  
FTS/Austron (Datum Companies)

Mr. Pete R. Lopez  
TRAK Microwave

Dr. Samuel R. Stein  
Timing Solutions Corporation

Mr. Jack McNabb  
TRAK Microwave

Mr. Michael R. Tope  
TrueTime, Inc.

Mr. Donald Mitchell  
TrueTime, Inc.

Mr. James L. Wright  
Computer Sciences Raytheon



## TABLE OF CONTENTS

<b>PTTI OPENING ADDRESS .....</b>	<b>1</b>
-----------------------------------	----------

**Captain Kent W. Foster  
Superintendent, U. S. Naval Observatory**

<b>PTTI DISTINGUISHED SERVICE AWARD .....</b>	<b>7</b>
---	----------

**Presented by  
Dr. Gernot M. R. Winkler  
U.S. Naval Observatory, Retired**

**to**

**Dr. James A. Barnes  
Austron, Inc., Retired**

<b>KEYNOTE ADDRESS .....</b>	<b>11</b>
------------------------------	-----------

**Progress of Timing in Telecommunications  
Mr. Ron Brown  
Bellcore**

### **SESSION I**

#### **Timing Systems**

**Chairman: John R. Vig  
U.S. Army Research Laboratory**

<b>GPS Monitor Station Upgrade Program at the Naval Research Laboratory ...</b>	<b>35</b>
Ivan J. Galysh and Dwin M. Craig, U.S. Naval Research Laboratory	

<b>The Role of Time and Frequency in Future Systems .....</b>	<b>51</b>
Samuel R. Stein, Timing Solutions Corporation; Al Gifford, U.S. Naval Observatory; and Tom Celano, The Analytical Sciences Corporation	

<b>Special Technology Area Review on Time and Frequency</b> . . . . .	<b>59</b>
John R. Vig, U.S. Army Research Laboratory	

## SESSION II

### UTC DISSEMINATION TO THE REAL TIME USER

Chairman: Al Gifford  
U.S. Naval Observatory

<b>Ideas for Future GPS Timing Improvements</b> . . . . .	<b>63</b>
Captain Steven T. Hutsell, U.S. Air Force, Falcon Air Force Base	
<b>UTC Dissemination to the Real Time User; Role of the USNO</b> . . . . .	<b>75</b>
Miranian, U.S. Naval Observatory	
<b>Role of the BIPM in UTC Dissemination to the Real Time User</b> . . . . .	<b>87</b>
Thomas J. Quinn and Claudine Thomas, Bureau International des Poids et Mesures	
<b>The Role of the International Telecommunications Union in Time and Frequency</b> . . . . .	<b>97</b>
Gerrit De Jong, NMI, Van Swinden Laboratorium	
<b>UTC Dissemination to the Real-Time User</b> . . . . .	<b>103</b>
Judah Levine, National Institute of Standards and Technology	

## SESSION III

### GPS PLANS AND ACTIVITIES

Co-Chairmen: Francine M. Vannicola  
U.S. Naval Observatory  
and  
Thomas R. Bartholomew  
The Analytical Sciences Corporation

<b>GPS Disciplined Oscillators for the Traceability to the Italian Time Standard</b> .	<b>113</b>
Franco Cordara and Valerio Pettiti, Istituto Elettrotecnico Nazionale Galileo Ferraris	



<b>Observations on the Reliability of Rubidium Frequency Standards on Block II/IIA GPS Satellites</b> .....	125
First Lieutenant Gary L. Dieter and Captain Gregory E. Hatten, U.S. Air Force Base	
<b>How Bad Receiver Coordinates Can Affect GPS Timing</b> .....	135
Harold Chadsey, U.S. Naval Observatory	
<b>Common View Time Transfer Using Worldwide GPS and DMA Monitor Stations</b> .....	145
Wilson G. Reid, Thomas B. McCaskill, and Orville J. Oaks, U.S. Naval Research Laboratory; and James A. Buisson and Hugh E. Warren, Sachs Freeman Associates, Incorporated	
<b>GPS/GLONASS Time Transfer with 20-Channel Dual GNSS Receiver</b> .....	159
Peter Daly and S. Riley, University of Leeds	

## SESSION IV

### ATOMIC STANDARDS AND RELATED DEVICES

Chairman: Malcolm D. Calhoun  
Jet Propulsion Laboratory

<b>Cesium and Rubidium Frequency Standards Status and Performance on the GPS Program</b> .....	167
Marius J. Van Melle, Rockwell Space and Operations Center	
<b>High Precision Time Transfer to Test a Hydrogen Maser on Mir</b> .....	181
Edward M. Mattison and Robert F.C. Vessot, Harvard-Smithsonian Center for Astrophysics	

## SESSION V

### TIME SCALES AND CLOCK ANALYSIS

Chairman: Franco Cordara  
Istituto Elettrotecnico Nazionale Galileo Ferraris

<b>Upper Limits of Weights in TAI Computation</b> .....	193
Claudine Thomas and Jacques Azoubib, Bureau International des Poids et Mesures	

<b>Tutorial: Clock and Clock Systems Performance Measures</b> . . . . .	<b>209</b>
David W. Allan, Allan's TIME	

<b>Appendix A: The Impact of the HP 5071A on International Atomic Time</b> . . . . .	<b>235</b>
David W. Allan, Allan's TIME; Alex Lepek, Tech Projects; Len Cutler and Robin Giffard, Hewlett-Packard Laboratories; and Jack Kusters, Hewlett-Packard SDC	

## SESSION VI

### SIGNAL PROCESSING

Chairman: Mark A. Weiss

National Institute of Standards and Technology

<b>Steering of Frequency Standards by the Use of Stochastic Linear Quadratic Gaussian Control Theory</b> . . . . .	<b>257</b>
Paul Koppang, U.S. Naval Observatory and Robert Leland, University of Alabama	

<b>Kalman Filtering USNO's GPS Observations for Improved Time Transfer Predictions</b> . . . . .	<b>269</b>
Captain Steven T. Hutsell, U.S. Air Force, Falcon Air Force Base	

<b>Simulation Study Using a New Type of Sample Variance</b> . . . . .	<b>279</b>
David A. Howe and K. J. Lainson, National Institute of Standards and Technology	

<b>Relating the Hadamard Variance to MCS Kalman Filter Clock Estimation</b> . . . . .	<b>291</b>
Captain Steven T. Hutsell, U.S. Air Force, Falcon Air Force Base	

## SESSION VII

### PRECISION TIME TRANSFER

Chairman: William J. Klepczynski

U.S. Naval Observatory

<b>Signal Delay Stability of a Ku-Band Two-Way Satellite Time Transfer Terminal</b> . . . . .	<b>303</b>
Dieter Kirchner, Technical University Graz and H. Rebler and R. Robnik, Space Research Institute	



<b>Data and Time Transfer Using SONET Radio .....</b>	<b>313</b>
Gary M. Graceffo, HRB Systems	
<b>Variance Analysis of Unevenly Spaced Time Series Data .....</b>	<b>323</b>
Christine Hackman and Thomas E. Parker, National Institute of Standards and Technology	
<b>Some Operational Aspects of the International Two-Way Satellite Time and Frequency Transfer (TWSTFT) Experiment Using INTELSAT Satellites at 307°E. ....</b>	<b>335</b>
James A. DeYoung and Angela Davis McKinley, U.S. Naval Observatory; John A. Davis, National Physical Laboratory; and Peter Hetzel and Andreas Bauch, Physikalisch-Technische Bundesanstalt	
<b>Preliminary Comparison of Two-Way Satellite Time and Frequency Transfer and GPS Common-View Transfer During the INTELSAT Field Trial .....</b>	<b>347</b>
John A. Davis, National Physical Laboratory; Wloedek Lewandowski, Bureau International des Poids et Mesures; James A. DeYoung, U.S. Naval Observatory; Dieter Kirchner, Technical University Graz; Peter Hetzel, Physikalisch-Technische Bundesanstalt; Gerrit de Jong, NMI, Van Swinden Laboratorium; Armin Söring, Forschungs-und Technologiezentrum, Deutsche Telekom; Françoise Baumont, Observatoire de la Côte d'Azur; William J. Klepczynski and Angela Davis McKinley, U.S. Naval Observatory; Thomas E. Parker, National Institute of Standards and Technology; K.A. Bartle, National Physical Laboratory; H. Ressler and R. Robnik, Space Research Institute; and Les Veenstra, RSI, Comsat World Systems	
<b>Results of the Calibration of the Delays of Earth Stations for TWSTFT Using the VSL Satellite Simulator Method .....</b>	<b>359</b>
Gerrit de Jong, NMI, Van Swinden Laboratorium; Dieter Kirchner, Technical University Graz; H. Ressler, Space Research Institute; Peter Hetzel, Physikalisch Technische Bundesanstalt; John Davis, Peter Pears, National Physical Laboratory; William Powell, Angela Davis McKinley, William J. Klepczynski, James A. DeYoung, U.S. Naval Observatory; Christine Hackman, Steve R. Jefferts, and Thomas E. Parker, National Institute of Science and Technology	
<b>Accurate Time/Frequency Transfer Method Using Bi-Directional WDMTransmission .....</b>	<b>373</b>
Atsushi Imaoka and Masami Kihara, NTT Optical Network Systems Laboratories	



## SESSION VIII

### APPLICATIONS I

Chairman: Henry F. Fliegel  
The Aerospace Corporation

<b>Limits to the Stability of Pulsar Time</b> .....	<b>387</b>
Gérard Petit, Bureau International des Poids et Mesures	
<b>GPS Moving Vehicle Equipment</b> .....	<b>397</b>
Orville J. Oaks and Wilson Reid, U.S. Naval Research Laboratory; James Wright, Christopher Duffey, and Charles Williams, Computer Sciences Raytheon; Hugh Warren, Sachs Freeman, Incorporated; Tom Zeh, Naval Undersea Warfare Center; and James Buisson, Antoine Enterprises	
<b>Bonneville Power Administration Timing System</b> .....	<b>409</b>
Kenneth E. Martin, Bonneville Power Administration	

## SESSION IX

### SYSTEMS AND SERVICES

Chairman: Judah Levine  
National Institute of Standards and Technology

<b>Direct-Y: Fast Acquisition of the GPS PPS Signal</b> .....	<b>419</b>
First Lieutenant O.M. Namoos, Space and Missile Center, Los Angeles Air Force Base and Dr. R.S. DiEsposti, The Aerospace Corporation	
<b>The WSMR Timing System: Toward New Horizons</b> .....	<b>433</b>
William A. Gilbert and Bob Stimets, White Sands Missile Range	
<b>Authentication, Time-Stamping and Digital Signatures</b> .....	<b>439</b>
Judah Levine, National Institute of Standards and Technology	

## SESSION X

### APPLICATIONS II

Chairman: Paul F. Kuhnle  
Jet Propulsion Laboratory

<b>Application of Millisecond Pulsar Timing to the Long-Term Stability of Clock Ensembles</b> .....	<b>447</b>
Roger S. Foster, U.S. Naval Research Laboratory and Demetrios N. Matsakis, U.S. Naval Observatory	
<b>A Novel Photonic Clock and Carrier Recovery Device</b> .....	<b>457</b>
X. Steve Yao, George Lutes, and Lute Maleki, Jet Propulsion Laboratory	
<b>Spacecraft Doppler Tracking as a Xylophone Detector</b> .....	<b>467</b>
Massimo Tinto, Jet Propulsion Laboratory	

# PTTI OPENING ADDRESS

**Captain Kent Foster  
Superintendent  
U.S. Naval Observatory  
Washington, D.C. 20392**

Good morning, ladies and gentlemen, and on behalf of the U.S. Naval Observatory, welcome to the 27th Annual PTTI meeting.

Before I get started on remarks, I feel I'd be remiss if I didn't mention a few people's names who have done a lot of behind-the-scenes work to provide these facilities and services this week. You all may be used to this kind of service, but this being my first time here at a PTTI meeting, I'm really impressed. I did press Sheila Faulkner to give me some names of some people who have done some of the behind-the-scenes work, and I'd like to recognize them this morning.

In the area of general assistance, folks from JPL, Dick Sydnor and Paul Kuhnle; from AlliedSignal, Clark Wardrip; from Hewlett-Packard, Len Cutler; from Timing Solutions, Sam Stein; and from TrueTime, Don Mitchell. A special thanks to Sheila Faulkner herself and Nikki Jardine for all the hours of work they put in for the registration and the overall coordination. Very, very nice job, folks.

To many of you, I'm sure this a longstanding recurring event in your lives. To me, it's a first, as I assumed command of the Naval Observatory just this past August. As is my style when dealing with anything new and unfamiliar to me, I will do a lot more listening than talking at this event. When I do talk, I'm sure I'm going to be asking a lot more questions than providing answers.

I did manage to recover some history at the Observatory while preparing to make these remarks this morning. I went back 25 years to the Second Annual PTTI meeting held at NRL in Washington in December of 1970. I looked at the objectives laid out for the 1970 meeting and compared those to this session (see Figure 1).

The 1970 objectives can be summarized as: Disseminating information about PTTI; reviewing present and future requirements for PTTI; and reviewing current and planned PTTI systems.

The objectives for this meeting are very similar: The first, second, and fourth objectives are essentially repeat items of the 1970 objectives. One additional item was thrown in, that is, to inform government officials of PTTI technology and its problems. This new item seems very closely associated with the fourth objective, and I therefore think I can say that the objectives of this meeting are essentially the same as they were at the meeting in 1970.

Without checking the records of every meeting between 1970 and now, I think it's fairly safe to assume that each year's objectives were similar to the ones listed here; and if they weren't, they probably should have been. So after 25 years of aiming at the same objectives, where are



we today?

When I look through the agenda of sessions one through ten of this meeting, they suggest the following to me: One, we are providing a lot of PTTI information to all attendees; and two, we are exchanging a lot of science and technology tied to PTTI. I think we could all feel confident about accomplishing objectives one, three and four here, based on the suggestions of this agenda; and I'm sure when this meeting adjourns, we will have our confidence verified.

What I don't feel confident about, however, is that objective number two, reviewing PTTI requirements, may not be getting a fair shake. I don't even see the word "requirements" in a single title in this agenda. I find this apparent inattention to requirements a little bit disturbing, and it's not the first time that I have found an absence of information-specific information--on this subject.

I know that I'm on a very steep learning curve in this new job of mine, and I know that I've got a long climb ahead of me before it even begins to level off. But the first easy lesson I learned is this: When you talk about current and future capabilities for precision accuracy involving time and positioning, especially those under development, the first question you get is "What is the requirement?" I've gotten the same question put to me by warfare-experienced Navy bean-counters--budgeteers--and laymen as well. When I turn to my prestigious ranks of PTTI experts at USNO for the requirements, especially the future requirements, I get a lot of looks of nervous uncertainty and a variety of very softly spoken numbers.

Figure 2 has been used in the past in USNO program briefs to show the long-term increases in USNO technology versus the increases in user requirements for precise time. I can tell you that the requirements line here is a rough quantitative estimate due to the uncertainty of precisely defined system-specific requirements. If, however, the slopes and the trends of this figure are generally correct, you can draw some inferences about the capabilities versus requirements.

From 1950 to about 1980, USNO technology preceded future requirements at any level of accuracy out to about 10 years. I guess this is probably a fairly comfortable margin. After about 1980, however, the technology development margin over future requirements shows a decreasing trend, as the lines beyond that point tend to converge. And by 1990, the relatively stable historical margin of USNO capabilities over current requirements begins to dwindle also.

These decreasing margins of capability over requirements should concern everyone here today. What this figure does not show is that the slope of the USNO capabilities line, which is of course the rate at which we can develop higher technology, is a partial function of resources, money, and people. Money and people are what all Navy and DoD activities are having to fight for on a continuing basis in order to minimize their losses. DoD is not a growth industry, and USNO is no exception to that rule.

USNO and other precise time activities do not launch combat aircraft; we do not put ships to sea; we do not aim and pull the trigger on any weapons system. We, therefore, in the eyes of war-fighters and defense bean-counters, don't do anything glamorous. But we do support marine and air navigation; we do support precise geo-location and putting weapons on target; and we do support synchronization of command, control, and communication systems. It's unfortunate, however, that these technical support functions are not well understood by war-fighters and bean-counters. The resources that provide these functions come under constant risk in competition with other more glamorous and high-priority requirements.

Our surest way to defend those resources against budget reduction drills, which are sure to continue, is through well-documented system-specific requirements, defined as precisely as possible and made understandable and appreciated by warfare commanders and bean-counters

alike. This will not happen without the proactive involvement of the PTTI expertise assembled in this room.

I would like to repeat that for emphasis. Systems-specific requirements defined as precisely as possible and made understandable and appreciated by warfare commanders and bean-counters will not happen without the proactive involvement of the people in this room.

So I urge all of you to begin thinking and focusing on the requirements review that has been, I think, an objective of this annual meeting for 25 years, and of the process used by the Defense Department in validating requirements. We need to come to grips with better requirements definition and to be a part of the continuing requirements process. This is especially true for future requirements that we must have to support continuing technology development.

Well, having overshot my precise time interval assigned to me by this agenda, I'll turn this podium over to someone who needs no introduction for any prior attendees at these meetings. Dr. Gernot Winkler, of course, was Director of Time at the Naval Observatory for 29 years, and culminated his enviable career with retirement earlier this year. I'm thankful, though, that we still see and welcome Dr. Winkler at USNO a day or two a week, and I'm happy to say that he's here with us now to present the Distinguished PTTI Service Award.

Ladies and gentlemen, I thank you for your efforts and your interest here this week. Please now welcome Dr. Winkler. Thank you.





# PTTI - Objectives

**1970**

- 1) Disseminate information associated with PTTI dissemination**
- 2) Review present & future requirements for PTTI dissemination**
- 3) Review status of current and planned systems for PTTI dissemination**

**1995**

- 1) Disseminate and coordinate PTTI information at the user level**
- 2) Review present & future PTTI requirements**
- 3) Inform government engineers, techs and managers of PTTI technology and its problems**
- 4) Provide an active exchange of new technology associated with PTTI**

Figure 1





# PTTI - Requirements & Capabilities

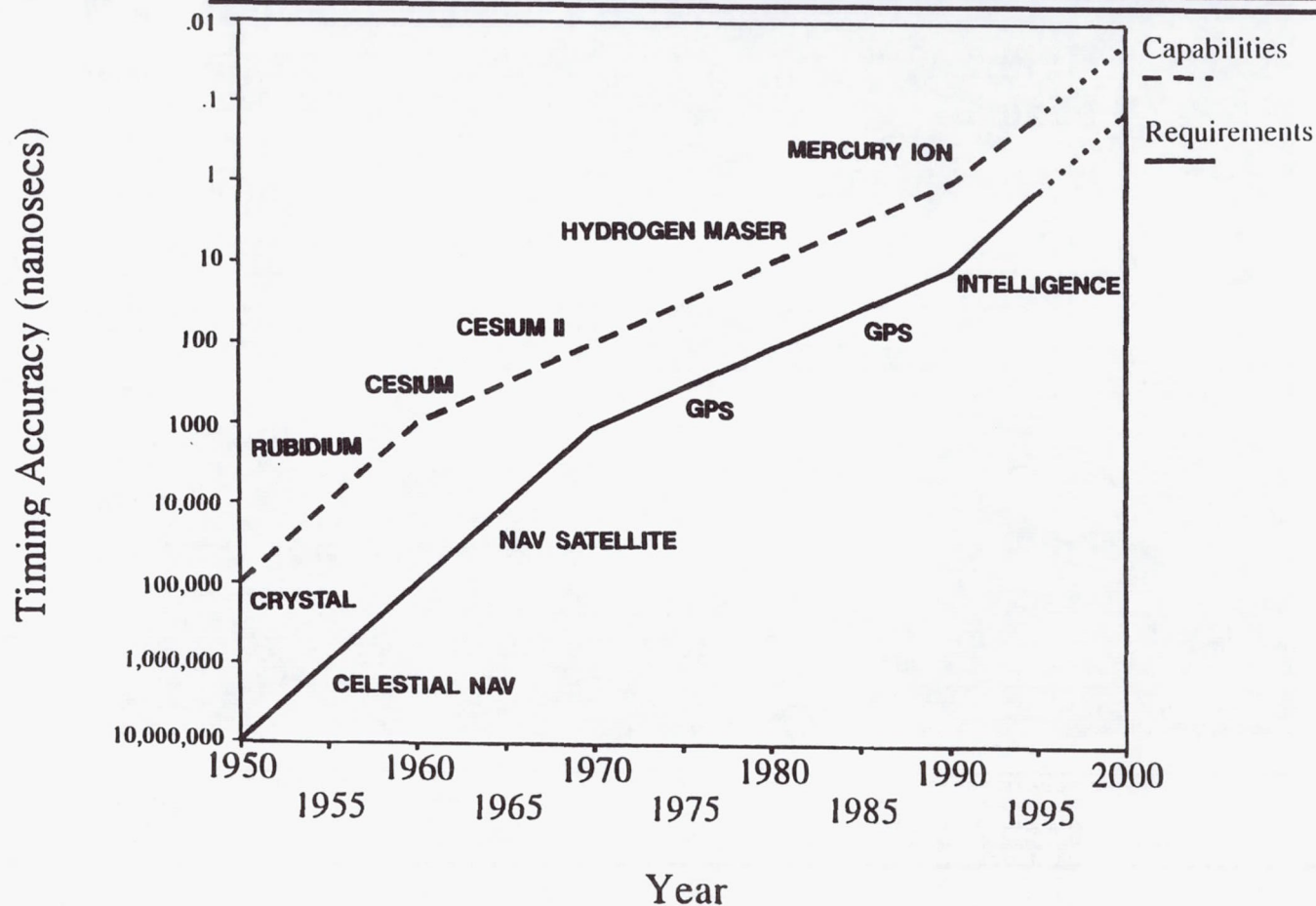


Figure 2



James A. Barnes



## PTTI DISTINGUISHED SERVICE AWARD

Presented by  
Dr. Gernot Winkler  
USNO, Retired

to

Dr. James A. Barnes  
Austron, Inc., Retired

Thank you very much, Captain. It is a very great pleasure for me to satisfy one requirement right here, and that is to recognize past achievements. I'm extremely happy that I can do that for my friend Jim Barnes, whom I have known for a long time, about 30 years. There is one thing which comes to mind immediately: his high personal qualifications, about which everyone agrees.

Jim's fairness has been recognized by quite a few people. And I want to read to you some of the comments which have been collected by David Allan, who wrote up the award citation. He has been an outstanding public administrator, bringing fairness and good will to his job. As the Time and Frequency Division Chief at the National Bureau of Standards (now NIST), he always treated outside agencies with respect and dignity. Dr. Cutler has added: "Jim has demonstrated both great depth and breadth in his solutions to problems. He is also a fine human being and an excellent leader. It is a real privilege to have known him for more than 30 years." These are the kinds of comments which have been made from old colleagues.

We owe him an enormous debt for his vision and follow-through in understanding and characterizing the random behavior of precision clocks. The tone of our whole community was set starting with his Doctor's thesis work in 1964 through his chairing the IEEE committee work leading to the classic publication in IEEE Transactions on Instrumentation Measurements entitled "Characterization of Frequency Stability," which has become a classic. The committee worked long and hard under his leadership to publish this pioneering work. In regard to this, Bob Vessot said "Jim's leadership helped pull together a coherent view by providing simple and elegant models to characterize the noise processes observed in clocks and oscillators."

Jim was born in Denver, Colorado. He will celebrate his birthday a week from this Thursday, at which time he will be 62. He received his BS from the University of Colorado, his Masters from Stanford, and his PhD back at the University of Colorado. He began summer work at NBS in 1956 with the Radio Broadcast Services Section, and the following summer worked



with the Atomic Frequency and Time Interval Standards Section. In 1958, he joined NBS full time, and in 1965 he was appointed Section Chief.

A long list of awards and recognitions have come to him over the years, which we will not highlight here, as we wish to focus on his service. His pride and joy, however, are his children Lisa, Leslie, and Jimmy, and his grandchildren.

Though his contribution to the understanding of statistical models for precision clocks and oscillators is monumental, he has made very important contributions in other areas as well. David Allan has printed out five pages of just the titles and authors of his publications while he was at NBS.

In his earlier career, he did some very important work in precision spectrum analysis of microwave signals. And among other things, he also was one of the two people who transported physically the time from the old Greenbelt WWV station to Boulder, Colorado.

In 1964, the IEEE and NASA sponsored a symposium on the definition and measurement of short-term frequency stability. Looking back with 20/20 hindsight, Jim's presentation at this conference probably had more long-term impact than any other, and was the beginnings of much of what we accept as standards for measurement in our field. Dr. Golay, during a panel discussion, had great vision, as he commented: "I would like to congratulate Mr. Barnes for having come with an extremely logical measure of instability."

Some very important clarification work was added by Bob Vessot, and Bob's paper and a classic overview paper by Dr. Cutler and Campbell Searle of MIT were published along with the above two theses in the special issue of the "Proceedings of the IEEE" in February of 1966, a classic today.

September of 1967 marked the birth of the Time and Frequency Division of NBS, with Dr. Barnes as its first chief. Roger Beehler said of this era: "It was very important in the Bureau to have a good beginning for this new division. Jim gave it the leadership, pulled together a very good staff, and launched (very successfully) the work of this important division." We are all the beneficiaries of Jim's fathering this division's efforts.

Because of his recognized stature in our field, he was asked in 1980 to write the section in the Encyclopedia of Physics on "Clocks, Atomic and Molecular." He represented NBS for many years on the Consultative Committee for the Definition of the Second, and he has helped to steer international time and frequency activities in a healthy direction.

His work now spans over nearly four decades. And it is now with great pleasure that we give Jim his award as we express to him our deep appreciation for his outstanding service and contributions to our community. Jim, may I ask you to come up here?

As we all know, the fitting token of this award is, of course, a clock. What else? This is what we would like to present to you. It's a PTTI clock, not keeping time as well as the clocks at the NBS or NIST, or the Naval Observatory, of course, but at least something which you may find as a remembrance to the service to our community. Congratulations!

**DR. JAMES BARNES:** I would like to make two very brief comments. One is that I'm

deeply honored by the award and I'm very pleased. I couldn't be more pleased with the chairman who just spoke to you. He was the first recipient of this award I understand. And I couldn't share it with better company.

One last thing is I've had some speech people help me at certain times. And they told me an interesting thing: If you have a lot of trouble, you say it very loud. And what I have to say then is **THANK YOU VERY MUCH!**



# KEYNOTE ADDRESS PROGRESS OF TIMING IN TELECOMMUNICATIONS\*

Ron Brown  
Bellcore  
Morristown, New Jersey 07960

## Abstract

*This talk provides an overview of why time and frequency are important in telecommunication networks. A historical perspective of the progress made in the telecommunication industry of both understanding and using PTTI are given. Switching, fiber-optic transmission, and wireless transmission are discussed. Finally, some prognostications about the future of PTTI in telecommunications are given.*

It is a pleasure to be with you today, particularly in San Diego with the beautiful weather. I spoke to my wife this morning, and back in New Jersey they got an inch of snow. She was not too happy about having to shovel it herself; I am happy to be out here.

I am going to be talking about the progress of timing in telecommunications. The punchline of my talk is that the telecommunications industry has come a long way in the field of synchronization over the past 10 years, but we still have a ways to go.

Let me give a little background of who I am; I work for Bellcore. Bellcore is a software and consulting firm that is owned by the seven baby bells, and we do most of our business with the seven baby bells. I am chairman of T1X1.3, which is the standards committee that sets standards for synchronization for telecommunication systems.

One example of how far we have come in telecommunications, goes back to when I began working at Bellcore seven years ago. When I hired in, my boss at that time was Joe Ohweiler. During my first week on the job he said "Right now there's only one person who really understands timing in telecommunications. His name is George Zampetti, he works at AT&T, and I want you to find out what he's talking about, if it makes sense, and if he's trying to somehow put one over on us." That was my mission. In the past seven years, I've had a chance to learn a tremendous amount from a lot of different people. In the telecommunications industry today, we have a lot more than one person who understands timing. We have come a long way.

---

\*Editor's note: This is a transcript of the oral presentation. Both the editor and the presenter have edited this paper.



One thing I want to say before I jump into my talk is Bellcore basically was created by lawyers and we have a lot of lawyers in our company. At Bellcore, it is very important for us to be unbiased. I'm going to talk about some specific companies in this talk. When I mention the companies, it is not an endorsement. In particular, I look at three companies that have really done a lot to drive progress in timing in the telecommunications industry. One of them is Bellcore, of course. The second one is AT&T Communications. The third one is Telecom Solutions, who builds timing equipment. So just because I mention those companies doesn't mean that I'm endorsing AT&T over MCI and Sprint or Telecom Solutions over HP, Austron, and all the other competitors in that field. I'm recognizing that they happen to have done a lot. I'm going to be around for pretty much the whole PTTI. If you want to get me off-line and ask about anything I bring up that we don't have time for questions and answers for, if you want to get in contact with me after the conference, my e-mail address is [sync2@cc.bellcore.com](mailto:sync2@cc.bellcore.com).

What I'm going to talk about is why do we bother to synchronize telecommunication systems. As I was going through this talk, it was a little bit long, so I'm going to go over this very briefly. Next, I'm going to talk about general milestones that have happened over the past 20 years in telecommunications; and then look at some specific topics that I think are of particular interest to this audience. Finally, I will take a quick look at the future.

Why do we bother to synchronize telecommunication networks? At a very general level (slide 3), it comes down to two things: delay and bandwidth efficiency. A synchronized system can have lower delay because you can have smaller buffers. A synchronized system will have better bandwidth efficiency for several reasons. One example is that you don't have to waste bandwidth on frequency difference accommodation. Another example is frequency reuse schemes in cellular systems. Every now and then you'll read that bandwidth, because of fiber optics, is free. This statement drives me crazy. Bandwidth is never free. There are always trade-offs. What we have found that the cost of synchronizing the system has benefits that outweigh the costs as far as bandwidth efficiency.

This leads us to design systems to be synchronous. When there are synchronization faults, they can lead to data errors that are usually related to buffers overflowing or underflowing. Those are sometimes called "slips." There are also impairments called "jitter" and "wander". All of these are impairments, but they're second-order effects due to the general things that I mentioned before of controlling delay and optimizing bandwidth efficiency.

Another area that I'm not going to talk about too much, because it's not my main area of expertise, is cellular or personal communication systems (slide 5). When I look to the future, I think cellular, as they move from the analog systems to the digital systems, is a big area of growth for synchronization.

Let me give you some rough numbers (slide 8). I think this is mostly a scientific and engineering audience, but for those who might have a marketing interest, I want to give you an idea of the market size. The baby bells, who are Bellcore's clients, sometimes called "local exchange carriers," (LECs) have roughly about 1,000 switching offices each. Each one of these offices has a clock. There are seven companies that are true baby bells that were formed when AT&T was broken up, and then there are many other independent LECs as well. GTE is the biggest, and is actually bigger than any of the baby bells. There are a handful of smaller players, Rochester



Tel for example. All together, I'd estimate that LECs in the U.S. have about 10,000 switching offices.

Inter-exchange carriers (IXCs) are companies that provide "long distance" service, like AT&T Communications, Sprint, and MCI. They have larger networks in terms of geography, but much smaller networks in terms of the number of offices, anywhere from 10's up to about 100 offices. They also have some large offices that don't have switches in them. Because of these network architecture differences, they tend to treat synchronization a little bit differently.

End users have their own networks with their own synchronization needs. I am not able to put a number on this, because there are a lot of private networks out there that vary all over the map in terms of size. For example, if you look at a company like General Motors, they have their own network for hooking their manufacturing operations and their dealer network together. Almost every large company has some form of private network. Some of them take synchronization from their carrier, and some of them have their own synchronization sources.

Cellular is an area that I've identified as a high growth area for synchronization needs. Another is the international market. North America has tended to be a little bit ahead of the international market in the synchronization area. I think in the near future carriers outside the US will be starting to catch up and doing a lot more in the synchronization area.

Let me jump into the milestones, starting with the 1970's (slide 9). I was very young in the 1970's, I was eight years old in 1972. So I certainly don't remember this, but I've been told that that's when the first triplicated cesium ensemble was built by AT&T to time the analog network. But things were happening in digital systems in the 1970's as well. First of all, in the early 1970's — I think that really might have been the late 1960's — digital transmission technology was developed, specifically the T-1 carrier system. It was a way of digitizing voice and carrying 24 voice channels within one circuit. In the late 1970's, digital switching was developed. Digital transmission has very clear benefits as far as signal-to-noise ratio; you can transmit data long distances and maintain your signal-to-noise ratio. I think most people understand the benefits of digital transmission. The benefits of digital switching are a little bit less clear and it took a little bit longer to gain acceptance. Digital switches were introduced in the late 1970's, but it didn't really grow until the mid-1980's. The main benefits have to do with the fact that if all your transmission facilities are digital, then it's easier to hook those digital transmission facilities together with a digital switch so that you don't have to convert back to analog. When the digital switches interconnected the digital transmission facilities synchronization became critical. In a simple point-to-point network, synchronization is not that important. It's when you're switching time slots that are created at Point A at Point B so that you can get to Point C that those time slots have to be of the same size and network synchronization is important.

Next we move into the 1980's (slide 10). The BITS concept was introduced in the early 1980's. The BITS concept stands for Building Integrated Timing Supply and simply states that you should have one master timing source in each office. When the BITS concept was first introduced, the master clock was usually the clock in the switch in the office. Switches were large and cost on the order of millions of dollars. They had pretty good oscillators in them, so it seemed to make sense to use that clock to time the rest of the office. It turned out not to work that well because the switch's main purpose in life was to switch telephone calls, and



it was not to be a synchronization box.

To address the shortcomings of the digital switch as a master synchronization source, Bellcore introduced the "True BITS" concept in 1986. The True BITS concept is differentiated from the BITS concept in that the master, or BITS, clock is a stand-alone clock rather than a clock embedded in a digital switch. Requirements for a dedicated, stand-alone synchronization system called a "Timing Signal Generator (TSG)" were published in a document called TA-378. The development of TSGs was important because now we had one box whose sole function in life was synchronization. By putting that emphasis on synchronization, we were really able to improve the quality of synchronization throughout the network.

1984 was the year of divestiture. Divestiture was a political event that drove a lot of technical innovations that happened later. In 1985, Pac Bell deployed their own cesium PRS's — I'm going to talk about PRS's as their own topic a little bit later.

In 1986, a rubidium Stratum 2 clock was developed. In telecommunications, we have a hierarchy of clocks. The T1.101 synchronization standard defines four strata in the hierarchy. Primary reference sources are Stratum 1 clocks and are the best clocks and are at the top of the hierarchy. As you go down, you go to lesser quality clocks. Stratum 2 is the second layer. Up until this point, Stratum 2 clocks have been double-ovenized crystal oscillators. Telecom Solutions made the decision to go with a rubidium oscillator for their Stratum 2 clock in their TSG. I think the rubidium turned out to be much more stable than the crystal and really helped to improve the performance of the network.

In 1987, AT&T started investigating GPS and started building a system to use it in their network — again, I'm going to talk about primary reference sources in detail later.

In the late 1980's, SONET started to be deployed. SONET stands for Synchronous Optical Network. It was the new fiber-optics standard. The important thing is that the 's' in SONET is for 'synchronous.' Before this, fiber-optic systems had been asynchronous. At this point, the industry made the decision to make optical systems synchronous, and there are a lot of reasons for that. I think in the bottom line, it goes back to delay and the bandwidth efficiency. For those of you with an international interest, SONET is the North American version of SDH. SDH stands for "Synchronous Digital Hierarchy."

Also in the late 1980's, there were some large network outages that were related to network synchronization and related to some problems with BITS boxes. The bottom line of these outages was not a precise time and interval-type issue, it was an availability issue. But the outages helped focus the telecom providers on synchronization. They saw that synchronization problems could bring down their network and create major outages. It was really right about when I started with Bellcore, so it made me kind of nervous whenever I was working in an office, knowing that I could bring down the network.

As we moved into the 1990's (slide 11), a big development was the adoption of TDEV as a performance parameter. I'm going to talk about parameters as a separate topic a little bit later. Also, SONET rings became the architecture of choice for SONET deployment. This is important because it impacts timing distribution architectures. Originally, switches were used to distribute timing. This led to a very simple star architecture. As SONET was being deployed,



we wanted to use SONET for timing distribution, but because it was in ring architectures, it is very hard to avoid timing loops. A timing occurs when a clock is disconnected from a primary reference source and somehow timed from itself. So SONET rings created a difficult planning issue.

Also in the early 90's a filter clock, Stratum 3E, was defined and built. As the industry was working on the performance specifications, it was clear that there was too much phase noise in the network and a clock that would filter out this phase noise was necessary. Up until this point most of the Stratum 3 clocks had been jitter filters, which meant their bandwidth was around 10 hertz. The industry decided we needed a clock that would filter to about 0.01 hertz. The 3E clocks that were developed were very neat pieces of engineering because there were some the very tough requirements on them. First of all, they needed a narrow bandwidth to do a lot of filtering, but also, when they had a good clean reference, we didn't want them generating a lot of wander, which implies a wider bandwidth. So there are a lot of design trade-offs to make both of those things happen.

TR-1244 was published by Bellcore and the ITU published G.812 in the early 90s. Up until this point, we had just had interface specifications and we didn't have any good detailed clock specifications. These documents were one of the first documents to say that this individual clock has to have this level of performance.

This year, we're seeing some primary reference sources using GPS with crystal being developed. There is a lot of excitement about this; it's helped drive down the cost of PRSs. Again, I'm going to talk about PRSs next. Let me jump into that.

PRS stands for "primary reference source." In the ITU terminology it's a PRC, a primary reference clock. They're at the top of the stratum hierarchy. Their main characteristics are an accuracy of  $10^{-11}$  and low wander. The peak-to-peak phase movement at one second is required to be less than 10 nanoseconds.

At divestiture (slide 12), there was one primary reference source for the Bell system; it was located in Hillsboro, Missouri. It was a triplicated cesium ensemble. Sprint and MCI had their own PRSs. They chose to go with LORAN technology and had quite a few distributed throughout their network. At this time, the baby bells were taking timing from AT&T.

Since divestiture (slide 13), as I said, the other IXC's were using LORAN and continue to do that, although I think they've started investigating GPS. In 1985, Pac Bell decided that the quality of synchronization they were getting from AT&T, as it was transported over the plains and then the Rocky Mountains and then the deserts of California, was not meeting their requirements. So they deployed their own primary reference sources, and they chose to use cesiums verified with LORAN. They had four of those distributed throughout California. That was the first of the baby bells to "break away" from AT&T.

Then in the late 1980's, AT&T, as I said before, started moving to GPS. Instead of having just one PRS in Hillsboro, they decided to have 16 sites throughout their network. Their PRS had 3 rubidium oscillators in conjunction with the GPS receiver. Their primary reference clocks are quite a rack of equipment, with GPS receivers, rubidium oscillators, time interval counters, and a lot of software.



As we look now in the 1990's, we see GPS gaining wider acceptance. But there's also a lot of interest in cesium, at least in the baby bells. There are a few reasons for this, the main one being the antenna required for either LORAN or GPS. The baby bells are very risk-adverse. When they see an antenna on a roof, they don't see that as a way of bringing timing into a building, they see it as a way of bringing lightning into a building and destroying equipment in the building. Certainly you can have lightning protectors, and that helps, but the lightning protectors need to be grounded. The baby bells are also very process-oriented, and so there are a lot of rules about how those things are grounded. This drives installation cost up.

We're seeing manufacturers being very aggressive in pushing GPS technology and driving the cost down. But the installation costs have been up to four times the equipment cost. That makes it very expensive. Cesium has no antenna, so the installation costs would be much less. There have been rumors about low-cost long-life cesiums, although I'm not aware of any products that have been announced. So the installed cost for the different technologies could end up being fairly close, even though the equipment cost will be higher for cesium.

Another thing about GPS is that telecommunications people have never been completely comfortable with it. The Selective Availability issue and the fact that the DoD retains the right to mess it up to any level at any time makes people a little nervous. Also the fact that it is not a completely mature system concerns people. I just started subscribing to *GPS World* since a lot of my clients have been deploying GPS, and the first issue that I received talked about a problem with the PRN-12 satellite. It doesn't seem like it was a terribly serious problem, but it's the type of thing that causes a sync coordinator in a Bell Company to ask if he can trust his telecommunications network to this system.

I tried to put together some rough projections on slide 14. We've had some cesium deployment up until now, as you can see in the second column, and we've had some LORAN deployment up until now as well. Given the 1994 FRP, I would be surprised to see much more deployment of LORAN equipment. GPS has taken a big step this year. Again, a lot of that has to do with the aggressive pricing by the suppliers.

I think the project for the year 2000 for the total number of PRSs is a good guess (4000). I think we're going to get to where we have about 40 percent of our offices timed by primary reference sources. It eliminates the distribution problems that we were talking about before. But the breakout between cesium and GPS, I think, is the big question. The competition between cesium and GPS will be an interesting thing to watch. I just kind of took a guess here that I think GPS might win out a little bit in the end, but it's anybody's guess right now.

As I was going over this talk last night, I realized that I left off a fairly important topic of interest to this audience; and it goes a little bit to the introductory speaker about what are our requirements. Right now, we have an accuracy requirement of  $10^{-11}$ . That's been around for a long time, since the mid-1980's. It is still our requirement, and I think it probably will be in the future. There's been talk of better accuracy,  $10^{-13}$ ,  $10^{-14}$ , and I think NTT out of Japan has taken this issue to some of the ITU standards groups.

I'm an engineer and I have a little bit of scientist in me, and I think it would be neat to develop a  $10^{-13}$  system just to say I did it, or we did it. But as an engineer, I need to know



the cost-benefit analysis: What are we going to gain with going to  $10^{-13}$ ? People usually cite higher byte rate systems. As you go up in byte rate, the size of your unit interval (nanoseconds per bit) decreases.

But that's not a driver this accuracy issue. The highest bit rate we have defined now is OC-192, which is a 10-gigabit system. But the 10-gigabit system is just a point-to-point system. The point where you need the synchronization is on the payload signals that you're switching or cross-connecting. Those signals are cross-connected at either the 50-megabit level or the 155-megabit level. That 10-gigabit signal — and this is kind of what SONET is all about — is made up of lots of these 155-megabit signals. So it doesn't matter how high you go in bit-rate, you're still cross-connecting the 155-megabit signal. That's where the synchronization comes in, at the cross-connected signal. So the bit rate is a non-issue in my opinion.

There could be other things that drive future accuracy requirements. One new technology is called "ATM," Asynchronous Transfer Mode. Without going into a lot of detail, one of the things in ATM is a time-stamping mechanism. Right now, it is purely a frequency time stamp, but it's conceivable that it would be a more robust system, if it used a true time of day time stamp.

Having said that, I was going to mention this in the introduction, the clocks I'm talking about are just recovering frequency, they're not recovering time of day. I'll talk about time of day a little bit more later. Currently our clocks are a bunch of either phase-lock loops or frequency-lock loops that are chained together. So they're recovering time from an upstream clock and not time of day.

We have improved some of our performance specifications. In the 1980's, there was a single number for wander, 18 microseconds. It related to the buffer size for DS-1 slip buffers. Basically the specifications were written to prevent more than a slip a day, by controlling the wander to 18 microseconds a day. 18 microseconds is a pretty large number.

In the 1990's, we finally completed those wander specs down to intervals shorter than a day. Wander is specified using MTIE, which is a peak-to-peak wander within a given observation window. For DS-1 signals, which is the one-and-a-half megabyte signal — the MTIE for observation times of 1 seconds is 300 nanoseconds; for SONET signals, it's 70 nanoseconds; and for the primary reference sources, it's 10 nanoseconds. Again, I don't see too much driving need to get too much tighter in the future.

Additionally, holdover specifications have evolved over the years. Holdover is when these PLLs go into a flywheel operation after a reference that they were locked to goes away. In the 1980's, there was just one number on this flywheel operation. In the 1990's, we decided to break that one number into components. What we saw is that clocks were very sensitive to temperature; so we could take that temperature component, break it out, and it becomes the largest component. The drift and the initial offset can become small compared to that temperature component. It leads you to the realization that the clocks were actually performing much better than the specification, because normally we don't have the wide temperature variations.

As we look to the future, I'd be surprised if we tightened up holdover specifications. The future is always a tough thing to guess at, but right now, at least for SONET, it seems like



we've nailed things down.

Another area of interest is performance parameters (slide 15). In the 1980's, we used two performance parameters, frequency accuracy and MTIE. In the late 1980's, we were using something called "RMS TIE." I joined Bellcore in 1988, so I don't accept any responsibility for this mistake. T1X1.3 quickly learned that RMS phase noise is a bad thing; it doesn't converge. We threw it out. This was an interesting time because we needed to make some big decisions. What we're finding out was there was too much wander in the network for our SONET systems to work. There were a whole bunch of issues that were interrelated; it was a very difficult problem to try to analyze. We didn't have a good measure of how much wander we had in the network, so we had to first pick a parameter to specify the wander in the network.

Working with Dave Allan and NIST, we chose TDEV. I must admit at the time I was a proponent of using a power spectral density parameter. I thought more information would be better. Since then, I've seen the light, and understand the power of TDEV to provide spectral information without being overly complicated.

As we get into the 90's now, we're nailing down a lot of definitions for parameters that have not been rigorously defined before. I want to credit one person in T1X1, Dan Wolaver, who is an old MIT professor. He's helped to bring some mathematical rigor to T1X1.3. We've nailed down a good mathematical definition for frequency drift and other items.

Another interest to a precise time group is our measurement methodology information (slide 16). Back in the mid-1980's, measurements were made with phase comparators and chart recorders. There is a company out of Rochester, New York, called Spectracom that puts these two together in a box and calls it a wander test set. We were still using these when I joined the group. We could get 100-foot-long tapes and we would stretch them out in the hallway and try to figure out what a clock was doing. This was not the easiest thing to do.

At this time, people in the industry were also using time interval counters that were hooked to printers. They'd get numbers; and they'd take the numbers and plot them. So this was getting a little bit more accurate, you had actual numbers you could work with, but it was still very difficult and tedious.

Finally in 1989, we programmed computers to control the time interval counters, and get the data electronically and automatically so that we could do analysis like MTIE and TDEV. Recently, there's been an integrated test set that does all this: Microwave Logic, which has since been bought out by Tektronix, developed a SONET test set called the SJ-300.

I put clock extractors on the slide. They're one of the banes of my life. Clock extractors serve a couple functions; they take data signals that have ones and zeros and create a square wave that is more useful with a time interval counter. They typically also do frequency division to give you a lower rate signal so that the edge crossing issue goes away as well. I have found them to be fairly unreliable and the largest source of measurement noise.

We're a little bit lucky in telecommunications because the level of noise we're measuring tends to be fairly high for wander: tens of nanoseconds. Therefore, we don't have to worry about things like the double-balanced mixer technique advocated by NIST. I think those techniques



are possible, but it would be that much harder to make the measurements.

However, for high-frequency phase noise called jitter, there are some very tight specifications that are more difficult to measure. For example, there's a 0.01 unit interval rms specification for OC-48, which is a two-and-a-half gigabit signal. 0.01 UI at two-and-a-half gigabits translates out to about four picoseconds. That's a very difficult thing to measure. Companies like Microwave Logic have developed test tests to do this, and I think they take advantage of balanced mixer techniques.

Another issue for Bellcore is that we're having trouble verifying PRS performance. I have a cesium in my lab that has an accuracy specified at 5 parts in  $10^{12}$ . I'm trying to measure the accuracy of GPS receivers that are specified to be at least as accurate, if not more accurate. I know I could buy a Hewlett-Packard cesium, but unfortunately I don't have the money. So we're looking at some cheap way to be able to verify accuracy performance for PRSs.

Finally, I will look into my crystal ball and share what I see in the future of timing in telecommunications (slide 18). The first item is pretty much a no-brainer. We definitely will see more PRS deployments. This goes back to the SONET deployment that is making it more difficult to distribute synchronization. So our synchronization coordinators want to either eliminate completely or minimize synchronization distribution, depending on who you talk to. The question here, I think, is which technology wins out in the end: GPS or cesium.

Time of day is something I have a question mark by. There's definitely a need for time stamping alarm events so that you can correlate them and figure out where problems actually are. Also time of day is need for billing. However, those applications don't have particularly tight time-of-day requirements, probably on the 10's to 100's of milliseconds.

Currently, I think people are going insert time of day at a few points in the network and then distribute it around using network time protocol (NTP). However, it seems if you had very accurate time of day, you could then use that for things like frequency synchronization, as well as other things such as encryption and secure digital signatures. The question is will the benefits of those applications justify the costs of much more time-of-day deployment.

PCS cellular seems like a big growth area to me. \$7 billion has just been spent on the spectrum by these carriers. They're all going with digital technology. I think both of the digital technologies, CDMA and TDMA, have synchronization concerns. I think these concerns are related to both the frequency reuse issue between the cell sites; and also to hand-off issues as phones move from one cell site to another.

Another issue I see on the horizon is better monitoring. Right now, we send synchronization to another office and we assume that they're using it correctly. We've seen that improper synchronization can degrade performance, and there's a feeling that we need to do more to make sure that performance is not being degraded. However, we're not completely sure exactly how to get there. The introduction of SONET only makes this more complicated.

The other thing that I see in the crystal ball is international markets. The international folks, I think, are starting to accept the BITS concept and the idea that you need stand-alone clocks. I think they're taking synchronization much more seriously now.

In conclusion (slide 19), I think we've come a long way but we have a long way to go. The telecommunications synchronization personnel will have jobs for awhile. To me, that's pretty important, given where I am in my career. If the government shuts down, we can take a few of you folks, but not all of you.





## Progress of Timing In Telecommunications

Ron Brown  
PTTI, December 1995

Copyright © 1995, Bellcore  
All Rights Reserved

### Outline

- Need for synchronization in telecommunications
- General milestones
- Evolution of specific topics
- Look to the future

slide 2



## Why Synchronize Telecom Networks?

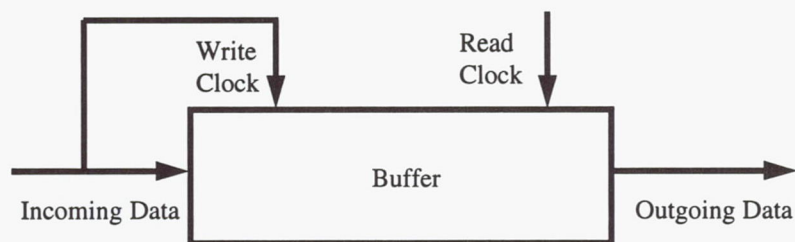
- General
  - Delay -smaller buffers
  - Bandwidth efficiency -bandwidth is not free
- Specific
  - Data integrity -slips, jitter
  - Frequency reuse - cellular

slide 3

**Bellcore**  
Bell Communications Research

## Elastic Stores

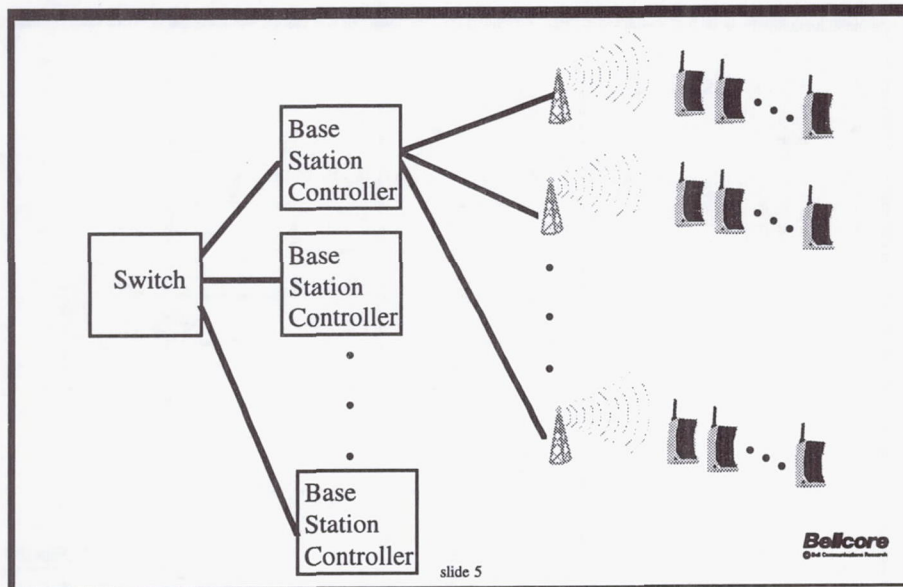
- Slip buffers, desynchronizers, pointer processors
- Read clock may be filtered version of write clock or independent



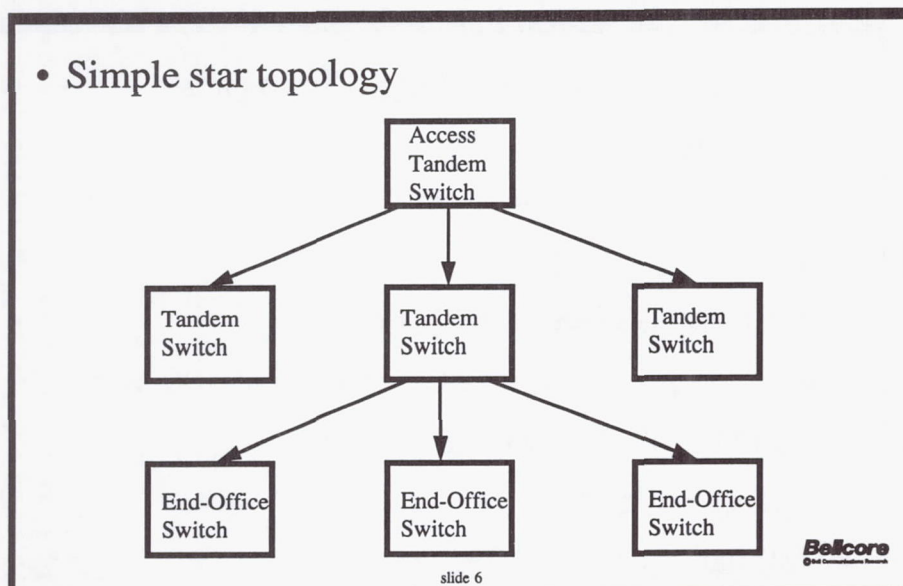
slide 4

**Bellcore**  
Bell Communications Research

## Cellular Networks

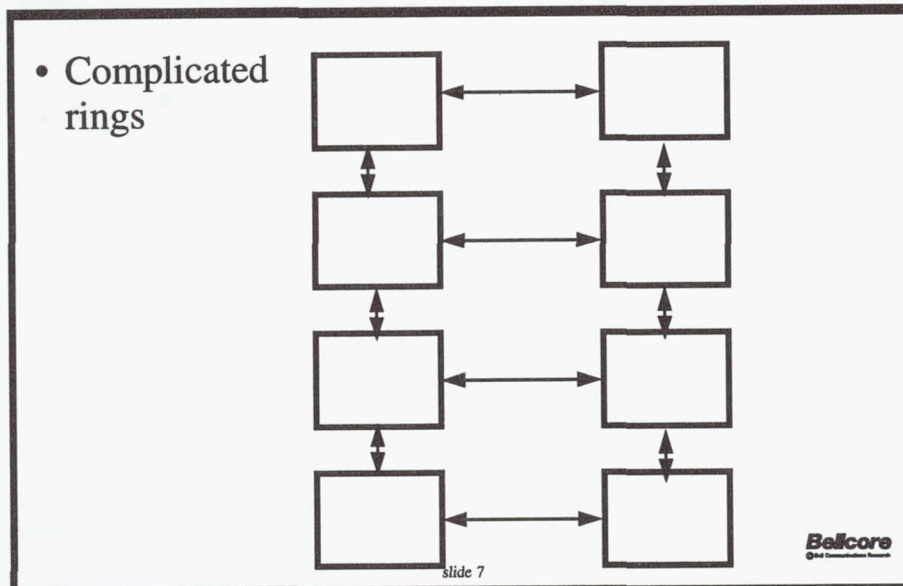


## Switched Based Timing Distribution





## SONET Based Timing Distribution



## Some Rough Numbers

- Baby bells - 1000 switching offices each
  - 7 baby bells & GTE
  - many independents with a few to 100 offices
- IXC's
  - 10s to 100 switching offices
  - also non-switching offices - 10s to 100 as well
- Large number of private networks
  - large variety in size
- Cellular -lots in the future

slide 8

**Bellcore**  
Global Communications Research

### Milestones of the 1970s

- 1972: Hillsboro triplicated Cesium ensemble
  - Analog network synchronization
- Early 70s: digital transmission equipment: T1 carrier
- Late 1970s: digital switching developed

slide 9

**Belcore**  
Global Communications Research

### Milestones -1980's

- Early 1980s: BITS Concept
- 1984: Divestiture
- 1985: Pac Bell deploys Cesium PRS
- 1986: True BITS -standalone clocks (TA-378)
- 1986: Rubidium ST2 clock
- 1987: AT&T decides to go to GPS
- 1988-90: SONET starts to be deployed
- 1989,90: Large sync related service outages: SS7

slide 10

**Belcore**  
Global Communications Research



## Milestones -1990's

- 1991: TDEV adopted by T1X1.3
- SONET rings architecture of choice
  - complicates sync planning
- 1992: ST3E filter clock developed-SONET driven
- 1993: TR-1244 "Synced Clock Requirements" published by Bellcore
- 1995: PRS using GPS with crystal developed

slide 11

**Bellcore**  
Bell Communications Research

## PRSs at Divestiture

- PRS at top of hierarchy
- AT&T 1 PRS in Hillsboro, MO
  - triplicated Cs
- Sprint & MCI
  - LORAN-C
- Baby Bells take timing from AT&T

slide 12

**Bellcore**  
Bell Communications Research

## PRS Since Divestiture

- 1989: AT&T moves to distributed GPS/Rb
- 1980s: Other IXC's use LORAN
- 1985: Pac Bell deploys 4 Cs verified w/LORAN
- 1990s: GPS gaining acceptance
- Interest in low-cost, long-life Cs
  - no antenna

slide 13

**Belcore**  
Global Communications Network

## Rough PRS Projections in 7 Baby Bells

•	Cs	LORAN	GPS	TOTAL
• 1990	10	10	1	21
• 1995	16	128	415	559
• 2000	1500?	200	2300?	4000

slide 14

**Belcore**  
Global Communications Network



## Performance Parameters

- 1984: Accuracy, MTIE
- 1988: rms TIE (!)
- 1991: TDEV adopted with help from NIST
- 1995: Defined methodology for frequency drift

slide 15

**Bellcore**  
Bell Communications Research

## Measurement Techniques Evolution:

- 1985: phase comparator & strip chart
- 1987: Time interval counter and printer (!)
  - clock extractors
- 1989: Computer controlled time interval counter
  - computer programs for MTIE, TDEV analysis
- 1993: Integrated Test Set (SJ-300)

slide 16

**Bellcore**  
Bell Communications Research

### Measurement Techniques Issues:

- Enough wander - mixer techniques not necessary
- Jitter measurements for high bit-rates harder
  - 0.01 UI rms at OC-48 = 4 picoseconds !
- Trouble verifying PRS performance
  - 10e-12 hard to measure

slide 17

**Belcore**  
Global Communications Research

### Crystal Ball

- Greater PRS deployment
  - eliminate distribution related issues
- Time-of-day
  - where? distribute with NTP? accuracy?
- PCS/Cellular
  - biggest growth area
- Better monitoring
  - get away from “send and pray”

slide 18

**Belcore**  
Global Communications Research



## Conclusion

- *We have come a long way, but we have a ways to go.*
- *Telecommunications sync personnel will have jobs for awhile.*

slide 19

**Belcore**  
© 1995 Communications Research

## QUESTIONS AND ANSWERS

**DR. GERNOT WINKLER (USNO, RETIRED):** Could you put the slide back on evolution of performance? The 18 microsecond per day wander is, of course, as you mentioned, the allowance for one slip of one frame per day. That requirement necessitated the absolute accurate specification of  $10^{-11}$ . In other words, that accuracy requirement comes from concern about the international connections, or the intercontinental connections.

Now if you look at development where you go to 300 nanoseconds, it goes to 300 nanoseconds, 70 nanoseconds, and so on at these increased bandwidths and higher communication speeds, I would expect that this would also then mean there would be a greater accuracy requirement for that. In other words, for the operation within your network, there is no benefit in having that accuracy. But for the interconnections between that, particularly accuracy, – so the accuracy requirement is an external requirement, and not an internal requirement.

**RON BROWN (BELLCORE):** My take on that again is that the higher bit rate signals, you can really view them as point to point; the 10-gigabit signal is point to point. You're going to need a buffer in the front end of your SONET equipment that needs to accommodate jitter.

One of the slides I skipped (slide 4) discussed elastic stores Elastic storage is the concept, I think, that probably most engineers are familiar with. An elastic store is a buffer that has a separate read and write clock. Elastic storage has a lot of different applications. One application is a DS-1 slip buffer. In a DS-1 slip buffer, the write clock is from the incoming data, the read clock is from the system clock. So if those two are different, eventually this buffer is going to overflow or underflow.

In the SONET system, there are actually several layers of these elastic storage. The first layer, in what I call the front end of the equipment, you have the relationship between the write and read clock in that the read clock is a filtered version of the write clock. It's not tied into the system clock. So if the system clock is different than the clock on the received data, it doesn't affect this buffer. It's the buffer at the next layer down that can be impacted. That next layer down is called the "point or processor buffer." That works on the 155-megabit or the 55-megabit signals. It's always going to work on the 155-megabit signals regardless of the line rate.

**DR. GERNOT WINKLER (USNO, RETIRED):** So if I understand you right, that suspicion that I voiced is not valid because you have buffering in an entirely different way.

But there is a second comment which I want to make, and that goes back to a need for having more precise definitions of these different requirements. You have five levels, and the five levels are to operate on the same frequency; to be on the same accurate frequency, an additional requirement which, of course, costs money; to be synchronized; to be synchronized in time – in other words, not allowing any steps, but without resolution of delays; and finally, to be on UTC, the time of day. If there is any requirement to be on time of day, then of course the use of GPS is far superior to the use of just the cesium standard.

**RON BROWN (BELLCORE):** Right. In the competition between cesium and GPS, I think time of day is a critical issue. If there is a time-of-day requirement, and that time-of-day



requirement gets tight enough where you can't distribute time of day, then GPS is clearly the technology of choice. I've seen a lot of articles by NTT and distributing time of day, and it seems like they can get fairly good accuracy. But if you need a nanosecond, or 10-nanosecond accuracy, I don't think you're going to be able to distribute it. So if that requirement becomes real, then GPS definitely will be the winner in that technology race.

The worse scenario, at least from my clients' point of view, is that that requirement isn't clear now, they choose cesium; the requirement becomes a requirement later on; and then they have to employ GPS on top of the cesiums they've already bought. But right now, there's no drive for 10 nanoseconds absolute UTC accuracy. Certainly if you have that, you can drive everything else into it. It's not a bad argument to say that why don't you just get that so that you derive everything else, and then you don't have to worry about where things go in the future. So, there's definitely a strong argument that can be made for GPS and getting that capability. By the way, I don't want to discourage people from developing  $10^{-13}$ ,  $10^{-15}$  cheap receivers. I'm sure if it becomes cheap enough, we'll definitely take advantage of it. So, there's always a cost benefit. As the cost comes down, it becomes easier to justify.

**CAPTAIN STEVEN HUTSELL (USAF):** You bring up a very good point about the amount of confidence that civilian users have in using GPS for time transfer. And I think it's important to point out that as with any costly expensive system that people decide to use for precise timing, whether it's a cesium ensemble, LORAN, or GPS, a lot of the confidence level that the user will have will greatly depend on the application and the implementation. I think it's important to point out that there are relatively simple techniques to identify and catch problems similar to what you were mentioning about PRN-12, as was mentioned in the *GPS World* article. Those include high-sampling checks of the parity and the help settings in the navigation message. That's probably a good first line of defense, and a good second line of defense would probably be something similar to a receiver set that could track all satellites in view and easily isolate a problem bird such as PRN-12.

**RON BROWN (BELLCORE):** Thanks for the input. We have tried to write requirements to make things as robust as possible, but we're not GPS experts. So, maybe I'll try and get with the GPS experts to get some more of those details.

**RON ROLOFF (DATUM):** One more question. You mentioned long life in cesiums. What is your long life?

**RON BROWN (BELLCORE):** My synchronization coordinators tend to be a little bit older group, so their definition is "As long as it's going to take me to retire!" But seriously, the number that I have heard thrown around is 15 years. I don't know if this is realistic or if it just the cesium suppliers trying to compete with the GPS suppliers. But, 15 years is the number that's getting people excited.

**RON ROLOFF (DATUM):** Why is that different than applied to your other equipment? Or is it?

**RON BROWN (BELLCORE):** You mean like other telecommunication equipment?

**RON ROLOFF (DATUM):** Yes.



**RON BROWN (BELLCORE):** Okay, telecommunication equipment life cycles is a bigger can of worms than you might realize. There are bigger depreciation cycles for different areas. So public utility commissions sometimes require 30-year depreciation cycles, whereas a normal business might look at it on a 5-year depreciation cycle. So, there's a bunch of depreciation issues there that are related to regulatory issues that I don't completely understand.

Then there's just a replacement cost. If you just look at lifetime cost of a product, you've got to look at how often it needs to be retrofitted, and how much that's going to cost you to do it.

**SAM STEIN (TIMING SOLUTIONS CORPORATION):** I would like to pursue this issue of the time synchronization in a network as opposed to frequency synchronization. I believe what's driving the interest of NTT in Japan is that the wander over 1000-kilometer networks is on the order of many microseconds. This is a substantial fraction of the allowable wander budget in the network. The issue being the ability to construct signals at the user end — to be able to reconstruct — in the phase-lock loop. So they would attempt to drive the wander due to — and alignment down from five microseconds to some small fraction thereof. — —. I was wondering whether there is support for that kind of approach within the United States in SONET and whether this is within long-term direction.

**RON BROWN (BELLCORE):** Let me raise a few issues. First SONET is a little bit ahead of SDH and there has been more SONET equipment deployed than SDH equipment. Anytime you look at changing the SONET standard, you are looking at possibly retrofitting a lot of equipment. So the carriers have to be convinced that the benefits are going to be significant to incur that cost, whereas the cost is maybe less for the SDH people because they do not have quite as much deployed. There is interest in going to higher accuracies; it has been brought up in T1X1.3 and when it gets brought up people say that it is interesting, better seems better, lets pursue that, and try and push for that. Which is not to say that won't happen in the future, but it is not clear to me what the NTT goal is.

**DR. GERNOT WINKLER (USNO, RETIRED):** I thought you were going to mention the Thursday evening seminar about "Robust Timing" techniques, which has a direct implication to what we have discussed here.

**SAM STEIN (TIMING SOLUTIONS):** I am going to talk about government interests in pursuing exactly that technology for reducing total wander across SONET links.



# GPS MONITOR STATION UPGRADE PROGRAM AT THE NAVAL RESEARCH LABORATORY

Ivan J. Galysh and Dwin M. Craig  
Naval Research Laboratory  
4555 Overlook Ave. SW  
Washington, D.C. 20375-5000

## Abstract

*One of the measurements made by the GPS Monitor Stations is to measure the continuous pseudo-range of all the passing GPS satellites. The pseudo-range contains GPS satellite and Monitor Station clock errors as well as GPS satellite navigation errors. Currently the time at the GPS Monitor Station is obtained from the GPS constellation and has an inherent inaccuracy as a result. Improved timing accuracy at the GPS Monitor Stations will improve GPS performance.*

*The U.S. Naval Research Laboratory (NRL) is developing hardware and software for the GPS Monitor Station Upgrade program to improve the Monitor Station clock accuracy. This upgrade will allow a method independent of the GPS satellite constellation of measuring and correcting Monitor Station time to U.S. Naval Observatory (USNO). The hardware consists of a high-performance atomic cesium frequency standard (CFS) and a computer which is used to ensemble this CFS with the two CFSs currently located at the Monitor Station by use of a dual-mixer system. The dual-mixer system achieves phase measurements between the high-performance CFS and the existing Monitor Station CFSs to within 400 femtoseconds.*

*Time transfer between USNO and a given Monitor Station is achieved via a two-way satellite time-transfer modem. The computer at the Monitor Station disciplines the CFS based on a comparison of one pulse per second sent from the master site at USNO. The Monitor Station computer is also used to perform housekeeping functions, as well as recording the health status of all three CFSs. This information is sent to USNO through the time-transfer modem.*

*Laboratory time synchronization results in the sub-nanosecond range have been observed and the ability to maintain the Monitor Station CFS frequency to within  $3.0 \times 10^{-14}$  of the master site at USNO.*

## INTRODUCTION

The GPS Monitor Station Timing Subsystem Enhancement (MSTSE) project will provide a timing subsystem to the existing GPS Monitor Stations in Hawaii, Kwajalein Island, Ascension Island, and Diego Garcia. The new timing subsystem will provide uninterrupted frequency output that is syntonized to Universal Time Coordinated from the U.S. Naval Observatory, UTC (USNO), via a Two-Way Satellite Time Transfer modem (TWSTT). A new cesium-beam frequency standard (CFS) will be ensembled with the existing clocks, which will increase reliability and stability. If one of the clocks at the Monitor Station (MS) site begins to fail, the KAS-2 (Kalman Filter Algorithm for Time Scale Computation) software will automatically deweight that CFS out of the system. This upgrade will also allow remote monitoring of the health and performance of the clocks in the ensemble. This will allow an independent means



to confirm the subsystems performance and the quality of the timing reference available to each MS. All of these functions will be automated and not require operator intervention.

The GPS Monitor Stations measure the continuous pseudo-range of all the passing GPS satellites. These data are sent to the Master Control Station (MCS) over a communications link. At the Monitor Stations there are three components that contribute to major errors in the pseudo-range measurements, errors from the clock in the space vehicle, errors in the ground receiver, and errors in the ground clock. If the problem involves the CFS, then the system must be switched over to the backup CFS. This manual switchover by the operator at the MCS may cause a phase discontinuity which can appear as a data anomaly. At the MCS the data that have been collected is preprocessed and input to the system Kalman filter. Recently measurements taken from the satellite constellation have been used to improve these error models, and system performance has improved. The purpose of the GPS MSTSE is to improve the reliability of the present system and to provide an independent method of measuring the clock performance of the ground station clocks, thus making possible improvements in the clock models and reducing noise from the ground clocks for the Kalman filter calculations.

## OBJECTIVES

The GPS Monitor Station Timing Subsystem Enhancement Project has the following objectives: to non-obtrusively enhance the existing Monitor Station systems using existing interfaces, to provide a higher degree of reliability at each monitor site, to syntonize the Monitor Station frequency to the USNO Master Clock, to provide an independent means to measure Monitor Station performance, and to provide for remote unmanned operation.

## MONITOR STATION INTERFACE

The new timing subsystem will appear, to the existing hardware interface at the GPS MS, as one of the CFSs already installed at the monitor site. The output from the MSTSE will be provided into the existing MS hardware as if it were the output of a single CFS. The MSTSE will also provide a clock health status signal into the existing hardware interface. Figure 1 is a diagram showing the way in which the MSTSE is integrated into the existing system.

## HARDWARE CONFIGURATION

As shown in Figure 2, the MSTSE hardware configuration consists of an HP5071 CFS, a dual-mixer phase measurement system, an autoswitch, a TWSTT, a system computer, a backup power system, and a watchdog timer. The equipment is contained in a single rack, excluding the Very Small Aperture Terminal (VSAT) for the TWSTT. The rack layout is shown in Figure 3. The HP5071 Primary Frequency Standard has the high-performance cesium beam tube option, which allows for time domain stability of  $2.0 \times 10^{-14}$  seconds in a 30-day period. This CFS has a microprocessor-controlled Voltage-Controlled Crystal Oscillator (VCXO) which is corrected several times a second so that it remains locked to the cesium transition frequency. The HP5071 can be accurately disciplined by ensemble software and the TWSTT modem.

To measure clock quality, a four-channel dual-mixer system is being employed. Measurements between the two existing HP5061 CFSs and the new HP5071 CFSs will be performed with precision in the 400 femtosecond range. The measurements are collected hourly. These data



are then applied to the KAS-2 ensembling software<sup>[1]</sup>. The resulting ensemble output is then used to discipline the HP5071 CFS.

The dual-mixer hardware consists of three elements, an offset reference oscillator, a crossover detector, and an event timer. The dual-mixer hardware uses a Guide Technology 401 event-timing controller. The GT401 has its own on board microprocessor and the ability to time-tag an event on any of four channels to 0.4  $\mu$ s accuracy. This card has a real-time clock which takes an external 10 MHz input supplied by the reference HP5071 CFS. This real-time clock is then the baseline reference for the time-tag generation. The 5 MHz outputs of the three CFS are fed into the distribution amplifier (DA). The outputs from the DA are then mixed with the output from the offset reference oscillator, thus providing the heterodyne effect, and is then sent to the event counter (GT401 Event-Timing Controller Monitor) for phase crossover detection and time-tagging. A more detailed description of the dual-mixer phase measurement system can be found in [2]. The dual-mixer software processes the time-tagged data and then outputs phase data on the different CFSs. The data generated by the dual mixer are integrated into the daily TWSTT message and sent during every time transfer.

The function of the autoswitch is to shut off the 5MHz RF signal to the MS in the event of a major failure; this is a failsafe feature. The existing MS system detects clock failure as a loss of signal and switches to the secondary CFS. The autoswitch hardware monitors the signal level and phase of the 5 MHz signals on all three CFS channels. The autoswitch has frequency drift and signal amplitude detection hardware. The autoswitch continuously tests the incoming signals. A comparison between all three inputs is done and a majority vote is taken to determine if any of the CFS outputs is drifting off frequency compared to the other two clock channels. If a CFS output frequency has drifted too far from the other CFSs, then that channel is shut down by the autoswitch. This provides a safeguard against a poorly performing CFS providing a bad frequency signal from the MSTSE.

The Two-Way Time Transfer modem is capable of precise time transfer with sub-nanosecond precision using commercial communications satellites. This modem allows for frequency synchronization of the HP5071 to the USNO Master Clock. This modem consists of a commercial PC/AT computer in an industrial chassis, an analog transmitter section, and a VSAT communications antenna. The system was developed at NRL and Allen Osborne Associates during the last 4 years<sup>[3]</sup>. The digital section of the modem is connected to the system computer using an RS-232 serial connection. The TWSTT modem can then not only send time-transfer results to the main system computer, but also CFS measurement data back through the modem. The TWSTT modem is configured as a target at the remote site, with USNO operating as the master station. The modem is configured for automated operation and will automatically perform a time transfer when initiated from the master site.

The system computer section of the timing subsystem is an PC in an industrial chassis. The computer has RS232 port connections to the Two-Way Time Transfer modem and the HP5071 CFS. The computer module also contains the dual-mixer hardware and the autoswitch module connected via its Industry Standard Architecture passive backplane. Along with the computer's power supply is a battery charger and voltage regulator for keeping the emergency batteries charged. The centronics parallel output of the computer is connected to a watchdog timer module. The watchdog timer is another failsafe feature of the timing subsystem. It controls the System Health Status line to the MS system and the MCS. A health status message will be indicated to the Monitor Station and the output of the autoswitch cut off if the system computer fails.



## SOFTWARE

The system computer operates under a multitasking operating system, with operations handled by small independent routines. There are separate routines to handle each portion of the timing subsystems' functionality. Tasks communicate to each other via files or pipelines. The operating system is Linux, which is a POSIX-compliant implementation of the UNIX operating system. Linux is an ideal operating system for implementation of the timing subsystem, and will accommodate possible future integration into a new MS open system architecture.

The MSTSE software consists of five software modules controlling the various parts of the data collection and control functions of the MSTSE, as shown in Figure 4. The five major software modules are: the control program, the dual mixer task, the autoswitch task, the cesium task, the modem task, and the watchdog task. Figure 4 illustrates the lines of communication between the different software modules.

The control program initializes all of the other software modules when the system first boots up. This program provides a display interface to the video output which shows the status of the autoswitch. This module also communicates with the cesium task to get status information from the HP5071 CFS. The control program provides a quick way to determine the health and status of the HP5071 CFS and the autoswitch.

The Dual Mixer task processes the dual-mixer data to provide the phase relationship between the Master Clock (HP5071) and the two existing HP5061s at the Monitor Station. The dual-mixer hardware collects hourly time-tagged data on four channels. The first channel is the reference HP5071, and the second and third channels are the two HP5061s. The fourth channel measures the reference HP5071 against itself as a noise channel and an extra check of dual-mixer performance. The GT401 event-timing controller monitor ISA bus card is checked continuously by the dual-mixer task to maintain the proper relationships between collected data. After data collection is complete, the dual-mixer software begins to perform postprocessing, which involves providing the correct time tags for each phase measurement. The dual-mixer task provides clock quality data to the modem task for inclusion into the daily time transfer.

After the phase data processing is complete, the dual-mixer task calls the KAS-2 software which generates the ensemble. The cesium task output then receives these data from the KAS-2 software for determination of the correct output frequency.

The autoswitch task monitors the autoswitch every 5 seconds and updates a status file. This software routine queries the hardware in the autoswitch to monitor the signal level and phase quality of the signals coming from the CFSs on all three channels.

The cesium task monitors and controls the HP5071 CFS. Every minute it checks the operating status of the HP5071. Once an hour the task collects the operating parameters from the CFS. The current discipline value generated by analysis of the TWSTT data is provided to the cesium task, which then disciplines the HP5071. In this way the reference HP5071 is syntonized to UTC (USNO).

The modem task monitors the operation of the TWSTT. After the time transfer has been initiated by USNO, the modem task collects the results of the transfer. The data from the transfer are then sent to the clock discipline task, where a calculation in the discipline algorithm determines if a command should be sent to the HP5071. The purpose of discipline task is to syntonize the reference HP5071 CFS to UTC (USNO). The disciplining algorithm estimates the frequency offset of the reference CFS to UTC (USNO) by using the slope of the data from a linear fit to the frequency data. The slope is calculated from a minimum of three



time-transfer measurements and is compared to a predetermined threshold. The threshold is preset. When the system is in the initialization process, a jam syntonization occurs between the reference CFS and USNO. This is a one-time gross adjustment of the remote clock after the first three time-transfer measurements are gathered. After the jam sync of the reference CFS, the discipline commands are limited to a maximum frequency value of 2 parts in  $10^{-14}$ . Discipline commands in this range should be well below the measurement threshold of the existing MS equipment and, therefore, transparent to its operation. The modem task also controls the packing task, which prepares the last three days of clock quality data to be sent to USNO during the transfer.

The watchdog task sends a reset signal to a watchdog timer every 60 seconds; failure to do so changes the health status message to the Monitor Station Frequency Standard Element and turns off the autoswitch. The MS system then switches to the secondary (backup) HP5061 as the frequency reference to the Monitor Station. This final switching occurs externally to the MSTSE.

## PERFORMANCE EVALUATION

### Clock Quality

Performance of the MSTSE software and hardware configuration was tested against the time and frequency reference systems at the NRL Precise Clock Evaluation Facility<sup>[4]</sup>. The time and frequency reference used at the NRL Precise Clock Evaluation Facility contains two Sigma Tau hydrogen masers. These masers produce 1PPS and 5MHz signals that are synchronized to UTC (USNO). The test configuration assigned each system under test consisted of one HP5071 as the primary or reference CFS. The other two CFS in the systems were two other HP5071s, which were also monitored by the precise clock evaluation facility's long-term clock measurement system. All three clocks have their 5MHz outputs routed into the Precise Clock Evaluation Facility's long-term measurement system. This dual-mixer system is capable of measuring 48 clocks simultaneously with a  $\tau$ -interval of one hour and a noise floor of  $6 \times 10^{-12}/\tau$ .

A test was run over a four-day period in which measurements of the three clocks were taken by the MSTSE system and NRL's precise clock evaluation facility. Figure 5 is a plot comparing the two systems. There is a intentional 1-nanosecond offset in the data to allow for easier comparison of the two phase plots. The correlation between the two sets of measurements is very good, as can be seen. Consequently the measurement precision and accuracy was verified.

### Two-Way Satellite Time Transfer

At NRL a test configuration was set up to verify the performance of the TWSTT that will be installed in the MSs. Two different configurations were used to evaluate the performance of the TWSTT. The first configuration tested involved taking two modems and connecting them directly without a using a satellite antenna. The second performance evaluation involved using a satellite link.

The first data plot (Figure 6) shows 16 days of data. As can be seen in the data, the original jam syntonization is on the order of 18 parts in  $10^{-14}$ . After this initial frequency correction, the reference CFS has very little drift in the next 13 days. The discipline algorithm doesn't sent a command to the CFS because the threshold frequency drift has not been crossed.



The second data plot (Figure 7) shows the modem performance using the satellite in the test configuration. Again, a jam sync occurs after the first three time transfers have occurred. After 33 days the CFS frequency drifted over the threshold set by the discipline algorithm and a command was sent to the cesium task to provide a correction. This demonstrates that the algorithm worked, and that the CFS can be syntonized remotely.

## CONCLUSIONS

The system improves performance at the monitor site by providing a very stable frequency standard with the HP5071. It allows measurement of the existing CFS against the new CFS and disciplines the new CFS to the UTC time provided by USNO. This upgrade will provide composite clock capability, which until now has only been available at the MCS. Greater reliability is realized through multiple safeguards to ensure continuous monitored performance at each ground site.

## REFERENCES

- [1] S. Stein 1995, "*KAS-2: Algorithm for time-scale computation and control of real-time clocks*," Report No. TS95.0046 Rev. 1 (Timing Solutions Corporation Boulder, Colorado).
- [2] S. Stein, D. Glaze, J. Levine, J. Gray, D. Hilliard, D. Howe, and L. Erb 1982, "*Performance of an automated high accuracy phase measurement system*," Proceedings of the 36th Annual Symposium on Frequency Control, 2-4 June 1982, pp. 314-320 = NIST Tech. Note 1337, pp. 241-247.
- [3] G.P. Landis, I.J. Galysh, G. Gifford, and A. Osborne 1992, "*A new two-way time transfer modem*," Proceedings of the 23rd Annual Precise Time and Time Interval (PTTI) Applications and Planning Meeting, 3-5 December 1991, Pasadena, California, pp. 247-257.
- [4] E.C. Jones, E.D. Powers, A.H. Frank, and J.A. Maury 1995, "*Static timing tests of the R-2332/AR, R2331/URN, MANPACK (RPU-1), and the Texas Instrument MANPACK AN/PSN-9 NAVSTAR Global Positioning System user equipment at the Naval Research Laboratory*," NRL MR/8150-95-7754 (Naval Research Laboratory, Washington, D.C.). A more up-to-date report will be forthcoming shortly.



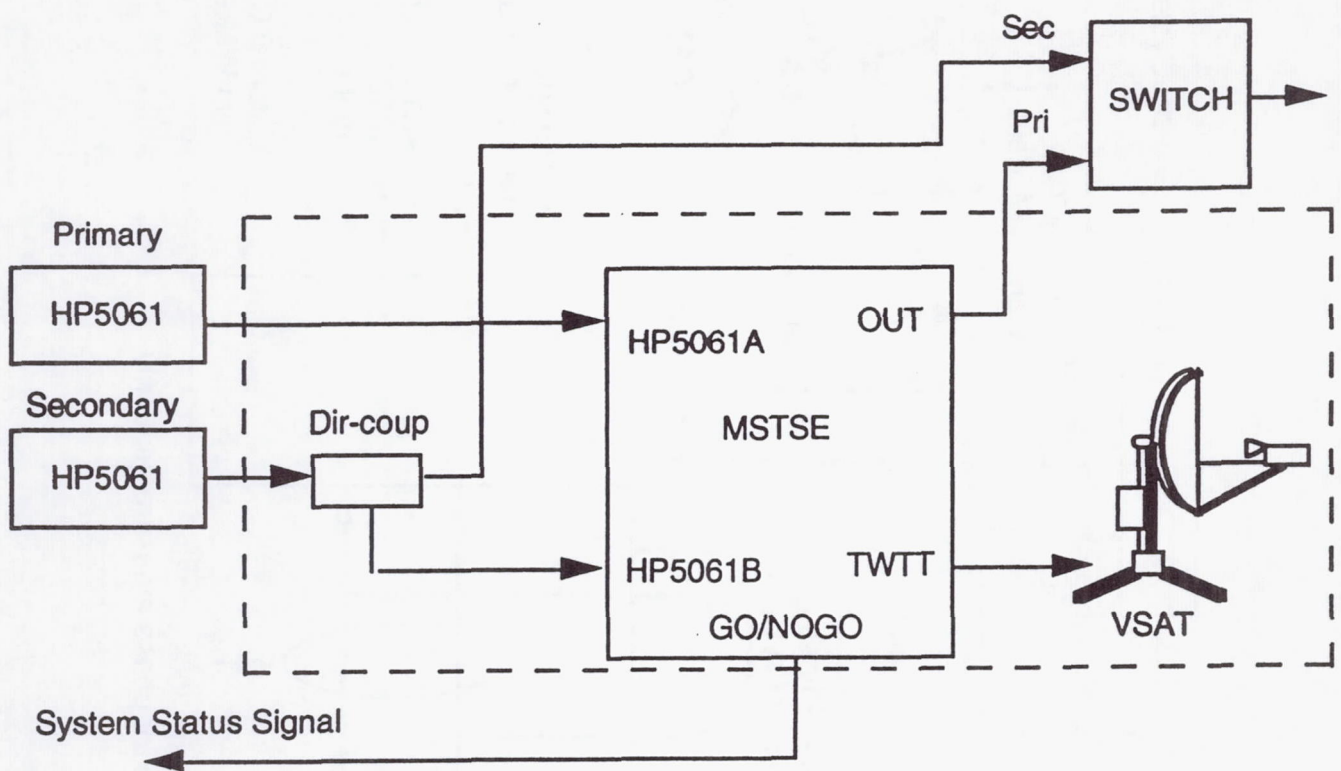


Figure 1

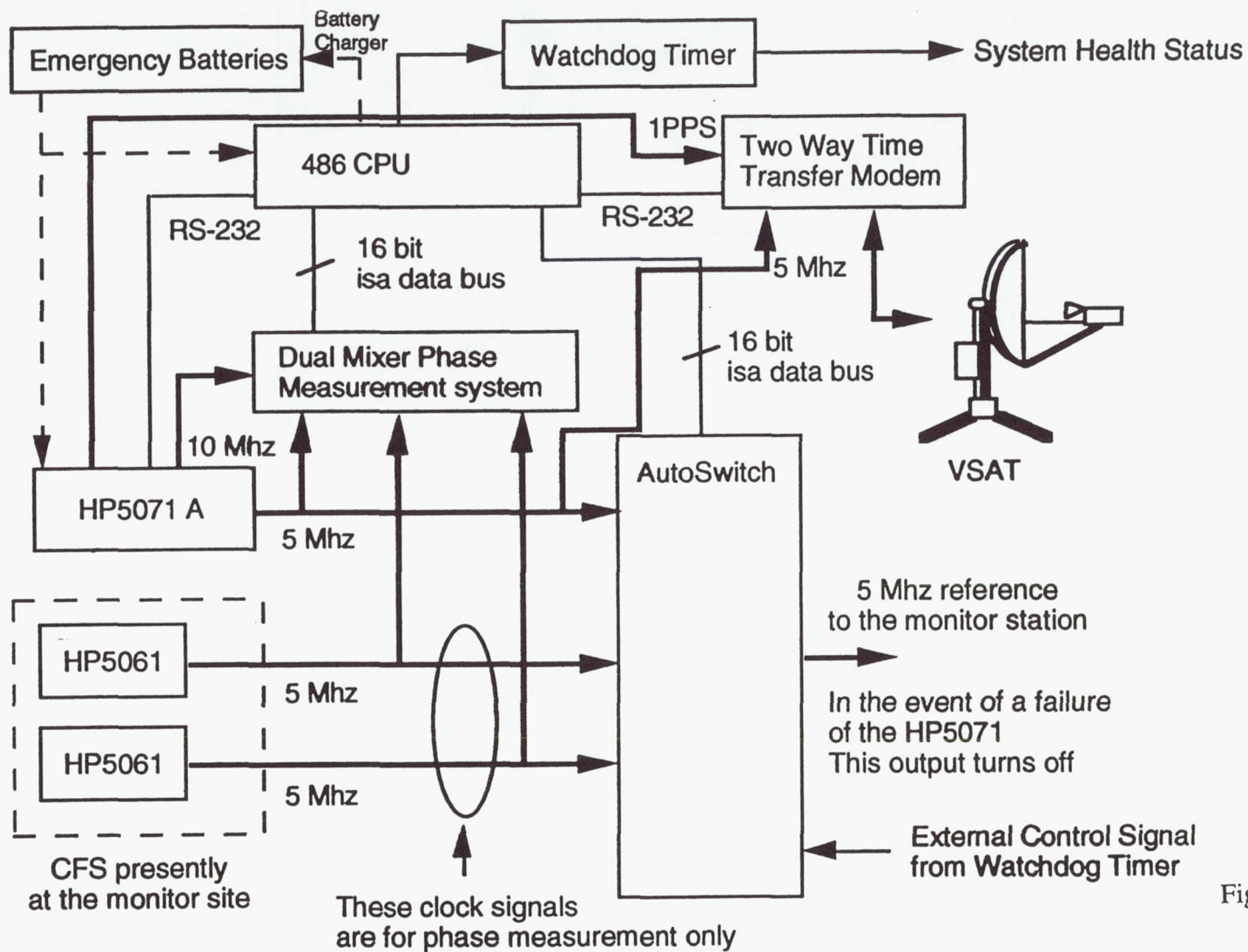


Figure 2



# TIMING SUBSYSTEM RACK ELEVATION

AC POWER CONTROL PANEL

FIBER OPTIC INTERFACE MODULE

COMPUTER, DUAL MIXER PHASE  
MEASUREMENT SYSTEM, AND  
AUTOSWITCH

HP5071 CESIUM FREQUENCY  
STANDARD

TWO-WAY TIME TRANSFER  
MODEM ANALOG CHASSIS

TWO-WAY TIME TRANSFER  
DIGITAL BOARD AND  
COMPUTER CHASSIS

BATTERY BACKUP POWER  
MONITOR

EMERGENCY BATTERIES

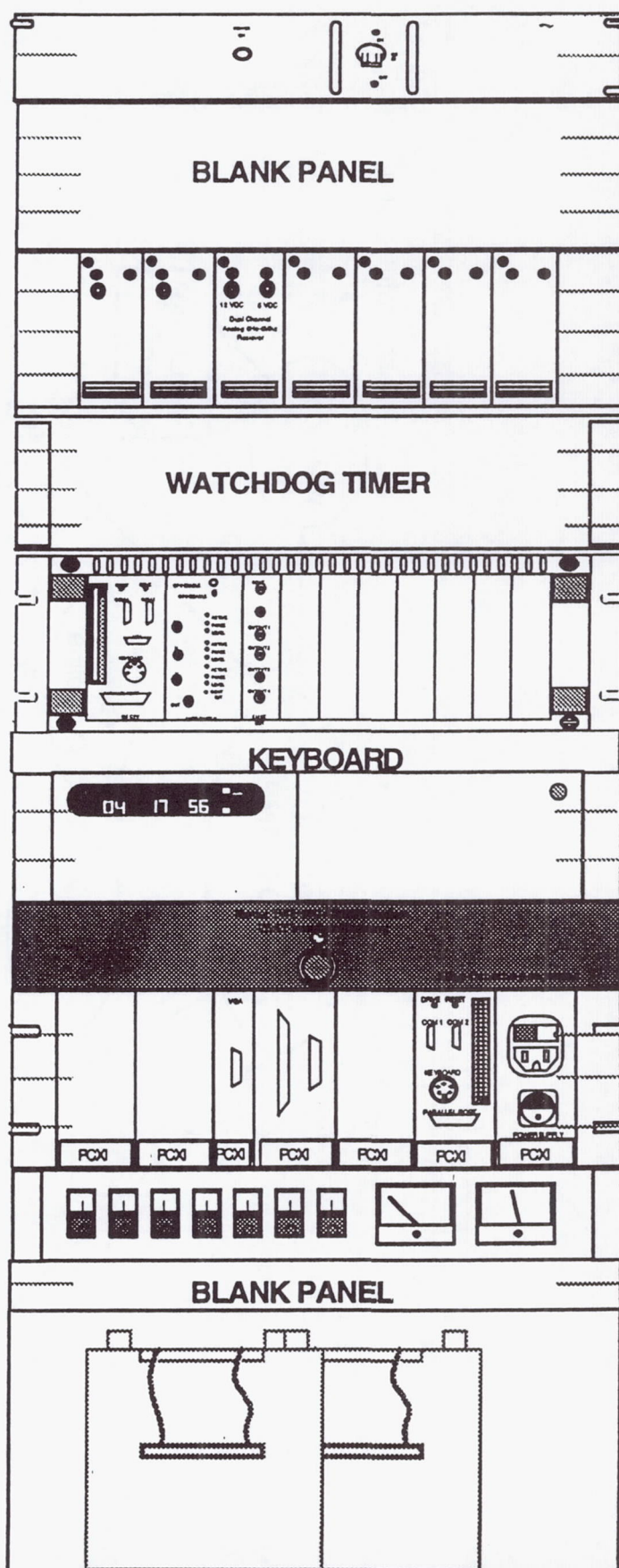


Figure 3

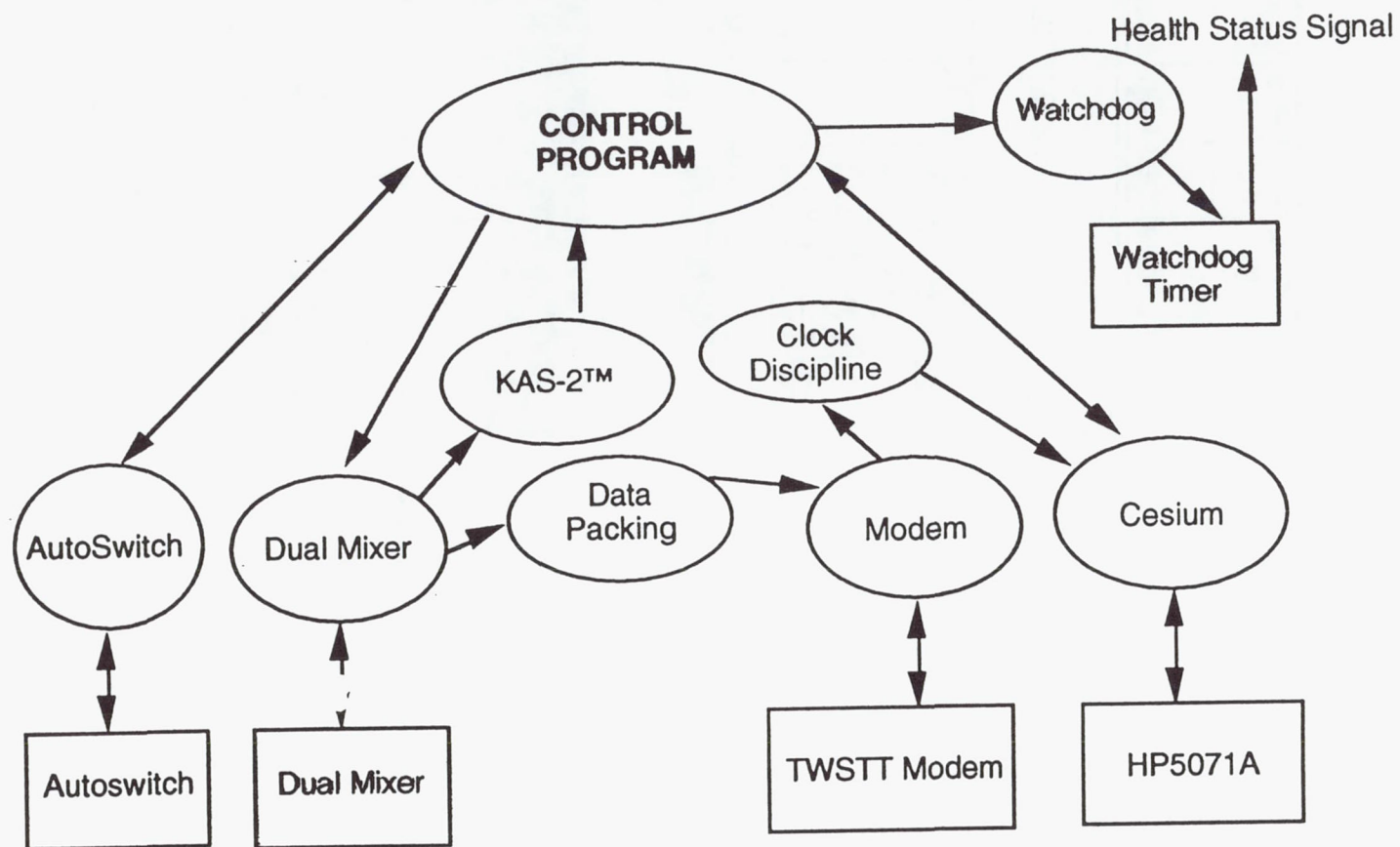


Figure 4



# RELATIVE PHASE COMPARISON TO NRL IN HOUSE SYSTEM

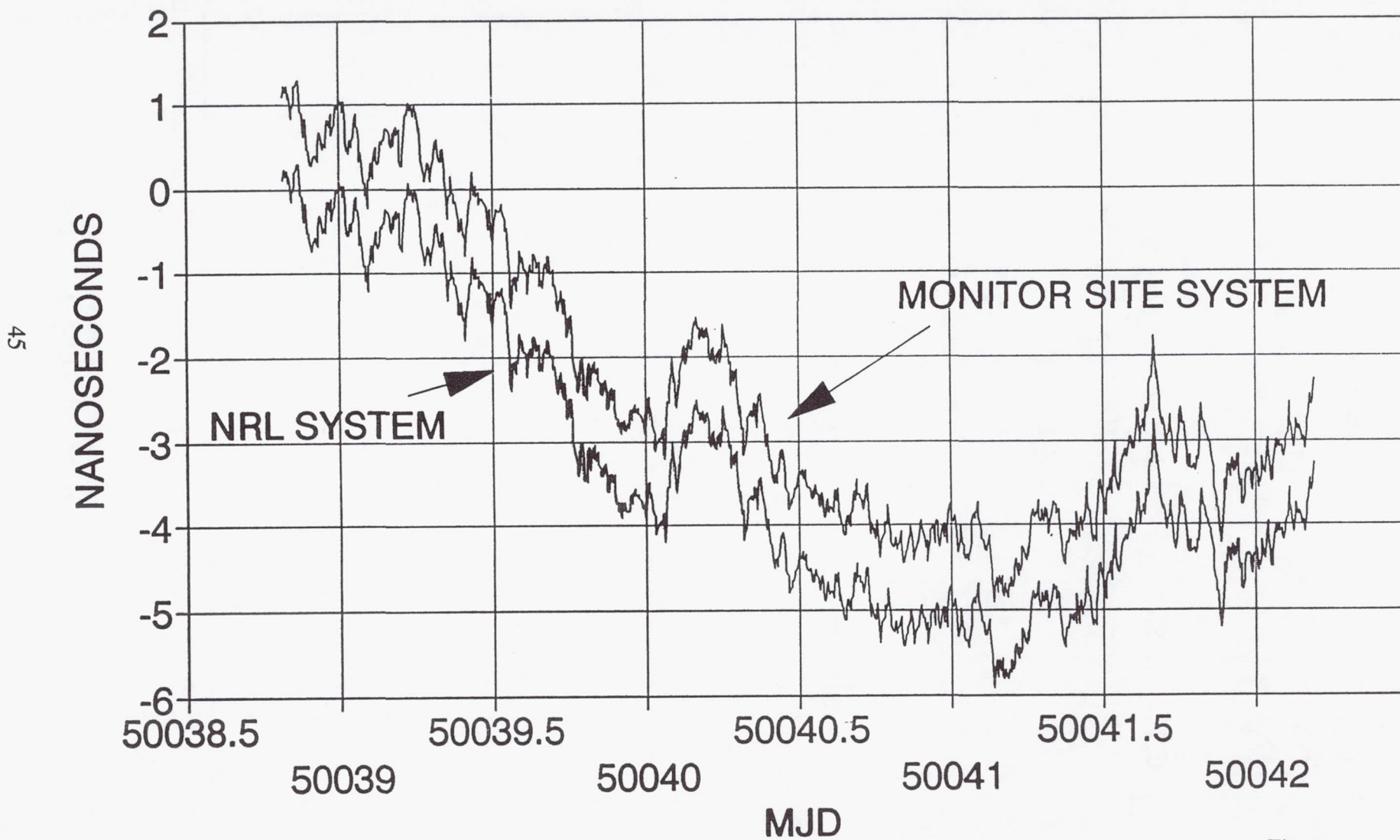


Figure 5

# HP5071 Disciplining via TWSTT via Wire

46  
Frequency Offset (x10E-14)

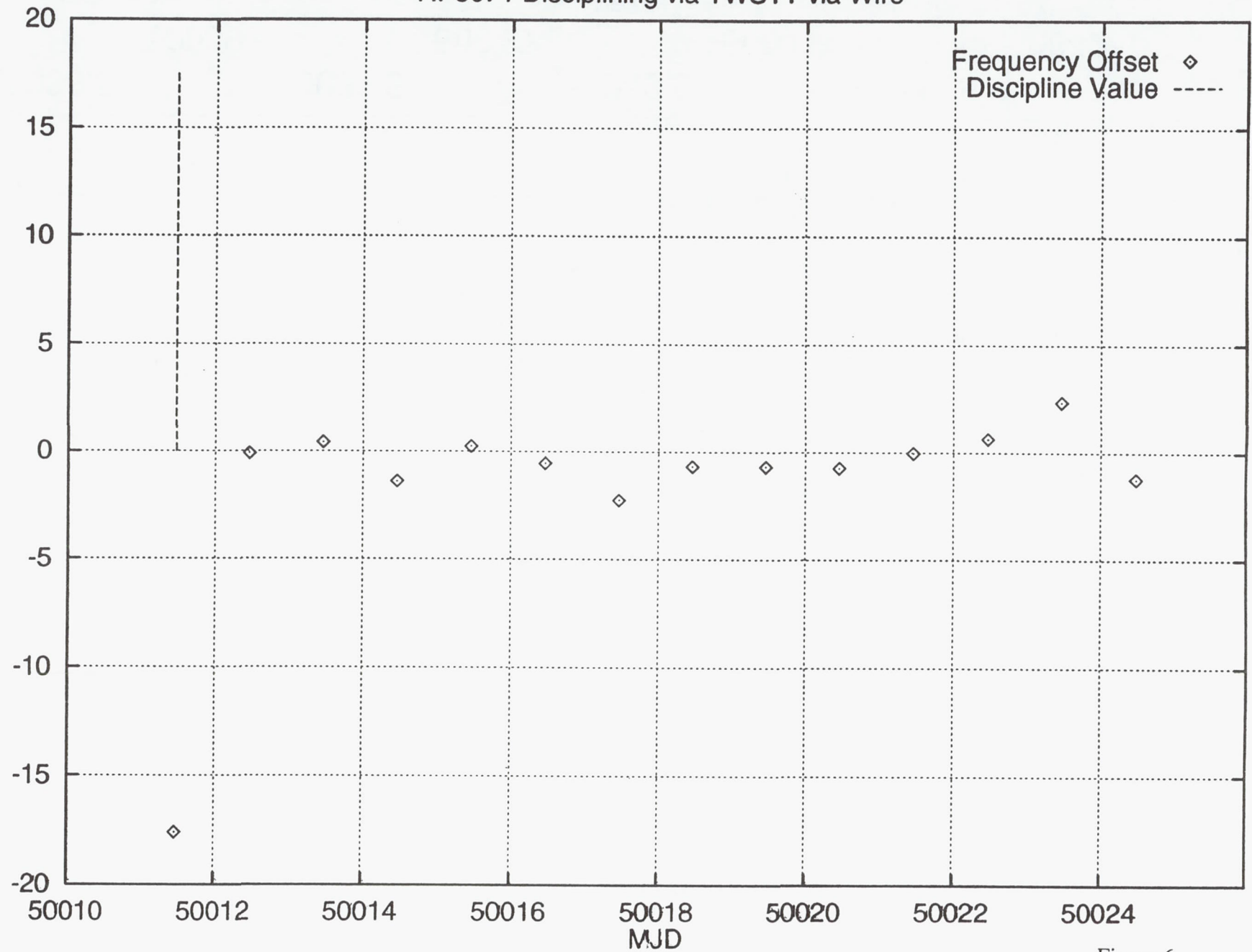


Figure 6



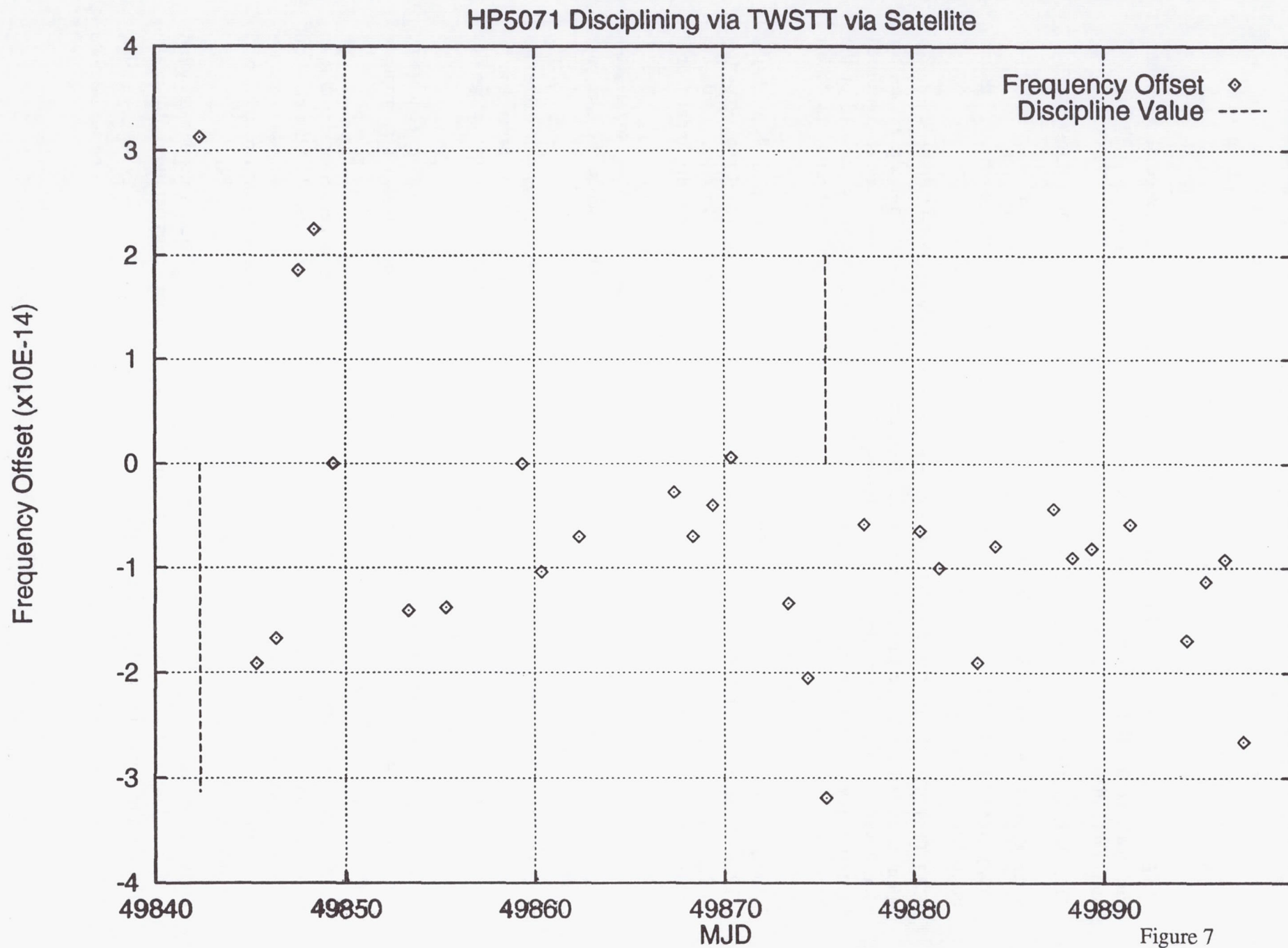


Figure 7

## Questions and Answers

**CAPT. STEVEN T. HUTSELL (USAF):** If my understanding of the proposal is current, the recalculation of the disciplining commands is going to be done once per day. Is that correct or is that current to your understanding?

**DWIN CRAIG (NRL):** There will be calculations going on after every time transfer.

**CAPT. STEVEN HUTSELL (USAF):** And is that going to be done once a day still?

**DWIN CRAIG (NRL):** My understanding is now for the operational deployment it should be a daily transfer.

**CAPT. STEVEN HUTSELL (USAF):** Because operationally one could make a safe argument that it would be disadvantageous to even do disciplining at all, and the reason for that is very simple. Disciplining, using a sampling of once per day, as far as we're concerned operationally, though it may improve the long-term stability of the frequency standard or the timing system at the monitor station, that's based on a sacrifice in the short term. By "short term" I mean that tau equal to or less than one day.

The real problem in this is currently MSTSE does not have any means to electronically notify the GPS composite clock that there are transients, if you will, being introduced that are completely independent of the natural noise that's occurring for that particular day. In other words, it's based off of information from previous days. I think one could make a safe argument that it would benefit us maybe not to consider disciplining the MSTSE.

In spite of that, we're very interested in the prospects of this. If we can have 5071s along with this ensemble algorithm at all of our sites, that would greatly benefit us. I'd like your comments on that.

**DWIN CRAIG (NRL):** Well, there are a lot of things that you could envision using this technology after it's been deployed. I personally look at it as an investment in infrastructure. And you're correct, a lot of your comments are correct. There have been some safeguards written into the software that performs the disciplining.

There's a gentleman here named Bill Reid who would be a good person to talk to concerning that. I did not write the disciplining algorithm, and that's why I don't think it's appropriate for me to go into depth.

**DR. GERNOT WINKLER (USNO, RETIRED):** I would like to make a comment to that. Look at Paper 21, which will begin tomorrow afternoon. The concern expressed by the question about degrading the stability of the local standard, it's just a question of how the servo loop is designed. You can completely avoid that if your main concern is the long-term correction. I would suggest looking at that after Paper 21 is given.

**DWIN CRAIG (NRL):** You're absolutely correct, Dr. Winkler. There's no debate about that at all. You're absolutely correct. Those things were taken into consideration. But again, I'm not the expert in depth on that particular algorithm.

I hope that I didn't leave anyone with the impression that there was going to be a discipline



sent to the clock on a very regular basis. If I did, I apologize. That's not the way the system operates.

**CAPT. STEVEN HUTSELL (USAF):** When we're talking about short-term versus long-term stability, it's important to point out that long-term stability is nice, but our primary concern is what I call "short-term stability," tau equals one day or less. The reason for that is because we update the navigation message in all of our satellites normally, as often as once per day or more. We're concerned about the predictability up to tau equals one day.

Yes, long-term stability is nice, but if we're making a sacrifice to short-term stability to maintain that, we could argue that well, it's maybe not as important as we'd like to think.

**DWIN CRAIG (NRL):** I agree with you, Sir. And I think one feature of the system that could actually contribute to helping you at the MCS would be the fact that you get the daily phase measurement data back, independent of the system as it exists now. That will provide you a second data source, sort of a sanity check on how the system is performing on a day-to-day basis.

# THE ROLE OF TIME AND FREQUENCY IN FUTURE SYSTEMS

Samuel R. Stein  
Timing Solutions Corporation  
Boulder, Colorado 80304

Al Gifford  
U.S. Naval Observatory  
Washington, D.C. 20392

Tom Celano  
The Analytical Sciences Corporation  
Reston, Virginia 22090

## INTRODUCTION

Over the last twenty years, the Global Positioning System (GPS) has revolutionized the performance and the geographical availability of time and frequency dissemination, while at the same time reducing the cost to the individual user. This paper examines the question of what comes next for time and frequency dissemination. The question has two motivations: How can improved performance be achieved in the future, and how can redundant sources of time and frequency be provided to critical systems? A model is developed for time and frequency dissemination based on the time management performed in GPS. Several candidate systems for future time and frequency distribution are identified. One system-SONET telecommunications-is discussed in detail. Performance requirements and hardware implementations are presented.

## SYSTEM MODEL

The implementation of time and frequency distribution begins with a model for the operation and management at the system level. In order to successfully integrate time and frequency into future systems, the time has to serve both internal system requirements as well external customer requirements. There are lessons to be learned from the GPS system on the requirements for the management of time. The GPS system provides a good model for the successful integration of internal and external requirements. Thus, the initial model for embedding time and frequency into future systems is based on the features and characteristics of how time is implemented in GPS.

GPS is an operational system serving military and civilian requirements. The system contains 24 satellite clocks as well as monitor station clocks, to form a distributed clock set which provides clock intercomparisons by virtue of the very operations of GPS itself. From the clock intercomparisons, GPS computes a composite time (a timescale that becomes the GPS time). The feature of time transfer within the system is built-in and automatic. It has a robust system architecture which is maintained, centrally managed, and globally available for recovery of



Universal Coordinated Time (UTC). GPS time itself is steered within what only a short time ago would have been considered to be very narrow limits. In addition to the steering of GPS time, GPS broadcasts UTC corrections, providing the user the capability to determine if and/or how the local time will be steered to UTC. No matter what steering algorithm is used, there is always a differential between the physically realized time at the user and the system time (UTC or GPS in this case). That differential is known and reported to the user, but not necessarily removed instantly.

The fundamental system requirement that is gleaned from the GPS model is that time and frequency within the system are provided as a by-product of the system operations. Unlike WWV, which was designed to disseminate time, the GPS system was designed to support a navigation mission with a timing sub-mission. GPS has set the standard for excellence in the field and time-transfer performance. Future systems that will be of interest for time dissemination are going to perform at comparable or better levels. They will probably have comparably very large costs. It will take billions of dollars to implement systems that can provide worldwide globally available timing to the tens-of-nanoseconds level as GPS does. So it is unlikely a stand-alone timing mission would be implemented with the phenomenal cost that would be involved. On the other hand, the cost of timing that is provided within major systems like GPS is only a few percent of the total system cost.

Just as the timing mission is not a stand-alone mission, the timing expertise must not be isolated, either. If the timing community is going to advance, the timing expertise must be distributed to the system level. It is important that on the operational level, people running these programs and systems truly have their own expertise, and not rely on experts located at centers of excellence.

## **FUTURE SYSTEMS**

One candidate for future systems which will require time and frequency distribution is a Department of Defense (DoD) project known as Global Grid. It's a concept for aggressive worldwide distribution of information, communications, and information processing. The Global Grid concept will use established government and commercial assets for communications, i.e. government and commercial satellites, optical fibers, and telecommunication systems utilizing established protocols such as SONET and ATM. Currently, there are many aspects of Global Grid that are being worked and demonstrated by multiple organizations. Three examples are the Global Broadcast System (GBS), Personal Communications Systems (PCS), and laser-based satellite communications (LASERCOM). These examples are discussed separately below.

The Global Broadcast System utilizes geosynchronous satellites for the one-way broadcast and dissemination of information. Adding the precise satellite position to the information downflow enables GBS to deliver precise timing to a user with a known position. Presumably, a stationary user with a known position can achieve 10 ns precision for time recovery. In fact this kind of precision has been demonstrated on an experimental basis by some of the commercial satellite companies. Such a system could also augment GPS by providing pseudolite signals.

In the Global Grid architecture, the Personal Communication Systems (PCS) represent the last mile of the communications systems. Often a commercial link exists (via satellite or cable) to an end point which does not serve the user, who may be deployed in an undeveloped or unstable area. The PCS systems are used to get information out to the individual in the field. Such systems often utilize wireless links. These links can be satellite-based or a combination of radio links and land lines. Time and frequency signals could be delivered to the user via



these PCS links for many military applications.

Laser communications (LASERCOM) will be used for satellite downlinks in future systems. Laser downlinks are occasionally interfered with by weather (Fig. 1), prohibiting the signal being received at a ground station. The impact of local weather on the ability of a ground station to receive the optical signal creates a requirement for multiple options for ground stations and the ability to seamlessly switch between ground stations. The transition from one ground station to another results in massive changes in signal path delay. The downlink is eventually fed to a synchronous optical communications system and it will be necessary to cope with the synchronization of data at the hub. The challenge of such a system is going to be the management of the path delays. Time recovery and synchrony at each ground station will be required to fuse the data at the high bit rates that are possible with LASERCOM systems.

## SONET IMPLEMENTATION

One possible implementation that will be applicable to future systems is the use of the Synchronous Optical Network (SONET) to disseminate time and frequency as a by-product of the transfer of payload data. SONET (or SDH) is being used to implement precision timing and precision frequency management both within the U.S. government and elsewhere. Nippon Telephone and Telegraph (NTT) has been publishing<sup>[1]</sup> and working with the ITU for many years in this area. In this paper we use a SONET system as an example of how precise timing (an order of magnitude better than GPS) may be implemented within a communications system. One of the advantages of using a communications system is that, for the most part, the traffic is two-way. This enables the implementation of two-way time transfer, which is the traditional technique for delivering high precision time. The current operating level of GPS with regard to delivering time is only quasi-two-way. One way is the management of the system through the monitor stations and master control station, and the other way is the delivery of the information to the user, but the two directions are asymmetric. Large offsets in time and large offsets in geolocation between the two links limit the performance of GPS time delivery to somewhere in the 10-25 ns range.

The implementation of precision timing within communications is being driven today by very high precision timing users with different agendas. However, the synchronization of networks in the time sense would be a significant benefit to all communications timing users. Time synchronization of network nodes can eliminate path changes as a source of wander on SONET or SDH networks. This results in allocating the entire wander budget to sources other than the path changes that currently dominate the calculation. This wander budget determines the ability to reconstruct analog signals, such as voice and facsimile, when the signals travel over the SONET network for long distances. Such a synchronization system will serve all time users (all the way down to the private branches) who in any way connect to the network at the OC-3 level or higher.

An architecture and a time code have been developed for SONET-based time and frequency dissemination. Hardware has been developed for this application and is currently under test. The implementation plan starts with point-to-point and extends to LAN, over the air, platform distribution, MAN, transoceanic cables, and WAN. The system conforms with the standard aspects of the NTT proposal and serves the long-term goal to be consistent with the standards that may be adopted by the ITU sometime in the future.

The SONET architecture is seen in Fig. 2. There are four network nodes with a multiplicity of network elements separating the nodes. One node is connected to a master timing unit that



provides the interface for an Ultra-High-Precision (UHP) clock system or a primary reference clock. Slave units connect to other nodes and re-derive signal sets which are steered to the master via two-way time transfer. The system also supports future goals of using the two-way SONET link to measure clocks which are connected to the slave nodes. This allows the clocks to be located at the remote slave nodes and still measured (via SONET two-way) at the nanosecond level for inclusion into the time scale. This concept of a distributed time scale (the clocks are distributed geographically) provides for clock ensembling without the requirement of maintaining the clocks in one central location. This increases the reliability and the robustness of the system without a performance trade-off.

The current goal for time and frequency distribution using SONET is to distribute a standard time and frequency set consisting of one standard frequency, high quality 1 PPS, and time code. The goal is to transfer performance that is representative of a cesium standard with a high-performance tube with time transfer accuracy of two nanoseconds. Two nanoseconds represents an improvement of approximately a factor of ten over what users are now able to do globally using GPS. The SONET system must be automatic, with no external calibration and support redundancy in automatic switch-over. Point-to-point time synchronization supported by such a system is limited by the SONET standards, which can communicate over ten kilometer fiber-optic cable. The system must also support higher quality future clocks and transfer that performance to the user.

This SONET system is an implementation and demonstration program (as opposed to a research program) which requires the use of standard, commercially available, telecommunications quality, zero dispersion single-mode fiber using standard connectors. Due to the path delay changes that are incurred on a fiber in a nominal environment, two-way time calibration is a requirement to support a 2 nanosecond accuracy specification. For example, a 10 km fiber with a 70 degree centigrade maximum environmental swing from dead of winter to heat of summer exhibits an approximately 60 nanosecond change in path delay. Extending this to a 3000 km SONET link in a network results in a 5 microsecond change. The basic approach is to use the synchronous SONET transport as a vehicle for the time code needed to perform two-way time transfer. The SONET payload is inappropriate for this application due to the ambiguity involved asynchronous data transfer. The transport for SONET at the physical layer supports synchronous data transfer, which is an appropriate vehicle for two-way time transfer.

The two-way time transfer is supported by a master/slave relationship between network nodes. The master encodes a time marker in the SONET overhead, which is measured at the time of transmission and measured once again at the slave at the time of reception. Similarly, the slave transmits a time marker that is received at the master. The two measurements performed at the master are transmitted to the slave in the time code, where they are used to compute the master-slave time difference, independent of the delay between the two locations. At the slave end, a clean-up loop recovers high quality frequency signals. It has been demonstrated that a clean-up loop with a bandwidth of 1 Hz can meet the specifications of a high-performance cesium standard. The clean-up loop uses one-way measurements. Therefore, its output is subject to temperature-variable delays, which are corrected based on the two-way measurements. This delay compensation is done by averaging the phase measurements in order to reduce the measurement jitter below the local clock time error. The slave local oscillator is held on frequency by calibration compared to the master clock.

## CONCLUSION

This paper uses GPS as a model for designing time and frequency systems which are embedded as by-products of primary mission objectives. This is done to defray the substantial cost of achieving high quality time synchronization. It is proposed that communications and data dissemination will be the next vehicle to provide system redundancy for GPS in the timing area and improvements in GPS timing performance. A SONET architecture is presented which conforms to the proposed model, and performance specifications are presented.

## REFERENCES

- [1] M. Kihara, and A. Imaoka 1995, "*SDH-based time and frequency transfer system*," Proceedings of the 9th European Time and Frequency Forum (EFTF), March 1995, Besançon, France.



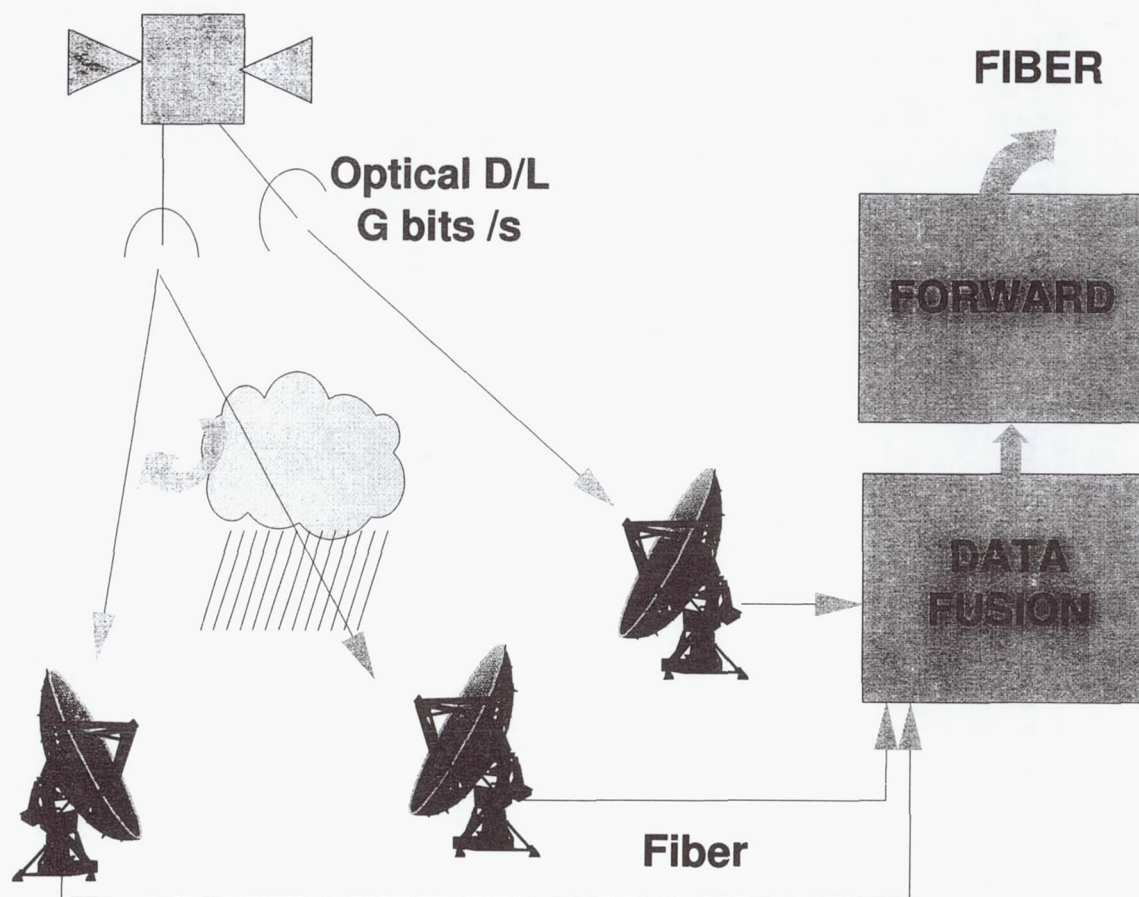


Figure 1. Switching LASERCOM downlinks changes the path delay.

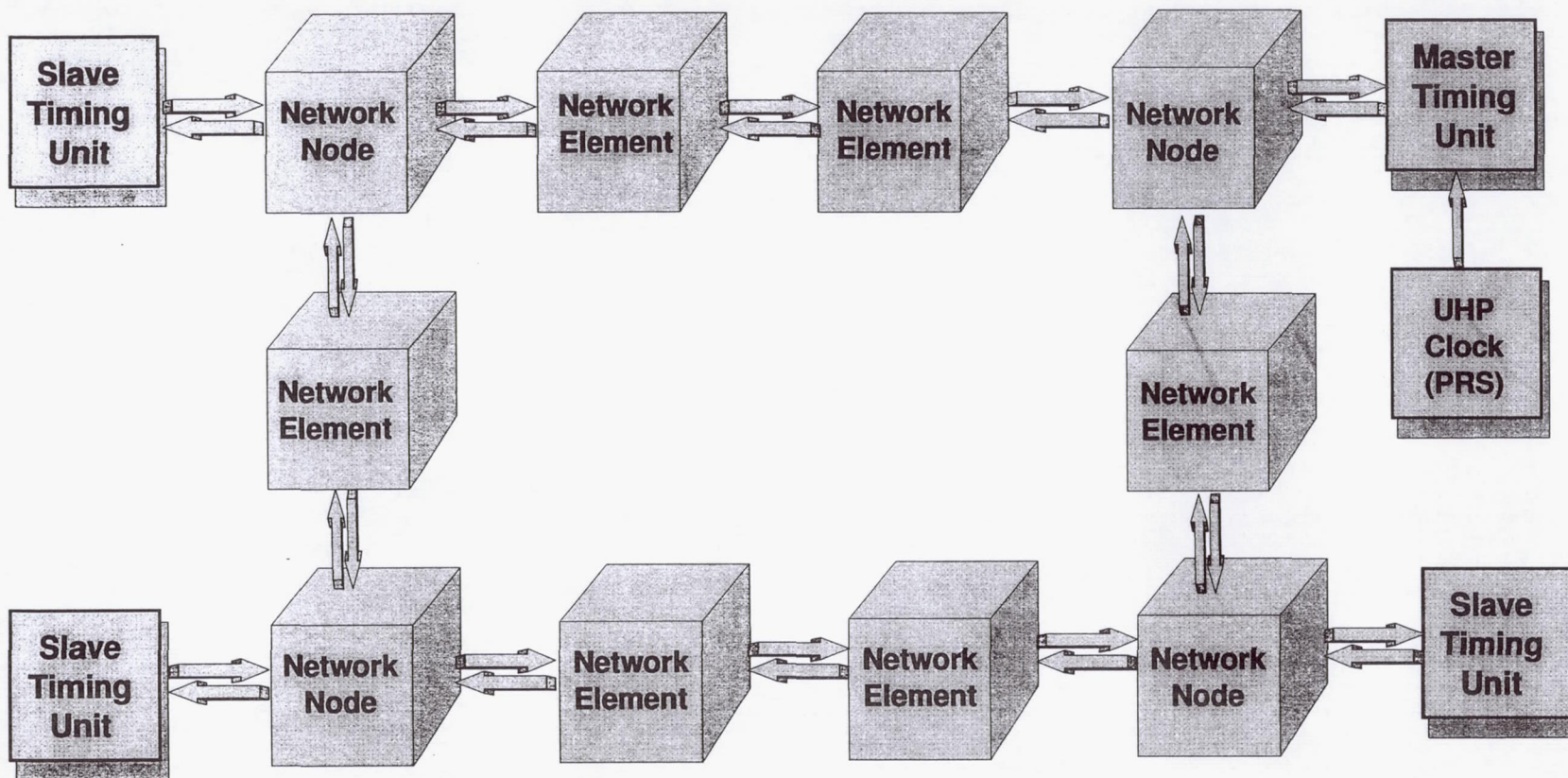


Figure 2. SONET loop with a master timing unit and three slaves.



# **SPECIAL TECHNOLOGY AREA REVIEW ON TIME AND FREQUENCY**

**John R. Vig  
U.S. Army Research Laboratory  
Fort Monmouth, New Jersey 07703-5601**

A Special Technology Area Review (STAR) of frequency control technology was held by Working Group A of the Department of Defense (DoD) Advisory Group on Electron Devices in March 1995. The goal was to develop a DoD investment strategy for research and development (R&D) on frequency control devices. The STAR sought answers to questions such as:

What are the DoD system needs and how critical are these needs?

Are DoD's needs being met?

What are the commercial needs, and to what extent can commercially available devices meet DoD needs?

What is the total R&D activity in the field - in government, industrial and university laboratories?

What critical-path R&D and manufacturability problems need to be solved, if any? Are there any "showstoppers"? What is the probability that solutions will be found? What will the solutions cost? What are the trade-offs if solutions are not developed?

What are the emerging technologies? To what extent can these technologies contribute to DoD capabilities in the future?

Are these technologies being adequately developed? If not, what would it cost? Who are the key organizations to make it happen?

What is the industrial base, and is the industrial base adequate for meeting the future R&D and manufacturing requirements of DoD?

What should be the role of DoD be in this technology area?

The conclusions and recommendations of this STAR are described in a report entitled "Special Technology Area Review on Frequency Control Devices." The report is available from:

Advisory Group on Electron Devices - Working Group A  
Palisades Institute for Research Services  
1745 Jefferson Davis Highway, Suite 500  
Arlington, VA 22202-3702, U.S.A.

## Questions and Answers

**RONALD L. BEARD (NRL):** Given the general mood of DoD to moving towards using commercial standards and getting away from military requirements, do you feel this is an area where adopting civilian or commercial standards might be practical?

**JOHN R. VIG (ARMY RESEARCH LAB):** I'll tell you my favorite story about the subject which some of you may already have heard. I was attending a NATO meeting a number of years ago, and we were discussing this subject over dinner. One of my colleagues — I think he was from the Netherlands — said that their defense department, some bean counter, was looking at purchases; and he noticed that the Dutch Navy was buying 40-watt light bulbs for \$10 apiece. And he said "Why are we doing this?" Nobody could answer. So he put in a suggestion saying "We should buy commercial. I could go down to the corner hardware store and buy light bulbs for three for a dollar."

His suggestion was adopted. He got a big award for saving money for the Dutch Navy. Gradually, all the light bulbs were replaced with these commercial light bulbs. Then they went out on NATO exercise, and were somewhere in the middle of the Indian Ocean when the command came, "Fire!" And all the lights went out.

They had one set of replacements, so they put in all the replacements. And the command came again, "Fire!" And all the light bulbs went out again. And then the commander had to meekly ask the permission to go home to get more light bulbs.

But the answer to the question is obviously there are some areas where commercial products can fill the need, and obviously there are some areas where commercial products cannot meet the need. Commercial products are not made to be radiation-hardened. So if you want to send an oscillator into space, the commercial products are definitely not the way to go. You need a radiation-hardened oscillator to send into space. Depending on what you envision for the scenario for future wars, you may or may not want to rad-harden tactical oscillators.

Things like vibrationless phase noise, things like gun-hardened oscillators — I mean, there are definitely some strictly DoD requirements which the commercial business will never address. There are no commercial requirements for an oscillator to be fired from a Howitzer. So if the DoD needs an oscillator that has to be fired from a Howitzer, the DoD better be prepared to pay for development of such an oscillator; otherwise, it will not be there.

**HARRY PETERS (SIGMA TAU STANDARDS CORPORATION):** Your chart of frequency standards and the amount expended on them in the potential market indicated H-masers estimated at 10 per year, and a nominal price of around 200k. The list of companies who produced these various standards which you put up there perhaps might have noted that the only commercial supplier of atomic H-masers in the West, that is, particularly those that have cavity tuning systems — at Sigma Tau Standards Corporation we have over 40 H-masers oscillating and a few more in the building stage at this time; and of course, there's been no government-funded research on H-masers within this company for the last 10 years. However, there has been input of funds from what is generated from profits; and all our research has been internal since 1985, but I think at least we might have merited a mention in your list of monies that are applied to research in frequency standards. I notice you didn't notice Sigma



Tau Standards Corporation. Thank you.

**JOHN VIG (ARMY RESEARCH LAB):** I said there were a number of companies under \$50 million that were not listed. So I apologize for not mentioning Sigma Tau. But the number I listed was 10 per year. So if you've built a total of 40, that doesn't seem to contradict the total production on the order of 10 per year, does it?

**HARRY PETERS (SIGMA TAU STANDARDS CORPORATION):** [Inaudible].

**JOHN VIG (ARMY RESEARCH LAB):** Okay, so it's even less than 10 per year. So I overestimated.

**DR. GERNOT WINKLER (USNO, RETIRED):** If you look at your horror stories, I think the overriding importance of communication is obvious. All of these things happened because we did not know about — I mean, systems engineers, system planners and system managers did not realize that it was a specific area, a special area requiring special knowledge and so on, the PTTI Conference, and Frequency Control Symposium and so on. Now the question is: Has this been discussed by that adjunct group? That the greatest improvement or the greatest savings could be accomplished if you get these system managers into the conferences?

**JOHN VIG (ARMY RESEARCH LAB):** Yes, it was discussed. In fact, unfortunately, as I pointed out, not only is there no incentive for a major contractor to come to a government lab, there's an incentive for them not to come to a government lab; because, government labs oftentimes are looked on as competitors. If Milstar's a problem, and the task of solving the problem goes to a government lab, Lockheed and TRW and Hughes Aircraft and Frequency Electronics don't make a profit. If Lockheed puts in a proposal for Lockheed to solve the problem, then Lockheed gets the money instead of government labs.

So in a sense, unfortunately, I'm not sure what to do about it, but the contractors look at government labs as competitors. And they have a disincentive for sending these problems to the government labs for solutions.

**DR. GERNOT WINKLER (USNO, RETIRED):** We are talking about the conferences, not the laboratories.

**JOHN VIG (ARMY RESEARCH LAB):** The conferences do address these questions, but unfortunately we can't get the systems people to attend these conferences. Okay? So again, we recognize the problem; we offer tutorials; we offer review papers; but the systems people, with a few exceptions, generally do not attend our conferences. If anybody has a solution to the problem, I would be more than happy to discuss it and listen to suggestions. But this is a problem — I think it all ties together, with the lack of university curricula, lack of communication, it often costs lots and lots of dollars.

The total budget of my group, for example, is on the order of a million dollars a year or less. This year it's less, a lot less. If you look at the cost of some of these problems, the cost of one of these major problems could fund frequency control research in the government indefinitely; you just take the money, put it in the bank, draw interest on it, and use that interest to fund the research. Again, it is not clear what we can do about it.



# IDEAS FOR FUTURE GPS TIMING IMPROVEMENTS

Capt Steven T. Hutsell, USAF  
2d Space Operations Squadron  
300 O'Malley Avenue Suite 41  
Falcon AFB CO 80912-3041

## Abstract

*Having recently met stringent criteria for Full Operational Capability (FOC) certification, GPS now has higher customer expectations than ever before. In order to maintain customer satisfaction, and to meet the even higher customer demands of the future, the GPS Master Control Station (MCS) must play a critical role in the process of carefully refining the performance and integrity of the GPS constellation, particularly in the area of timing.*

*This paper will present an operational perspective on several ideas for improving timing in GPS. These ideas include the desire for improved MCS-USNO data connectivity, an improved GPS-UTC prediction algorithm, a more robust Kalman Filter, and more features in the GPS reference time algorithm (the GPS Composite Clock), including frequency step resolution, a more explicit use of the basic time scale equation, and dynamic clock weighting.*

*Current MCS software meets the exceptional challenge of managing an extremely complex constellation of 24 navigation satellites. The GPS community will never want to risk losing the performance and integrity that we currently have. The community will, however, always seek to improve upon this performance and integrity.*

## INTRODUCTION

The GPS community will never experience a period of accepted complacency. Customer demands for accuracy will continue to increase. The increasing dependence on GPS as the primary mechanism for precise time transfer incurs the expectation for extremely high reliability within the GPS architecture. The community is quickly understanding the need to delicately balance integrity with performance improvements.

The GPS Master Control Station (MCS) software plays an integral role in this balance. The current release, version 5.41, is largely responsible for GPS maintaining Full Operational Capability (FOC). Generating, integrating, testing, and installing over two million lines of code is not an easy task, to say the least, especially when this code is responsible for the command and control of a 24 navigation satellite constellation.

This paper focuses on an operational perspective of various methods the GPS community could consider for refining the measurement, estimation, and prediction of timing within the MCS software.



## MCS-USNO CONNECTIVITY

The United States Naval Observatory (USNO) is the official Department of Defense (DoD) source for precise time and time interval (PTTI) information. USNO provides the DoD reference for Coordinated Universal Time (UTC). Precise time transfer is one of the three very important missions of GPS, and GPS is the primary means to disseminate precise time to the vast majority of DoD time transfer users [6].

This rather great responsibility depends hugely on the interface between the 2d Space Operations Squadron (2 SOPS) and USNO. The interface control document, ICD-GPS-202, defines the working relationship between these two agencies. The GPS Joint Program Office (JPO) will soon publish an update to this 11-year old ICD [3].

The Time Transfer mission in GPS currently operates in a closed daily feedback loop, as described in figure 1. The MCS transmits UTC information in navigation uploads to all operational satellites. The satellites, in turn, broadcast estimates of the GPS-UTC bias and drift in subframe 4, page 18 of the navigation message. In order for the MCS to properly generate GPS-UTC correction parameters for broadcast, USNO must compare GPS's broadcast of UTC to the USNO Master Clock, and feed back this offset information to the MCS.

### The USNO Download

USNO employs an authorized (keyed) GPS receiver, connected to the Master Clock, to monitor the GPS broadcast. USNO generates a smoothed measurement for each successive 13-minute track. These measurements contain estimates of, among other parameters, the offset of satellite time with respect to UTC, the offset of GPS time with respect to UTC, and the time transfer error, based on that single-satellite track [6].

Every day, at approximately 1500z, the MCS downloads a data file from USNO. This file contains roughly 160 of these smoothed 13-minute track measurements, along with daily averages of the constellation-wide GPS-UTC offset and time transfer error. The MCS uses Procomm, installed on a PC-based computer connected to a keyed modem, to execute the daily download.

Unlike the interfaces with most other outside agencies, the MCS's computer interface with USNO is not currently governed by formal configuration management. Various problems with the hardware, software, and even the communication lines can interfere, and have interfered, with the time transfer loop on dozens of occasions over the last several years. On 20 Oct 95, 2 SOPS and USNO installed more current hardware and software to ease the operational headache, but some challenges still exist today.

Additionally, because the MCS downloads the UTC information into a PC, operators must manually extract and enter information onto the MCS mainframe. This process is susceptible to human error, and restricts the ability to pump large quantities of data into the mainframe for processing. Human error, such as typing the GPS-UTC sign incorrectly, can be devastating. The inability to receive large quantities of data renders the MCS mainframe less capable of measuring the true GPS-UTC offset, and hence, less capable of *predicting* GPS-UTC for time transfer.



## GPS-UTC PREDICTION

As alluded to earlier, MCS operators enter a daily estimate of GPS-UTC into the mainframe. USNO generates this estimate by mapping a least-squares fit onto 38 hours worth of their 13-minute smoothed measurements of GPS-UTC. We at 2 SOPS call this the daily UTCBIAS point. The MCS predicts GPS-UTC using only *two* daily UTCBIAS points. Using two data points only 24 hours apart for calculating the GPS-UTC drift does not make the best use of the available optimal estimation techniques that most of us are familiar with.

By piping USNO-smoothed measurement data directly into the mainframe, the MCS could take advantage of techniques to a) apply corrections for known observables, b) edit outliers, and c) Kalman Filter the USNO data for optimum GPS-UTC estimation and prediction.

2 SOPS and Det 25, Space and Missile Systems Center (SMC) are currently addressing two software change requests related to the above concerns.

## A ROBUST KALMAN FILTER

The current MCS Kalman Filter estimates the ephemeris, solar pressure, and clock states for 25 satellites, and the clock states for five monitor stations. The MCS Kalman Filter is capable of estimating the phase, frequency, and frequency drift states for all operational clocks.

## Systematics/Periodics

The Kalman Filter does not currently perform explicit estimation of 12- or 24-hour periodic terms for our clocks. During earth eclipse seasons, our spaceborne atomic clocks may exhibit significant periodics with amplitudes of several nanoseconds, due possibly to thermal and/or electromagnetic systematics. To a large extent, other degrees of freedom in the Filter, particularly the ephemeris and solar pressure states, can help to artificially compensate for satellite clock periodics--the eccentricity and solar pressure parameters can, many times, help to model the effects of these periodics. In counterpoint, however, many could argue that this same feature can open the door for ephemeris-clock cross-corruption.

Because the Operational Control Segment (OCS) uses only five monitor stations, the MCS can only monitor a GPS satellite for, at most, 22 hours a day. When monitor stations are undergoing maintenance, this visibility lessens dramatically. Not only does this lack of coverage prevent the MCS from ensuring the integrity of the constellation full-time, but it also restricts the MCS's ability to decouple ephemeris, solar pressure, and clock errors. More monitor stations could help to minimize this cross-corruption.

Currently, the MCS does not estimate troposphere height. The MCS is *capable* of tropospheric estimation, based on measurements corrected with environmental sensor data. Unfortunately, the environmental sensor data we receive from most of our monitor stations has historically been very inconsistent. Until we can realize acceptable reliability from our sensor data, we will continue to use fixed (default) values for troposphere height states. Improving tropospheric state estimation could help to remove much of what we commonly may see as 24-hour periodics.



## A Fully Correlated Kalman Filter

What we know as the MCS Kalman Filter is actually an ensemble of several mini-Kalman Filters, known as partitions. Each partition can estimate the states of, a maximum of, *six* satellites. Each partition estimates the states of all monitor stations, and a partition reconciliation algorithm keeps these monitor station states consistent between the estimating partitions. The partitioned architecture significantly reduces the computational burden within the MCS mainframe [5].

In future architecture, 2 SOPS hopes to utilize a fully correlated Filter capable of estimating the states of *all* satellites. The current partition architecture works very well, but a fully correlated Filter could reduce some of the short-term noise caused by temporary deviations between the MS states of the respective estimating partitions. Advances in CPU capability will hopefully meet the extra burden imposed by a fully correlated Filter.

## THE FUTURE GPS COMPOSITE CLOCK

GPS, like most timing systems, uses a reference time scale. GPS time is defined by the Composite Clock software, installed in June 1990. The Composite Clock presented a remarkable solution to the need for a stable, continuously operating reference against which all GPS ephemeris, solar pressure, and clock states are referenced. The GPS Composite Clock is largely responsible for time transfer performance and GPS time stability that are both exceeding specifications [1,5].

Five years of operational use of the Composite Clock have helped 2 SOPS learn how to best utilize its capability. Similarly, the same five years have given us ample time to create a wish list for extra features.

### Frequency Step Resolution

MCS software algorithms have historically provided excellent visibility into clock phase discontinuities. Software version 5.41 alarms, displays, and rejects unacceptably large phase discontinuities. Frequency step detection has been more of a challenge, however [2].

At approximately 0200z, 21 Dec 94, the primary timing input for the Colorado Springs monitor station (COSPM) failed. Due to a technical error, in recovering from the failure, COSPM experienced a discrete frequency jump of, approximately,  $1.25 \text{ E-12 s/s}$ . Since COSPM, at the time, had a long-term weighting factor of about 20 % in the Composite Clock [1], GPS time experienced a run-off on the order of -22 ns/day, with respect to UTC, as a direct result of the discrete frequency jump.

The impacts of this run-off were significant. The Control Segment (CS) component of error in GPS Time Transfer, usually within  $\pm 10 \text{ ns}$ , jumped to -19 ns. Though -19 ns was smaller than the overall ICD-GPS-202 time transfer specification (at the time, 110 ns) [6], many important authorized users greatly depend on an error magnitude less than 25 ns. Had the COSPM jump been any larger, we could have seriously impacted many important users in late December 1994 (figure 2).

In addition to the time transfer error, the GPS-UTC divergence itself was also noteworthy. By the time the MCS had completely steered out the GPS-UTC frequency offset of -22 ns/day, the GPS-UTC phase offset had grown to as large as -257 ns, on 17 Jan 95. Again, though well inside the system specification of  $\pm$



1000 ns [6], -257 ns was a much larger magnitude than the typical offset (within  $\pm 30$  ns), and substandard to what the timing community should reasonably expect from the Control Segment (figure 3).

This incident revealed the need for improved integrity monitoring, and a better capability to handle frequency jumps. The new L-Band Monitor (LBMON) software, installed in February 1995, has greatly helped the MCS in *detecting* frequency steps. LBMON scans ranging measurements once every six seconds for anomalies, alerts operators when anomalies are discovered, and provides real-time plots of ranging errors. LBMON's anomaly detection algorithm employs qualifying, forward, and backward-in-time filters optimized for detecting phase and frequency changes.

Several real-world incidents have allowed LBMON the opportunity to validate its role in the MCS's integrity monitoring capability. For example, at approximately 1930z, 20 Mar 95, the operational Rubidium frequency standard on SVN36 experienced a discrete frequency jump on the order of  $-1.58 \text{ E-11 s/s}$ , during a period of earth eclipse. On the previous GPS software release, this error would likely have only appeared as successive increases in the ranging measurement residuals, once every K-point (every 15 minutes). With this limited information, the operator would have had trouble properly identifying the nature of the satellite ranging error. In particular, the GPS analyst would *not* have been able to quickly a) determine if this were a phase error or a frequency error, b) minimize the ranging error experienced by users, or c) minimize the effect on the GPS Composite Clock. This type of corruption could possibly have progressed for over an hour before being properly characterized, under the older software.

Just 28 minutes after the jump, LBMON flagged SVN36's anomalous behavior. Subsequently, the Navigation Analyst viewed a display called NPLSVSUM, which shows the near-real time (once every six seconds) observed ranging error for one or more satellites. When displaying NPLSVSUM for SVN36, the navigation analyst noticed the rather discernible change in ranging error. (Figure 4 is an EXCEL reconstruction using the NPLSVSUM display data).

Because the analyst visually noticed the unusual run-off in ranging error, he was able to quickly increase specified portions of the system covariance matrix. This expedient reaction allowed the Filter to lock on to SVN36's new characteristics, permitted the operators to quickly upload new clock estimates for satellite broadcast, and minimized the degradation to the GPS Composite Clock.

Of course, not all anomalies are detected as easily as in this particular case. For instance, the Control Segment won't necessarily have visibility into the anomaly, and, in many cases, the anomaly may not be as noticeable as the above. Nonetheless, LBMON now allows operators to have a better "seat-of-the-pants" grasp of some of the more significant satellite and monitor station problems that can occur. LBMON has given the MCS more capability to identify, analyze, and reconcile some types of frequency step anomalies.

Ultimately though, MCS analysts would benefit from software that, in addition to detecting frequency steps like the above mentioned, would also *automatically* reconcile the step. Software that could automatically compensate Kalman Filter state estimates and covariances would reduce the dependency on operator input--humans are only so reliable in terms of catching anomalies, and a frequency step is one of the more difficult anomalies to detect.

## Dynamic *q*-ing

The GPS Composite Clock is an implicit ensemble of over 20 of GPS's spaceborne and ground-based atomic frequency standards. Clock weighting is implicitly defined by the state covariances located within



the functionality of the Kalman Filter. Covariances are primarily a function of the measurement noise, the number of measurements, and the continuous time update process noise ( $q$ ) values.

Analysts have the freedom to change clock  $q$  values periodically. Once per quarter, 2 SOPS derives new  $qs$  using independent Allan Variance data from the Naval Research Laboratory (NRL). 2 SOPS has successfully performed this fine tuning since October 1994. By uniquely tuning satellite clock state estimation based on empirical data, representing the true performance of each clock, 2 SOPS, thanks to NRL and other agencies, has improved the one-day stability of GPS time by approximately 10 % [4].

This quarterly activity should be viewed only as a short-term initiative, however. Manually updating the data base  $q$  values for each satellite incurs the risk of potentially hazardous typographical errors. The more often we update the  $qs$ , the higher the risk. Ideally, we'd like software that automatically and dynamically updates these  $qs$ . Besides alleviating the risk associated with manual updates, dynamic  $q$ -ing allows the capability to expediently reduce the effective weighting of clocks that have begun to behave anomalously. Obviously, dynamic  $q$ -ing has its *own* risks. Most sophisticated time scale algorithms can perform this task safely, and when we can utilize such a capability in the future, we must ensure that the MCS's version is at least as safe as those on existing, proven time scale algorithms.

## Using the Basic Time Scale Equation

One noted difference between the Composite Clock and other time scale algorithms is the issue of separate control for clock weighting. The MCS's  $qs$  actually serve a multi-role purpose. Primarily, MCS  $qs$  increase covariances during time updates, and hence, are integral to Kalman Filter estimation. As stated earlier,  $qs$  also effectively control the weighting of clocks within the implicit ensemble. Additionally, the MCS calculates the user range accuracy (URA) values broadcasted in the navigation message, using these  $qs$ .

Other time scale algorithms, such as A1(USNO), AT1(NIST), and KAS-2(TSC), explicitly generate system time, using a *version* of the following equation [8]:

$$\sum_{i=1}^N A_i X_i \langle t + \tau | t + \tau \rangle = \sum_{i=1}^N A_i X_i \langle t + \tau | t \rangle, \text{ where } \sum_{i=1}^N A_i = \begin{bmatrix} 1 & 0 & 0 \\ 0 & 1 & 0 \\ 0 & 0 & 1 \end{bmatrix},$$

$X_i$  is the state vector of the corrected clock  $i$ , and  $A_i$  is the user-controlled weighting matrix for clock  $i$ . This equation essentially mandates that the weighted sum of the corrected clock states (at a time  $t + \tau$ ) is equal to the weighted sum of the time scale algorithm's predictions (from  $t$  to  $t + \tau$ ) for those same corrected clock states. The Composite Clock is defined *implicitly* within the workings of the MCS Kalman Filter, which is responsible for the immense task of sorting out ephemeris and solar pressure state error, as well as clock error. The Composite Clock is not explicitly controlled by this time scale equation [8].

Use of this time scale equation would introduce the ability to control the weighting of clocks independently of the effective Kalman Filter weighting. This would generate a more explicit ensemble time separate from the implicit ensemble time generated within the Composite Clock.



The weights for each clock ( $A_i$ ,  $i = 1, 2, \dots, N$ ), could have the capability for both operator control and automatic control. Meaning, at the same time the system would be dynamically updating the weights, the operator would have the option to override and reduce the weight of any clock, for whatever reason.

The following example illustrates the utility of operator-controlled weighting. The MCS Kalman Filter operates under the premise of stochastic, optimal estimation. The currently operating Cesium frequency standard aboard SVN22 does not behave very stochastically, and therefore, somewhat violates a basic assumption of Kalman Filtering. SVN22 experiences frequency jumps on the order of  $-5 \text{ E-13}$  once every 45-64 days [7] (figure 5 is an EXCEL reconstruction using NRL data). When these frequency steps are removed, SVN22 has a 10-day stability of around  $5 \text{ E-14}$ . Unedited, the 10-day stability is around  $9 \text{ E-14}$  (figure 6). Ideally, one would like to keep the Kalman Filter  $q$ -ed based on its average performance, but prevent the frequency steps from corrupting Kalman Filter estimation, and thus, from distorting the mean time scale. A separate time scale with user-controlled weights, along with automatic frequency step resolution and dynamic  $q$ -ing, could help to reach this ideal.

The GPS Composite Clock fulfills the need for a stable, continuously operating reference against which all GPS ephemeris, solar pressure, and clock states are estimated. Without the GPS Composite Clock, we would not have been able to realize the time transfer performance and GPS time stability that we currently experience [5]. When introducing these ideas for improving the Composite Clock in the future, we must be careful not to introduce software that could impose unacceptable risk, or generate operational problems caused by being too complex to understand and operate. Let's take what we have now, value its advantages, and *refine*.

## CONCLUSION

The time transfer mission of GPS has gained increasing attention in recent years. We all continue to appreciate how much timing is the pivotal physical phenomenon that helps all three missions of GPS to realize their capabilities. Both from an accuracy and integrity perspective, we must not take our current capability for granted; rather, we must take advantage of the continually advancing PTTI technology, as well as CPU technology.

Hand in hand, these two can be combined to make long-term improvements to MCS software, with safety as the guiding principle. Now is the opportunity to apply our operational experience and lessons learned, and exercise consideration towards the above ideas for improving GPS timing performance in the future.

## ACKNOWLEDGMENTS

The author wishes to thank the following people and agencies for their generous assistance:

Kenneth R. Brown, Loral Federal Systems Division  
M. K. Chien, Loral Federal Systems Division  
The Defense Mapping Agency  
William S. Mathon, Loral Federal Systems Division  
Sam R. Stein, Timing Solutions Corporation  
The people of the 2 SOPS  
Francine Vannicola, USNO



## REFERENCES

- [1] Brown, Kenneth R., *The Theory of the GPS Composite Clock*, Proceedings of ION GPS-91, 11-13 Sep 91
- [2] Brown, Kenneth R., Chien, Ming Kang, Mathon, William S., Hutsell, Steven T., Capt, USAF, and Shank, Christopher M., Capt, USAF, *L-Band Anomaly Detection in GPS*, Proceedings of ION's 51st Annual Meeting, 5-7 Jun 95
- [3] Hutsell, Steven T., Capt, USAF, *A Statistical Analysis of the GPS Time Transfer Error Budget*, Proceedings of ION's 51st Annual Meeting, 6-8 Jun 95
- [4] Hutsell, Steven T., Capt, USAF, *Fine Tuning GPS Clock Estimation in the MCS*, Proceedings of PTTI-94, 5-8 Dec 94
- [5] Hutsell, Steven T., Capt, USAF, *Recent MCS Improvements to GPS Timing*, Proceedings of ION GPS-94, 20-23 Sep 94
- [6] ICD-GPS-202, 21 Nov 84
- [7] NRL Quarterly Report 95-3, 3 Aug 95
- [8] Stein, S. R., *Advances in Time-Scale Algorithms*, Proceedings of PTTI-92, 1-3 Dec 92

# *GPS Time Transfer*

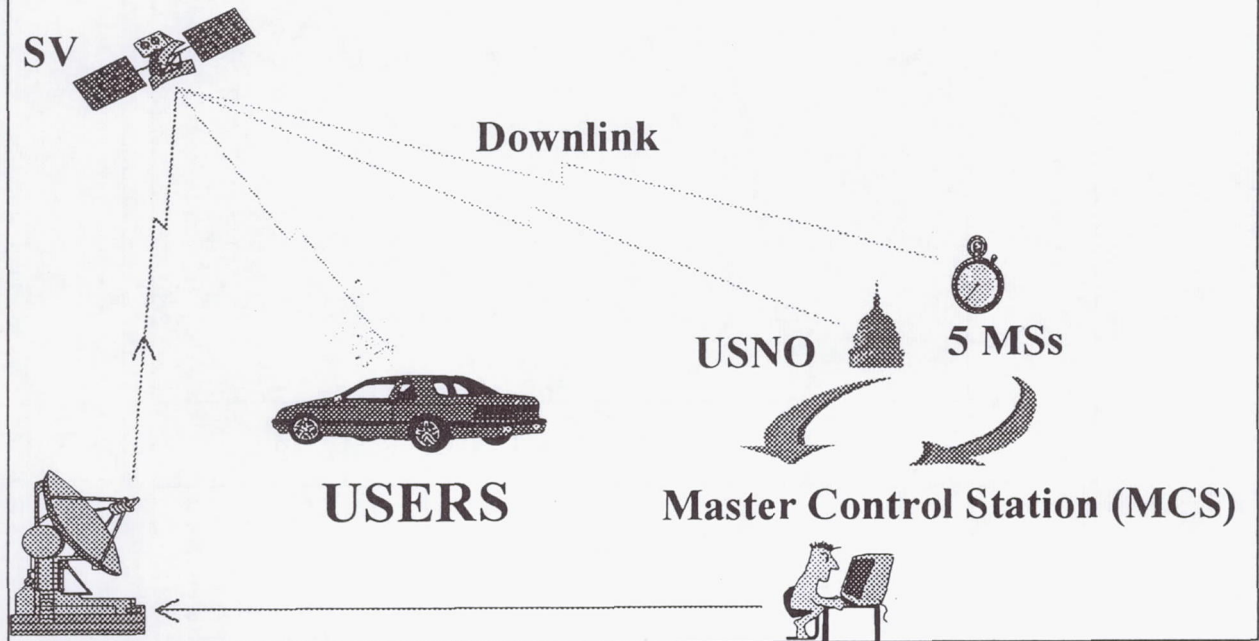


Figure 1

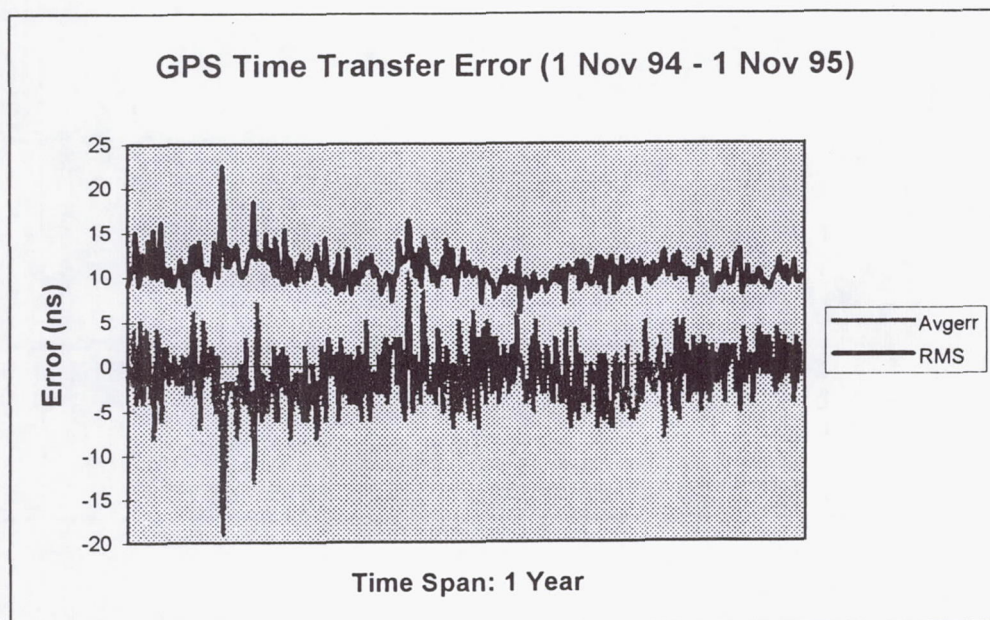


Figure 2



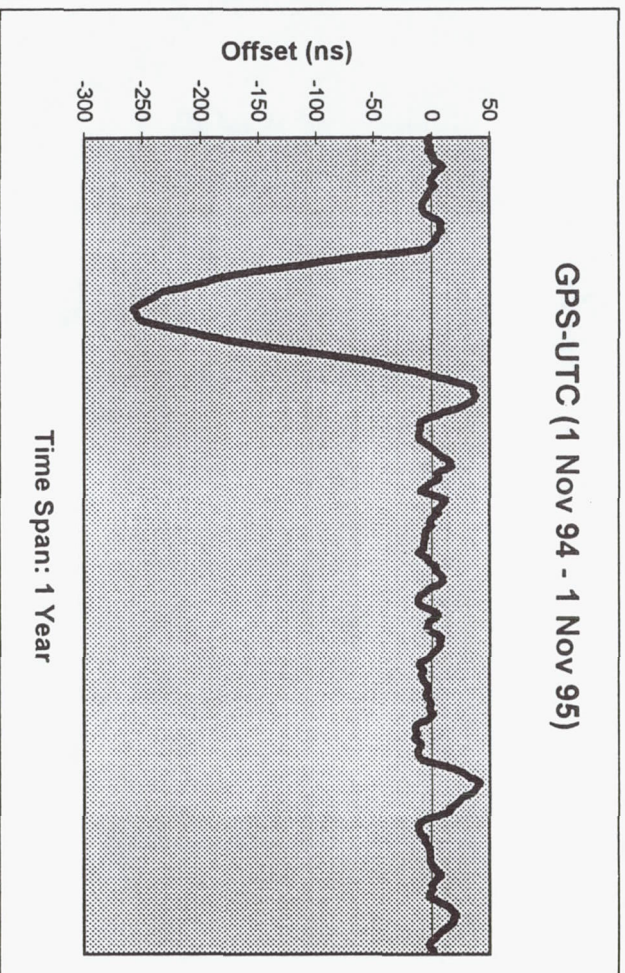


Figure 3

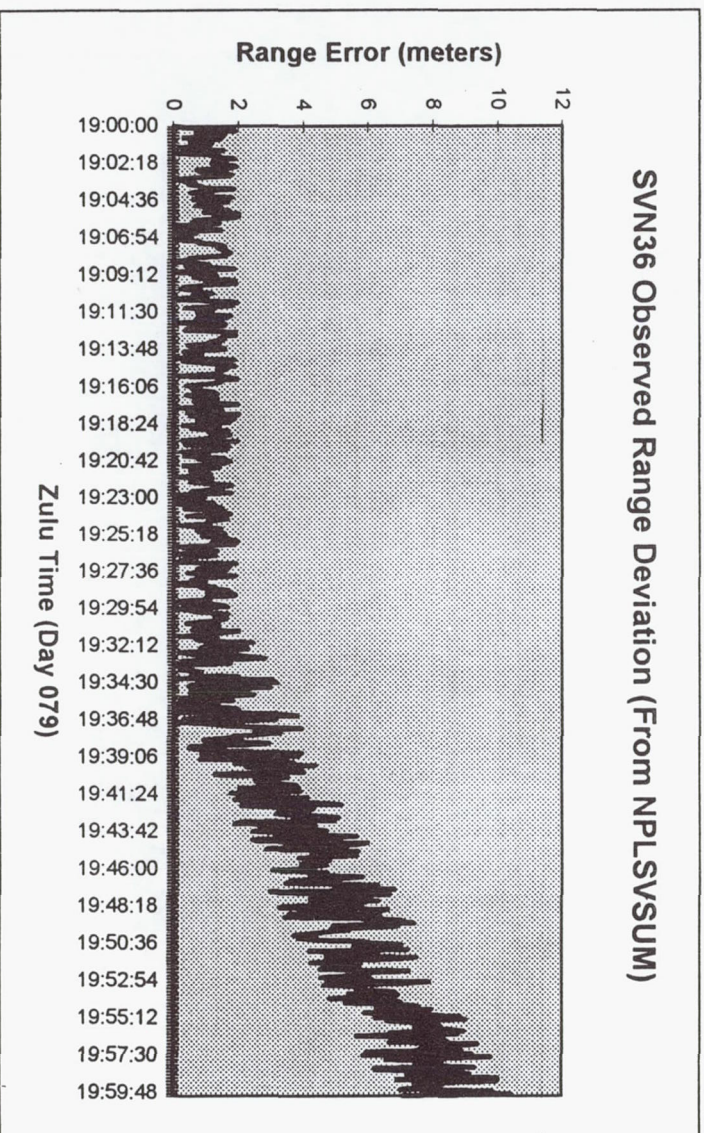


Figure 4



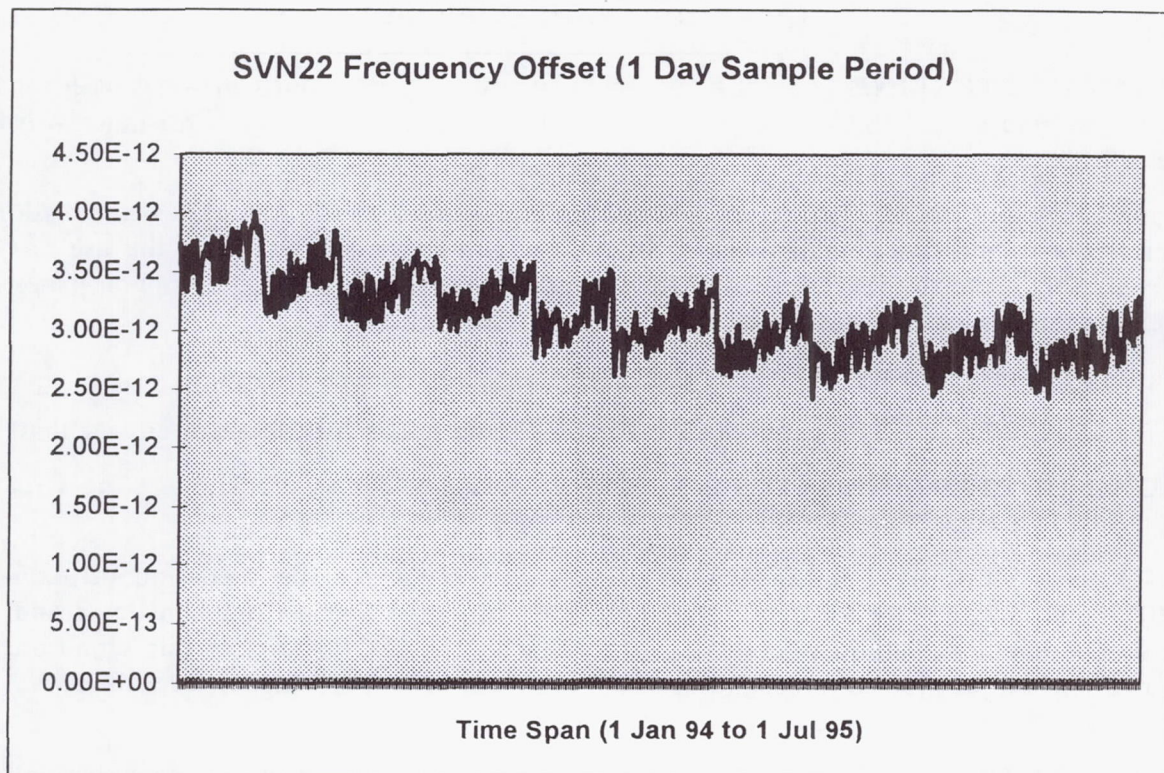


Figure 5

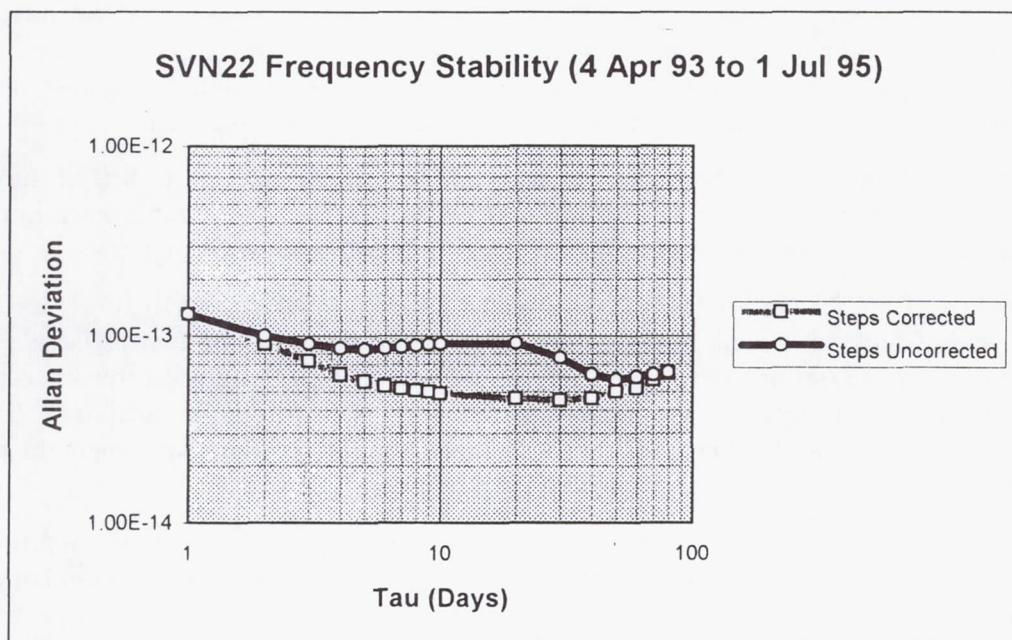


Figure 6



## Questions and Answers

**EDGAR BUTTERLINE (AT&T):** As long as you were giving your Christmas wish list, I'd like to give you what I think is the number one item on the "civil users" Christmas wish list: Turn off SA.

As you know, and I realize you're not in a controlling position, the President has commissioned several blue ribbon civil commissions to come up with a recommendation for the use of GPS for civil users. And the last GPS Civil Users Conference, results of that blue ribbon panel was published and issued and discussed. On that list is "Turn off SA."

What are the prospects?

**CAPT. STEVEN HUTSELL (USAF):** I certainly am not in a position to answer that.

**EDGAR BUTTERLINE (AT&T):** Nothing is cooking as far as you know? And I realize you're not in a controlling position.

**CAPT. STEVEN HUTSELL (USNO):** I'm sure it's going to be a continuously-cooking matter. I'm sure it always comes up at both the Air Force Space Command level and the National Command Authority level. I can say that at the 2SOPS level at our squadron, we are really in no position to affect the decision; it's made at a much higher level than what we operate at. We are the implement.

**EDGAR BUTTERLINE (AT&T):** I understand, I understand. You're not making policy.

Let me make an offer. One of your big problems seems to be that telephone line. I really worry about that telephone line also; and if that telephone line happens to be an AT&T telephone line, let me give you my card. I assure you, I can get that fixed.

**CAPT. STEVEN HUTSELL (USAF):** Thankfully, with the backup that we have, I work with some very helpful people out at the Naval Observatory — when we do have communication problems, they're very helpful about getting the necessary information to us over the phone; and they help out on weekends and drive in, if necessary, to fix a problem.

But I complain about it a lot. We're not in seriously dire shape with that. But, it makes sense that in the long term we work on something that's a government-paid communication line and not something that we don't know for sure whether it's going to work or not.

**WILLIAM KLEPCZYNSKI (USNO):** In regard to the connectivity to the USNO, we are in the process of moving our alternate master clock out to Falcon. The first phase is sort of set up now and it's in operation there. And I'm sure that will go a long ways toward establishing better communications between Washington and Falcon; in addition to telephone lines, we'll be using satellite links and things like that. So there should be some improvement with time — and refinement.

**CAPT. STEVEN HUTSELL (USAF):** Right. It would offer, also, a good dual path for us in case if, for whatever reason, the connectivity is lost, we can always rely on a backup, whether it's the alternate master clock or Washington, D.C.

# UTC DISSEMINATION TO THE REAL-TIME USER: THE ROLE OF USNO

Mihran Miranian  
U.S. Naval Observatory  
Washington, D.C. 20392

## Abstract

*Coordinated Universal Time (UTC) is available worldwide via the Global Positioning System (GPS). The UTC disseminated by GPS is referenced to the U.S. Naval Observatory Master Clock, UTC(USNO), which is regularly steered and maintained as close as possible to UTC(BIPM), the international time scale. This paper will describe the role of the USNO in monitoring the time disseminated by the GPS and the steps involved to ensure its accuracy to the user. The paper will also discuss the other sources of UTC(USNO) and the process by which UTC(USNO) is steered to UTC(BIPM).*

## INTRODUCTION

The United States Department of Defense (DoD) Instruction 5000.2 charges the U.S. Navy and specifically the U.S. Naval Observatory (USNO) with the requirement to maintain the timing standard for all precise time and time interval (PTTI) operations within DoD. The accomplishment of this task involves a coordinated effort by the USNO and the electronic navigation systems that are synchronized to USNO time. The USNO monitors the time emanating from these systems and reports their offsets with respect to the USNO timing standard. The navigation systems operators then make the necessary adjustments for synchronization with the USNO.

The timing standard or Master Clock (MC) of the USNO is a hydrogen maser which is continuously steered to the USNO time scale. This time scale is based on an ensemble of 50 to 60 cesium frequency standards and 8 to 12 hydrogen masers which are located in environmental chambers throughout the observatory facility in Washington and at the USNO Alternate Station in Richmond, Florida<sup>[1]</sup>. This is the largest assembly of atomic clocks for any single timing operation in the world. Furthermore, the USNO collection of atomic clocks constitutes nearly forty percent of the International Atomic Time Scale (TAI) which is formulated at the Bureau International des Poids et Mesures (BIPM) in Paris, France. Moreover, to establish a backup MC in a secure facility and to better support GPS timing operations, the USNO will soon have an Alternate Master Clock (AMC) at Falcon Air Force Base in Colorado Springs, Colorado. This AMC will replace the USNO AMC at Richmond, Florida and will be fully integrated into the USNO MC System.



## COORDINATED UNIVERSAL TIME (UTC) AND UTC(USNO)

Coordinated Universal Time was revised in 1971 and the new system became effective on January 1, 1972. On that date, UTC was set to be exactly 10 seconds behind TAI. This difference was caused by the divergence of the two time systems from January 1, 1958 when TAI and the time based on the rotation of the Earth (UT1) were set nearly together. During this period variations in the rotation of the Earth which resulted in a longer day, when compared to the more precise atomic time, accumulated to a difference of 10 seconds. Therefore, the more stable atomic time was adjusted to agree on the average with UT1. This adjusted atomic time is UTC.

By international agreement, UTC is maintained within 0.9 seconds of UT1. This is accomplished by making periodic one second adjustments to UTC. These one-second adjustments are referred to as "Leap Seconds" and they can be either positive or negative depending on the variations of the Earth's rotation. Leap seconds are usually added or deleted on June 30 or December 31, but under unusual circumstances the adjustment can be made at the end of any month (Figure 1).

Most timing laboratories that contribute to the TAI steer their reference clocks to UTC(BIPM). However, this is not an easy task and consequently there is always a difference between the reference clocks at each of these laboratories. Therefore, when referring to UTC, it is necessary to define which laboratory clock is being referenced, such as UTC(USNO), UTC(NIST), or UTC(PTB).

## STEERING UTC(USNO) TO UTC(BIPM)

The reason steering to UTC(BIPM) is not easy, is because timing reports from the BIPM are usually more than 30 days old. Consequently, timing offsets from the BIPM must be predicted more than one month into the future. This can only be done if a laboratory has a very stable time scale on which to base the predictions. Fortunately, the USNO has such a time scale, due to its large ensemble of state-of-the-art clocks in stable environments with close monitoring, and an optimal mean time scale algorithm.

The USNO predictions of UTC(BIPM) - UTC(USNO) are based on the latest 180 days (18 data points) of data in the monthly Circular T report from the BIPM. These data points are compared to the USNO unsteered time scale and a linear least-squares computation is made for the frequency and drift, with more weight given to the most recent data. Predictions are then made based on the extrapolation of the unsteered time scale in relation to UTC(BIPM) incorporating the computed frequency and drift.

The steering philosophy at the USNO is to make very small ( $1.0 \times 10^{-15}$ ) frequency adjustments to its steered time scale to keep it on time with respect to the predicted UTC(BIPM). Once the steered time scale has been coordinated with UTC(BIPM), UTC(USNO) is steered to this time scale by making daily frequency adjustments of no more than  $3.5 \times 10^{-15}$ . To maintain the stability of UTC(USNO), these adjustments are determined using 10-day averaging and a damping factor of 100. This simple process has proven to be very effective and has maintained UTC(USNO) to within  $\pm 20$  nanoseconds of UTC(BIPM) for the past year (Figure 2).



## GPS TIME AND THE UTC CORRECTION

The Global Positioning System has become the most accurate widely accessible source of UTC throughout the world. With a constellation of 24 satellites, there are at least four satellites in view continuously and a user need only track one of these satellites to obtain precise time, if the user's location is known. Otherwise, all four satellites must be tracked to determine location first. Although we take UTC via GPS for granted, it is important to understand how it is disseminated by the satellites.

Even though GPS time originated from UTC, it is not UTC. At 0h on January 6, 1980, GPS time was synchronized to UTC. But unlike UTC, GPS time is not adjusted for leap seconds. Consequently, whenever there is a leap second applied to UTC, the difference between GPS time and UTC changes. While the two time scales may differ by an integral number of leap seconds, they will always be very close at the sub-microsecond level, because GPS time is steered to be in phase with UTC(USNO). However, due to the variations of the two time scales, there will always be a small difference between them. The accumulated leap seconds plus this small phase offset is the correction for UTC.

Leap second adjustments are announced three to four months in advance, so the accumulated leap second correction is clearly defined and easily accounted for. Phase corrections, most often no more than  $\pm 20$  nanoseconds, are determined at the USNO and sent via secure communications to the GPS Master Control Station (MCS) at Falcon AFB. The data are processed at the MCS and uploaded to the satellites. Page 18 of subframe 4 in the GPS broadcast from the satellites includes the parameters needed to relate GPS time to UTC. User sets must apply these parameters according to the following relationship in order to estimate UTC(USNO). This then becomes a source of UTC referred to as UTC(via GPS):

$$UTC(\text{via GPS}) = t_{GPS} - \Delta t_{UTC}$$

where  $UTC(\text{via GPS})$  is in seconds and

$$\begin{aligned}\Delta t_{UTC} &= \Delta t_{LS} + A_0 + A_1(t_{GPS} - t_{RT}) \\ \Delta t_{LS} &= \text{delta time due to leap seconds} \\ t_{GPS} &= \text{GPS time} \\ A_0 &= \text{phase correction} \\ A_1 &= \text{the first-order term} \\ t_{RT} &= \text{reference time for the UTC data.}\end{aligned}$$

Due to Selective Availability (SA) and Anti-Spoofing (A-S) imposed by the GPS, an unauthorized real-time user can experience a time transfer accuracy degradation of 150 nanoseconds (one sigma) or worse, while the user correcting for SA/A-S can expect an accuracy of 28 nanoseconds (one sigma). However, some manufacturers have incorporated smoothing algorithms and other techniques, which have been shown to improve accuracy by a factor of 2 or greater in their uncorrected timing receivers<sup>[3]</sup>.

## MONITORING GPS TIME

The USNO monitors GPS system time to provide a reliable and stable coordinated time reference for the satellite navigation system. There are several GPS timing receivers in constant operation in Washington, D.C. and at the USNO Alternate Sites. Each location monitors GPS time using both authorized Precise Positioning Service (PPS) and uncorrected



Standard Positioning Service (SPS) receivers. The receivers are scheduled to track satellites according to a recommended common-view tracking schedule, which is provided by the BIPM, for international time comparisons. Satellite track times are chosen to maximize elevation angles between pairs of stations and open tracking periods are filled with the emphasis on providing a balanced coverage of all satellites.

Data from the SPS receivers are collected and processed on the general purpose computers and, to maintain security, the PPS data are collected and processed on a dedicated computer. Each receiver outputs a measure of GPS time referenced to UTC(USNO) and also the correction for UTC, from individual satellites every six seconds. The six-second data are grouped into thirteen-minute intervals to produce one processed data record. The values within each record are computed for the mid-point of the track and are a measure of the difference between UTC(USNO) and GPS time (Figure 3, column 5) and the difference between UTC(USNO) and UTC(via GPS) (Figure 3, column 14)<sup>[4]</sup>. The latter is a measure of how well the satellite is disseminating UTC(USNO).

The USNO has adopted what it calls the "melting pot" technique for data reduction. With this technique, the thirteen-minute data from all satellites are grouped into running two-day intervals and a filtered linear least-squares solution is made, solving for the beginning of the second day. These daily values are a very good gauge of the time dissemination performance for the entire GPS constellation. The smooth data in Figure 4 shows that GPS time is most often maintained to within  $\pm 10$  nanoseconds of UTC(USNO). It also shows that on rare occasions there can be a large divergence. However, Figure 4 also shows that, during periods when GPS time runs off, UTC(via GPS) can remain stable because the USNO reports the magnitude of the run-off to the MCS so that the UTC correction can be adjusted accordingly.

## OTHER SOURCES OF UTC(USNO)

There are many ways in which UTC(USNO) is disseminated to the real time user. These range from a simple telephone call to a voice announcer at the USNO to specialized receiving equipment for tracking Earth-orbiting navigation satellites. With accuracies ranging from  $\pm 0.05$  seconds to less than  $\pm 100$  nanoseconds, users can select the system that best fills their requirements. Figure 5 lists the principal sources of UTC(USNO) and the accuracy a user can expect when using one of these systems. It should be noted that while all of the systems provide a reference for making phase comparisons, Loran-C and Omega do not provide the time of day.

The USNO Time Announcer, Computer Time via modem, and Network Time Synchronization (NTP) satisfy the needs of most users and are relatively inexpensive. In fact, with the possible exception of GPS, NTP is the most accessed source of UTC(USNO), with over 500,000 requests daily. The NTP is a free service and the software is available via anonymous FTP from "louie.udel.edu". All three of these services provide UTC(USNO) to an accuracy of  $\pm 0.05$  seconds or better. In addition, the commercial Leitch system has a direct link to the USNO Master Clock and provides UTC(USNO) to subscribers via its time dissemination system.

For those who need time in the microsecond range, the Navy Transit Satellite System and the Omega navigation system are synchronized to UTC(USNO) via GPS and can provide a time reference which is accurate to less than  $\pm 25$  microseconds. However, both of these systems will stop operations in the near future. The Transit system will discontinue its service at the end of 1996 and Omega will stop transmitting at the end of 1997.

As a service to the U.S. Coast Guard (USCG), the USNO has been monitoring the timing



of the Loran-C system since the mid 1960s. This is in compliance with Public Law 100-223, which requires that all USCG controlled Loran-C master stations shall be synchronized to UTC. The monitoring of Loran-C transmissions by the USNO has made it possible for the USCG to control the timing of the Loran-C signals to within  $\pm 300$  nanoseconds of UTC(USNO)[2]. Therefore, a user can obtain UTC(USNO) to an accuracy of  $\pm 500$  nanosecond from Loran-C, allowing for errors in the computation of the propagation path of the signal. The USCG recently relinquished control of all foreign Loran-C stations to the host nations. Consequently, we cannot guarantee that these stations will continue to be synchronized to UTC. Therefore, it is recommended that users only monitor USCG-controlled Loran-C transmissions for the purpose of time transfer. But even this will not last long, because the USCG has announced that Loran-C transmissions controlled by them will be turned off by the year 2000, and replaced with differential GPS.

## CONCLUSION

The USNO plays an important role in the formulation and dissemination of UTC. As the major contributor to the TAI, the USNO clocks have become a critical ingredient in the formulation of the International Atomic Time Scale. This is an important responsibility which the USNO will continue to meet in its support of the world timing community. The GPS now provides continuous accessibility to UTC throughout the world. As the primary reference to UTC for the GPS, UTC(USNO) has been steered to within  $\pm 20$  nanoseconds of UTC(BIPM) for the last 400 days and within  $\pm 10$  nanoseconds for the last 150 days (Figure 2). By maintaining UTC(USNO) as close as possible to UTC(BIPM), the USNO will ensure that all time dissemination systems that are synchronized to UTC(USNO) will also be synchronized to UTC.

## REFERENCES

- [1] L.A. Breakiron 1992, "*Timescale algorithms combining cesium clocks and hydrogen masers*," Proceedings of the 23rd Annual Precise Time and Time Interval (PTTI) Applications and Planning Meeting, 3-5 December 1991, Pasadena, California, pp. 297-305.
- [2] H. Chadsey 1992, "*Loran-C data reduction at the U.S. Naval Observatory*," Proceedings of the 23rd Annual Precise Time and Time Interval (PTTI) Applications and Planning Meeting, 3-5 December 1991, Pasadena, California, pp. 103-110.
- [3] J.A. Kusters, R.P. Gifford, L.S. Cutler, D.W. Allan, and M. Miranian 1995, "*A globally efficient means of distributing UTC time and frequency through GPS*," Proceedings of the 26th Annual Precise Time and Time Interval (PTTI) Applications and Planning Meeting, 6-8 December 1994, Reston, Virginia, pp. 235-254.
- [4] M. Miranian, and W.J. Klepczynski 1991, "*Time transfer via GPS at USNO*," Proceedings of ION GPS-91, 11-13 September 1991, Albuquerque, New Mexico, pp. 215-221.



# HISTORY OF UTC

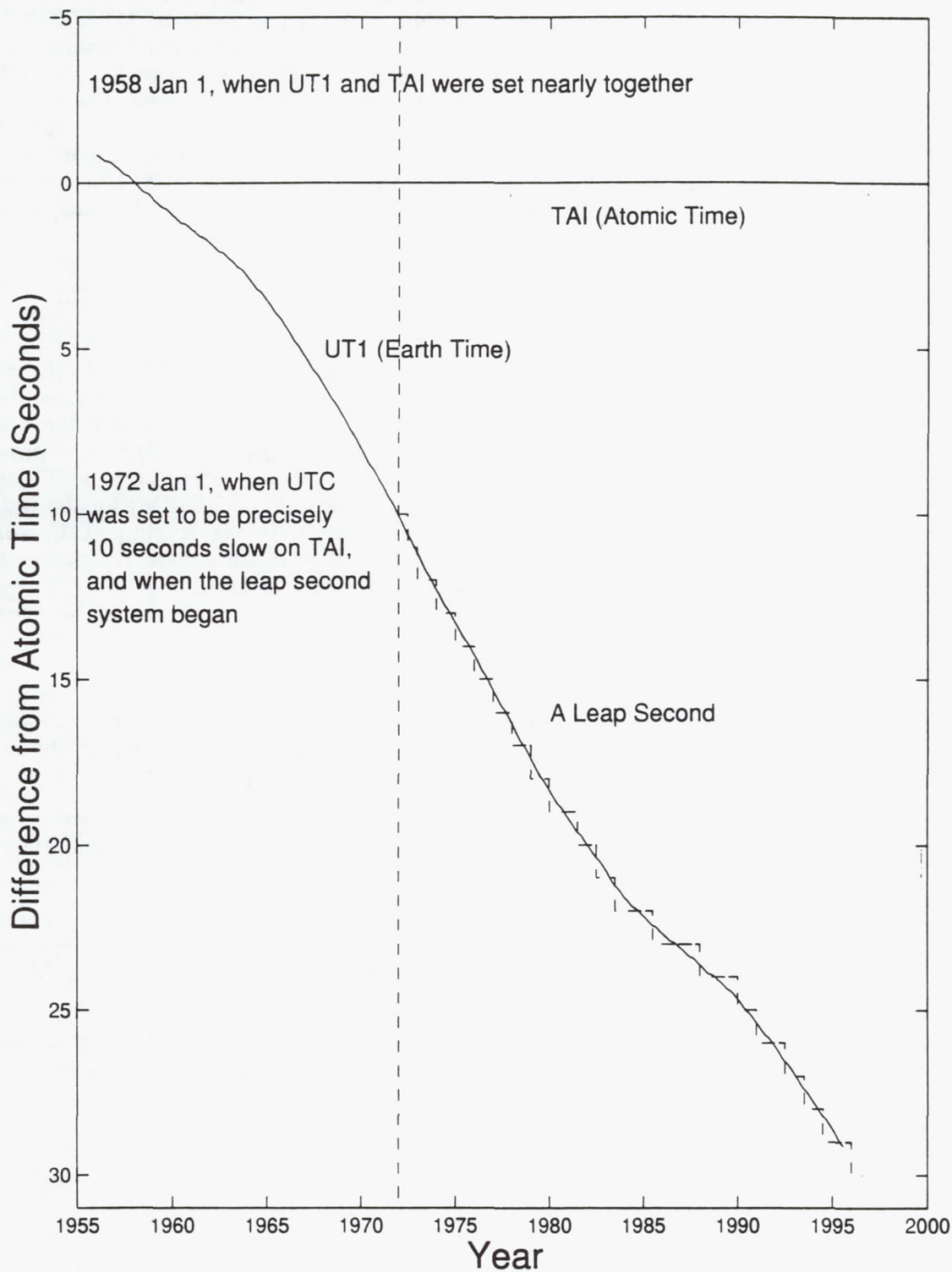


Figure 1

# UTC(BIPM) - UTC(USNO)

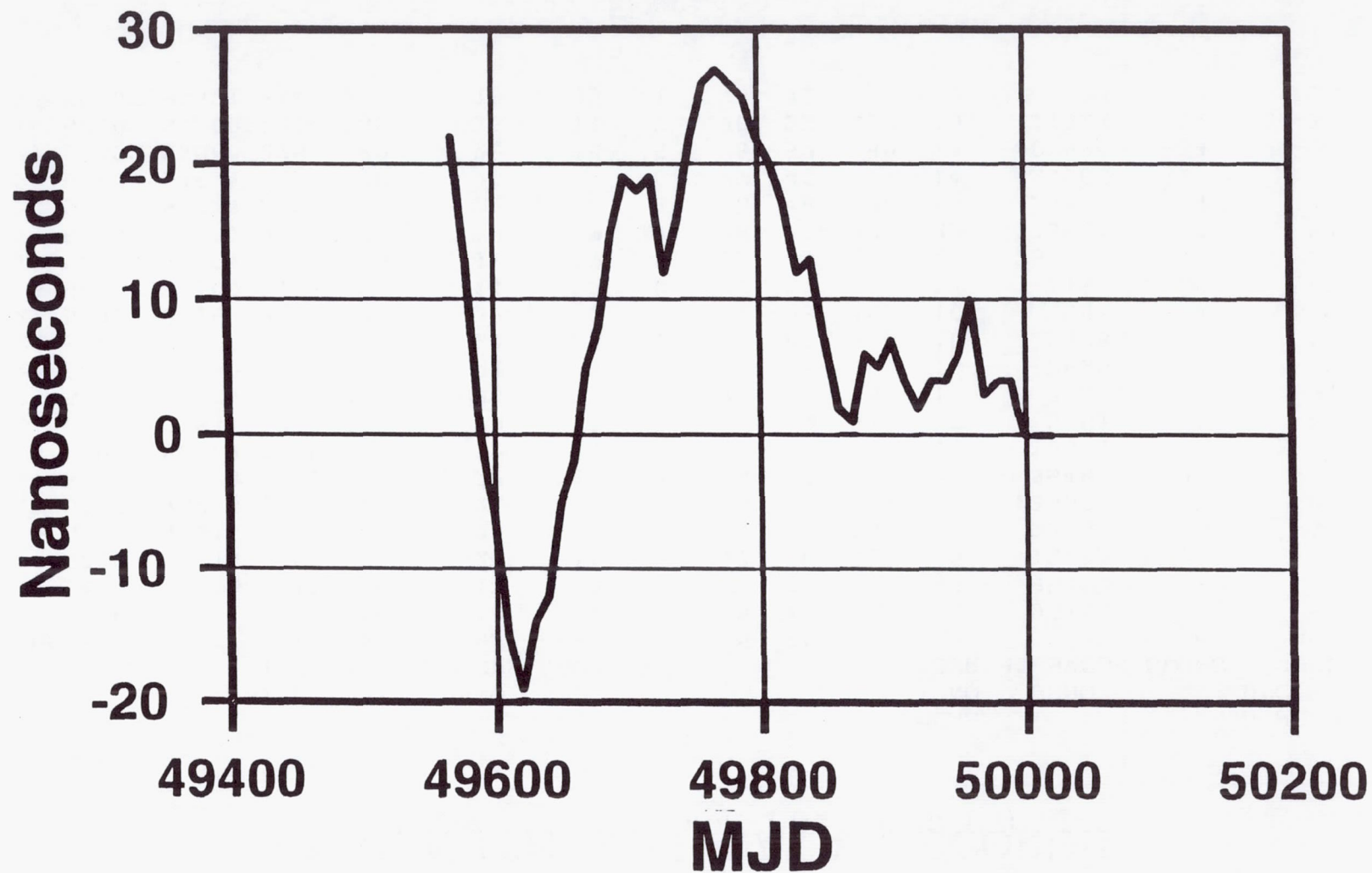


Figure 2



# 13-MINUTE PPS DATA RECORDS

PRN	MJD	START TIME	TRK TIME	USNO MC-GPS	SLOPE	RMS				MEAS IONO CORR	USNO MC-SVCLK	SLOPE	USNO MC-UTC (via GPS)
	MID-POINT	UTC	s	ns	ps/s	ns	N	EL	AZ	ns	ns	ps/s	ns
17	50007.71705	1706	780	-18	-5	7	78	46	315	15	95466	0	4
17	50007.72608	1719	780	-17	2	3	78	66	316	19	95470	6	5
9	50007.75316	1758	780	-24	14	7	77	40	138	19	12682	17	-3
9	50007.76219	1811	780	-23	-12	5	78	45	132	20	12684	-9	-2
12	50007.78233	1840	780	-26	5	8	78	26	51	27	-236089	55	-5
17	50007.79483	1858	780	-22	19	8	78	57	181	20	95487	22	-1
9	50007.80663	1915	780	-22	0	4	78	56	84	15	12694	2	-1
21	50007.81844	1932	780	-29	31	5	75	49	314	18	5481	32	-8
23	50007.83927	2002	780	-20	-9	2	78	70	88	17	-2624	-9	2
23	50007.84830	2015	780	-21	7	3	78	66	103	16	-2625	7	1
21	50007.87260	2050	780	-24	1	1	69	84	331	10	5498	-8	0
21	50007.88157	2103	770	-22	0	4	77	88	152	10	5501	4	0
5	50007.89407	2121	770	-14	12	8	77	32	74	15	-4151	10	8
15	50007.90524	2137	780	-19	-12	9	78	19	309	24	-233545	-14	2
15	50007.91427	2150	780	-17	9	17	78	21	303	22	-233544	10	5
20	50007.93927	2226	780	-22	14	3	78	46	80	16	-29963	4	-1
20	50007.94824	2239	770	-20	-7	6	77	45	71	14	-29968	-17	1
1	50007.96080	2257	780	-29	-15	6	78	57	80	13	-607994	-13	-7
14	50007.97260	2314	780	-25	11	7	78	22	317	19	-11324	11	-3
25	50007.99621	2348	780	-19	33	11	78	71	8	9	-793	33	3

Figure 3

# UTC(USNO) - GPS and UTC(USNO) - UTC(via GPS)

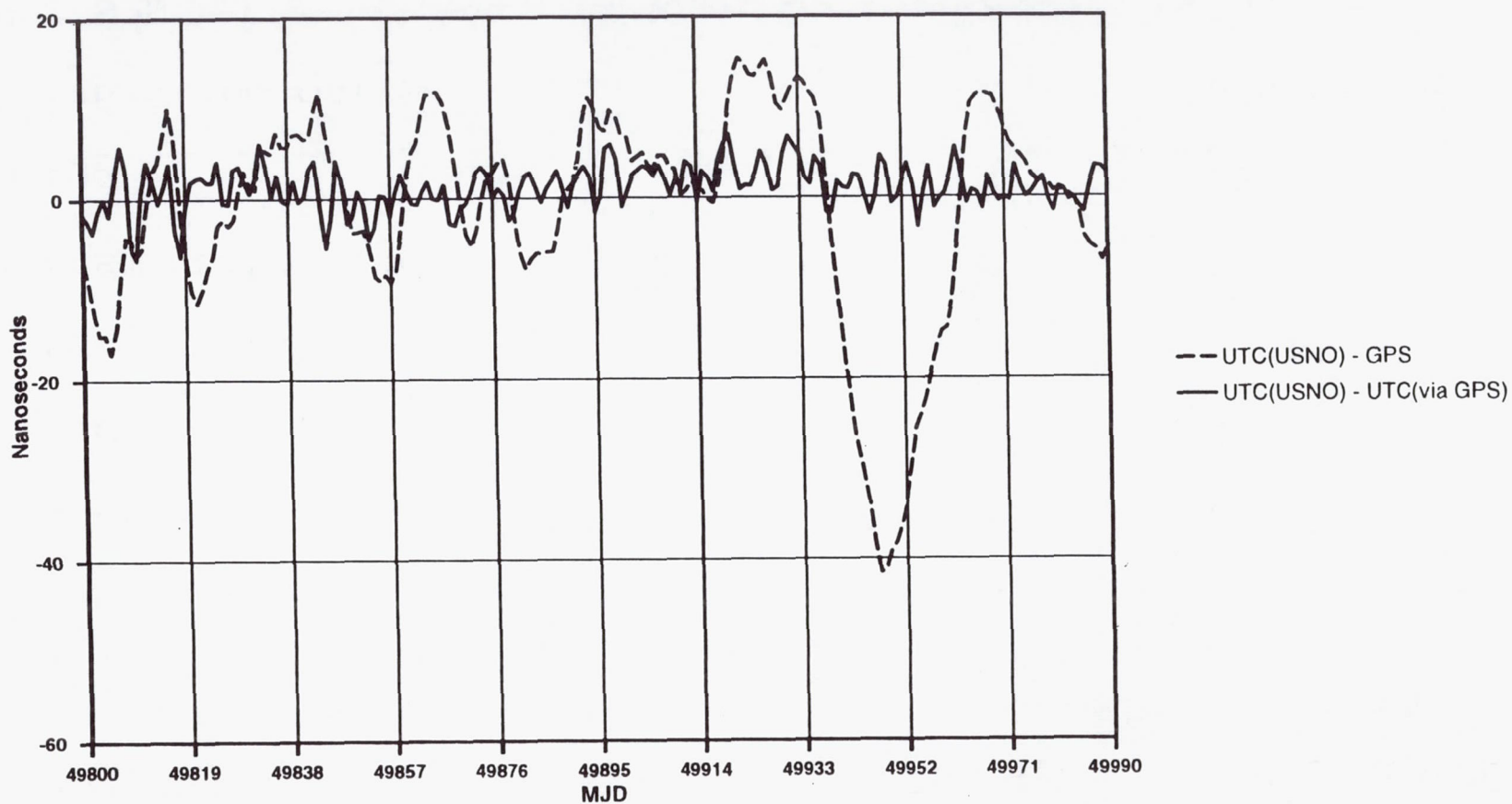


Figure 4



# SOURCES OF UTC (USNO)

(Real Time)

SOURCE	TIME	PHASE	ACCURACY
			>
Voice Announcer	X	X	0.05 seconds
Computer Time	X	X	0.01 "
Leitch	X	X	0.01 "
Internet (NTP)	X	X	0.01 "
Transit Satellite	X	X	25 microsec.
Omega		X	2 "
Loran-C (US only)		X	500 nanosec.
GPS SPS	X	X	300 "
GPS PPS	X	X	50 "

Figure 5

## Questions and Answers

**SAMUEL STEIN (TIMING SOLUTIONS CORPORATION):** Mihran, I was wondering if it would be possible for you to put some numbers to the bullets you had on your conclusion graph. For example, if I'm in an industrializing nation and I'm setting up a time and frequency laboratory to provide calibrations for local industry, and I want to establish frequency accuracy using GPS, I go through UTC, USNO; and the frequency accuracy I get is determined by the maximum steering rate that USNO will ever use in order to keep its time close to UTC. Do you publish that maximum rate?

**MIHRAN MIRANIAN (USNO):** The maximum rate – let's see – that we're using right now is about  $3 \times 10^{-15}$ . That's a maximum. But it's usually not that much; it's no more than about one part daily. So it's pretty stable.

**SAMUEL STEIN (TIMING SOLUTIONS CORPORATION):** The other question I had was that I think you gave a very conservative specification of 300 nanoseconds for the performance an SPS commercial receiver, but more commonly, people bandy about approximately 100 nanoseconds. Can you comment on that?

**MIHRAN MIRANIAN (USNO):** Yes. There are a number of techniques that are being used. I think the HP receiver, the new HP receiver, we just tested one for a short time at the Observatory. It's amazing what it can do. It's performing around 50 to 70 nanoseconds.

The Motorola receiver – I just showed you that one – there are a number of receivers. There are a lot of techniques that are now being used for averaging. Actually, maybe Dave could talk about that, Dave Allan. I know you're involved with that. Do you want to, Dave?

**DAVID ALLAN (ALLAN'S TIME):** The idea of averaging is a little different because, of course, these receivers are built for telecom, and they have to be real time. So you're not really averaging, you're looking at the SA spectrum and reducing its effects; looking at the clock spectrum and designing a filter so that you can do a real-time estimate of what is UTC. The rms numbers on the HP receivers are about 20 nanoseconds. Peak-to-peak will go up to like 70 each day.

So one can do very well. That's with a quartz-phase simple receiver. So once you understand the SA, it goes extremely well.

The question I had, Mihran, I know there's legislation for LORAN to be within 100 nanoseconds. How is that proceeding?

**MIHRAN MIRANIAN (USNO):** Yes, there is a public law that says that LORAN is supposed to be within that specification, but they never defined what. And we think they mean 100 nanoseconds rms. But it was never clearly defined. So I don't know what to tell you. But I can tell you that when you look at our Series Four, where we published the offset between LORAN stations – most of them are within about 100 nanoseconds.

But again, to the user – and I'm going to the real time user now – what can he expect? I'd say it's safe to say 500 nanoseconds.



# ROLE OF THE BIPM IN UTC DISSEMINATION TO THE REAL TIME USER

T. J. Quinn and C. Thomas  
Bureau International des Poids et Mesures  
Pavillon de Breteuil  
92312 Sèvres Cedex  
France

## Abstract

*The generation and dissemination of International Atomic Time, TAI, and Coordinated Universal Time, UTC, are explicitly mentioned in the list of the principal tasks of the BIPM, that appears in the Comptes Rendus of the 18e Conférence Générale des Poids et Mesures, in 1987. These time scales are used as the ultimate reference in the most demanding scientific applications and must, therefore, be of the best metrological quality in terms of reliability, long-term stability, and conformity of the scale interval with the second, the unit of time of the International System of Units. To meet these requirements, it is necessary that the readings of the atomic clocks, spread all over the world, that are used as basic timing data for TAI and UTC generation, must be combined in the most efficient way possible. In particular, to take full advantage of the quality of each contributing clock calls for observation of its performance over a sufficiently long time. At present, the computation period treats data in blocks covering two months. TAI and UTC are thus deferred-time time scales that cannot be immediately available to real-time users.*

*The BIPM can, nevertheless, be of help to real-time users. The predictability of UTC is a fundamental attribute of the scale for institutions responsible for the dissemination of real-time time scales. It allows them to improve their local representations of UTC and, thus, implement a more thorough steering of the time scales diffused in real time. With a view to improving the predictability of UTC, the BIPM examines in detail timing techniques and basic theories in order to propose alternative solutions for timing algorithms. This, coupled with a recent improvement of timing data, makes UTC more stable and, thus, more predictable. At a more practical level, effort is being devoted to putting in place automatic procedures for reducing the time needed for data collection and treatment: monthly results are already available ten days earlier than before.*

## 1 INTRODUCTION

The Comité International des Poids et Mesures, CIPM, reviewed the role of the Bureau International des Poids et Mesures, BIPM, in the 1980s. Its conclusions were made known in the Convocation to the 18e Conférence Générale des Poids et Mesures<sup>[1]</sup>; insofar as it concerns the time activities, they were as follows: "The purpose of the BIPM is to provide the physical



basis necessary to ensure worldwide uniformity of measurements. Therefore, its principal tasks are [among others]: ...to establish and disseminate the International Atomic Time, and in collaboration with the appropriate astronomical organizations, Coordinated Universal Time;...

The definition of TAI was approved by the CIPM in 1970, and recognized by the CGPM, in 1971<sup>[2]</sup>. It reads as follows: "International Atomic Time (TAI) is the time reference coordinate established by the Bureau International de l'Heure on the basis of the readings of atomic clocks operating in various establishments in accordance with the definition of the second, the unit of time of the International System of units." An addition was made to this definition in 1980<sup>[3]</sup> in order to place TAI in the context of General Relativity. In 1988 responsibility for TAI was transferred to the Time Section of the BIPM, fulfilling one of the explicit missions given above.

To be used as the ultimate time reference in the most demanding scientific applications, TAI must be of the best metrological quality, in particular in respect of long-term stability. This calls for observation of the performance of each contributing clock over a sufficiently long period of time. At present, the computation takes two-month blocks of data, so TAI, and consequently UTC, are deferred-time time scales that present an *intrinsic* delay of access to the real-time users of two months. In addition, the definition given above also implies that TAI and UTC are the results of a collective effort: national laboratories provide timing data to the BIPM, which in turn produces TAI and distributes it as time corrections to national time scales. An additional *material* delay of access is thus linked to the time needed for data exchange and analysis. For example, the definitive UTC updates for the months of September and October 1995 were made available to users on the 17th of November 1995.

Real-time users have access to local representations of UTC, UTC(k), maintained by national laboratories, and to derived time scales, such as GPS time and GLONASS time, diffused by global satellite systems. These real-time time scales are often linked to the output of a physical clock. Their close agreement to UTC then supposes both an excellent stability performance of the physical clock on site, and also an excellent predictability of UTC over an averaging time of from 1 to 2 months.

In December 1993, the recent commercial availability of HP 5071A cesium clocks and of active auto-tuned hydrogen masers, both presenting a remarkable frequency stability, led the BIPM to propose, in collaboration with D. Allan, of Allan's TIME, the realization of a real-time prediction of UTC, UTCp<sup>[4]</sup>. As shown in Figure 1, it was suggested that the proposed UTCp be directly linked to the output of a physical clock, kept for instance at the BIPM, steered on a software clock, UTCs. UTCs is obtained with a delay of a few days from data of a small number of very good clocks kept in only some laboratories. At the time, this proposal gave rise to much discussion inside the time community and in the face of the many arguments advanced against, the project was abandoned. The subject was again evoked during the meeting of the CCDS Working Group on TAI, which was held in March 1995<sup>[5]</sup>. It then appeared that the UTCp as previously proposed is only another local representation of UTC, with the same quality as most of the UTC(k) kept by national centers having at their disposal the data from a sufficient number of clocks. Rather than providing UTCs and UTCp, it was then concluded that the role of the BIPM was, in the first instance, to improve the predictability of UTC so as to facilitate the steering of real-time time scales to UTC. The progress that has been made in this is discussed in Section 2. In Section 3, we examine the possible reduction in that part of



the delay of access which results from the time taken for data collection and treatment, already mentioned above.

## 2 IMPROVING THE PREDICTABILITY OF UTC

The predictability of UTC over averaging times of between 1 and 2 months can be quantitatively examined by studying its medium-term stability. We refer here to the stability of the freely running time scale EAL<sup>[6]</sup> with the hypothesis that the full stability of EAL is transferred to UTC without any degradation.

Table 1 illustrates the stability of EAL: values of the Allan deviation  $\sigma_y(\tau)$  have been computed by application of the N-cornered hat technique to data obtained in comparisons between EAL and five of the best independent time scales in the world. These are those maintained at the NIST (Boulder, Colorado, USA), the VNIIFTRI (Moscow, Russia), the USNO (Washington DC, USA), the PTB and the LPTF (Paris, France).

Table 1 Stability of the time scale EAL estimated from data covering the period January 1993 – April 1995	
$\tau/d$	$\sigma_y(\tau)$
10	$4.0 \times 10^{-15}$
20	$3.4 \times 10^{-15}$
40	$3.1 \times 10^{-15}$
80	$3.7 \times 10^{-15}$
160	$4.6 \times 10^{-15}$

The best performance is obtained for averaging times of 40 days and corresponds to  $\sigma_y(T) = 3.1 \times 10^{-15}$ . In terms of predictability, it means that the time error accumulated over  $T = 40$  d, which can be roughly estimated by the quantity  $\sigma_y(T)T$ , is about 12 ns ( $1 \sigma$ ). Already, several timing centers take advantage of this performance by combining it with high quality local time scales obtained, for instance, in near real time from a set of HP 5071A clocks. This is the case for UTC(USNO), which is used as the basis of GPS time, and which has remained within less than 5 ns of UTC for several months.

In fact, the predictability of UTC has quite naturally improved over the last two years, simply because the quality of the timing data has itself improved over the same period. This is now well known<sup>[7]</sup>, and is linked to:

- (a) the massive replacement of older clock designs by the new HP 5071A. For instance, in May – June 1995, 69 of the 232 weighted clocks in UTC computation were HP 5071A units, most of them presenting a flicker floor level characterized by an Allan deviation of about  $6 \times 10^{-15}$  over averaging times from 20 to 40 days,
- (b) the operation in timing centers of several auto-tuned and active hydrogen masers presenting frequency drifts smaller than several parts in  $10^{17}$  per day, which make them outstanding tools for timekeeping, and

- (c) the efficient smoothing of time comparison data collected over only a few days, including intercontinental distances, thanks to the worldwide use of the GPS common-view technique.

The natural improvement of UTC is felt in another way. Although definitive values of UTC are delivered only every two months, provisional values are given after collecting timing data over one month and published in the BIPM *Circular T*: for example, on the 17th of October for the month of September, definitive values for September-October being available on about the 17th of November. As shown in Table 2, the time differences between provisional and definitive values have always been less than 4 ns over the last year. Thus, timing laboratories maintaining a UTC(k) can already use the provisional UTC values with some confidence.

Table 2 Time differences between definitive and provisional values of UTC for a one year period beginning in September 1994		
Computation interval	Date $t$	$\Delta t$ / ns
September – October 1994	49599	+1
	49609	+2
	49619	+4
	49649	0
November – December 1994	49659	0
	49669	-1
	49679	-1
	49709	0
January – February 1995	49719	-5*
	49729	-8*
	49739	-10*
	49769	0
March – April 1995	49779	+1
	49789	+3
	49799	-4
	49829	0
May – June 1995	49839	+1
	49849	-1
	49859	-1
	49889	0
July – August 1995	49899	0
	49909	0
	49919	0
	49929	+1
	49959	0
September – October 1995	49969	+1
	49979	+1
	49989	+2
	50019	0
* Artificially large values for the month of January 1995 were caused by the absence of timing data from one laboratory.		



Further improvement in the predictability of UTC would require a revision of the stability algorithm which produces EAL. Several possible changes have been the subject of experiments on real clock data collected at the BIPM. These studies mainly concern the use of hydrogen masers, a change in the upper limit of weights, and shortening of the computation time of TAI.

It has been shown that the introduction of hydrogen maser data in the EAL computation did not degrade its stability for the period 1988 – 1994, although frequency drifts were not taken into account<sup>[8]</sup>. For averaging times close to the EAL computation time (60 days), the variation of the maser frequencies relative to EAL was dominated by an important drift in just one of them, which, in consequence was given a small weight. However, EAL stability is improving and the frequency drift of some hydrogen masers may become significant when compared with the intrinsic EAL noise, without leading to their deweighting. If this proves to be the case, it will be necessary to use a specific weighting procedure and mode of frequency prediction for hydrogen masers, based on estimates of their frequency drift. The CCDS Working Group on TAI has not yet taken any decision on this point and tests are being carried out. It is already recognized, however, that periods of observation of at least one year are necessary to make good estimates of frequency drifts.

Another research study concerns the possible shortening of the computation time of EAL. So far, however, no definitive results have been obtained on this point: averaging over 30-day periods rather than 60-day periods, improves the long-term stability of EAL only if it is associated with an increase in the upper limit of weight<sup>[9]</sup>. Following a decision of the CCDS Working Group on TAI, the maximum allowable weight of a clock in EAL was increased from 1000 to 2500<sup>[5]</sup> beginning with the computation over the two-month interval May – June 1995, but with no reduction of EAL computation time.

In addition, following the advice of the Working Group, studies are in hand to assess the advantages of using an upper limit of relative weights, rather than one of absolute weights. Tests show that an upper contribution of 1.4% for any individual clock would have helped to improve the stability of EAL for all averaging times during the period May 1993 – August 1994<sup>[10, 11]</sup>. This criterion imposes a very severe discrimination even among HP 5071A clocks and primary standards, some of these not being stable enough to reach the upper limit. It also deweights laboratories for which GPS data are not of the first quality. It does, however, result in an improvement in the stability of the resulting time scale for all averaging times. In particular,  $\sigma_y(T) = 2.0 \times 10^{-15}$  for  $T = 40$  d leading to an accumulated time error of less than 8 ns ( $1 \sigma$ ) over the same averaging time. The next step is the combination of the use of an upper limit of relative weight with a reduction of the computation time of EAL. If convincing results are obtained, they will be presented during the March 1996 CCDS meeting with a view to possible changes in the TAI algorithm. In order to help national laboratories keep their local UTC as close as possible to UTC, two additional decisions were taken by the CCDS Working Group on TAI and were put into operation immediately after the meeting: all time differences published in *Circular T* are given within  $\pm 1$  ns, and the frequency steering corrections applied by the BIPM for improving TAI accuracy are published in advance. Finally, clock data are now requested every five days rather than every ten days. When this is fully implemented, possibly at the beginning of 1996, local time scale prediction will be based on a larger number of points and is, thus, likely to be more efficient.



### 3 REDUCING THE DELAY OF ACCESS DUE TO DATA COLLECTION AND TREATMENT

Besides the intrinsic delay of access to UTC due to the mode of computation, there exists an additional delay related to the time needed for data collection and analysis at the BIPM. The use of electronic mail and of INTERNET anonymous FTPs has significantly reduced the transfer time of timing data, and has increased their reliability: it avoids 'hand manipulation' of data and, thus, reduces trivial errors. The ideal configuration would be a complete automation of the complete process according to standardized procedures. The BIPM is working on this in collaboration with national laboratories and appropriate CCDS Working groups. Good progress has already been made, which we illustrate by taking the TAI computation over the period September – October 1995.

The TAI computation relies on timing data made available to the BIPM by 45 national laboratories or timing centers, all of them keeping a local representation of UTC. Some of these laboratories, such as the OP or CH, collect data inside their country before sending it to the BIPM. The total number of contributing laboratories can, thus, reach 65, but the BIPM has only 45 direct contacts. For September – October 1995, 3 of the 45 centers provided no data because of local operating problems.

The first type of data requested from a laboratory is a set of GPS common-view observations obtained on site. Raw data collected directly, on a weekly basis, from the output of the GPS time receiver are preferred. The transfer of these data to the BIPM works remarkably well through electronic mail. Some laboratories, three in September – October 1995, send a monthly file on a floppy disk through Express Mail, this is also quite convenient to us. A small problem lies in the fact that there exists a number of different formats for these files. The CCDS Group on GPS Time Transfer Standards has already worked on it in publishing the Technical Directives for GPS Time Receivers<sup>[12]</sup> which, in particular, include a standardized format for GPS data. This is now being implemented in local GPS receivers: already 10 laboratories were using this standardized format for the period September – October 1995. Besides facilitating the task of the BIPM, it should also lead to a reduction of the noise of GPS time links.

The second type of data requested from a laboratory is a set of time differences between its local UTC and individual free-running clocks. Since the last meeting of the CCDS Working Group on TAI, clock data for month  $n$  are requested on the 5th of month  $(n + 1)$ , in a file arranged according to a specified format. It is also recommended to collect data for MJDs ending in 4 and 9, that is to say every 5 days rather than 10 days, over a short epoch surrounding 0 h UTC. Except for laboratories keeping a large number of clocks, the monthly clock data file includes only a few lines, very often less than 10 lines.

Over the period September – October 1995, all clock data files received through electronic mail corresponded to the specified format and could immediately be analyzed. Only one of them did not yet include data for MJD ending in 4. Some contributing laboratories do not yet have at their disposal electronic mail and send their data on a paper sheet transmitted by fax. This was the case for five laboratories during the period September – October 1995. In these cases, we copy by hand these data and check it as far as we can. Generally, the same laboratories do



not yet have at their disposal a GPS receiver specifically designed for time and can only give occasional values of a rough estimation of  $UTC(k) - GPS$  time. A poor quality time link also leads to some deweighting of the clocks involved. However, the role of the BIPM includes the distribution of time to all contributing laboratories and we try to publish our *Circular T* only when the whole set of laboratories has sent their data.

For the period September – October 1995, a provisional UTC was computed and published in mid-October, with data covering the month of September. Data for the seven standard dates of October were requested by the 5th of November. On the 13th of November, only two laboratories had still omitted to send their data. One of these laboratories had experienced an interruption in data of several months in the spring and summer 1995, so that its clocks were still in their test period. The TAI could, thus, be safely computed with these missing data. Unfortunately, it was impossible to contact the second laboratory, which contributes about 1.5% of the total weight, and we finally issued the results of UTC for October in *Circular T94* on the 17th of November.

The last standard date of this two-month computation is MJD = 50019 and corresponds to the 29th of October. That part of the material delay of access to TAI due to data collection and analysis was, thus, about 19 days, which still seems very long. However, progress on this point is soon expected and it is intended to issue *Circular T* before the 12th of the month during 1996.

## 4 CONCLUSIONS

The Time Section of the BIPM produces time scales which are used as the ultimate reference in the most demanding scientific applications. They also serve for the synchronization of national time scales and local representations of UTC, upon which all time signals used in current life are based. This work is, thus, in complete accordance with the fundamental missions of the BIPM.

To fulfill the metrological requirements these time scale are necessarily computed after the fact and cannot, therefore, be distributed to real-time users. This apparent disadvantage can, however, be almost completely overcome by ensuring that the predictability of UTC is such that individual laboratories maintaining their own  $UTC(k)$  can use it to predict the differences  $UTC-UTC(k)$  with the required accuracy. Considerable effort at the BIPM is now being devoted to making this possible through a better combination of the contributing data and through the reduction of the delay of access due to data exchange and treatment by the automation of data transfer procedures.

## REFERENCES

- [1] Comptes Rendus 18e Conférence Générale des Poids et Mesures, 1987, BIPM Publications, p. 23.
- [2] Le Système International d'Unités (SI), 6th edition, 1991, BIPM Publications, p. 110.

- [3] Comité Consultatif pour la Définition de la Seconde, 1980, BIPM Publications, 9, p. S15.
- [4] C. Thomas, and D.W. Allan 1994, "*A real-time prediction of UTC*," Proceedings of the 25th Annual Precise Time and Time Interval (PTTI) Applications and Planning Meeting, 29 November-2 December 1993, Marina del Rey, California, pp. 217-230.
- [5] G. Petit 1995, "*Report on the discussions and decisions of the meeting of the CCDS Working Group on TAI*," BIPM Publications, 13 pages.
- [6] C. Thomas, P. Wolf, and P. Tavella 1994, *Time Scales*, BIPM Monograph 94/1, 52 pages.
- [7] C. Thomas, and J. Azoubib 1995, "*A modified version of the TAI algorithm under test*," Report to the CCDS Working Group on TAI, GT-TAI/95-9, 15 pages.
- [8] J. Azoubib, and C. Thomas 1995, "*The use of hydrogen masers in TAI computation*," Proceedings of the 9th European Frequency and Time Forum (EFTF), 1995, Bessançon, France, pp. 283-287.
- [9] J. Azoubib, and C. Thomas 1995, "*Shortening of the definitive computation time of TAI*," Report to the CCDS Working Group on TAI, GT-TAI/95-7, 28 pages.
- [10] C. Thomas, and J. Azoubib 1995, "*TAI computation: Study of an alternative choice for implementing an upper limit of clock weights*," submitted to *Metrologia*.
- [11] C. Thomas, and J. Azoubib 1996, "*Upper Limit of Weights in TAI Computation*," Proceedings of the 27th Annual Precise Time and Time Interval (PTTI) Applications and Planning Meeting, 29 November-1 December 1995, San Diego, California.
- [12] D.W. Allan, and C. Thomas 1994, "*Technical directives for standardization of GPS time receiver software*," *Metrologia*, 31, 69-79.



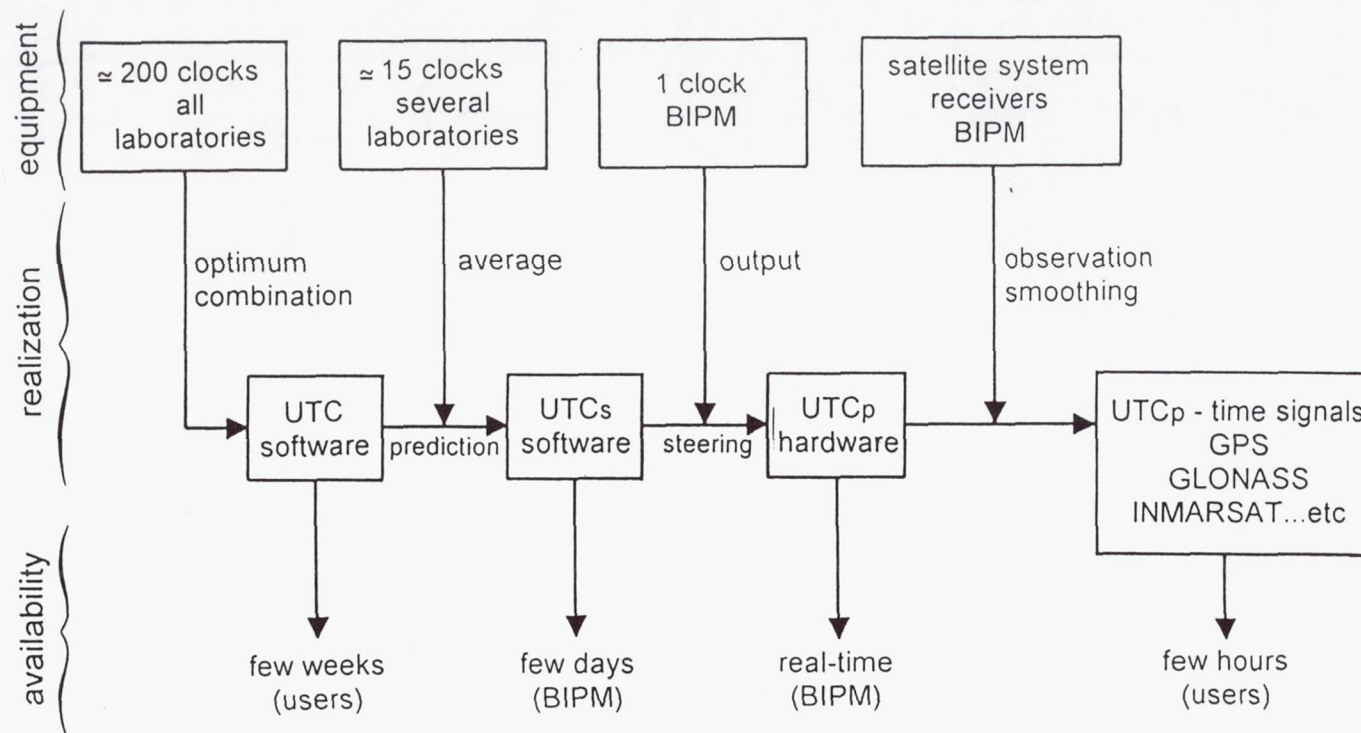


Figure 1. Block diagram of the realization of the real-time prediction of UTC, UTCp

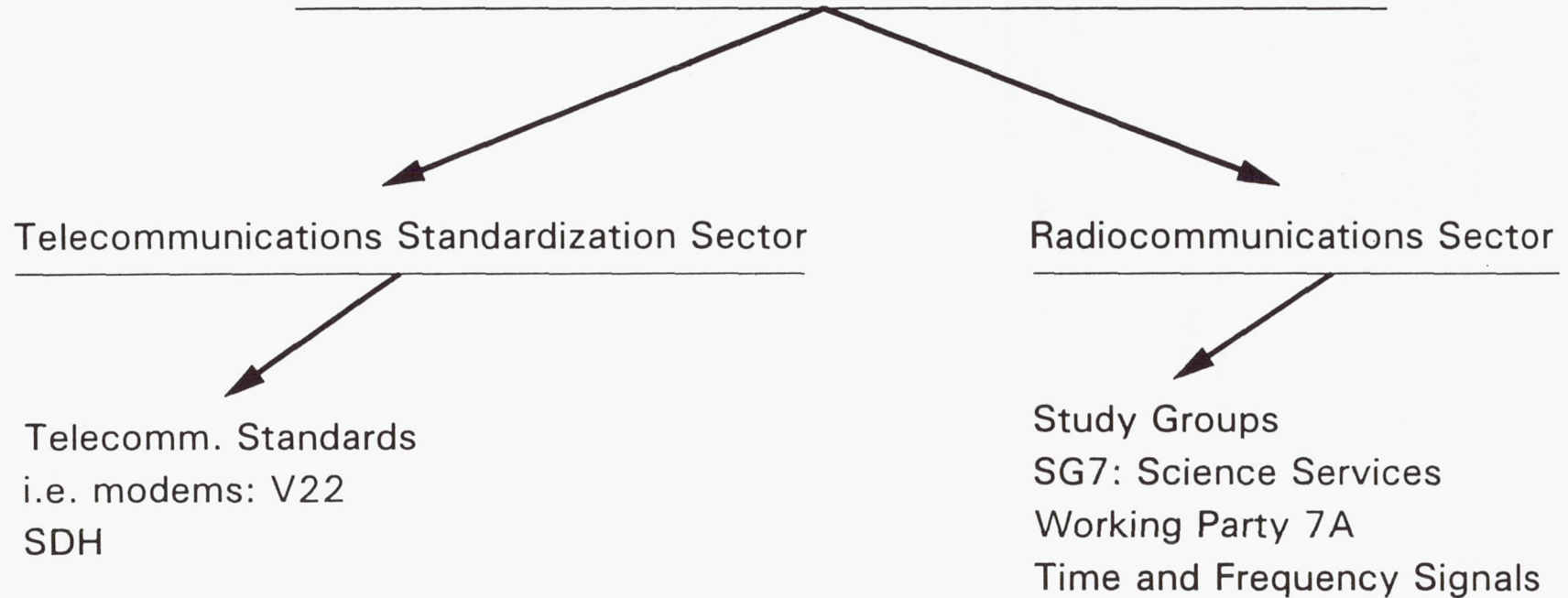
# THE ROLE OF THE INTERNATIONAL TELECOMMUNICATIONS UNION IN TIME AND FREQUENCY

Gerrit de Jong  
NMI, Van Swinden Laboratorium  
Delft, the Netherlands

**EDITOR'S NOTE:** *The author originally planned for this paper was ill and could not attend the meeting. Gerrit De Jong of NMI Laboratory, Delft, the Netherlands, who is the Chairman of Working Party 7A of the ITU-R, presented the following slides after only 5 minutes to prepare. It is felt that the information presented is important and thus the slides are reproduced here.*



# International Telecommunications Union



86

Figure 1. ITU Structure

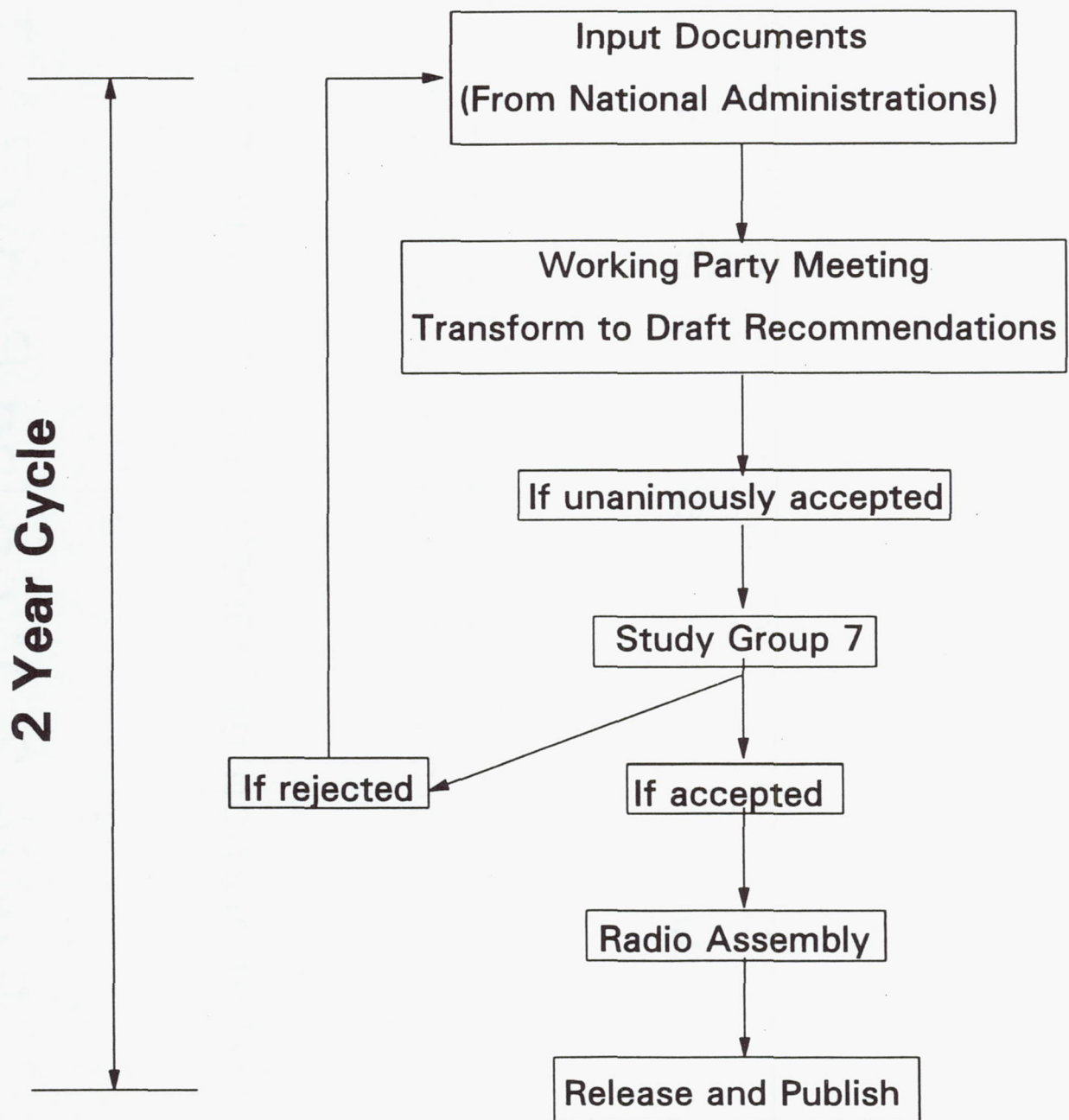
## Recent Topics

- \* Recommendation on the use of Two Way Satellite Time and Frequency Transfer
- \* Proposal on the use of SDH overhead bits for the purpose of precise time transfer
- \* Preparation of Handbooks on Time and Frequency

Figure 2. Working Party 7A Tasks



# Figure 3 ITU Working Method



## Questions and Answers

**DR. GERNOT WINKLER (USNO, RETIRED):** One of the greatest difficulties and obstacles in making the recommendations more useful is that they're so difficult to get. Users write to the Observatory, for instance, and ask for copies, which is not the function of the Observatory. Is there any recommendation which could be made to the ITU Headquarters to make them more readily available?

In connection with that there is, of course, the idea of why not include the most important recommendations in the handbook. Are they going to be included or is that separate?

**GERRIT de JONG (NMI VAN SWINDEN LAB):** They will remain separated. Maybe one of the editors is here who can comment. Dr. Allan?

**DAVID ALLAN (ALLAN'S TIME):** Thank you, I appreciate your bringing up the handbook. Dr. Sydnor and I are editors of this handbook; and we've been able to get some of the best people in the world to write the chapters for it. The title of the handbook is "Selection and Uses of Precision Time and Frequency Systems." It treats systems, because nowadays we have satellites connected with clocks and things are much more complicated than when we were children.

In regard to Dr. Winkler's question, one thing that's included in this handbook is the glossary, a complete glossary of definition of terms. But beyond that, we have no charter, we can't put any of the recommendations in; even though there's some outstanding information in those recommendations, we don't have the charter to include them.

**GERRIT de JONG (NMI VAN SWINDEN LAB):** Concerning the documentation, I think you could order through a book seller, and they can get it in Geneva with the ITU. It's not so well known, but it is not difficult to obtain that.

**DR. GERNOT WINKLER (USNO, RETIRED):** They are sinfully expensive, and a user may need only one recommendation out of the whole thing.

**GERRIT de JONG (NMI VAN SWINDEN LAB):** Yes, but they're smaller than they used to be, more specific.

**DAVID ALLAN (ALLAN'S TIME):** There may be one solution. NAVTEC became aware of this — this is an organization that provided seminars and tutorials at the last ILN meeting in Palm Springs in September; and they approached me because they make this available. And the answer is yes, we've contacted the ITU and they can become a resource within the states, for example, for handbooks and for some of these documents which have critical time and frequency information. They have to pay the sinful price, probably with a little commission, but at least they'd be more accessible. They would have advertising so that people would know what's available.

**ATTENDEE:** I have a question. When will the handbook be released?

**GERRIT de JONG (NMI VAN SWINDEN LAB):** The handbook is not completed at this moment. But after that, the draft will go to Geneva; they will print it there; and it may have to be translated also in Spanish and French. I'm not sure of that. Normally, they do not release anything before it's translated also into French and Spanish, but I don't know if this is mandatory. I'm not sure if that's still the policy. I hope not, but it's beyond my control.



# UTC DISSEMINATION TO THE REAL-TIME USER

Judah Levine  
Time and Frequency Division  
National Institute of Standards and Technology  
Boulder, Colorado 80303

## Abstract

*This paper concludes the tutorial session on the delivery of UTC to the real-time user. The first paper of the session describes the technical problems and other issues that impede the ability of users to achieve synchronization and syntonization. The next four papers describe the activities of several national and international organizations that provide critical time and frequency services. These papers address many of the questions, explain the roles of the organizations and describe some of the improvements that the future may bring.*

*This paper summarizes the session. It synthesizes the individual presentations to provide an overall assessment of how well the real-time user can perform synchronization and syntonization using the existing infrastructure. Finally, it highlights areas where improvements can be made by providing additional information or services.*

## THE DEFINITION OF UTC

The current definition of Coordinated Universal Time (UTC) dates from 1972<sup>[1]</sup>. The duration of a UTC second is defined in terms of the frequency of a hyperfine transition in the ground-state of cesium. This standard frequency is realized in a number of different laboratories using ensembles of commercial cesium clocks and a few primary frequency standards. The data from all of these devices are transmitted periodically to the Bureau International des Poids et Mesures (BIPM) in Sevres, France, where they are combined in a statistical procedure to produce International Atomic Time (TAI)<sup>[2]</sup>. The time of this scale is adjusted as needed ("Coordinated") by adding or dropping integer seconds so as to keep it within  $\pm 0.9$  s of UT1, a time-scale based on the observations of the transit times of stars and corrected for the predicted seasonal variations in these observations. When the leap seconds are included into TAI, the result is called UTC. The difference between TAI and UTC is therefore an exact integer number of seconds. This difference is currently 29 s and will become 30 s at 0 UTC on 1 January 1996.

## THE COMPUTATION OF TAI AND UTC

The algorithm used by the BIPM to compute TAI is called ALGOS, an algorithm designed to optimize the long-term stability of the average frequency of the ensemble. It is computed retrospectively using data from about 250 clocks located in many different laboratories. The computation is performed at the end of each month and the results are usually available in about 3 weeks: the computation for October, 1995, for example, was published on 16 November.

The BIPM is planning to reduce this delay, but it can never be zero because of the retrospective nature of ALGOS and because of the time needed to collect the data from the contributing laboratories. In addition, the BIPM computations use relatively infrequent measurements: timing laboratories currently report clock data to the BIPM on a 10-day mesh (at 0 UTC on every MJD ending in 9); the intervals between data points will be reduced to 5 days in the near future. The monthly computation cycle will not be changed.

Estimating UTC in real time therefore requires both extrapolation from the most recent computation of ALGOS and interpolation to a time grid more suited to real-time applications. These computations are simple in principle, but they can have significant uncertainties because the underlying noise processes in the data are not well known. Even when the noise process is known, extrapolation is an uncertain business, especially for processes characterized by flicker or random-walk spectral distributions. In addition to the uncertainties in estimating UTC in real time, the BIPM does not transmit a physical realization of UTC, so that users with real-time requirements must obtain UTC from a timing laboratory.

## THE REALIZATION OF UTC BY A TIMING LABORATORY

In addition to operating ensembles of clocks, timing laboratories generally average the readings of these devices in some way to compute a local realization of UTC called UTC(lab) to distinguish it from the scale computed by the BIPM, which is written as simply UTC. As part of its monthly analysis, the BIPM computes  $UTC - UTC(lab)$  for each laboratory that contributes clock data and publishes these differences in a monthly bulletin called Circular T. This publication gives the value of  $UTC - UTC(lab)$  on the same 10-day mesh that is used to submit the clock measurements: currently at 0 UTC on every MJD that ends in 9.

The method used to realize UTC(lab) varies from laboratory to laboratory. In some cases UTC(lab) is the output of a "principal" clock whose output may be either free-running or steered towards UTC using data from Circular T. Other laboratories define a UTC scale based on a weighted average of the times of their local clocks. This is the procedure used at NIST.

The NIST clock ensemble consists of a number of commercial cesium standards and hydrogen masers. The data from these devices are combined in a time scale called AT1, which is computed automatically every 2 hours. The weight of each clock in AT1 is based on its previous performance except that no clock can have a weight greater than 30%. The algorithm is designed to average the white frequency noise that usually characterizes cesium clocks at relatively short periods of a few days or less. The scale is normally free-running — its time and frequency are not adjusted administratively. Clocks are added and dropped from the scale



as needed: a clock is added only after its performance has been evaluated for some time so as to minimize the perturbation to the ensemble average and a clock that appears to be nearing the end of its life is dropped before it actually fails.

UTC(NIST), in turn, is computed from AT1 using an equation which is designed to steer UTC(NIST) towards UTC with a time constant of several months. The parameters of the equation are estimated using the most recent 36 values (an interval of 360 days) of UTC - UTC(NIST) from Circular T. The parameters of the equation are published in the monthly NIST Time and Frequency Bulletin; each issue gives older values, the official parameters for the current month and the provisional values for one month in the future. The equation is only changed at 0 UTC on the first day of every month and includes data from the most recently-received Circular T; the equation for December, for example, is based on the BIPM computations of UTC - UTC(NIST) through the end of October. Only the rate offset is changed from month to month (time steps are never used), and the change in rate is limited administratively to be not more than  $\pm 2$  ns/day (a fractional frequency change of not more than  $\pm 2.3 \times 10^{-14}$ ).

The time of UTC(NIST) is realized physically using a computer-controlled phase-stepper, which operates at 5 MHz. The input is from one of the clocks in the ensemble and the output is monitored every 12 minutes; these measurements are used to control the phase-stepper so as to lock the physical signal to the predicted value of UTC(NIST) - AT1. The difference between the definition of UTC(NIST) and its physical realization is about 0.2 ns RMS. This difference arises from two effects: (1) the time dispersion during the 12 minutes between measurements due to the frequency-noise of the clock driving the phase-stepper, and (2) by the white noise in the measurement process itself. The adjustments applied by the phase-stepper are typically on the order of ps, so that the frequency stability of UTC(NIST) is essentially the same as that of its parent scale AT1 for averaging times longer than the 12 minutes cycle time of the control loop.

We are experimenting with other ways of realizing UTC(NIST). In one experiment, we have added a clean-up oscillator after the phase-stepper to improve the spectral purity of the steered 5 MHz signal. This is advantageous for satellite time-transfer equipment and other systems that use the 5 MHz as a reference frequency in addition to the 1 pps output that is used by the GPS receivers. In a second experiment, we have changed the steering algorithm to emphasize frequency smoothness at the expense of time accuracy. The phase-stepper is driven from a hydrogen maser in this case, but both the amplitude and the frequency of the phase adjustments are controlled to provide maximum frequency smoothness at intermediate periods of a few days or less. The resulting output has the frequency of UTC(NIST) on the average, with almost the stability of the hydrogen maser reference. (The price of frequency smoothness is time-dispersion, and this implementation is therefore designed for users whose primary need is for frequency stability rather than time accuracy.)

In all realizations, the reference plane for the time is at a specified input to a counter located in the clock room; delays in the distribution system after that point must be measured and are included as offsets in subsequent analyses.



## THE ACCURACY AND STABILITY OF UTC(lab)

Both NIST and USNO steer their respective UTC(lab) scales so that the difference UTC - UTC(lab) is small — on the order of 10 ns or less. This is not universally true, however. Many laboratories have significant offsets (both in time and in frequency) between UTC and UTC(lab). In general, therefore, the scale UTC(lab) can not be used as a replacement for UTC without estimating the difference between the times and rates of the two scales. The accuracy with which this can be done is determined by the stability of the frequency difference UTC - UTC(lab). For labs such as USNO, NIST or PTB, this value can be on the order of  $(5 \pm 3) \times 10^{-15}$  for an averaging time of about 30 days, so that data from a previous Circular T can be used to predict the current value of UTC - UTC(lab) with an uncertainty of about 10 – 20 ns RMS.

## SYSTEMATIC OFFSETS IN GPS DATA

Many users with demanding time or frequency requirements use data from GPS satellites to estimate UTC. These data may be used directly to estimate UTC(USNO) from the received values of GPS time and its offset to UTC(USNO). Alternatively, some of the noise in the observations may be at least partially canceled using the common-view method in which two laboratories observe a given satellite simultaneously. Common-mode errors (such as the satellite clock and a portion of the unmodeled atmospheric delay) cancel in the differences of the two measurements. (The BIPM issues tracking schedules which facilitate the simultaneous observations that are needed for common-view observations. All timing laboratories adhere to these schedules; the data from these observations form the basis for international time coordination.)

Direct and common-view observations are affected in first order by fluctuations in the transmission delay through the antenna and the receiver, by delays introduced by multi-path effects, and by fluctuations in the transit time of the reference pulse from the reference plane of the laboratory to the receiver hardware. These effects can be on the order of 50 ns or more; they are also likely to be temperature-dependent and therefore hard to measure accurately.

In addition, some laboratories use a reference for their GPS receiver that is intentionally offset from the corresponding UTC(lab) for some administrative reason. Determining these offsets accurately may be difficult because of the variations in the input impedance of the receivers which change the effective arrival time of the 1 pps pulse. Variations of this kind also change the voltage-standing-wave ratio of the cable that delivers the 1 pps; these fluctuations may be important for long cables but are quite difficult to characterize.

The BIPM has conducted several differential calibrations using a single portable receiver that is operated at each laboratory in parallel with the permanent equipment there, but the results of these comparisons are somewhat ambiguous. At some of the laboratories, the calibration constants have changed by as much as 10 ns over periods of months, while other laboratories show essentially no change over many years. The BIPM attributes some of these fluctuations to the effects of changes in the local temperature on the long cable between the antenna and the receiver, but this cause is probably not the whole story, and these effects are not completely



understood at this time<sup>[3]</sup>.

## MEASUREMENT NOISE

The largest source of noise in GPS measurements is likely to be the fluctuations in time delay introduced by Selective Availability. The effect of SA can be seen in Figure 1, which shows the time difference between a local cesium clock and GPS time as measured using two satellites: SV 12 which does not have SA and SV 14 which does. Each point on the figure is a 5-minute average of the time-difference; the lines connecting the points are to make it easier to identify them and are not otherwise significant. The RMS scatter of the data from SV 14 is about 60 ns; frequency estimates computed by dividing the first difference of these data by 300 s will therefore have a scatter of about  $4.2 \times 10^{-10}$ .

If the frequency of the local clock is sufficiently stable, both the time and the frequency estimates can be improved by averaging. The spectrum of the GPS time-difference measurements is usually characterized by white phase noise out to averaging times on the order of  $10^4$  s or so; if fluctuations in the frequency of the local clock are not important on this time scale, the uncertainty in the time estimate can be reduced by about a factor of 6 by averaging for about  $10^4$  s. (Longer averaging times can be used as long as the residuals are still characterized by white phase fluctuations. These longer averaging times generally require additional post-processing of the data, which is not useful in a real-time context.) It is often possible to improve the estimate of the frequency offset of the local clock by additional averaging without the need for extensive post-processing; the maximum averaging time for a frequency estimator will usually be set by the time at which the fluctuations in the frequency of the local clock are no longer white. This may be several days for a good cesium standard. A number of effects may produce a variation in the time difference data with a period of 1 day, and any averaging algorithm must be designed with this in mind.

It is important to remember that averaging is only useful until the noise floor set by the characteristics of the local clock (or clock ensemble) is reached. Furthermore, while increased averaging may improve the noise performance, it degrades the transient response of the system. This means that it will take longer for the estimator to reach equilibrium initially and to recover from a glitch in steady-state operation.

## CONCLUSIONS

Most real-time users who need UTC time or frequency information use the signals from the GPS satellites to get it. They can either recover UTC(USNO) using the broadcast signal directly or they can use the common-view method in which they receive signals from satellites that are being observed at the same time by a timing laboratory which realizes a local estimate of UTC.

Both of these methods of receiving UTC are limited by a number of problems. For non-authorized users, the largest problem is usually the intentional degradation imposed on the GPS signals by selective availability (SA), but systematic errors in the receiver hardware and

uncertainties in the relationship between UTC(lab) and UTC are also significant. Authorized users are not affected by SA in principle, so that the remaining effects become their dominant sources of noise.

It would be nice if SA were switched off. Lacking that, it is important to design data acquisition algorithms that minimize its impact. The acquisition algorithms for GPS data that are used by all timing laboratories were designed before SA was implemented, and it is not clear that they are still optimum in this new environment. Furthermore, the increasing availability of multi-channel receivers suggests that the traditional track schedules should be augmented or modified to make better use of this hardware.

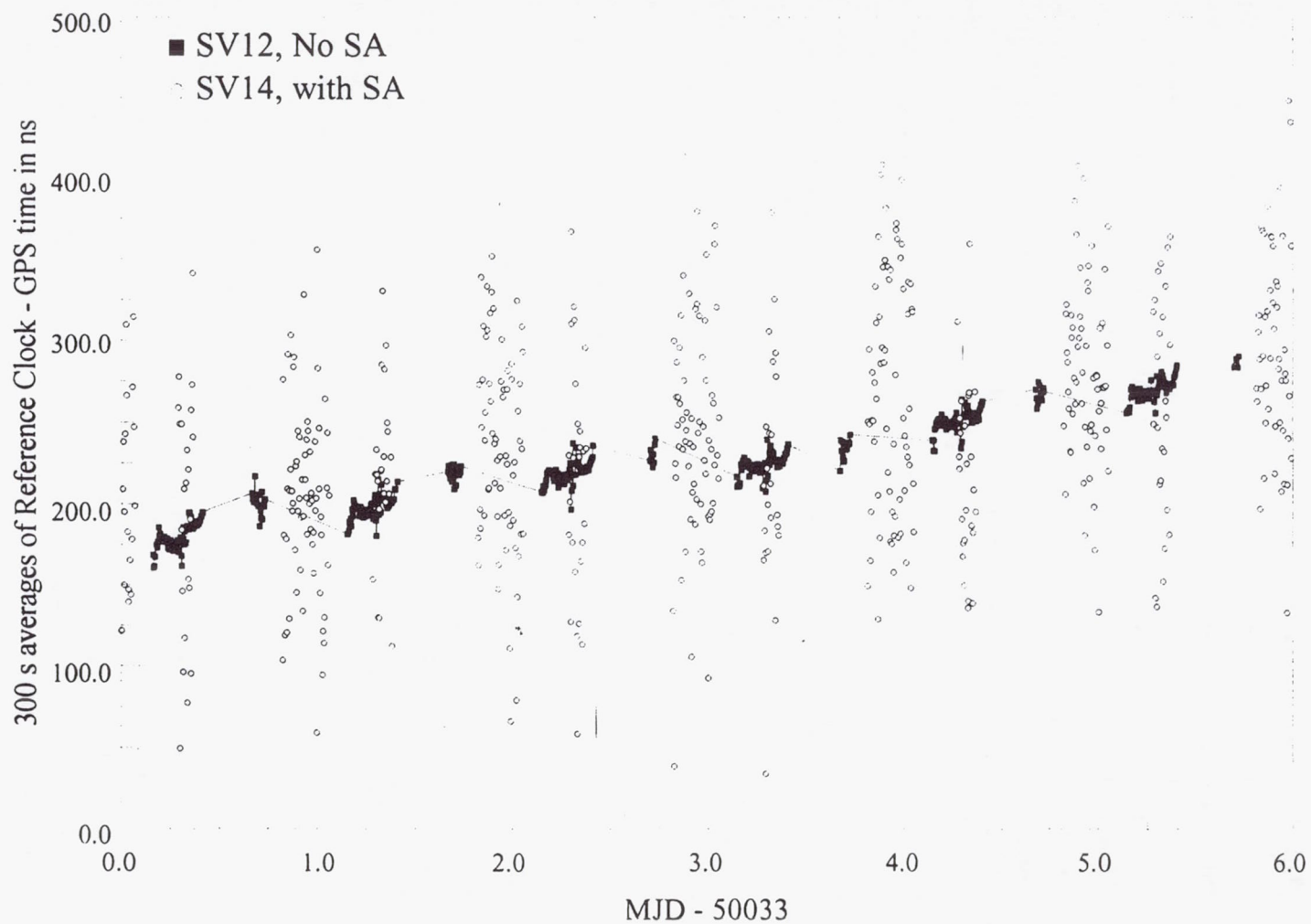
Finally, it is important for users to understand how each timing laboratory realizes its UTC(lab). In particular, it is important for users to know when time or frequency steps are applied and how large they are expected to be. These effects are probably smaller than the degradations due to SA in most cases, but this is not true for authorized users now and may not be true in the future if SA is ever turned off or if alternate distribution methods, such as two-way satellite time transfer or distribution via fibers, become widely used.

## REFERENCES

- [1] T.J. Quinn 1991, "*The BIPM and the Accurate Measurement of Time*", Proceedings of the IEEE, **79**, 894-905.
- [2] B. Guinot, and C. Thomas 1989, "*The Establishment of International Atomic Time*", Annual Report of the Time Section, BIPM, Sèvres, France.
- [3] W. Lewandowski, and C. Thomas, BIPM, private communication.



Fig. 1. The effect of Selective Availability on GPS data.



## Questions and Answers

**CAPT. STEVEN HUTSELL (USAF):** I appreciate your comments on this. You mentioned that you believe that there might be a systematic in GPS time transfer on the order of 10 nanoseconds?

**JUDAH LEVINE (NIST):** Yes.

**CAPT. STEVEN HUTSELL (USAF):** One thing that I presented in my slides earlier, we run a daily feedback loop, and theoretically – and I'd like your opinion – if there is a systematic error in time transfer by getting the daily feedback from the Naval Observatory, the Naval Observatory would be telling us how far off we are and what corrections to make. Your comment on that.

**JUDAH LEVINE (NIST):** Well, there are two issues here. The first one is that that loop is an authorized loop and I am a non-authorized user. Not only am I a non-authorized user, but all the data that I have access to is non-authorized data. The result of that is that it depends very critically on how you average the SA. Okay?

The second issue is that some of the data that the BIPM uses is post-processed. Therefore, there's a difference between the post-processed ephemerides and the broadcast ephemerides. Just remember that a real time user doesn't have the luxury of post-processing and has to deal with real time. And the result of that is there may be an offset between what's calculated using a post-processed ephemeris and what's calculated in real time using a broadcast ephemeris.

So it's not obvious that this problem is your problem. It may very well be my problem. It may not be in the loop between the Naval Observatory and Falcon because that's an authorized loop.

**DR. GERNOT WINKLER (USNO, RETIRED):** That's a very interesting discussion. I have to agree that there are systematic problems in the absolute delay in GPS receivers; and that there are some things which we do not quite understand; and I would agree that probably the level of uncertainty is on the order of 10 nanoseconds.

But the way in which you arrived to that conclusion is completely wrong. Because, you don't see UTC(USNO). You don't get it. What you get is mean USNO, and that's not being steered. And Mr. Miranian explained this morning, we have the difference between the unsteered time scale and the steered time scale. The steered time scale, you don't see. The only instrument which sees that is the servo-loop that controls the Master Clock. So you cannot base your conclusions on that.

What you could base it on, however, is something which is very inconvenient. This is a difference if you compare in the Circular T the values given by the Paris Observatory and the Naval Observatory, they would find a discrepancy. That discrepancy is entirely viewed to the difficulty of guaranteeing, in an absolute sense, the calibration of the GPS delays.

That is a problem, and I think we have to address that sooner or later. At the moment, however, nobody is worried about it because everything is relative and you calibrate these receivers side-by-side. But, the absolute value is uncertain, and we have never actually been able to have all the receivers in one place. That would solve the problem.



**JUDAH LEVINE (NIST):** To answer your question, the data — when I said UTC(USNO), that came from Circular T; that's a Circular T number. I cannot see inside your servo-loops, I just looked at the Circular T.

**DR. GERNOT WINKLER (USNO, RETIRED):** But, it is not UTC(USNO).

**JUDAH LEVINE (NIST):** It says "UTC, USNO" on the piece of paper.

**DR. GERNOT WINKLER (USNO, RETIRED)** It also says A.1. A.1 is the unsteered time scale.

**CLAUDINE THOMAS (BIPM):** On Circular T, there is a note about that. What we call "UTC(USNO)" is, in fact, the USNO Master Clock. I think it's on the equation, which was wrong. What you wanted to say is that there is a difference between taking the raw data from two labs, computing the common-view observation, and the results which are in Circular T. That's what you - - -

**JUDAH LEVINE (NIST):** No. When I get a file from your computer, or when I get a file from the USNO computer, it says on the top of the heading "Master Clock minus GPS." When I take that number, I take that number as Master Clock minus GPS. And when I said "USNO Master Clock," that's where the number came from. It came from that column.

**DR. GERNOT WINKLER (USNO, RETIRED):** The servo-control of the GPS timing is derived from a different receiver, as compared to that which are publically available. They have to be. We have to keep that separate. It's a completely separate receiver, and there is also a question about how constant these are. There isn't a moment that this is going on between a GPS receiver, which is on loan from the BIPM, and the 502 reference receiver that we have at the Observatory, and there is no large variation.

Mr. Miranian, you have conducted that test between the two receivers. What was the result of that?

**MIHRAN MIRANIAN (USNO):** We've had the two receivers running side-by-side since July. And we see no more than a variation of a couple of nanoseconds. I think I showed you this last night, Judah.

And we've had temperature changes of up to 40 degrees. So this is one of the things we were trying to check on.

**JUDAH LEVINE (NIST):** Let me make clear what I did, okay? When I say "USNO Master Clock," that comes from the data which you put on your computer, which the Naval Observatory puts on its computer. It says on a top of a column "Master Clock minus GPS." Then I took that data and went around to the various laboratories which published the same data and took the differences. And then I compared that number against the values that are published by Dr. Thomas in Circular T. That's where that difference comes from.

**CLAUDINE THOMAS (BIPM):** Yes, because the time comparisons, which are computed at the BIPM, the computation is chosen so that to get the most precise result, but also the most accurate result. So we have already shown that to improve accuracy, we need to use, for instance, measurements, post-processed, precise ephemerides and so on. And we also add some

differential delays between some receivers, which have been obtained through experimental calibration trips. And that's why you get those differences, for sure.

**WLODZIMIERZ LEWANDOWSKI (BIPM):** I'm working with Mihran Miranian on this comparison between USNO and the Paris Observatory. Just a comment about the differences that we have found and what is going on.

It happens that in June '94 we compared USNO receivers to the ones we have at the Paris Observatory. We found a 13 nanosecond difference, which is not the same as the correction we just added in Circular T. This is an experiment. In Circular T, I believe there is like 20 nanoseconds now. We found 13 nanoseconds and a very clear indication that USNO receivers have a problem with temperature. We even made the determination of the coefficient which was a half of nanosecond per degree Celsius.

Then we repeated the comparison in March of 1995. And the comparison was then 20 nanoseconds between the Paris Observatory and USNO, seven nanoseconds off the previous review, and this matched exactly with the coefficient of temperature.

Then we shifted the receiver at the beginning of August, and theoretically we should receive 10 nanoseconds, according to this coefficient, and we received 10 nanoseconds. The trouble is that after several months, this is still 10 nanoseconds, and it should go down. It was going up. So there is a problem. Yesterday Dr. Gifford showed us some data which shows that the receiver jumped in behavior from one year to another, it changed behavior. So there is some work that needs to be continued concerning the calibration of receivers.



# GPS DISCIPLINED OSCILLATORS FOR TRACEABILITY TO THE ITALIAN TIME STANDARD

Franco Cordara and Valerio Pettiti  
Istituto Elettrotecnico Nazionale Galileo Ferraris  
Corso M.d'Azeglio, 42 - 10125 Torino, Italy

## Abstract

*The Istituto Elettrotecnico Nazionale (IEN) is one of the Italian primary institutes which is responsible for the accreditation of secondary laboratories belonging to the national calibration system SNT, established by law in 1991. The Time and Frequency Department, that has accredited in this frame 14 calibration centers for frequency, performs also the remote calibration of their reference oscillators by means of different synchronization systems.*

*The problem of establishing the traceability to the national time standard of GPS disciplined oscillators has been investigated and the results obtained are reported.*

## INTRODUCTION

The dissemination of the SI units realized in the primary laboratories down to the users, has always been a matter of concern of all the international organizations involved in metrology or in standardization. The importance of developing, at the industrial level, calibration structures traceable to the national standards and using appropriate measurement procedures, is also recognized and requested in some written standards of the International Organization for Standardization (ISO), namely the ISO 9000 for Quality Assurance Systems and the ISO Guide 25 for Calibration and Test Laboratories<sup>[1]</sup>.

For traceability to a national standard, that should be guaranteed for any relevant quantity in a production process, it is intended what follows: "the property of the results of a measurement or the value of a standard, whereby it is related to a national standard through an unbroken chain of comparisons all having stated uncertainties"<sup>[2]</sup>.

The national standard is defined by the same source as: "a standard recognized by an official national decision to serve in a country, as the basis for fixing the value of all other standards of the quantity concerned."

The demand for traceability, that has been constantly increasing worldwide, led some countries to organize networks of accredited laboratories under the label of Calibration Services, consisting of calibration laboratories both independent or included in large companies or educational

institutions. These national calibration services operate surveillance programs to assess the traceability to the national standards of the accredited laboratories. This assures the confidence level of the calibration system and allows to recognize a technical equivalence between the calibration certificates issued by the primary laboratories and the accredited centers, apart from their different uncertainty levels.

At present, the implementation of ISO Standard 10012, concerning the metrological confirmation system for measuring equipment and regarding not only manufacturers but also the suppliers of services, is having a great impact on the Italian calibration market.

This document prescribes, in fact, that all the measuring equipment should be calibrated against measurement standards that are traceable to national or international standards, and that the measurement standards must have a calibration certificate with a statement of uncertainty.

## THE NATIONAL CALIBRATION SYSTEM

To organize a network of calibration centers, the national Commission for Metrology of the National Research Council (CNR), established in 1977 the Italian Calibration Service SIT which is managed by a Secretariat where the three primary institutes, namely IEN, IMGC and ENEA, are involved.

The accreditation organization is technically supported by a Committee with experts involved in the accreditation or standardization activity. More than 70 calibration centers have been accredited, up to now, in the different metrological fields according to the SIT and EAL (European Cooperation for the Accreditation of Laboratories) rules, that are based on the ISO and European standards on testing, certification and accreditation activities.

In August 1991 finally, it was established by law the National Calibration System SNT, consisting of the three primary institutes (IEN for electrical quantities, IMGC for mechanical and thermal quantities, ENEA for the ionizing radiations) and of accredited calibration centers, which is under the responsibility of the Ministers of the University and Research and of the Industry and Trade.

The primary institutes main duties consist in studying and realizing the primary standards, in comparing these standards internationally and in disseminating them within the SNT context.

The primary standards maintained in the three institutes became "national standards" by decree in 1993; in this document the realization of each standard is reported and its uncertainty is declared.

The calibration centers agreed by the primary institutes and taking part to the SNT, are secondary level calibration laboratories, selected according to their technical competence and organization and equipped with secondary standards periodically compared to the national standards.

The IEN Time and Frequency Department, that realizes the national standard of time and frequency, is responsible for the accreditation of laboratories in these fields and for the calibration of their reference standards.



## TRACEABILITY TO THE NATIONAL TIME STANDARD

The national standard of time is actually realized by a HP5071-High Performance cesium clock, selected among an ensemble of 4, generating the reference time scale UTC(IEN) that is traceable to the international standard UTC computed by the Bureau International des Poids et Mesures (BIPM), by means of the reception of the GPS satellites. An independent atomic time scale TA(IEN) is also generated from the clock ensemble<sup>[3]</sup> and, since May 1995, the data are reported to the BIPM. UTC(IEN) time scale is steered on UTC to maintain a long term agreement within  $0.5 \mu\text{s}$  or better as recommended in 1993 by the CCDS (Recommendation S5).

The traceability to the national time standard of the secondary standards maintained in the accredited laboratories, can be obtained by means of three different synchronization systems: the passive television method, the coded time signals generated by the IEN and broadcasted by the national radio company RAI and the GPS signals<sup>[4]</sup>.

The uncertainty level recognized to the centers, at the moment being, can range from  $1 \times 10^{-9}$  to  $3 \times 10^{-12}$ , depending on the reference oscillator selected and on the metrological chain implemented. To establish the traceability for frequency and time, every laboratory must perform daily an agreed number of time interval measurements and periodically send the results to IEN, where the same kind of measurements are performed. Every three months, the accredited laboratory is supplied with a calibration certificate reporting the reference oscillator parameters, the relative frequency departure and the frequency drift in the case of the television and GPS synchronization systems.

A typical uncertainty value obtainable in the evaluation of the oscillator accuracy is of the order of  $1 \times 10^{-13}$  ( $2\sigma$ ) for observation times of one month, in the case of the television method and of  $2 \times 10^{-14}$  ( $2\sigma$ ) for  $\tau = 1$  week in the case of GPS in common view.

In the case of reference oscillators disciplined by standard signals, the frequency offset and the drift of the oscillator are continuously compensated and therefore a different approach has to be followed especially if the time signals used do not disseminate the national standard.

## GPS DISCIPLINED OSCILLATION

The use of disciplined oscillators as reference standards also in European calibration laboratories is rapidly increasing due to the wide offer of such equipment on the market featuring, in the case of GPS disciplined system, long term near cesium stability performances using quartz or rubidium oscillators and suitable control algorithms<sup>[5]</sup>. Such devices in fact are capable to evaluate and compensate, using a suitable time constant, the long term instabilities of an oscillator, with good short-term features, due to the frequency drift and to the environment variations and to transfer locally the accuracy of the time scale disseminated by the standard signals received.

The use of the GPS time signals in a one-way mode, allows one to trace the local oscillator to the GPS time scale which is kept in agreement with UTC(USNO) within  $100 \text{ ns}$ <sup>[6]</sup>.



As the traceability of the national laboratories to the international time scale UTC is based on the GPS signals measured in the common-view technique and according to a daily schedule organized by the BIPM, it is possible to refer a GPS disciplined oscillator to a national time standard, as requested in the national accreditation systems, through the GPS synchronization results.

A typical block diagram of an oscillator disciplined by the GPS signals is depicted in Figure 1. It is a microprocessor controlled device made of a multichannel OEM GPS receiver card, a local reference oscillator that can be voltage controlled, a time interval counter, a digital divider and phase stepper and a control loop including a filter and a Digital to Analog Converter (DAC).

A Central Processing Unit (CPU) controls all the major functions: collects the time differences between the 1 PPS from GPS and the local time scale, applies a statistical filter to the measured data to reduce the effect of the noise, computes the frequency corrections to steer the local reference and the phase steps to be applied to the frequency divider to keep the local 1 PPS synchronized with the GPS time. Moreover, it allows the user to introduce initialization parameters, to modify the operation mode and to read the operational status of the system through an I/O port.

The oscillator can either be a temperature compensated or an ovenized quartz, a small rubidium or a still better source. Some instruments can also discipline external oscillators already available in the laboratory. The most commonly delivered output signals are a 1 PPS derived from the GPS card and one or more standard frequencies from the disciplined oscillator. Additional information such as the UTC or local time, the antenna coordinates, the local oscillator disciplining process and the time tagging of external events, can be obtained through the display or an interface. In some cases a frequency error multiplier function is also implemented to characterize oscillators to be calibrated.

As the GPS time signals are affected by a degradation due to the Selective Availability (SA), the most critical element to be implemented is the filter that reduces the effects of the SA modulation and allows one to better estimate the oscillator offset and drift. It has been demonstrated<sup>[7]</sup>, that the decorrelation time of the GPS signals is of the order of 200 s to 300 s and that for longer observation times it is predominant the white phase noise that can be reduced by an averaging process. In Figure 2 are reported the  $\text{Mod}\sigma_y(\tau)$  (MDEV) and the  $\sigma_x(\tau)$  (TDEV) of the GPS signals received from a 4-channel OEM module and measured versus UTC(IEN), showing this typical behavior for observation times longer than 230 s.

To get accurate evaluation of the oscillator parameters, the time constant of the filter must therefore be higher than the decorrelation time and find a trade-off with the long term instability of the oscillator to be steered. In some devices, different time constants are used to distinguish the oscillator offset and drift from the temperature effects; others are also capable of modeling the oscillator long term behavior and to maintain its output frequency and time within stated limits when the system enters in a holdover mode due to the temporary loss of GPS signals.

The operational sequence of one of such devices can be exemplified as follows. First the GPS multichannel receiver searches for the satellites in view and tracks at least 4 of them to



determine the antenna coordinates. When this operation has been successfully completed, a 1 PPS output signal synchronized to GPS is available and the procedure of evaluation of the local clock error can start. To this purpose, a composite satellite clock obtained by averaging the phase differences of all the satellites tracked, is used to determine the oscillator offset and drift after having applied to the data the statistical filter designed. At this point, the computed correction is converted by the DAC into a voltage applied to the oscillator frequency control input.

A digital phase-stepper can instead perform the corrections needed to maintain the 1 PPS derived from the local oscillator in close agreement with the GPS time scale.

In some instruments, after having reached a steady state condition, only frequency corrections are applied to maintain the time synchronization. The philosophy followed in applying these corrections can be of two types, nearly continuous or periodic, resulting in different short-term instability characteristics.

## LABORATORY TEST RESULTS

To get practical knowledge about the performances of this kind of instruments, necessary to solve the problem of their traceability to UTC(IEN), some devices have been tested in 1994 and 1995 at the IEN time and frequency laboratory.

The measurement set-up used is shown in Figure 3; the frequency and time interval measurements have been referred to UTC(IEN) and the differences between UTC(IEN) and the GPS time scale have been determined with the NBS/GPS receiver used for the international traceability. The mean frequency departure between the IEN and the GPS time scales never exceeded  $1 \times 10^{-13}$  during the instruments testing periods.

Four devices from three different manufacturers, labeled in the following as A, B, C, and D, with quartz crystal oscillators or rubidium frequency standards inside, have been checked as regards to their capability to reproduce GPS time, their short and long-term instability, their frequency accuracy and the supplying of information useful to establish a traceability to an external reference standard. All the instruments have been operated in the "time mode" and in all but one case, the reference coordinates of the IEN site have been inserted. The normalized frequency departure values for a period of 54 days, obtained from time interval measurements on instrument A equipped with a high performance rubidium oscillator, are reported in Figure 4 and the corresponding time and frequency instability data in Figure 5. From the frequency data it can be seen that the steering process eliminates the frequency drift; the average value of the frequency offset of the disciplined oscillator corresponds to the difference existing at that time between UTC(IEN) and GPS. The  $\text{Mod}\sigma_y(\tau)$  for  $\tau = 5$  days, exhibits a flicker floor at the  $3 \times 10^{-14}$  level. In Figures 6 and 7 are reported the same kind of data computed for a period of 22 days on instrument B, having a standard rubidium inside, showing that a lower accuracy and stability are obtained and that sometimes the oscillator frequency momentarily exceeds the specifications. Eight hours of the oscillator frequency departures versus GPS, averaged over the disciplining time constant and supplied every 10 seconds by the instrument via its serial interface, are reported in Figure 8. These data can be collected by the user to check that the



system is operating properly. The frequency and stability results obtained over a period of 28 days with instrument C, a steered ovenized quartz oscillator, are shown in Figures 9 and 10. If we compare these results with those obtained for instrument B, we notice that they are not only comparable, but even better as regards to the frequency accuracy. The last instrument evaluated, identified as D and equipped with a small rubidium oscillator, has been checked also for its warm up characteristic. The frequency results reported in Figure 11, show the effect of the correction of the oscillator offset occurred after three hours from the power-on, corresponding to its disciplining time constant, lowering the frequency error down to the  $10^{-11}$  level. The accuracy specification of this instrument was met after 24 hours of operation. The time error versus UTC(IEN) of instrument D, computed from time interval measurements 12 hours apart for a period of 35 days, has been found equal to  $\bar{x} = (0.29 \pm 0.02) \mu\text{s}$ . Meanwhile the frequency offset was in the range between  $-1.8 \times 10^{-12}$  and  $1.9 \times 10^{-12}$ . The instability data, computed from frequency measurements, are reported in Figure 12. As a comment to these data, that are very alike to those of C, it should be said that: i) instruments C and D come from the same manufacturer and differ only for the oscillator option, ii) in the case of D the position determination was made by the instrument itself, iii) that both devices in the long term correct only the oscillator frequency and not the 1 PPS phase.

To check if the compensation of the oscillator drift is effective, in these devices a user can collect the data of the oscillator control voltage, convert them into frequency corrections and compare with the oscillator long term specifications. This has been verified for instrument D and found compliant.

Concerning the overall delay of the instruments tested, it has been found of the order of  $0.2 \mu\text{s}$ .

## ESTABLISHING TRACEABILITY TO UTC(IEN)

Using instrument D, a detailed investigation has been made on the use of GPS as transfer standard for the traceability to IEN of a secondary standard. To this purpose, the time interval measurements performed twice a day between UTC(IEN) and 1 PPS (instr. D) output have been compared with those made by the instrument itself against 1 PPS GPS (2 data a day) and with the UTC(IEN) – GPS data obtained from the averaging of the results coming from the common view schedule (46 data a day). Figure 13 reports the frequency and time instability data of the averaged values of UTC(IEN) – GPS used for this test, showing a slope typical of a white phase noise process for  $0.5 < \tau < 3d$ . On the residuals obtained by subtracting the three sets of time interval readings mentioned before, taken over 35 days, the TDEV and the MDEV have been computed to find the overall uncertainty limit of this traceability system. The results in Figure 14 prove that it is possible to refer the frequency of a GPS disciplined oscillator to a national standard with an uncertainty of  $7 \times 10^{-13}$  for  $\tau = 1$  day that decreases for longer averaging times with a slope of about  $-3/2$ .

## CONCLUSIONS

The problem of establishing the traceability of disciplined oscillators to the Italian reference of time using the GPS signals as transfer standard has been investigated. It has been demonstrated



that this is possible, using adequate measurement protocols, at an uncertainty level of  $7 \times 10^{-13}$  for observation times of 1 day and that it can improve for longer periods. For the instruments of different manufacturers tested, it has been generally found that the long term accuracy declared is very well met, but some discrepancies were found for shorter observation times.

If these kind of instruments are to be used as references in calibration laboratories, a characterization of their short term instability in a metrological laboratory is suggested to help in evaluating the uncertainties of the calibration procedures implemented.

## REFERENCES

- [1] V. Kose 1995, "*Dissemination of Units in Europe – Traceability and its Assurance in a National and Regional Context*", *Metrologia*, **31**, 457-466.
- [2] *International Vocabulary of Basic and General Terms in Metrology (VIM)*, 1993, International Organization for Standardization (ISO), Geneva, Switzerland.
- [3] F. Cordara, G. Vizio, P. Tavella, and V. Pettiti 1994, "*An algorithm for the Italian atomic time scale*", Proceedings of the 25th Annual Precise Time and Time Interval (PTTI) Applications and Planning Meeting, 29 November-2 December 1993, Marina del Rey, California, pp. 389-400.
- [4] F. Cordara, V. Pettiti, and P. De Giorgi 1994, "*Time and frequency traceability sources in the Italian Calibration Service*", Proceedings of the 8th European Frequency and Time Forum (EFTF), Germany, 1994.
- [5] J. Kusters, K. Ho, R.P. Gifford, L.S. Cutler, and D.W. Allan 1994, "*A no-drift and less than  $1 \times 10^{-13}$  long-term stability quartz oscillator using a GPS SA filter*", Proceedings of the 1994 IEEE International Frequency Control Symposium, 1-3 June 1994, Boston, Massachusetts, pp. 572-577.
- [6] C. Thomas 1993, "*Real-time restitution of GPS time*", Proceedings of the 7th European Frequency and Time Forum (EFTF), Switzerland, 1993.
- [7] D.W. Allan, and W. Dewey 1993, "*Time-domain spectrum of GPS SA*", Proceedings of the ION GPS-93 Conference, 22-24 September 1993, Salt Lake City, Utah, pp. 129-136.

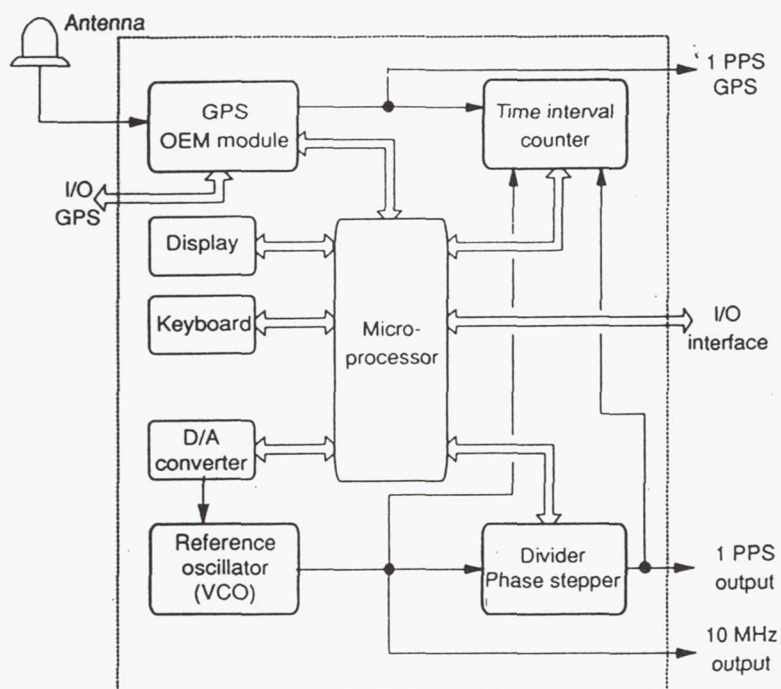


Fig. 1 - GPS disciplined oscillator block diagram

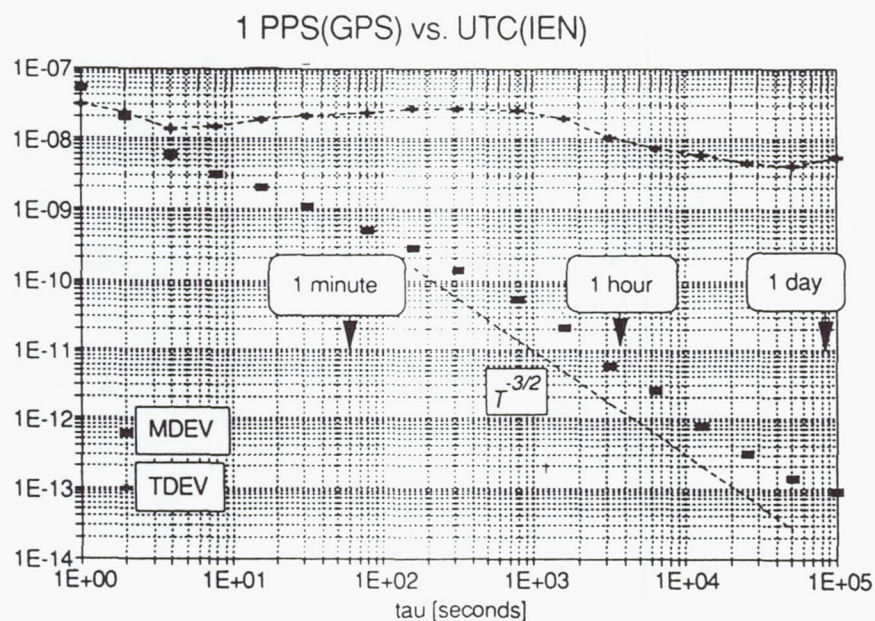


Fig. 2 - MDEV and TDEV analysis of GPS data



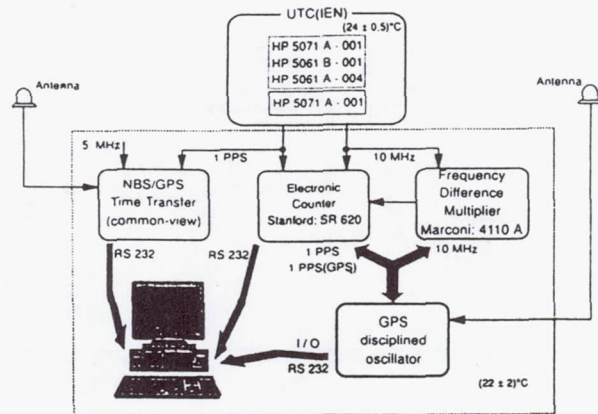


Fig. 3 - Block diagram of the measuring system

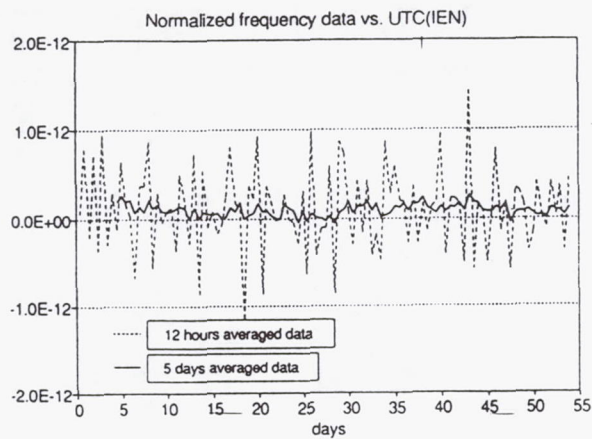


Fig. 4 - Normalized frequency departures of instrument A computed every 12 hours

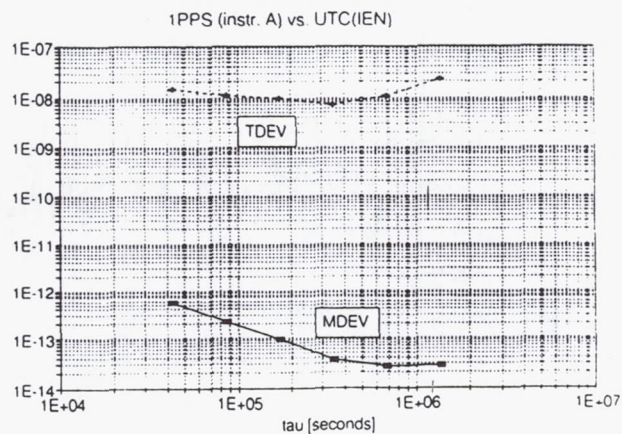


Fig. 5 - Time and frequency instabilities of instrument A

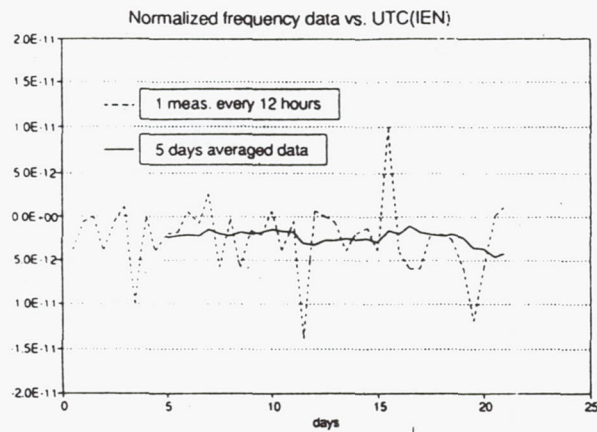


Fig. 6 - Normalized frequency departures of instrument B measured every 12 hours

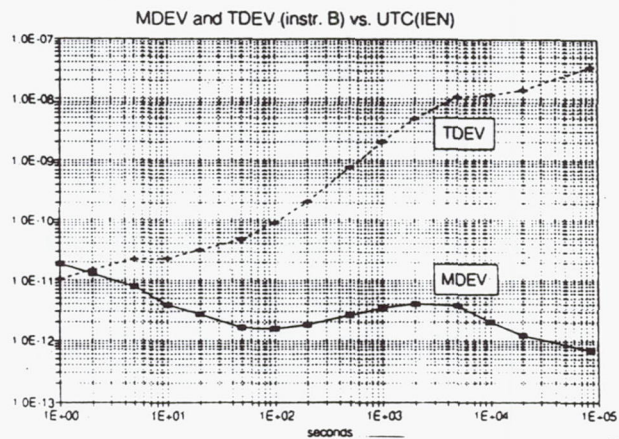


Fig. 7 - Time and frequency instabilities of instrument B from frequency data

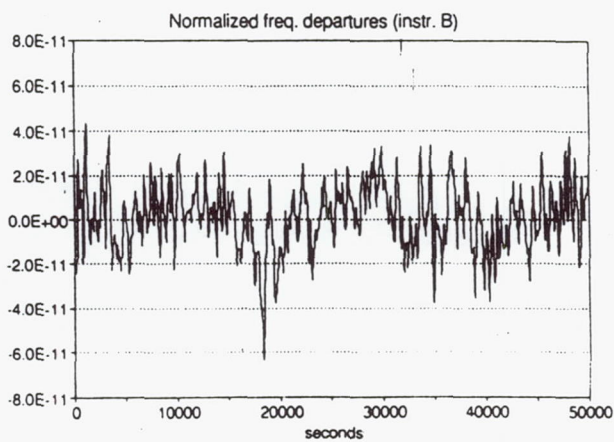


Fig. 8 - Normalized frequency departures versus GPS as given by instrument B



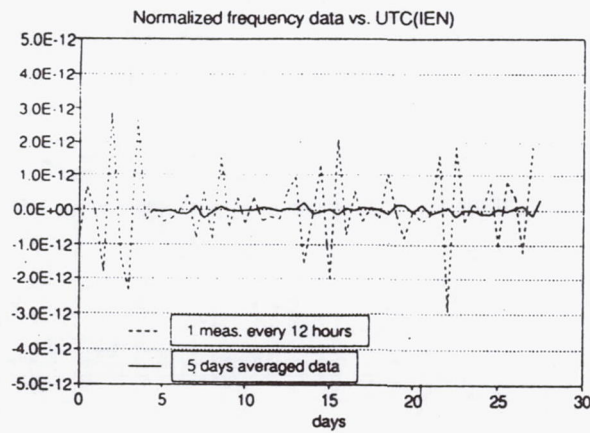


Fig. 9 - Normalized frequency departures of instrument C computed every 12 hours

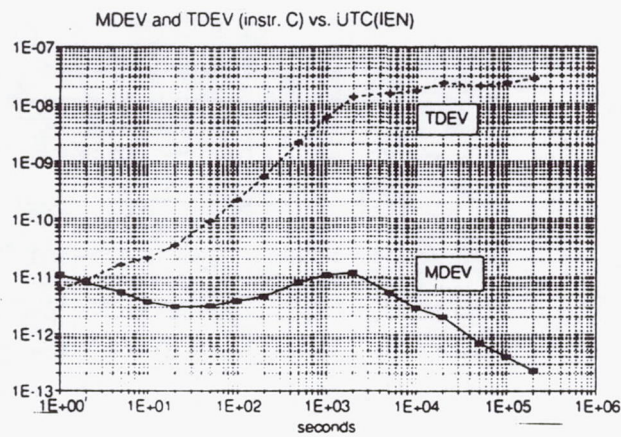


Fig. 10 - Time and frequency instabilities of instrument C

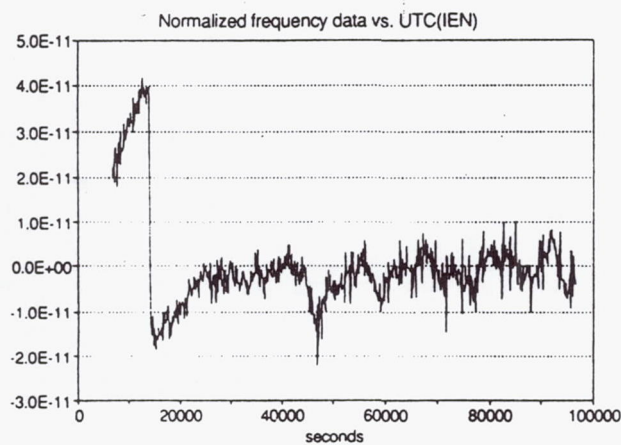


Fig. 11 - Warm up characteristic of instrument D, one measurement every 100 s

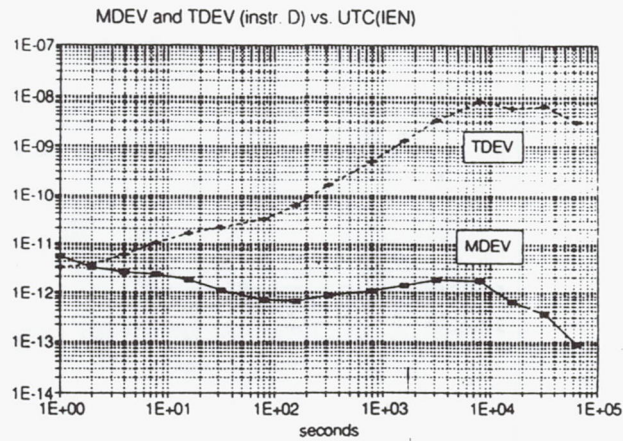


Fig. 12 - Time and frequency instabilities of instrument D

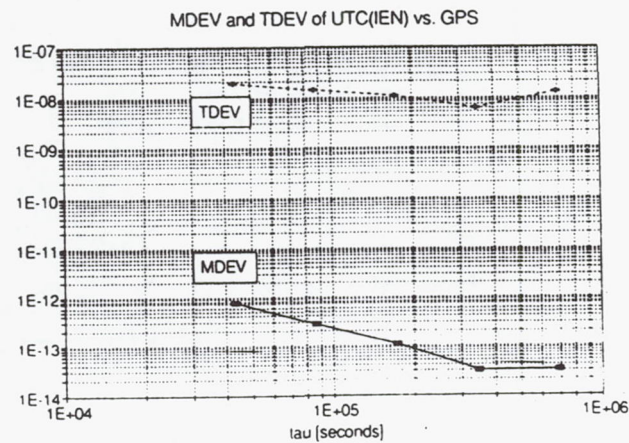


Fig. 13 - Frequency and time instabilities of UTC(IEN) versus GPS from the common-view schedule

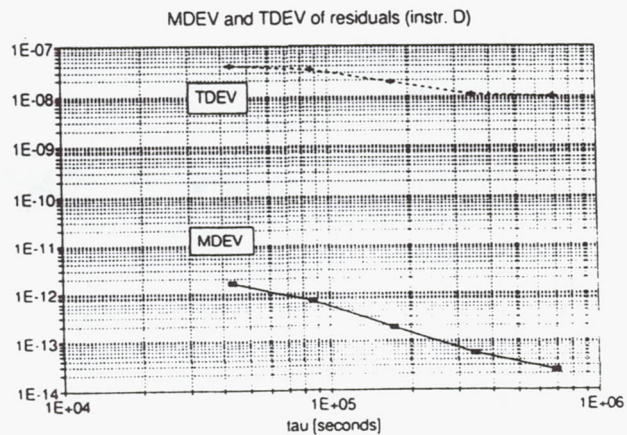


Fig. 14 - Instabilities of the residuals in establishing the traceability chain



# OBSERVATIONS ON THE RELIABILITY OF RUBIDIUM FREQUENCY STANDARDS ON BLOCK II/IIA GPS SATELLITES

1Lt. Gary L. Dieter  
Capt. Gregory E. Hatten  
US Air Force, Falcon AFB, Colorado Springs, CO 80912

## Abstract

*Currently, the Block II/IIA Global Positioning System (GPS) satellites are equipped with two rubidium frequency standards. These frequency standards were originally intended to serve as the back-ups to two cesium frequency standards. As the constellation ages, the Master Control Station is forced to initialize an increasing number of rubidium frequency standards. Unfortunately, the operational use of these frequency standards has not lived up to initial expectations.*

*Although the performance of these rubidium frequency standards has met and even exceeded GPS requirements, their reliability has not. The number of unscheduled outage times and the short operational lifetimes of the rubidium frequency standards compare poorly to the track record of the cesium frequency standards.*

*Only a small number of rubidium frequency standards have actually been made operational. Of these, a large percentage have exhibited poor reliability. If this trend continues, it is unlikely that the rubidium frequency standards will help contribute to the navigation payload meeting program specification.*

## INTRODUCTION

The GPS program was designed with atomic frequency standards at the heart of the navigation payload. The choice of available frequency standards limited the number of options available to the program designers. Although different atomic frequency standards were available on the commercial market, only rubidium standards could meet Air Force space qualification and be set into production quickly enough to meet the planned launch date of the first Block I satellites<sup>[2]</sup>.

The first few satellites of the GPS Block I program provided the test bed for space rated rubidium frequency standards. Changes in the composition of the glass in the rubidium lamp and the amount of rubidium contained within the lamp enabled Rockwell and the Air Force to improve the design of the rubidium frequency standard. By the first Block II launch in 1989, the GPS rubidium frequency standard was in its eleventh and final production model.

Cesium frequency standards were subjected to a much slower production schedule. Delays in production and space qualification prevented the introduction of the production model cesium



frequency standard into the GPS payload until 1983, when it was included in the launch of SVN 8. A single cesium frequency standard was also included in each of the subsequent Block I nav payloads, each of which also included three rubidium standards. Not until the introduction of the Block II satellite in 1989 did the nav payload include two rubidium and two cesium clocks.

Rubidium frequency standards had several features that made them the obvious choice for precise time generation. They were small, lightweight, and their history suggested that they would be more reliable than the newly available cesium frequency standards. Despite these advantages, they also had certain drawbacks. They were very temperature sensitive and required occasional control segment intervention to maintain the proper frequency and phase offset. Perhaps most importantly, their relatively poor long-term stability prevented accurate extended navigation capability.

This extended navigation capability is essential to ensure continued GPS coverage in the event that the control segment is damaged or destroyed. Although not a consideration during the research and development phase of Block I, extended navigation was an important consideration in the Block II design. For this reason, the cesium frequency standard was advanced as the primary source of precise timing. The rubidium standard was included as insurance because its performance had been more thoroughly evaluated during the Block I phase.

This is the irony of the situation. The cesium frequency standard was included for its superior long-term stability, deemed necessary in an effective wartime asset. In the event of a catastrophic failure of the control segment, the extended navigation feature would require the long-term stability of a cesium standard. Fortunately, the GPS constellation has never required extended navigation and hopefully never will. Therefore, long-term stability is of lesser importance to routine daily operations. In fact, stability at periods longer than one day are, for the most part, invisible to the user due to control segment intervention.

The rubidium standard was included as a backup due to its reliable service in the Block I program. Although its stability was deemed inferior, past performance indicated that it should be included in order for the nav payload to meet reliability requirements. The cesium standards did not have enough history to accurately determine their reliability coefficient<sup>[2]</sup>.

The experience of the personnel of the 2 SOPS and the GPS Master Control Station has contradicted these expectations. The typical stability of rubidium clocks is not inferior to that of typical cesium standards as measured under current operational procedures. In fact, the one-day stability of rubidium clocks is usually better than that of the cesium frequency standards. The reliability issue is also reversed. The previously unproven cesium standards have actually experienced longer lifetimes than the rubidium frequency standards.

This paper will attempt to show some concrete examples of the reliability and stability of the two types of frequency standards. A side-by-side comparison will show that rubidium atomic clocks, when viewed from the perspective of the Master Control Station, do not provide the level and consistency of operation demanded by the GPS community. In fact, they are frequently a source of error and frustration for the operators of the GPS program.



## STABILITY

The stability of an atomic frequency standard is critical for its use as a timing source in the GPS navigation payload. The 2 SOPS operational definition of stability differs slightly from the definition used in the original program specifications. Both of these differ from the definition used by some independent analysis agencies.

The U.S. Naval Research Laboratory (NRL) periodically provides 2 SOPS with reports which summarize the performance of the on-board frequency standards. NRL uses data from a keyed receiver which can properly account for Selective Availability. The accumulated phase offset of each operational clock is measured daily by USNO. These data, gathered over a period of several months, allows NRL to generate reports detailing GPS clock performance. These reports provide insight into several different clock characteristics, including stability, frequency offset, phase offset and linear frequency drift.

NRL's stability plots show frequency stability as a function in the time domain:  $\sigma_y(\tau)$  (Allan Deviation). NRL applies a constant "aging" correction to the raw data in order to remove a linear drift. This approach is warranted for evaluating rubidium frequency standards since the MCS also calculates a frequency drift value and adjusts the broadcast clock values to reflect this change in frequency. The difference between the two frequency drift values lies in the methodology used to measure the frequency drift. NRL applies a flat aging rate to the entire time span of collected data. The MCS updates the frequency drift value every 15 minutes and thus estimates aging more dynamically. Fortunately, the MCS-derived value of frequency drift changes very little over the lifetime of a rubidium clock (once it has fully warmed up).

The frequency drift values for cesium GPS clocks are negligible when viewed over the span of one day. Because of this, the MCS does not calculate a frequency drift value for cesium clocks. Hence, the correction applied at NRL is not reflected in the navigation signal.

The GPS stability specifications for rubidium ( $5 \times 10^{-13}$  at one day) and cesium ( $2 \times 10^{-13}$  at one day) clocks do not assume that an aging correction is applied<sup>13, 41</sup>. Therefore, although the  $\sigma_y(\tau)$  plots (with aging correction included) from NRL are useful to the MCS as a measuring stick for GPS performance, they do not indicate adherence to the GPS program specifications.

To compare NRL collected data with the  $\sigma_y(\tau)$  plot provided in the program spec, the following approach was taken to remove the aging correction from NRL's data. This method assumes that any frequency drift values are completely uncorrelated with other noise types. If this assumption is made, the instability due to aging is added to the corrected stability via the root sum squared (RSS) method<sup>15</sup>:

$$\sigma_y(\tau) = \text{Allan Deviation} \quad (1)$$

$$\sigma_{yNRL}(\tau) = \text{NRL's } \sigma_y(\tau) \text{ (Corrected for Drift Rate)} \quad (2)$$

$$A = \text{Aging Value (Calculated by NRL)} \quad (3)$$

$$\sigma_{yD}(\tau) = \text{Allan Deviation due to Aging} \quad (4)$$

$$\sigma_{yU}(\tau) = \text{Uncorrected Allan Deviation} \quad (5)$$



$$\sigma_{yD}^2(\tau) = 1/2(A\tau)^2 \quad (6)$$

$$\sigma_{yU}^2(\tau) = \sigma_{yD}^2(\tau) + \sigma_{yNRL}^2(\tau) \quad (7)$$

$$\sigma_{yU}(\tau) = [\sigma_{yD}^2(\tau) + \sigma_{yNRL}^2(\tau)]^{1/2} \quad (8)$$

This method allows us to compare stability data collected independently by NRL with the stability requirements outlined in the program specifications. The results of this comparison are shown in Table 1.

A comparison of data points corrected for aging to those not corrected found that NRL's aging correction for cesium clocks was minimal for  $\tau$  equal to one day. The stability component due to aging was, however, significant at one day for the rubidium clocks. The magnitude of these aging coefficients suggest that the looser, non-corrected specification was appropriate. In order for a rubidium standard to conform to the tighter cesium specification, an aging correction would have to be included.

Two important considerations must be taken into account when looking at the one-day stability of GPS clocks. The first is that relatively few Block II/IIA rubidium frequency standards have been powered on. This skews the results of the analysis, as the rubidium clocks represent a smaller pool of data. Statistically, a greater percentage of the total number of cesium standards have been powered on. With more than half of all available cesium standards included in this survey, the occasional poor performer does not carry as much weight.

The second consideration is the lack of confidence in the measurement process for a newly enabled frequency standard. "Infant mortality" forced the authors to exclude data gathered from two clocks that were never set healthy. One of SVN 32's rubidium frequency standards never settled down to the point where it could be declared fully operational. Its abnormal behavior eventually resulted in a situation where the clock was powered down and the stand-by was powered up. Because this rubidium clock behaved so poorly and was never declared operational, it was excluded from the average. The same is true with an improperly modeled cesium standard on SVN 22. Although the cesium clock itself has since been excluded from blame, poor modeling of the orbital states by the MCS Kalman filter led to inaccurate phase measurements. This, in turn, led to incorrect modeling of the frequency standard stability. For this reason, this cesium frequency standard was excluded from the stability average.

The most obvious result of this analysis is that, with the aging coefficient accounted for, the average one-day stability of a rubidium frequency standard is no worse than the that of a cesium clock. Although the sample size is not large enough to provide a definitive answer, it appears that the corrected one-day stability of the rubidium standards surpasses that of the cesium frequency standards.

Even with the aging coefficient included, the rubidium clocks more than meet their stability specification of 5 parts in  $10^{13}$ [3]. In fact, if aging is accounted for, the rubidium clocks meet the much stricter cesium spec of 2 parts in  $10^{13}$ [4]. The cesium clocks also perform within specification. According to NRL, rarely does a GPS frequency standard's one-day stability exceed 2 parts in  $10^{13}$ [1].



How does this result compare with the experience of the operators in the MCS? We measure frequency standard stability by the ability of the MCS to model and predict the phase, frequency, and frequency drift parameters. When a clock shows poor stability, the uploaded predictions diverge from reality. When this occurs, the operators are forced to update the navigation message in the satellite more frequently than once per day in order to prevent an accumulation of ranging errors. Good short-term stability leads to an improved ranging signal and eliminates the need for additional navigation uploads.

A one-day stability greater than approximately 2 parts in  $10^{13}$  (corrected for aging) corresponds to an increased demand on the MCS to provide updated navigation uploads. If the stability is better than this, the normal upload frequency of once per day is sufficient. If the frequency of the clock is much less stable than this, the MCS Kalman filter will not be able to accurately predict the clock's behavior. At this point, no amount of navigation uploads will maintain the ranging error within tolerances. When this extreme instability occurs, the usual course of action is to power down the clock and select a redundant frequency standard.

Tracking frequency standard stability according to daily ranging errors is only approximate. Daily and long-term analysis of all clock parameters as well as independent analysis by NRL and the Defense Mapping Agency (DMA) allows the MCS to maintain confidence in the performance of our frequency standards.

## RELIABILITY

Because the GPS frequency standards are physically inaccessible, reliability is very important for maintaining system integrity. Each GPS satellite contains four frequency standards (two cesium and two rubidium). In order to meet the required mission lifetime of 7.5 years, each of the four clocks should be expected to operate within stability specifications for approximately two years. Based on the lifespans of frequency standards that have been disabled, rubidium clocks fall short of this goal. The rubidium clocks which have been powered down averaged only 13 months of operation each. By comparison, cesium clocks have averaged 25 months of operation before being powered down. These figures are detailed in Table 2.

It is important to qualify these numbers with respect to clock lifetime. The numbers given above represent the average age of the cesium and rubidium clocks when they were powered down. The MCS will power down a frequency standard when it does not perform adequately; however, this may occur before every spark of life is extinguished. Because extensive control segment maintenance may provide limited use of a poorly performing frequency standard, the MCS may try to revive a previously used frequency standard before declaring the payload non-operational and disposing of the satellite. Therefore, these lifespans may not represent the total operational use of the clock. Instead, they are a good representation of the time during which the clock has performed to an acceptable level.

In order to gain a more representative sampling of frequency standards, it may be helpful to analyze the lifetimes of the currently operating cesium and rubidium clocks. The average life of the operating cesium standards is 44 months. The average life of the operating rubidium standards is 10 months. If every active clock were to fail in December 1995, the average



lifespan of expired frequency standards would improve. When the data from the active clocks are included in the total lifetime averages, the cesium lifespan increases from 25 to 37 months and the average rubidium lifespan is relatively unchanged (13 to 12 months).

The longevity figures for operational clocks must be taken in context. The MCS has only recently begun powering up rubidium clocks in relatively greater numbers. This recent change in operations is responsible for the low average lifespan of operational rubidium clocks. The cesium clocks more accurately represent the performance of the Block II/IIA program. Their greater longevity may be attributed to the reliance upon cesium standards in the early days of the Block II/IIA program. If rubidium standards had been powered up in greater numbers following the first few launches, it is possible that the MCS would now be operating rubidium frequency standards as old as the oldest cesium clocks.

The performance of GPS frequency standards as a whole is satisfactory. Active cesium frequency standards approach an average lifetime of four years. The GPS constellation may need this type of performance from the cesium clocks as the lifespan of the rubidium clocks lags behind. Based solely upon data from disabled clocks, the rubidium frequency standards do not show the type of longevity necessary to maintain a navigation payload lifetime of 7.5 years. As the constellation matures, more performance data will be available for analysis. These data may show that the initial sampling of rubidium standards does not accurately represent the entire collection as a whole. If this initial sampling of data does accurately represent all rubidium clocks, the GPS constellation will have to rely heavily on the performance of cesium standards to complete each satellite's 7.5 year mission.

## MCS OPERATIONS

The MCS continuously monitors the 24 orbiting satellites via the L-band downlink. L-BAND MONITOR examines each six second bundle of data for inconsistencies. If the ranging signal begins to creep out of tolerance, an alarm triggers alerting the operations crew to the presence of an anomaly. Once an active contact is opened between the satellite and a ground antenna, the MCS operators can begin analyzing S-band telemetry. Often this telemetry pinpoints the cause of the ranging errors; other times it is not as helpful. In either case, once a satellite begins transmitting an unstable navigation signal, it is set unhealthy until the problem is resolved.

If further analysis indicates that the problem lies with the frequency standard, it may be necessary to swap to a redundant clock. When this is the case, the MCS operators often have the option of choosing between a rubidium and a cesium standard. There are several different factors that determine the choice of frequency standard.

Because of better short-term stability, the MCS benefits from the inclusion of rubidium clocks in the paper ensemble, called the GPS Composite Clock. An effective mixture of cesium and rubidium standards can only be maintained by selectively powering up the appropriate clock.

The MCS is still relatively unfamiliar with the maintenance of rubidium clocks. By slowly increasing our knowledge of the operating characteristics of these frequency standards, we can prevent the sudden and unexpected use of rubidium clocks in the waning days of the Block II/IIA constellation. By mixing the operation of rubidium and cesium clocks now, we can



ensure the availability of both rubidium and cesium clocks at a later date.

Despite the advantages of rubidium clocks, their suspect reliability has made the operators at the MCS reluctant to power them up. During the first several months of operation, rubidium standards are prone to sudden and unpredictable phase jumps as well as a rapidly changing frequency drift rate. The MCS operators can quickly and easily fix these, but confidence in the constellation as a whole is reduced.

Outage time is also a major factor. Rubidium clocks require a longer initial warm up period than cesium clocks. Due to the rapidly changing frequency drift term (A2), the MCS can not accurately model or predict the future states of a new rubidium clock. Because of this, initializing a new rubidium clock necessitates an average outage of 7.7 days, while a cesium clock only stays unhealthy an average of 4.3 days. If the operational situation necessitates a minimal outage time, a cesium clock will probably be chosen over a rubidium clock.

The age of the satellite as well as the condition of the various support systems may indicate a limited available lifetime for a particular satellite. For those satellites with a limited expected lifetime, the choice of a cesium clock will reduce the amount of required maintenance. There are two main reasons why rubidium clocks need more control segment intervention. The large frequency drift requires occasional "Frequency Biasing" in which the MCS alters the output frequency of the timing signal. Also, since rubidium clocks require an external heat source, the entire payload operates at a higher temperature. This requires more frequent "Ion Pump Maintenance" for any stand-by or suspect cesium clocks. Since both of these procedures require several hours of down time, avoiding them entirely is an operational advantage.

## CONCLUSION

The MCS has gained experience in the operation of cesium and rubidium frequency standards. This experience has shown a few trends. Rubidium clocks tend to be better performers with respect to short-term (one-day) stability. Since every satellite in the GPS constellation is provided with a fresh navigation upload every day, this improved stability is revealed by a more accurate ranging signal.

In order to meet program specifications, the GPS signal must not only be accurate, it must also be dependable. This dependability is directly related to the reliability of the on-board atomic clocks. Analysis of a limited number of GPS frequency standards shows that the expected lifetime of rubidium standards lags behind that of cesium clocks. Luckily, the overall lifetime of GPS clocks appears to be sufficient to fulfill the intended mission.

The combination of frequency stability and reliability makes the decision difficult when the time comes to power up a new clock. The importance of GPS timing stability and the need for an appropriate mixture of frequency standards in the constellation make the inclusion of rubidium clocks a necessity. Although only a case by case review of the appropriate factors will determine the new type of operational clock, the improved reliability and decreased maintenance time makes the cesium standard a more attractive option.

## ACKNOWLEDGEMENTS

The authors would like to thank the following for their assistance and encouragement:

- Captain Steven Hutsell, 2 SOPS
- Mr. M.J. Van Melle, Rockwell Space Operations Company
- The men and women of the 2nd Space Operations Squadron

## REFERENCES

- [1] NAVSTAR Global Positioning System Quarterly Reports, 1992-1995, Naval Center for Space Technology, Space Applications Branch, US Naval Research Laboratory, Washington, DC.
- [2] Personal interview, Dr. Brad Parkinson, 28 September 1995.
- [3] MC474-0030 *Rubidium Frequency Standard Performance, Design Development and Test Requirements*, 5 May 1988.
- [4] MC474-0031 *Cesium Frequency Standard Performance, Design Development and Test Requirements*, 2 October 1987.
- [5] *2 SOPS Mission Support Study Guide 3-16: Timing Stability*.

Table 1 1 Day Stability				
Frequency Standard	Number of Data Points	$\sigma_y(\tau)$ $\tau$ = one day (corrected for aging)	$\sigma_y(\tau)$ $\tau$ = one day (NOT corrected for aging)	Specification (NOT corrected for aging)
Rubidium (active)	4	$0.94 (\times 10^{-13})$	$2.23 (\times 10^{-13})$	$5.0 (\times 10^{-13})$
Rubidium (dead)	4	$2.35 (\times 10^{-13})$	$3.84 (\times 10^{-13})$	$5.0 (\times 10^{-13})$
Rubidium (all)	8	$1.79 (\times 10^{-13})$	$3.14 (\times 10^{-13})$	$5.0 (\times 10^{-13})$
Cesium (active)	18	$1.34 (\times 10^{-13})$	$1.36 (\times 10^{-13})$	$2.0 (\times 10^{-13})$
Cesium (dead)	10	$1.37 (\times 10^{-13})$	$1.37 (\times 10^{-13})$	$2.0 (\times 10^{-13})$
Cesium (all)	28	$1.36 (\times 10^{-13})$	$1.37 (\times 10^{-13})$	$2.0 (\times 10^{-13})$

Table 2 Average Operational Lifetime		
Frequency Standard	Number of Data Points	Life in Months
Rubidium (active)	5	10.2
Rubidium (dead)	6	12.7
Rubidium (all)	11	12.2
Cesium (active)	19	43.7
Cesium (dead)	12	24.9
Cesium (all)	31	36.6



## Questions and Answers

**KEN MARTIN (BONNEVILLE POWER ADMINISTRATION):** I'm trying to figure out — it looked like when you have standby time and "on" time that, I take it, it's operating on one oscillator; and then the other ones are just completely turned off for a couple of years; and they turn those on, and turn the other ones off; and each one wears out in a couple of years or a year. Is that - - - ?

**1st LT. GARY L. DIETER (USAF):** I'm a little bit confused when you say "standby" time and "on" time. Could you please - - - ?

**KEN MARTIN (BONNEVILLE POWER ADMINISTRATION):** I'm not sure. It looks to me like all the clocks will wear out in maybe a couple or three years, and that must not be the case. So - - -

**1st LT. GARY L. DIETER (USAF):** Right, three years is definitely not a cutoff time for clocks to stop dying. Some of them can last a lot longer than that.

**KEN MARTIN (BONNEVILLE POWER ADMINISTRATION):** So what you're saying is that you use a cesium clock for like 33 months and then it dies; and then you turn a different one on?

**1st LT. GARY L. DIETER (USAF):** Yes, there are four clocks on each satellite. Obviously, we use a clock as long as it can operate within stability specifications. Once either it has a hard death or it starts to operate outside of specs and is causing problems, we will swap a redundant clock on a satellite. So, we'll pick from one of the three remaining clocks.

**KEN MARTIN (BONNEVILLE POWER ADMINISTRATION):** So the clocks that are not being used are actually turned off? And that's not shelf life, that's standby life while it's heated up?

**1st LT. GARY L. DIETER (USAF):** Right, yes. The clocks that aren't being used for the signal are turned off.

**UNKNOWN:** Do you have any insight into possible reasons for the poor reliability of rubidium in GPS?

**1st LT. GARY L. DIETER (USAF):** That's a good question. I'm sure there's much speculation on that topic. I personally cannot give a good official reason for why this is.

One thing, as I said before, it's important to keep in mind the numbers — we're not looking at a great number of data points for rubidiums. So, as I said, hopefully this isn't a trend; hopefully, this is some bad beginning luck. I'm not sure why we're having bad luck now; I'm not sure anyone knows for sure what the problem is, if there is a problem. It may just be, like I said, some initial bad luck. Sorry I can't answer your question better.

**ALBERT KIRK (JPL):** I notice on your cesium lifetime that the disabled clock had a shorter lifetime than the other clocks. Can you explain what "disabled" really means in this context?

**1st LT. GARY L. DIETER (USAF):** In this context it means — for instance, say we turn on a cesium clock first on a satellite. As soon as it starts to perform poorly, or if it dies, we'll

turn it off and turn another one on. And that disabled number is the average lifetime for the clocks that we've already turned off.

**ALBERT KIRK (JPL):** But then the clocks, if they have a lifetime of 40, then that means they're disabled after 40. So they're all disabled eventually, right?

**1st LT. GARY L. DIETER (USAF):** That's if they were to die today. If all the cesium clocks that are on right now were to die today, their average lifetime would be 44 months.



# HOW BAD RECEIVER COORDINATES CAN AFFECT GPS TIMING

H. Chadsey  
U.S. Naval Observatory  
Washington, D.C. 20392

## Abstract

*Many sources of error are possible when GPS is used for time comparisons. Some of these errors have been listed by Lewandowski<sup>[1]</sup>. Because of the complexity of the system, an error source could have more than one effect. This paper will present theoretical and observational results by offsetting a receiver's coordinates. The calculations show how an error as small as 3 meters in any direction can result in a timing error of more than 10 nanoseconds. The GPS receiver must be surveyed to better than 0.2-meter accuracy for the timing error to be subnanosecond.*

## INTRODUCTION

GPS is a receive-only system. The user's equipment does not transmit a signal other than the intermittent frequencies used internally to the receiver. The system relies on knowing the position of the transmitter (the GPS satellite), the time of signal transmission, and the position of the receiver so the receiver can determine its time and time offset from some reference (for time transfer operations). For mobile operations, the information from at least four satellites is needed so the receiver can find its position, time, and time offset. If the satellite is at its stated location and the corrections for propagation are correct, the source of error in time transfer mode of operation must be the receiver coordinates.

## THEORETICAL CALCULATIONS

A person must first understand the different coordinate systems used and put all positions in a common system. The GPS antenna used was surveyed by The Defense Mapping Agency into the World Geodetic Survey 1984 (WGS-84) coordinates<sup>[2]</sup>. The WGS-84 is based on the Earth's center of mass. The Z-axis is in the direction of the Conventional Terrestrial Pole (CTP) for polar motion. The X-axis is the intersection of the WGS-84 reference meridian plane and the plane of the CTP's equator. The reference meridian is the zero meridian as defined by the BIH for epoch 1984.0 on the basis of the coordinates adopted for the BIH stations. The Y-axis completes a right-handed, Earth-fixed orthogonal coordinate system. Programs from the Defense Mapping Agency and Mihran Miranian (USNO) were used to convert the WGS-84 coordinates to Earth-Centered, Earth-Fixed (ECEF), which is used by the GPS system.

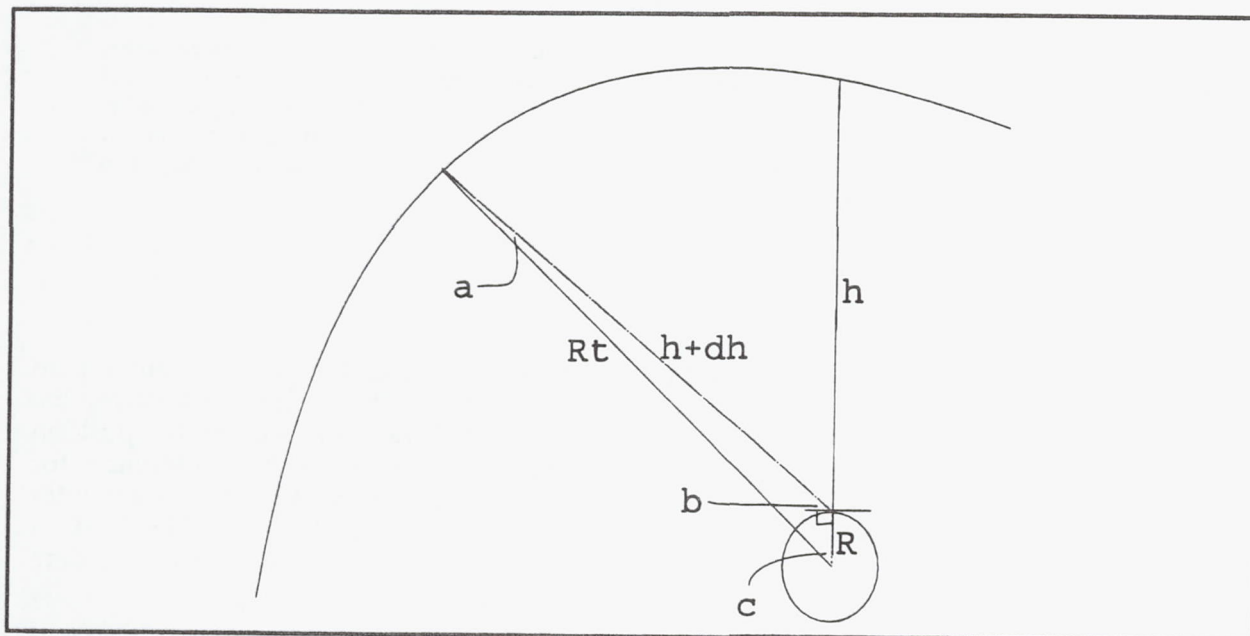
The coordinates for one GPS antenna at USNO are:

	WGS-84		ECEF		ECEF
N	38°55'13.397"	X	1112168.189m	$R_e$	6369795.132m
W	77°03'58.431"	Y	-4842863.286m	$\Theta$	-77.0662308386°
A	55.5m	Z	3985479.536m	$\Phi$	38.7324162285°
				$\Phi'$	51.2675837715°

where  $R_e$  is the radius of the Earth (ECEF) at the receiver's location, and  $\Phi'$  is measured from the Z-axis rather than from the X-Y plane.

A satellite directly at zenith is 26407545 meters from the receiver according to actual measured values. The height of the satellite above the receiver is 20037749.868 meters.

The next step is to understand how changing the position of the satellite will change the geometry of the satellite-receiver relationship and the path length.



Let:

$R$  = radius of Earth

$R_t$  = height of satellite above center of Earth (assumed constant)

$h$  = height of satellite above receiver

$h+dh$  = height of satellite above receiver plus additional distance due to change of satellite-receiver geometry

$c$  = angle between zenith of receiver and location of the satellite

$b$  = angle satellite is above the horizon

We have the following relations:

$$a = \arcsin \left( \frac{R \times \sin(b + 90)}{R_t} \right)$$



$$c = 180 - (b + 90) - a$$

$$h+dh = \frac{R_t \times \sin(c)}{\sin(b + 90)}$$

The angle  $b$  was varied from  $90^\circ$  to  $0^\circ$ . This resulted in  $c$  varying from  $0^\circ$  to  $76.375^\circ$  and  $dh$  varying from 0 meters to 5477587.0874 meters. These variations were then transformed to those seen by the individual receiver coordinates. These values were then converted to ECEF coordinates  $X$ ,  $Y$ ,  $Z$ .

This assumes that the receiver is at its proper coordinates. In order to understand of how  $dh$  changes as the satellite changes position when the receiver is NOT in its proper location, one must vary the surveyed latitude, longitude, and altitude (in WGS-84 coordinates) and determine the "new" coordinates in the ECEF coordinate system.

The altitude changes in direct proportion to the radius. However, latitude and longitude do not have such a simple transform. The latitude of the satellite is given by:

$$SLAT = \frac{S}{2\pi \times B}$$

where  $S$  is seconds per 360 degrees (1296000) and  $B$  is the Earth's polar radius (6356752.3142 meters). For the USNO receiver,  $SLAT = .032448''$  per meter.

The longitude is given by:

$$SLON = \frac{S}{2\pi \times \cos(Lat) \times A}$$

where  $A$  is the Earth's equatorial radius (6378137.0 meters). At USNO's Latitude of  $38^\circ 55' 13.397''$ ,  $SLON = .04156624''$  per meter.

The receiver offsets, symmetric about zero, were 15m, 10m, 5m, 4m, 3m, 2m, 1m, .9m, .8m, .7m, .6m, .5m, .4m, .3m, .2m, .1m, and .05m. These offsets were transformed to altitude, latitude, and longitude offsets in the WGS-84 coordinate system. The new positions were then transformed into the ECEF coordinate system.

With the satellite and receiver in ECEF coordinates and knowing the non-offset  $h+dh$  values, a simple computer program can solve the time error equation. The time error equation is:

$$dt = \frac{\sqrt{(X_s - X_r)^2 + (Y_s - Y_r)^2 + (Z_s - Z_r)^2} - (h+dh)}{c}$$

where  $s$  and  $r$  represent satellite and receiver respectively.

The results are plotted as time offset vs. offset vs. angle of satellite above the horizon in Figure 1. An error of as small as 3 meters offset in any of the three coordinates can result in

a time error of more than 10 nanoseconds. For the time error to be subnanosecond, the GPS antenna must be surveyed to better than 0.2 meter accuracy.

Theoretical calculations for offsetting a receiver's coordinates, holding the other variables fixed, show some interesting results. First, a time error of 20 nanoseconds would require an antenna's coordinates to be off by more than five meters. Second, the errors are three-dimensionally symmetric.

## OBSERVATIONAL RESULTS

The theoretical results are interesting, but mean nothing without some proof of observation. For this, two keyed dual-frequency receivers were used. First, both receivers were set in the time transfer mode of operation with their correct coordinates in their databases (Figures 2 and 3). After several days of observation, receiver 1 continued to operate with the correct coordinates, while receiver 2 had its coordinates offset changed daily. Receiver 2's offset were 15m, 10m, 5m, 1m, .5m, and back to 0m (for two days) to verify each offset run. The offsets were applied in altitude (Figures 4, 5, and 6), latitude (Figures 7 and 8), and longitude (Figures 9, 10, and 11). The closure checks of zero offset showed that no parameters changed during the observations. The bias of approximately 5.6 nanoseconds was between this pair of receivers. In a follow-on observational set between one of these receivers and another, the bias was 3.5 nanoseconds. All receivers were calibrated by the manufacturer.

## CONCLUSION

The theoretical and observational results agree with common sense that an approximate three nanoseconds per meter error would be present because of receiver coordinates being offset. However, more important facts were found from the observational data. First, although the receivers used to collect the observational data met specification, there was an offset between them. In a follow-up observation series, using one of these two receivers and a third, this offset was found to still be present but of a different value. (The offset values differed by 2-3 nanoseconds.) Further investigation is needed to resolve these differences for higher precision time transfers. Second, although keyed dual-frequency receivers were used, evidently there are some differences between satellites. Averaging does decrease this effect. Higher accuracy time transfers will require more investigation of this effect. One needs to know if averaging is the right thing to do or if some problem must be fixed.

## REFERENCES

- [1] W. Lewandowski 1994, "GPS common-view time transfer," Proceedings of the 25th Annual Precise Time and Time Interval (PTTI) Applications and Planning Meeting, 29 November-2 December 1993, Marina Del Rey, California, pp. 133-148.
- [2] "Department of Defense World Geodetic System 1984," 1992, Defense Mapping Agency Technical Report 8350.2.



# Time Error vs. Receiver Offset

Figure 1

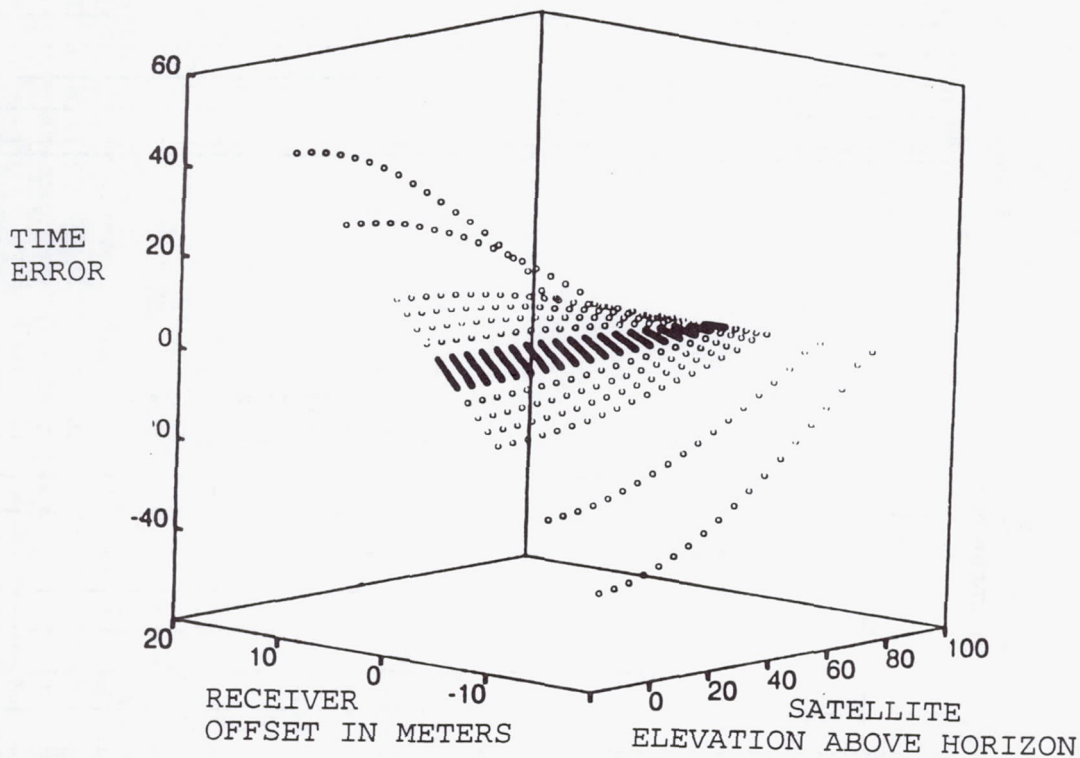


Figure 2 Theoretical minus Experimental Results  
each satellite observation averaged independently

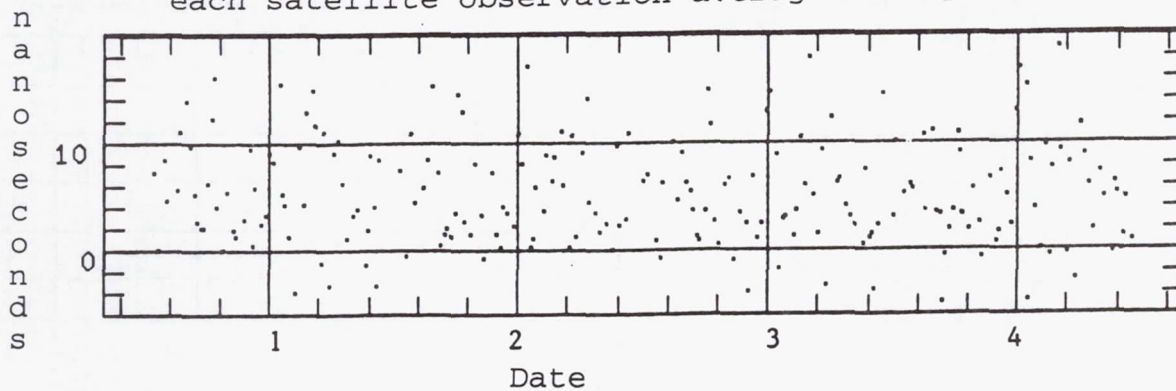


Figure 3                      Theoretical minus Experimental Results  
all satellite observations averaged daily

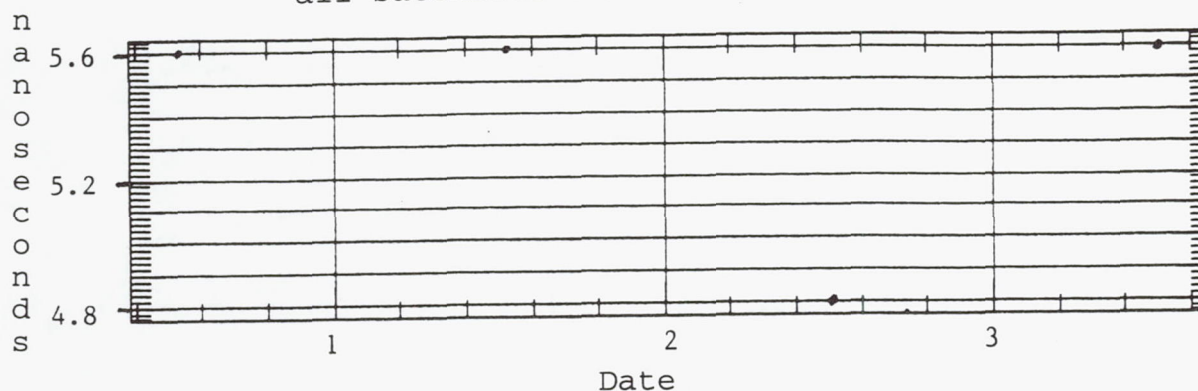


Figure 4                      Receiver Altitude Coordinate Offset  
each satellite observation averaged independently

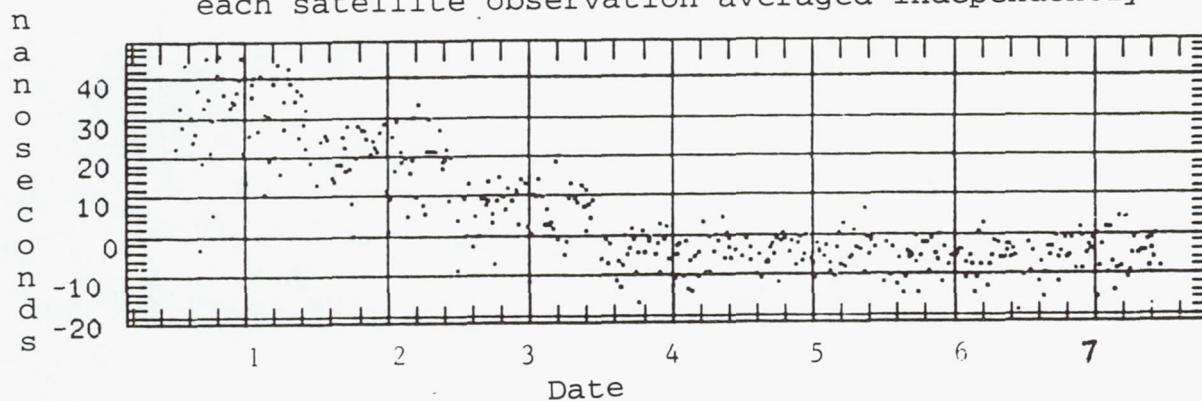


Figure 5                      Theoretical minus Experimental Results  
each satellite observation averaged independently

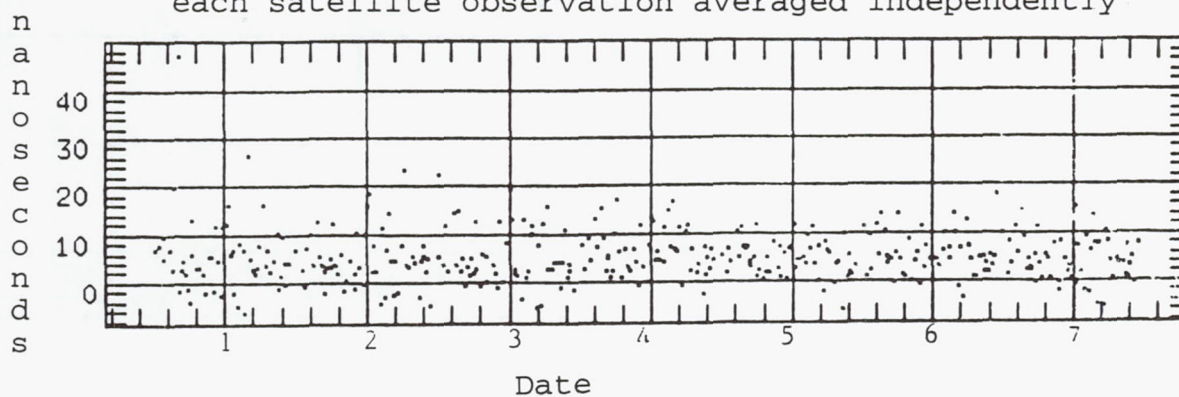




Figure 6

Theoretical minus Experimental Results  
all satellite observations averaged daily

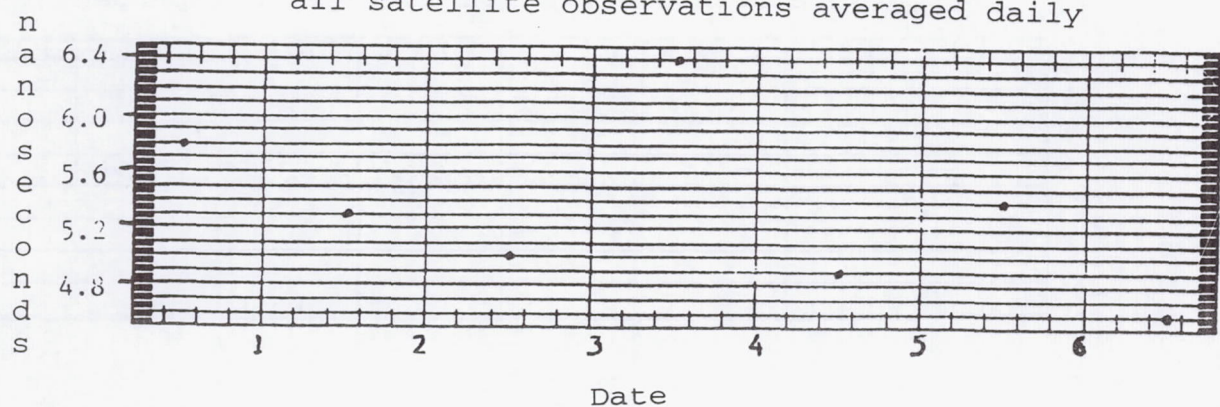


Figure 7

Theoretical minus Experimental Results  
each satellite observation averaged independently

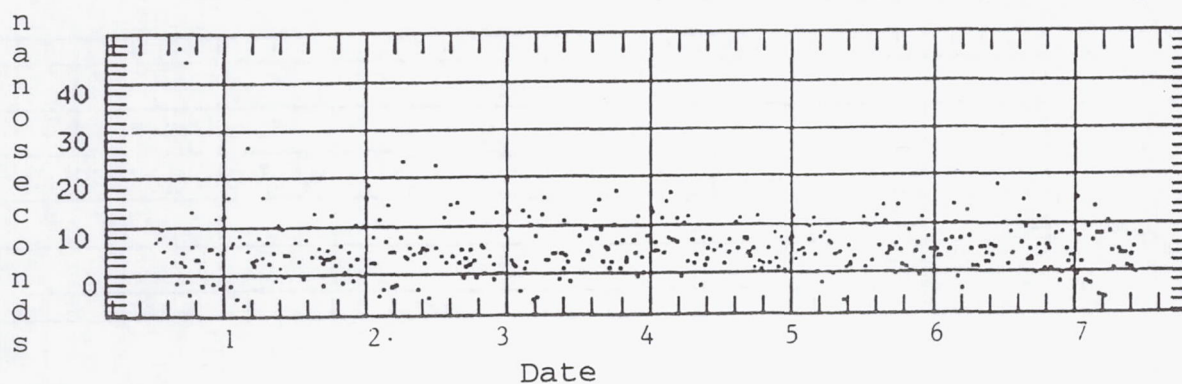


Figure 8

Theoretical minus Experimental Results  
all satellite observations averaged daily

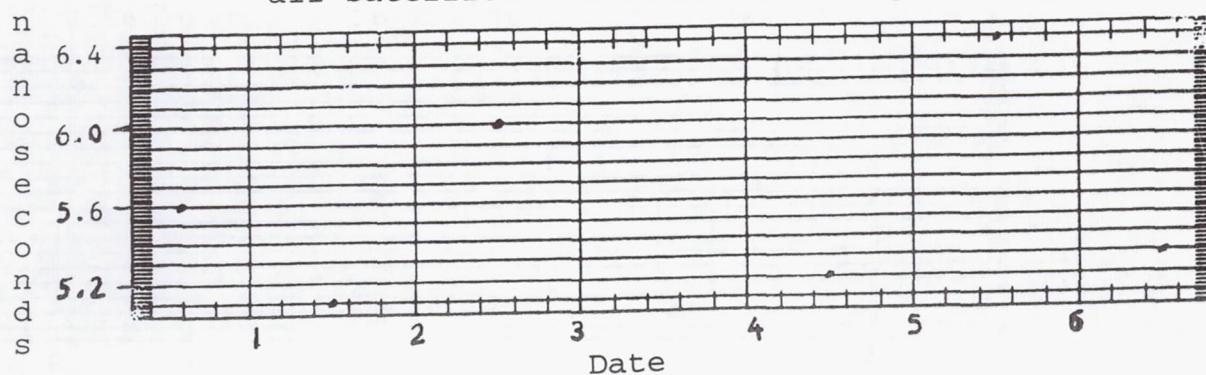


Figure 9

Receiver Longitude Coordinate Offset  
each satellite observation averaged independently

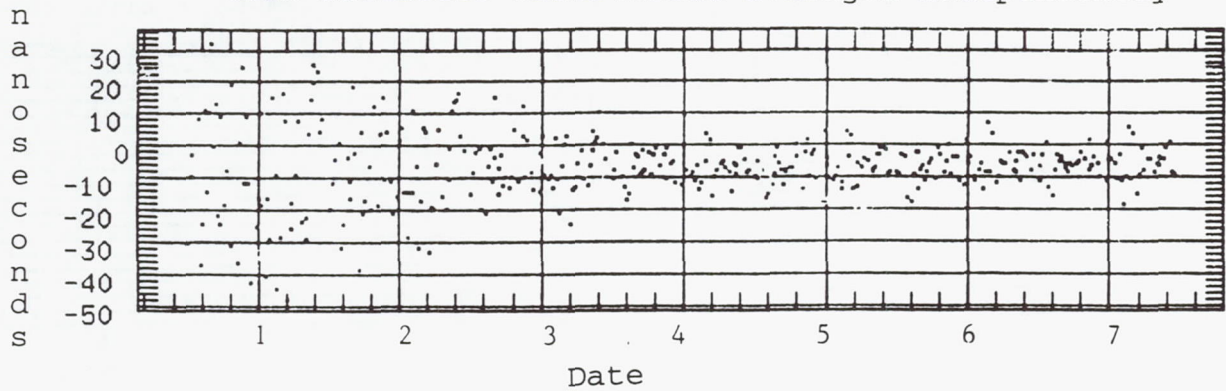


Figure 10

Theoretical minus Experimental Results  
each satellite observation averaged independently

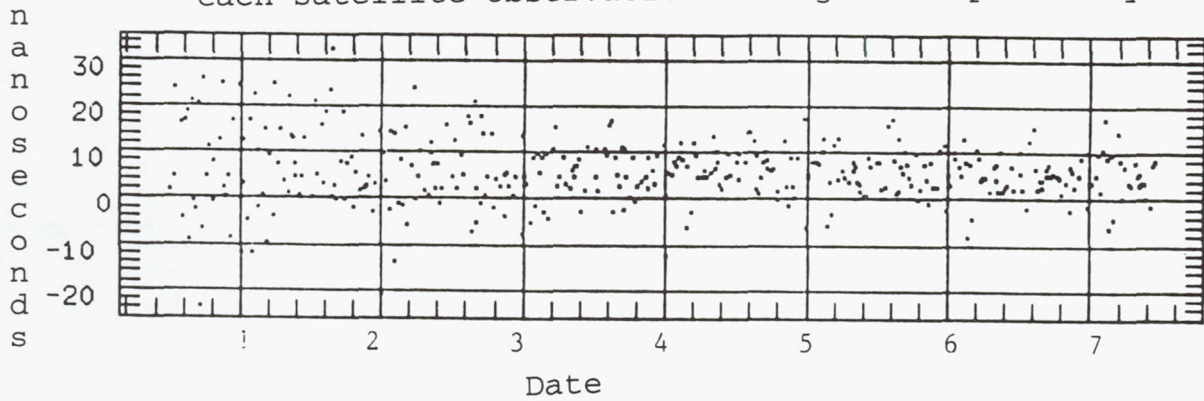
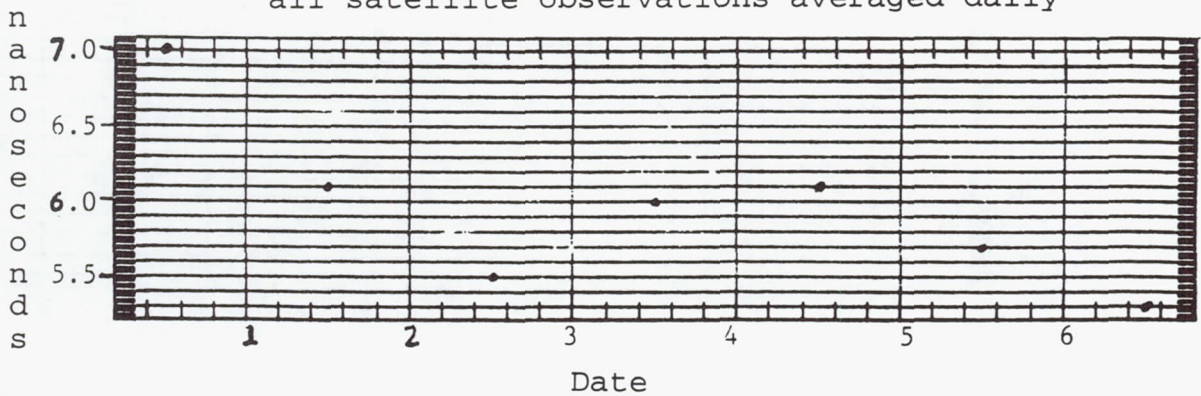


Figure 11

Theoretical minus Experimental Results  
all satellite observations averaged daily





## Questions and Answers

**WLODZIMIERZ LEWANDOWSKI (BIPM):** The receivers you had compared, they had exactly the same software or were they different?

**HAROLD A. CHADSEY (USNO):** These were two identical receivers running the same software and firmware internally.

**WLODZIMIERZ LEWANDOWSKI (BIPM):** The differences were not coming, for example, anomalies from the software?

**HAROLD A. CHADSEY (USNO):** It definitely wasn't a problem of one was a TrueTime receiver and one was an S-TEL or something like that. There is a slight possibility that there may have been a small fractional difference in the software. But in talking with the manufacturer, they said that those two receivers had the same software and same firmware versions in them. And when they left the factory, they were calibrated.

# COMMON VIEW TIME TRANSFER USING WORLDWIDE GPS AND DMA MONITOR STATIONS

Wilson G. Reid  
Thomas B. McCaskill  
Orville J. Oaks  
U.S. Naval Research Laboratory  
Washington, DC 20375-5000

James A. Buisson  
Hugh E. Warren  
SFA, Inc.

## Abstract

*Analysis of the on-orbit Navstar clocks and of the GPS monitor station reference clocks is performed by the Naval Research Laboratory using both broadcast and postprocessed precise ephemerides. The precise ephemerides are produced by the Defense Mapping Agency (DMA) for each of the GPS space vehicles from pseudo-range measurements collected at five GPS and at five DMA monitor stations spaced around the world. Recently, DMA established an additional site co-located with the U.S. Naval Observatory precise-time site. The time reference for the new DMA site is the DoD Master Clock. Now, for the first time, it is possible to transfer time every 15 minutes via common view from the DoD Master Clock to the 11 GPS and DMA monitor stations. The estimated precision of a single common-view time transfer measurement taken over a 15-minute interval was between 1.4 and 2.7 nanoseconds. Using the measurements from all Navstar space vehicles in common view during the 15-minute interval, typically 3-7 space vehicles, improved the estimate of the precision to between 0.65 and 1.13 nanoseconds. The mean phase error obtained from closure of the time transfer around the world using the 11 monitor stations and the 25 space vehicle clocks over a period of 4 months had a magnitude of 31 picoseconds. Analysis of the low-noise time transfer from the DoD Master Clock to each of the monitor stations yields not only the bias in the time of the reference clock, but also focuses attention on structure in the behavior of the reference clock not previously seen. Furthermore, the time transfer provides a uniformly sampled database of 15-minute measurements that makes possible, for the first time, the direct and exhaustive computation of the frequency stability of the monitor station reference clocks. To lend perspective to the analysis, a summary is given of the discontinuities in phase and frequency that occurred in the reference clock at the Master Control Station during the period covered by the analysis.*

## BACKGROUND

The initial work of transferring time by means of a satellite clock between points widely separated on the Earth's surface was demonstrated by Easton<sup>[1]</sup>, who obtained an average time-transfer

<sup>1</sup>This work was sponsored by the GPS Joint Program Office.



time-transfer accuracy to 120 nanoseconds between sites in the continental U.S. Easton *et al.*[3], using the TIMATION II satellite, transferred time between the U.S. Naval Observatory and the Royal Greenwich Observatory with an accuracy of 270 nanoseconds. Buisson *et al.*[4], using the Navigation Technology Satellite NTS-1 in a 7500 nautical-mile orbit, obtained in common-view mode for three closely spaced monitor sites a closure with a mean phase error of 9 nanoseconds and an rms phase error of 43 nanoseconds. Time was also transferred to England and to Australia with an accuracy of 240 and 700 nanoseconds respectively. Allan *et al.*[5], using four Navstar satellites in 10000 nautical-mile orbits and three timing centers in Boulder, Colorado, in Braunschweig, Germany, and in Tokyo, Japan, transferred time in a common-view mode over a 3-month period and obtained a mean phase error upon closure of 5.2 nanoseconds. Using measurements of ionospheric delays, precise ephemerides from DMA, and a consistent set of antenna coordinates, Lewandowski *et al.*[6] achieved time transfer over intercontinental distances by the GPS common-view method with a precision of 2 nanoseconds by averaging several measurements over a day. Around-the-world closure using three intercontinental links was verified to within a few nanoseconds.

## INTRODUCTION

Prior to establishment at the U.S. Naval Observatory (USNO) of the new DMA monitor station, time transfer via the common-view method<sup>2</sup> from the DoD Master Clock to a GPS monitor station, for use in analysis of the performance of the monitor station time reference, was limited by a number of factors. For example, measurements<sup>2</sup> of the offset of the space vehicle clocks from the DoD Master Clock were obtained from a linear least-squares fit to 13 minutes of six-second phase-offset measurements, and these measurements were nominally timed according to a schedule issued by the Bureau International des Poids et Mesures (BIPM) for establishment of International Atomic Time (TAI). Although this schedule was adequate for the purpose intended, the number of measurements was sparse compared to those taken by the other monitor stations, which made observations every 15 minutes during each pass of the space vehicle. Moreover, these measurements utilized the broadcast ephemeris, and the receiver operated for some period of time on a single frequency requiring use of the ionospheric model broadcast in the navigation message. Measurements made by the monitor stations, on the other hand, were synchronized to GPS system time and were scheduled every 15 minutes. The phase offset was obtained using post-fit precise ephemerides supplied by DMA, and the receivers operating at dual frequencies measured the ionospheric delay. The dissimilarity in the nature of the measurements made by the Naval Observatory compared to those made by the ten monitor stations and the lack of synchronization of the Naval Observatory measurements with those made by the other monitor stations introduced significant error. But most limiting was the sparse number of measurements made by the Naval Observatory, resulting in a single raw estimate of the time transfer at a given time.

## TIME TRANSFER

While the time reference for both the DMA site in Washington, D.C., and the Naval Observatory precise-time site is the DoD Master Clock, as expected there is considerable difference in the time transfer from each of these sites. Figure 1 is a plot of the time transfer from the Naval Observatory to the Colorado Springs monitor station for the first ten hours of Thursday, 1 June 1995. Immediately obvious is the lack of multiple estimates of the time transfer at the

---

<sup>2</sup>All measurements utilized in this study were corrected for Selective Availability.



measurement times even though, during the ten hours shown, there were between five and seven Navstar space vehicles in common view. So sparse was the measurement schedule that as few as two measurements were made from 0500 to 0600. In addition to the paucity of the estimates, there is considerable scatter in the measurements, as evidenced by a standard deviation of 11 nanoseconds.

Using the DMA site in Washington, D.C., which made synchronized measurements every 15 minutes, produced the raw estimates of the time transfer to the Colorado Springs monitor station shown in Figure 2. Here the number of simultaneous measurements—indicative of the number of Navstar space vehicles in common view—varied between five and seven. If the noise in the raw measurements for a specified measurement time were white, the optimum estimator of the time transfer at that time would be the sample mean. Figure 3 is a plot of the sample mean at each of the measurement times over the 10-hour time span. If the sample mean in Figure 3 is subtracted from the raw measurements in Figure 2, the plot of the measurement noise shown in Figure 4 is obtained. Doing this for the 4 months from 1 June 1995 to 1 October 1995 results in the time transfer and the corresponding measurement noise shown in Figures 5 and 6. In Figure 5 the frequency offset of the Colorado Springs time reference from the DoD Master Clock has been removed to emphasize the detailed behavior of the reference clock. An appreciation for the stability of the time transfer using the DMA site in Washington, D.C., can be had by examining the comparison in Figure 7 of the time transfer to Colorado Springs from both the DMA site in Washington, D.C. (dark trace) and the Naval Observatory (scattered dots) for the same 4 months.

## MEASUREMENT STATISTICS

The histogram in Figure 8 shows the measurement noise for the Washington, D.C., to Colorado Springs link to be predominantly normal. In Figure 9 the normalized integrated periodogram of the measurement noise lies well within the 95 percent Kolmogoroff-Smirnov<sup>[8]</sup> confidence interval, supporting the hypothesis that the noise is white, or uncorrelated.

To estimate the precision of the time-transfer measurement requires computation of the standard deviation of the distribution of the sample mean—the sample being the 5–7 raw time transfer measurements made during the same 15-minute interval. If the measurements in the sample are independent and identically distributed random variables, the standard deviation of the sample mean will be the standard deviation of the population from which the sample was taken reduced by  $1/\sqrt{n}$ , where  $n$  is the number of measurements in the sample. The number of noise measurements ( $n_{noise}$ ) in Figure 6 was 59497. The number of estimates ( $n_{mean}$ ) of the time transfer obtained by taking the mean of each sample of raw measurements at the measurement times was 10364. Dividing the two yields  $n_{sample} = 5.74$  for the average size of the samples for which the mean was found. With the standard deviation of the measurement noise  $\sigma_{noise} = 2.67$  nanoseconds, the standard deviation of the sample mean is

$$\sigma_{mean} = \frac{\sigma_{noise}}{\sqrt{n_{sample}}} = 1.1 \text{ ns.}$$

The same analysis was performed for the other ten links and the results summarized in Table 1. It is interesting to note that the two links involving Colorado Springs show the least precision even though the reference clock at Colorado Springs was an HP5071 high-performance cesium beam tube. In addition, the reference clock at the DMA Washington site was a hydrogen maser steered by a very large ensemble of atomic clocks. The fact that the noise on the Washington-to-Quito link is considerably lower establishes Colorado Springs as the problem.



Of the 11 links, eight had subnanosecond measurement precision. The link between Hawaii and Kwajalein Island showed the greatest precision at 650 picoseconds.

*Table 1*  
SUMMARY OF TIME TRANSFER  
BETWEEN ADJACENT PAIRS OF MONITOR STATIONS  
1 June 1995 to 1 October 1995

Link	$n_{noise}$	$n_{mean}$	$n_{sample}$	$\sigma_{noise}$ (ns)	$\sigma_{mean}$ (ns)
CSP--WAS	59497	10364	5.74	2.67	1.11
HAW--CSP	49470	10554	4.71	2.46	1.13
KWJ--HAW	60369	10688	5.65	1.40	0.65
SMF--KWJ	47509	10633	4.47	1.49	0.70
DGI--SMF	33268	9717	3.42	1.52	0.82
BAH--DGI	49671	9928	5.00	1.86	0.83
ENG--BAH	47884	10766	4.45	2.12	1.01
ASC--ENG	40855	10234	3.99	1.55	0.78
ARG--ASC	49258	10852	4.54	1.43	0.67
QUI--ARG	57927	11348	5.10	1.81	0.80
WAS--QUI	53269	11149	4.78	1.66	0.76

The time transfer links listed in the table utilized the five GPS monitor stations in Colorado Springs (CSP), Hawaii (HAW), Kwajalein Island (KWJ), Diego Garcia Island (DGI), and Ascension Island (ASC), and the six DMA monitor stations in Washington, D.C. (WAS), Smithfield, Australia (SMF), Bahrain (BAH), England (ENG), Argentina (ARG), and Quito, Ecuador (QUI).

## ANOMALY DETECTION

Previous to the availability of the uniformly sampled database of 15-minute low-noise time transfer measurements between the DoD Master Clock and a monitor station, analysis of an anomaly in the behavior of the monitor station time reference relied upon the 15-minute measurements made during a pass of a Navstar space vehicle over the monitor station. While voids between passes could be filled in with observations from other space vehicles, always the analysis was hampered by the behavior of the less stable Navstar clock.

Figure 10 is a plot of the residuals of a linear fit to the phase offset of several Navstar clocks from the Colorado Springs reference clock and the Colorado Springs reference clock from the DoD Master Clock. The bottom trace was obtained from time-transfer measurements. A 7-nanosecond break is clearly visible in the low-noise time-transfer measurements. The break in the time transfer was traced to initialization of the Colorado Springs monitor station. The break was not detectable in the measurements from Navstar 13 and Navstar 29 because it occurred between passes of the space vehicles over the monitor station. The break, on the other hand, occurred during the time the Navstar 20 and the Navstar 36 space vehicles were in view of the monitor station. While the evidence of a break in the time-transfer measurements is compelling, such a small break in the phase offset of the Navstar clocks from the monitor station

reference clock is much more difficult to detect. It was only a review of these time-transfer measurements that revealed the anomaly.

Figure 11 presents the time-transfer measurements—the mean of the raw measurements at each measurement time—between the time reference at the Hawaii monitor station and the DoD Master Clock for the month of August. The abrupt changes in the slope of the phase reflect repetitive breaks of  $2 \text{ pp}10^{13}$  in the frequency of the Hawaii time reference, which was an HP5061 cesium beam tube. Such breaks in the frequency of an HP5061 are not unusual, and a review of the operations log for the monitor station revealed no switching of frequency standards during this time.

In Figure 12 is plotted the behavior of the Colorado Springs time reference for 5 days in July. The data were smoothed by a moving average filter to reduce the short-term noise. Immediately apparent is a 12-hour periodic component. It needs to be emphasized that the peak-to-peak variation of 2 nanoseconds would have been difficult to detect in the observations by the monitor station of any of the Navstar space vehicle clocks.

## DATA CORRECTIONS

A summary is given in Table 1 of the corrections that were made to the data from the Colorado Springs monitor station during the period covered by the analysis. That there were no breaks in the frequency is not surprising, since the time reference for the entire period was never switched from the single HP5071 cesium clock. Each of the breaks in phase requiring correction were confirmed to have been the result of actions taken by the Master Control Station. The corrected data, except for a constant bias, represent what would have been the unperturbed behavior of the reference clock.

*Table 2*  
**DATA CORRECTIONS**  
Colorado Springs Monitor Station  
1 June 1995 to 1 October 1995

(date)	Time (hour)	(MJD)	Phase (ns)	Frequency ( $\text{pp}10^{14}$ )
06 JUN 95	1607	49874.67188	94	0
14 JUN 95	1700	49882.70834	-446	0
12 JUL 95	1707	49910.71354	-238	0
25 AUG 95	1552	49954.66146	-155	0
25 AUG 95	1800	49954.75000	-7	0
14 SEP 95	1622	49974.68229	-10	0

## FREQUENCY STABILITY

The time transfer provides a uniformly sampled database of 15-minute measurements, which makes possible for the first time the direct and exhaustive computation of the frequency stability of the monitor station reference clocks. Figure 13 is a plot of the frequency-stability profile for the time reference at Colorado Springs for sample times of 15 minutes to 12 days. By exhaustive calculation is meant that the frequency stability is calculated for every multiple of



the basic sample interval of 15 minutes up to the maximum sample time. The maximum sample time is limited to one-tenth of the time spanned by the measurements to ensure meaningful confidence limits on the estimates of the stability.

Superimposed on the plot is a solid line corresponding to the Allan deviation of simulated white phase noise with a standard deviation of 1 nanosecond, which was approximately the estimated deviation of the sample means (Figure 5) of the raw time-transfer measurements. This might be expected to represent a floor below which the estimates of the stability would not fall. That the stability for 15 minutes does fall slightly below this line suggests that the estimate of 1 nanosecond for the precision of the time-transfer measurements without smoothing is a conservative one.

The stability for a sample time of one day is  $3 \text{ pp}10^{14}$  which is the upper bound on the specification<sup>[9]</sup> of the HP5071A high-performance cesium beam tube. While the specified upper bound on the flicker floor for this frequency standard is  $2 \text{ pp}10^{14}$ , at 12 days the Colorado Springs time reference had a stability of  $5 \text{ pp}10^{15}$  and had not yet reached the flicker floor.

Of particular interest is an oscillation with a period of 3 hours which is clearly visible in the stability profile. The oscillation was only visible in the stability profile for the reference clocks at the Colorado Springs and the Smithfield, Australia, monitor stations. The source of the oscillation is under investigation.

## CLOSURE

The path indicated in Figure 14 for calculating closure of the time transfer was chosen to minimize the distance between station pairs. Figure 15 is a plot of the time transfer from the DMA site in Washington, D.C., to the same site using the ten intervening GPS and DMA monitor stations and the 25 Navstar space vehicle clocks over a period of 4 months. The periods of missing data are the cumulative effect of outages at the various monitor stations. No smoothing of the data was done. While there were almost one million measurements in the analysis, only five were purged as statistical outliers. The magnitude of the mean phase error obtained from closure of the time transfer around the world measured 31 picoseconds. Figure 16, which is a history of the magnitude of the mean phase error of closure for time transfer around the world, shows an almost linear trend with time.

## CONCLUSIONS

Now, for the first time, it is possible to transfer time every 15 minutes via common view from the DoD Master Clock to the 11 GPS and DMA monitor stations. The estimated precision of a single common-view time-transfer measurement taken over a 15-minute interval was between 1.4 and 2.7 nanoseconds. Using the measurements from all Navstar space vehicles in common view during the 15-minute interval, typically 3–7 space vehicles, improved the estimate of the precision to between 0.65 and 1.13 nanoseconds. With the uniformly sampled database of 15-minute measurements afforded by the time transfer, it is also possible for the first time to directly and exhaustively calculate the stability of the time reference for each of the monitor stations—the exhaustive calculation in one case leading to detection of systematics that would otherwise have been missed. The uniformly sampled database of low-noise time-transfer measurements provides a very sensitive analysis tool for detecting anomalous behavior in the monitor station clocks. Finally, closure of the time transfer around the world was achieved



with an error of 31 picoseconds.

## REFERENCES

- [1] R.L. Easton 1972, "The role of time/frequency in Navy navigation satellites," *Proc. IEEE*, 60, pp. 557-563.
- [2] J.A. Buisson, D.W. Lynch, and T.B. McCaskill 1973, "Time transfer using the TIMATION II satellite," NRL Report 7559 (Naval Research Laboratory, Washington, D.C.).
- [3] R.L. Easton, D.W. Lynch, J.A. Buisson, and T.B. McCaskill 1974, "International time transfer between the U.S. Naval Observatory and the Royal Greenwich Observatory via the TIMATION II satellite," NRL Report 7703 (Naval Research Laboratory, Washington, D.C.).
- [4] J.A. Buisson, T.B. McCaskill, T.B., H. Smith, P. Morgan, and J. Woodger 1977, "Precise worldwide station synchronization via the Navstar GPS Navigation Technology Satellite (NTS-1)," Proceedings of the 8th Annual Precise Time and Time Interval (PTTI) Applications and Planning Meeting, 30 November-2 December 1976, Washington, D.C., pp. 55-84.
- [5] D.W. Allan, D.D. Davis, M. Weiss, A. Clements, B. Guinot, M. Grandveaud, K. Dorenwendt, B. Fischer, P. Hetzel, S. Aoki, M. Fujimoto, L. Charron, and N. Ashby 1985, "Accuracy of international time and frequency comparisons via Global Positioning System satellites in common-view," *IEEE Trans. Instr. Meas.*, IM-34, pp. 118-135.
- [6] W. Lewandowski, G. Petit, and C. Thomas 1992, "Accuracy of GPS time transfer verified by closure around the world," Proceedings of the 23rd Annual Precise Time and Time Interval (PTTI) Applications and Planning Meeting, 3-5 December 1991, Pasadena, California, pp. 331-339.
- [7] D.W. Allan, and M.A. Weiss 1980, "Accurate time and frequency transfer during common-view of a GPS satellite," Proceedings of the 34th Annual Symposium on Frequency Control, 28-30 May 1980, Ft. Monmouth, New Jersey, pp. 334-346.
- [8] G.M. Jenkins, and D.G. Watts 1968, *Spectral Analysis and Its Applications*, (Holden-Day, San Francisco), pp. 234-237.
- [9] "Operating and programming manual HP 5071A primary frequency standard," 1st ed., September 1993, Manual Part No. 05071-90025 (Hewlett-Packard Company, Santa Clara Division, 5301 Stevens Creek Boulevard, Santa Clara, California 95052-8059), p. 6-2.



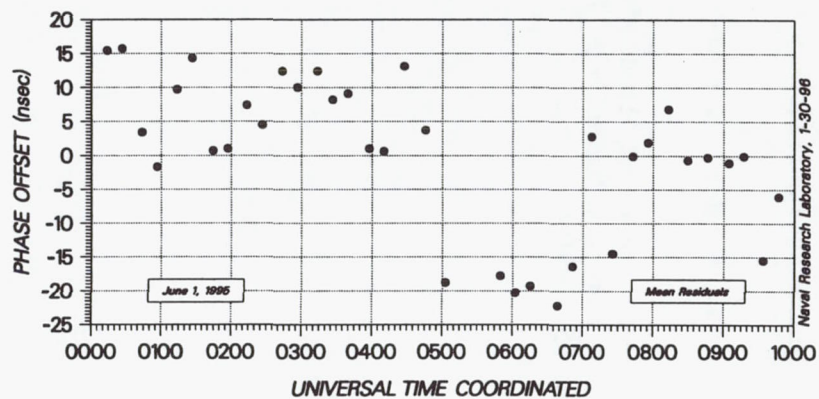


Figure 1

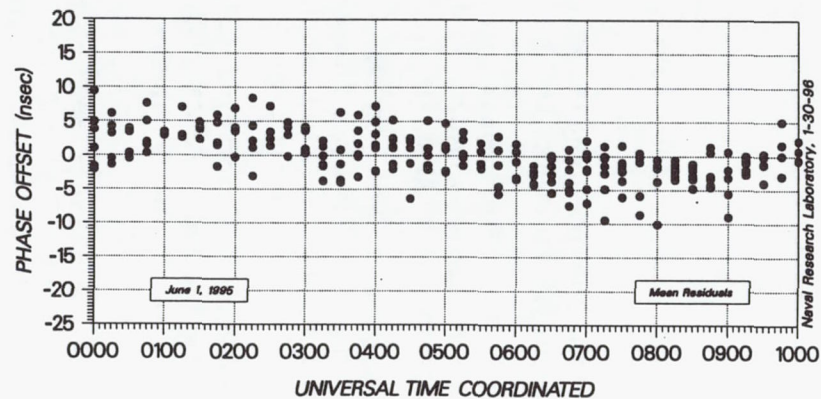


Figure 2

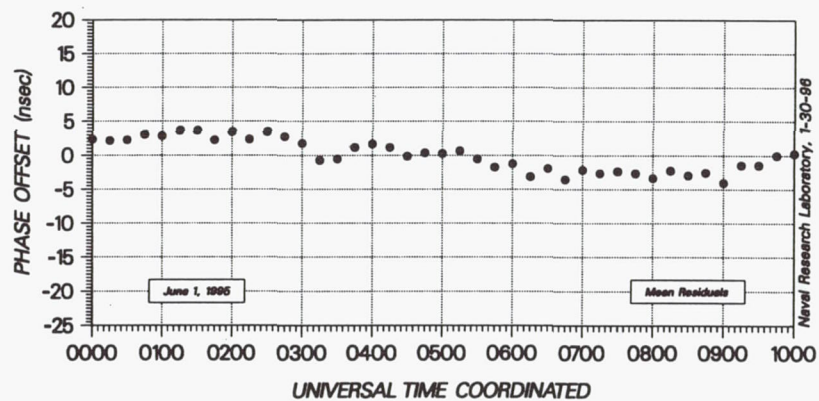


Figure 3

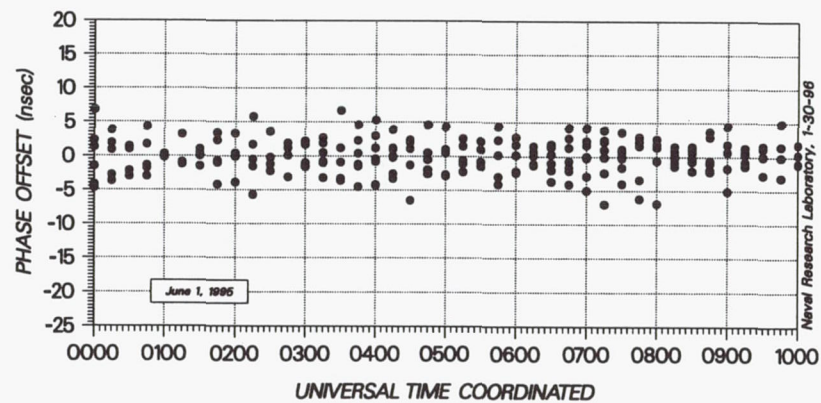


Figure 4

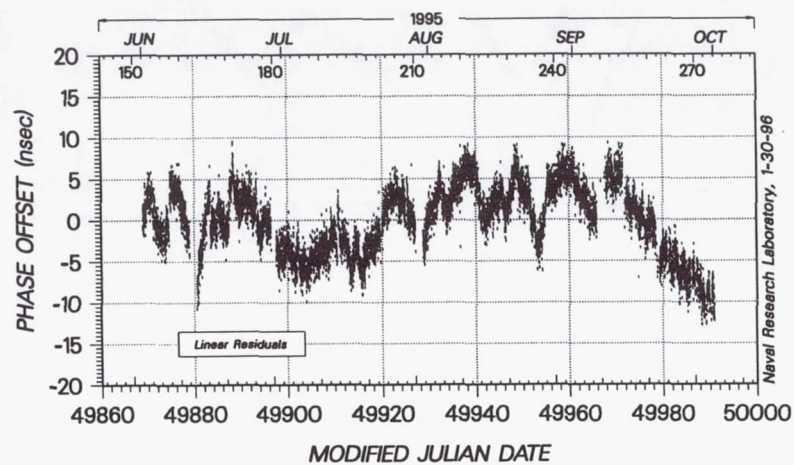


Figure 5

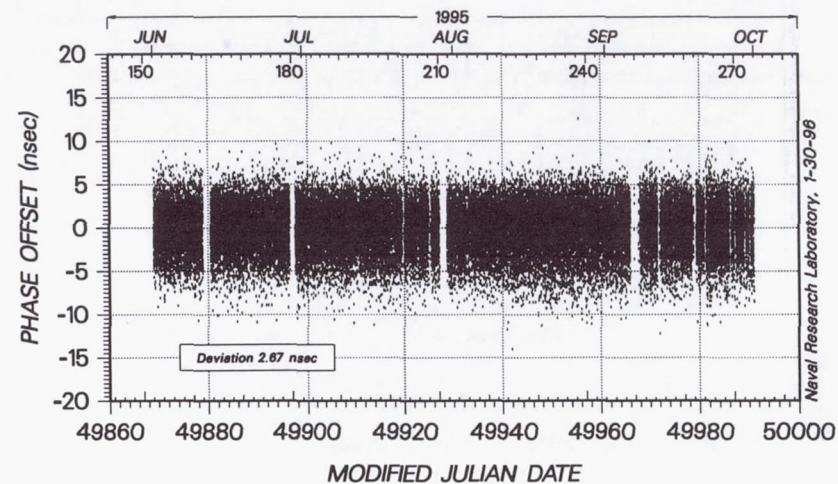


Figure 6

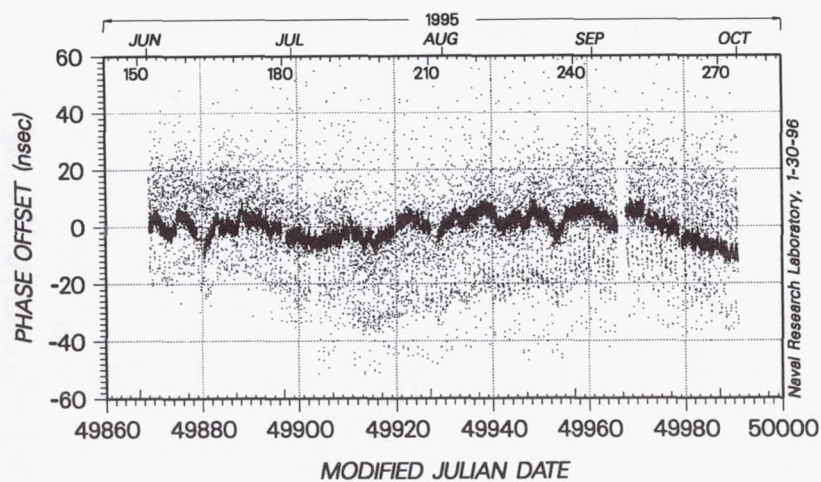


Figure 7

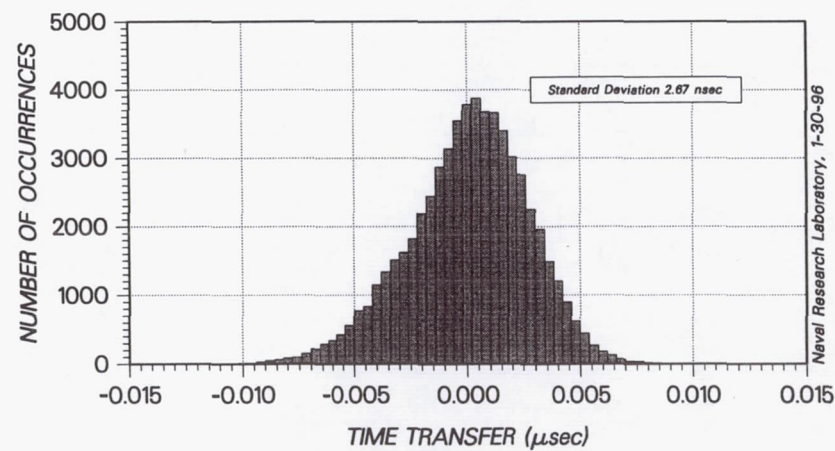


Figure 8



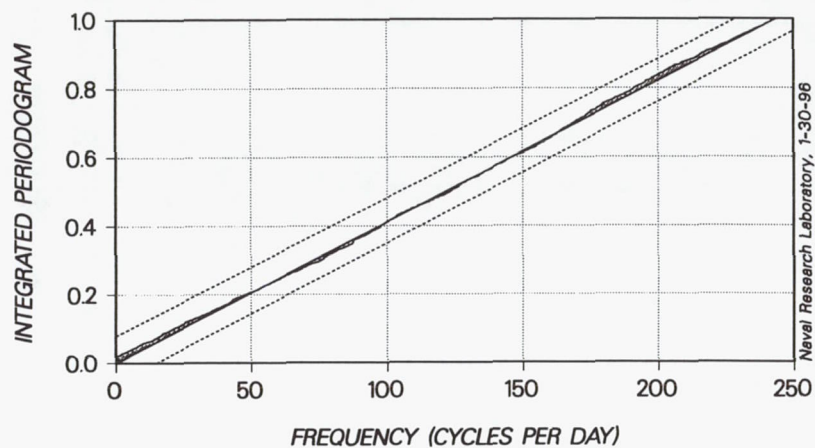


Figure 9

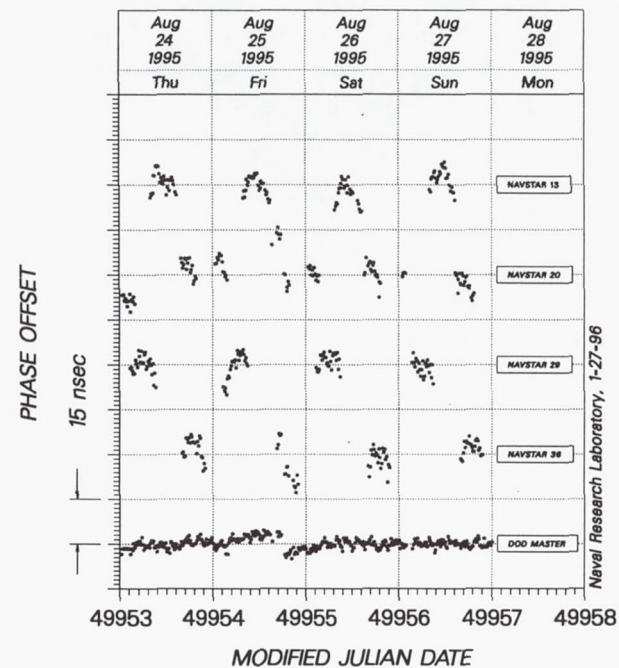


Figure 10

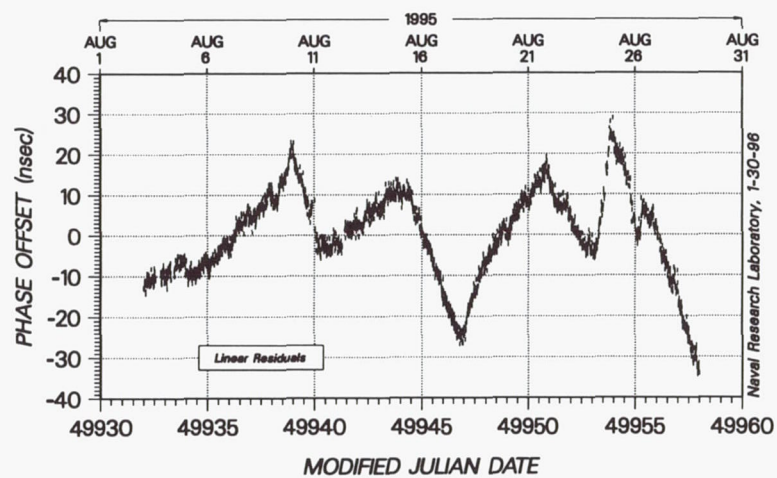


Figure 11

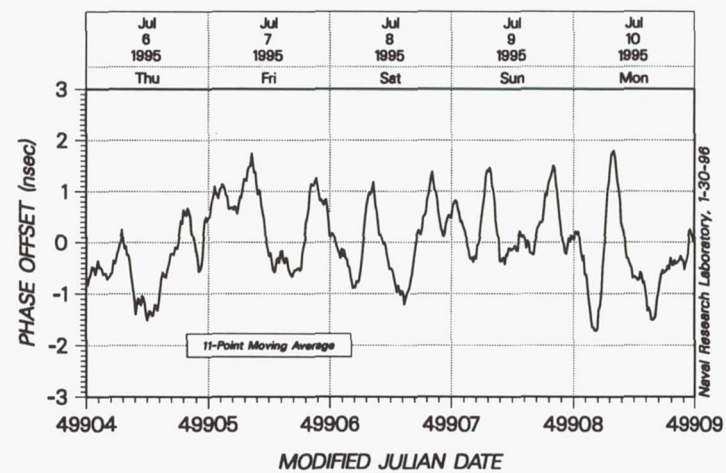


Figure 12

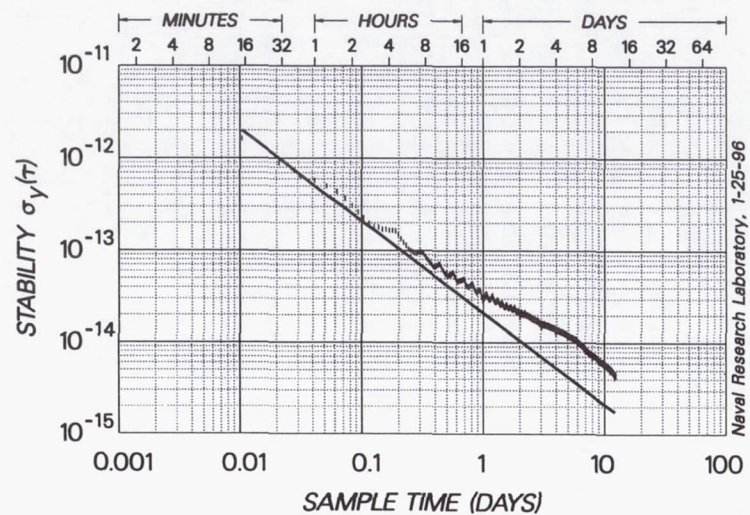


Figure 13

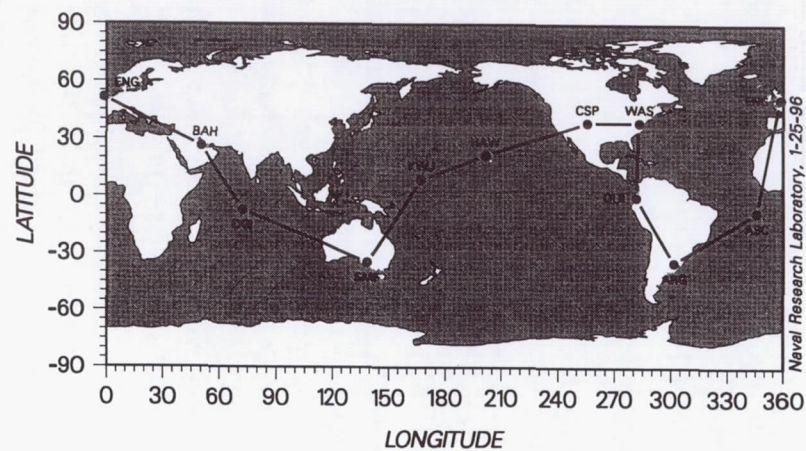


Figure 14

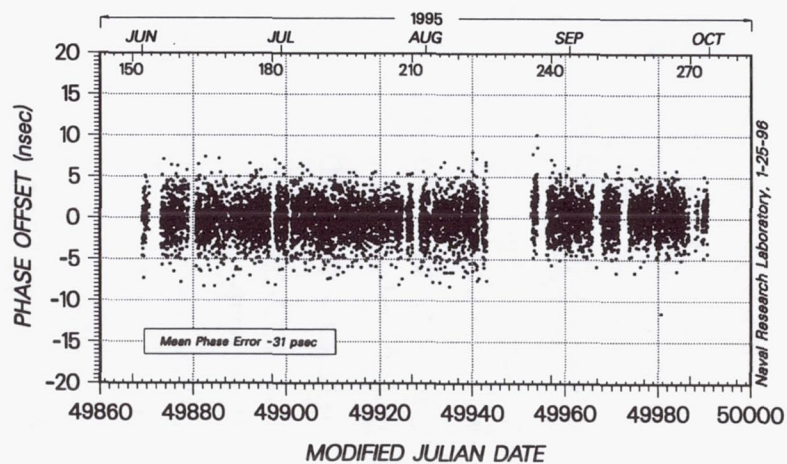


Figure 15

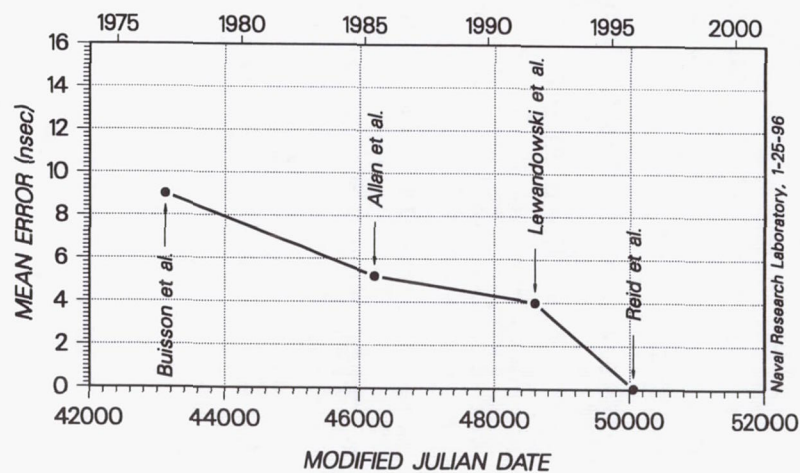


Figure 16



## Questions and Answers

**CAPT. STEVEN HUTSELL (USAF):** If you could, could you put up the plot of the Diego Monitor Station, rather the Hawaii Monitor Station? No, the plot that led you to conclude that there were frequency standard swaps being performed at Hawaii Monitor Station.

**WILSON G. REID (NRL):** You mean Kwajalein. Right here?

**CAPT. STEVEN HUTSELL (USAF):** Yes. I'm trying to find out if you have any additional information that would lead you to believe that there are actually frequency standard swaps occurring. Because, I can tell you that unless the site folks are doing something they're not telling us about, we did not swap any frequency standards at Hawaii that often, let alone that many times, over the course of the summer.

My conclusion, or I surmise from this that we've actually had a very chronic problem over this past year, not with Hawaii, but also — in fact, the reason why I said "Diego" earlier — with very huge changes in frequency which we can't absolutely pinpoint because we're not out at the site. We do know that Diego, for example, has experienced temperature changes within the timing rack on the order of tens of degrees. Whether it's a very good performing cesium frequency standard or not, that 25-degree temperature change will affect the frequency output. I'm wondering if you would agree that that would be the most likely cause of this.

**WILSON G. REID (NRL):** As I go back and look, if we examine the file that we've been sent in the past of special events which affect what we see, sometimes for these monitor sites we would switch to Frequency Standard One, switch to Frequency Standard Two; and then again switch to Frequency Standard Two, which indicates that maybe in the log the switching back to One was left out.

So I don't know. Sure, you do. So if you tell me that no switches were made, I believe you. But without having that information, I assume that they might have been clock switches.

**CAPT. STEVEN HUTSELL (USAF):** Oftentimes those logs will include times when the operator will re-select the frequency standard that it's intended to be on. Oftentimes, when we perform an initial program load, what we call an "IPL," of the site, sometimes the Series I computer will automatically switch to One. In many cases, the operator will need to immediately re-select the frequency standard that we desire it to be on. And I can safely say we have not had any scheduled frequency standard swaps nearly that often over that time period. If there were any frequency standard swaps, they were unauthorized.

**DR. GERNOT WINKLER (USNO, RETIRED):** Can I make a comment to that? This is a 5061 standard?

**WILSON G. REID (NRL):** Yes, I believe so.

**DR. GERNOT WINKLER (USNO, RETIRED):** Some of those standards have a very great environmental sensitivity. It is entirely possible that it is due to environmental shocks.

Let me ask a question. Monitor station receivers, is it correct that DMA stations all have the Ashtech-12 channel?

**WILSON G. REID (NRL):** I believe that's what they have.

**DR. GERNOT WINKLER (USNO, RETIRED):** But the GPS monitor stations have the S-TEL monitor receiver.

**WILSON G. REID (NRL):** I think so.

**DR. GERNOT WINKLER (USNO, RETIRED):** So they are different receivers. In addition, you have the tremendous difference in performance between the 5071 in Colorado Springs and the 5061 in Hawaii.

**WILSON G. REID (NRL):** Oh, yes.

**DR. GERNOT WINKLER (USNO, RETIRED):** That is exactly the point, because you have been trying to preach for a number of years that they should be replaced.

**DAVID ALLAN (ALLAN'S TIME):** I would like to follow up on what Dr. Winkler said in terms of the environmental sensitivity of the 5061s. In fact, all commercial cesiums we studied when I was back at NIST, they all have temperature and humidity coefficients. And given the length of time over which you are seeing these frequency shifts, one would wonder about storm systems and humidity; that if in fact you plotted the humidity during that period, you might see a correlation with those frequency steps. Because, the humidity coefficients for the 5061, along with all other commercial standards, except for the 5071, are quite high.

**WILSON G. REID (NRL):** That's a good suggestion. We don't get that data, and I'm not sure — did I hear this morning that there's a problem with the sensors on the environment? I think that was mentioned this morning. So, it might be difficult to get that data, but it would certainly be useful.



# GPS/GLONASS TIME TRANSFER WITH 20-CHANNEL DUAL GNSS RECEIVER

P. Daly & S. Riley

CAA Institute of Satellite Navigation  
Department of Electronic and Electrical Engineering  
University of Leeds, Leeds LS2 9JT, United Kingdom

## Abstract

*One of the world's two global satellite navigation systems, GPS, is already fully operational (April 1994) and the other, GLONASS, will become operational by the end of 1995 or early 1996. Each will offer, independently of the other, precise location and time transfer continuously anywhere in the world and indeed in space itself. Many potential users, in particular the civil aviation community, are keenly interested in a joint GPS/GLONASS operation since it would offer substantial advantages in defining and maintaining the integrity of the navigation aid. Results are presented on the characterisation of GPS/GLONASS time comparison using a 20-channel dual receiver developed & constructed at the University of Leeds, UK.*

## INTRODUCTION

GLONASS provides worldwide time dissemination and time transfer services in the same manner as Navstar GPS with both exhibiting substantial advantages over other existing timing services. Time transfer is both efficient and economic in the sense that direct clock comparisons can be achieved via GLONASS between widely separated sites without the use of portable clocks. Event time tagging can be achieved with the minimum of effort and users can reacquire GLONASS time at any instant due to the continuous nature of time aboard the satellites.

The first release from the Soviet Union of detailed GLONASS information occurred at the International Civil Aviation Organisation (ICAO) special committee meeting on Future Air Navigation Systems (FANS) in Montreal in May 1988. In full operation GLONASS, like GPS, will have 24 satellites in orbit, 8 satellites separated by 45 degrees in phase in each of three planes 120 degrees apart. Currently 22 GLONASS satellites are in full operation, 8 each in planes 1 and 3 and 6 in plane 2. In the event of no failures before the next triple launch planned for early December 1995, a full constellation will be available around the end of 1995.

## TIME FROM GPS/GLONASS

Time transfer from GPS/GLONASS is achieved in a straightforward manner. Each satellite transmits signals referenced to its own on-board clock. The Control Segment monitors the

satellite clocks and determines their offsets from the common GPS/GLONASS system time. The clock offsets are then uploaded to satellites as part of their transmitted data message. A user at a known location receives signals from a satellite and by decoding the data stream modulated on to the transmission, is able to obtain the position of the satellite, as well as the satellite's clock offset from the common system time. Hence the signal propagation time can be calculated at any instant. The time at which the signals are transmitted is also contained in the data message; by combining this with the propagation time and correcting first for atmospheric effects and other delays and then for the satellite's own clock offset, the user can effect transfer to GPS/GLONASS system time. Correction to an external time scale (such as UTC(USNO) or UTC(SU)) is then possible since the relevant offset is one of the transmitted data parameters. Any other user who has the same satellite visible is also able to transfer to the same common time scale.

## SATELLITE CLOCK OFFSETS

GLONASS clock offsets [1] are transmitted as part of each satellite's ephemeris data once every half-hour. The clock information arrives in the form of two parameters (i) the SV clock phase offset from GLONASS system time,  $a_0$  and (ii) the SV clock fractional frequency offsets from the GLONASS system reference,  $a_1$ . The clock offset  $a_2$ , the second rate of change of phase used in GPS, is not employed by GLONASS as the half-hour update makes this unnecessary. GLONASS does transmit one additional timing parameter — the phase offset between system time and its reference standard,  $A_0$ . This last offset is normally only updated once a day. There is again a parallel here between the two satellite navigation systems as GPS also transmits a phase offset between GPS system time and its reference standard, UTC(USNO).

## GPS/GLONASS TIME TRANSFER MEASUREMENTS

A series of tests<sup>[2]</sup> was conducted during November 1994 between UTC(LDS) and UTC(NPL) in the UK using dual, multi-channel GNSS receivers developed in the University of Leeds capable of simultaneous GPS and GLONASS code-phase time transfer. Position coordinates at the Leeds venue are known to better than 2 m while the National Physical Laboratory, UK (NPL) are certainly much better. The object of this test was to establish the degree to which time could be transferred between the two UTC references using first GPS and then GLONASS. Each receiver was synchronised to the local UTC reference and set to run for 24 hours continuously.

In the first instance the UTC reference was compared to satellite system time with each receiver operating independently in a non-differential mode. In this way the measurement made over a satellite pass of several hours duration would show up the totality of the systematic & random errors to which this kind of test is naturally subject. In the case of GPS the outstanding error source is "selective availability" (SA) as can readily be observed in Figure 1. The effect is displayed dramatically in this Figure — measured pseudo-range from PRN 4 corrected to refer to system time. In comparison results for the same test (see Figure 2) relating to GLONASS over an equally long satellite pass on the same day using GLONASS 1 (almanac slot 1) show



no SA effect, dispersion due to random noise and a clear linear slope deriving from the (small) frequency differences between the clocks involved. The increased level of noise at the beginning and end of the test results from effects experienced at very low satellite elevation.

Subtraction of the data sets taken at Leeds and NPL eliminates the common system time reference and most of the systematic errors in the measurement, including SA, satellite orbit & clock errors, local position and clock errors and the ionosphere. The results relating UTC(LDS) to UTC(NPL) are shown in Figure 3 (GPS) and Figure 4 (GLONASS) agreeing to about 1.5 ns with spreads of 4.4 and 7.0 ns respectively. Clearly there are other data sets whose mean values do not agree so closely as the set chosen.

## RELATIVITY CORRECTIONS in GLONASS

In an excellent discussion<sup>[3]</sup> on the effect of relativity corrections on GPS satellite signals, it is shown how both general and special relativity corrections are transmitted in the GPS data message so as to allow the user to correct ranging measurements. Due to the high stability of GNSS satellite on-board clocks, the relativistic variations are, in fact, larger than the effects of clock stability itself. Because of the effect of special relativity alone, clock oscillators have to be offset on the ground before launch, in the case of GPS, by  $-4.45 \times 10^{-10}$  in frequency. Including the effects of both special and general relativity, the time-varying component of relativity is shown to be as large as 45.8 ns for a GPS orbit with maximum eccentricity,  $e = 0.02$  (this orbital parameter expresses the non-circularity of the orbit).

It is a fact that GLONASS satellites have orbits which are normally more circular than GPS satellites. This means that the general relativity correction which depends on the distance of the satellite from the centre of the earth is smaller for GLONASS satellites than for GPS satellites simply because the distance variation is less. The combined relativistic effects are shown<sup>[3]</sup> to produce a variation in the satellite frequency with peak-to-peak fractional frequency linearly dependent on eccentricity ( $e$  small). The variation is cyclic with period the same as the orbital period with the minimum value occurring at time of perigee. The GLONASS satellite with the largest eccentricity was GLONASS 47 (channel 4) with  $e = 0.0060$ . The next largest eccentricity is  $e = 0.0038$  for GLONASS 48 (channel 13) — all other GLONASS satellites have  $e$  less than 0.0025. Calculation shows that the fractional frequency peak-to-peak change over an orbit amounts to 4.2 ps/s for GLONASS 47 and 2.6 ps/s for GLONASS 48. For all other satellites the magnitude of the effect is of the order of the clock frequency data resolution (0.9 ps/s) and is difficult to observe. The only satellite currently in action which exhibits the effect is GLONASS 76 ( $e = 0.0037$ ).

Since no relativistic corrections are transmitted by GLONASS in the data message, yet the corrections must be implicit in the ranging scheme, the question arises — how are the relativity terms included? We have found that the corrections are included directly in the phase and frequency offsets transmitted by GLONASS satellites. By logging GLONASS ephemerides (updated every half-hour) over a satellite pass with high elevation, it is possible to obtain values of clock phase and frequency offset over more than 5 hours, slightly less than half the orbital period. Should the observation interval coincide with the time which encompasses a minimum and maximum of the phase and frequency changes, it is possible to extract the peak-to-peak



values for an orbit. It is observed that the peak-to-peak values of a cyclic fractional frequency in GLONASS 47 are 4.5 ps/s (cf 4.2 ps/s) and for GLONASS 48 are 2.7 ps/s (cf 2.6 ps/s). It is also confirmed from satellite data that the minimum value of the relativistic fractional frequency correction occurs at the time of perigee. The cyclic effect is also clearly observed in residuals of the clock phase data transmitted by these satellites. It is concluded that relativistic corrections to GLONASS orbits are transmitted as phase and frequency corrections within the GLONASS data message and require no intervention on the part of the user.

When analysing GLONASS satellite clock data for the purpose of establishing estimates of clock stability, it is important to remove the effects of relativistic effects first; otherwise these corrections are interpreted as satellite clock instability.

## **FREQUENCY RE-USE & BAND RELOCATION**

Frequency re-use would involve antipodal satellites in the GLONASS system using the same transmit frequency. In this way satellites on opposite sides of the earth would not interfere with each other, allowing the entire space segment to be implemented with only 12 channels. One exception to this rule would be high-flying receivers on-board satellites attempting to use GLONASS for navigation purposes. However even in cases such as these, modern receiver techniques are sophisticated enough to distinguish between the two mutually-interfering signals. Currently (November 1995) 18 of the 22 operational satellites have a paired frequency allocation. The removal of the top 12 channels of GLONASS would reduce the required bandwidth by 6.75 MHz, saving spectrum where it is most needed – at the top of the band.

A second solution to the problems raised above would be to relocate the entire frequency band occupied by GLONASS down towards the GPS band. Between the lower edge of the current GLONASS band and upper end of the GPS band, there is already room for a shift of almost 12 MHz. With the anti-interference properties enjoyed by both GPS and GLONASS (spread-spectrum processing gain), there is room possibly for an even larger shift. The relocation solution has the potential to resolve all of the interference difficulties being met. This course of action as well as frequency re-use is currently under consideration by the GLONASS administration. Relocation of the frequency band would clearly have a large impact on receiver implementation, resulting in a major upheaval amongst current users of the system.

A “half-way” solution has also been suggested whereby GLONASS would use both frequency re-use and re-location by halving the number of channels used not by removing the top 12 channels but rather by removing the top 18 channels and adding 6 channels at the lower end of the spectrum. In this way, the “old” channel 1 at 1602.5625 MHz would become the “new” channel 7. The “new” spectrum would then extend from 1594 - 1610.5 MHz.

## **ACKNOWLEDGEMENTS**

The authors wish to thank the UK National Physical Laboratory for their support during the November 1994 GNSS time transfer tests between UTC(NPL) and UTC(LDS).



## REFERENCES

- [1] P. Daly & I. D. Kitching: *"Progress in transferring time using GLONASS satellites"*, Proceedings of the 21st Annual Precise Time & Time Interval (PTTI) meeting, Nov.28-30, 1989, Redondo Beach, pp.59-68.
- [2] S. Riley: *"Provisional GNSS results from November 1994 data collection at Leeds (UK), NPL (UK) and ESA/ESTEC(NL)"*, CAA ISN, University of Leeds report to National Physical Laboratory, 1994.
- [3] P. S. Jorgensen: *"Relativity correction in GPS user equipment"*, IEEE Plans'86, Las Vegas, pp. 177-183.

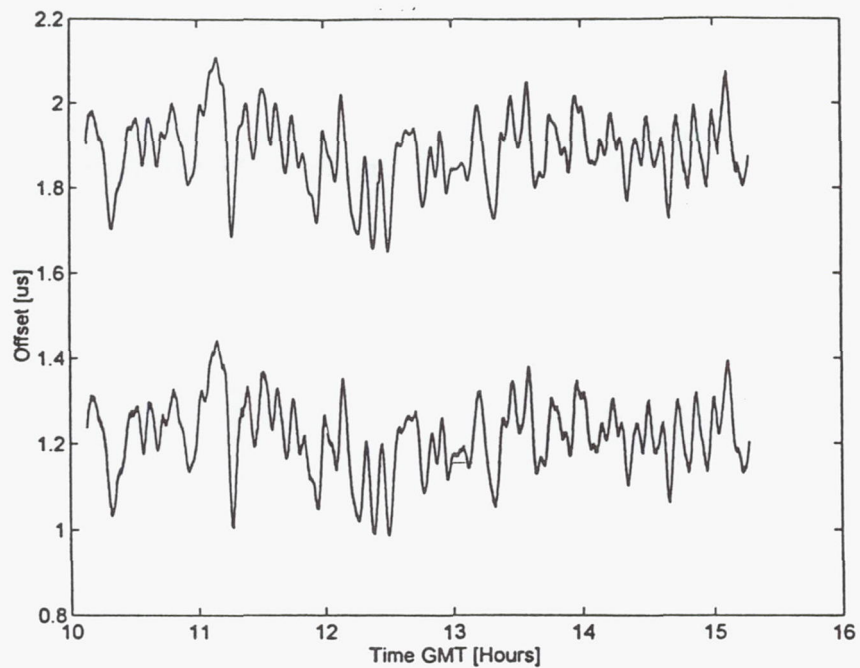


Figure 1: UTC(LDS) & UTC(NPL2) - GPS system time  
PRN 4 → 4 Nov '94

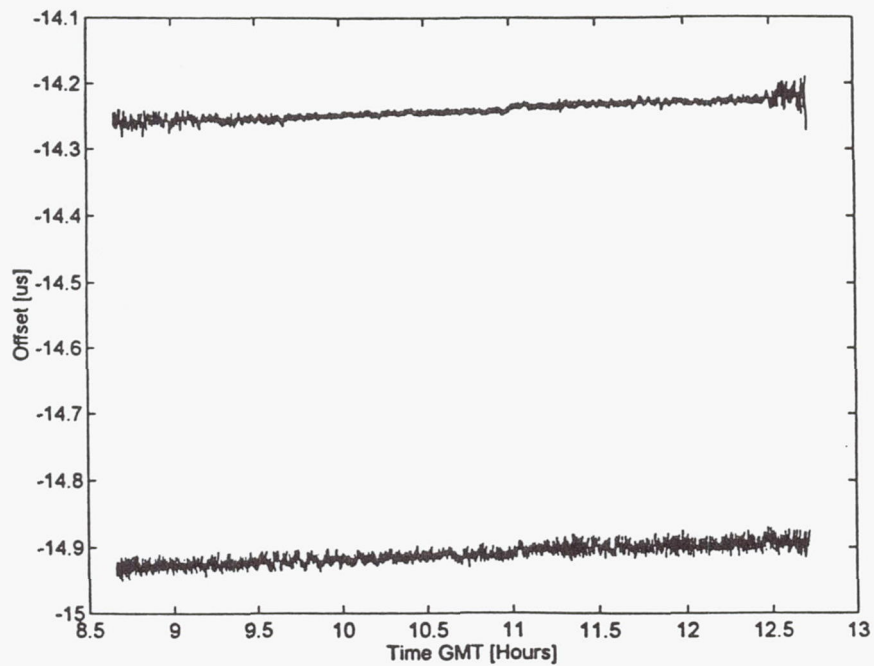


Figure 2: UTC(LDS) & UTC(NPL2) - GLONASS system time  
GLONASS 1 → 4 Nov '94



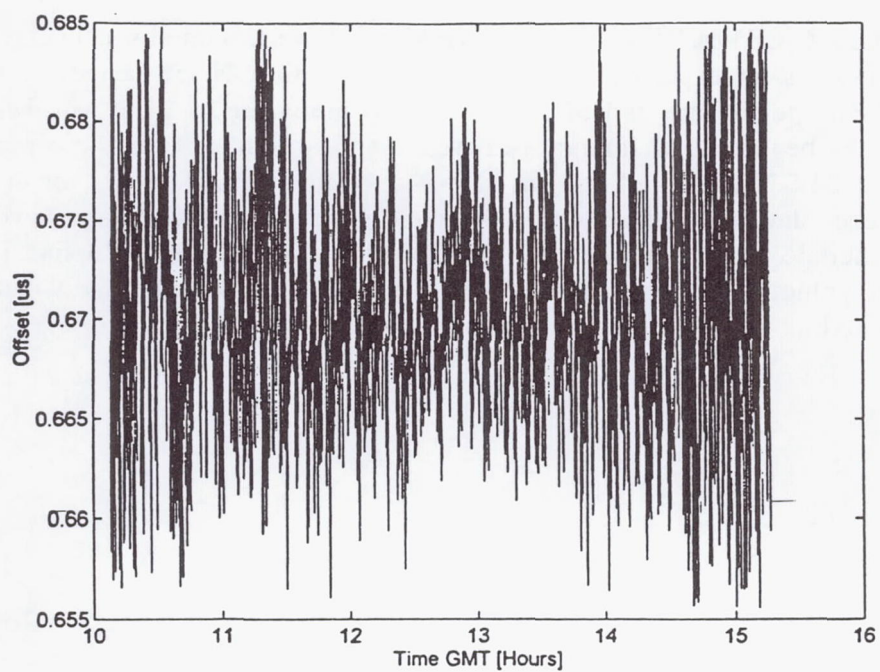


Figure 3: UTC(LDS) - UTC(NPL2)  $\rightarrow$  PRN 4 on 4 Nov '94  
mean value = 670.3 ns;  $1-\sigma = 4.4$  ns

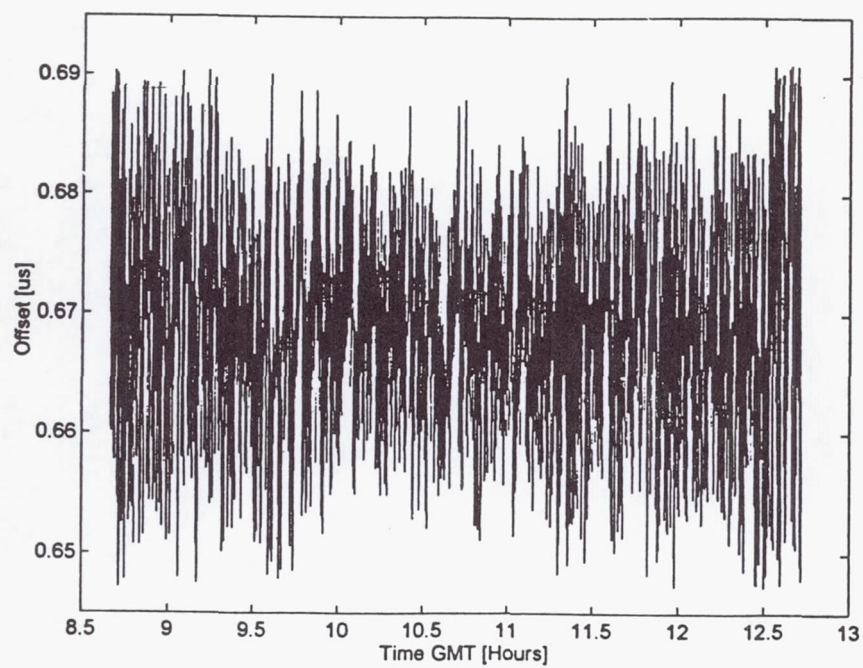


Figure 4: UTC(LDS) - UTC(NPL2)  $\rightarrow$  GLN 1 on 4 Nov '94  
mean value = 668.8 ns;  $1-\sigma = 7.0$  ns

## Questions and Answers

**WLODZIMIERZ LEWANDOWSKI (BIPM):** I have comments concerning GLONASS schedules. There is an experiment schedule in use, a GLONASS schedule, between North America and Europe for the end of June. We are preparing to issue worldwide GLONASS schedules for the beginning of January next year. This schedule is for the observation of slots — not specific GLONASS satellites, but slots — which are moving by, you have to subtract four minutes each day. So we have about the same pattern as for GPS, and have an automated GLONASS schedule, which doesn't have changes often, as is done in Russia. This is to prove it works, now going on for five months. So we hope next January we will have a regular GLONASS schedule.



# CESIUM AND RUBIDIUM FREQUENCY STANDARDS STATUS AND PERFORMANCE ON THE GPS PROGRAM

M. J. Van Melle  
GPS NAVSTAR Operations  
Rockwell Space and Operation Center  
Falcon Air Force Base  
Colorado Springs, CO

## Abstract

*This paper is an update of the on-orbit operational performance of the frequency standards on the last Block I NAVSTAR satellite (GPS-10), the complete Block II NAVSTAR satellites (GPS-13 to 21) and the Block IIA NAVSTAR (GPS-22 to 40) satellites. Since the status of the GPS constellation is now at Full Operational Capability (FOC), a minimum of twenty-four satellites are in position with all the necessary tests successfully completed. The evolution of frequency standards on board the GPS vehicles will be presented with corresponding results.*

*Various methods and techniques will be presented to show on-orbit life time, down time, state of health telemetry, on-orbit trending and characterization of all the frequency standards. Other topics such as reliability, stability, clock quirks and idiosyncrasies of each vehicle will be covered.*

## INTRODUCTION

The evaluation of the space-rated frequency standards on the GPS program started with the Block I concept validation program and the full-scale development vehicles of which only one is still functional: GPS-10 (PRN-12). The production vehicles are divided into two groups, Block II (GPS-13 through 21) and Block IIA (GPS-22 through 40). Each vehicle includes two Rubidium Frequency Standards (made by Rockwell) and two cesium Frequency Standards (made by Frequency and Time Systems as the primary source and, Kernco and Frequency Electronics Inc. as secondary sources on selected vehicles).

The cesium clocks are considered primary because of their degree of radiation hardness, their extremely low frequency drift, or aging, which does not require any Kalman filter modeling, and the shorter modeling time between turn-on and activation for GPS users.

The actual on-orbit GPS Frequency Standard operating history (shown in Figure 1 for the last Block I and all Block II satellites, and in Figure 2 for the Block IIA satellites minus the four

vehicles in the Eastern Launch Site awaiting launch) illustrates the results of these hardware implementations.

The operating life history of the production models of both cesium and rubidium frequency standards will be briefly discussed. This will be reviewed in order to calm the doubting Thomas's or Henny Pennies, that the sky is not falling in regard to (1) the amount of disabled clocks that have recently been occurring, Dec 94 – July 95, (2) the reliability of the clocks and (3) the combined projected lifetime of the four clocks (7.5 years) on each of the vehicles.

A brief history of the rubidium clocks on the Block I vehicles is given in Table 1. The major problems were corrected via modifications (the final modified clock for Block II/IIA is Modification number 12). The non-generic problems were never repaired. From the sample of 30 Block I rubidiums launched, the average age was 1.5 years with a maximum of 12.5 years and a minimum of one day. The minimum acceptable hardware reliability requirement for a five-year life rubidium clock was 0.765, which equates to a 3.8 year projection life.

The history of the rubidium clocks on the Block II/IIA vehicles is given in Table 2. Of the six disabled clocks, four may be retried with possible degraded performance. The final production model #12 RFS's have not acquired much on-orbit operating time, since the cesium clocks have traditionally been preferred over the rubidiums. This is because of the advantage of cesium over rubidiums in terms of radiation hardness, lower drift rate by a factor of 100, no C-field tuning or frequency biasing needed, and a shorter warm-up time before the vehicle can be set healthy (2.6 days versus 6.4 days on the average). There have been eleven turn-ons with six powered down, for a total time of 120 months or 87,380 operational hours, as of 30 November 1995. Since the hours of operation (sample size) are so small, a point-in-time failure rate estimate must be used. If the two failures are used, then the calculated failure rate is  $26.5 \times 10^{-6}$  or an Mean Time Between Failure (MTBF) of 4.3 years. If the six disabled clocks are considered complete failures, then the failure rate is  $79.6 \times 10^{-6}$  and an MTBF of 1.4 years.

The operating history of the cesium clocks on the Block I vehicles is as follows: a total of six clocks (three pre-production models and three Model 1 production clocks) with an average life time of 5.9 years (Maximum of 9.3 years and a minimum of 3.3 years). Since five of the failures were caused by cesium depletion, the final production model (Model 2) had an increase of cesium fill (1.0 grams to 1.5 grams).

The history of the cesium clocks on Block II/IIA vehicles is given in Table 3. Of the thirty-one CFS's powered-up, nineteen are still operating, with an age range of 6.5 years to seven months. Of the twelve clocks which have been disabled, six have been labeled failures and six may be given a second chance with possible degraded performance. If the five failures, excluding one GFE clock, are used, then the calculated failure rate (via the point-in-time failure rate estimate) is  $7.2 \times 10^{-6}$  and the MTBF is 15.8 years. If the ten disabled clocks (excluding the two GFE clocks) are considered failures, then the failure rate is  $14 \times 10^{-6}$  and the MTBF is equal to 7.9 years. The manufacturer signed up for a minimum acceptable hardware reliability requirement for a 7.5 year life of 0.663, or 4.3 years per clock. Taking the reliability numbers of both rubidium and cesium clocks, plus having to meet the navigation payload reliability number of 0.934 for 7.5 year life, the number of clocks per vehicle came out to be two rubidiums and



two cesiums. Another figure to remember is the mean mission duration value of six years, a specification which five vehicles have already surpassed. In summary, the complete GPS Block II/IIA clock status is included in Table 4.

## ON-ORBIT PERFORMANCE

In order to acquire the exact performance characteristics of the operating on-orbit frequency standard, the L-Band signal must be evaluated. This signal is affected by the (Frequency Synthesizer Distributor Unit) FSDU (which is commanded by the NDU), atmospheric effects, ephemeris uncertainties, monitor station variations, spacecraft effects and other factors. All of these factors are fed into a Kalman filter, which is a computer algorithm for processing discrete measurement data in an optimal fashion.

There are several parameters which are instrumental in evaluating the operational performance of the frequency standards. The first two parameters are in the navigation message. One is  $a_1$ , which is the frequency offset (sec/sec). This is the filter's estimate of the frequency difference, or offset between the satellite's frequency standard and the GPS composite clock (a nominal frequency). This is a continuous absolute value. One can also take the daily average of the difference between the minimum and maximum values of  $a_1$  as a possible trending signature. Another parameter is the frequency drift in  $\text{sec/sec}^2$ ,  $a_2$  term. This is the rate of change of the drift term.

Another parameter that is used daily to evaluate the clock's performance is the Estimated Range Deviation (ERD). An ERD is the difference between a range determined from the a posteriori state estimates during a Kalman interval and the range determined from the navigation upload data that is valid for the same time. These ERD's compare the current filter estimates each 15 minute period to the prediction made from previous filter estimates (considered to be a minimum range error either induced primarily, by clock movement or satellite positional change). Examples of these ERD's are in Figures 3 and 4. Plots of these estimates provides us one more clue of evaluating the performance of each spacecraft's clock.

Continuing the investigation of a potential clock problem, a correlation of these ERD plots to the telemetry monitor values must be examined. Along with these clock monitor values, the  $a_1$  and  $a_2$  terms must be observed for movement.

One important aspect of Kalman filter operation is to provide accurate continued measurement updates, every fifteen minutes. Unfortunately, there are periods when the spacecraft is not in view of a monitor station, and the filter must estimate aging through the  $a_2$  term, with no real measurement verification. Also, different monitor stations (with obvious different clock errors) contribute errors into the filter estimation and subsequently the prediction process.

An operating limit is set on the ERD value in terms of meters (eg. 10 meters or 8 meters). When the limit is exceeded, a new upload must be sent to the vehicle to correct the new terms in the navigation message. A new experimental limit has recently been defined as 5 meters, resulting in a fifteen percent improvement in the URE. This also has increased the work load on the Master Control Station (MCS) crew, which now performs approximately twelve more uploads per day on the 25 vehicles. As a rule, the MCS contacts each vehicle twice a day,

once to update the navigation message. This equates to a total of 60 to 70 supports per day for the MCS crew.

Another set of parameters which appear to effect the clock's performance are environmental effects, such as prolonged radiation effects (i.e. passing through the Van Allen belts every twelve hours) and irregular solar activities. Thermal variations, either induced by delta-v maneuvers or eclipse seasons, appear to be causing the older cesium clocks ( $> 5$  years) the most problems in terms of ERD's. Maybe aging of the electronics, resulting in a degraded temperature coefficient causes frequency changes. The eclipse season causes the cesium clock's temperature to decrease by three degrees centigrade with a  $\pm 1^\circ \text{C}$  variation. The rubidium does not have this problem since a heater (ABTCU) keeps the rubidium clock at a stable temperature,  $\pm 0.1^\circ \text{C}$ . When the satellite enters eclipse season especially during the first eclipse season, an ephemeris change could also occur, which is corrected by manual intervention from the operators.

## ON-ORBIT TRENDING

The most important objective of trending analysis is to determine when a particular frequency standard is no longer useful for providing a navigation signal. Particularly elusive is the time frame - whether it be in days or months - when a clock will expire. Note that this is different than not meeting specifications. The stability specification of the clock,  $2 \times 10^{-13}$  at one day for the cesium clock, is so tight, that if the clock is performing at  $3 \times 10^{-13}$  at one day, the URE of 4.8 meters (1 s) can still be met with extra maintenance by the MCS, for the space segment. There are several vehicles now that do not meet the stability specification, but the Air Force is reluctant to switch to another clock. The Air Force will determine when a clock will be disabled by many factors. These factors include:

1. how burdensome to the MCS crew are extra daily uploads and/or Kalman maintenance in order to correct the a1 and a2 terms?
2. how old is the clock ( $> 5$  years)?
3. how old is the vehicle ( $> 6$  years)?
4. how many clocks are left to be tried?
5. what is the world situation (conflicts/trouble spots)?
6. what is the condition of the vehicle in terms of performance operation and other subsystems? and
7. what is the condition of the entire constellation?

The navigation signal must be made available 98% of the time with 21 spacecraft. In predicting the useful operating lifetime of the clock, the most important performance parameter is the stability of the clock. This is what most effects the user, and is the most sensitive parameter.



The next set of parameters are the  $a_1$  and  $a_2$  terms and their deterioration and/or fluctuations, and the ERD's. The last set of parameters which effect the performance of the clock and that of the navigational signal is internal to the clock. The cesium clock has 18 monitors (combination of analog and digital) and the rubidium clock has 11 monitors (combination analog and digital). Of all the telemetry monitors on the cesium clock, there are only a few that could vary and not effect the performance of the clock. The rest of the monitors will cause an upset of the performance by any detectable movement (minimum step size). One of the monitors having particular character or individuality is the cesium beam current monitor. This trending parameter is hard to interpret in the sense that each of the 19 operating clocks has a slightly different signature as seen in Figure 5. SVN-17 has the normal stair-stepping decline in beam current. Since each clock starts off at a different absolute value, each has a different rate of decline (the higher it starts, the faster it drops) and each has a different final plateau. So each drop in beam current may or may not effect the stability,  $a_1$  or  $a_2$  terms, or ERD's. Furthermore, each clock will degrade or age at a different rate. Even though each clock is built to the same specification and from the same set of drawings, when one compares stability performance in terms of parts in  $10^{14}$ , there will be variations in their outputs.

The other parameter that might change without detrimental effects on the performance is the loop-control voltage, which normally will move slightly one way or another, depending on what electronic changes or aging occur in the loop in order to keep the same 10.23 MHz frequency output to the FSDU. The parameters which are catastrophic to clock performance if any movements are observed are the cesium oven temperature, RF level (power shift and or spectrum change), electron multiplier gain changes, ionizer voltage, and any input current changes to the total clock or to individual units such as the quartz oven.

The rubidium clocks have the same type of monitors and the same type of loop control voltages. The lamp voltage monitor which detects pressure changes and photo cell degradations is somewhat similar to the cesium beam current in terms of end-of-life predictions.

To predict the exact (one week) end-of-life of either type of clock is extremely hard. This was tried on SVN-20 with Cesium No. 3. After 4.5 years of operation, the stability was  $> 2 \times 10^{-13}$  one-day with four to five extra uploads needed per week. Maybe two to three months of less than useful life could have been squeezed out of the clock.

Other parameters that are incorporated into the trend analysis include on-orbit temperature of the spacecraft, any FSDU - NDU influence, or L-Band effects.

## SCHEDULES

The last of the Block I satellites, NAVSTAR 10 (PRN 12), launched in 1984, is scheduled to be disposed of in the June 1996 time period. The main problem is that the solar arrays have lost their efficiency (design life of five years) and can no longer support the navigation payload. On November 18, 1995, the payload was set unhealthy. Kalman filter tests, frequency standard tests, sun sensor test, etc., will be performed in February and March 1996. The two rubidium frequency standards, yet to be powered up after 12 years of on-orbit storage, will be tested for stability, temperature coefficient, VCXO and turn-on characteristics and any other tests the

clock community would like to have performed.

The last Block IIA satellite launched, GPS-37, reached orbit in March 1994. This completed the 24 satellite constellation. There are four vehicles in the Eastern Launch Site in storage waiting to be launched. The next launch is planned to be positioned in "Plane C" in March 1996. There are available launch slots for summer 1996 time frame.

The total on-orbit times for both rubidium and cesiums are staggering for the first operational satellite system ever to utilize both types of production frequency standards. The on-orbit times for all rubidiums exceed 60 years of operation, while the cesium on-orbit times are more impressive with over 125 years of operation. The GPS clock utilization times in their operational sequence are shown in Figure 6.

## CONCLUSION

As verified by on-orbit performance data, most of the major generic problems, especially with the rubidiums, have been corrected. I will admit that the rubidium short life times, the phase jumps that occur within the first 3 to 4 months of operation and the changing drift rate within the first 6 months are on-going problems. There have been 31 out of 48 cesium clocks activated with 19 currently operating. Of the 12 disabled clocks, half may be reactivated with possibly degraded performance. There have been eleven rubidium clocks activated with 37 remaining to be turned on. Of these eleven clocks, five are still operating and four to be reactivated for future use.

The average age of all the disabled clocks is 1.65 years. The average age of the currently operating clocks is 2.9 years. The average age of the space vehicles is 4.5 years, which equates to 60% of the design life (7.5 years). The total number of clocks turned on is 42, which equates to using only 44% of the available clocks. The usage and performance to date indicates that the number of clocks (four), originally determined in the 1982 proposal, will support both the spacecraft design life of 7.5 years and the mean mission duration of 6.0 years.

For the more quick-look-managerial type, a user-friendly smiley face chart, Figure 7, has been concocted in order to eliminate reviewing all the Kalman drift rate residuals, Allan variance stability curves, and ERD's figures. Each little quirk and idiosyncrasies of the vehicles combined with clock performance in terms of ERD's are for your (management) eyes only.

## ACKNOWLEDGMENTS

The author would like to acknowledge the following companies and services who were involved and contributed to the GPS frequency standard program over the past twenty years:

- Air Force Space Division (JPO) and 2SOPS (FAFB)
- Naval Research Laboratory (NRL)
- National Institute of Standards & Technology (NIST)
- Aerospace



- Rockwell (RFS Manufacturer)
- Frequency and Time System (CFS Manufacturer)
- Kernco & Frequency Electronics Inc. (Second Source CFS Manufacturers)

TABLE 1 RUBIDIUM FREQUENCY STANDARDS - BLOCK I

TYPES OF PROBLEMS	NO.	AGE (YR)	HOW FIXED
		Hi - Low	
TRANSFORMER	3	0.53	MOD. P/N 3
RUBIDIUM FILL	8	1.0 - .3	MOD. P/N 4
		2.7	
C-FIELD TUNING HITS	3	12.5 - 0.4	MOD. P/N 11
		1.9	
VCXO	1	5.1 - 0.03	NON-GENERIC
DRIFT RATE	2	2.8	NON-GENERIC
		0.5	
ATOMIC LOOP *	1	0.5 - 0.5	NON-GENERIC
		1 DAY	
		1.77	
OPERATIONAL TO END *	7	12.5 - .003	N/A
		1.2	
		3.5 - 0.1	
NOMINAL TURN-ON (TESTS)	2	1 MONTH	N/A
NEVER TURNED-ON *	3	-	N/A
		-	
TOTAL	30	1.5	
		12.5 - .003	

\* ONE STILL AVAILABLE

TABLE 2 RUBIDIUM FREQUENCY STANDARDS - BLOCK II

• DISABLED 6 CLOCKS

AGE (YRS.)	SYMPTOMS
1.7	ERRACTIC MONITORS
1.4	HEATER CIRCUITRY; LAMP VOLTAGE ERRACTIC
1.4	DRIFT RATE LARGE; DESERT STORM DECISION
1.1	TEMPERATURE SENSITIVE; FREQUENCY MOVEMENTS
0.2	INSIDE TEMPERATURE CONTROLLER; FREQUENCY MOVEMENTS
0.2	DRIFT RATE LARGE

AVE. = 1.0 YR.

• OPERATIONAL 5 CLOCKS

- OLDEST = 1.3 YRS.
- AVERAGE = 0.8 YRS.

TABLE 3 CFS BLOCK II VEHICLES

No. of CFS - 19 Operating	AGE
2	> 6 YRS.
2	> 5 YRS.
2	> 4 YRS.
4	> 3 YRS.
3	> 2 YRS.
3	> 1 YR.
3	< 1 YR.

12 - DISABLED AGE

REASONS

4.3 YRS.	* $\sigma > 2 \text{ E-13}$ at 1 day
3.5 YRS.	VCXO OR SERVO
2.8 YRS.	FUSE
2.5 YRS.	* VCXO; $\Delta f$
2.3 YRS.	* SECOND SOURCE - RF
2.2 YRS.	* 35 DAY CYCLIC PATTERN
2.1 YRS.	CBI LOW, HIGH BACKGROUND NOISE
1.8 YRS.	SECOND SOURCE - RF
1.1 YRS.	EMULT; $\Delta f$
.7 YRS.	VCXO, DAC, SERVO or EMULT
0.1 YRS.	* SOLAR COEFFICIENT
0.1 YRS.	* DESERT STORM; $\Delta f$

\* AVAILABLE FOR POSSIBLE DEGRADED OPERATION



TABLE 4 - GPS BLOCK I/II/IIA CLOCK STATUS - NOV. 30, 1995

SVN	CLOCK	STATUS	PART	PLN/ SLT	TURN ON-OFF	NEXT IPO	RECENT COMMENTS
13	1Rb 2Rb 3Cs 4Cs	SPARE SPARE OPERATING SPARE	I	B/3	6/17/89	MAR '96	$\sigma = 1.4 \times 10^{-13} \pm 10^3$ S, $0.86 \times 10^{-13}$ @ 10 days. Aging - $3.6 \times 10^{-15}$ /day on 3/Cs.
14	1Rb 2Rb 3Cs 4Cs	SPARE SPARE DEAD OPERATING	II	E/1	2/23/89-8/30/92 8/30/92	NONE	$\sigma = 1.1 \times 10^{-12}$ @ $10^3$ S, $0.47 \times 10^{-12}$ @ 10 days. Aging - $2.0 \times 10^{-15}$ /day on 4/Cs. VCXO or Servo had, not in Cesium tube on 3/Cs.
15	1Rb 2Rb 3Cs 4Cs	SPARE SPARE DEAD OPERATING	II	D/2	10/6/90-11/10/92 11/10/92	NONE	$\sigma = 1.3 \times 10^{-12}$ @ $10^3$ S, $0.51 \times 10^{-12}$ @ 10 days. Aging - $0.3 \times 10^{-15}$ /day for 4/Cs. Low beam current and high noise on 3/Cs caused turn-off
16	1Rb 2Rb 3Cs 4Cs	SPARE SUSPECT OPERATING SPARE	VI	E/3	8/24/89 - 1/7/91 1/7/91	DEC 95	$\sigma = 3.0 \times 10^{-12}$ @ $10^3$ S, $1.0 \times 10^{-12}$ @ $10^3$ S. Aging + - $17.0 \times 10^{-15}$ /day; Low Beam current < 1.1 nA on 3/Cs. Suspect clock with many frequency discontinuities, large drift rate, along with the Desert Storm time period, caused change from 2/Rb
17	1Rb 2Rb 3Cs 4Cs	SPARE SPARE OPERATING SPARE	II	D/3	12/24/89	MAR '96	$\sigma = 1.2 \times 10^{-12}$ @ $10^3$ S, $0.47 \times 10^{-12}$ @ 10 days. Aging - $0.8 \times 10^{-15}$ /day on 3/Cs
18	1Rb 2Rb 3Cs 4Cs	SPARE SPARE OPERATING SPARE	I	F/3	2/5/90	MAY '96	$\sigma = 1.4 \times 10^{-12}$ @ $10^3$ S, $0.35 \times 10^{-12}$ @ days. Aging is $3.6 \times 10^{-15}$ /day on 3/Cs
19	1Rb 2Rb 3Cs 4Cs	SUSPECT OPERATING SUSPECT DEAD	II	A/4	10/16/94-12/30/94 12/30/94 11/1/89-1/2/92 1/2/92-10/16/94	AUG '96 NONE	$\sigma = 1.8 \times 10^{-12}$ @ 1 day for 2/Rb. Freq change on 11/20/94 and temperature controller instable for 1/Rb. Suspect 3/Cs had 35-day freq offset cyclic pattern with large aging of $16 \times 10^{-15}$ /day. $\sigma = 1.2 \times 10^{-12}$ @ $10^3$ S. Instant Off on 4/Cs.
20	1Rb 2Rb 3Cs 4Cs	SPARE OPERATING SUSPECT SPARE	I	B/2	8/6/94 4/8/90-8/6/94	JUL '96 JUL '96	Disturbance on 8/20/94; ABTCU - Range C, $\sigma = 0.6 \times 10^{-12}$ @ 1 day. Aging - $80 \times 10^{-15}$ /day on 2/Rb, $\sigma = 1.9 \times 10^{-12}$ @ $10^3$ S, 4 extra ERD weekly; CH1 < 1.6 nA on 3/Cs. Proactive move
21	1Rb 2Rb 3Cs 4Cs	SPARE SPARE OPERATING SPARE	IV	E/2	8/14/90	JUL '96	$\sigma = 2.0 \times 10^{-12}$ @ $10^3$ S, $1.0 \times 10^{-12}$ @ 10 days; Aging $8.4 \times 10^{-15}$ /day 4 extra uploads needed weekly; low cesium beam current; = 3.5 nA; LTC = 1.36 sec, gain decrease of 11 in 4.5 years on 3/Cs.
22	1Rb 2Rb 3Cs 4Cs	SPARE SPARE SUSPECT OPERATING	IV	B/1	2/14/93-3/17/93 3/17/93	FEB '96	$\sigma = 1.4 \times 10^{-12}$ @ $10^3$ S, $0.81 \times 10^{-12}$ @ 10 days; Aging - $10 \times$ $10^{-15}$ /day for 4/Cs. Incorrect solar coefficient in Kalman filter estimate during eclipse season, influenced 3/Cs change.
23	1Rb 2Rb 3Cs 4Cs	SPARE SPARE SUSPECT OPERATING	IV	E/4	12/5/90-1/4/91 1/4/91	JUL '96	$\sigma = 1.2 \times 10^{-12}$ @ $10^3$ S, $0.32 \times 10^{-12}$ @ 10 days. Aging - $1.6 \times 10^{-15}$ /day for 4/Cs. Frequency jumps along with Desert Storm caused change for 3/Cs.
24	1Rb 2Rb 3Cs 4Cs	DEAD/SUSPECT OPERATING SUSPECT SPARE	III	D/1	1/24/94-7/1/95 7/1/95 7/1/91-1/24/94	MAY '96 MAY '96	Healthy on 7/7/95; $\sigma = 0.7 \times 10^{-12}$ @ $10^3$ S, for 2/Rb; Heater loop control voltage changes with A Freq on 1/Rb; VCXO suspect on 3/Cs.

TABLE 4 - GPS BLOCK I/II/IIA CLOCK STATUS - NOV. 30, 1995

SVN	CLOCK	STATUS	PART	PLN/ SLT	TURN ON-OFF	NEXT IPO	RECENT COMMENTS
25	1Rb 2Rb 3Cs 4Cs	SPARE DEAD OPERATING DEAD	III	A/2	3/14/92-12/1/93 1/10/95 12/1/93-1/10/95	NONE	$\sigma = 1.1 \times 10^{-12}$ @ 1 day, aging $1.0 \times 10^{-15}$ for 3/Cs. Frequency jumps occurred in 1/93 with erratic lamp voltage and control voltages on 2/Rb. EMUL TV and CH1 toggling after $1 \times 10^{-11}$ M. Large ERD run-off for 4/Cs.
26	1Rb 2Rb 3Cs 4Cs	SPARE SPARE OPERATING SPARE	II	F/2	7/17/92	JUL '96	$\sigma = 1.0 \times 10^{-12}$ @ $10^3$ S, $0.73 \times 10^{-12}$ @ 10 days. Aging + $4.5 \times 10^{-15}$ /day
27	1Rb 2Rb 3Cs 4Cs	SPARE SPARE OPERATING SPARE	IV	A/3	9/24/92	AUG '96	$\sigma = 1.2 \times 10^{-12}$ @ $10^3$ S, $0.45 \times 10^{-12}$ @ 10 days. Aging $0.6 \times 10^{-15}$ /day
28	1Rb 2Rb 3Cs 4Cs	SPARE SPARE OPERATING SPARE	I	C/2	4/18/92	MAR '96	$\sigma = 1.1 \times 10^{-12}$ @ $10^3$ S, $0.26 \times 10^{-12}$ @ 10 days. Aging - $1.0 \times 10^{-15}$ /day
29	1Rb 2Rb 3Cs 4Cs	SPARE SPARE SPARE OPERATING	III	F/4	12/30/92	AUG '96	Second Source Cesium of Keroco, $\sigma = 0.8 \times 10^{-12}$ @ $10^3$ S, $0.23 \times 10^{-12}$ @ 10 days. Aging - $0.5 \times 10^{-15}$ /day
31	1Rb 2Rb 3Cs 4Cs	SPARE OPERATING SPARE SUSPECT	III	C/3	1/18/95 4/8/93-1/18/95	JAN '96 JAN '96	$\sigma = .91 \times 10^{-12}$ @ 1 day, aging - $300 \times 10^{-15}$ /day on 2/Rb. Second Source Cesium of FEL, Temperature sensitive VCXO. SRD & P.S. variations for 4/Cs.
32	1Rb 2Rb 3Cs 4Cs	SUSPECT OPERATING SPARE DEAD	IV	F/1	3/18/95-5/8/95 5/8/95	MAY '96 NONE	Second Source Cesium of FEL; SRD problem on 4/Cs. Aging $400 \times 10^{-15}$ /day large ERD's and drift rate changes for 1/Rb. Healthy on 5/12/95. $\sigma = 1.4 \times 10^{-12}$ @ 1 day for 2/Rb.
33							LAUNCH IN MARCH 1996 (C-PLANE)
34	1Rb 2Rb 3Cs 4Cs	SPARE SPARE SPARE OPERATING	II	D/4	11/15/93	NOV '96	Second Source Cesium of Keroco, $\sigma = 0.8 \times 10^{-12}$ @ $10^3$ S, $0.6 \times 10^{-12}$ @ 10 days. Aging $2.0 \times 10^{-15}$ /day on 4/Cs.
35	1Rb 2Rb 3Cs 4Cs	SPARE SPARE OPERATING SPARE	I	B/4	9/21/93	SEP '96	$\sigma = 1.5 \times 10^{-12}$ @ $10^3$ S, $1.2 \times 10^{-12}$ @ 10 days. Aging - $1.5 \times 10^{-15}$ /day on 3/Cs.
36	1Rb 2Rb 3Cs 4Cs	SPARE SUSPECT SPARE OPERATING	I	C/1	3/18/94 - 5/01/95 5/01/95	MAR '96	$\Delta V$ on 2/10/95, Problems on next eclipse 3/16/95. Frequency movements on 2/Rb. $\sigma = 0.8 \times 10^{-12}$ @ 1 day. C-field monitor high on 4/Cs. Aging - $5.5 \times 10^{-15}$ /day.
37	1Rb 2Rb 3Cs 4Cs	SPARE SPARE DEAD OPERATING	III	C/4	5/20/93-3/31/94 3/31/94	NONE	$\sigma = 1.1 \times 10^{-12}$ @ $10^3$ S, $0.3 \times 10^{-12}$ @ 10 days. Aging - $0.1 \times 10^{-15}$ /day on 4/Cs. VCXO, DAC, Servo, or Multiplier suspect on 3/Cs.
39	1Rb 2Rb 3Cs 4Cs	SPARE SPARE OPERATING SPARE	III	A/1	7/4/93	JUN '96	$\sigma = 0.8 \times 10^{-12}$ @ $10^3$ S, $0.42 \times 10^{-12}$ @ 10 days. Aging + $3.0 \times 10^{-15}$ /day on 3/Cs.

Figure 1: BLOCK II FREQUENCY STANDARD CONFIGURATION

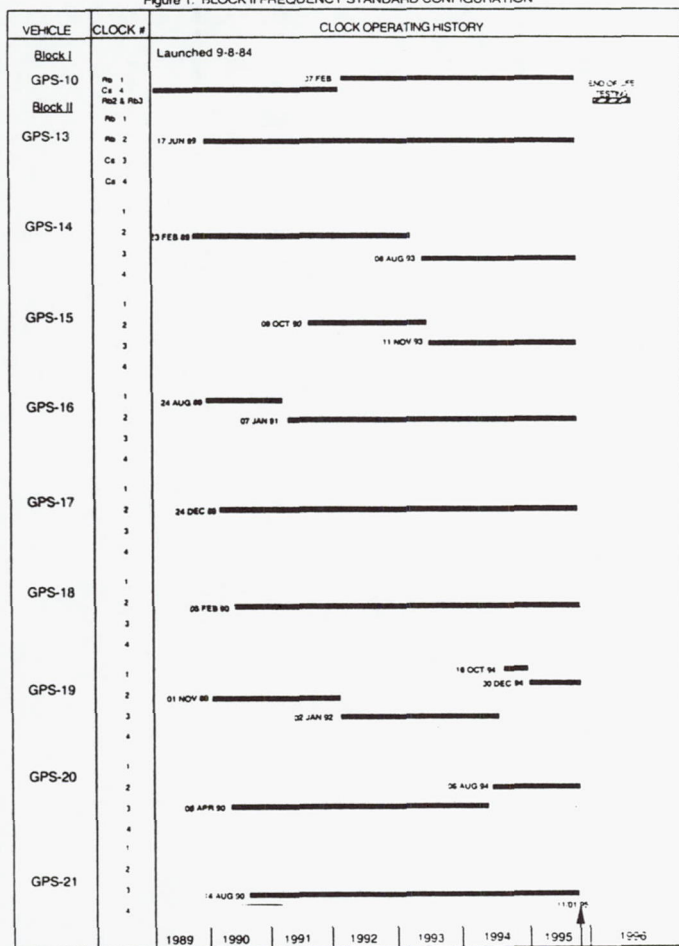


Figure 2: BLOCK IIA FREQUENCY STANDARD CONFIGURATION

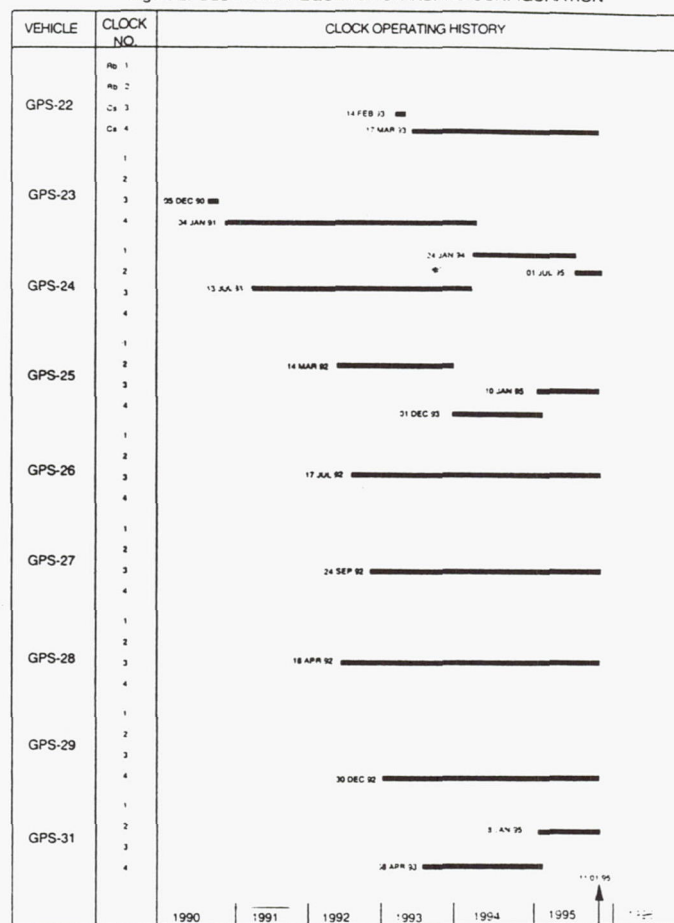
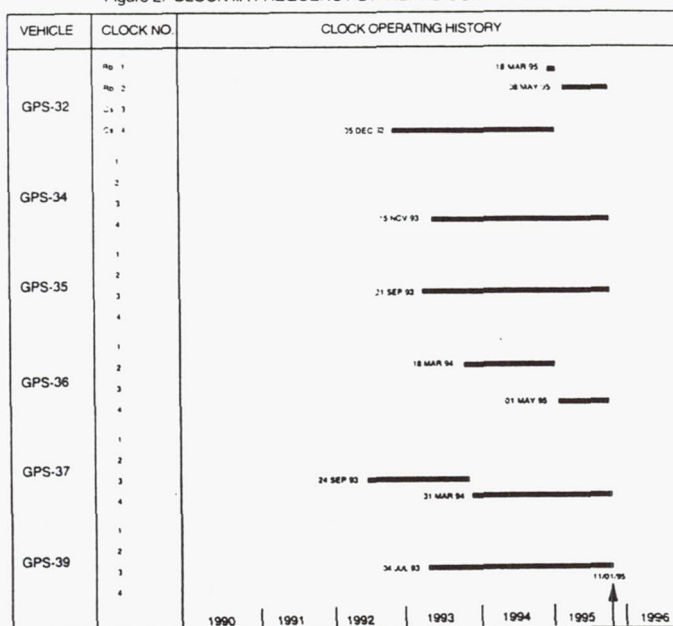
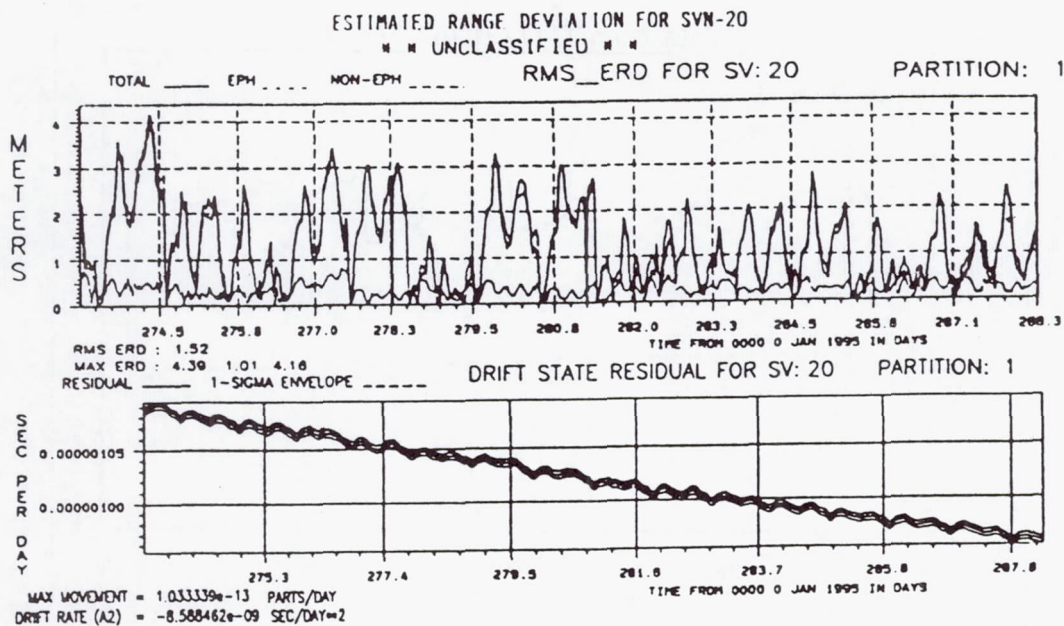


Figure 2: BLOCK IIA FREQUENCY STANDARD CONFIGURATION

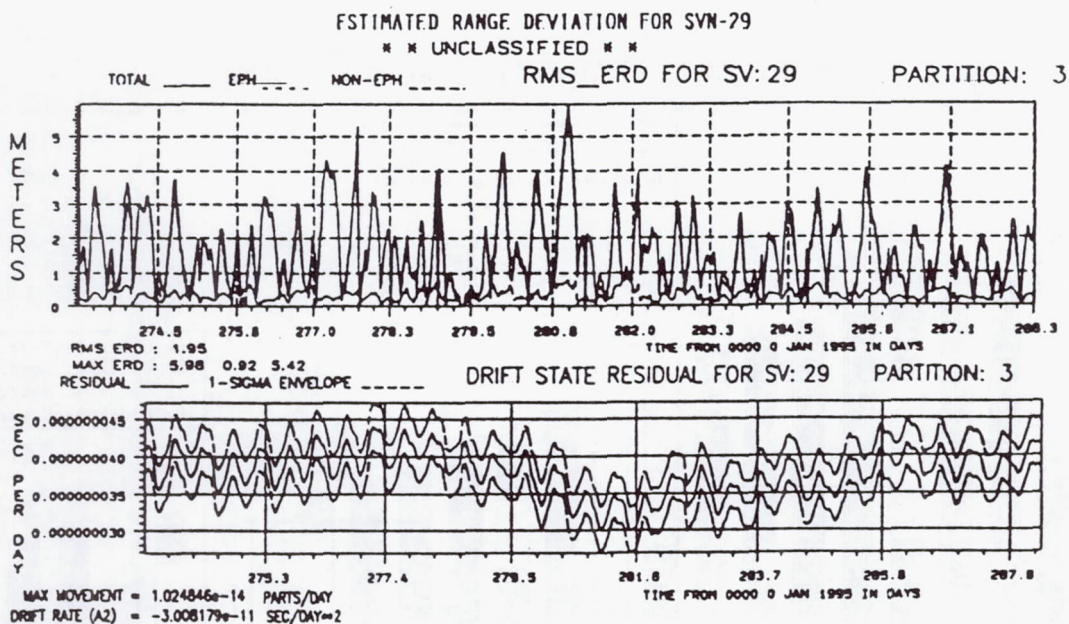






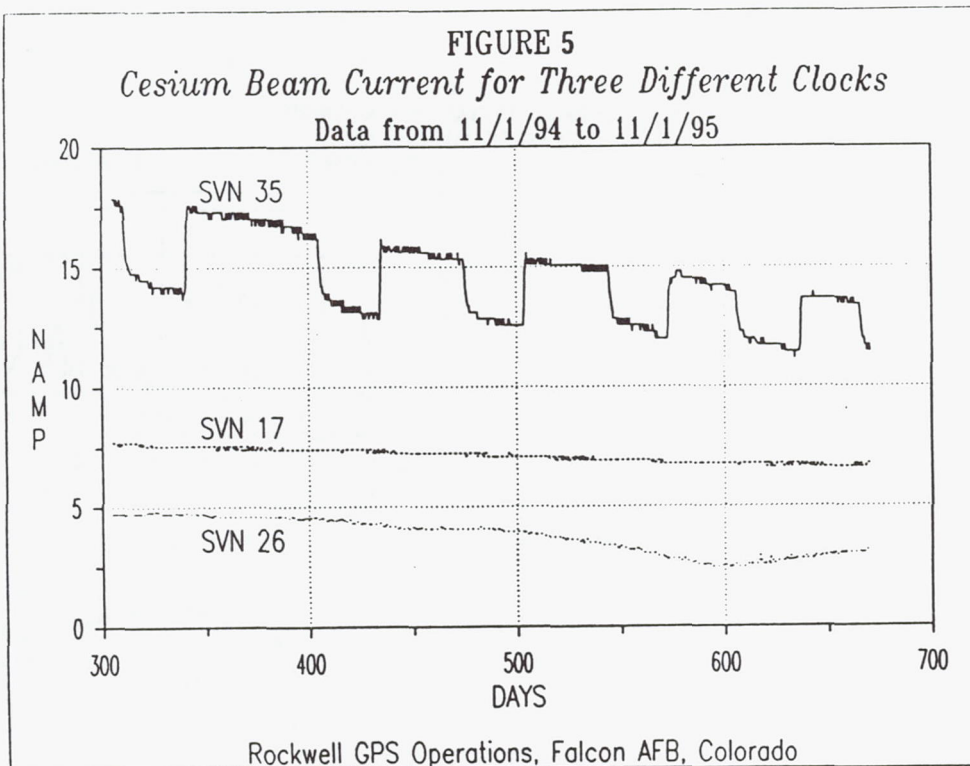
Plot 009 of 052

\*\* UNCLASSIFIED \*\*  
 FIGURE 3



Plot 018 of 052

\*\* UNCLASSIFIED \*\*  
 FIGURE 4



### GPS CLOCK UTILIZATION IN OPERATIONAL SEQUENCE

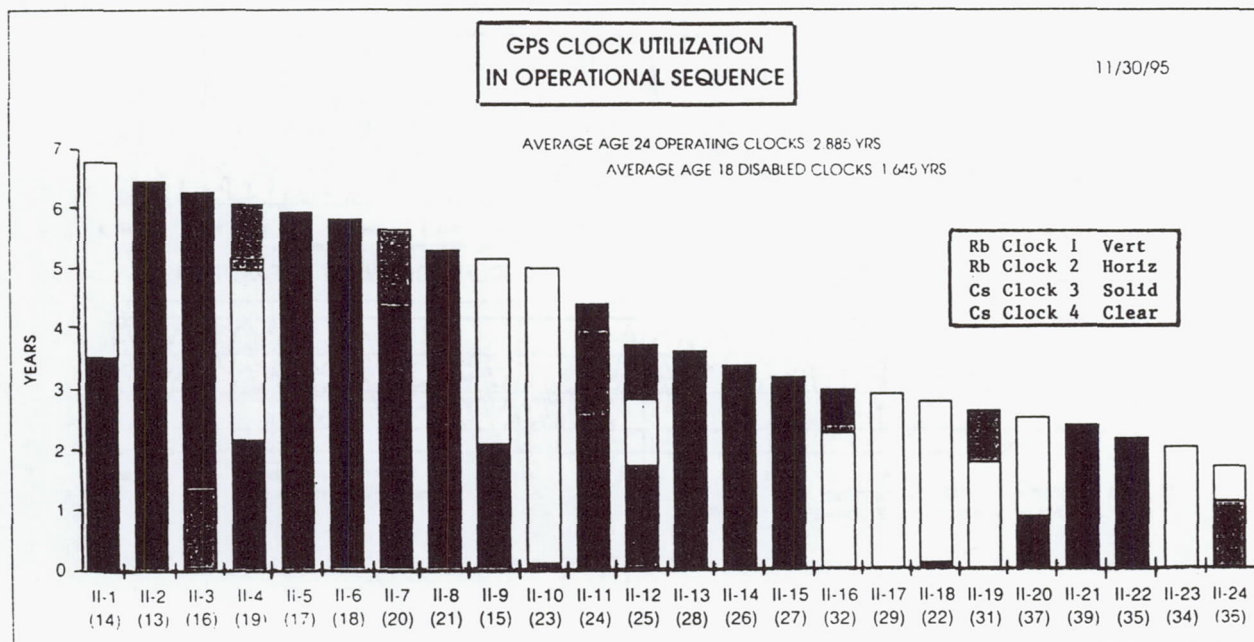


FIGURE 6





ROCKWELL Aerospace

NAVSTAR GPS Operations

November 01, 1995

CLOCK OPERATIONAL PERFORMANCE October, 1995

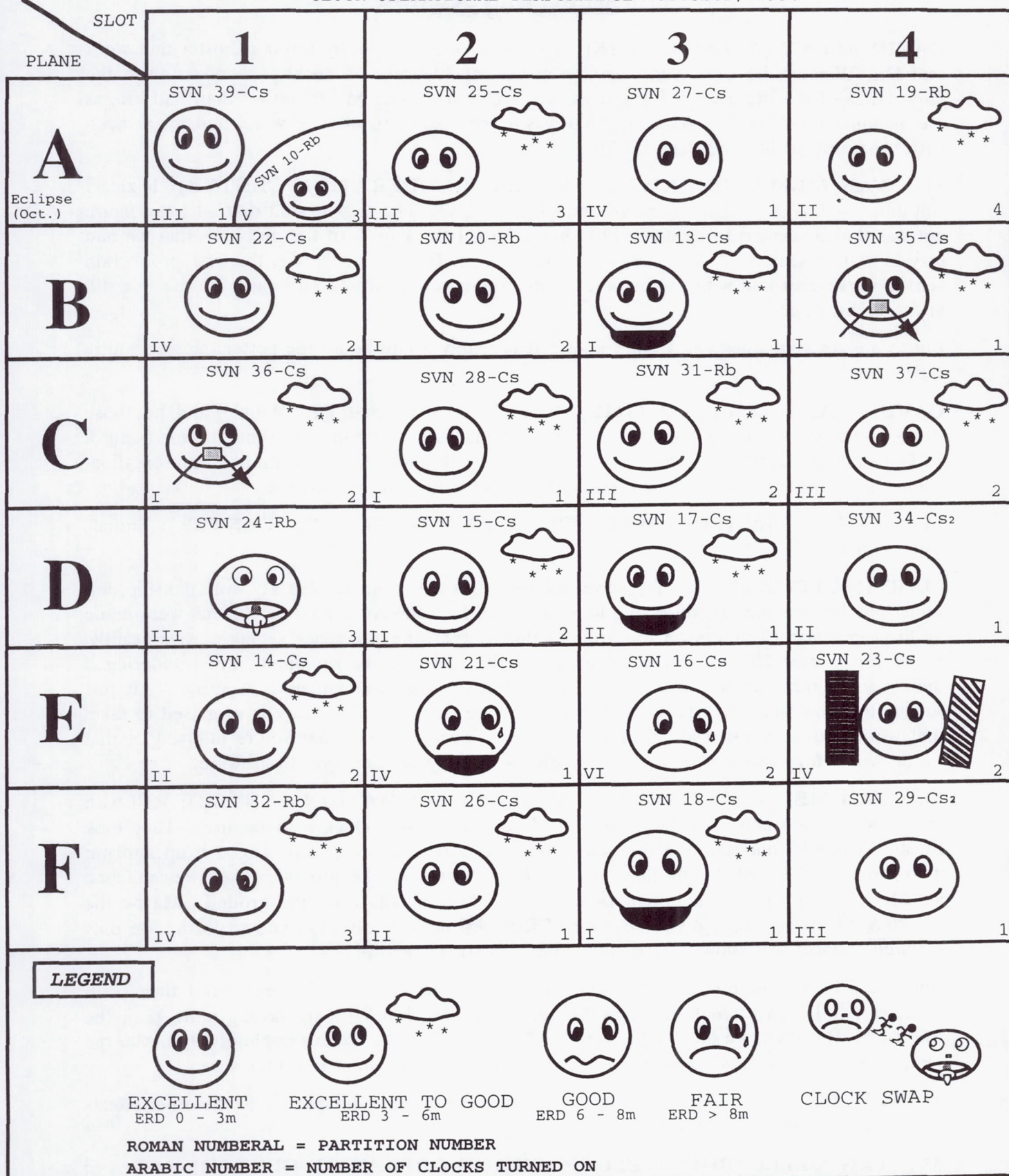


FIGURE 7



## Questions and Answers

**DAVID ALLAN (ALLAN'S TIME):** Given our opening talk by Captain Foster and work that Dr. Winkler did some years ago on measuring lifetimes of clocks, I wonder, given the importance of the lifetime of this system, why we're still using MTBF rather than half-life, as was recommended by Dr. Winkler. That was a very excellent piece of work, and it's a much better measure of lifetime than MTBF.

**M.J. VAN MELLE (ROCKWELL SPACE AND OPERATION CENTER):** Right, I still don't — this is a reliability person that I gave all the data to who said that all I can figure out was that it seemed to be a little high. Plus, I think most of the problems that we had may be workmanship. I don't know how hard it is. Remember, this is the first production vehicle we've ever had with production rubidium and cesium clocks on board. To me, it's still in the infant stages.

But to answer your question, I don't know. It probably would be a little better the way you're suggesting.

**DAVID ALLAN (ALLAN'S TIME):** Well it's the work that Dr. Winkler did on those clocks some years ago, and it's a very excellent measure. Perhaps, in terms of this being a PTTI planning meeting, it's something we should think about for some future representation. I don't know whether we can do anything here, but it certainly is an issue.

**M.J. VAN MELLE (ROCKWELL SPACE AND OPERATION CENTER):** Sounds good to me.

**MARTIN BLOCH (FEI):** Van, we've discussed this many times. You say workmanship, but something bothers me. If you take a look at the performance of similar clocks that were made by the same manufacturers on the ground, they outperform the space segments significantly, where life is over 10 years on the cesium and the same on the rubidium. I'm wondering if there's some other reason that we're overlooking on what is happening in space — it just sounds that the number of failures, with all the care that space hardware is supposed to take, that workmanship doesn't sound to me is a good excuse; unless what you're implying is that we do worse for space hardware than we do for military or commercial hardware.

**M.J. VAN MELLE (ROCKWELL SPACE AND OPERATION CENTER):** Well with the rubidium, you know, Rockwell made it, Rockwell is not a clock manufacturer. They took Efratom's physics package and they took your oscillator, and we just packaged it up and put it together; and tested it only like three or four months on the ground. Then we launched it. Maybe during the six-month period, it would have a failure on the ground. Maybe the launches affected it, but we still do a lot of fault testing with vibration and so forth. We only vibrated it once; you know, maybe the second vibration killed it.

But, the FTDS's are production clocks made by the cesium manufacturers, and they seem to have a little longer lifetime. I can't explain why the Block-I's are lasting more than the Block-II's. But then, we only had a sample of six; and here we had a sample of 19; maybe the sample size was too small compared to the complexity of the standards themselves.

**MARTIN BLOCH (FEI):** I wonder if anybody else has some thoughts as to the other effects that influence the life performance.

**M.J. VAN MELLE (ROCKWELL SPACE AND OPERATION CENTER):** And we're talking about if it goes to  $5 \times 10^{-13}$ , it's no good.



# HIGH PRECISION TIME TRANSFER IN SPACE WITH A HYDROGEN MASER ON MIR

Edward M. Mattison and Robert F.C. Vessot  
Harvard-Smithsonian Center for Astrophysics  
Cambridge, Massachusetts 02138

## Abstract

*An atomic hydrogen maser clock system designed for long term operation in space will be installed on the Russian space station, Mir, in late 1997. The H-maser's frequency stability will be measured using pulsed laser time transfer techniques. Daily time comparisons made with a precision of better than 100 picoseconds will allow an assessment of the long-term stability of the space maser at a level on the order of 1 part in  $10^{15}$  or better. Laser pulse arrival times at the spacecraft will be recorded with a resolution of 10 picoseconds relative to the space clock's time scale. Cube corner reflectors will reflect the pulses back to the earth laser station to determine the propagation delay and enable comparison with the earth-based time scale. Data for relativistic and gravitational frequency corrections will be obtained from a GPS receiver.*

## INTRODUCTION

Space qualified frequency standards having the frequency stability of the hydrogen (H) maser have a variety of potential applications in space, including very long baseline interferometry, improved navigation systems, tests of relativistic gravitation, and high precision world-wide time transfer. The Hydrogen Maser Clock (HMC) project is a NASA-sponsored experiment to design, build, and test in space an active-oscillation atomic hydrogen maser. The HMC maser instrument, which is being built by the Smithsonian Astrophysical Observatory, will be transported to the Russian Space Station Mir by the NASA Space Shuttle. It will be installed and operated on Mir in the last quarter of 1997.

The space maser's frequency will be measured by means of high-precision time transfer between the space-borne and earth-based clocks, using laser pulse timing. In this system time kept by a clock located at an earth-based laser ranging station (LRS) is compared with the space clock's time by measuring the arrival time of a laser pulse at the spacecraft in terms of both the space and earth time scales. A laser pulse transmitted from the LRS is detected at the spacecraft, and its arrival time is recorded with a resolution of 10 ps in terms of the space clock's time by a high-speed electronic event timer. The pulse is also reflected back to the earth by a retroreflector array mounted on the spacecraft, and is received at the LRS as a return pulse. The two-way propagation delay, measured in terms of the earth clock's time by an event timer located in the LRS, yields the pulse arrival time in terms of the earth clock. The measured

earth and space times provide a comparison of the respective clock time scales. Figures 1 and 2 are block diagrams of the major system components.

The Mir space station is in an orbit inclined at  $51^\circ$  and at an altitude of approximately 450 km. The earth-based LRS for measuring the frequency stability of the HMC hydrogen maser will be at the NASA Goddard Space Flight Center (GSFC), latitude  $38^\circ$ . GSFC is within range of Mir at least once, and sometimes several times, per day. With the expected system precision of better than 100 ps, we will be able to measure the space maser's frequency stability to a level of 1.2 parts in  $10^{15}$  or better. The HMC time transfer system would be suitable for international high precision time transfer by other laser ranging stations within view of Mir.

## **INSTRUMENT OVERVIEW**

The HMC instrument consists of:

- (i) the hydrogen maser physics unit;
- (ii) the electronics required to operate the maser and interface with the spacecraft;
- (iii) two laser event timer units that incorporate retroreflectors and photodetectors;
- (iv) a GPS receiver; and
- (v) a rechargeable silver-zinc backup battery system that will provide continuous operation of up to several hours during power outages.

The instrument is housed in a cylindrical support structure that will be mounted on the outside of Mir's Space Shuttle docking adaptor, shown in Figure 3. The complete HMC instrument package is 43.1 cm in diameter and 83.9 cm long, and has a mass of 200 kg. The instrument will consume on average approximately 156 to 188 watts of 28 volt d.c. power, depending on thermal conditions owing to the orientation of Mir as it orbits the earth.

The HMC instrument is operated by a microprocessor, called the Dedicated Experiment Processor, that monitors the maser's operation, gathers scientific data from the event timers and the GPS receiver, and controls the maser's operating parameters according to commands sent from the ground station and entered by Mir Cosmonauts. The GPS receiver will provide orbital position and velocity data that will be used to correct the space maser's time scale for relativistic and gravitational effects. In addition, the GPS receiver will send pulses to the event timers that will allow us to compare the HMC time scale with GPS time, and thus uniquely identify the laser pulses for comparison with the ground station.

## **THE HYDROGEN MASER PHYSICS PACKAGE**

The H maser oscillator shown in cross-section in Figure 4 is the next generation of the maser built and flown in the 1976 Gravitational Redshift Experiment<sup>[1, 2]</sup>.



The TE-011 mode microwave resonant cavity made of Cer-Vit, within which is mounted a quartz hydrogen storage bulb, is contained in a titanium alloy vacuum tank. A double Belleville spring clamps the cavity endplates to the cylinder and is adjusted so that the compressive force is nominally independent of the length of the clamping structure, thus reducing the effect of thermal expansion on the cavity's resonance frequency. The cavity mounting base plate is attached in cantilever at its center to the base of the vacuum tank to isolate it from dimensional changes in the outer vacuum envelope. The maser signal is picked up by a coupling loop at a level of approximately -100 dBm and sent through an isolator and amplifier to a heterodyne receiver. A second loop within the cavity incorporates a reverse-biased varactor tuning diode to make small frequency adjustments to the cavity's resonance frequency.

Hydrogen is supplied from about 50 grams of lithium aluminum hydride contained in a heated stainless steel container whose temperature is controlled to maintain a constant hydrogen pressure within the container. Hydrogen flow to the maser's dissociator is controlled by sensing the pressure in the dissociator by means of a thermistor Pirani gauge, and regulating the temperature of a heated palladium-silver diaphragm through which hydrogen flows to the dissociator. Expended hydrogen is absorbed by two sorption cartridges that capture only hydrogen. Two small ion pumps with self-contained high voltage supplies remove other outgassing products. Frequency shifts from variation of the magnetic field within the maser storage bulb are controlled by 4 layers of passive shielding and by active field compensation. Magnetic field leakage through the outer shield is sensed by a flux-gate magnetometer and nulled by a compensating coil wound on the next innermost magnetic shield. This combination provides a shielding factor,  $S = \Delta B_{ext} / \Delta B_{int} > 2 \times 10^6$ , for external field variations of  $\pm 0.5$  Gauss. A two-layer flexible printed circuit solenoid closely fitted to the inside of the innermost shield produces a 0.5 milligauss uniform axial magnetic field within the cavity. With the available shielding factor, we can limit the fractional frequency effects of external field variations to less than 1 part in  $10^{15}$ .

The temperature dependence of the resonance frequency of the cavity bulb combination is about -800 Hz/degree C. For frequency stability at  $1 \times 10^{-15}$  we require temperature stability on the order of  $10^{-4}$  degrees C. This level of temperature stability is provided by a multi-zone microprocessor-controlled temperature stabilizing system.

## LASER PULSE TIMING STSTEM

The main components of the HMC time transfer system are the retroreflector array; an omnidirectional fiber-optic light collector; a photodetector and preamplifier; and the event timer, which consists of a constant-fraction discriminator and a time interpolation circuit (TIM) with a resolution of 10 ps. This system is shown in Figure 5. The space-qualified TIM, which has exhibited excellent repeatability and low systematic variation of measured time, is useful for a variety of precise space and earth timing applications.

The HMC retroreflector array consists of 20 fused silica cube corners, each 1 cm in diameter, mounted in a hemispherical base. This shape provides a hemispherical field of view, permitting reflections independent of spacecraft attitude. Laser pulses impinging on the retroreflector array are brought to a photodetector tube by an omnidirectional fiber optic light collector. The



collector consists of a 22-cm long bundle of 127 optical fibers, each 100  $\mu\text{m}$  in diameter. At one end of the bundle the fibers are splayed out into a hemispherical pattern and inserted through holes drilled in a 1.5-cm diameter hemispherical shell that is mounted at the apex of the retroreflector array. The hemispherical fiber array ensures that at least one fiber is illuminated by light coming from anywhere in a hemispherical field of view. The other end of the fiber bundle connects to a photodetector tube (PMT) that detects the laser pulses.

The time transfer system's ability to resolve sub-nanosecond intervals results from a high-precision space-qualified event timer developed at the Los Alamos National Laboratory that is capable of timing with a resolution of 10 ps. The output pulse from the photodetector is sent to a constant-fraction discriminator (CFD), which produces a pulse whose shape is largely independent of the input pulse amplitude<sup>[3, 4, 5]</sup>. This property of the CFD reduces the variation in triggering time that would otherwise result from the orders-of-magnitude variation in laser pulse intensity that can result from changes in atmospheric conditions and in spacecraft attitude and altitude.

The CFD's output pulse goes to the time interpolator<sup>[6, 7]</sup>, which is a combined digital and analog hybrid circuit that has the effect of subdividing the period of a 100 MHz clock signal by a factor of 1000. When a pulse triggers the time interpolator, a constant current  $I_c$  charges a capacitor until the next clock edge arrives. The capacitor is then discharged by a second constant current  $I_d = I_c/1000$ , and the discharge time is measured in terms of clock periods. By this technique the interpolator divides the 10 ns clock period into 1000 "bins", providing 10 ps resolution.

We have built and tested engineering models of the photomultiplier and event timer circuits. Measurements of the interpolator's integral linearity, which measures the total timing error for any bin compared to an ideal perfect interpolator, are shown in Figure 6. The maximum excursion of the integral linearity is less than 10 ps, with test-to-test repeatability of less than 1 ps, and variation of less than 5 ps in any bin from 10°C to 30°C. The resulting systematic variations in measured time are repeatable and can be calibrated to a few picoseconds.

## DATA RETRIEVAL AND COMMAND

Data from the dedicated experiment processor will be stored in a specially modified IBM 750-C laptop computer located within the Mir cabin. Data will be transferred daily for transmission to the Russian Space Agency's ground stations.

The instrument's Dedicated Experiment Processor buffers telecommand signals exchanged between the HMC and the IBM 750-C. Pre-recorded command sequences, stored in the laptop will be executed by keystroke entry by a Russian Cosmonaut. These command sequences include the instrument power-up sequence, cavity resonator tuning, RF dissociator operating level, automated magnetic field measurement and functions for various diagnostic programs.



## ACKNOWLEDGMENTS

The HMC contract is supported by NASA's George C. Marshall Space Flight Center, Huntsville, Alabama under contract number NAS 8 39194.

## REFERENCES

- [1] R.F.C. Vessot, M.W. Levine, E.M. Mattison, E.L. Blomberg, T.E. Hoffman, G.U. Nystrom, B.F. Farrell, R. Decher P.B. Eby, C.R. Baugher, J.W. Watts, D.L. Teuber, and F.D. Wills 1980, "*Tests of relativistic gravitation with a space-borne hydrogen maser,*" *Phys. Rev. Lett.*, **45**, 2081-2084.
- [2] R.F.C. Vessot, M.W. Levine, E.M. Mattison, T.E. Hoffman, E.A. Imbier, M. Tetu, G. Nystrom, J.J. Kelt, H.F. Trucks, and J.L. Vaniman 1977, "*Spaceborne hydrogen maser design,*" Proceedings of the 8th Annual Precise Time and Time Interval (PTTI) Applications and Planning Meeting, 30 November-2 December 1976, Washington, D.C., pp. 277-333.
- [3] R.C. Smith 1988, "*Optimal design of high speed analog APD receivers,*" SPIE Proceedings, 987 = Los Alamos National Laboratory Report LA-UR-88-3731.
- [4] B.T. Turko, and R.C. Smith, "*A precision timing discriminator for high density detector systems,*" Lawrence Berkeley Laboratory Report LBL-30602.
- [5] B.T. Turko, W.F. Kolbe, and R.C. Smith 1990, "*Ultra-fast voltage comparators for transient waveform analysis,*" *IEEE Trans. Nucl. Sci.*, **NS-37**, 424.
- [6] R. Nutt 1968, "*Digital time interval meter,*" *Rev. Sci. Instr.*, **39**, 1342.
- [7] B. Turko 1984, "*Multichannel interval timer,*" *IEEE Trans. Nucl. Sci.*, **NS-31**, 167.

## Hydrogen Maser Clock experiment overview

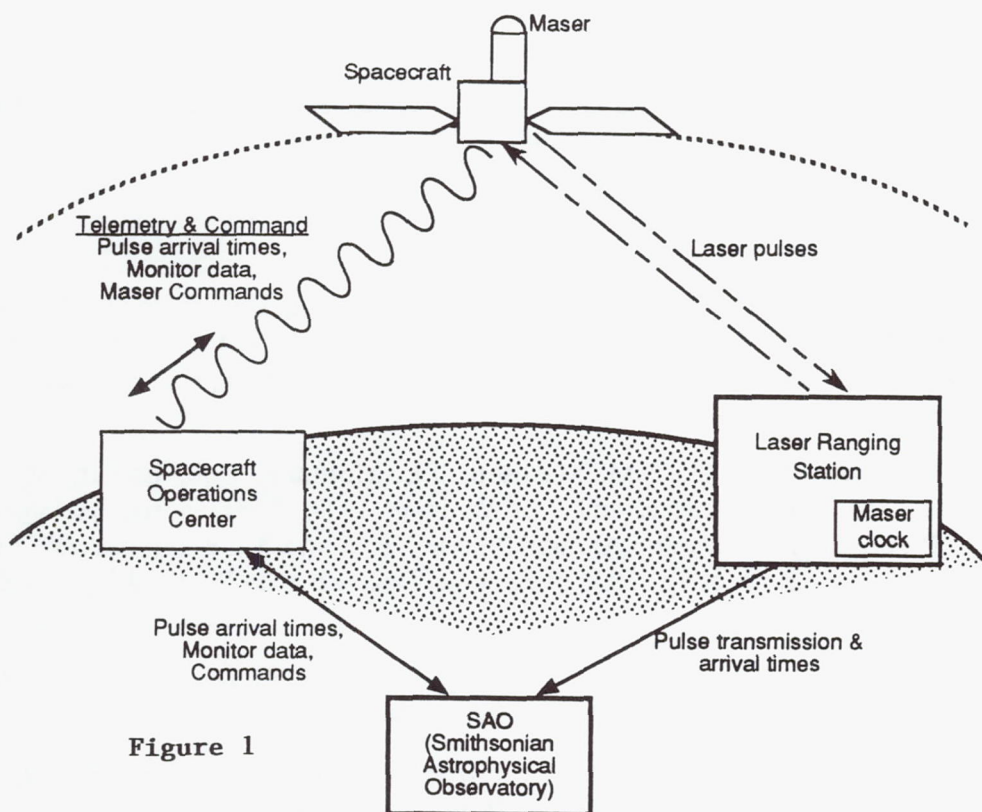
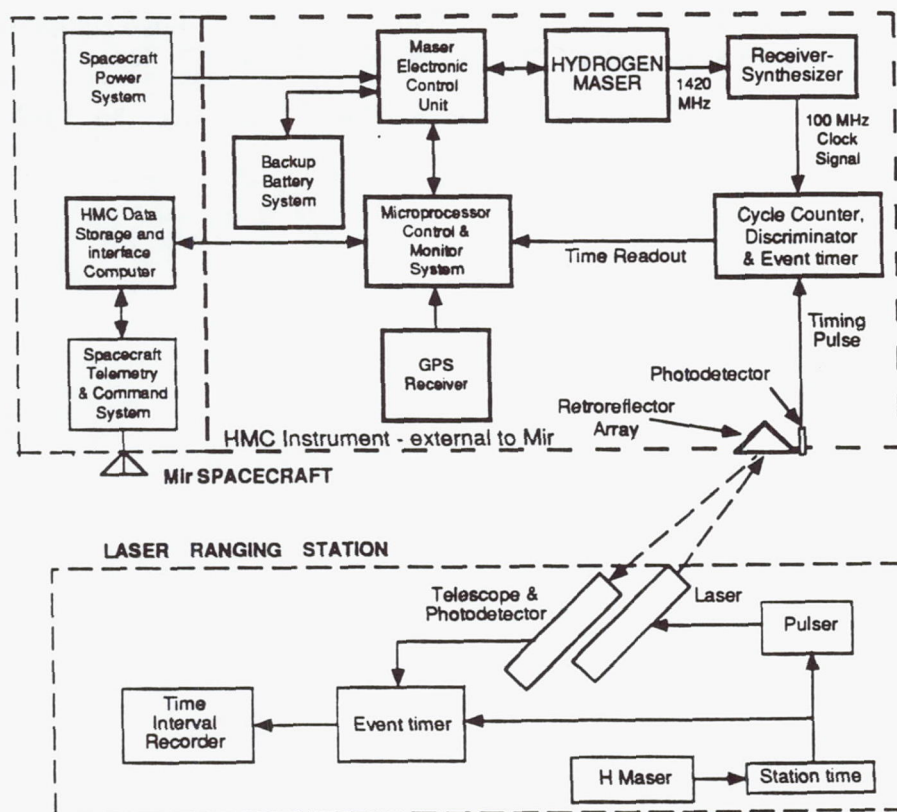


Figure 1



Block diagram of major HMC experiment components

Figure 2



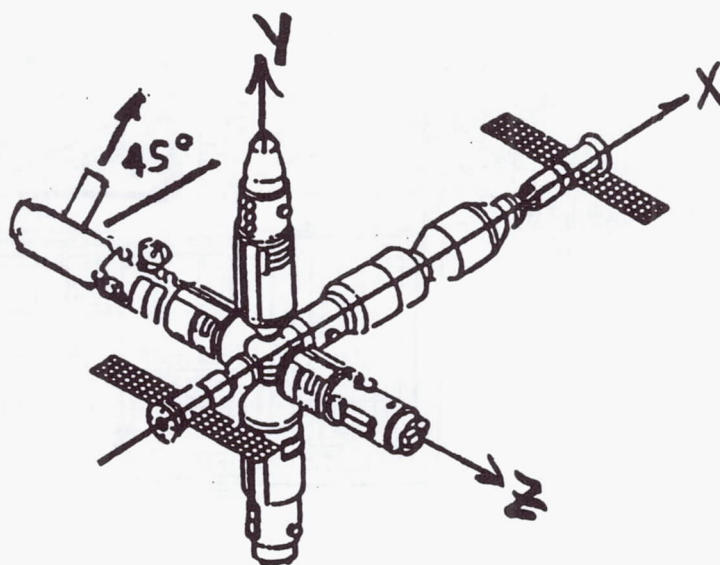
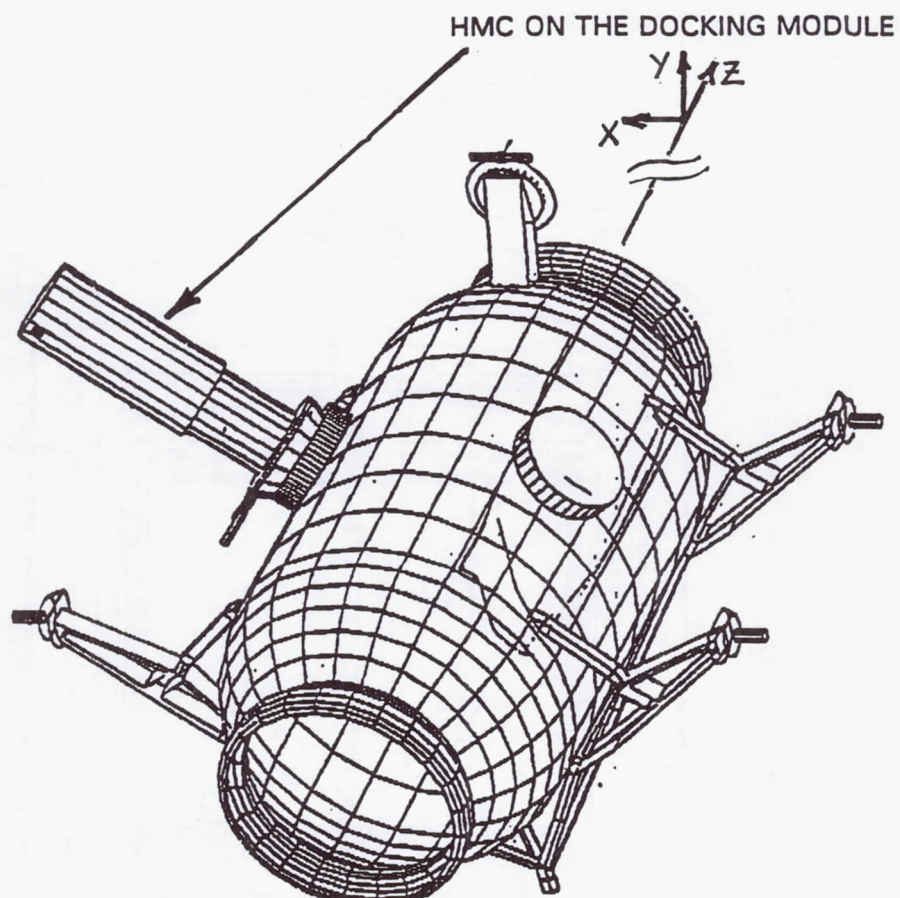


Figure 3 Location of HMC on Mir

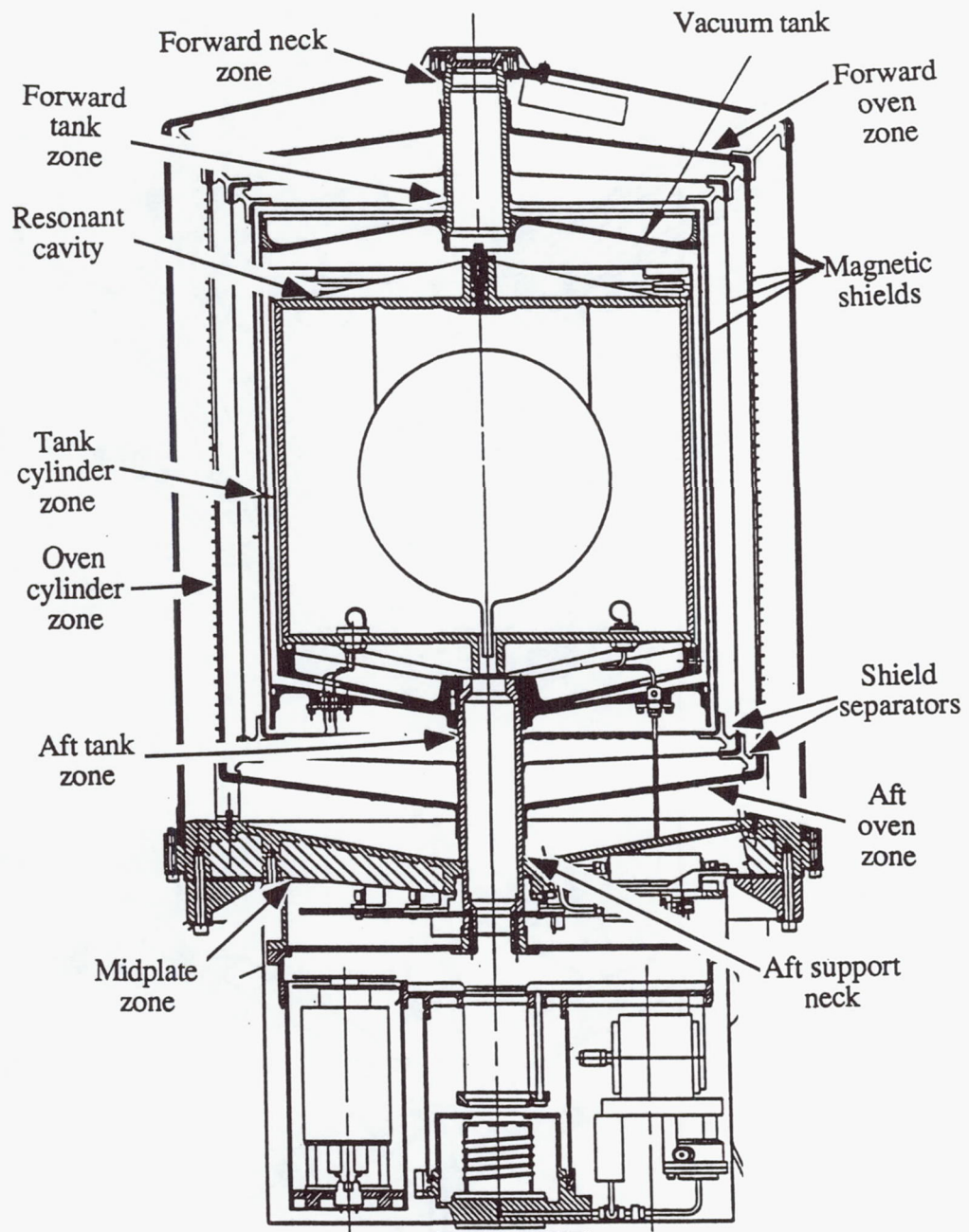
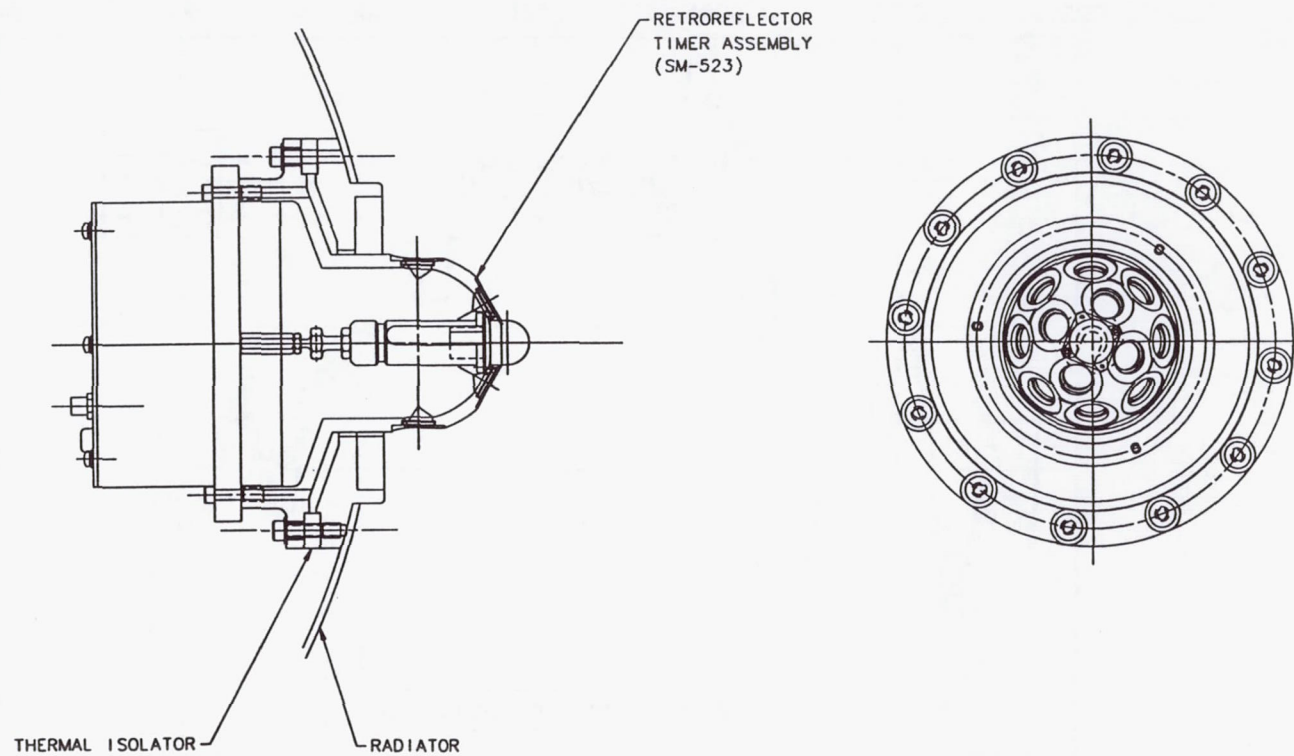


Figure 4 Cross section of Hydrogen Maser Oscillator





RETROREFLECTOR LAYOUT

Figure 5

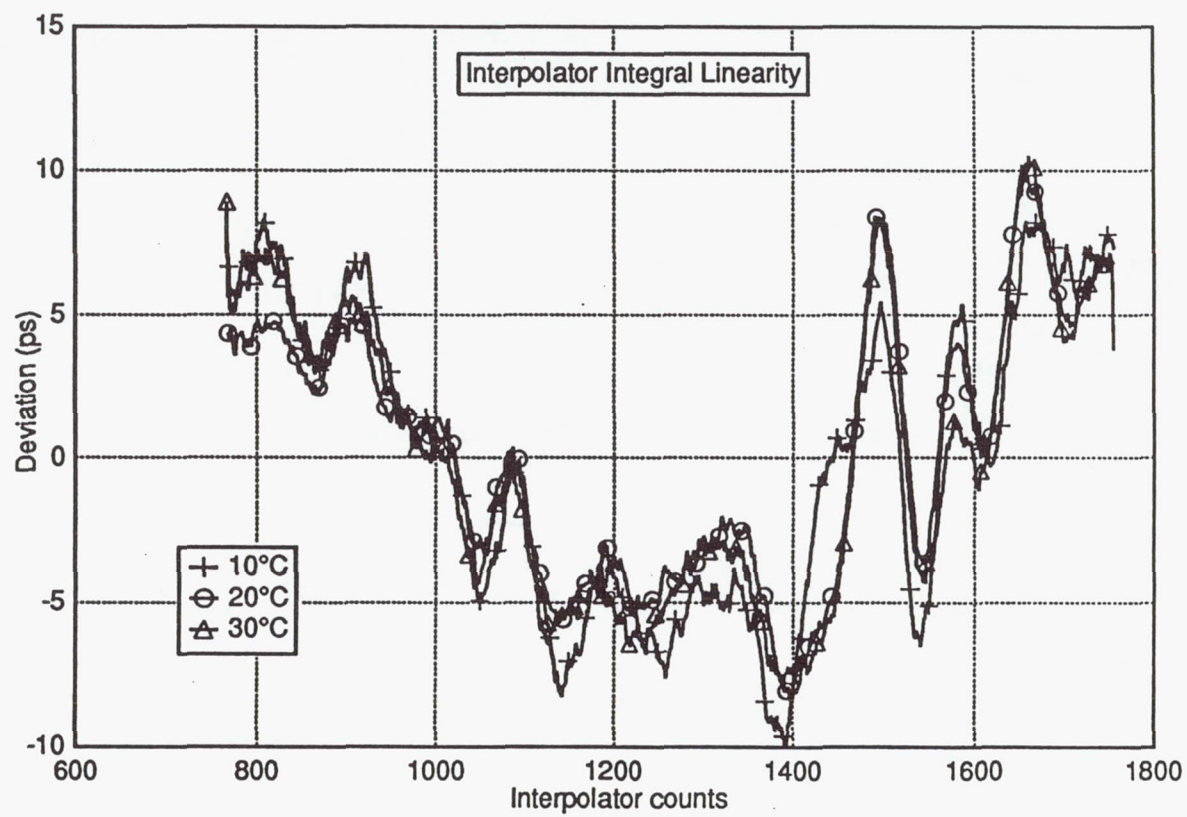


Figure 6



## Questions and Answers

**PIERRE J-M UHRICH (BNM-LPTF, PARIS OBSERVATORY):** In the frame of the FARO Project, we have not yet chosen the space vehicle, and your maser will be launched on a space vehicle, which is not a geo-stationary one. In that case, you have a problem with following the satellites. You don't think you will have any problems following the satellite by using your laser pulse? That's my first question.

**EDWARD M. MATTISON (SMITHSONIAN ASTROPHYSICAL OBSERVATORY):** The worldwide laser ranging network does a lot of ranging to low-earth orbiting satellites. This is a little bit lower than they usually do, and there's a problem with tracking with a slew rate. But according to John Degnan at Goddard, there shouldn't be a problem. If I understand your question correctly.

**PIERRE J-M UHRICH (BNM-LPTF, PARIS OBSERVATORY):** Maybe we'll talk about this later.

**EDWARD M. MATTISON (SMITHSONIAN ASTROPHYSICAL OBSERVATORY):** As Christian said, you'll only see the satellite for maybe five minutes at a time. But, there is not an operational problem in following the spacecraft. Because it's low, you get a huge signal. There's not a problem with intensity.

**PIERRE J-M UHRICH (BNM-LPTF, PARIS OBSERVATORY):** The second point is that unfortunately laser links between the earth and satellites are sometimes subjected to perturbation and sometimes you have clouds over the countries. So there is a need — and this is also the case for the FARO Project — there is a need for a radio-wave link between the space vehicle and the ground. And as far as I know, you intend to do a radio-wave link. Could you comment on this?

**EDWARD M. MATTISON (SMITHSONIAN ASTROPHYSICAL OBSERVATORY):** We have in the past proposed an experiment "STFT," Satellite Time and Frequency Transfer, that uses a radio link with a pseudorandom code modulated signal to establish phase and to compare time. Frankly, we didn't have the money in this experiment to implement that. So, that would be an alternative method of transferring time.

You're absolutely right, we are limited by clouds, by weather; and that is the interest in having, for example, GPS as an absolute farout backup; but, of course, it doesn't give the kind of precision that we can get with the laser ranging. We could get, at best, 30 to 50 nanoseconds instead of on the order of 100 picoseconds resolution.

**C. ANDY WU (THE AEROSPACE CORPORATION):** What is the size and the power consumption required for this device?

**EDWARD M. MATTISON (SMITHSONIAN ASTROPHYSICAL OBSERVATORY):** The maser itself is about "that" big. The entire experiment includes the maser, its electronics; it's all housed in basically a cylindrical structure that is roughly a meter and a half long and about three-quarters of a meter in diameter; and the mass is currently 200 kilograms. That includes the outer structure, battery pack, which was necessitated by being on year, and a variety of other things.

# UPPER LIMIT OF WEIGHTS IN TAI COMPUTATION

Claudine Thomas and Jacques Azoubib  
Bureau International des Poids et Mesures  
Pavillon de Breteuil  
92312 Sèvres Cedex  
France

## Abstract

*The international reference time scale TAI computed by the BIPM relies on a weighted average of data from a large number of atomic clocks. In it, the weight attributed to a given clock depends on its long-term stability. In this paper the TAI algorithm is used as the basis for a discussion of how to implement an upper limit of weight for clocks contributing to the ensemble time. This problem is approached through the comparison of two different techniques:*

- *In one case, a maximum relative weight is fixed: no individual clock can contribute more than a given fraction to the resulting time scale. The weight of each clock is then adjusted according to the qualities of the whole set of contributing elements.*
- *In the other case, a parameter characteristic of frequency stability is chosen: no individual clock can appear more stable than the stated limit. This is equivalent to choosing an absolute limit of weight and attributing this to the most stable clocks independently of the other elements of the ensemble.*

*The first technique is more robust than the second and automatically optimizes the stability of the resulting time scale, but leads to a more complicated computation. The second technique has been used in the TAI algorithm since the very beginning.*

*Careful analysis of tests on real clock data shows that improvement of the stability of the time scale requires revision from time to time of the fixed value chosen for the upper limit of absolute weight. In particular, we present results which confirm the decision of the CCDS Working Group on TAI to increase the absolute upper limit by a factor 2.5. We also show that the use of an upper relative contribution further helps to improve the stability and may be a useful step towards better use of the massive ensemble of HP 5071A clocks now contributing to TAI.*

## 1 INTRODUCTION

The Bureau International des Poids et Mesures, BIPM, is responsible for the generation of worldwide reference time scales, among them International Atomic Time, TAI, and Coordinated Universal Time, UTC. The TAI relies basically on measurements taken from commercial atomic clocks and primary frequency standards maintained in national timing centers. Since 1977, the procedure used for combining these data has been carried out in two steps:



- The first step in the generation of TAI is the computation of the free atomic time scale, EAL (échelle atomique libre), obtained as a weighted average of a large number  $N$  of free-running and independent atomic clocks spread worldwide. The corresponding algorithm, ALGOS, is optimized for long-term stability and postprocesses measurements taken over a basic sample period of  $T = 60$  d[1, 2, 3].
- In a second step, TAI is derived from EAL by frequency steering with the aim of maintaining the accuracy of its scale unit. The steering corrections, determined by comparing the EAL frequency with primary frequency standards, are of the same order of magnitude as the EAL instability[4, 5].

The relative weight  $\omega_i$  attributed to a given clock  $H_i$  reflects its long-term stability. It uses clock measurements covering a full year and is designed to deweight both clocks which are highly sensitive to seasonal changes and hydrogen masers which show a large frequency drift. In practice,  $\omega_i$  is proportional to the reciprocal of the individual classical variance  $\sigma_i^2(6, T)$  computed from the frequencies of the clock, relative to EAL, estimated over the current 60-day interval and over the past five consecutive 60-day intervals. The  $\omega_i$  are numbers between 0 and 1, often expressed as a percentage, which add to 1 over the full set of clocks. They are computed using a temporary value  $\omega_{iTEMP}$  given by:

$$\omega_{iTEMP} = \frac{1}{\sigma_i^2(6, T)} \left[ \sum_{i=1}^N \frac{1}{\sigma_i^2(6, T)} \right]^{-1} \quad (1)$$

The usual problem in such a design is that if one of the contributing clocks is much more stable than others it makes an ever more important relative contribution to the resulting time scale, and finally dominates it. Similarly, a small group may become dominant. This threatens the reliability of the time scale and leads to large instability if one of the high-weighted clocks fails. One of the theoretical solutions to this problem is to set an upper limit of weight. In practice there exist two different possibilities for implementing this limit: one can choose a minimum value  $\sigma_{MIN}^2$  for the variance  $\sigma_i^2(6, T)$  of any individual clock, or a maximum value  $\omega_{MAX}$  for the relative contribution  $\omega_i$  of any individual clock. These two solutions are not equivalent as shown in the following.

In ALGOS, the weight limit has always been chosen following the first of the possibilities described here. However, as the quality of the clocks contributing to EAL rapidly evolves, it is necessary to update the value chosen for the upper limit, and to examine alternatives.

## 2 UPPER LIMIT OF WEIGHTS IN THE PRESENT EAL COMPUTATION

In the present ALGOS configuration, the individual clock contribution is limited by setting a maximum individual stability, characterized by a minimum value,  $\sigma_{MIN}^2$ , of the classical variance computed from six consecutive 60-day frequencies of clock  $H_i$ , relative to EAL. This condition is written in the form:

$$\text{if } \sigma_i^2(6, T) \leq \sigma_{MIN}^2, \text{ then } \sigma_i^2(6, T) = \sigma_{MIN}^2, \quad (2)$$

which means that some of the stability that could be brought to the resulting time scale by clocks for which  $\sigma_i^2(6, T) \leq \sigma_{MIN}^2$  is given up for sake of reliability.

Table 1 gives values of  $\sigma_{MIN}$  used to produce different time scales, published or analyzed for tests, with ALGOS: for example, since 2 May 1995, the value of  $\sigma_{MIN}$  has been set at 2 ns/d.

Period of Computation	Time scale	$p_{MAX}$	$\sigma_{MIN}$ , (ns/d)	$\sigma_{yMIN}(T)$ , $10^{-14}$
1 Jan 88 – 2 May 95	EAL	1000	$\sqrt{10}$	2.11
2 May 95 – still valid	EAL	2500	2	1.34
Mar 92 – Jun 95	E5000	5000	$\sqrt{2}$	0.94
Mar 92 – Jun 95	E10000	10000	1	0.67

Table 1 Values of  $\sigma_{MIN}$  used to produce different time scales with ALGOS: EAL (published), and E5000 and E10000 (analyzed in this paper). The corresponding upper limit of weight,  $p_{MAX}$  is deduced from (8) and the minimum Allan deviation,  $\sigma_{yMIN}(T)$ , is related to  $\sigma_{MIN}$  through  $\sigma_{yMIN}(T) = \sigma_{MIN}/\sqrt{3}$  assuming random walk frequency modulation of clocks over the averaging time  $T = 60$  d<sup>[3]</sup>

An objective criterion to safeguard EAL against abrupt steps of clock frequencies is also required. For each clock  $H_i$  the average  $\bar{y}_i$  and the variance  $\sigma_i^2(5, T)$  of the frequencies  $y_i$  over the last five 60-day intervals, are first computed. Assuming a random walk frequency modulation, a six sample variance  $s_i^2(6, T)$  is calculated using the two criteria:

$$s_i^2(6, T) = (6/5)\sigma_i^2(5, T), \text{ and} \quad (3)$$

$$\text{if } s_i^2(6, T) \leq \sigma_{MIN}^2, \text{ then } s_i^2(6, T) = \sigma_{MIN}^2. \quad (4)$$

Abnormal behavior of clock  $H_i$  is considered to occur if, over the interval of computation,

$$r_i = (y_i - \bar{y}_i)/s_i(6, T) > 3. \quad (5)$$

In this case the weight of clock  $H_i$  is set to zero.

Equation (4) is a direct consequence of using the criterion of maximum stability expressed in (2). It has the effect that the weight of a clock which is more stable than the allowed maximum is not necessarily turned to zero even if it experiences a frequency step greater than  $3s_i(6, T)$ . Such a clock is given a "reserve of stability" which allows it to be maintained close to the upper weight even although its stability has degraded. The result is that the ratio in (5) is not independent of the choice of the value of  $\sigma_{MIN}$ .

Although an absolute value for  $\sigma_{MIN}$  is fixed over a number of years, the maximum contribution of any individual clock  $\omega_{MAX}$  fluctuates with time according to the global quality of the whole



ensemble of clocks. This is shown in Figure 1 for the period January 1988 – April 1995 during which  $\sigma_{MIN}$  remained constant (see Table 1):  $\omega_{MAX}$  has decreased since mid-1990 and has remained below 1% since mid-1993, following the massive input from the newly designed HP 5071A clocks which show outstanding long-term stability. The value of  $\omega_{MAX}$  thus cannot be deduced uniquely from the value of  $\sigma_{MIN}$  and a better way to represent  $\sigma_{MIN}$  is to introduce an absolute weight  $p_i$  rather than a relative weight  $\omega_i$ . There exists an infinity of choices for the definition of the absolute weight  $p_i$ , which allow  $p_i$  to be inversely proportional to  $\sigma_i^2(6, T)$  and:

$$\omega_i = p_i \left[ \sum_{i=1}^N p_i \right]^{-1} . \quad (6)$$

In practice, the weight  $p_i$  is computed in terms of a temporary value  $p_{iTEMP}$  according to:

$$p_{iTEMP} = \frac{10000}{\sigma_i^2(6, T)}, \text{ where } \sigma_i^2(6, T) \text{ is expressed in } (\text{ns/d})^2. \quad (7)$$

It follows that there exists a maximum value for the absolute weight defined by:

$$p_{MAX} = \frac{10000}{\sigma_{MIN}^2}, \text{ where } \sigma_{MIN}^2 \text{ is expressed in } (\text{ns/d})^2. \quad (8)$$

For example, since 2 May 1995, the value of  $p_{MAX}$  has been fixed at 2500. For the 60 day interval of computation May–June 1995, 172 clocks contributed to TAI. Of these, 93 showed a stability better than the stated limit ( $\sigma_{MIN} = 2 \text{ ns/d}$ ) and thus received the maximum absolute weight  $p_{MAX}$ . Each of these clocks contributed a weight of 0.92% to the ensemble.

The absolute weight  $p_i$  of each clock  $H_i$  is deduced from (5), (7) and (8): it is zero,  $p_{iTEMP}$  or  $p_{MAX}$  independent of the other clocks of the ensemble. The set of relative weights  $\omega_i$  is then obtained using (6).

It is not an easy task to fix the value of  $\sigma_{MIN}$ : to make the system reliable a sufficient number of clocks should reach the limit, but some discrimination should be exercised, even among the best clocks. The choice is thus empirical and should evolve with time as the global quality of data improves. For example, faced with the massive input to the EAL computation of data from the very stable HP 5071A units, the CCDS Working Group on TAI decided to increase  $p_{MAX}$  a factor of 2.5, a decision which was applied on 2 May 1995<sup>[6]</sup>. The distribution of the absolute weights attributed through ALGOS is illustrated in Figure 2 for the two consecutive 60 day intervals March–April 1995 and May–June 1995. In each histogram four sets of clocks are distinguished:

- clocks with null weight resulting from abnormal behavior,
- clocks with a small weight, less than 20% of  $p_{MAX}$ , but not null,



- clocks with a non-negligible weight, less than  $p_{MAX}$  but greater than 20% of  $p_{MAX}$ , and
- clocks at  $p_{MAX}$ .

The agreed increase in  $p_{MAX}$  took place between the two 60 day intervals under study, although the clocks themselves were nearly unchanged. The figure shows that the increase of  $p_{MAX}$  helps to equilibrate the distribution of weights: very stable clocks experience stronger discrimination, the detection of abnormal behavior operates more often and intermediate weights are attributed to a larger amount of clocks. All these features improve the stability of the resulting time scale.

The choice of the value of  $\sigma_{MIN}$  should also reflect the physical characteristics of the contributing clocks. The Allan deviations  $\sigma_{yMIN}(T = 60 \text{ d})$  corresponding to the different values of  $\sigma_{MIN}$  which have been used or tested are given in Table 1. The value of  $\sigma_{yMIN}(T)$  corresponding to  $p_{MAX} = 2500$  is small for most of the cesium clocks which are not HP 5071A units: these may not be stable enough to reach the maximum weight. This is not the case for the HP 5071A units. In Figure 3 values of  $\sigma_{yMIN}(T)$  are compared with Allan deviations for the least stable HP 5071A unit to contribute to EAL. It may be seen that this particular clock can hardly reach  $p_{MAX} = 5000$  and cannot reach  $p_{MAX} = 10000$ . Most HP 5071A clocks present a flicker floor at  $6 \times 10^{-15}$  for averaging times ranging from 20 d to 40 d; to discriminate between the best units thus calls for values of  $p_{MAX}$  larger than 10000 or for an alternative way of choosing the upper limit.

### 3 ALTERNATIVE CHOICE FOR THE UPPER LIMIT OF WEIGHTS IN EAL COMPUTATION

Another way to limit individual clock contributions is to choose a value of  $\omega_{MAX}$ , expressed as a fraction (percentage or number between 0 and 1). In this case no criterion exists for individual clock stability and the weight computation requires a two-step iterative procedure:

- A first set of iterations starts from (1). In each, a cut is made at  $\omega_{MAX}$  and the temporary weights are normalized. Several iterations are necessary because each normalization increases the temporary weight of those clocks which have not reached  $\omega_{MAX}$  and may thus lead to another cut. This first set of iterations is convergent: it ends when no more cuts are necessary. It follows that there exists one particular clock which is the last to reach  $\omega_{MAX}$  in the iteration process. This clock is the least stable at  $\omega_{MAX}$  and the variance characteristic of its stability  $\sigma_i^2(6, T)$  is the minimum allowed in the ensemble of clocks at  $\omega_{MAX}$ . It thus plays the role of  $\sigma_{MIN}^2$  defined in 2. The criterion for detection of abnormal behavior can thus operate according to (5). This process affects a number of clocks taken from the whole set with either  $\omega_{iTEMP} = \omega_{MAX}$  or  $\omega_{iTEMP} < \omega_{MAX}$  [3].
- A second set of iterations should then be run to normalize the data and cut off the new temporary relative weights obtained after detection of abnormal behavior. This second set of iterations is also convergent: it delivers a set of normalized relative weights making it possible to compute the weighted average.



The important feature of this process is that it does not independently assign a weight to each clock. Rather the set of clocks is treated globally. Another way to consider this point is to note that the value of  $\sigma_{MIN}$ , the minimum stability required to reach the upper relative weight, is not fixed as in the case of the current ALGOS. It is free to fluctuate: if the global stability of the clocks is improving, the value of  $\sigma_{MIN}$  decreases and the criterion of reaching  $\omega_{MAX}$  becomes more difficult to satisfy. There is thus an automatic discrimination among the best clocks which improves the stability of the time scale. In the case of the current ALGOS this must be done "by hand", through a change of  $p_{MAX}$ .

The choice of the value of  $\omega_{MAX}$  is empirical, as was the choice of  $\sigma_{MIN}$  in the current ALGOS. If we had to implement this new choice for EAL computation at a given date, the most reasonable solution for the choice of  $\omega_{MAX}$  would be that giving the best continuity. This could be realized by setting  $\omega_{MAX}$  to the value it would have had over the current 60 day interval if the computation had been done with the current ALGOS.

## 4 TESTS ON REAL DATA

In this section five different time scales are compared. They are all computed by running the algorithm ALGOS over real clock data, but differ in the way of implementing the upper limit of weight and in its value. They are:

- EAL with  $p_{MAX} = 1000$  over the period March 1992 – April 1995,
- E2500 with  $p_{MAX} = 2500$  over the period March 1992 – June 1995,
- E5000 with  $p_{MAX} = 5000$  over the period March 1992 – June 1995,
- E10000 with  $p_{MAX} = 10000$  over the period March 1992 – June 1995,
- ER with  $p_{MAX} = 1.37\%$  over the period January 1993 – June 1995.

The EAL is the free atomic time scale which was effectively the first step in the calculation of the published TAI over the period March 1992 – April 1995, just before the implementation of  $p_{MAX} = 2500$  on 2 May 1995. For E2500, E5000 and E10000, the value of  $p_{MAX}$  is simply increased. The ER scale is computed using a maximum relative contribution, as explained in Section 3. The period of computation is chosen to cover the two years in which large numbers of HP 5071A clocks entered the TAI ensemble. The value of  $p_{MAX}$  is held constant throughout the period of computation, its value being 1.37%, the value of the maximum relative weight assigned to clocks in the EAL computation, with  $p_{MAX} = 1000$ , in the 60 day interval January–February 1993. The ER and the EAL are thus very close to one another over this particular interval.

Figure 4 shows the comparative variation with time of the number of clocks reaching the maximum weight for the five time scales under study. Four different 60 day intervals are chosen, March – April 1992, 1993, 1994 and 1995, and three clock types are distinguished: hydrogen masers, HP 5071A clocks and other cesium clocks. It follows that:

- The number of HP 5071A clocks reaching the maximum weight increases with time for the five time scales under study.
- Nearly all HP 5071A clocks are weighted at the maximum absolute weight  $p_{MAX}$ , independent of the value of  $p_{MAX}$ , as soon they enter the ensemble.
- Increasing the value of  $p_{MAX}$  yields a decrease in the number of highly weighted hydrogen masers and cesium clocks which are not of the HP 5071A type.
- The time scale ER which was initiated in January – February 1993 is very close to EAL for its first 60 day intervals of computation so, for each clock type, the number of clocks at the upper weight is identical for EAL and ER for the period March – April 1993.
- The use of a constant value of  $\omega_{MAX}$  in ER produces a discrimination with time among hydrogen masers and those cesium clocks which are not of the HP 5071A type, similar to that obtained by increasing  $p_{MAX}$ . However, it also discriminates among the HP 5071A clocks, only maintaining the best of them at  $\omega_{MAX}$ . The discrimination is more important than in the case of E10000 for which the value of  $p_{MAX}$  was already multiplied by a factor 10 relative to the value of  $p_{MAX}$  used in the published EAL.

It follows that increasing  $p_{MAX}$  or fixing  $\omega_{MAX}$  makes the algorithm more sensitive to the frequency drift of hydrogen masers and to the instability of cesium clocks which are not of the HP 5071A design. In addition, the use of a constant  $\omega_{MAX}$  provides some discrimination among HP 5071A units as they progressively enter the ensemble.

It is difficult to set an objective criterion to test the reliability of the time scale. Intuitively, reliability is ensured if a sufficient fraction of the total number of clocks reaches the upper limit of weight and if this fraction does not vary too much. The fraction is given in Table 2 for the four 60-day intervals already chosen for Figure 4. The time scale ER appears to be the most reliable among the five under test:

- The fraction of clocks at the upper limit of weight increased rapidly with time for the four time scales which use an absolute upper limit, while it remains nearly constant at a value close to 25% when a relative upper limit is used.
- Less than 12% of the clocks reached the upper weight during the first eighteen months of computation of E5000 and E10000, so these two time scales are not sufficiently reliable.
- May 1995 was a good time to increase the value of  $p_{MAX}$  in EAL by a factor 2.5. Indeed as more than half of the clocks were at upper limit of weight, a stronger discrimination was necessary.



Interval	EAL	E2500	E5000	E10000	ER
Mar-Apr 92	18.3%	9.1%	5.1%	4.6%	
Mar-Apr 93	23.5%	12.9%	7.8%	5.1%	22.6%
Mar-Apr 94	40.3%	32.1%	28.0%	24.4%	25.8%
Mar-Apr 95	52.1%	43.1%	38.0%	32.4%	28.2%

**Table 2** Ratio of the number of clocks at upper weight to the total number of clocks (expressed as a percentage) for the computation of five different time scales.

Figure 5 shows the variation with time of the relative weight of a clock reaching  $p_{MAX}$  for the four values of  $p_{MAX}$  under study. The limit  $\omega_{MAX} = 1.37\%$  is also indicated. The individual maximum relative weight varies much more with time for  $p_{MAX} = 10000$  than for smaller values. A convergence may be seen for the three last 60 day intervals, from November – December 1994 to March – April 1995, towards values between 0.7% and 1.2% for all values of  $p_{MAX}$ . These are too small relative to the value of 1.37% for  $\omega_{MAX}$  which delivered the most reliable time scale in the period under study.

Values of the Allan deviation  $\sigma_y(\tau)$  have been computed by application of the N-cornered hat technique to data obtained in comparisons between EAL, or E2500, or E5000, or E10000, or ER and five of the best independent time scales in the world maintained at the NIST (Boulder, Colorado, USA), the VNIIFTRI (Moscow, Russia), the USNO (Washington DC, USA), the PTB and the LPTF (Paris, France). They are given in Table 3, and shown graphically in Figure 6 for EAL, E2500 and ER.

	$\sigma_y(\tau)$				
	$\tau = 10 \text{ d}$	$\tau = 20 \text{ d}$	$\tau = 40 \text{ d}$	$\tau = 80 \text{ d}$	$\tau = 160 \text{ d}$
EAL <sup>1</sup>	$4.0 \times 10^{-15}$	$3.4 \times 10^{-15}$	$3.1 \times 10^{-15}$	$3.7 \times 10^{-15}$	$4.6 \times 10^{-15}$
E2500 <sup>2</sup>	$3.7 \times 10^{-15}$	$2.8 \times 10^{-15}$	$2.5 \times 10^{-15}$	$3.1 \times 10^{-15}$	$3.9 \times 10^{-15}$
E5000 <sup>2</sup>	$3.7 \times 10^{-15}$	$2.7 \times 10^{-15}$	$2.3 \times 10^{-15}$	$3.1 \times 10^{-15}$	$4.4 \times 10^{-15}$
E10000 <sup>2</sup>	$3.4 \times 10^{-15}$	$2.5 \times 10^{-15}$	$2.1 \times 10^{-15}$	$3.1 \times 10^{-15}$	$4.8 \times 10^{-15}$
ER <sup>3</sup>	$2.8 \times 10^{-15}$	$2.0 \times 10^{-15}$	$2.0 \times 10^{-15}$	$2.6 \times 10^{-15}$	

**Table 3** Values of the Allan deviation  $\sigma_y(\tau)$  computed for five time scales under study by application of the N-cornered hat technique, using data covering the periods: <sup>1</sup>January 1993 – April 1995, <sup>2</sup>January 1993 – June 1995, <sup>3</sup>July 1993 – June 1995.

The time scale ER is obviously the most stable, with a flicker floor of 2 parts in  $10^{15}$ . In addition, one can clearly see typical frequency noise: white frequency noise for  $\tau$  between 10 d and 20 d and random walk frequency modulation for  $\tau$  between 40 d and 80 d. Unfortunately, not enough data are available to allow a safe estimation of the stability of ER at longer averaging times.

The time scale E2500 shows better stability than EAL for all averaging times. It was thus justified to increase  $p_{MAX}$  from 1000 to 2500 in May 1995.

The noise characteristics of EAL and E2500 are not as pure as those for ER, probably due to residual systematic effects. In particular, Table 3 shows that the  $\sigma_y(\tau)$  values obtained for



E2500, E5000 and E10000 with  $\tau = 80$  d are identical: a limit of about  $3.1 \times 10^{-15}$  seems to have been reached. This suggests the presence of a 'bump' of the type which characterizes a seasonal frequency dependence, an effect which was not apparent in EAL but is revealed by increasing  $p_{MAX}$ . Notice also that this seasonal effect decreases for ER with  $\sigma_y(\tau = 80 \text{ d}) = 2.6 \times 10^{-15}$ .

## 5 CONCLUSIONS

From the beginning, an absolute upper limit of weight has been set in computation of the free atomic time scale EAL. This has the effect that the stability of the most stable clocks is artificially degraded, their characteristic frequency variances being limited to a minimum value. This technique is very simple to put in operation since the weight attributed to a given clock reflects its own behavior independent of the other participating clocks. However, from time to time it is necessary to adapt the value chosen for the minimum variance to match the global quality of the clock ensemble. After tests carried out at the BIPM on real clock data covering the last few years, the CCDS Working Group on TAI decided in March 1995 to reduce the minimum variance by a factor 2.5, an action implemented in the EAL computation on 2 May 1995. This change helps to improve the stability of the resulting time scale by discriminating among participating hydrogen masers and those commercial cesium clocks which are not newly designed HP 5071A units.

More generally, an upper limit of weight could be set for the maximum relative contribution from any one clock. The corresponding weighting procedure is more complicated, since the weight of each clock should be adjusted according to the quality of the whole set of contributing elements, but it gives very encouraging results. With the progressive entrance of very stable clocks, such as the HP 5071A units, fixing an upper limit of relative weight removes from the highest weight category some of those with the weakest stability. This technique is robust and automatically leads to a time scale more stable than the equivalent one computed with a maximum absolute weight. Tests carried out on real clock data covering 1993, 1994, and the beginning of 1995 largely confirm this result, showing a flicker floor level of the resulting time scale at the level of 2 parts in  $10^{15}$  and a reduction of all systematic effects. These results suggest that the stability of the international reference time scale TAI could be improved by setting an upper relative contribution for individual contributing clocks.

## REFERENCES

- [1] P. Tavella, and C. Thomas 1991, "Comparative study of time scale algorithms," *Metrologia*, 28, 57-63.
- [2] C. Thomas, P. Wolf, and P. Tavella 1994, *Time scales*, Monograph BIPM 94/1, 52 pages.
- [3] C. Thomas, and J. Azoubib 1995, "TAI computation: study of an alternative choice for implementing an upper limit of clock weights," *Metrologia*, in press.
- [4] J. Azoubib, M. Granveaud, and B. Guinot 1977, "Estimation of the scale unit duration of time scales," *Metrologia*, 13, 87-93.



- [5] *"Differences between the normalized frequencies of EAL and TAI,"* 1994, Annual Report of the BIPM Time Section, 7, Table 5, p. 35.
- [6] G. Petit 1995, *"Report on the discussions and decisions of the meeting of the CCDS Working Group on TAI,"* 7 pages.

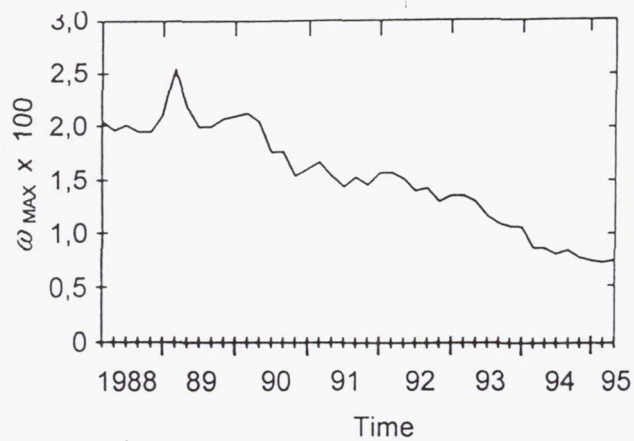


Figure 1: Variation with time of the maximum relative contribution  $\omega_{\max}$  of an individual clock in EAL computation for the period January 1988 - April 1995 ( $\sigma_{\min} = 2 \text{ ns/d}$ ).

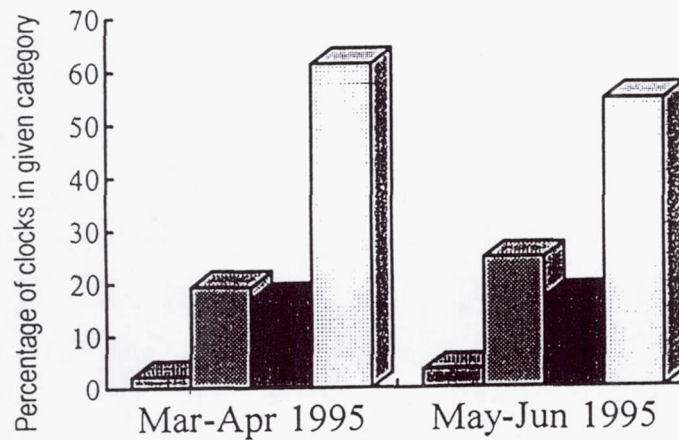
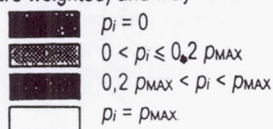
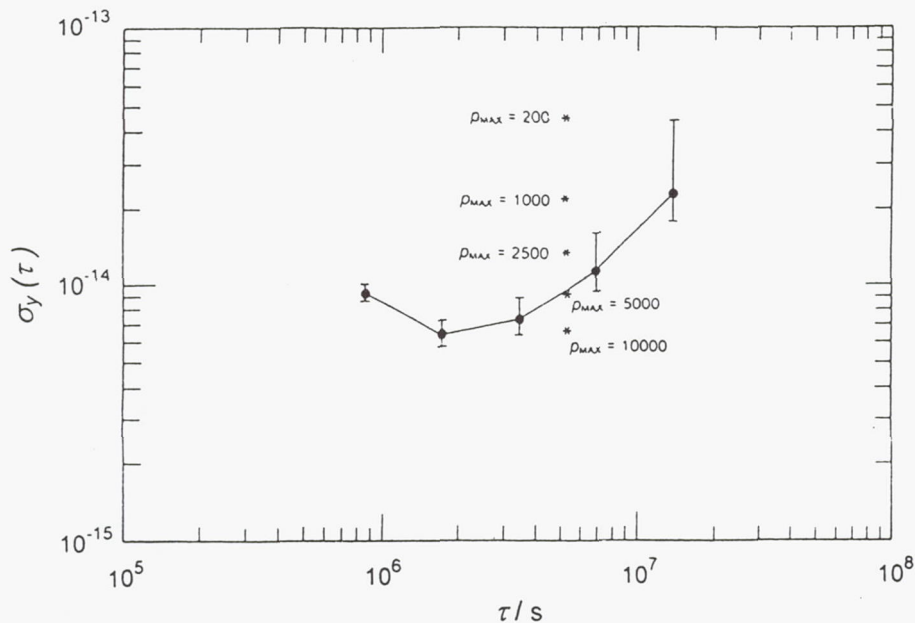


Figure 2: Histograms showing the distribution of clocks assigned a weight  $p_i$  for two consecutive 60 day intervals of 1995: March - April 1995 ( $p_{\max} = 1000$ , 181 clocks are weighted) and May - June 1995 ( $p_{\max} = 2500$ , 170 clocks are weighted).







**Figure 3.** Curve characterizing the stability of the least stable HP 5071A unit contributing to EAL. The values of the Allan deviation  $\sigma_{yMIN}(T = 60 \text{ d})$  corresponding to the minimum stability necessary for reaching  $\rho_{MAX} = 200, 1000, 2500, 5000$ , and  $10000$  are also indicated (see also the 5th column of Table 1).

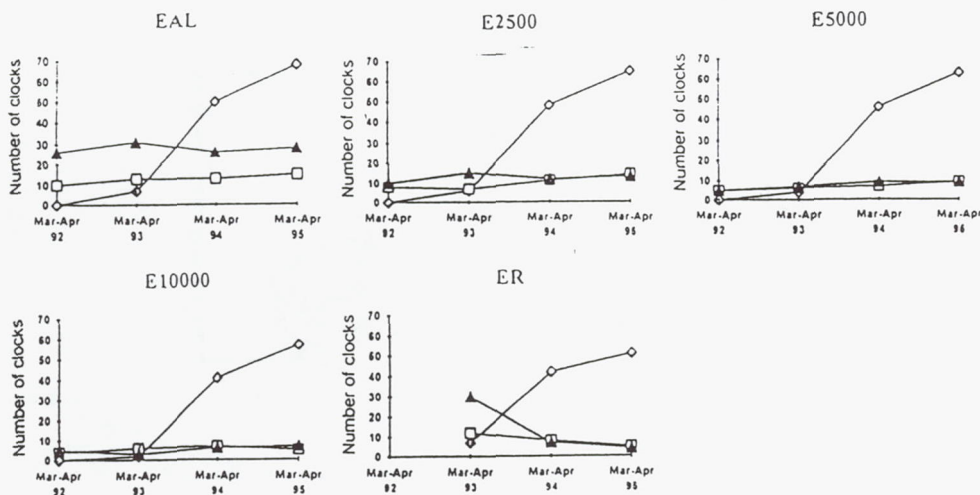


**Figure 4:** Variation with time of the number of clocks reaching the upper limit of weight in the computation of five different time scales: EAL, E2500, E5000, E10000 and ER. Three different types of clocks are distinguished: HP 5071A ( $\diamond$ ), hydrogen masers ( $\square$ ) and other caesium clocks ( $\blacktriangle$ ).

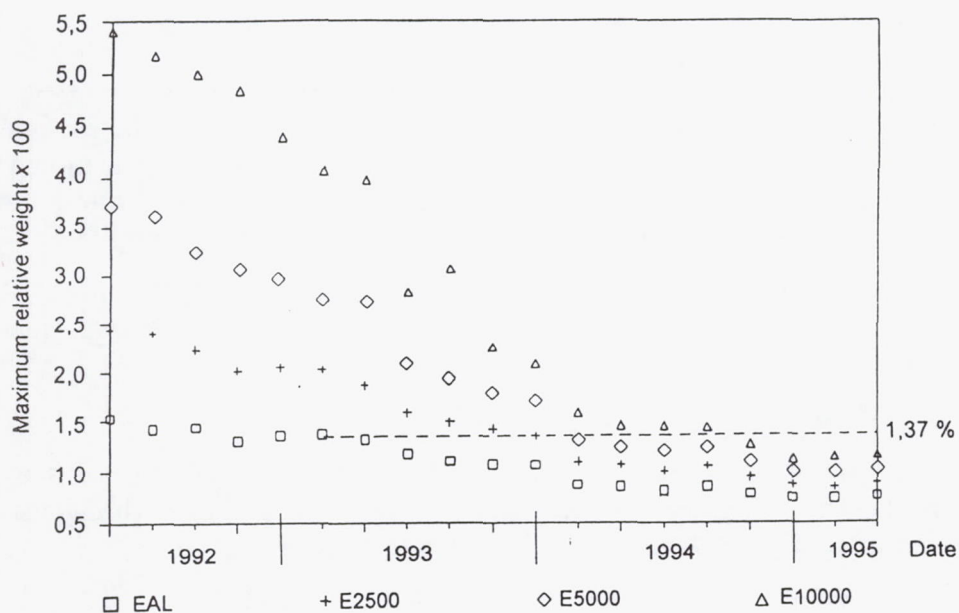


Figure 5. Maximum relative weight reached by individual clocks in the computation of the time scales EAL, E2500, E5000 and E10000 over the period March-April 1992 to March - April 1995. The upper limit of relative weight  $\omega_{\max} = 1,37\%$  used for computation of the time scale ER is indicated in the figure.

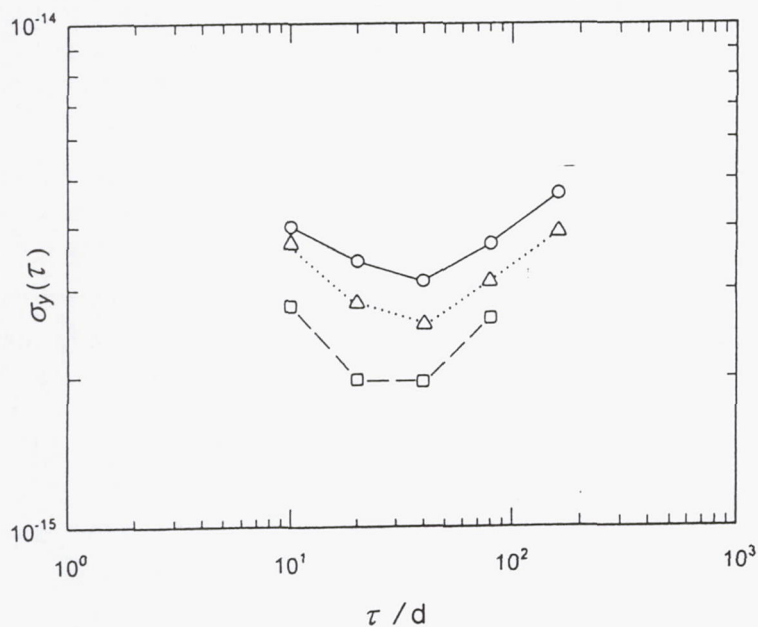


Figure 6: Variation with the averaging time  $\tau$  of the Allan standard deviation  $\sigma_y(\tau)$  computed by application of the N-cornered hat technique on the data of time comparisons between EAL, or E2500, or ER, and 5 of the best independent time scales of the world. The data involved covers the periods January 1993 - June 1995 for EAL and E2500, and July 1993 - June 1995 for ER.



## Questions and Answers

**DR. GERNOT WINKLER (USNO, RETIRED):** I remember that the original argument in favor of maximizing of setting a limit to the maximum weight has been the concern, that that time scale should not become dependent on a few very good performers. So it was a question of reliability and robustness. I think that's a very important point.

On the other hand, if you increase relative weight or go, as you said, with your ER scale and you still have about 25 percent of your clocks reaching that upper limit, that seems to be an entirely acceptable compromise. Do you agree?

**CLAUDINE THOMAS (BIPM):** Yes, I completely agree.

**SERGEY V. ERMOLIN (HEWLETT-PACKARD CO.):** My question is about the lower limit of stability. Why do you set a lower limit and artificially bring in the poorer performance clock to this lower limit to include it into the scale?

**CLAUDINE THOMAS (BIPM):** I'm not sure what you mean.

**SERGEY V. ERMOLIN (HEWLETT-PACKARD CO.):** Well, if I understood it correctly, you set a lower limit of stability, which was about, I think, 10 nanoseconds per day; and then you saved the clock below 10 nanoseconds per day. You still made it 10 nanoseconds per day. It seems to me that for you to include this inferior clock, you artificially bring the stability of the clock up. Why do you do it?

**CLAUDINE THOMAS (BIPM):** We do that because it is absolutely necessary to do that; because, if one clock was much more stable than others, it would, during time, when time is passing, completely dominate the time scale. That's what we cannot accept; because, if this clock fails, we would have a time step in our time scale.

Of course, we are losing stability for some very, very good clocks. It is a compromise, you know. We must improve the stability, so use the best clocks. But, on the other side, we must not have only one or a very small ensemble of clocks completely dominating the time scale. It is not possible because of availability. So it's a compromise.

**SERGEY V. ERMOLIN (HEWLETT-PACKARD CO.):** Yes, I understand it. I'm not sure I stated my question right. You also have clocks with bad performance which, on your report, you assign a higher stability.

**CLAUDINE THOMAS (BIPM):** You mean clocks with bad performance?

**SERGEY V. ERMOLIN (HEWLETT-PACKARD CO.):** Yes.

**CLAUDINE THOMAS (BIPM):** Which was reaching the limit, you mean?

**SERGEY V. ERMOLIN (HEWLETT-PACKARD CO.):** Yes, a lower unit.

**CLAUDINE THOMAS (BIPM):** I'm not sure I understand. Well, what I showed, this clock was maybe a bad clock for this kind of clock. But it's already a very good clock, it was below  $10^{-14}$ .

**ALBERT KIRK (JPL):** Do you only consider measured performance data? Or do you also

use as an input reported discontinuities on these clocks, that are reported to you from around the world?

**CLAUDINE THOMAS (BIPM):** Do you mean if we are only using real clock data?

**ALBERT KIRK (JPL):** I mean, suppose somebody makes a small frequency adjustment of a few parts in  $10^{14}$ .

**CLAUDINE THOMAS (BIPM):** We take these things into account - - -

**ALBERT KIRK (JPL):** If they are reported only.

**CLAUDINE THOMAS (BIPM):** If they are reported. We are asking people to report such operation. And if we see something which has not been reported, we ask people if they did something on their clock. So we try to monitor all these things the best we can, of course.



# **TUTORIAL: CLOCK AND CLOCK SYSTEMS PERFORMANCE MEASURES**

David W. Allan  
Allan's TIME

## **Introduction**

This tutorial contains basic material — familiar to many. This will be used as a foundation upon which we will build — bringing forth some new material and equations that have been developed especially for this tutorial. These will provide increased understanding toward parameter estimation of clock and clock system's performance.

There is a very important ITU Handbook being prepared at this time which goes much further than this tutorial has time to do. I highly recommend it as an excellent resource document. The final draft is just now being completed, and it should be ready late in 1996. It is an outstanding handbook; Dr. Sydnor proposed it to the ITU-R several years ago, and is the editor with my assistance. We have some of the best contributors in the community from around the world who have written the ten chapters in this handbook. The title of the Handbook is, "Selection and use of Precise Frequency and Time Systems." It will be available from the ITU secretariat in Geneva, Switzerland, but NAVTEC Seminars also plans to be a distributor.

## **Definitions and Concepts**

If we ask the very simple question, "What is a clock?" We discover that essentially all clocks can be considered two-part devices: a resonator or frequency source and counter or divider for keeping track of the number of oscillations. As an example, we have the definition of a second: when 9,192,631,770 oscillations occur of the photon associated with the quantum ground-state of the cesium-133 atom, we have a second. The electronics for counting are more sophisticated than for the ordinary clock, but the concepts are the same.

Given this concept, it is important to remember that the counter (divider) will always deteriorate the signal. In other words, the phase noise of the sine wave of the source, for example, will be more stable than the clock's output. We will come back to this when we talk about measurement noise and optimization algorithms.

Consider another very important concept: If we have two clocks, we feel obligated to ask the question, which is correct under the basic statistical theorem that every clock disagrees with

every other clock? The disagreement may be very small, but they will always disagree except at most an instant. In fact, you can make the very strong statement that it is impossible to have two clocks perfectly synchronized, except at an instant, because of noise. So, you can never have two clocks perfectly synchronized on a continuous basis.

In a fundamental sense, what is the difference between frequency and time? We can talk about frequency in an absolute sense as in the definition of the second. Time is not absolute. It is an artifact — depending on when we set the integrator as we started counting seconds, for example. Independently, a frequency standard built in Braunschweig, Germany will agree with one built in Boulder, Colorado within their accuracy limits because they are based on the same fundamental phenomena within physics.

Time, on the other hand, depends upon when you set the integrator for counting the seconds. Hence, two clocks may be arbitrarily different in their readings. There is no absolute time with which to compare a clock.

Figure 5 compartmentalizes the perceived causes of clock deviations into four areas:

- 1) How we process the data is very important. Clock performance can be made worse by improper processing.
- 2) The measurement noise limits our ability to see the true performance of a clock. A classic example is GPS SA. If it were turned off, the venetian blinds would go up, and we would be able to see the GPS satellite clocks very clearly. The measurement noise should always be considered; it may be negligible compared to the clock noise, but often it is not.
- 3) Every clock has intrinsic mechanisms which perturb its output time. By nature it is convenient to have two sub-categories for the intrinsic clock perturbations — typically denoted by the random variations and by the systematic variations. Random and systematic variations also occur in measurement systems as well as in the environmental perturbations. The environment perturbations can look like a random process, depending upon how it couples into the clock. And
- 4) the environmental perturbations often adversely impact the long-term performance of a clock. Clearly, it is desirable to design to minimize the environmental perturbing effects.

Let us now review some fundamental clock concepts (see Figure 6) A working definition of time is the apparent reading of a clock. Synchronization is to have two or more clocks with the same apparent time reading. In principle, this has to be within some level of uncertainty since every clock disagrees with every other clock except at most an instant. Syntonization is to have two or more clocks with the same apparent rate. In the telecommunication industry, they word “synchronization” is often used when, in fact, what is meant is “syntonization.” These are two different useful concepts, and if used properly can help avoid a lot of confusion in specifications and in system performance descriptions. Syntonization also needs to be specified with an uncertainty.



Simultaneity doesn't really require a clock. Here two or more events occur at the same moment, as perceived in some reference frame.

The environmental elements which we often see that perturb clocks are listed in Figure 7. This list contains some of the more important ones. One of the fundamental breakthroughs with the HP model 5071A cesium clock is that by active electronic control and feedback the effect of the environment can be greatly reduced. This approach has improved the long-term stability by more than an order of magnitude over other models.

There is a new IEEE standard, 1193-1994, which gives guidelines for the measurement of environmental sensitivities. Later, we will use some of the messages from this standard. This standard is another good reference document. The place to order it is shown in Figure 8.

## Measurement Models, Terminology and Concepts

Figure 9 shows the usual model for an oscillator's output. The frequency,  $\nu(t)$ , always varies with time; hence, its period,  $\tau(t)$ , also varies. One of our main goals in this tutorial is to clearly and in a parsimonious way quantify these variations so that there is good communication between the vendor and the user, and so that the designer or planner may work effectively and efficiently. The output need not always be a sine wave. The following characterization procedures have been kept general enough to work as well for square wave or for any periodic signal. But since sine waves are fundamental to nature, this is the common representation.

Using the sine-wave as a conceptual model, we usually have a nominal frequency at which the standard is designed to work,  $\nu_0$ . By definition it does not vary with time. We then use  $\phi(t)$  to denote all the phase variations around the nominal accumulated phase,  $2\pi\nu_0 t$ . The cycles of an oscillator are counted to create a clock. Again, the divider noise will degrade the signal from the oscillator. Hence, without some special filtering, the integrated clock noise will always be greater than the integrated oscillator noise.

As illustrated in Figure 10, what is measured in practice is never the time of a clock, since we have no absolute reference with which to measure it alone. What, in fact is measured is the time difference between two clocks. The time difference can be measured with arbitrary precision. Today there exists instrumentation which can measure time differences at the femtosecond level using the carrier phase.

Figure 11 shows the normalized representation of frequency offset  $y(t)$ . This is a dimensionless quantity which is simply defined as the free-running frequency,  $\nu(t)$  of the clock, minus its nominal frequency,  $\nu_0$ , all divided by the nominal frequency. Even though this is a conceptual value, in practice it is very useful because  $\nu_0$  can be the reference oscillator of the pair being measured. In addition, there is the big advantage that  $y(t)$  is a small number compared to  $\nu(t)$ . Conceptually  $y(t)$  represents the offset from the ideal. It is often referred to as parts in  $10^{10}$ , for example, or equivalently  $1 \times 10^{-10}$ .

On the other hand, the time offset,  $x(t)$ , is the exact integral of the frequency offset,  $y(t')$ , integrated from 0 to  $t$ . It also can be written exactly in terms of the  $\phi(t)$  shown in Figure 9,  $x(t) = \frac{\phi(t)}{2\pi\nu_0}$ . We often talk about time deviations or phase deviations interchangeably, and since



they are directly proportional this is okay.

Because of the integral relationship shown in Figure 11, the fractional frequency offset,  $y(t)$  is the time derivative of the time offset. Hence, the slope on a phase plot is proportional to the frequency offset.

Figure 12 gives a simple parsimonious model for the time offset or time error of a clock. The first term represents the synchronization error,  $x_0$ . The second term contains the syntonization error,  $y_0$ . It gets multiplied by the running time to calculate its effect on the total time error. The third term contains the linear frequency drift. Its dimensions will be fractional frequency change per unit time interval, per second or per day, as examples. All of the rest of the deviations are included in  $\epsilon(t)$ . Here, we often hide a multitude of sins! This last term, for example, could represent all of the effects due to environmental perturbations while also containing the random noise deviations. In addition, it may contain side-band components due to diurnal effects, or to modulation or RFI.

If we subtract off the effects of the first three systematic terms, then  $x(t) = \epsilon(t)$ . Analyzing these residuals is very helpful in diagnosing the effects of the random and other perturbations on the clock. Once the level and kind of random perturbations are known, then optimum estimation procedures can be used to better estimate the systematic effects as well as being able to calculate optimum predictions, for example.

Taking the derivative of the model equation in Figure 12 yields:  $y(t) = y_0 + Dt + \dot{\epsilon}(t)$ . Writing the equation this way will be useful later as we get into optimum parameter estimation.

## Frequency and Time Accuracy and Stability

Figure 13 shows an example of two very simple systematic situations: a positive frequency offset, and a negative frequency drift. The first drawing illustrates  $y(t)$  and the second one its integral,  $x(t)$ . The constant frequency offset turns into a ramp for the time error, and the drift into a quadratic. We assume the same synchronization error (constant of integration) for both situations.

In 1988, IEEE Standard 1139-1988 was published providing a recommended set of measures for time and frequency characterization. Figure 14 gives some of those measures from this standard. The exception is  $\sigma_x(\tau)$ , as it had not been developed at that time. Subsequently, it has been adopted by the telecommunications community and by the ITU-R. As we need them, we will describe the functionality of some of these measures.

Figure 15 gives some time-domain definitions and some useful measures. For example,  $y(t)$  is a direct indicator of frequency accuracy if the reference,  $\nu_0$ , is the definition of an agreed upon standard. Similarly,  $x(t)$  is a direct indicator of the time inaccuracy if it is taken with respect to UTC, which is the correct time by definition. The other three sigma measures shown are for determining the level and kind of instabilities, as will be shown later.

As was mentioned before, the design of the relatively new HP 5071A cesium-beam clock was for increased accuracy and improved immunity to environmental perturbations — resulting in



greatly improved long term stability. Figure 16 is a histogram of  $y(t)$  for the 94 HP 5071A clocks contributing to TAI/UTC during 1994. Figure 17 shows the 311 total participating clocks during 1994 plotted with the same abscissa. It is apparent that the design goals have nicely been met. The accompanying paper gives more details as well as documenting the performance of TAI/UTC<sup>[1]</sup>. The introduction of the HP 5071A clocks, as Dr. Thomas has pointed out, is having a major impact toward improving the performance of International Atomic Time.

In both Figures 16 and 17 the mean is significantly larger than the standard deviation of the mean. So in both cases the standards would not be considered in statistical control. Hence, the need for primary standards, so that calibrations with same can provide frequency accuracy; i.e. agreement with the definition of the second.

Figure 18 a frequency stability diagram — using  $\sigma_y(\tau)$  — showing the range of values available for most of the important clocks to our community. This stability diagram is taken from an ITU-R document giving the characteristics of these clocks<sup>[2]</sup>. QZ stands for quartz crystal oscillators, RB stands for rubidium-gas-cell frequency standards, CS stands for cesium-beam frequency standards, and HM stands for hydrogen-maser frequency standards. For CS stabilities, an extended line has been drawn in representing the improved long-term frequency stability of the relatively new HP 5071As.

Figure 19 is a plot of the time accuracy of three time scales over the last approximately 200 days: UTC(NIST), UTC(OP), and UTC(USNO-MC). These three time scales are taken with respect to UTC, the official time for the world. By definition, how well a clock agrees with UTC is a measure of its true time accuracy. All three have been within nominally 100 nanoseconds for about the last half year. The time accuracy of many of the worlds time scales have improved significantly over the last three years. This has been primarily driven with the introduction of the HP 5071As into these sundry time scales.

One of the most significant challenges that a timing center has toward time accuracy is in predicting where UTC will be at the current time, because UTC is calculated and distributed about one and one-half months after the fact. Each country maintains its own real-time estimate of UTC — denoted UTC(i) for the  $i^{th}$  timing center. Clearly, if UTC were available in real-time, it would be far simpler to have a high-level of time accuracy. Through international cooperation, this direction is being pursued.

The limiting noise for the cesium clocks contributing to TAI/UTC is white-noise FM. The optimum RMS prediction error for this noise is  $\tau_p \sigma_y(\tau_p)$ , where  $\tau_p$  is the prediction interval. For the USNO data over the last half of year, the RMS error is 6 ns. This is not the same as the standard deviation; the 6 ns is with respect to the truth, which is UTC by definition.

An RMS error of 6 ns with  $\tau_p$  = about 45 days implies that  $\sigma_y(\tau_f) \leq 1.5 \times 10^{-15}$ , since any prediction algorithm cannot be better than optimum. If the USNO time scale and UTC were independent, then this number would be directly related to the square root of the sum of the variances from each scale. The weight of the USNO clocks contributing to TAI/UTC is about 40 percent. The effect of the bias of a time scale contributing is given approximately by  $1/(1 - \text{weight})$ . Hence, we can conclude that either of the two time scales is equal to or better than  $2.6 \times 10^{-15}$  at  $\tau = 45$  days, and one of the scales is better than this number divided by  $\sqrt{2}$ , or



than  $1.8 \times 10^{-15}$ .

This level of stability represents a major advancement during the last three or four years. And again, it comes mainly as a result of the introduction of the HP 5071A clocks with their excellent environmental insensitivity. One would also conclude that the prediction algorithm used by USNO is very close to optimum.

## Random Processes, Models and Measures

Characterizing the random deviations in a clock's performance allows us to determine the noise type. Knowing the type of noise then allows us to design optimum parameter estimation procedures. Figure 20 illustrates two very important types of noise. Since one flip of a coin is independent of the next flip, a series of flips generates a random and uncorrelated series. In other words, a flip of heads at one point in time has no bearing on whether the coin will come up heads or tails at another time. The spectral density of these flips is then a white-noise process.

We can integrate these flips by taking one step forward with heads and one step backwards with tails. Our displacement from the origin is now a random-walk process and has an  $f^{-2}$  spectral density. These same arguments are very analogous as to why the random time deviations out of most atomic clocks are a random-walk process. The atomic-clock servo hunts for the resonance frequency being limited by white noise in the search; the integral of these white frequency deviations generates a random-walk in the time deviations. *Vice-versa*, if a derivative or first difference is taken of random-walk time deviations, the process turns into one with a white-noise spectrum.

The HP 5071A is an excellent example of a clock with classical white-noise frequency spectrum over many decades of Fourier space. This kind of noise causes  $\sigma_y(\tau)$  to go as  $\tau^{-1/2}$ , and for the high-performance model of this clock the white-noise behavior extends from about 10 seconds to as long as  $10^7$  seconds in some cases with a performance specification given by the top equation in Figure 21. Such behavior results in long-term stabilities well below  $1 \times 10^{-14}$ .

As also illustrated in Figure 21, whereas white-noise FM is the ideal classical noise for most atomic clocks, white PM is the ideal classical measurement noise. That measurement noise can, of course, contribute to  $\epsilon(t)$  in the general model equation for the time error between two clocks.

As shown in Figure 22, typically five different noise processes are employed to model clocks, oscillators and measurement systems. These seem to be fairly basic in nature. Figure 23 gives the Fourier transformation relationships between the time-domain measures and the frequency-domain representation, as well as the region of applicability. Using these relationships and going back to Figure 17, one can see both the regions of applicability (from the different slopes corresponding to the  $f$  values) as well as the different levels of random variations.

Figure 24 gives the abbreviation, the name and the mathematical expression for each of these three time-domain measures. Their square roots are: ADEV, MDEV and TDEV, respectively. The first two measures are explained in detail in NIST Technical Note 1337<sup>[3]</sup> and all three



in the upcoming ITU-R Handbook. The transformation coefficients from the time-domain to the frequency-domain or *vice-versa* (preserving the noise type and level) may be found in reference[4] and for AVAR and MVAR in NIST TN 1337.  $\text{TVAR} = \tau^2 \text{Mod.}\sigma_y^2(\tau)/3$  has been shown to be a very good measure for measurement system stability, network stability, and time dissemination stability. TVAR was developed after the publication of NIST TN 1337.

Note that the equations for AVAR, MVAR and TVAR in Figure 24 are all represented in terms of a second difference of the time deviations,  $x$ . In the case of MVAR and TVAR, the  $x$  values making up the second difference are each averaged over a separate, but sequentially adjacent interval  $\tau$  — rather than being a time error measurement at a point as for AVAR. The effect of averaging the data in an appropriate way, applies a filter in the software so that it effectively modulates the bandwidth of the software processor. This bandwidth modulation removes the ambiguity associated with AVAR; i.e. AVAR has essentially the same slope ( $\mu = -2$ ) value, for either white-noise PM or for flicker-noise PM. MVAR and TVAR can distinguish between white-noise PM and flicker-noise PM — having different slopes when plotted logarithmically versus  $\tau$ .

## Applications of Optimum Parameter Estimation and Prediction

As shown in Figure 25, optimum parameter estimation means that once a model parameter has been determined, the residuals around that parameter model have been minimized in a squared-error sense. Similarly, for prediction, the errors of prediction are minimized in a squared-error sense. Of course, both parameter estimation and prediction will depend upon the type and the level of the noise processes involved. Hence, knowing the noise type and level is essential for optimum parameter estimation and prediction.

The statistical theorem given in Figure 26 is important, as well as useful and simple. In particular, it is useful for parameter estimation and for prediction. Since nature gives us white PM and white FM, this theorem is directly applicable in these cases. In addition, the long-term performance of most clocks may be reasonably well modeled as a random-walk FM process; this is sometimes called white acceleration because the second derivative of  $x$  ( $d^2x/dt^2$ ) has a white spectrum. Here again we may use the above theorem.

Two very important examples are the following. In Figure 21 it was pointed out that white FM is the classical noise for most atomic clocks, and white PM is the classical noise for an ideal time-difference measurement system. Hence, as illustrated in Figure 27, in the presence of white FM, AVAR is the optimum estimator of frequency change (or instability). This is true since each of the average frequencies, taken over an interval  $\tau$ , is the optimum estimate of frequency over that interval. Comparing an optimum with an optimum causes the difference to be an optimum estimate of the change. AVAR then is an RMS computation of this optimal estimate of change over the interval  $\tau$ . Similar arguments hold for TVAR in the presence of white-noise PM making it an optimal estimate, in an RMS sense, of the change in the time each averaged over an interval  $\tau$ .

Flicker models also are very common; they are more arduous to deal with, but filters have been designed that turn flicker residuals into white noise — providing the opportunity of developing



optimum estimation and prediction procedures for  $1/f$  type noise processes. These have only been partially developed because of their complexity.

Figure 28 gives the uncertainties associated with optimum estimation for three different circumstances. The first equation is an applicable model if the same clock signal is fed into both input ports of a time-difference measurement system. In the ideal case  $\epsilon(t)$  would have a white-noise PM spectrum with mean zero. Hence, the mean value over a data set would be the optimum estimate of the time-delay difference,  $x_0$ , in the cable delays feeding the two input ports. The standard deviation of the measurements is given by  $\sigma_x(\tau_0)$ , and the uncertainty in this estimate is given by the standard deviation of the mean, where  $N$  is the number of measurements. Such a model may also be appropriate if two very good atomic clocks, remote from each other, were being compared using the GPS common-view technique. The day-to-day measurement noise is often characterized by white-noise PM, and if this noise is significantly higher than the clock noise at  $\tau = 1$  day, then the simple mean gives the optimum estimate of the time difference between the remote clocks as averaged over the interval  $\tau$ .

The second equation in Figure 28 would be a reasonable model if two independent clocks had negligible noise as compared to the measurement system's white PM level over the time of the measurement. This model also assumes there is no frequency drift between these two independent clocks. In this case, a linear regression provides the optimum estimate of the synchronization error,  $x_0$ , and the syntonization error,  $y_0$ , between the two clocks, since the residuals will have a white spectrum. The uncertainty is given at the right; notice that the confidence on the frequency-difference estimate improves as  $N^{-3/2}$ , whereas the confidence on the time-difference estimate only improves as  $N^{-1/2}$ . This is because we are estimating frequency in the presences of white-noise time residuals, and frequency and time are related by a derivative,  $y = dx/dt$ . We will show later that this  $N^{-3/2}$  factor may be used to significant advantage in some frequency transfer experiments, such as with GPS and with Two-Way Satellite Time and Frequency Transfer.

In the third equation in Figure 28, the model, for example, could be for two clocks with relative frequency drift between them along with having time and frequency offsets. Again, the clock's random noise is negligible as compared to the white-noise PM measurement noise over the length of the measurement. This model could also be applicable for a clock with intrinsic white-noise PM, such as active hydrogen masers and quartz crystal oscillators have in the short-term. In this case, the quadratic regression line is the best fit, because the time residuals,  $\epsilon(t)$ , have a white spectrum. For similar arguments, the confidence of the estimate of the drift term improves as  $N^{-5/2}$ . That is,  $4D = d^2x/dt^2$  is being optimally estimated in the presence of white-noise time residuals.

If we apply the second equation in Figure 28 to Dr. Mattison's experiment, reported in this conference<sup>[5]</sup>, we get some very impressive results. With data taken once a second, having 100-picosecond white PM measurement noise, and having the satellite in view for 5 minutes, the uncertainty on the frequency measurement would be about  $6.7 \times 10^{-14}$ . Now if the data rate could be speeded up to a 1 ms rate, then the uncertainty becomes  $2.1 \times 10^{-15}$  — a factor of 30 improvement for the period of observation. The uncertainty expression at the right of the second equation in (28) is equivalent to  $2 \text{ Mod.} \sigma_y(\tau)$ , where  $\tau$  is the observation interval.



Figures 29 through 31 apply to the case where classical white-noise is predominant as for most atomic clocks. The first equation in Figure 29 represents the true average normalized frequency over the interval  $\tau_0$  as determined from the time difference at the beginning and the end of the interval. Such a measurement is much like is done in a time interval counter over its gate time. The second equation is the definition of the average over the whole data length. Hence, if the first equation is substituted into the second equation, the result is the third equation. Therefore, the end point time-difference values yield the optimum estimate of the frequency in the presence of white-noise FM. The algorithm is extremely simple: the difference of the last point minus the first point divided by the data length. It is well to check either visually or statistically that neither of these two points is an outlier, which would contaminate the result. It is always good practice to check the data visually. Looking at the time residuals after subtracting the systematics is one of the most useful visual inspection techniques.

Since it is not uncommon for people to subtract a linear regression from the phase or time residuals to determine the frequency of their atomic clock from the slope thus derived, Figure 30 is a simulation showing the degradation in this estimate as compared with the optimum. This figure gives the results from a Monte Carlo analysis of 100 simulations of 100 points each. The mean frequency from the regression line slope was 72% worse than optimum. The standard deviation of the frequency residuals was 8.5% worse. The simulations were derived from a normally distributed set with unit variance for the white-noise FM frequency residuals. The column denoted "Mean  $x_0$ " is the average value of the synchronization term derived at the origin of each set and is zero by design in the optimum estimation procedure. The optimum value for time prediction is the last value, which is the value used in the optimum estimate of the frequency for the measurement period.

USNO has 40 HP 5071A clocks. They are well modeled by the first pair of equations in Figure 31 for  $\tau$  values out to the 45 day prediction time needed to bring the UTC estimate forward to the current time. Using the white-noise model equation for the HP 5071A clock given in Figure 21, and the uncertainty relationship given at the right in (31), we obtain for the frequency measurement uncertainty, for  $\tau = 45$  days and for 40 independent clocks,  $6.4 \times 10^{-16}$ . We previously deduced from the data an upper limit of  $2.6 \times 10^{-15}$  as derived from the actual prediction error in UTC(USNO-MC) as observed over the last half year.

The prediction upper limit is about a factor of four worse than optimum. From the previous analysis, we cannot tell whether the major contributor to the instability is TAI/UTC or USNO. It is possible that the white-noise FM model starts to break down for some of the clocks for  $\tau$  values of the order of a couple of months. An other explanation for the disparity could be that optimum parameter estimation and prediction may not be used in the generation of TAI/UTC. In talking to personnel at USNO, it seems that their procedure is very close to optimum. Regardless, the results obtained are greatly improved over what they were a few years ago.

One may notice that the expression for the uncertainty at the right of the first pair of equations in Figure 31 is the same as the standard deviation of the mean. The second pair of equations in Figure 31 is the model for two clocks having relative frequency drift and where the predominant noise is white FM. In this case the linear regression on the frequency is the optimum estimator, because the residuals around that regression line are white. The uncertainty on that drift



estimate decreases as  $N^{-3/2}$ . This kind of regression analysis is often used in our community, and is obviously very useful.

Figure 32 considers the random-walk FM model as the predominant noise. This is often the model used for clocks for their long-term stability performance. The model in Figure 32 assumes the presence of frequency drift. The second difference of the  $x(t)$  data has a white spectrum. Hence, from our statistical theorem the mean value of the second difference is an optimum estimator. This mean value is directly relatable to the drift as shown and which has an uncertainty given at the right. This uncertainty is equivalent to the standard deviation of the mean.

Unfortunately, as shown in Figure 33, life is not so simple. We almost never have single noise processes in a data set. But a filter can almost always be designed which will give white residuals. It may be a complex filter.

Figure 34 is an illustration useful to our community: the case of white PM and/or white FM with long-term random-walk FM. An appropriate filter may be designed to average down the white-noise PM and/or the white-noise FM, and then we can analyze the random-walk FM residuals. If the random-walk FM is the predominant noise in the long-term, as it often is, then a simpler algorithm for determining a near optimum estimate of the frequency drift is as follows. If the first, the middle, and the last time-difference points are used to compute the estimate of the frequency drift,  $D$ , this estimate has two distinct advantages. First, as a second-difference estimate it is optimum for random-walk FM. Second, the effect of the higher frequency noise processes (e.g. white-noise PM and white-noise FM) is diminished if the  $\tau$  for half the data length is long compared to those  $\tau$  values where the higher frequency noise processes predominate. If these higher frequency noise processes have been filtered, so much the better.

In the case of white-noise FM and frequency drift a linear regression to the frequency gives the optimum estimate of the drift. But in this case, if the second-difference estimator per equation Figure 34 were used, how much worse than optimum would it be? The uncertainty is given in Figure 35, and it is only 15% worse than optimum. However, in the case of random-walk FM, the three-point estimator is optimum and the linear regression is worse by some similar factor.

In telecommunications, very often the frequency drift of quartz oscillators as it affects the time-interval-error (TIE) is an important specification. Figure 36 gives a relationship between  $\sigma_x(\tau) = \text{TDEV}$ , the frequency drift,  $D$ , and the corresponding TIE.

Figures 37 and 38 show the effect of modulation on  $\sigma_y(\tau)$  and on  $\sigma_x(\tau)$ . In the latter case, a background noise of white PM is also included in the simulation. Notice that the effect of the modulation averages down as  $1/\tau$ .

If there is a need to estimate an effect due to temperature, pressure, humidity, etc., then the following procedure will be helpful. Suppose the clock has a  $\sigma_y(\tau)$  diagram something like that shown in Figure 39. Denote  $\tau_{\text{floor}}$  as the averaging time where the clock reaches its flicker floor. Now average the frequency for this length of time with the parameter in question fixed at some value. Switch the parameter to some new value, allowing for settling, and measure the frequency again for an interval  $\tau_{\text{floor}}$ . Switch the parameter back to its original setting, again



allowing for settling, and measure the average frequency for the third time. Keep repeating the switching of the parameter setting as often as needed to get the uncertainty desired. In principle, the uncertainty in the size of the effect of this particular parameter on the frequency will decrease as  $1$  over the square root of the number of the independent switches. In this way, we are not limited by the flicker floor, and can determine the size of the effect arbitrarily well.

Now consider optimum procedures in using some of the clocks contributing to TAI/UTC. Figure 40 is a stability plot for 78 of the HP 5071As contributing to TAI/UTC during 1994. Clearly, there is not a single representative model for all of these clocks. The best possible stability obtainable from these clocks is given by the equation at the bottom right of Figure 41 and represented by the 'x's. These results are reasonably modeled by the equation given:  $\sigma_y(\tau) = 8.7 \times 10^{-13} \tau^{-1/2}$ , where  $\tau$  is in units of seconds. The dots are the estimated stabilities under the assumption that the 78 clocks are all equal; square root of the average variance divided by the square root of the number of clocks. These two stability plots give an upper and a lower bound to the actual stability one could obtain using these clocks. The circles are the composite stabilities for the hydrogen masers used in TAI/UTC for this same period.

The above are only theoretical estimates since there is no clock good enough with which to measure this level of stability. In an effort to estimate the actual stability, a three-cornered hat experiment was performed between a time scale generated for each of three clock sets: the primary standards running as clocks, the hydrogen masers contributing to TAI/UTC, and 78 HP 5071A cesium clocks analyzed in Figure 40. The two plus '+' points were the resulting estimated stability for the HP 5071A clocks. The  $\tau^{-3/2}$  slope would indicate we are only seeing measurement noise and are not limited by the clocks for these  $\tau$  values.

Figure 42 is the time stability,  $\sigma_x(\tau)$ , and Mod. $\sigma_y(\tau)$  for several important time and/or frequency transfer techniques. Both can be plotted on the same graph since  $\sigma_x(\tau) = \tau \text{ Mod.}\sigma_y(\tau)/\sqrt{3}$ . Most of the plots are for state-of-the-art techniques except for Loran-C, which is plotted for comparison purposes.

The Two-way Satellite Time Transfer Technique has excellent short-term stability, but due to equipment delay variations to date it only reaches somewhat better than  $1 \times 10^{-13}$  before these variations significantly contaminate the estimation process. In the very long-term these instabilities start to average down again.

The enhanced GPS, EGPS, technique was developed to utilize the new multichannel GPS receivers and to overcome to some degree the effects of the Selective Availability (SA) degradation present for the civil users of GPS. The degree to which the SA can be filtered away is a function of the quality of clock used with the multi-channel GPS receiver; i.e. quartz, rubidium or cesium. For example, if a very good quartz oscillator is properly used and servoed to GPS and the SA is optimally filtered, then the short-term stability will be that of the quartz oscillator, which is usually excellent, and the very long-term will be that of GPS. The intermediate-term stability will depend on the intermediate-term stability of the quartz oscillator, which is not as good as a rubidium gas-cell frequency standard; and the rubidium in turn is not as good as a cesium-beam frequency standard for the intermediate term.

The GPS carrier phase technique has outstanding frequency transfer capability — reaching



about  $2 \times 10^{-15}$  in  $10^5$  seconds (about one day). The data plotted here came from a comparison of hydrogen masers located in Goldstone, California and in Algonquin Park, Canada. The baseline distance is about 3.2 Mm (2,000 miles); the circumference of the Earth is about 40 Mm. Some 35 tracking stations were used to determine accurate orbits. Notice that the classical measurement noise only persists for about five minutes, then some random-walk errors start to come in. Notice also that the time instability averages down to below 10 ps; that is the time it takes a light signal to travel 3 millimeters! Clearly, Earth tides had to be included in this analysis. One also sees the power of these kinds of measurements to study plate tectonics for the Earth.

The GPS common view (GPS CV), which has been used since 1981 and still is the best operational means of comparing time and frequency standards remote from each other, starts at  $\tau = 1$  day and integrates down to below the  $10^{-14}$  level. This is the main means of time and frequency transfer for the clocks and frequency standards providing input into TAI/UTC.

If we go back to the second equation in Figure 28 — remembering that the confidence of the estimate of frequency improves as the degrees of freedom  $N$  to the  $3/2$ s power — one can think of some very exciting opportunities with the new multi-channel GPS receivers. These receivers are able to take one second data. If the measurement noise is white PM at a level of 8 ns and four satellites could always be tracked in common-view with another site, then the frequency transfer uncertainty would be  $1.4 \times 10^{-16}$  for a one day's regression analysis. This technique is called the Advanced Common-view approach (GPS ACV).

Two eight-channel receivers were tested with common clock and common antenna to study instrumentation noise and to check the theory of the above paragraph. The results are plotted in Figure 42. A complex digital filter was developed to take advantage of all the degrees of freedom while increasing the averaging time to ten seconds in order to reduce the data rate. This digital filter explains the little hump at about 30 seconds. The curve generally follows the white-noise PM power-law spectral model with the data averaging as  $\tau^{-1/2}$  down to a level of about 70 picoseconds. This data is taken from the accompanying paper<sup>[1]</sup>, and is thanks to Dr. Robin Giffard. We next need to study the performance with separate antennas, as a function of temperature, and with the receivers located at sites remote to each other. The effects of the ionosphere, the troposphere and multipath can be measured and/or averaged and can be driven below the nanosecond level. Much work is yet to be done, but the GPS ACV technique appears to have the potential to be very practical and useful.

Notice the effects of diurnal and annual variations in the Loran-C stability. As better and better standards are being compared, it may be that in some cases temperature control will be necessary to avoid such variations as they may occur in other techniques as well. As we move time and frequency metrology forward, it is always well to keep in mind the basic concepts and methodologies for parameter estimation and prediction. Those presented here are not a complete set, but it is hoped that they will be useful to those interested in utilizing the powerful time and frequency resources and tools we now have available within our community.



## References

- [1] Our PTTI paper
- [2] ITU-R  $\sigma_y(\tau)$  Sydnor performance plot
- [3] NIST TN 1337
- [4] Allan, Weiss & Jespersen
- [5] Mattison PTTI paper, '95

## Which Is Correct?



Figure 3

Every clock disagrees with every other clock—except at most an instant.

Disagreement is only a matter of degree.



## Frequency VS. Time

### Frequency

(from an atomic resonance) IS ABSOLUTE; hence is the basis of the definition of "the second."

### Time

(clock reading) is an artifact of man; we define it to be what we want it to be. IT IS NOT ABSOLUTE.

Figure 4

Time is an artifact



## Q: What Is A Clock?

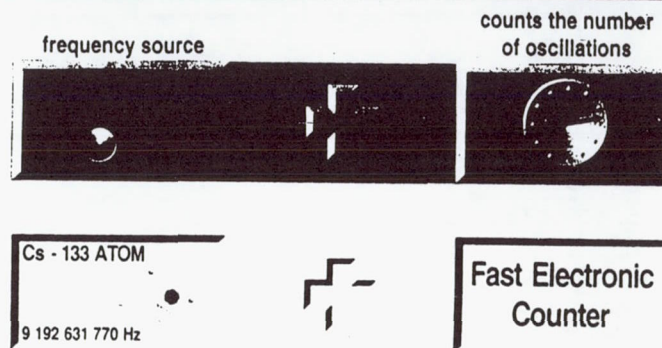


Figure 2

A: an oscillator + a counter

**Clocks & Clock Systems  
Performance Measures**  
by  
**David Allan**

-----

**ITU Handbook**  
"Selection and Use  
of Precise Frequency  
and Time Systems"

Figure 1



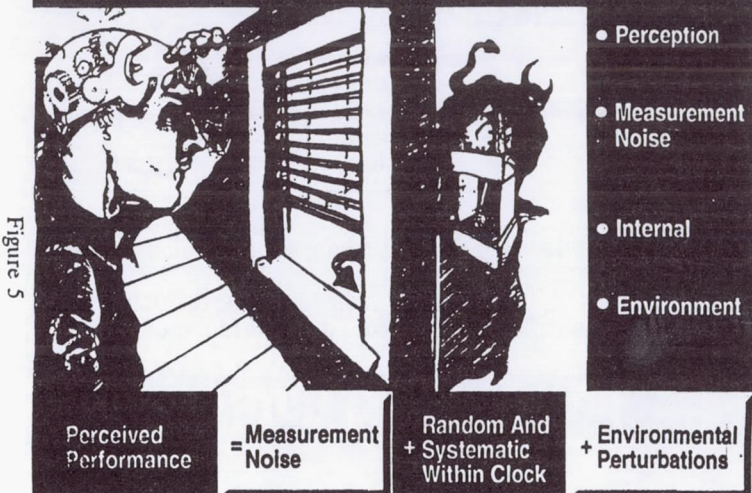
## Model Elements Dependent On Environment

Operator Interference  
Shock and Vibration  
Supply Voltage  
Magnetic Field  
Temperature  
Pressure  
Humidity  
Load  
Etc.

Figure 7

All clocks affected by environment

## Perceived Causes Of Clock Deviations



## Clock Concepts

- **Time (in practice)**  
the apparent reading of a clock
- **Synchronization**  
two or more clocks have the same apparent time
- **Syntonzation**  
two or more clocks have the same apparent rate
- **Simultaneity**  
two or more events occur at the same moment  
(does not require a clock)

Figure 6

Time is a definition

## IEEE Std 1193-1994

### IEEE Guide for Measurement of Environmental Sensitivities of Standard Frequency Generators

Sponsor  
IEEE Standards Coordinating Committee 27 (SCC27)  
Time and Frequency

Approved July 25, 1994  
IEEE Standards Board

Abstract: Standard frequency generators that include all atomic frequency standards and precision quartz crystal oscillators are addressed.

Keywords: environmental sensitivities, standard frequency generators

The Institute of Electrical and Electronics Engineers, Inc.  
345 East 47th St.  
New York, NY 10017-2394, USA

copyright © 1994  
ISBN 1-55937-487-X

Figure 8

## Define: Normalized Freq. & Time Residual

$$y(t) = \frac{v(t) - v_o}{v_o} \quad \text{Dimensionless Normalized Freq.}$$

$$x(t) = \frac{\phi(t)}{2\pi v_o} \quad \text{Time Residual}$$

Then  $y(t) = \frac{dx(t)}{dt} \equiv \dot{x}(t)$

And  $x(t) = \int_0^t y(t') dt'$

Measures of departure

## Model Time Residual

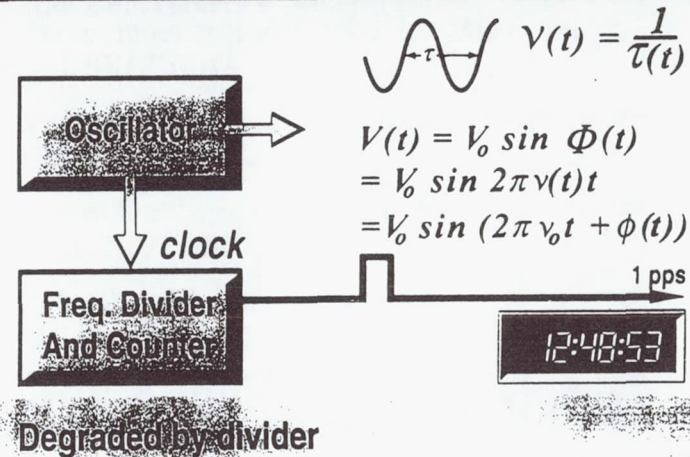
$$x(t) = x_o + y_o t + \frac{1}{2} D t^2 + \epsilon(t)$$



Subtracting first three terms from data, then  $x(t) = \epsilon(t)$

Separate random from systematics

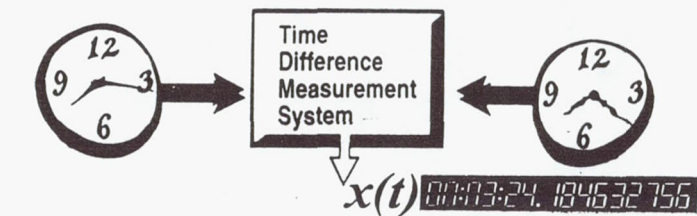
## Characterizing an Oscillator Clock Performance



## That Which Is Measured

We cannot measure the time of a clock against absolute time because absolute time does not exist.

We can measure the time difference between two clocks with great precision.



Time is not absolute



## Time - Domain Measures

- **Frequency Accuracy:**  
The degree of conformity with a standard or a definition.
- **Frequency Instability:**  
Change, typically averaged over an interval,  $\tau$ , with respect to another frequency.
- **Time Accuracy:**  
The degree of conformity with UTC or some agreed upon time-scale.
- **Time Instability:**  
Change, in residual readings, typically averaged over an interval,  $\tau$ , with respect to nominal or other averaged interval(s).

Figure 15

$y(t)$   $x(t)$   $\sigma_y(\tau)$   $\sigma_x(\tau)$   $Mod. \sigma_y(\tau)$   $UTC$

HISTOGRAM OF FREQUENCY OFFSETS (TAI - CLOCK) FOR 1994  
(ALL 8071As)

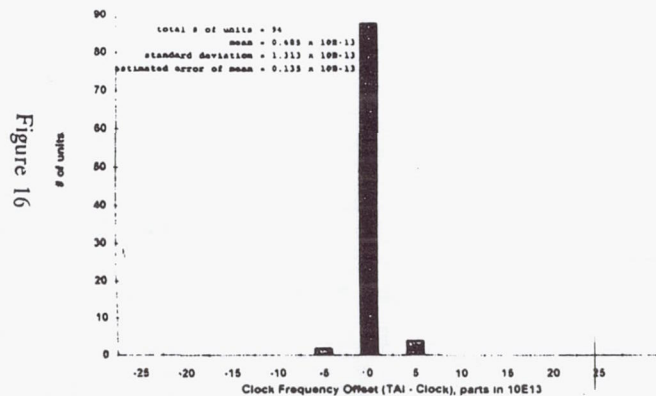
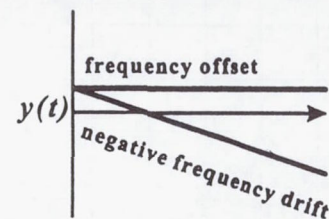


Figure 16

normalized frequency error vs. time



time error vs. time

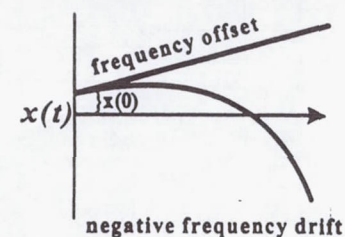


Figure 13

Synchronization error and frequency drift

## IEEE Recommended Measures

for clock/oscillator

$$\begin{cases} S_y(f), S_\phi(f) \\ \sigma_y(\tau), Mod. \sigma_y(\tau) \end{cases}$$

for measurement system or network

$$\begin{cases} S_x(f), S_\phi(f) \\ \sigma_x(\tau), Mod. \sigma_y(\tau) \end{cases}$$

$\sigma_y(\tau), \sigma_x(\tau)$  optimum for classical noises

Figure 14

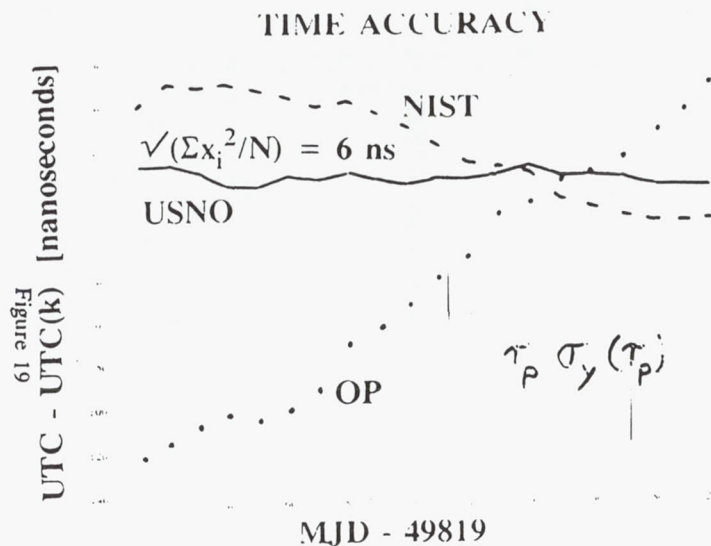


Figure 17

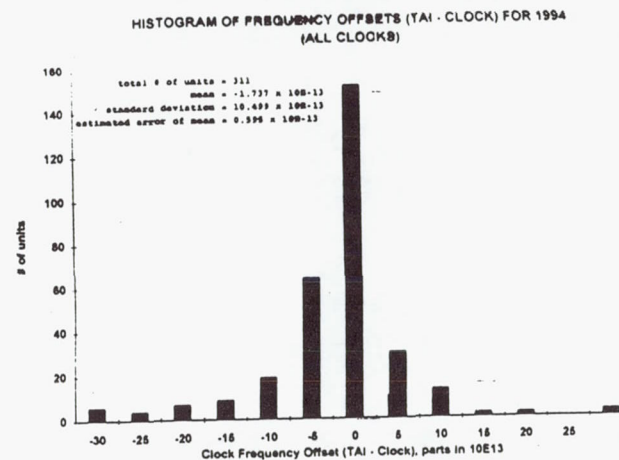


Figure 18

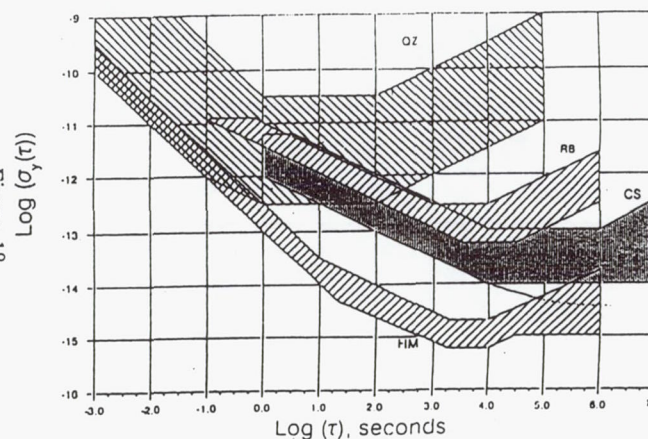


FIGURE 2  
Stability Ranges of Various Frequency Standards

## Flip Coins For White Noise

Flip of a coin is a random, uncorrelated process:  
(white noise spectrum)

Integrating these flips generates a random-walk process:  
(heads = one step forward)  
(tails = one step backward)

After  $N$  flips of a coin, will be  $\sqrt{N}$  away from the origin  
(ensemble rms)

Since  $y = dx/dt$ ,

Taking a first difference of a random-walk process turns it  
into a white process.

...and random walks

$$S_x(f) \sim f^{-0}$$

$$S_x(f) \sim f^{-2}$$

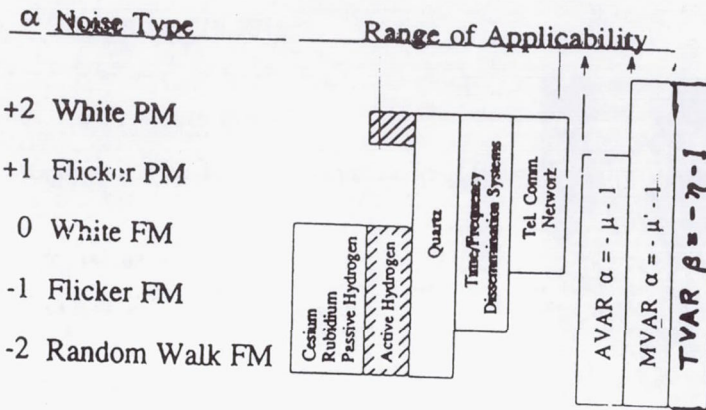
$$S_y(f) \sim f^{-0}$$

$$y = \Delta x/\tau$$



Figure 20



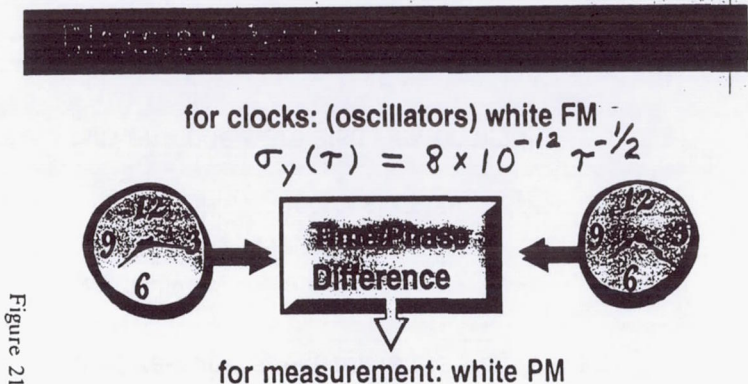


$$\sigma_y^2(\tau) \sim \tau^\mu \quad \text{Mod. } \sigma_y^2(\tau) \sim \tau^{\mu'}$$

$$\sigma_x^2(\tau) \sim \tau^\eta \quad \eta = \mu' + 2$$

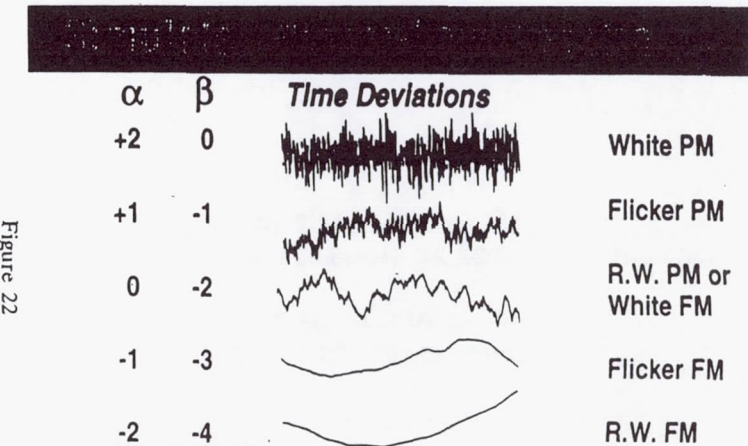
**Figure 24**

ABBREVIATION	NAME	EXPRESSION
AVAR	ALLAN VARIANCE	$\sigma_y^2(\tau) = \frac{1}{2} \langle (\Delta y)^2 \rangle$ $= \frac{1}{2\tau^2} \langle (\Delta^2 x)^2 \rangle$
MVAR	MODIFIED ALLAN VARIANCE	$\text{Mod } \sigma_y^2(\tau) = \frac{1}{2\tau^3} \langle (\Delta^2 x)^2 \rangle$
TVAR	TIME VARIANCE	$\sigma_x^2(\tau) = \frac{1}{6} \langle (\Delta^2 x)^2 \rangle$



$$x(t) = x_0 + y_0 t + \frac{1}{2} D t^2 + \epsilon(t)$$

Model for time difference



$$S_y(f) \sim f^{-\alpha} \quad S_x(f) \sim f^{-\beta}$$

## Optimum Estimation & Prediction

- ▼ Optimum means parameter estimation with
- *minimum* squared error residuals

Goal: to minimize errors for parameter estimation and/or for time and frequency prediction.

Figure 25

Depends on noise type

## Statistical Theorem:

*The optimum estimate of the mean of a process with a white-noise spectrum is the simple mean.*

Figure 26

Naturally we have:

White PM, White FM,  
R.W. FM (white acceleration,  $\ddot{x}(t)$ )

Flicker models are also very common.

Seek for white residuals

$$\sigma_y^2(\tau) = \frac{1}{2} \langle (\Delta \bar{y})^2 \rangle$$

$$\bar{y} = \frac{x(t+\tau) - x(t)}{\tau}$$

is optimum for  
white FM

$$\sigma_x^2(\tau) = \frac{1}{6} \langle (\Delta^2 \bar{x})^2 \rangle$$

$\bar{x}$  = avg. of  $x$  over  $\tau$   
is optimum for  
white PM

Figure 27

## White PM

$x(t) = x_0 + \epsilon(t)$   
simple mean

$x(t) = x_0 + y_0 t + \epsilon(t)$   
linear regression

$x(t) = x_0 + y_0 t + \frac{1}{2} D t^2 + \epsilon(t)$   
quadratic regression

Figure 28

## Uncertainty

time:  
 $\sigma_x(\tau_0)/\sqrt{N}$

freq:  
 $\frac{\sqrt{12} \sigma_x(\tau_0)}{\tau_0 N^{3/2}}$

drift:  
 $\frac{12\sqrt{5} \sigma_x(\tau_0)}{\tau_0^2 N^{5/2}}$

Optimum estimate



## White FM

$$x(t) = x_0 + y_0 t + \epsilon(t)$$

$$y(t) = y_0 + \dot{\epsilon}(t)$$

simple mean

$$x(t) = x_0 + y_0 t + \frac{1}{2} D t^2 + \epsilon(t)$$

$$y(t) = y_0 + D t + \dot{\epsilon}(t)$$

linear regression

Uncertainty

freq:

$$\sigma_y(\tau_0)/\sqrt{N}$$

drift:

$$\frac{\sqrt{12} \sigma_y(\tau_0)}{\tau_0 N^{3/2}}$$

Optimum estimate

Figure 31

## Random Walk FM

$$x(t) = x_0 + y_0 t + \frac{1}{2} D t^2 + \epsilon(t)$$

$$y(t) = y_0 + D t + \dot{\epsilon}(t)$$

$$z(t) = D + \ddot{\epsilon}(t)$$

simple mean

$$D = \frac{\Delta^2 x}{\tau_0^2}$$

Uncertainty

drift:

$$\frac{\sqrt{2} \sigma_y(\tau_0)}{\tau_0 \sqrt{N-1}}$$

Optimum estimate

Figure 32

## Optimum Estimate For White FM

Given: Discrete  $x(i)$  values spaced  $\tau_0$  from a time difference series

Then 
$$y(i) = \frac{x(i) - x(i-1)}{\tau_0} = \frac{\Delta x(i)}{\tau_0}$$

Figure 29

Average Frequency 
$$\bar{y} = \frac{1}{N} \sum_{i=1}^N y(i)$$
 Simple Mean

$$= \frac{x(N) - x(0)}{N\tau_0}$$

Optimum Estimate for white FM

Optimum based on simple mean

GIVEN: CLASSICAL WHITE NOISE FM

(as from Cs or Rb)

THIS IS THE SAME AS RANDOM WALK PM

(100 simulations of 100 points)

Difference between end-point and regression for determining the frequency and time

	Mean Freq.	$\sigma_y$	Mean $x_0$
REGRESSION	-0.0005	0.0970	0.44
END POINTS	-0.00029	0.0894	0

Figure 30

## Given White FM & Frequency Drift

linear regression to:

$$y(n) = y_o + Dn\tau_o$$

or using 3-point  $\Delta^2 x$ :

$$y(n) \quad \bar{y}(1:\bar{y}) \quad \bar{y}(\bar{y}:N)$$

Uncertainty  
Drift:

$$\frac{\sqrt{12} \sigma_y(\tau_o)}{\tau_o N^{3/2}}$$

$$\frac{4\sigma_y(\tau_o)}{\tau_o N^{3/2}}$$

$$\frac{4}{\sqrt{12}} = 1.15$$

Optimum and near optimum

Figure 35

## Life Is Not Simple

Any given time series may be modeled by more than one Noise Model

There will always be a filter which will produce white residuals

Figure 33

Optimum may be complex filter

## Some Multiple Noise Type Examples

White PM and White FM and/or R.W. FM

Average white PM  
Then analyze residuals

White FM and R.W. FM

Average white FM  
Then analyze residuals

Optimum Freq. DRIFT estimation in both cases

$$D = \frac{X_N - 2X_{N/2} + X_o}{\tau^2}, \quad \tau = \frac{N}{2} \tau_o$$

Effective estimate for most clocks

Figure 34

TIME INTERVAL ERROR due to DRIFT

Given:

$$x(t) = 1/2 D t^2$$

Then:

$$\text{TIE} |_{\text{drift}} = \sqrt{6/2} \sigma_x(\tau)$$

$$= 1.2 \text{ TDEV}$$

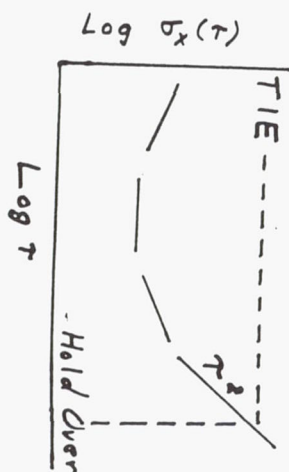


Figure 36



# EFFECTS OF SINGLE FREQUENCY MODULATION ON $\sigma_y(\tau)$

$$S_y(f) = 2.5 \times 10^{-15} (1 \cdot 10^3 \text{ Hz})$$

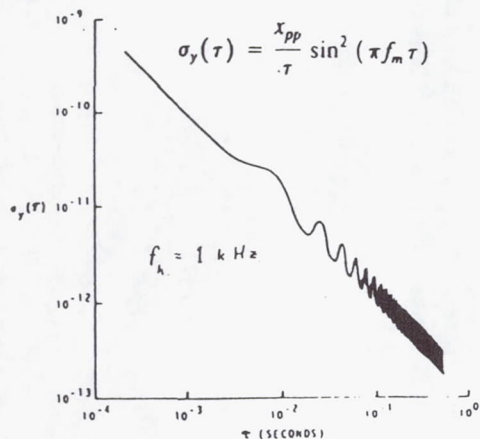


Figure 37

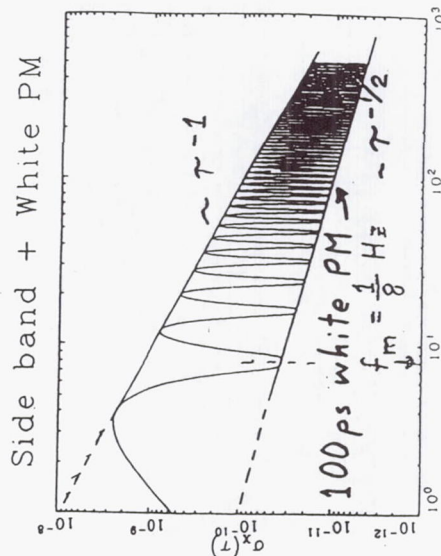


Figure 38

## Given White FM and flicker-floor:

To Measure an environmental steady-state effect, hold the parameter constant and average the frequency for an interval such that the  $\sigma_y(\tau)$  curve starts changing from  $\tau^{-1/2}$  toward a flattening (flicker floor). Then change the environmental parameter being evaluated and repeat the integration time to measure the frequency change. If "N" is the number of changes back and forth, then the confidence on the frequency change is the value of  $\sigma_y(\tau_{\text{floor}})$  times  $1/\sqrt{N}$ .

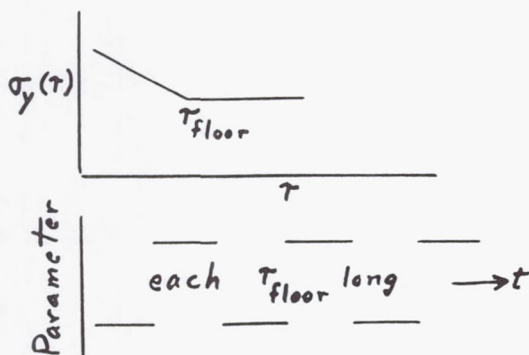


Figure 39

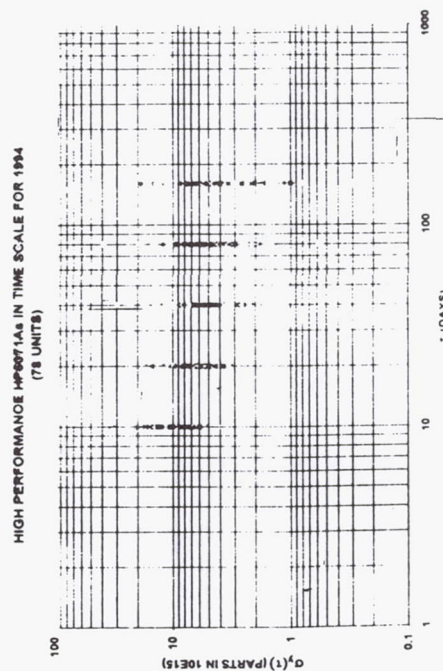


Figure 40

Hand-drawn graph showing the relationship between  $\sigma_1(t)$  (PARTS IN  $10^{10}$ ) on the y-axis and  $t$  (HOURS) on the x-axis. The y-axis ranges from 0 to 100, and the x-axis ranges from 0 to 10. A sine wave is plotted, with a peak labeled  $\sigma_1(t) = 8.7 \times 10^{-10}$ . A dashed line indicates the envelope of the signal. A small diagram shows a sine wave with peak-to-peak amplitude  $2A$  and average value  $A$ .

1928

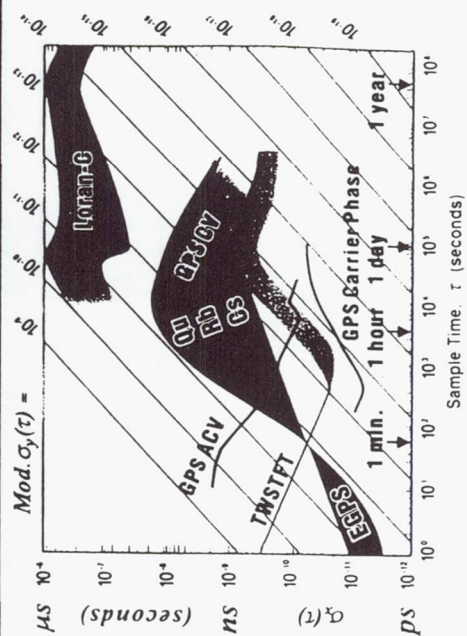


Figure 42



## Questions and Answers

**MICHAEL GARVEY (FREQUENCY AND TIME SYSTEMS):** You showed the slide in which you were trying to pull an environmental sensitivity out of the noise; and you said "Wait until you hit the flicker floor." Is there any reason not to modulate the environmental effect at a faster rate?

**DAVID ALLAN (ALLAN'S TIME):** You have to wait for settling, so that increases the amount of time it takes to do the experiment.

**MICHAEL GARVEY (FREQUENCY AND TIME SYSTEMS):** I know. But if I wait for the flicker floor in a cesium standard, I might wait weeks.

**DAVID ALLAN (ALLAN'S TIME):** Yes, and if you can't hold the environmental parameter stable for that long, you should change it more often. For cesium and rubidium clocks the frequency averages as  $\tau^{-1/2}$ . If you can hold the parameter constant, then you're much better off to let the clock do the averaging because of the delay associated with settling for each switching time. If the parameter can be held sufficiently constant, then average all the way down to the flicker floor.

**MICHAEL GARVEY (FREQUENCY AND TIME SYSTEMS):** Rather than wait for the square root of  $N$  in the denominator.

**DAVID ALLAN (ALLAN'S TIME):** Yes, you buy information at the same rate except for the settling time. It is a trade-off between the parameter's instability and the length of the settling time. In the case of humidity effects in quartz, for example, the settling time can be very long.

# APPENDIX A

## THE IMPACT OF THE HP 5071A ON INTERNATIONAL ATOMIC TIME

David W. Allan, Allan's TIME, Fountain Green, UT  
Alex Lepek, Tech Projects, Jerusalem, Israel  
Len Cutler and Robin Giffard, HP Labs, Palo Alto, CA  
Jack Kusters, HP SCD, Santa Clara, CA

### Abstract

*The international clock ensemble, which contributes to the generation of International Atomic Time (TAI and UTC), has improved dramatically over the last few years. The main change has been the introduction of a significant number of HP 5071A clocks. Of the 313 clocks contributing to TAI/UTC during 1994, 94 of these were HP 5071As. The environmental insensitivity of the HP 5071A clocks is more than an order of magnitude better than that of previous contributing clocks. This environmental insensitivity translates to outstanding long-term stability — with a typical flicker floor of a few  $\times 10^{-15}$ . In addition, there are now several hydrogen masers with cavity tuning contributing to TAI/UTC. These not only have outstanding short-term stability, but comparatively low frequency drifts and excellent intermediate-term frequency stability.*

*By analyzing the data available from the international ensemble, we have obtained two important results. First, the frequency stability obtainable with an optimum algorithm is about  $10^{-15}$  for both the intermediate and long-term regions. It could be as good in the short-term if time transfer measurement instabilities were reduced sufficiently. Second, with cooperation, this performance can be made available on an international basis in near real time. The recent enhancements in the contributing clocks are already providing a significant improvement in the accuracy with which UTC is made available to the world from several of the national timing centers, such as NIST and USNO.*

### Introduction

The accuracy improvement rate in atomic frequency standards has been about one order of magnitude every seven years since the first one was built in 1948. Notable events along the way have contributed to that improvement, and more are anticipated that should significantly enhance frequency accuracy. The most recent events have been the operational establishment of NIST-7 optically-pumped primary cesium-beam frequency standard with an accuracy of  $1 \times 10^{-14}$ . Recently, a cesium fountain primary frequency standard was reported to have an accuracy of  $3 \times 10^{-15}$ . The development of the new HP 5071A cesium-beam commercial frequency standard is, as will be shown, a major contributor after its introduction a few years ago.



New frequency standards are imminently expected that could provide accuracies in the vicinity of  $1 \times 10^{-15}$ . One of the purposes of this paper is to suggest techniques for evaluation and comparison of these standards<sup>[1]</sup>. The standards will often be remote from each other and there will be a local reference adequate to check their performance. The results reported herein should assist substantially toward improving international time and frequency metrology.

The HP 5071A clocks have demonstrated an improvement of more than an order of magnitude in both accuracy and in environmental insensitivity over previous commercial clocks. The excellent long-term stability of these clocks along with the excellent intermediate- and short-term stability of the several contributing hydrogen masers with cavity tuning provides the opportunity of having a combined reference clock with a stability of about  $1 \times 10^{-15}$  for averaging times,  $\tau$ , ranging from about 1,000 seconds out to the order of a year<sup>[2]</sup>.

Though the above stability is only available in theory, by analyzing the data publicly available from the BIPM ensemble, we have obtained two important results. First, the potential frequency stability obtainable in practice with an appropriate algorithm is about  $1 \times 10^{-15}$  for both the intermediate and long-term regions. It could be as good in the short-term if time transfer measurement instabilities were reduced sufficiently. Second, with cooperation, this performance can be made available on an international basis in near real time. The paper will also demonstrate how  $1 \times 10^{-15}$  is available by using post processing. Some guidelines and suggestions are made in the paper on how a  $1 \times 10^{-15}$  stable real-time frequency reference could be constructed.

The rate of TAI/UTC is syntonized with the primary cesium-beam frequency standards in the world in accordance with the SI (System International) definition. The data analyzed for this paper cover 1991 through 1994, and, during this period, there were three primary standards in continuous operation as clocks. All the contributing clocks act as "flywheels" in preserving the rate or length of the SI second as given by the primary standards. As the rate of TAI/UTC has instabilities, algorithmic procedures are chosen to maintain syntonization within some reasonable limit.

The length of the second is the same for TAI and UTC. In other words, they are perfectly syntonized in the way they are constructed. Their times differ by an exact number of seconds, which changes about annually as leap-seconds are used to steer UTC to stay within 0.9 seconds of UT1 (earth time). As of 1 January 1996,  $\text{TAI} - \text{UTC} = 30 \text{ s}$ .

## Performance of Individual Clocks Contributing to UTC

In this section, the frequency accuracy of the contributing clocks is analyzed. This is important for TAI/UTC, because frequency accuracy almost always translates to long-term frequency stability resulting in the preservation and perpetuation of a best estimate of the SI second.

### Factors Contributing to Frequency Accuracy

The goal in making a primary cesium-beam frequency standard is to determine all effects that cause the physical output frequency of the standard to depart from the definition. These effects



are evaluated and removed either 'on paper' or by frequency synthesis in order to provide an estimate of the SI second. The uncertainties introduced by these effects combine to determine the accuracy of the standard.

The factors contributing to cesium-beam frequency standard inaccuracy are: magnetic field, electric field, phase shifts in and between the microwave interrogation regions, velocity of the cesium beam, detuning of the cavity, interference from adjacent quantum transitions to the wanted ground-state transition, stray microwave radiation seen by the atoms, and imperfections in the associated electronics. The current reported accuracy of the second for TAI/UTC is  $1 \times 10^{-14}$ , which is the number reported for NIST-7[3]. The value for the new cesium fountain frequency standard should be included soon.

To obtain accuracy, both the size of the frequency offset caused by each of the above contributors to inaccuracy must be determined as well as the uncertainty associated with this estimate. In addition, for an operating clock to be long-term stable these frequency offsets cannot change with time. That is a difficult challenge in the design of a clock, and has occupied large amounts of effort. Hence, having better operational accuracy almost always guarantees better long-term stability. Having such operational accuracy is one of the main advantages of the HP 5071A.

The accuracies of the commercial clocks contributing to TAI/UTC can be further improved. Two fundamental systematic frequency offsets in well designed and constructed cesium-beam frequency standards (besides that due to the magnetic field (C-field)) are:

- 1) the relativistic offset due to beam velocity, also known as the second order Doppler shift, and,
- 2) the offset due to end-to-end microwave cavity phase shift.

The second-order Doppler shift depends on cesium-beam velocities and is typically  $1$  to  $3 \times 10^{-11}$ . It can be estimated within 20 to 30% using the velocity calculated from the measured atomic-resonance line-width. If the velocity distribution of the detected beam were known in detail, then the second-order Doppler shift could be calculated accurately. The offset due to end-to-end cavity phase shift can be measured in principle by sending the beam through the cavity in the opposite direction, but this is impractical in commercial standards. Both second order Doppler and the end-to-end cavity phase shift offsets, however, lead to small asymmetries in the atomic-resonance line shape. These are independent and additive in lowest order terms. If the velocity distribution of the beam is known, the asymmetry due to second-order Doppler can be calculated and subtracted out. The residual asymmetry can then be attributed to end-to-end phase shift and the resulting frequency offset can be calculated. This is only possible if asymmetries due to neighboring quantum mechanical transitions are negligible.

One of the authors (Cutler) has developed an accurate technique for determining the velocity distribution of the detected beam in the HP 5071A from a measurement of the beam current versus applied microwave frequency while the standard is off-line. An iterative technique is used to solve the integral equation for the velocity distribution assuming rectangular microwave distribution in the cavity ends. The detailed shape of the excitation, however, is not critical in this technique for determining the velocity distribution. Results appear to be accurate to



better than one percent. In the HP 5071A, the microwave interrogation technique permits one aspect of the total line asymmetry to be measured while the standard is in operation. This allows a long averaging time to reduce the measurement noise to an acceptably low value. The only equipment required is a personal computer with appropriate software tied to the standard through its RS232 port. This overall technique should allow both offsets to be calculated accurately enough so that the absolute frequency of the cesium standard will be known to within  $1 \times 10^{-13}$ . This is an improvement of an order of magnitude to the current specification, and could effectively turn all of the HP 5071As contributing to TAI/UTC into primary standards.

## Histogram Study of Frequency Accuracies

In this sub-section, only the most recent data available (for the year 1994) from the BIPM for the clocks contributing to TAI/UTC were used. The frequency reference used was the length of the second for TAI/UTC. The data are reported in histogram form to simplify the presentation. For convenience of comparison, all values in this subsection are given in units of  $1 \times 10^{-15}$ . For histogram Figures 1 through 3a the units for the bins are  $500 \times 10^{-15}$  and  $100 \times 10^{-15}$  for Figures 3b and 4.

The EAL - clock(k) data were provided by Mr. Jacques Azoubib of the BIPM for the years 1991 through 1994, inclusive. The data listed each clock contributing to TAI/UTC against EAL, which is the BIPM free time scale. As needed these data were related to TAI/UTC as well as to the SI second as given by the primary frequency standards. During 1994 the frequency difference  $y(\text{EAL}) - y(\text{TAI})$  was  $740 \times 10^{-15}$ .

The average frequency of TAI/UTC for the year 1994 was  $-3 \times 10^{-15}$ . However, the frequency calibration data supplied by the PTB did not reflect the black-body radiation correction. There were no steering corrections applied to TAI/UTC during this year. In the BIPM annual report for 1994 the listed uncertainty for the SI scale unit for TAI/UTC is  $20 \times 10^{-15}$ . The deviations of the scale unit with respect to the weighted average of the primary standards stayed well within this uncertainty. One may note that the mean frequency of the primary frequency standards is not equal to the weighted mean used as the BIPM best estimate of the SI second.

Figure 1 shows the frequency distribution of all the contributing clocks during 1994. In partial agreement with the skewness, the mean was  $-174 \times 10^{-15}$ . The standard deviation was  $1050 \times 10^{-15}$ , and the standard deviation of the mean (estimated error of mean) was  $60 \times 10^{-15}$ . The standard deviation of the mean, under the assumption of independence among the standards, is computed in the usual way by dividing the standard deviation by the square root of the number of clocks. This assumption may not be valid for commercial clocks as there may be frequency biases that are not adequately dealt with in the production process. In Figure 1, for example, the mean is nearly three times the standard deviation of the mean.

Figure 2 is a similar plot for the contributing hydrogen masers. The abscissa scales have been kept the same for Figures 1 through 3a for convenience of comparison. The mean, the standard deviation and the standard deviation of the mean were, respectively,  $-130$ ,  $319$ , and  $52 \times 10^{-15}$ . It must be noted that the hydrogen masers are generally calibrated and are not independent frequency sources better than their intrinsic accuracies of about  $1000 \times 10^{-15}$ .



Figure 3a is the histogram for the 94 Hewlett Packard model 5071A standards — including both the high-performance option as well as the standard performance units. These two options were studied separately, but the distribution curves did not seem to be significantly different. The mean, the standard deviation and the standard deviation of the mean were, respectively, 48, 131, and  $14 \times 10^{-15}$ . For the third time, the assumption of independence may not be valid as the mean differs by more than 3.5 times the standard deviation of the mean. However, in this case the standard deviation of the mean is of the same order as that given by the best primary frequency standards in the world. The published accuracy specification for HP 5071A is  $1000 \times 10^{-15}$ , and the mean is 20 times better than the specification.

Figure 3b is the same data as in Figure 3a, but plotted with a different abscissa to compare with the distribution of frequencies as given by the laboratory primary frequency standards shown in Figure 4. In the case of the primary standards, the mean, the standard deviation, and the standard deviation of the mean are, respectively, 32, 57, and  $33 \times 10^{-15}$ . Though the sample size is only three, the standard deviation of the mean is consistent with the mean. This result, however, is somewhat artificial since the second for TAI is steered to be in agreement with the primary standards.

If future experiments confirm the theory that allows the HP 5071A to be considered a primary frequency standard, this will considerably increase the data base for Figure 4. In addition, the mean, the standard deviation, and the standard deviation of the mean could be decreased dramatically for the data shown in Figure 3. It should not be anticipated that the accuracy of  $N$  standards will improve the combined accuracy by  $1/\sqrt{N}$  because the frequency inaccuracies among the standards may be correlated.

### Independent Estimates of Frequency Instabilities

The same data from the international clock ensemble was used to calculate the stability,  $\sigma_y(\tau)$ , for each of the Hewlett Packard 5071A high performance cesium beam frequency standards over the year 1994. Since each standard contributes at most only a few percent to the computation of TAI/UTC, the resulting stabilities will be optimistically biased at most by a few percent. The results for 78 of the HP 5071As are shown as  $\sigma_y(\tau)$  scatter diagram in Figure 5. Four of the 82 clocks were not used because there was either insufficient data or the data were pathological. The BIPM reports data every 10 days, so calculations were made for  $\sigma_y(\tau)$  for each clock for frequency averaging times,  $\tau$ , of 10, 20, 40, 80, and 160 days. The confidence of the estimate for  $\sigma_y(\tau)$  ( $\tau = 160$  days) of each clock is poor due to the small number of data samples available at this averaging time. The maximum overlapping technique was used in analyzing the data to obtain a good confidence of the estimate<sup>[4]</sup>.

Figure 5 also demonstrates the great improvement in the stability of TAI/UTC with the inclusion of the HP 5071As, since each clock is relatively independent of the international set of clocks. Over the four year period, while the HP 5071As were being added into the computation of TAI/UTC, the stability performance of international timing has improved well over an order of magnitude.

Figure 6 shows the  $\text{RMS}/\sqrt{N}\sigma_y(\tau)$  values for the 78 clocks. These values give an estimate of ensemble performance under the assumption that the clocks are about the same in their stability.



performance. Figure 5 shows a fairly wide distribution of stabilities. Hence, the  $\text{RMS}/\sqrt{N}$  values will be a pessimistic estimate. As can be seen, the flicker floor is about  $8 \times 10^{-16}$ , which is an order of magnitude better than the stability of TAI/UTC prior to 1991.

Figure 6a also shows an optimum weighted estimate for the ensemble for each  $\tau$  value. In other words, an optimum weighted combination of the clocks could not be better than these values. The degree to which these values can be approached will be both a function of the algorithm employed as well as of the consistency of the stability behavior of each contributing clock. There is nothing with which to measure this performance. The best laboratory clocks in the world have not demonstrated this level of long-term stability. The problem of measuring the performance will be dealt with in the next section.

Some additional very important messages from this data are: the stability performance of EAL is very impressive — at about  $1 \times 10^{-15}$  in the long-term. Several of the HP 5071As perform at similar levels. The diversity of the long-term frequency stability of these standards varies by more than an order of magnitude. Hence, an optimum weighting approach for combining their readings is essential to take advantage of and to properly utilize such diversity. This is illustrated in the next section.

A long-term frequency drift exists on several of the clocks contributing to EAL. If not properly dealt with, these drifts could cause significant long-term instabilities in EAL. Fortunately, the ALGOS algorithm used in generating EAL de-weights drifting clocks.

## Ensemble Performance of Contributing Clocks

It is well known that combining algorithmically the contributing-clock readings in an optimum way has several distinct advantages. The computed time can have better stability than any of the contributing clocks both in the short-term and in the long-term. Detection of and immunity against errors of individual contributing clocks is part of the process. The ideal algorithm should have adaptive characteristics so as to respond to improvements or degradations in the individual contributors — gradual or otherwise. The better a clock performs, the better it must perform or it will get de-weighted in the algorithm's computation. In other words, each clock's errors are tested each measurement cycle; if the errors are consistent with its weight, that error value is used to perpetuate its weighting factor. If the error is too large, the clock is rejected. If the error degrades with time, the weighting factor is degraded. If the error improves with time, the weighting factor increases. It can further be shown that even the worst clock enhances the algorithm's output and adds robustness to the ensemble time calculation. The algorithm generates a real-time estimate of the figure of merit of each clock, which is not only used in the optimum weighting procedures, but also as a diagnostic measure. Knowing the weighting factors for all the contributing clocks provides the necessary information to calculate an estimate of the ensemble's performance against a perfect clock. The algorithm needs to handle the addition and removal of clocks optimally.

An often overlooked point is that if an optimum weighting procedure is not used, then the worst clocks in the ensemble contribute adversely. This effect has been observed very dramatically over the last few years with TAI/UTC. The ALGOS algorithm generating these time scales has



an upper-limit of weight, which is arbitrarily set. In the past, because it was set too low, the worst clocks contributing to TAI/UTC caused a significant annual term to be introduced. As the upper-limit of weight is increased, the annual term in TAI/UTC decreases. This is because ALGOS weightings approach the theoretical ones for the HP 5071As, which are environmentally insensitive and have almost no detectable annual terms.

Since each clock, in principle, contributes to the algorithm's output, if that clock is compared with the output, it is being compared, in part, with itself. This biases the measured stability toward zero. Carefully designed algorithms can remove these biases — prohibiting the best clock from getting too much weight or from taking over the time scale's output. Not accounting for such biases would make the time scale less robust.

Such algorithms have been tested and utilized for many years with significant success. Taking advantage of the marked improvements in the contributing clocks to TAI/UTC and of appropriate algorithms allows the significant reference frequency improvements reported in this paper.

The results documented in this paper lead to another significant potential improvement in international time and frequency metrology. Heretofore, UTC has only been available about a month or two after the fact. The procedures outlined herein provide a real-time estimate of UTC at an accuracy level of better than 10 ns along with also providing a real-time stable frequency reference good to the order of  $1 \times 10^{-15}$ .

Because the character of clocks contributing to TAI/UTC has changed so dramatically over the last few years, using adaptive algorithms is very important. The basic algorithm used for this paper is based on the AT1 algorithm, initially written in 1968 for the NBS time scale system. Updates and revisions of this algorithm have been made over the years and a significant level of experience and improvements have now been obtained with these approaches to time keeping. A PC version of this algorithm with further adaptive characteristics has been written and is now employed in the generation of the Israeli time scale, UTC(INPL). The results shown below are the output of this PC version of the algorithm<sup>[5, 6]</sup>.

## Independent Estimate of Stability of Algorithm Outputs

Because of the different character of the clocks, they were divided into four different groups:

- 1) the primary standards contributing to the definition of the SI second;
- 2) the hydrogen masers;
- 3) the HP 5071A standards, which just became available in 1991; and
- 4) all of the rest of the clocks which contributed over this four year period.

The number of clocks that participated in each of the four sets for the following analysis were: 3 primaries, 40 masers, 80 HP 5071As and 100 other clocks. Each group of clocks was used to produce an ensemble using the algorithm described above.

Because the number of HP 5071A standards available during the beginning of the data period was small, the best stability results were obtained by excluding the first part of the data.



There are three contributions to the variations in the data:

- i. the noise of the individual clocks being measured,
- ii. the measurement noise or transmission or processing errors, and
- iii. the noise of the reference time scale, in this case, EAL (which is TAI without steering).

Since the measurements made at each site to provide the data are made at the same time, the reference (EAL) was subtracted out and comparisons made between the individual clocks — leaving only the first two kinds of contributions. The measurement noise is non-negligible and contributes noticeably at the shorter times as evidenced by the  $1/\tau$ -like slope at  $\sigma_y(\tau = 10\text{days})$ . The performance at longer times is affected by apparent phase jumps, some of which were removed in the original data and some in the data processing. Probably, not all were caught. In addition, some of the clocks showed frequency drifts which were not removed and this shows up as a  $\tau^{+1}$  dependence at the longest sample times in a  $\sigma_y(\tau)$  or  $\text{Mod.}\sigma_y(\tau)$  stability diagram.

In order to obtain an independent estimate of stability, the three-cornered hat technique was used:  $\sigma^2(i) = (\sigma^2(i, j) + \sigma^2(i, k) - \sigma^2(j, k))/2$ , where  $i, j$  and  $k$  represent three independent clocks. This technique has the disadvantage that the worst of the three can be observed with the best confidence, and the best of the three has the worst confidence of the estimates. The longer the data length the better the estimates of stability; the last 710 days of data was used. Because of the above mentioned disadvantage the “other” clocks were not used. Figure 6b is the  $\text{Mod.}\sigma_y(\tau)$  plot of the results of this analysis.  $\text{Mod.}\sigma_y(\tau)$  was used because the measurement noise is significant. These independent estimates are consistent with the estimates in Figure 6a for the reasons outlined above and documenting that the long-term stability of the HP 5071A ensemble is best, followed by that of the hydrogen masers and then the primary cesium clocks. The primary clocks undergo some disturbances in order to maintain their accuracy. This may contribute to the long-term instabilities, but eventually such disturbances should average out and there is indication in the  $\text{Mod.}\sigma_y(\tau)$  slope as  $\tau$  increases that this is the case.

### Real-Time Estimate of Time and Frequency

Given that the optimally combined frequency stability of the clocks contributing to TAI/UTC is about  $1 \times 10^{-15}$  for averaging times longer than about two hours, there are two basic problems in making this available in real-time at any location desired on the earth. First, the current time and frequency transfer techniques are inadequate to sustain this level of performance for either the short-term (seconds) or the intermediate-term (days) stability regions. Only in the long-term (months and years) are the comparison methods adequate. This inadequacy problem will be addressed in the next section. Second, TAI/UTC is calculated more than one month after the fact; hence, to have a real-time traceable reference to UTC requires prediction to the current time over an interval of about a month and a half.

The optimum predictor in the presence of white-noise FM (the classical noise for cesium-beam clocks) is to use the last time available from the clock, and the mean frequency over the life of the clock as the rate with which to predict forward. Because of the excellent environmental



immunity of the HP 5071As, the white-noise FM model fits over a very large region of prediction times ranging from about 10 seconds to about a month or longer for some of the best performing units. As can be seen from Figure 5, for sample times of the order of a few weeks to a few months, some of these units begin to exhibit flicker-noise and/or random-walk FM like behavior. If such is the case, near optimum prediction techniques have been developed to deal with these more dispersive noise processes.

Over the last six months (since 22 April 1995), the USNO has had an RMS prediction error for their UTC(USNO MC) with respect to UTC of 6 ns. Their prediction algorithm takes advantage of optimum estimation techniques — using the simple mean frequency assumption (white-noise FM). The RMS optimum prediction error for white-noise and random-walk-noise FM cases is given by  $\tau \times \sigma_y(\tau)$ . If the prediction interval is about 45 days (1 1/2 months), then this implies  $\sigma_y(\tau = 45 \text{ days}) = 1.5 \times 10^{-15}$ . This represents the relative instability between the USNO ensemble of clocks used for prediction and that of TAI/UTC. Since the clocks at USNO contribute about 40% to the generation of TAI/UTC, this stability number is biased low by the factor  $1/(1 - \text{weight})$ , where the weight is that part the USNO clocks have in the ALGOS computation of TAI/UTC. The actual percentage of weight varies over the course of the data since clocks come in and go out of ALGOS computation. As an example, if this weight is 40%, then the measured stability needs to be multiplied by 1.67 to obtain an unbiased estimate. This unbiased estimate is about  $\sigma_y(\tau = 45 \text{ days}) = 2.6 \times 10^{-15}$  for the combined instabilities of EAL and USNO. It is safe to say that one of these two scales has a stability better than this number divided by  $\sqrt{2}$  or  $1.8 \times 10^{-15}$ . USNO has about 40 of the HP 5071A clocks in their ensemble.

The current specification level for the stability of the high-performance HP 5071A is approximately  $\sigma_y(\tau) = 8 \times 10^{-12} \tau^{-1/2}$ . If a timing center has an ensemble of these standards, a simple equation, relating the number of these clocks in the ensemble and the integration or averaging time necessary to reach a stability of  $1 \times 10^{-15}$ , is  $N\tau = 6.4 \times 10^7$ . Hence, if  $N = 1$ , almost two years of averaging would be necessary. Most of these clocks would exhibit non-white-noise instabilities before  $1 \times 10^{-15}$  could be reached. If  $N = 4$ , six months are needed, which is not impractical. If  $N = 10$ , then two and one-half months are needed. And if  $N = 40$ , then less than three weeks are needed.

Having 10 or more of these clocks optimally used would allow a laboratory to have a real-time predicted frequency reference with about  $1 \times 10^{-15}$  traceability to TAI/UTC. Having 4 or more of these clocks would probably provide a real-time frequency estimate of about  $2 \times 10^{-15}$ .

## Accuracy and Stability of Methods of Distributing Time and Frequency

A perfect clock is limited by the means of distributing its time and frequency. This is, of course, true both within a laboratory setting as well as for remote distribution and comparisons.

As atomic clocks have improved at a rate of about one order of magnitude every seven years, this rate of improvement has placed significant demands on the methods of distribution and comparison. Natural limits have been reached for many different methods so that they are no longer useful for state-of-the-art clocks. HF broadcasts, such as WWV, are limited at the



millisecond level due to propagation path delay variations as the ionosphere moves up and down. LF and VLF transmissions, such as Loran-C, are limited at the microsecond level due also to propagation path delay variations.

New techniques are needed and satellite timing systems have opened up opportunities. There are systems which will work at the 10 picosecond level, but it is often a question of operational complexity and cost. Today's operational time scales have sub-nanosecond day-to-day predictabilities. To meet these needs a systems approach should be taken. In addition to satellite techniques, the potential of using optical-fiber communications is very promising. Now that the communications industries are laying fibers extensively and they also need time and frequency, a closer cooperation between them and the time and frequency community could be very beneficial.

Figure 7 is a summary plot of some of the best methods of time and frequency comparisons. The stability measure used is called the time variance, TVAR, and is given by  $\sigma_x^2(\tau) = \langle (\Delta^2 x)^2 \rangle / 6$ , where  $\Delta^2$  is the second difference operator,  $x$  is the time differences averaged over an interval  $\tau$ , and the brackets " $\langle \rangle$ " denote the expectation value. What is plotted is  $\sigma_x(\tau)$  for each of the different techniques. Since  $\sigma_x(\tau) = \tau \text{Mod}.\sigma_y(\tau) / \sqrt{3}$ , the  $\text{Mod}.\sigma_y(\tau)$  stability values are also shown for each decade. This is of particular value since the confidence on the estimate of the frequency difference measured over an interval  $\tau$  is given by  $2 \times \text{Mod}.\sigma_y(\tau)$  if the residuals are modeled by white-noise PM. If this model is not valid, the  $2 \times \text{Mod}.\sigma_y(\tau)$  value is still an approximate estimate of the confidence for using a particular technique for frequency transfer.

Figure 7 includes both time and frequency distribution techniques as well as time and frequency transfer techniques. In all cases, the clocks can be remote from each other, but in some cases there are limitations. Loran-C is plotted as a well-known stability reference. The Loran-C values are limited by the ground-wave propagation path, which is about two to four Megameters. The ground-wave signals vary because of distance, terrain variations, and atmospheric conditions; the effects of diurnal and annual variations are also shown. Loran-C can be used as a real-time time and frequency distribution system or in the common-view mode. The latter provides better accuracy and stability. The disadvantage of the common-view method is that it is an after-the-fact computation. The range of stabilities plotted covers both methods.

The GPS common-view technique depends not only on the baseline distance, but also on the receiver hardware and processing techniques. The maximum baseline distance is about 13 Mm (the circumference of the earth is about 40 Mm). Over the longest baselines the tropospheric and ionospheric delays are the limiting uncertainties. In this case the satellite's ephemeris must also be known well. For short baselines, this technique provides a lot of common-mode cancellation of errors. The common-view technique was a major break-through for international time and frequency comparisons and is still today the main means of communicating the times of most of the contributing clocks in the generation of TAI/UTC<sup>[7]</sup>.

Originally, day-to-day stabilities of as good as 0.8 ns were obtained between baselines as far apart as Boulder, Colorado and Ottawa, Canada. Global accuracies of about 4 ns have been obtained with careful post-processing.

Since the original GPS common-view receivers were designed, built and experiments conducted,



there seems to have been a gradual degradation in the performance of this technique. Day-to-day stabilities of from 2 to 8 ns are now more typical, and significant temperature coefficients have been measured due to antenna and lead-in cable sensitivities. Problems have crept into the common-view technique at about the 10 ns level. The source of these is being investigated at this time.

The GPS advanced common-view (ACV) technique is a systems approach. With digital GPS multichannel receivers, new opportunities become available that could provide major advancements in time and frequency metrology among clocks remote from each other. The basic benefits of the common-view technique can be built upon because of the large increase in the available data.

The ability to track several satellites continuously at a single observing location means that a more productive common-view schedule can be used, particularly between less-distant sites. The increased diversity of the measurement should reduce multipath effects since the multipath tends to average across the sky. Ionosphere and troposphere modeling errors will be basically the same for both techniques; except, comparing multiple tracks allows a comparison of an individual track from day-to-day. Since the geometry stays the same from one sidereal day to the next for a fixed site, the scatter in a given common-view track could be used in a time series weighting procedure to minimize errors for the remote clock comparison.

From a simple "degrees of freedom" argument there is significant advantage to the GPS ACV technique. If the measurement noise is white PM, then the confidence on the estimate of the frequency difference between two ideal reference clocks, as determined from a linear regression to the time-difference residuals taken between the two clocks, is:  $\sqrt{12} \times \sigma / (\tau_0 \times n^{3/2})$ , where  $\sigma$  is the standard deviation of the white-noise residuals,  $\tau_0$  is the measurement interval, and 'n' is the degrees of freedom (the number of independent measurements).

Since GPS common-view instrumentation errors have apparently gotten worse as time has gone on, and these original techniques involved a lot of analog circuitry, the question arises that perhaps the delays and delay stabilities may be better in these new miniaturized digital circuits. Hence, understanding and documenting instrumentation errors would be useful.

With some of the new digital multi-channel GPS timing receivers, it is possible to track several satellites at a time and to obtain a solution each second for each satellite. This has the potential of increasing the data density more than three orders of magnitude over the original common-view technique outlined above. If this white-noise model persisted, this would allow  $1 \times 10^{-15}$  confidence interval to be reached on a one-day regression line between two standards. The question is: can this GPS ACV approach significantly and efficiently increase the effective number of degrees of freedom over the original common-view technique?

An experiment was set up at HP labs in Palo Alto, CA using two eight-channel GPS receivers with the same reference clock feeding both and the same antenna providing the signal for both. All errors should cancel except for instrumentation errors and cable length differences. A multi-channel digital filter was designed to provide 10 s averages in order to decrease the volume of data and still take advantage of the available degrees of freedom. Each receiver and associated counting and computing system produced the 10 s average time difference between



each satellite clock and the common local-reference clock. These time series were differenced satellite by satellite and averaged across the satellites for each 10 s interval to produce the time difference between the two common times of the reference clock.

A plot of the time stability of these measurements is shown in Figure 7. The above equation for the confidence on the frequency estimate is equivalent to  $2 \times \text{Mod.}\sigma_y(\tau)$ . If the white-noise FM,  $\tau^{-1/2}$  level were to persist, then indeed the  $1 \times 10^{-15}$  level could be reached for an averaging time of 1 day. The little hump for  $\tau$  just longer than 10 s is probably due to our digital filter. For longer  $\tau$  values the stability level reached below 100 ps for  $\tau$  greater than about 1 hour. Environmental effects need still to be evaluated.

Also in Figure 7, The upper and lower values for the two-way satellite time and frequency transfer (TWSTFT) technique are the stabilities for continuous operation. The bottom curve is a measured instrumentation stability limit achievable. The upper curve is a more typical performance stability observed between two sites remote to each other. The upper limit is dotted on the right end as a reminder that TWSTFT is not typically used in the continuous mode for this range of sample times, but rather three times per week, and the frequency transfer uncertainty will not be as good as that shown, but would be nominally given by  $1 \text{ ns}/\tau$ .

The TWSTFT technique both transmits and receives, and cannot be used for dissemination, but for after-the-fact time and frequency transfer. Because the typical mode is for intermittent operation, it is more amenable for after-the-fact time transfer. The baseline distances between clocks being compared is limited by the position of the geostationary communications satellite being used. Distance up to about 9 Mm have been realized.

The enhanced GPS (EGPS) technique can be used both for time and frequency transfer and for real-time distribution. It is also a systems approach and is highly dependent on the reference clock used; hence, the different levels of performance when a quartz oscillator is used, or a rubidium frequency standard, or a cesium-beam frequency standard. Because EGPS employs an SA filter and is phase-locked to GPS, the long-term stabilities all approach the GPS stability regardless of the reference clock used. The upper curve is dotted on the right end as a projection of theoretical behavior. The other values are based on experimental analysis. If SA is removed, the stability of EGPS will be significantly improved — especially in the intermediate-term region of averaging times.

Because GPS is global, there is no limit on the baseline separation of the clocks being compared or which are receiving the distributed time and frequency information. Hence, this approach is excellent as a telecommunication network-node synchronization and syntonization technique. With an excellent reference clock the instrumentation residual errors have been documented at about 1.5 ns. It is also extremely cost effective — producing in real time a simple 1 pps output that is very stable. An EGPS receiver can lock either to GPS system time or to the broadcast estimate of UTC(USNO MC). The latter is usually kept within about 20 ns of the master-clock at the observatory.

A potentially very useful experiment that has not been conducted would be to treat GPS system time (the composite clock) as a common-clock. Assume there are two perfect clocks remotely located with respect to each other anywhere on the earth. If these two clocks were



to perform the same kind of optimum regression analysis estimate of the frequency of GPS system time using EGPS receivers over the same integration interval, and then the difference in these frequency estimates were calculated, the uncertainty in this estimate should improve with the length of integration. In other words, each of the two sites is measuring the same clock in the same way within some noise band. Subtracting their measured values from each other subtracts out the common clock. If for long integration times, the time-difference residuals had a white-noise spectrum, the uncertainty on frequency transfer could improve as fast as  $\tau^{-3/2}$ . It should only take a few weeks of averaging time to reach  $1 \times 10^{-15}$  very cost effectively and with straight-forward data processing.

The GPS Carrier-phase technique has the smallest uncertainty for frequency comparison of remote clocks. Experiments have been conducted comparing hydrogen masers remote to each other by having geodetic type receivers at both sites. By locking to GPS common carrier-phase at the two sites, RMS residuals of 30 ps have been measured. The data plotted in Figure 7 are between Goldstone, California and Algonquin Park, Canada. The baseline distance is about 3.4 Mm (2,000 miles). About 35 monitor stations were involved in determining accurate ephemerides for the satellites. Both sites have to view the same satellites at the same time. The main problems with this technique are the difficulty in the data processing and the expense of the receivers. Both of these problems could be overcome, and this technique could be among the best for minimizing remote frequency comparison uncertainty.

Time accuracies of the order of 10 ns may eventually come out of the FAA's Wide Area Augmentation System (WAAS) via the signals from the INMARSAT satellites. These could also be very useful to the timing community.

## Conclusions

Intrinsically, the proper algorithmic combination of the global set of clocks contributing to the composition of TAI/UTC provide a reference as good as  $1 \times 10^{-15}$  or better for sample times,  $\tau$ , longer than about two hours. More than a month after the fact, the long-term stability of TAI/UTC is available from the BIPM Circular-T and it approaches the ideal stability intrinsically available. The measurement noise limits the stability of TAI/UTC at  $\sigma_y(\tau = 10 \text{ days})$  to about  $1 \times 10^{-14}$ . The paper discusses ways to improve the intermediate stability ( $\tau = 1 \text{ day to a month}$ ) measurement noise for international comparisons to better than  $1 \times 10^{-15}$ . The paper also suggests ways to transfer optimally the stability of the international clock set to a local clock set so that frequency standards at two different locations can compare frequencies with uncertainties at or below  $1 \times 10^{-15}$ . This can be done for both the intermediate and long-term stability ranges and in real-time or in post processing. The post processed data intrinsically have better uncertainties.

Existing local clock sets properly utilized and optimally predicted forward can project to the current time much of the intrinsic stability of the international clock set. This can be done at the  $1 \times 10^{-15}$  or better level for frequency comparisons or to better than 10 ns of UTC timing accuracy. The outstanding long-term stability of a new commercial cesium-beam clock contributes a key element to the  $1 \times 10^{-15}$  comparison ability now available. The well known short-term stability of hydrogen masers can contribute substantially to the frequency comparison



effort — especially if they also have excellent intermediate and long-term stabilities.

The BIPM data analyzed in this paper were for the period 1991 through 1994. The data base has only improved since then, and an international cooperative, using the Internet, for example, could make available much of the intrinsic stability of the international clock set for both the intermediate as well as the long-term stability comparisons of remote clocks. This could be done at or below the  $1 \times 10^{-15}$  level and in near-real time.

## Acknowledgements

The authors are very grateful for the extended effort of Mr. Jacques Azoubib for providing much of the data used in the analysis. Mr. Mihran Miranian of USNO has been very helpful with some of the comparisons and in making data available. Mr. Mike King of Motorola has been extremely helpful toward optimally utilizing the new multi-channel digital GPS receivers. The service and support of the time and frequency staff at NIST are much appreciated.

## Figure Captions

**Figure 1** Histogram of offsets from TAI for all clocks, 311 total, reporting in the international time scale for 1994. There are several outliers plotted in both the  $-30$  and  $+30 \times 10^{-13}$  bins. The large number of units in the 0 bin are mainly due to the primary standards and the HP 5071As.

**Figure 2** Histogram of offsets from TAI for all hydrogen masers, 37 units, reporting in the international time scale for 1994.

**Figure 3a** Histogram of offsets from TAI for all HP 5071As, 94 units, reporting in the international time scale for 1994.

**Figure 3b** Same as Fig. 3a but with bin size reduced to  $1 \times 10^{-13}$ .

**Figure 4** Histogram of offsets from TAI for the three primary standards reporting in international time scale for 1994.

**Figure 5** Scatter plot of  $\sigma_y(\tau)$  for high performance HP 5071As (78 units) reporting in the international time scales for 1994. The ideal theoretical white-noise FM slope on this plot should be proportional to  $\tau^{-1/2}$ . With some outliers, many of the units tend to follow this slope within the confidence of the estimates. The slope tends to be slightly steeper between  $\tau = 10$  days and 20 days. This may be caused by residual measurement noise. For the longest  $\tau$  values, some of the clocks tend to be flatter than the  $\tau^{-1/2}$  behavior. In these clocks there appears a slight frequency drift, flicker or random-walk noise. Those indicating drift are of the order of a few parts in  $10^{-16}$  per day.

**Figure 6a**  $\text{RMS}/\sqrt{N}$  of sigmas for the data in Fig. 5. The  $\text{RMS}/\sqrt{N}$  values are also plotted for the hydrogen masers. The  $\text{RMS}/\sqrt{N}$  will typically give a pessimistic estimate for ensemble stability because the values with larger sigmas are weighted heavier. The results using optimum weighting for the HP 5071A ensemble are also plotted.



**Figure 6b** The  $\text{Mod.}\sigma_y(\tau)$  stability results from an independent three-cornered hat analysis. The three independent ensembles were the primary clocks, the hydrogen masers and the HP 5071As. The  $\tau^{-3/2}$  behavior is consistent with white PM measurement noise at a level of 1.3 ns. Apparently, the HP 5071A ensemble is sufficiently better than the measurement noise or the other two ensembles that its stability cannot be measured with confidence because of only having 71 data points.

**Figure 7** A plot of the time stability of state-of-the-art techniques for time and/or frequency comparison at locations remote to each other, and showing Loran-C as a well-known stability reference. The Loran-C values are for ground-wave signals and vary because of distance and terrain and atmospheric conditions; the effects of diurnal and annual variations are also shown. GPS common-view technique also depends on the baseline distance, but more importantly on the receiver hardware and processing techniques. The GPS advanced common-view (ACV) technique shows the first experimental results for the hardware only. The upper and lower values for the two-way satellite time and frequency transfer (TWSTFT) technique are the stabilities for continuous operation. The bottom curve is a measured instrumentation stability limit achievable. The upper curve is a more typical performance stability observed between two sites remote to each other. The upper limit is dotted on the right end as a reminder that TWSTFT is not typically used in the continuous mode for this range of sample times, but rather three times per week, and the frequency transfer uncertainty will not be as good as that shown, but would be nominally given by  $1 \text{ ns}/\tau$ . The enhanced GPS (EGPS) technique can be used both for time and frequency transfer and for real-time distribution. It is a systems approach and is highly dependent on the reference clock used; hence, the different levels of performance when a quartz oscillator is used, or a rubidium frequency standard, or a cesium-beam frequency standard. Because EGPS employs an SA filter and is phase-locked to GPS, the long-term stabilities all approach the GPS stability regardless of the reference clock used. The upper curve is dotted on the right end as a projection of theoretical behavior. The other values are based on experimental analysis. All GPS methods basically assume that SA will stay at the current level.

## References

- [1.] D. W. Allan, A. Lepek, L. Cutler, R. Giffard, and J. Kusters, "A  $10^{-15}$  International Frequency Reference Available Now," Proceedings of Fifth Symposium on Frequency Standards and Metrology, Woods Hole, MA, October 1995.
- [2.] A.A. Uljanov, N.A. Demidov, E.M. Mattison, R.F.C. Vessot, D.W. Allan, and G.M.R. Winkler, "Performance of Soviet and U.S. Hydrogen Masers," submitted to Proc. of 22nd Annual Precise Time and Time Interval (PTTI) Applications and Planning Meeting, 1990.
- [3.] Jon H. Shirley, W.D. Lee, and R. Drullinger, "The Evaluation of NIST-7 A New Era," Proceedings of the Symposium on Frequency Standards & Metrology, Woods Hole, Massachusetts, 15-19 Oct. 1995 (World Scientific Publishing)



- [4.] D.B. Sullivan, D.W. Allan, D.A. Howe, and F.L. Walls, "*Characterization of Clocks and Oscillators, NIST Tech Note 1337,*" 1990.
- [5.] A. Lepek, A. Shenhar, and D. W. Allan, "*INPL Virtual Time Scale, UTC(INPL),*" to be published, Metrologia.
- [6.] M.A. Weiss, D.W. Allan and T.K. Pepler, "*A Study of the NBS Time Scale Algorithm,*" IEEE Transactions on Instrumentation and Measurement, 38, 631-635, 1989.
- [7.] D.W. Allan, D.D. Davis, M. Weiss, A. Clements, B. Guinot, M. Granveaud, K. Dorenwendt, B. Fischer, P. Hetzel, S. Aoki, M.-K. Fujimoto, L. Charron, and N. Ashby, "*Accuracy of International Time and Frequency Comparisons Via Global Positioning System Satellites in Common-View,*" IEEE Transactions on Instrumentation and Measurement, IM-34, No. 2, 118-125, 1985.

# HISTOGRAM OF FREQUENCY OFFSETS (TAI - CLOCK) FOR 1994 (ALL CLOCKS)

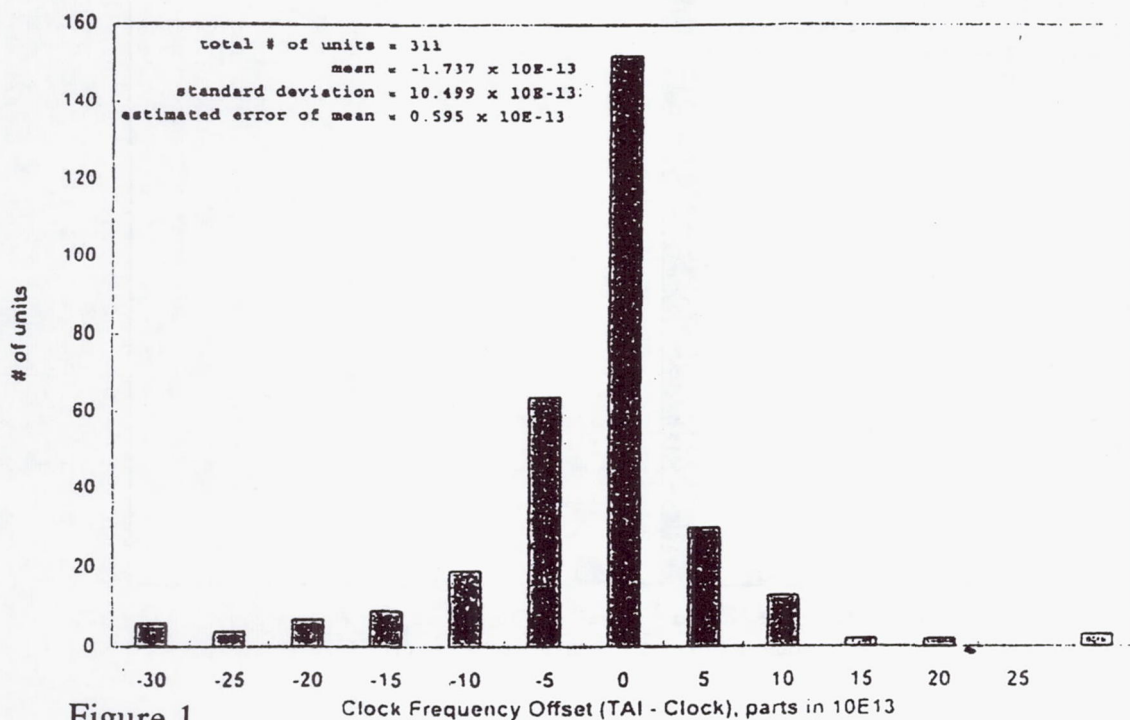


Figure 1

# HISTOGRAM OF FREQUENCY OFFSETS (TAI - CLOCK) FOR 1994 (HYDROGEN MASERS)

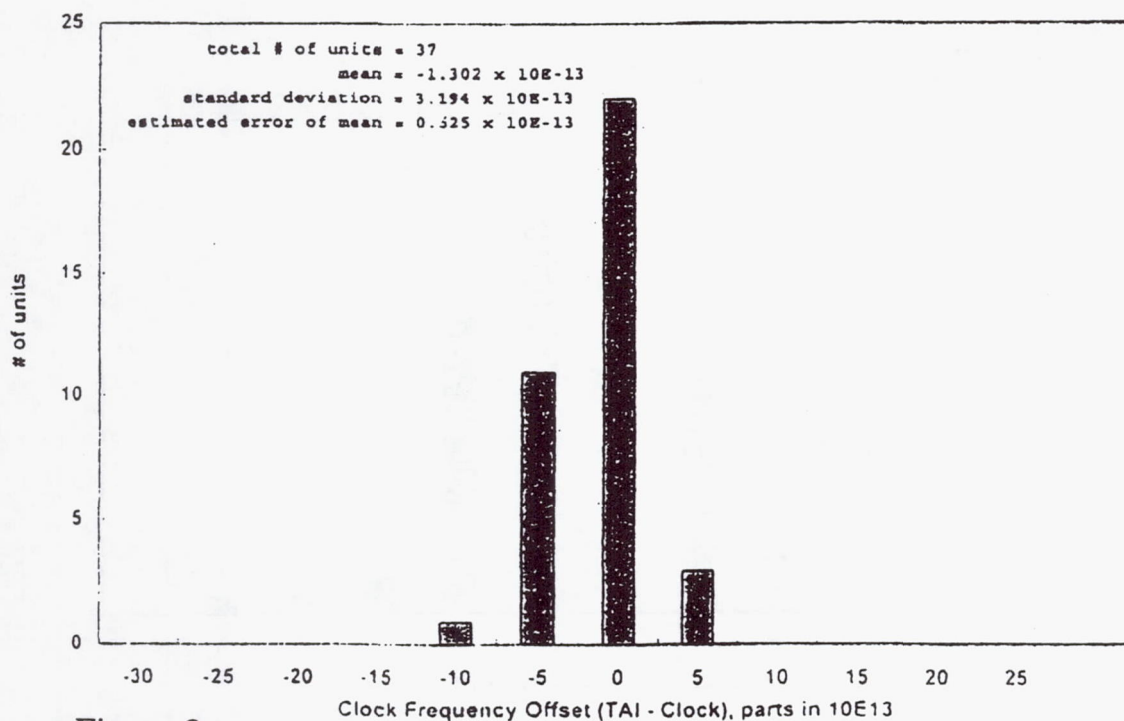


Figure 2



# HISTOGRAM OF FREQUENCY OFFSETS (TAI - CLOCK) FOR 1994 (ALL 5071As)

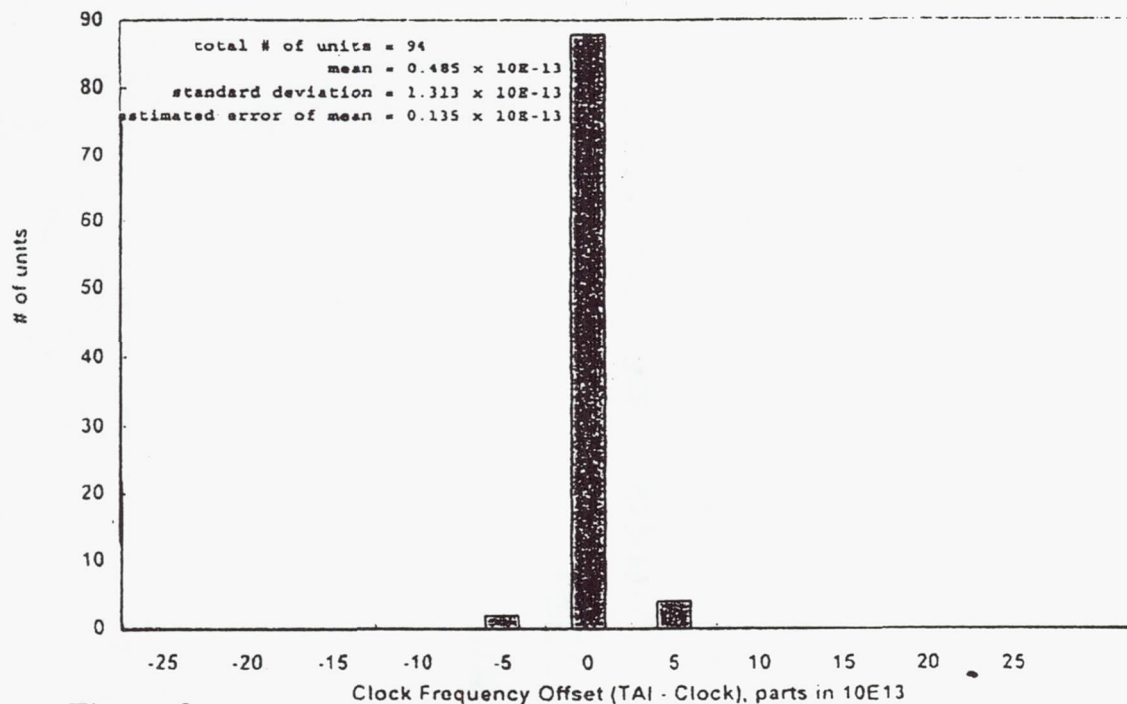


Figure 3a

# HISTOGRAM OF FREQUENCY OFFSETS (TAI - CLOCK) FOR 1994 (ALL 5071As)

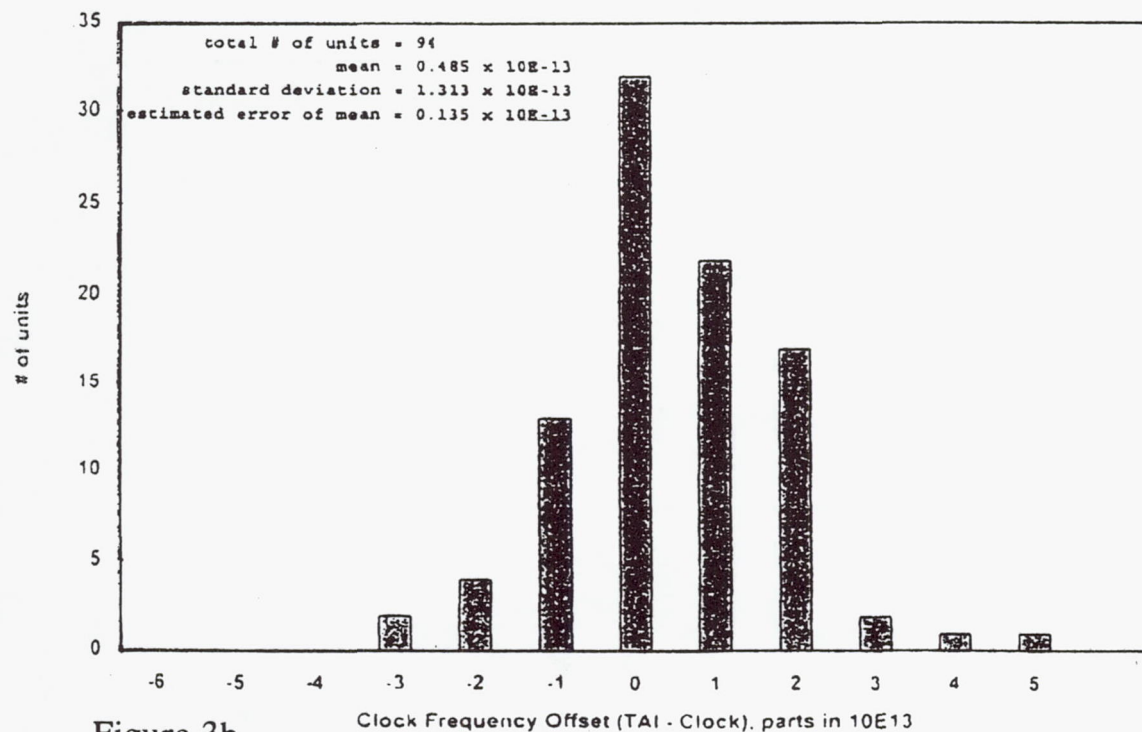


Figure 3b

# HISTOGRAM OF FREQUENCY OFFSETS (TAI - CLOCK) FOR 1994 (PRIMARY STANDARDS)

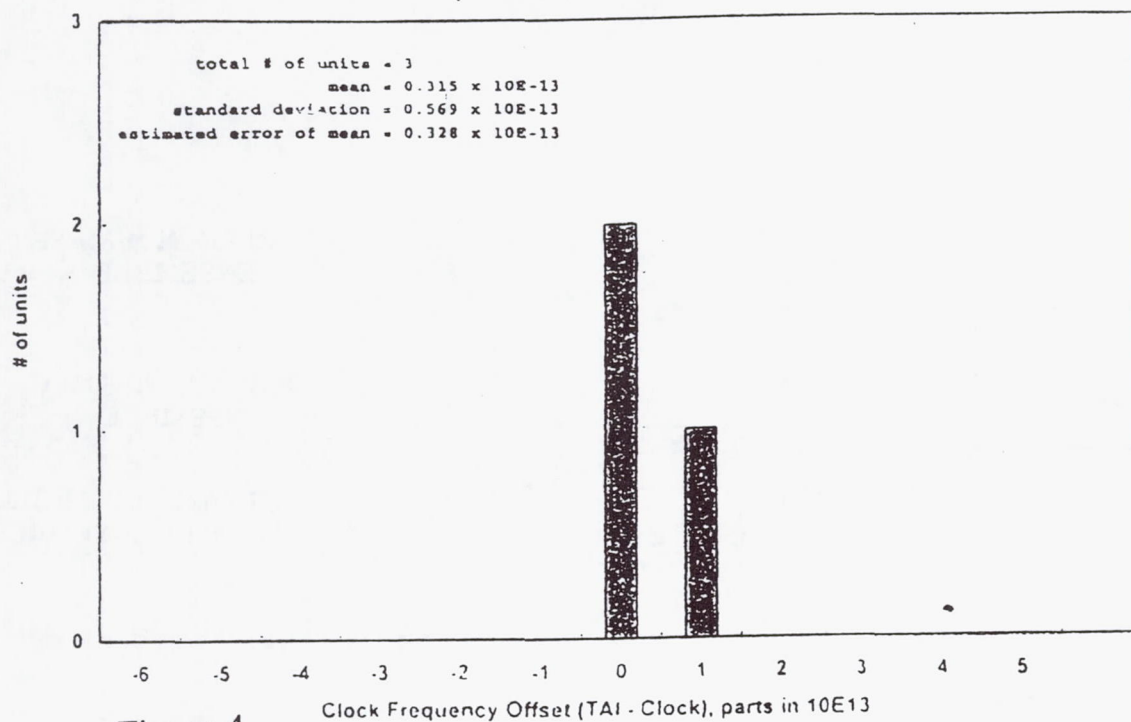


Figure 4

# HIGH PERFORMANCE HP5071As IN TIME SCALE FOR 1994 (78 UNITS)

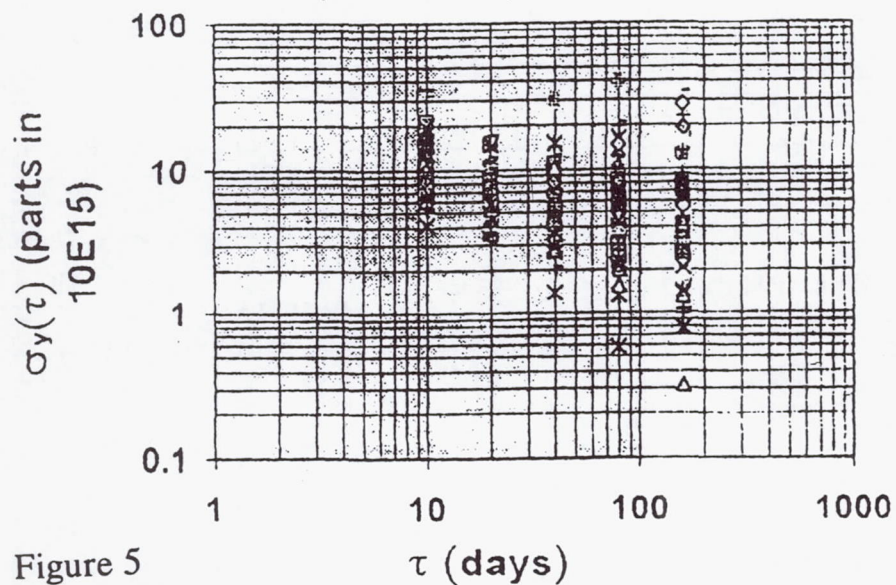


Figure 5



# ENSEMBLE FREQUENCY STABILITY of HP 5071As and HYDROGEN MASERS vs. EAL

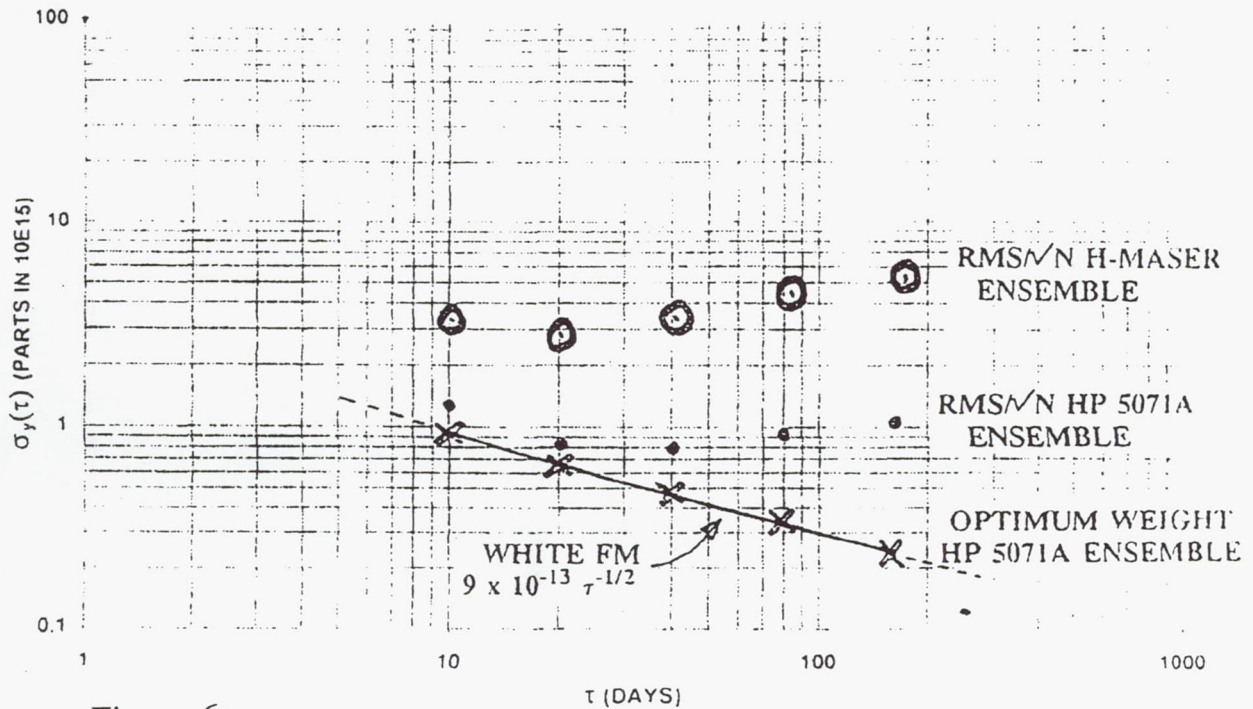


Figure 6a

# THREE CORNERED-HAT ESTIMATE OF STABILITY OF INDEPENDENT ENSEMBLES

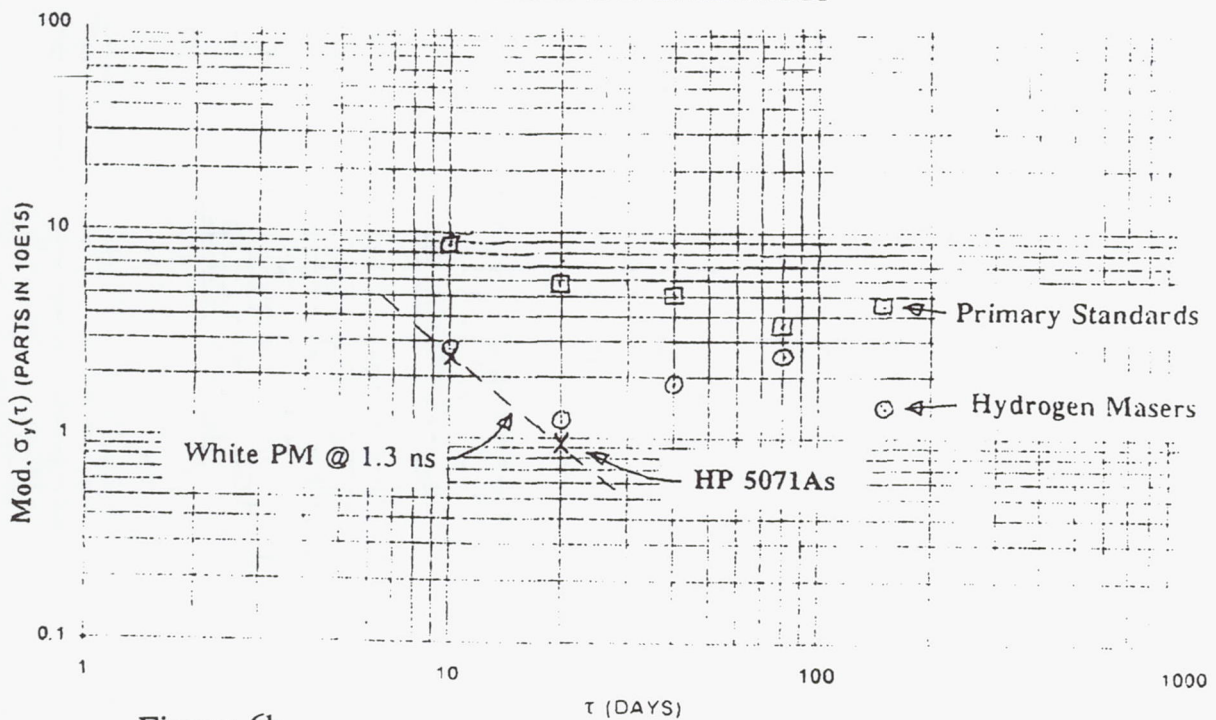


Figure 6b

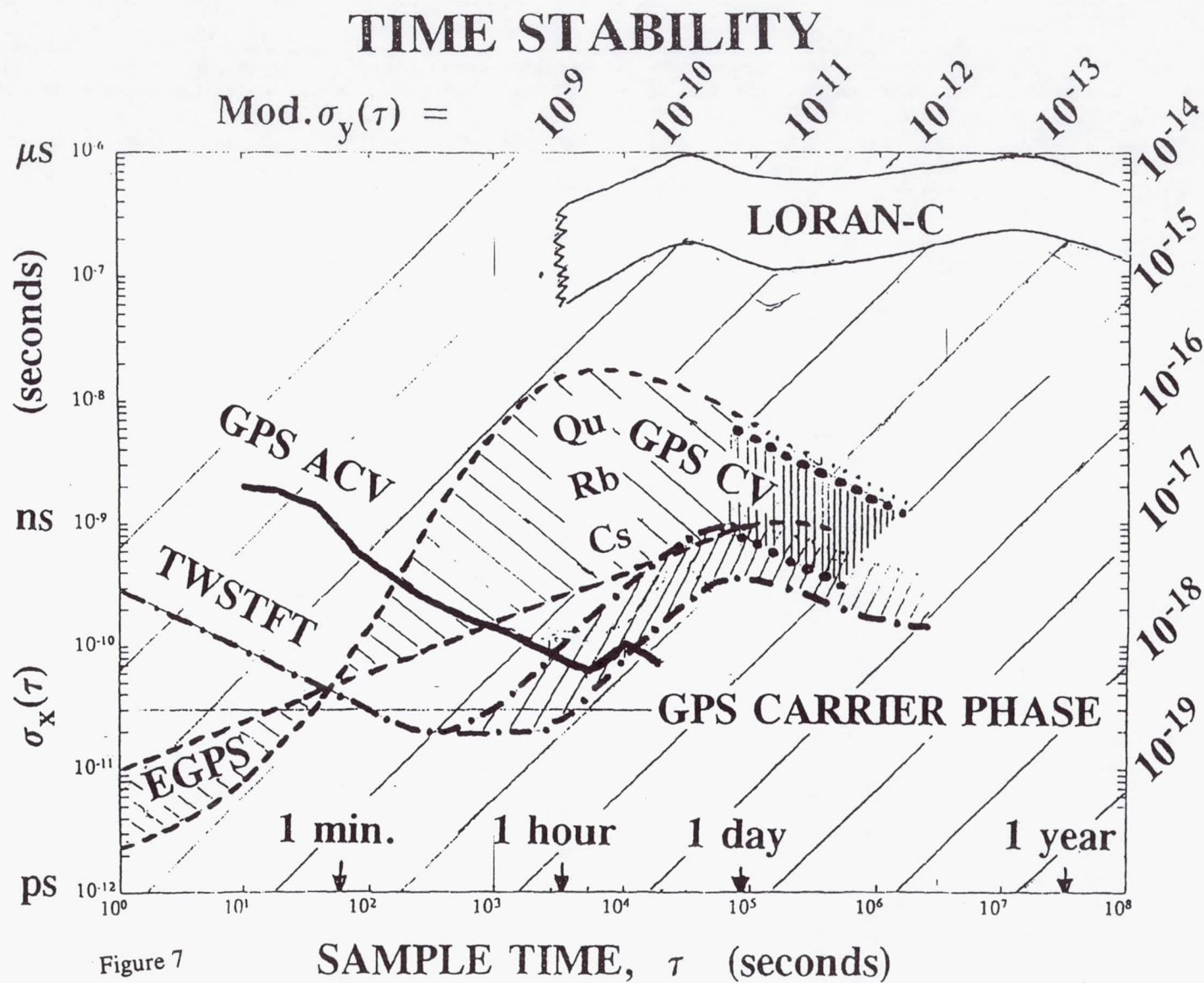


Figure 7



# STEERING OF FREQUENCY STANDARDS BY THE USE OF LINEAR QUADRATIC GAUSSIAN CONTROL THEORY

Paul Koppang  
U.S. Naval Observatory  
Washington, D.C. 20392

Robert Leland  
University of Alabama  
Tuscaloosa, Alabama 35487

## Abstract

*Linear quadratic Gaussian control is a technique that uses Kalman filtering to estimate a state vector used for input into a control calculation. A control correction is calculated by minimizing a quadratic cost function that is dependent on both the state vector and the control amount. Different penalties, chosen by the designer, are assessed by the controller as the state vector and control amount vary from given optimal values. With this feature controllers can be designed to force the phase and frequency differences between two standards to zero either more or less aggressively depending on the application. Data will be used to show how using different parameters in the cost function analysis affects the steering and the stability of the frequency standards.*

## INTRODUCTION

The steering of frequency standards (atomic clocks) is a very important procedure in the timing community. Steering is used to synchronize remote clocks using very accurate time transfer methods such as two-way time transfer and the Global Positioning System. Also in time scale applications a standard is steered to a paper, or calculated, clock in order to give the time scale a physically realizable output. This paper will discuss how the linear quadratic Gaussian (LQG) technique applies to the designing of control systems to steer frequency standards.

In any real world application, a control system must deal with some amount of uncertainty, whether it comes in the form of sensor noise, process modeling error, or any other noise sources. The LQG technique is used for designing optimal control systems for uncertain physical processes. An important feature of this technique is that the stability of the control system is assured if system parameters have the properties of observability and controllability. Kalman filtering is used in order to estimate the actual state variables from measurements made of the stochastic system.

## TWO-STATE LQG THEORY FOR FREQUENCY STANDARDS

In the LQG theory<sup>[1,2,3]</sup> the state equation is assumed to be given as a linear function of a state vector and a control vector:

$$\mathbf{x}(k+1) = \Phi \mathbf{x}(k) + \mathbf{B} \mathbf{u}(k) + \mathbf{w}(k), \quad (1)$$

where

$$\mathbf{x}(k) = \text{state vector} = \begin{bmatrix} x_1(k) \\ x_2(k) \end{bmatrix},$$

$x_1(k)$  is the phase difference, and  $x_2(k)$  is the fractional frequency difference, between the reference and the steered standard,

$u(k)$  = control vector which is a scalar in this case corresponding to the fractional frequency change of the synthesizer controlling the steered standard,

$$\Phi = \text{transition matrix} = \begin{bmatrix} 1 & \tau \\ 0 & 1 \end{bmatrix}, \tau \text{ is the time interval between measurements,}$$

$w(k)$  = white noise characterized by covariance  $Q_k$ ,

$Q_k = \begin{bmatrix} \frac{1}{2}h_0\tau + 2h_{-1}\tau^2 + \frac{2}{3}\pi^2h_{-2}\tau^3 & \pi^2h_{-2}\tau^2 \\ \pi^2h_{-2}\tau^2 & 2\pi^2h_{-2}\tau \end{bmatrix}$ , and the  $h$ 's are calculated from the two-sample (Allan) variance of the comparison between two standards[4,5].

The noisy measurement  $z(k)$  is related to the state vector by

$$z(k) = \mathbf{H}\mathbf{x}(k) + v(k) \quad (2)$$

where

$z(k)$  = measurement, in our case a scalar phase difference,

$\mathbf{H}$  = connection matrix =  $[1 \ 0]$ , and

$v(k)$  = white noise characterized by covariance  $R_k$  = measurement noise.

The linear state equation (1) is an approximation to the state modeling equation that includes higher order terms. In order to help give the linear approximation validity, the control vector  $u(k)$  is chosen such that the quadratic cost function

$$J = \sum_k [\hat{\mathbf{x}}(k)^T \mathbf{W}_Q \hat{\mathbf{x}}(k) + u(k)^T \mathbf{W}_R u(k)] \quad (3)$$

is minimized.

$\mathbf{W}_Q$  and  $\mathbf{W}_R$  are matrices that are chosen by the designer in order to set the relative penalties assessed to the state vector estimate  $\hat{\mathbf{x}}(k)$  and control vector  $u(k)$  as they vary from zero. In general, if  $\mathbf{W}_R$  is large compared to  $\mathbf{W}_Q$ , the penalty is large for the system attempting to drive the state vector toward zero too rapidly. Conversely, if  $\mathbf{W}_Q$  is large compared to  $\mathbf{W}_R$ , the system faces a smaller penalty for large control effort and the system is driven toward zero more quickly.

Due to the noisy measurement of  $\mathbf{x}(k)$ , we are faced with a compound problem of optimal control and estimation. A very useful theorem from control theory known as the separation principle allows us to solve the optimal control and the estimation problem independently. Kalman filtering is the technique used to estimate the true state  $\mathbf{x}(k)$  from the noise. The Kalman filter is calculated as usual[3] with the exception that the update estimate must now include control terms:

$$\hat{\mathbf{x}}(k+1) = \Phi \hat{\mathbf{x}}(k) + \mathbf{B}u(k) + \mathbf{K}_g[z(k+1) - \mathbf{H}(\Phi \hat{\mathbf{x}}(k) + \mathbf{B}u(k))] \quad (4)$$



where  $K_g$  is the Kalman filter gain,  $\hat{x}(k)$  is the state estimation, and  $B = \begin{bmatrix} 1 \\ 1 \end{bmatrix}$  for the two-state model with a frequency synthesizer as the control mechanism. The optimal control for the given cost equation is

$$u(k) = -\hat{G}_0 \hat{x}(k) \quad (5)$$

where

$$\hat{G}_0 = (B^T \hat{K}_0 B + W_R)^{-1} B^T \hat{K}_0 \Phi \quad (6)$$

and  $\hat{K}_0$  is a solution to the steady state Ricatti equation

$$\hat{K}_0 = \Phi^T \hat{K}_0 \Phi + W_Q - \Phi^T \hat{K}_0 B (B^T \hat{K}_0 B + W_R)^{-1} B^T \hat{K}_0 \Phi. \quad (7)$$

This gives us a statistically optimal control  $u(k)$  for the given cost function with the designer specified parameters  $W_Q$  and  $W_R$ . Now that the control is optimized, we need to be concerned with the stability of the control design. Stability is assured if the pair  $(W_Q, \Phi)$  are observable, the pair  $(\Phi, B)$  are controllable, the Kalman filter is stable, and the model is reasonably good (see [2]). Controllability is the ability to steer the system from an initial state to another state in a finite amount of time, and observability is the ability to determine the state at any time from a finite number of measurements.

## SIMULATIONS

Actual data measured from frequency standards at the United States Naval Observatory (USNO) were used in the simulations. An LQG control was applied to the data as if one of the standards frequency was being adjusted by a frequency synthesizer. Thus, the only assumption in the simulations is that the synthesizer works ideally.

The hydrogen maser NAV8 was chosen to be steered to the USNO Mean<sup>[6]</sup>. The Mean is a paper clock that is calculated using an ensemble of hydrogen masers and cesium frequency standards. Maser NAV8 has excellent short-term stability, but due to the poor environment that it was in during the data collection, its long-term stability suffered. One of the best performing standards at USNO is maser NAV4. Figure 1 shows the performance differences between NAV8 and the Mean versus NAV4. As can be seen, we face an interesting problem of steering maser NAV8 to the Mean in phase and frequency while attempting to preserve the short-term stability of the maser and gain the long-term stability of the USNO Mean. The phase difference between NAV8 and the Mean is given in Figure 2. In order to minimize initial offsets, a frequency offset was removed from the data, and a constant was subtracted out giving the initial phase difference point to be near zero.

In trial 1 we set  $W_R = 10^5$  and  $W_Q = \begin{bmatrix} .001 & 0 \\ 0 & .001 \end{bmatrix}$ , which gives

$$\hat{G}_0 = \begin{bmatrix} 6.50277 \times 10^{-5} & .57714 \end{bmatrix}$$

after solving equations (5) and (6). Figure 3 shows the phase difference between the Mean and NAV8 after steering NAV8 using the above solution. The phase difference is kept very small with the difference having a standard deviation of 140 picoseconds.



In trial 2 we set  $W_R = 10^{12}$  and  $W_Q = \begin{bmatrix} .001 & 0 \\ 0 & .001 \end{bmatrix}$  which gives

$$\hat{G}_0 = \begin{bmatrix} 3.3185 \times 10^{-8} & .014976 \end{bmatrix}$$

after solving equations (5) and (6). Figure 4 shows the phase difference between the Mean and NAV8 after steering NAV8 using the trial 2 parameters. The phase differences after the initial settling have a standard deviation of 691 picoseconds.

A plot of the two-sample deviation of NAV4 versus the steered NAV8 for both trial 1 and trial 2 parameters is shown in Figure 5. This plot shows that the short-term stability of the maser in trial 1 has been perturbed by the fairly aggressive steering. While for trial 2, the stability exhibits the short-term stability of the maser and excellent performance in the long term.

Another application of the LQG technique is the steering of remote clocks to UTC (USNO) via GPS. Figure 6 shows data obtained between a keyed GPS receiver and Hewlett-Packard HP5071 cesium standard #249. The initial data had 50 nanosecond phase and  $4.0 \times 10^{-14}$  frequency offsets. Also shown in Figure 6 is the phase difference after a simulation run with the LQG control using the parameters of trial 1. We assume that there are two remote clocks being compared by a noisy GPS measurement system. The stability plot in Figure 7 shows how the cesium performed during the steers compared to a hydrogen maser after the initial settling of the controlled system. The solid line on the plot shows the performance specification for the 5071 cesium. The slightly worse stability near 10 hours is most likely due to modelling errors incurred from assuming whiteness of the GPS data.

The parameters chosen for the LQG depend on the systems being used, the desired outcome, and the individual designer. This can be seen in the differences between the results in trial 1 and 2. In trial 1 the short-term stability is sacrificed slightly for a tight control in the differences between the standards. The stability is still good, but if this does not meet the frequency stability needs for a system then the parameters of trial 2 could be used, or any other parameter set that gives the desired results as determined through simulation.

## EXPERIMENTAL RESULTS

One of the great concerns in designing a controller is whether or not it will be stable and robust. This was tested by offsetting an external synthesizer, called an Auxiliary Output Generator manufactured by Sigma Tau Standards Corporation, driven by maser NAV2. The phase offset made was approximately 8 milliseconds compared to maser NAV4. Figure 8 shows how the controller with parameters given in trial 1 of the simulations reacted to this phase step that was nearly 7 orders of magnitude greater than would be expected in practice. The system remained stable and brought the signals within 300 picoseconds in approximately 6 days.

Figure 9 shows experimental data of maser NAV2 being steered to the USNO Master Clock using an Auxiliary Output Generator that received its input from a distribution amplifier driven by NAV2. The several hundred picosecond humps in the data are caused by temperature changes in the testing lab where the 5 MHz distribution amplifier with a poor temperature coefficient resides. Temperature control of the lab was poor during the installation of a back-up air conditioning system.



## CONCLUSION

The LQG design philosophy is a robust, statistically optimal method for steering frequency standards. Simulations can be run without undue difficulty in order for the designer to characterize how different parameters will affect system responses. This technique could also be used to steer one standard very tightly to another, thus creating an independent back-up that is in phase and on frequency with its reference. Testing is now under way for implementing the LQG technique to synchronize remote systems using the Global Positioning System and two-way satellite time transfer methods.

## REFERENCES AND NOTES

- [1] M. Athans 1971, "The Role and Use of the Stochastic Linear Quadratic Gaussian Problem in Control System Design," *IEEE Trans. Auto. Control*, pp. 529-552.
- [2] K. Ogata 1987, *Discrete-Time Control Systems* (Prentice Hall, Englewood Cliffs, New Jersey).
- [3] R. Brown, and P. Hwang 1992, *Introduction to Random Signals and Applied Kalman Filtering* (John Wiley and Sons, New York).
- [4] I. Ahn, and R. Brown 1987, "Assessing the Validity of Suboptimal 2-State Clock Models," *Proceedings of the 18th Annual Precise Time and Time Interval (PTTI) Applications and Planning Meeting*, 2-4 December 1986, Washington, DC, pp. 421-436.
- [5] Ahn gives several Q matrix models. For the data used in this paper, we did not find a significant difference in LQG results based on the different models. Simulations should be run in order to determine the best modeling for different applications.
- [6] The USNO Mean is presently composed of an ensemble average of 58 frequency standards (10 hydrogen masers and 48 cesium standards).

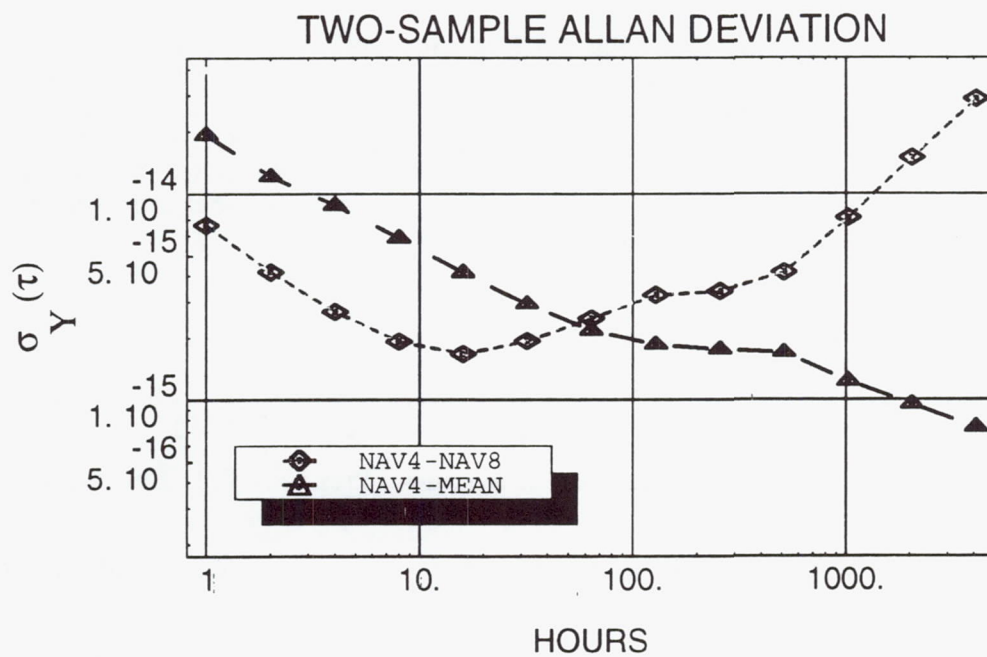


Figure 1

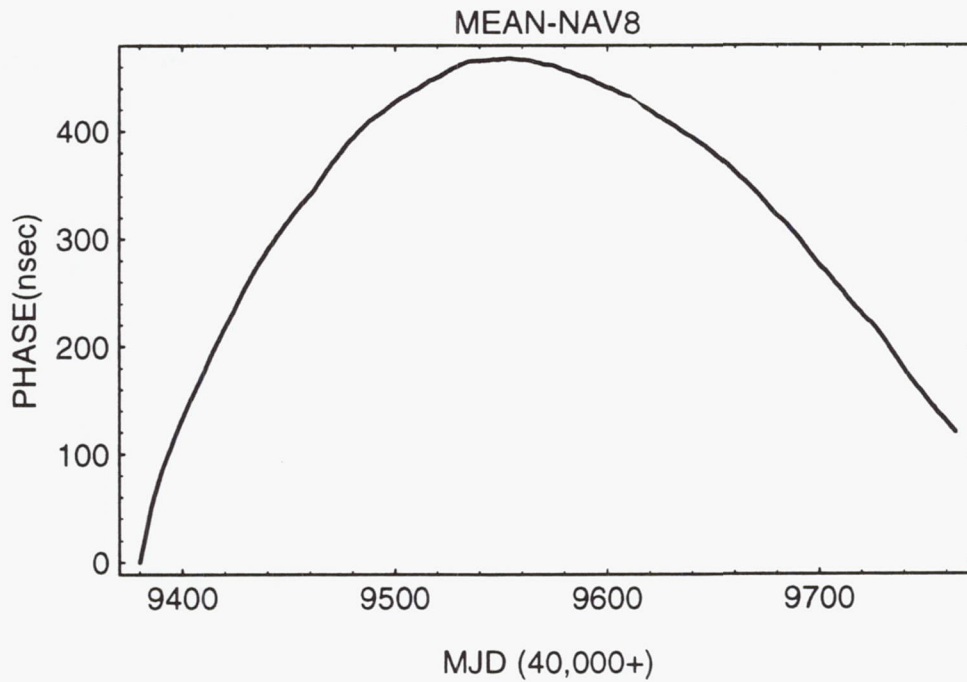


Figure 2



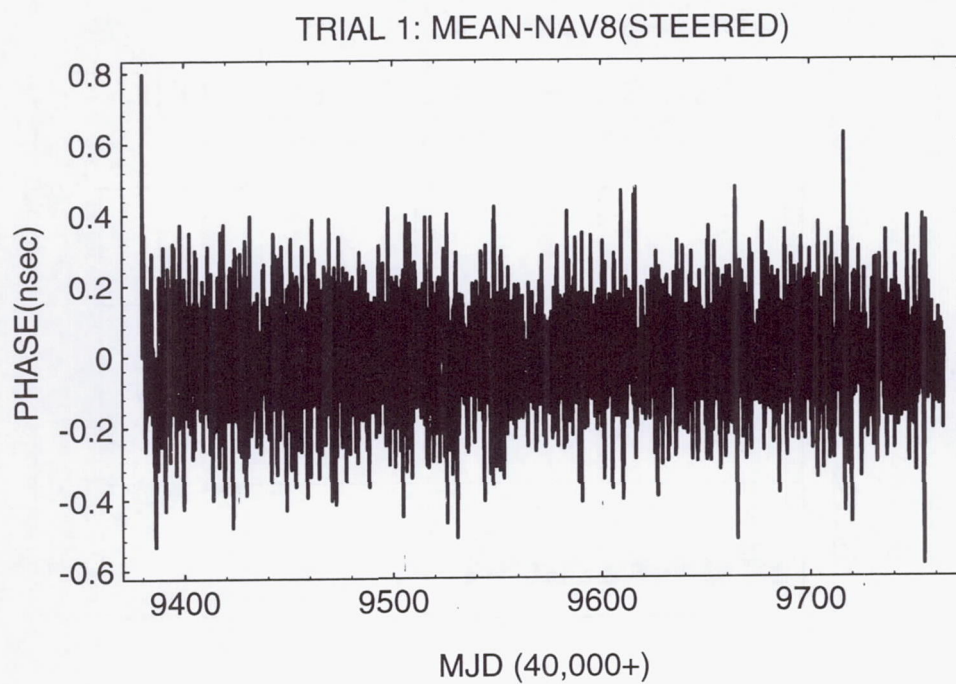


Figure 3

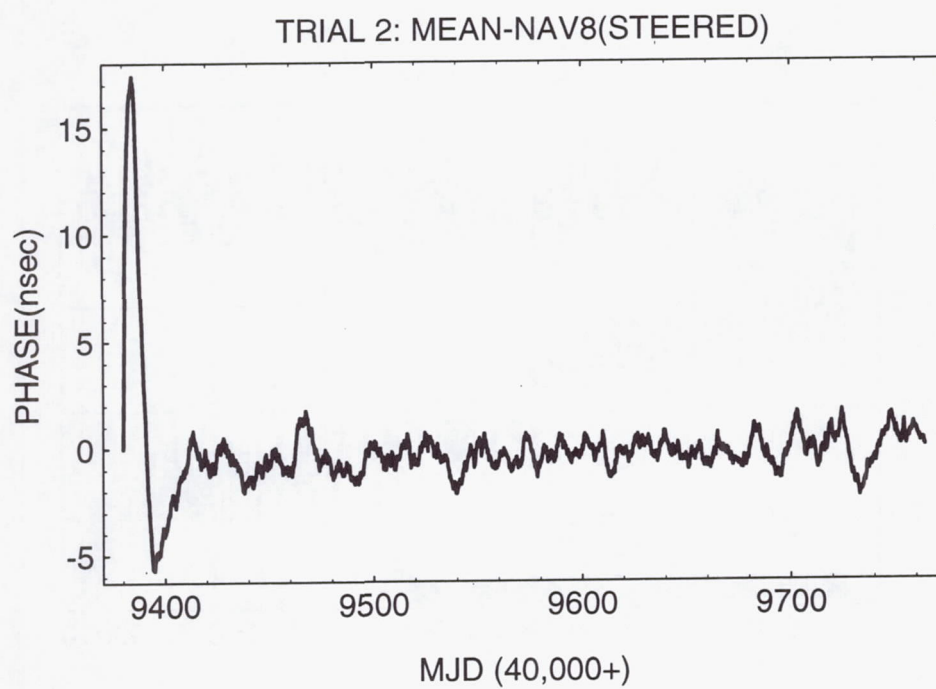


Figure 4

# TWO-SAMPLE ALLAN DEVIATION NAV4 - NAV8(STEERED)

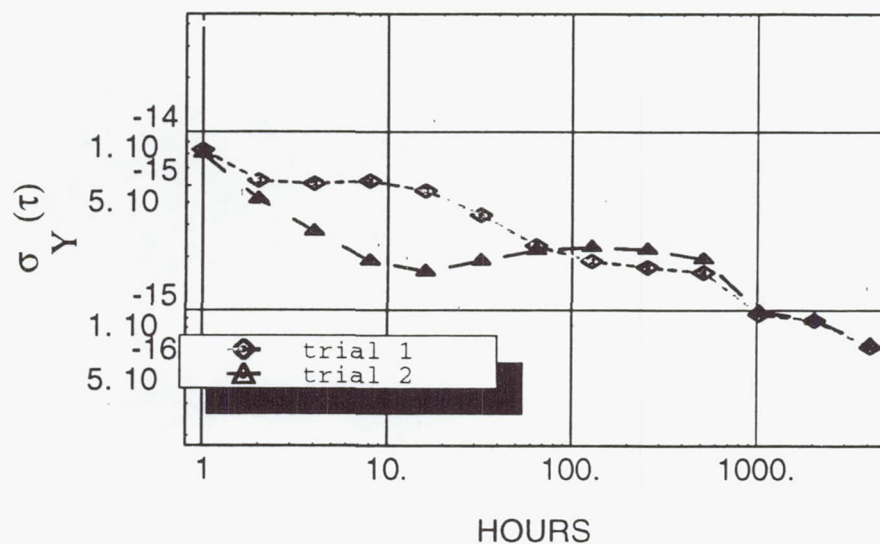


Figure 5

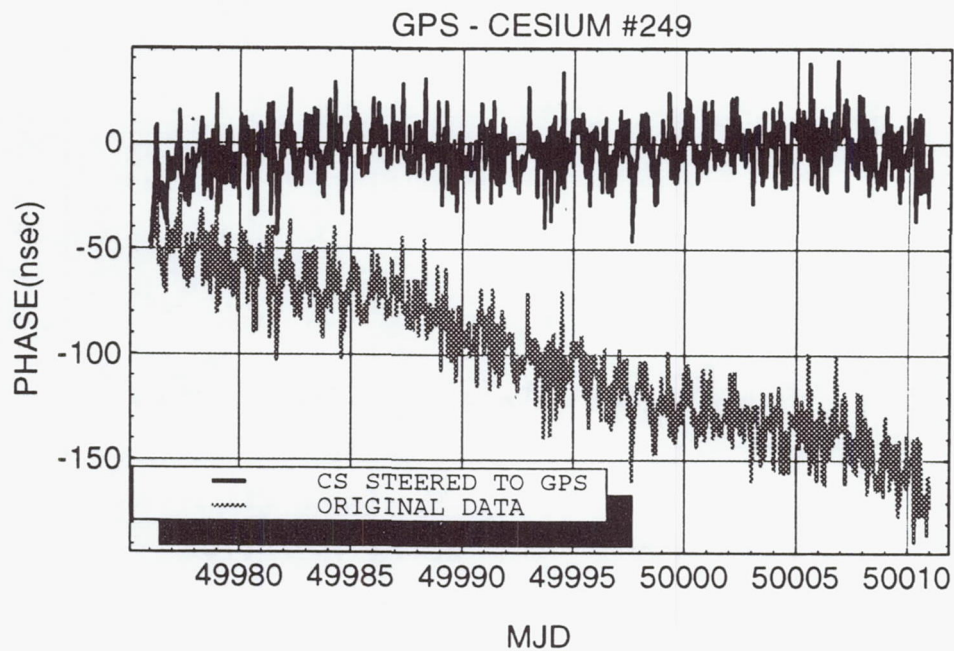


Figure 6



# TWO-SAMPLE ALLAN DEVIATION Cs #249(STEERED) VS. HYDROGEN MASER(MC2)

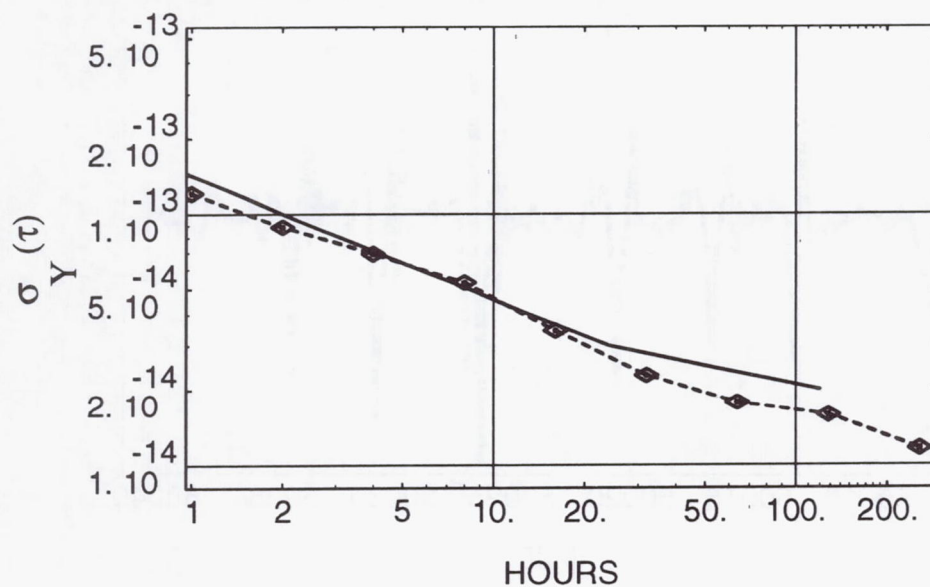


Figure 7

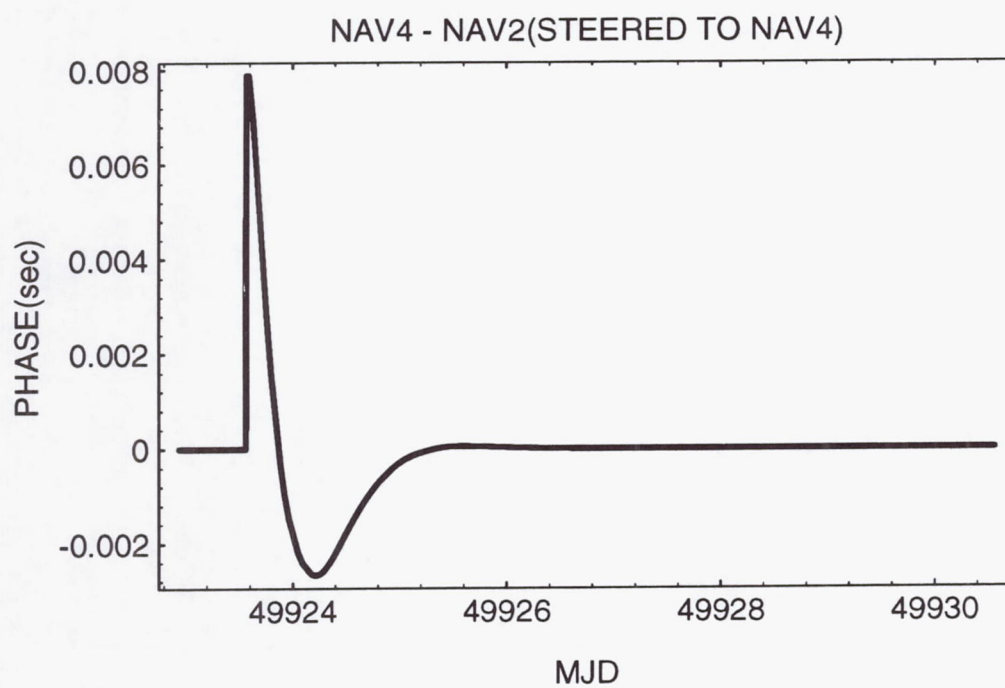


Figure 8

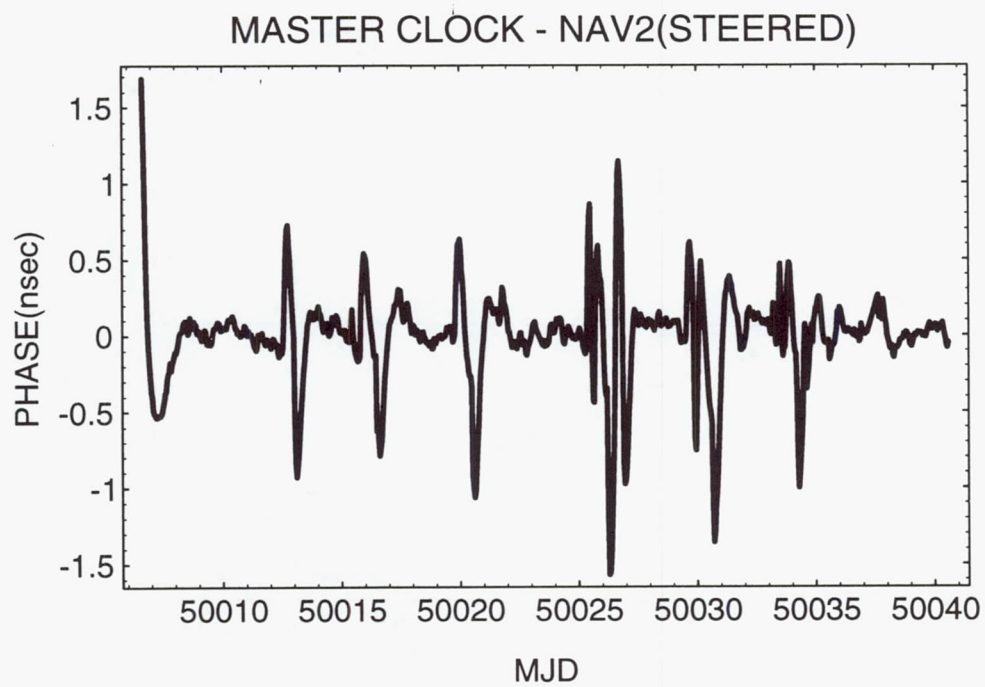


Figure 9



## Questions and Answers

**ALBERT KIRK (JPL):** I have actually three questions. The first one, what are the temperature variations in your laboratory?

**PAUL KOPPANG (USNO):** They were approximately five to six degrees C.

**ALBERT KIRK (JPL):** I see. The second question is: What is the smallest step you can use on your synthesizer to correct the frequency?

**PAUL KOPPANG (USNO):**  $10^{-19}$

**ALBERT KIRK (JPL):** The final question is: How do you determine, or how does your system determine, the loop time constant for each maser in response to — you know, to steer the maser to some average that you mentioned here?

**PAUL KOPPANG (USNO):** That's done by the Kalman filtering; it would steer to a Kalman filter value.

**ALBERT KIRK (JPL):** Can you select that, then, for each particular maser, depending on its characteristics?

**PAUL KOPPANG (USNO):** Yes.

# KALMAN FILTERING USNO's GPS OBSERVATIONS FOR IMPROVED TIME TRANSFER PREDICTIONS

Capt Steven T. Hutsell, USAF  
2d Space Operations Squadron  
300 O'Malley Avenue Suite 41  
Falcon AFB CO 80912-3041

## Abstract

*The GPS Master Control Station (MCS) performs the UTC time transfer mission by uploading and broadcasting predictions of the GPS-UTC offset in subframe 4 of the GPS navigation message. These predictions are based on only two successive daily data points obtained from USNO. USNO produces these daily smoothed data points by performing a least-squares fit on roughly 38 hours worth of data from roughly 160 successive 13-minute tracks of GPS satellites. Though sufficient for helping to maintain a time transfer error specification of 28 ns (1 Sigma), the MCS's prediction algorithm does not make the best use of the available data from USNO, and produces data that can degrade quickly over extended prediction spans.*

*This paper investigates how, by applying Kalman Filtering to the same available tracking data, the MCS could improve its estimate of GPS-UTC, and in particular, the GPS-UTC  $A_1$  term. By refining the  $A_1$  (frequency) estimate for GPS-UTC predictions, error in GPS time transfer could drop significantly. Additionally, the risk of future spikes in GPS's time transfer error could similarly be minimized, by employing robust Kalman Filtering for GPS-UTC predictions.*

## INTRODUCTION

The UTC time transfer mission of GPS depends on daily connectivity with the official Department of Defense (DoD) agency for PTTI, the United States Naval Observatory (USNO) [4]. Currently, the GPS Master Control Station (MCS) downloads a daily file from USNO (called FALCON), containing smoothed GPS tracking data, estimates of GPS-UTC, and time transfer performance metrics. Every morning, the on-duty operations crew at the MCS enters the daily estimate of the GPS-UTC phase offset (called the daily UTCBIAS value), based on USNO's least-squares fit of approximately 38-hours worth of the smoothed GPS tracking data. This tracking data consists of a series of measurements, each smoothed over a 13-minute tracking interval.

Current MCS software calculates the GPS-UTC frequency (slope) based on a linear fit of only two successive daily GPS-UTC phase (bias) values. Calculating a slope based on only two data points assumes that GPS-UTC predictions are optimal when using only a 24 hour span of data points. Intuitively, since most of the frequency standards within the GPS reference time scale (the GPS Composite Clock [1]) are Cesium clocks, the ensemble time should theoretically behave as a paper clock with noise characteristics roughly proportional to, and a fraction of, that of a single Cesium clock. Since white FM is the predominant noise type for  $\tau \leq$  several days on most GPS Cesium clocks, intuitively, white FM should dominate for GPS time itself. Hence, a GPS-UTC slope calculated from a data span of only 24 hours contradicts these intuitions.



This paper presents the results of testing an off-line computer program that a) estimates GPS-UTC using a Kalman Filter optimized for the empirical noise characteristics of GPS time, and b) applies this Filter onto the same smoothed data currently used for calculating the least-squares fit estimate of the GPS-UTC phase offset.

## A GPS-UTC KALMAN FILTER

The following is a description of a PC-based computer program written in Quick Basic, designed for applying Kalman Filtering to USNO's smoothed 13-minute measurements. The program is similar in design to the MCS's miniature Kalman Filter designed to estimate the states of the backup vs. operational frequency standards at the GPS monitor stations (MSs). This GPS-UTC Filter reads successive text files that the MCS downloads daily from USNO, and calculates a smoothed estimate of the GPS-UTC phase and frequency, via a modified two-state Kalman Filter.

### Equations

The GPS-UTC Kalman Filter employs the following equations, similar to those of many small Kalman Filters [5]:

Notes:  $\hat{\phantom{x}}$  = *Aposteriori*  
 $\tilde{\phantom{x}}$  = *Apriori*  
 $t$  = *Kalman Time*  
 $\tau$  = *Time update prediction span*

(1) State Vector:

$$X(t) = \begin{bmatrix} x_1(t) \\ x_2(t) \\ x_3(t) \end{bmatrix}$$

$x_1(t)$  is the bias (phase) estimate (s)

$x_2(t)$  is the drift (frequency) estimate (s/s)

$x_3(t)$  is slaved to the time steering drift rate (s/s<sup>2</sup>), currently  $\pm 1.0 \text{ E-}19 \text{ s/s}^2$

(2) State Covariance Matrix:

$$P(t) = \begin{bmatrix} p_{11}(t) & p_{12}(t) & 0 \\ p_{21}(t) & p_{22}(t) & 0 \\ 0 & 0 & 0 \end{bmatrix}$$

Units:  $p_{11}(t)$   $s^2$   
 $p_{12}(t), p_{21}(t)$   $s^2/s$   
 $p_{22}(t)$   $s^2/s^2$

(3) Process noise values:

$$Q = \begin{bmatrix} q_1 \\ q_2 \\ q_3 \end{bmatrix}$$

$q_1 =$  The bias (phase)  $q$  (set to  $1.11 \text{ E-}23 \text{ s}^2/\text{s}$ )

$q_2 =$  The drift (frequency)  $q$  (set to  $2.22 \text{ E-}33 \text{ s}^2/\text{s}^3$ )

$q_3 = 0$

(4) Noise addition matrix:

$$N(\tau) = \begin{bmatrix} q_1\tau + q_2(\tau^3/3) & q_2(\tau^2/2) & 0 \\ q_2(\tau^2/2) & q_2\tau & 0 \\ 0 & 0 & 0 \end{bmatrix}$$

(5) The measurement:

$$Z = \begin{bmatrix} z \\ ns \end{bmatrix} (ns)$$

(6) The measurement transformation

$$Z = \begin{bmatrix} z \\ ns \end{bmatrix} \cdot [1.0\text{E-}9] (s)$$

(7) Measurement noise:

$$R = [r] \text{ (set to } 3.6 \text{ E-}16 \text{ s}^2\text{)}$$

(8) Transition matrix:

$$\Phi(\tau) = \begin{bmatrix} 1 & \tau & \frac{1}{2}\tau^2 \\ 0 & 1 & \tau \\ 0 & 0 & 1 \end{bmatrix}$$

(9) Identity matrix:

$$I = \begin{bmatrix} 1 & 0 & 0 \\ 0 & 1 & 0 \\ 0 & 0 & 1 \end{bmatrix}$$



(10) Unity vector:

$$H = [1 \ 0 \ 0]$$

(11) The Time Update:

$$\tilde{X}(t_k) = \Phi(\tau) \cdot \hat{X}(t_{k-1})$$

$$\tilde{P}(t_k) = \Phi(\tau) \cdot \hat{P}(t_{k-1}) \cdot \Phi^T(\tau) + N(\tau)$$

(12) The Kalman Gain equation:

$$K(t_k) = \tilde{P}(t_k) \cdot H^T \cdot \left( H \cdot \tilde{P}(t_k) \cdot H^T + R \right)^{-1}$$

(13) Measurement Acceptance:

$$\left( Z(t_k) - H \cdot \tilde{X}(t_k) \right) < Tolerance$$

(14) The Measurement Update:

$$\hat{X}(t_k) = \tilde{X}(t_k) + K(t_k) \cdot \left( Z(t_k) - H \cdot \tilde{X}(t_k) \right)$$

$$\hat{P}(t_k) = \left( I - K(t_k) \cdot H \right) \cdot \tilde{P}(t_k)$$

## Data Base Values

The GPS-UTC Kalman Filter uses several important data base values:

(a) The process noise values,  $q_1 = 1.11 \text{ E-}23 \text{ s}^2/\text{s}$ , and  $q_2 = 2.22 \text{ E-}33 \text{ s}^2/\text{s}^3$ , are based on the stability performance of GPS-UTC, as visualized in figure 1, and the following equation [1]:

$$\sigma_y^2(\tau) = (q_1)/\tau + (q_2)\tau/3$$

(b) The measurement noise value,  $R = 3.6 \text{ E-}16 \text{ s}^2$ , is based on a User Range Accuracy (URA) index of 3, equivalent to 5.67 meters, or  $\sim 18.9 \text{ ns}$ .  $(18.9 \text{ ns})^2 \cong 3.6 \text{ E-}16 \text{ s}^2$ .

(c) The rejection tolerance,  $4.0 \text{ E-}08 \text{ s}$ , is based on a maximum estimated range deviation (ERD) of 12 meters.

- (d) The MCS currently steers GPS time at a maximum value of  $1.0 \text{ E-19 s/s}^2$  [3].

## Filter Processing

The following is a synopsis of the functionality of the GPS-UTC Filter program. The program:

- (a) Inputs values from PC data base files.
- (b) Initializes the Filter using the most recent state estimates, which reside in the PC state files.
- (c) Inputs the daily USNO file, or if requested, an archived USNO file. If the operator requests an archived file, he/she may enter successive files during the same execution of the GPS-UTC Filter program.
- (d) Cycles through the following steps (for each measurement):
  - Reads columns 2 and 4, from the DFR24 subfile of USNO's FALCON file. (These are the time tag and the corresponding single-satellite GPS-UTC estimate, respectively).
  - Accounts for the current time steering sign and magnitude.
  - Performs a time update of the current phase and frequency estimates.
  - Performs a residual check on the measurement. If the measurement is rejected, the program reads the next measurement, and continues.
  - Performs a measurement update if the measurement is accepted.
  - Displays the current state estimates and variances on the PC screen.

As a side note, if GPS-UTC experiences a substantial excursion in bias and/or drift, due to, for instance, an undetected single clock frequency jump, the GPS-UTC Kalman Filter may be manually re-initialized, by re-setting the covariance matrix elements to default values (below) and by restarting the Filter:

$$P_I(t) = \begin{bmatrix} 1.0 \text{ E-15 s}^2 & 0 & 0 \\ 0 & 1.0 \text{ E-25 s}^2 & 0 \\ 0 & 0 & 0 \end{bmatrix}$$

## TESTING THE FILTER

The author processed the GPS-UTC Kalman Filter against two months' worth of daily USNO files. The author chose this period primarily because of the relatively erratic performance of GPS time, caused, in part, by a frequency jump at the Colorado Springs monitor station, at  $\sim 0200z$ , 21 Dec 94 [2].



## Test Plan

As stated earlier, the Kalman Filter produces daily estimates of GPS-UTC phase and frequency. The test compared the current linear model's 24-hour prediction error against that of the Kalman Filter. The test:

- (a) Produced daily Kalman Filter estimates of the GPS-UTC phase and frequency:  $X_{\text{posteriori}}(t)$ .
- (b) Propagated the daily Filtered estimates 24 hours in the future:  $X_{\text{priori}}(t + 1\text{Day})$ .
- (c) Compared the predicted estimates against the next day's Filtered estimates:

$$\text{Filter Error} = X_{\text{priori}}(t + 1\text{Day}) - X_{\text{posteriori}}(t + 1\text{Day})$$

- (d) Compared the Filter error to the daily operational average time transfer error.

The test included a re-initialization of the Kalman Filter on 22 Dec 94, to compensate for the known GPS-UTC frequency excursion.

## Test Results

Figure 2 compares the GPS-UTC phase estimate produced by the least-squares fit, to that produced by the Kalman Filter. The test indicated only a *small* improvement in GPS-UTC prediction. Figure 3 shows a plot of the actual GPS time transfer average error (using the current linear model) for 1 Dec 94 - 31 Jan 95, and the simulated systematic (average) time transfer error (based on the Kalman Filter) for the same period.

The linear model's RMS of daily average error was 4.81 ns, and its overall average was -2.13 ns. By comparison, the Kalman Filter model's RMS of average error was 4.04 ns, and its overall average was 0.22 ns.

## Test Findings

No test can completely simulate reality, and hence, the test results may paint a picture nicer than reality.

(a) The Kalman Filter allows the operator to generate GPS-UTC predictions based on optimal estimation, with data base values tailored towards the true (empirical) noise characteristics of GPS time. This optimal estimation could theoretically produce a small reduction in time transfer error.

(b) The theoretical reduction in time transfer error may not be significant enough to justify the extra operational burden at the MCS, at the present time. The computer setup that the MCS currently employs to download daily GPS-UTC information already has some operational problems, including numerous communication drop-outs, and occasional errors caused by the manual processing of data. The extra hassle imposed on operations crews, caused by new, intricate software, may very well *degrade* GPS-UTC predictions, if the number of operator-related errors were to increase. The undetected corruption of one PC file could theoretically prove disastrous for time transfer.

(c) The GPS-UTC Kalman Filter was unable to detect (and hence, reconcile) the -22 ns/day jump in GPS time that occurred on 21 Dec 94. The above test results were based on the assumption that the operator would detect and manually re-initialize the Filter to compensate for the frequency step. If the

operator couldn't have detected the jump, the Filtered GPS-UTC prediction, based on a theoretical frequency predictability longer than 24 hours, could have been unacceptably late in converging on a new frequency estimate, and hence, could have degraded time transfer performance.

## CONCLUSION

This test of the PC-based GPS-UTC Kalman Filter produces several recommendations:

(a) For the time being, continue with the current operational approach for GPS-UTC prediction.

(b) Pursue a study on a more refined Kalman Filter. This PC-based filter processed *raw* measurements, based on the broadcasted navigation message of 25 GPS satellites. Since the MCS typically updates the navigation message only once every 24 hours, these GPS measurements can, and will, have up to 40 ns of noise. This high measurement error causes the Filter to produce very coarse estimates of GPS-UTC, which are only predictable to about 4-5 ns over one day.

(c) Incorporate the USNO Download into MCS mainframe architecture. By introducing solid configuration management into the data connectivity between USNO and the MCS, the MCS could a) receive more timely measurements from USNO, for improved accuracy and integrity monitoring, b) refine these USNO measurements by subtracting known observables (ERDs), and c) employ a more reliable setup for the MCS to perform its critical role in GPS's time transfer mission.

## ACKNOWLEDGMENTS

The author wishes to thank the following people and agencies for their generous assistance with this paper:

Loral Federal Systems Division  
The people of the 2 SOPS  
Francine Vannicola, USNO

## REFERENCES

- [1] Brown, Kenneth R., *The Theory of the GPS Composite Clock*, Proceedings of ION GPS-91, 11-13 Sep 91
- [2] Brown, Kenneth R., Chien, Ming Kang, Mathon, William S., Hutsell, Steven T., Capt, USAF, and Shank, Christopher M., Capt, USAF, *L-Band Anomaly Detection in GPS*, Proceedings of ION's 51st Annual Meeting, 5-7 Jun 95
- [3] Hutsell, Steven T., Capt, USAF, *Recent MCS Improvements to GPS Timing*, Proceedings of ION GPS-94, 20-23 Sep 94
- [4] ICD-GPS-202, 21 Nov 84
- [5] Maybeck, Peter S., *Stochastic Models, Estimation and Control*, 1979



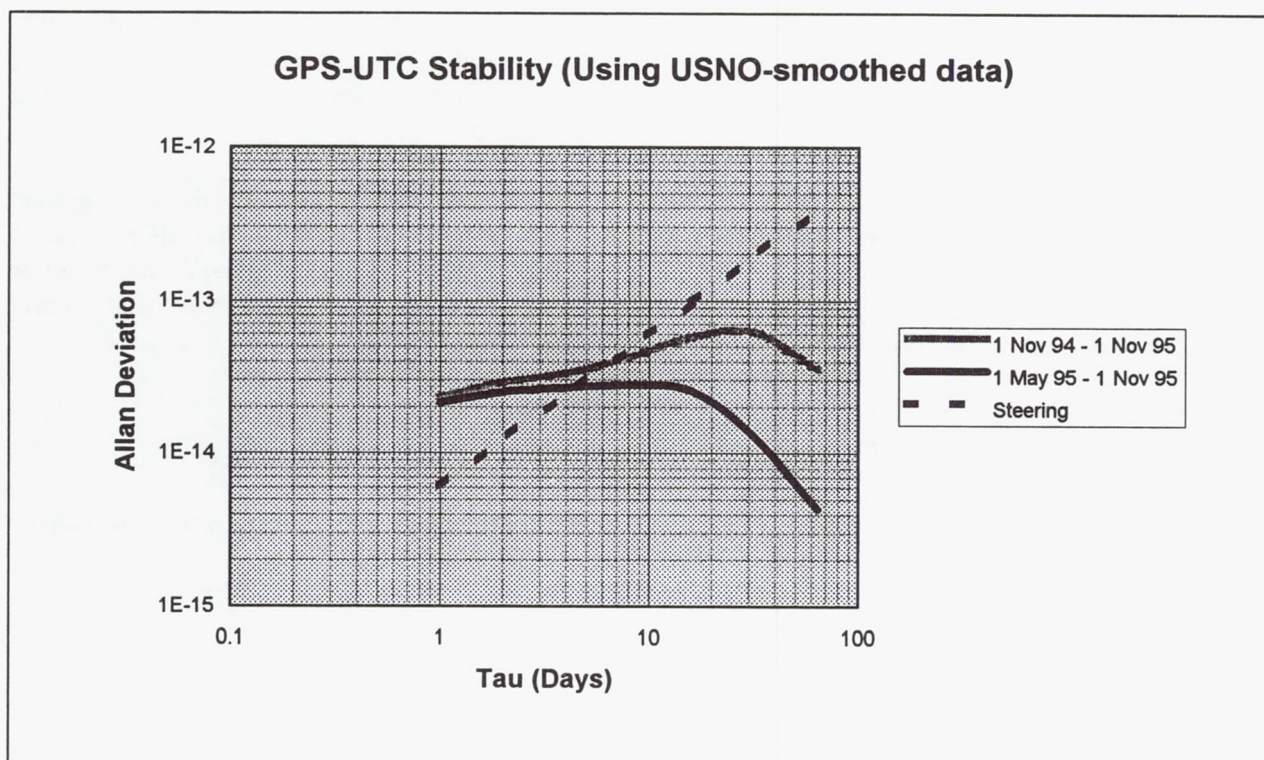


**Figure 1**

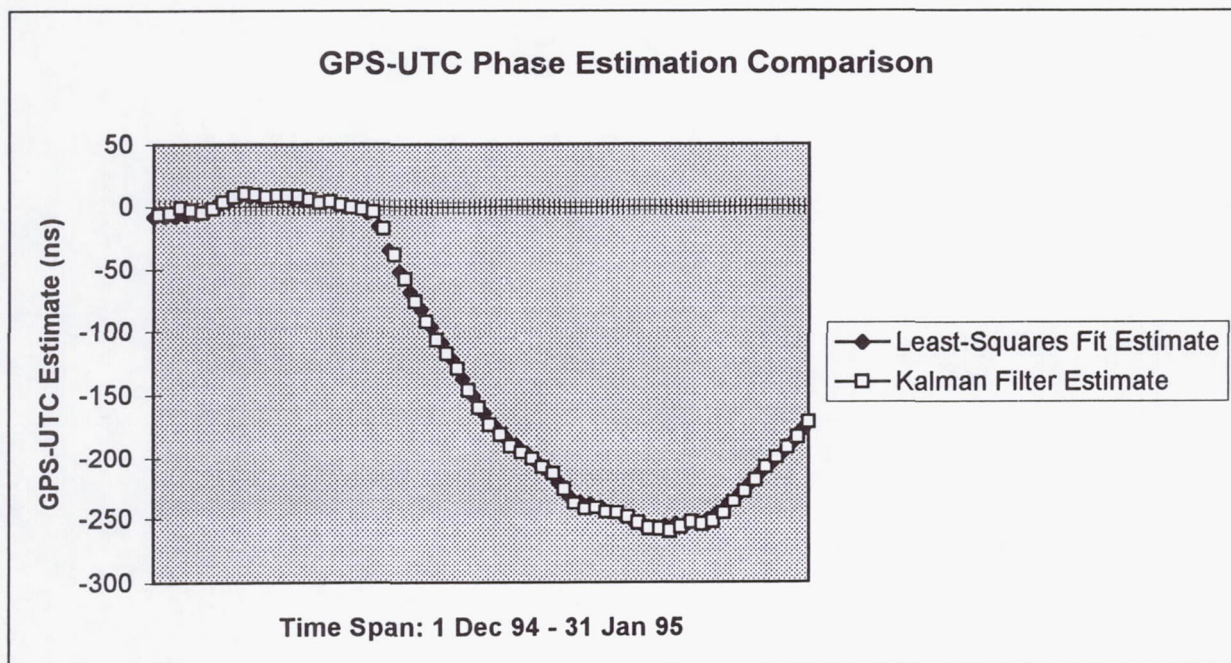


Figure 2

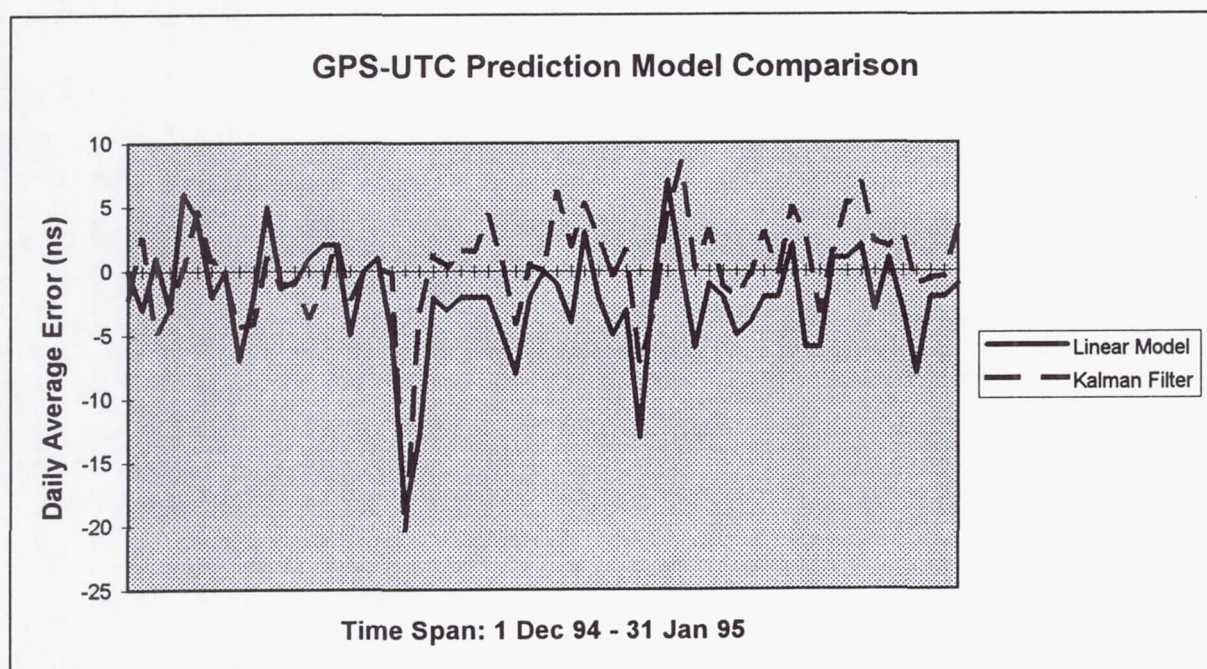


Figure 3



# SIMULATION STUDY USING A NEW TYPE OF SAMPLE VARIANCE\*

D.A. Howe and K.J. Lainson  
Time and Frequency Division  
National Institute of Standards and Technology  
Boulder, CO 80303

## Abstract

*We evaluate with simulated data a new type of sample variance for the characterization of frequency stability. The new statistic (referred to as TOTALVAR and its square root TOTALDEV) is a better predictor of long-term frequency variations than the present sample Allan deviation. The statistical model uses the assumption that a time series of phase or frequency differences is wrapped (periodic) with overall frequency difference removed. We find that the variability at long averaging times is reduced considerably for the five models of power-law noise commonly encountered with frequency standards and oscillators.*

## INTRODUCTION

The most common method of quantifying frequency stability between oscillators is to evaluate the RMS of the fractional frequency changes vs. averaging time  $\tau$ , dubbed the Allan deviation<sup>[1]</sup>. For any sequence of average fractional frequency deviations  $\{\bar{y}_t\}$ , the widely used quantity  $\hat{\sigma}_y(\tau)$  is ideally suited as a reliable, easily interpretable statistic for the characterization of frequency stability for common kinds of FM oscillator noise<sup>[2, 3]</sup>.

There is a considerable literature on various methods and candidate statistics for the characterization of relative oscillator frequency stability. Suffice it to say that for a given system and noise, a statistic can be constructed to be nearly optimum. A single, unified approach will have its compromises. The Allan deviation, however, has a remarkable range of applicability in quantifying frequency and phase stability. This is because as a function of averaging time  $\tau$ , it is particularly well-suited in identifying the model of the *trend* in frequency stability or what is called the underlying "power-law" over a range of  $\tau$  values. The power-law is the slope on a typical log-log  $\sigma_y(\tau)$  plot, and  $\sigma_y(\tau)$  is suitably the RMS prediction error of frequency stability. Predicting the long-term stability of a frequency reference rests ultimately on predicting (correctly identifying) its power-law behavior. For an estimate of stability longer or different than the measurement at hand, simply extrapolate from or directly apply an expected

---

\*Contribution of the U.S. Government, not subject to copyright.

trend (power-law slope). Lastly, we can estimate the evolution of a squared phase error as proportional to  $\tau^2$  times the modified Allan variance for a uniquely identified power-law slope. This is the time variance or TVAR<sup>[4]</sup>.

A long-standing problem is that the best statistic, the two-sample Allan deviation, has rather poor confidence at longer and longer  $\tau$ -values, where confidence is often needed most. A new statistic has been developed which retains the intuitive simplicity of the RMS fractional frequency changes (Allan deviation) and which has improved confidence at long-term averaging times<sup>[5]</sup>. The model for the new statistic uses the assumption that a time series of phase or frequency differences is wrapped (periodic) with overall frequency difference removed<sup>[6]</sup>. Figure 1 illustrates the procedure. This variance (thus its square root) reduces estimation errors universally seen in previous treatments, thereby providing a better estimate of frequency stability for measurement times longer than say 20% of the data length.

We compare the response of the new statistic (as a variance) to the traditional Allan variance by simulation of the five models of power-law noises commonly encountered with oscillators and frequency standards. Results show that the new variance shows a promise for greatly reduced variability hence uncertainty compared to the traditional Allan variance.

## DISCUSSION

The sample Allan deviation  $\hat{\sigma}_{\bar{y}}(\tau)$  and  $\text{mod}\hat{\sigma}_{\bar{y}}(\tau)$  are square roots of two types of tau-domain sample variances (AVAR and MVAR)<sup>[1, 7]</sup>. They are recommended statistics in quantifying frequency stability between oscillators. In certain situations their responses have high variability at long averaging times  $\tau$ , as indicated by traditional simulation studies using common noise types, because the traditional sample Allan statistics are time-shift dependent. Therefore these statistics have degraded confidence at long averaging times. The method of complex demodulation motivates another statistic which is an improved sample variance for the characterization of frequency stability<sup>[5]</sup>. For average fractional frequency fluctuations  $\{\bar{y}_{k'}\} = \bar{y}_1, \dots, \bar{y}_{N-1}$  with overall frequency difference removed, this sample variance is given by:

$$\hat{\sigma}_{total}^2(\tau) = \frac{1}{N-1} \sum_j^{N-1} \left[ \frac{1}{2(M-1)} \sum_{k=1}^{M-1} (\bar{y}_{k+1,j} - \bar{y}_{k,j})^2 \right], \quad (1)$$

where  $\{\bar{y}_{k',j}\} = \bar{y}_{j+1}, \bar{y}_{j+2}, \dots, \bar{y}_{N-1}, \bar{y}_1, \bar{y}_2, \dots, \bar{y}_j$  are spaced by  $\tau_0$  and  $\{\bar{y}_{k'}\}$  is therefore wrapped and re-indexed by  $j$ . Series  $\{\bar{y}_{k,j}\}$  – with unprimed  $k$  – are averages implied over  $\tau = m\tau_0$ . Hence, as with traditional AVAR (and MVAR), the new sample variance  $\hat{\sigma}_{total}^2$  is implicitly dependent on dimensionless quantity  $m$ , a scale parameter which determines  $\tau$  and which for efficiency can be limited to rational powers of 2, that is,  $2^i = m$ ,  $i = 0, 1, 2, 3, \dots$ .

Measurements of relative phase differences  $\{x_{k'}\}$  are preferred to average frequency  $\{\bar{y}_{k'}\}$  as in Equation (1). We have  $k' = 1, 2, 3, \dots, N$  and separated by interval  $\tau_0$  and overall frequency difference removed; therefore  $x_1 = x_N$ . Furthermore  $\{x_{k'}\}$  is wrapped and assumed periodic; hence  $x_1 = x_{N+1}$  and we eliminate the increment  $x_N$  to  $x_{N+1}$  to avoid bias (see Figure 1). We have



$$\hat{\sigma}_{total}^2(m\tau_0) = \frac{1}{N-1} \sum_j^{N-1} \left[ \frac{1}{2m^2\tau_0^2(M-2m)} \sum_{k'=1}^{M-2m} (-x_{(k'-m)-j} + 2x_{(k')-j} - x_{(k'+m)-j})^2 \right], \quad (2)$$

where the argument in the brackets "[\*]" has stride  $k' - m$  and is time-shifted by  $j\tau_0$  and averaged for all  $N - 1$  possible shifts. This notation centers the second-difference operation (argument in parenthesis) at  $k'$  with a span of  $\pm m$  which seems more intuitive especially considering the wrap procedure.

## STATISTICS COMPARED

The primary reasons for using  $\hat{\sigma}_y(\tau)$  are that it is well-known, it is simple to calculate, it is the most efficient estimator for FM noise, and it has a unique value for all  $\tau$ . The primary disadvantage of using  $\hat{\sigma}_y(\tau)$  is that the results can be too conservative, sometimes very optimistic at the long  $\tau$ -values. It can take much longer than the longest reportable  $\tau$ -values (often orders of magnitude longer) to accurately quantify the underlying low-frequency variations between the frequency standards being evaluated<sup>[3]</sup>. For example, quantifying the frequency stability at, say,  $\tau$  equals two weeks often requires no less than two months of actual measurement time.

We compare the new sample variance  $\hat{\sigma}_{total}^2(\tau)$  (also called TOTALVAR) to traditional AVAR  $\hat{\sigma}_y^2(\tau)$  using simulation studies of five common integer power-law noise types. These noise types are white PM, flicker PM, white FM, flicker FM, and random walk FM. A version of  $\hat{\sigma}_{total}^2(\tau)$  called  $\text{mod}\hat{\sigma}_{total}^2(\tau)$  exists for MVAR; however since our present emphasis is on confidence at long  $\tau$ -values, AVAR is of interest. MVAR's advantage is in distinguishing white PM from flicker PM which usually are associated with short  $\tau$ -values. MVAR has no advantage for flicker PM and beyond, which occur at long  $\tau$ -values. Furthermore, a chief disadvantage to MVAR is that it only extends to 1/3 the total data length, whereas AVAR extends to 1/2 the same length.

For highly divergent noise types, the new statistic is not expected to be unbiased<sup>[8, 9]</sup>. However, this report indicates that the new statistic essentially estimates the same unbiased quantity as traditional AVAR for the five common integer power-law noise types but has better confidence than AVAR.

## GENERATION OF SIMULATED $\{x'_k\}$ DATA

Most high level computer program languages can return random variables which we then order as a time series  $\{a_n\}$ . The usual assumption is that variables are uncorrelated and normally (Gaussian) or uniformly distributed. Thus  $\{a_n\}$  forms the basis for a white-noise-of-phase process which is characterized by a constant power spectral density,  $S_a(f) \propto f_0$ . We build from  $\{a_n\}$  the other four noise processes: flicker ( $\propto f^{-1}$ ), random walk ( $\propto f^{-2}$ ), flicker walk ( $\propto f^{-3}$ ), and random run ( $\propto f^{-4}$ ). The treatment of non-integer power law noise types has recently been explored<sup>[10]</sup>. We limit our simulations to the five common integer power laws.

Random walk of phase (RWPM) is equivalent to white noise of frequency (WHFM) and is one integration (single summation) of  $\{a_n\}$ . Random run of phase (RRPM) is random walk

in frequency (RWFM) and is two integrations (double summation) of  $\{a_n\}$ . These operations are among the simplest autoregressive (AR) procedures.

Flicker processes can be generated using an AR operation but must also include an (integrated) moving average (MA). The ARIMA model used in generating the five integer noise processes is adequately described by

$$x_n = \phi_1 x_{n-1} + \phi_2 x_{n-2} + a_n - \theta a_{n-1} , \quad (3)$$

where  $a_n$  is an input random variable and  $x_n$  is an output.

For flicker of phase (FLPM):

$$\begin{aligned} \phi_1 &= 1.549, \\ \phi_2 &= 0.56, \\ \theta &= 0.88 \end{aligned}$$

Flicker walk of phase is flicker of frequency (FLFM) and is one integration (single summation) of an FLPM series.

As mentioned, random run of phase (or random walk FM, RWFM) could be adequately realized as only a double summation of  $a_n$  which means  $\phi_1 = 2$  and  $\phi_2 = -1$ , and  $\theta = 0$  in Equation (3). Cleaner representations of RWFM are realized for  $\theta = \sqrt{3} - 2$ [11]. Thus we use:

$$\begin{aligned} \phi_1 &= 2, \\ \phi_2 &= -1 \\ \theta &= \sqrt{3} - 2 = -0.268 \end{aligned}$$

For the simulations here, some thought went into initializing each sequence to obtain a representation for the flicker and random run noise types.  $a_1$  was chosen to be between 0 and 1;  $x_{n-1}$ ,  $x_{n-2}$ , and  $a_{n-1}$  were derived from the end of previous simulations.

In each of the noise types, the top of Figures 2 to 6 show plots of 100 calculations of  $\hat{\sigma}_{total}(\tau)$  followed below by plots of 100 calculations of  $\hat{\sigma}_y(\tau)$  from the same 100 simulations. At the bottom of each figure is a plot of the square root of the mean of  $\hat{\sigma}_y^2(\tau)$  derived from the 100 simulations in order to see its agreement or disagreement with theory, that is, the theoretical square root of a mean of an infinite set. Flicker of phase (FLPM) is the only type which does not have a straight-line (log-log scale) theoretical slope owing to a logarithmic dependence on bandwidth.



## WHITE PM (WHPM) AND FLICKER PM (FLPM) CASES

For short  $\tau$ -values, we usually find noise modulation of the phase (not frequency) originating from noisy electronics not involved in the frequency-determining elements. White PM (WHPM) noise is broadband phase noise and has little to do with the resonance mechanism. Stages of amplification are usually responsible for white PM noise. This noise can be kept very low with good amplifier design, hand-selected components, the addition of narrowband filtering at the output, or increasing, if feasible, the power of the primary frequency source.

Flicker PM (FLPM) noise may relate to a physical resonance mechanism in an oscillator, but it usually is added by noisy electronics. This type of noise is common, even in the highest quality oscillators, because in order to bring the signal amplitude up to a usable level, amplifiers are used after the signal source. Flicker PM noise may be introduced in these stages. It may also be introduced in a frequency multiplier or frequency synthesizer.

Figures 2(a) and 3(a) show 100 plots of calculations of the square root of  $\hat{\sigma}_{total}^2(\tau)$  for 100 simulations of white PM noise and flicker PM respectively. Equation (2) is used for these calculations and  $N=1024$  for each simulation. Each of the simulation averages of two-sample variances at  $\tau = 1$  is equal to one. Figures 2(b) and 3(b) are traditional square root of maximally overlapped  $\hat{\sigma}_y(\tau)$  for the same 100 simulations. The bottom plot is the 100-simulation-total square-root of the mean of the sample Allan variances and shows excellent agreement with theory. The spread in the estimates is greater using AVAR instead of the new statistic  $\hat{\sigma}_{total}^2(\tau)$ .

White and flicker of PM both exhibit a  $\tau^{-1}$  slope in  $\sigma_y(\tau)$  and hence  $\hat{\sigma}_{total}(\tau)$ . These noise types differ from the others in an important regard: their amplitudes are significantly affected by measurement (software and/or hardware) bandwidth [3, Introduction]. Because of this,  $\text{mod}\hat{\sigma}^2(\tau)$  or modified Allan variance (MVAR) was invented (for analyzing phase data only,  $\{x_{k'}\}$ ) to take full advantage of the  $1/n\tau_0$  slope in the standard variance of  $\{x_{k'}\}$  for white PM and  $\frac{1}{\ln(n\tau_0)}$  slope for flicker PM. As mentioned earlier, we limit our present discussion to a comparison between  $\sigma_y^2(\tau)$  and  $\hat{\sigma}_{total}^2(\tau)$ . This is because the present interest is an improved confidence at long  $\tau$ -values where more dispersive noise types are encountered and ultimately limit accurate characterization of frequency stability. Again a significant disadvantage to MVAR is that a single longest reportable  $\tau$ -value is limited to  $1/3$  the total measurement time; 50% more time is required for equivalent results using MVAR vs. AVAR. It suffices to say, however, that for white PM and flicker PM, the improvement in confidence in the long term is dramatic using the new statistic  $\hat{\sigma}_{total}^2(\tau)$  as shown in Figures 2 and 3.

## 6. WHITE FM (WHFM) CASE

The cases of white FM, flicker FM, and random walk FM are of particular importance since they are physically traceable noise types encountered in virtually all precision frequency standards, and they often occur at long  $\tau$ -values.

White FM noise ( $\sigma_y(\tau) \propto \tau^{-1/2}$ ) is the type found in common passive-resonator frequency standards. These contain a slave oscillator, often quartz, which is locked to a resonance feature of another device which behaves as a high-Q filter. High quality cesium, rubidium,



and passive hydrogen standards have white FM noise characteristics<sup>[12]</sup>. Howe has previously presented results using white FM simulation that show that the new statistic TOTALVAR is an improved estimate of the mean-square frequency deviations between oscillators, particularly at long  $\tau$ -values<sup>[5]</sup>. Figure 4 reproduces those results for the comparison here.

## 7. FLICKER FM (FLFM) CASE

Flicker FM ( $\sigma_y(\tau) \propto \tau^0$ ) is a noise whose physical cause is not fully understood but may typically be related to the physical resonance mechanism of an active oscillator, the design or choice of parts used for the electronics, or environmental conditions<sup>[12]</sup>. Flicker FM noise is considered the quantum limit of resonance devices<sup>[13]</sup>. Flicker FM is common in the highest quality oscillators but may be masked by white FM or even white PM and flicker PM in lower quality oscillators.

Figure 5(a) shows 100 plots of calculations of  $\hat{\sigma}_{total}(\tau)$  for 100 simulations of flicker FM noise and Figure 5(b) is the same set of calculations using traditional square-root of maximally overlapped AVAR. The square root of the mean of the AVAR's of the 100 simulations as shown in Figure 5(c) show a slight downward offset which can commonly occur at  $\tau = 512\tau_0 = T/2$ . Even though the power law is not exact, it is sufficient for the comparison of the spread in the responses between  $\hat{\sigma}_{total}(\tau)$  and traditional  $\hat{\sigma}_y(\tau)$ . Again, the new statistic is preferred since it is generally less susceptible to large variations at long  $\tau$ -values.

## RANDOM WALK FM (RWFM) CASE

Of the five models of power-law noise types, random walk FM noise ( $\sigma_y(\tau) \propto \tau^{1/2}$ ) is most difficult to measure since its power is concentrated mainly very close to the carrier. This translates to near DC when considering phase differences  $\{x_k\}$  or average frequency differences  $\{\bar{y}_k\}$ . Random walk FM usually relates to an oscillator's physical environment. If random walk FM is a predominant noise type then mechanical shock, vibration, humidity, temperature, or other environmental effects may be causing "random" shifts in the carrier frequency<sup>[14, 15]</sup>.

Figure 6(a) and 6(b) are 100 plots of calculations of the square roots of  $\hat{\sigma}_{total}^2(\tau)$  and  $\hat{\sigma}_y(\tau)$  respectively, for 100 simulations of random walk FM noise. Again, even though the simulated power-law is assumed to be not exact as interpreted from the square root of the mean of AVAR's in Figure 6(c), the important point is the comparison of the spread between square roots of TOTALVAR and AVAR (Figures 6(a) and 6(b)). And again, the square root of TOTALVAR is preferred since the spread and skews are reduced at long  $\tau$  values.

## CONCLUSION

We compare the response of the traditional sample Allan deviation  $\hat{\sigma}_y(\tau)$  with a new similar sample statistic  $\hat{\sigma}_{total}(\tau)$  referred to as TOTALDEV (square root of TOTALVAR) for the five models of integer power-law noise types. These integer noise types are white PM, flicker PM, white FM, flicker FM, and random walk FM. Using traditional plots of sigma vs. tau and 100



simulations of each noise type, we find the variability in  $\hat{\sigma}_{total}(\tau)$  to be less than in  $\hat{\sigma}_y(\tau)$  in all cases. As a result, we can expect a reduction in the actual measurement time involved to characterize the long-term frequency stability of a standard or oscillator.

## ACKNOWLEDGEMENTS

We thank Chuck Greenhall for the origination of  $\theta = \sqrt{3} - 2$  in the ARIMA model of random walk FM and Jim Barnes for the flicker PM and FM modeling. We gratefully acknowledge the comments and help of Dave Allan and Jim Barnes in interpreting the simulation results. Finally we thank Don Percival and Francois Vernotte for useful insights into the statistical procedure incorporated in TOTALVAR.

## REFERENCES

- [1] Allan, D.W., "Statistics of Atomic Frequency Standard," Proc. IEEE, 54, 221-231, 1966.
- [2] Barnes, J.A., Chi, A.R., Cutler, L.S., Healey, D.J., Leeson, D.B., McGunigal, T.E., Mullen, J.A., Smith, W.L., Sydnor, R.L., Vessot, R.F.C., and Winkler, G.M.R., "Characterization of Frequency Stability," IEEE Tran. Instrum. Meas., IM-20, 105-120, 1971.
- [3] Sullivan, D.B., Allan, D.W., Howe, D.A., and Walls, F.L., "Characterization of Clocks and Oscillators," Natl. Inst. Stand. Technol. Technical Note 1337, 1-342, 1990.
- [4] Allan, D.W., Weiss, M.A., and Jespersen, J.L., "A Frequency-Domain View of Time-Domain Characterization of Clocks and Time and Frequency Distribution Systems," Proc. of 45th Ann. Freq. Control Symp., 1991, pp. 667-678
- [5] Howe, D.A., "An Extension of the Allan Variance with Increased Confidence at Long Term," Proc. 1995 IEEE Int. Freq. Control Symp., 95CH3446-2, 445 Hoes Lane, Piscataway, NJ, 08854, pp. 321-329.
- [6] Howe, D.A., "Circular Representation of Infinitely Extended Sequences," Proc. 1995 IEEE Int. Freq. Control Symp., 95CH3446-2, 445 Hoes Lane, Piscataway, NJ, 08854, pp. 337-345.
- [7] Allan, D.W. and Barnes, J.A., "A Modified 'Allan Variance' with Increased Oscillator Characterization Ability," Proc. of 35th Ann. Freq. Control Symp., Philadelphia, PA, May 27-29, 1981, pp. 470-475.
- [8] Fougere, P.F., "On the Accuracy of Spectrum Analysis of Red Noise Processes Using Maximum Entropy and Periodogram Methods: Simulation Studies and Application to Geophysical Data," 90, pp. 4355-4366, May 1, 1985.
- [9] Vernotte, F., private communications, 1995, with reference to Vernotte, F., Zalamansky, G., McHugh, M., and Lantz, E., "Cutoff Frequencies and Noise Power Law Model of Spectral Density: Adaptation of the Multi-Variance Method for Irregularly Spaced

*Timing Data Using the Lowest Mode Estimator Approach*," Proc. 1995 IEEE Int. Freq. Control Symp., 95CH3446-2, 445 Hoes Lane, Piscataway, NJ, 08854, pp. 330-336.

- [10] Walter, T., "Characterizing Frequency Stability: A Continuous Power-Law Model with Discrete Sampling," IEEE Trans. Instrum. Meas., Vol. 43, 69-79, 1994.
- [11] Audoin, D., Dimarcq, N., "Stochastic Models of Stable Frequency and Time Sources and their Relationship," IEEE Trans. Instrum. Meas., 42, 1993.
- [12] Howe, D.A., Allan, D.W., and Barnes, J.A., "Properties of Signal Sources and Measurement Methods," Proc. 35th Freq. Control Symp., Philadelphia, PA, May 27-29, 1981, pp. A1-A47.
- [13] Vig, J.R. and Walls, F.L., "Fundamental Limits on the Frequency Stabilities of Crystal Oscillators" IEEE Trans. Ultrason., Ferroelec., and Freq. Cont., 42, 576-589, 1995.
- [14] Gray, J.E., Machlan, H.E., and Allan, D.W., "The Effect of Humidity on Commercial Cesium Beam Atomic Clocks," Proc. of 42nd Ann. Freq. Control Symp., Baltimore, MD, June 1-4, 1988, pp. 514-518.
- [15] Walls, F.L., "The Quest to Understand and Reduce  $1/f$  Noise in Amplifiers and BAW Quartz Oscillators," Proc. 9th European Freq. and Time Forum, Besancon, France, March 8-10, 1995, pp. 227-244.



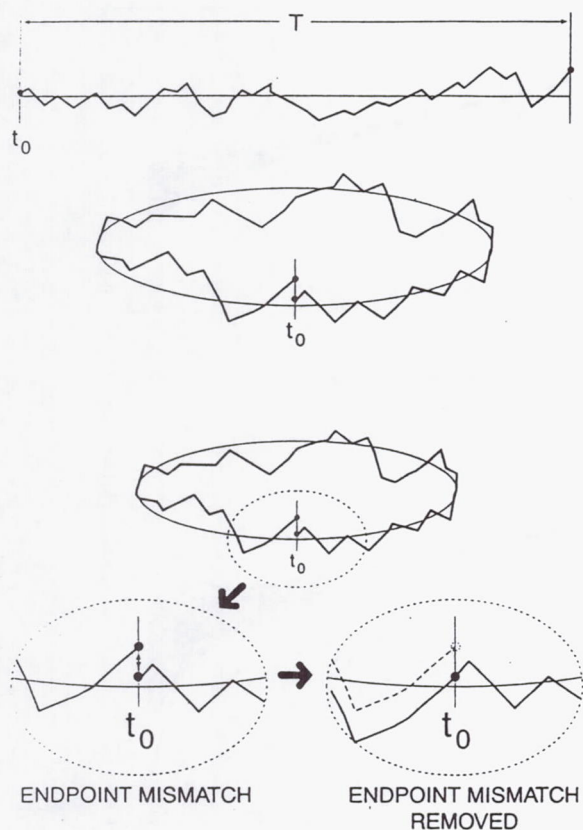


Fig. 1

The new statistic (referred to as TOTALVAR and its square root) uses the model that a time series of phase difference  $x_i$  are wrapped with period  $T$  and overall frequency difference removed. The periodic assumption means that the data are circularly represented and the time-origin is no longer  $t_0$  but is shiftable by  $j\tau_0$  where  $\tau_0$  is the minimum measurement interval. TOTALVAR is traditional AVAR averaged over  $N-1$  possible shifts. Removal of the overall frequency difference eliminates an end-match step by making  $x_1 = x_N$ , hence  $x_1 = x_{N+1}$  and we eliminate the increment  $x_N$  to  $x_{N+1}$  to avoid bias. We use

$$\hat{\sigma}_{\text{total}}^2(m\tau_0) = \frac{1}{N-1} \sum_j \left[ \frac{1}{2m^2\tau_0^2(M-2m)} \sum_{k=1}^{M-2m} (-x_{(k'-m)-j} + 2x_{(k'-j)} - x_{(k'-m)-j})^2 \right],$$

where the argument in the brackets is traditional AVAR shifted by  $j$ .

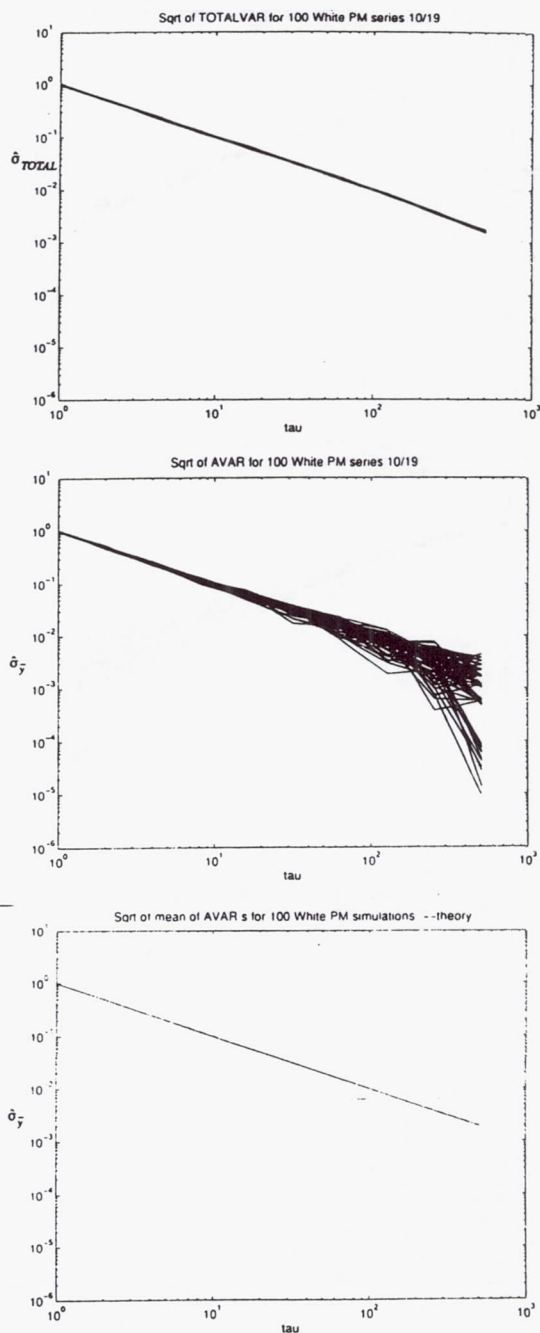


Fig. 2

Top(a): Square root of TOTALVAR calculated for 100 WHPM simulations with unit (two-sample) mean at  $\tau=1$ .

Middle(b): For comparison, traditional square root of maximally-overlapped AVAR calculated for the same 100 WHPM simulations as used at top for square root of TOTALVAR.

Bottom(c): Square root of 100-total mean of maximally-overlapped AVAR's, an indication of the desired result. Dashed line is the theoretical mean of an infinite set.

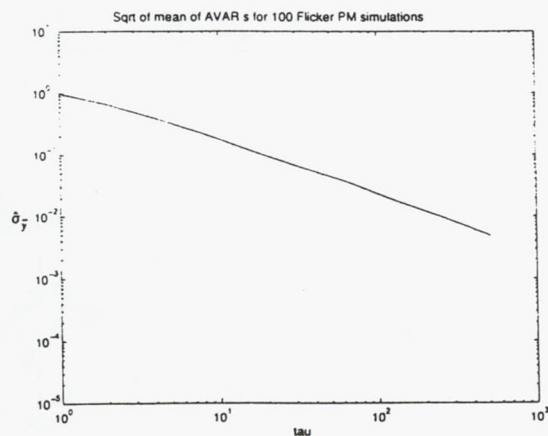
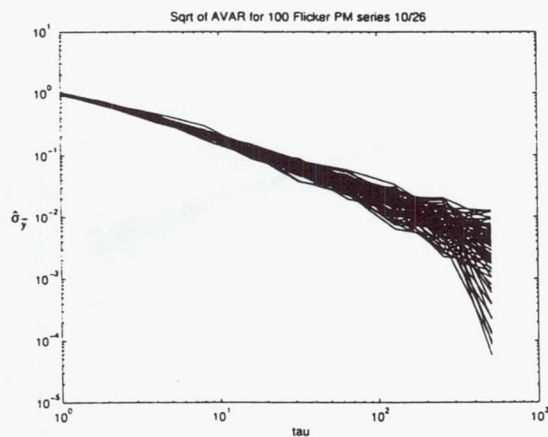
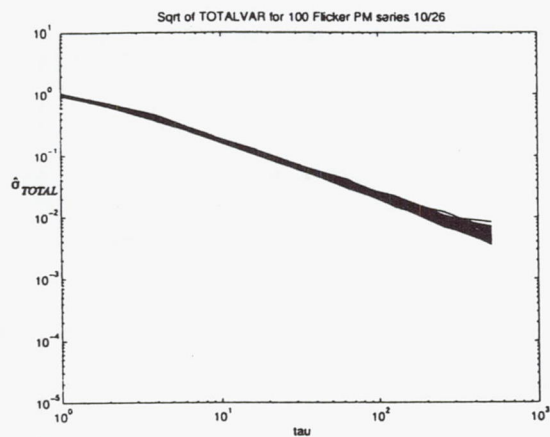


Fig. 3

Top(a): Square root of TOTALVAR calculated for 100 FLPM simulations with unit (two-sample) mean at  $\tau=1$ .  
 Middle(b): For comparison, traditional square root of maximally-overlapped AVAR calculated for the same 100 FLPM simulations as used at top for square root of TOTALVAR.  
 Bottom(c): Square root of 100-total mean of maximally-overlapped AVAR's, an indication of the desired result.

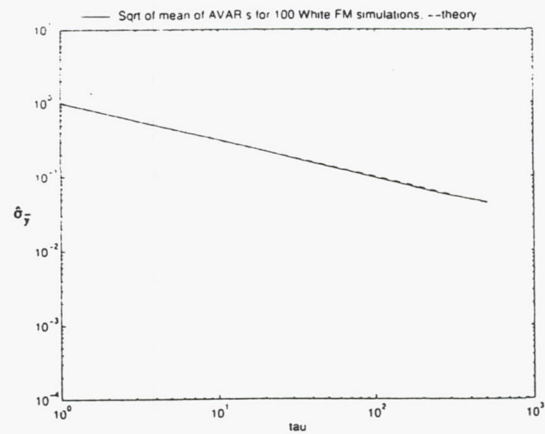
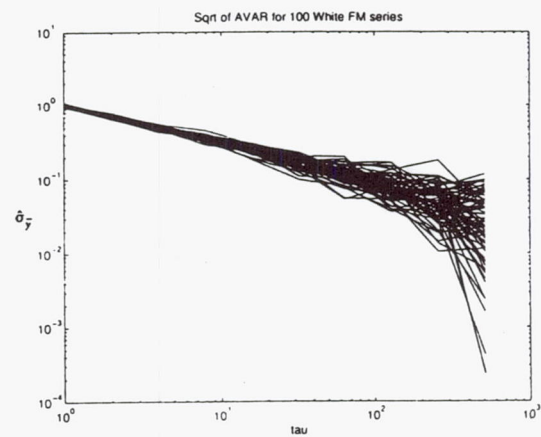
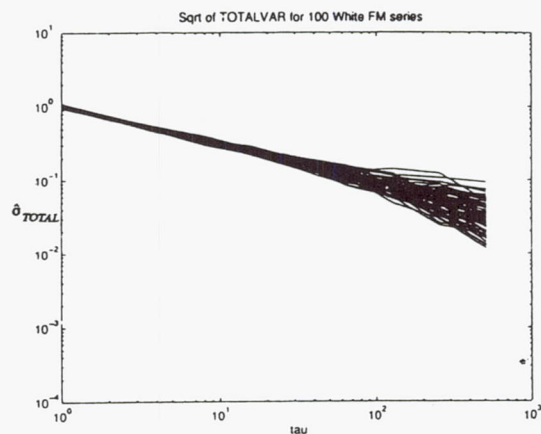


Fig. 4

Top(a): Square root of TOTALVAR calculated for 100 WHFM simulations with unit (two-sample) mean at  $\tau=1$ .  
 Middle(b): For comparison, traditional square root of maximally-overlapped AVAR calculated for the same 100 WHFM simulations as used at top for square root of TOTALVAR.  
 Bottom(c): Square root of 100-total mean of maximally-overlapped AVAR's, an indication of the desired result. Dashed line is the theoretical mean of an infinite set.



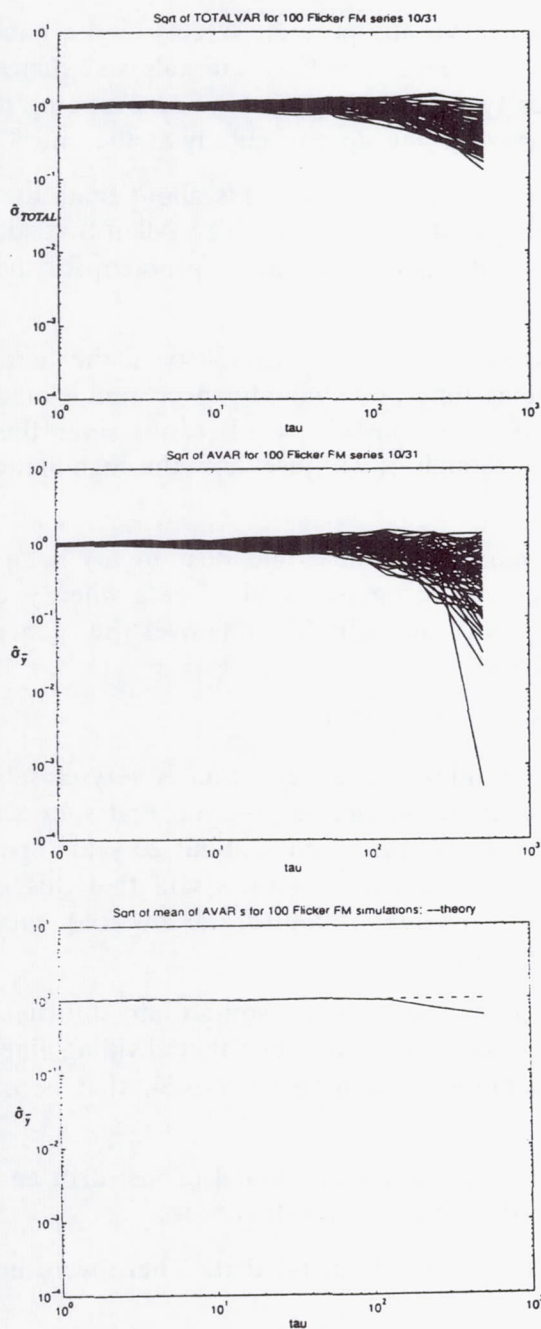


Fig. 5

Top(a): Square root of TOTALVAR calculated for 100 FLMF simulations with unit (two-sample) mean at  $\tau=1$ .  
 Middle(b): For comparison, traditional square root of maximally-overlapped AVAR calculated for the same 100 FLMF simulations as used at top for square root of TOTALVAR.  
 Bottom(c): Square root of 100-total mean of maximally-overlapped AVAR's, an indication of the desired result. Dashed line is the theoretical mean of an infinite set.

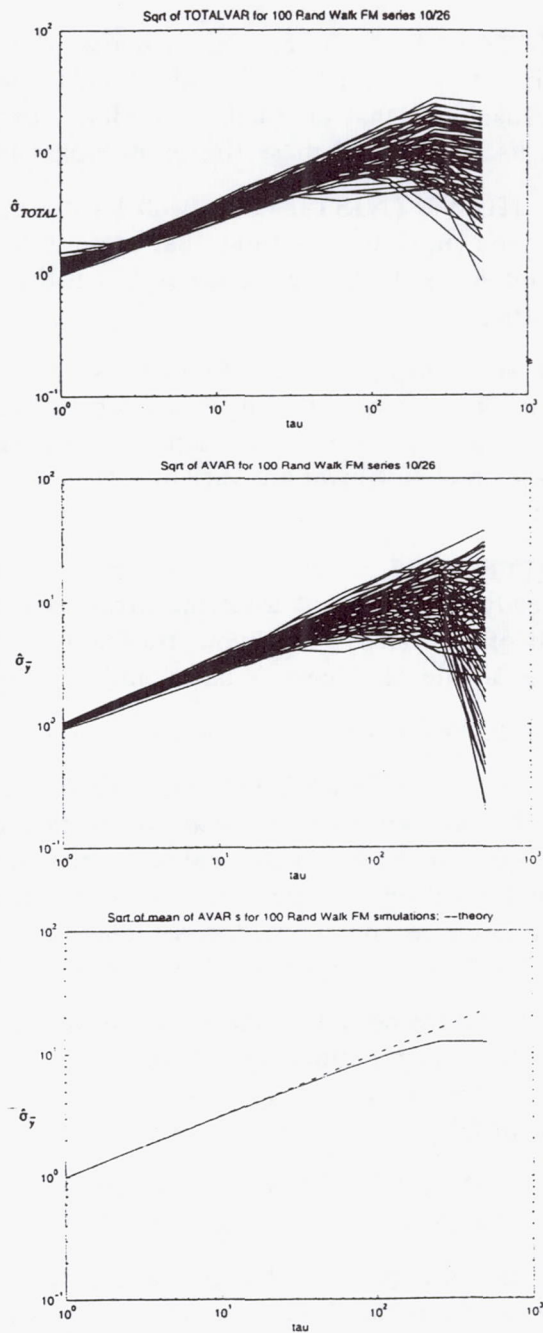


Fig. 6

Top(a): Square root of TOTALVAR calculated for 100 RWFM simulations with unit (two-sample) mean at  $\tau=1$ .  
 Middle(b): For comparison, traditional square root of maximally-overlapped AVAR calculated for the same 100 RWFM simulations as used at top for square root of TOTALVAR.  
 Bottom(c): Square root of 100-total mean of maximally-overlapped AVAR's, an indication of the desired result. Dashed line is the theoretical mean of an infinite set.

## Questions and Answers

**JOE WHITE (NRL):** Dave, what happens when you have any periodic effects in the data that goes into this sample? Real world data, for instance, since they have diurnals and things like that, what does that do to the confidence of this type of thing where we're wrapping it around on itself now, and these things no longer necessarily line up particularly at the ends?

**DAVE A. HOWE (NIST):** Okay, well let me make a couple of comments about that, Joe. One is that the simulations assume that there is no periodicity in the data. The Allan Statistic is ideally suited for stochastic processes, but if there is a diurnal, then that's a problem for the Allan Statistic.

On that, I would expect the results to be similar; that is, if there's a periodicity in the data, then once again, as you go to longer and longer averaging times, one would expect some would expect some nulls to occur. But actually thinking about it, maybe not. Because since this variance is a time shift invariant variance, then I think, though, it will just show the high value throughout the run. So, that's a good question.

**JOE WHITE (NRL):** Let me follow up with one more that's near and dear to my heart: Are you ready to talk about what the error bars ought to be on this kind of data when you do this sort of approach? You know, traditionally they run something like one over the square root of  $N$  as a rule of thumb. What would you say here?

**DAVE A. HOWE (NIST):** I'm not in a position to talk about that.

**DR. GERNOT WINKLER (USNO, RETIRED):** I think the old question is very closely related to the problem of how much systematics, how many systematics, do you first subtract before you go into the statistical analysis. I remember that we discussed it about 20 years ago, why this sudden drop in  $\sigma_\tau$ . And Jim Barnes, in fact, at that time said that this is inevitable as soon as you subtract a systematic part. You remove, of course, the low frequency part; and therefore, the  $\sigma_\tau$  has to drop at that point.

Now when you have periodic content, again the description is that before you go into statistical evaluation, you must remove systematics. But how much, where you put that dividing line, whether you stop at the linear subtraction or a quadratic or a simple sinusoid, that is, of course, the problem and the real question.

**DAVE A. HOWE (NIST):** Well, I understand. Typically, we use the model of just drift and linear rate. That's as far as we go. We assume the rest of it is the residual noise.

I do appreciate the question, I'm not sure I can shed any more light on that. There were no systematics in this data. There was no drift introduced.



# RELATING THE HADAMARD VARIANCE TO MCS KALMAN FILTER CLOCK ESTIMATION

Capt Steven T. Hutsell, USAF  
2d Space Operations Squadron  
300 O'Malley Avenue Suite 41  
Falcon AFB CO 80912-3041

## Abstract

*The GPS Master Control Station (MCS) currently makes significant use of the Allan Variance. This two-sample variance equation has proven excellent as a handy, understandable tool, both for time domain analysis of GPS Cesium frequency standards, and for fine tuning the MCS's state estimation of these atomic clocks.*

*The Allan Variance does not explicitly converge for the noise types of  $\alpha \leq -3$ , and can be greatly affected by frequency drift. Because GPS Rubidium frequency standards exhibit non-trivial aging and aging noise characteristics, the basic Allan Variance analysis must be augmented in order to a) compensate for a dynamic frequency drift, and b) characterize two additional noise types, specifically  $\alpha = -3$  and  $\alpha = -4$ . As the GPS program progresses, we will utilize a larger percentage of Rubidium frequency standards than ever before. Hence, GPS Rubidium clock characterization will require more attention than ever before.*

*The three-sample variance, commonly referred to as a renormalized Hadamard Variance, is unaffected by linear frequency drift, converges for  $\alpha > -5$ , and thus has utility for modeling noise in GPS Rubidium frequency standards. This paper demonstrates the potential of Hadamard Variance analysis in GPS operations, and presents an equation that relates the Hadamard Variance to the MCS's Kalman Filter process noises ( $qs$ ).*

## INTRODUCTION

The two-sample variance, or what we commonly refer to as the Allan Variance, has been an excellent device for time domain characterization of GPS Cesium frequency standards over the past few years. Over the past year, the GPS Master Control Station (MCS) has also applied the Allan Variance towards fine tuning the MCS's state estimation of these Cesium clocks [3].

In terms of Power-Law Spectral Density exponents, the Allan Variance does not explicitly converge for noise types of  $\alpha \leq -3$ , and may be greatly affected by frequency drift [5]. Because GPS Rubidium frequency standards exhibit significant aging and aging noise characteristics, the Allan Variance analysis must be augmented to dynamically compensate for this frequency drift, and to characterize two additional noise types, specifically  $\alpha = -3$  and  $\alpha = -4$ . As the GPS program progresses, we will utilize a larger percentage of Rubidium frequency standards than ever before. In particular, the Block IIR satellite platform will house three atomic frequency standards, and two of these three will be Rubidium. Clearly, the characterization of GPS Rubidium clocks will soon require more attention than ever before.

In contrast, the three-sample variance, commonly referred to as a renormalized Hadamard Variance, is *unaffected* by linear frequency drift, converges for  $\alpha > -5$  [8], and hence has a potential utility for modeling the various noise types resident in GPS Rubidium frequency standards. This paper demonstrates this potential for Hadamard Variance analysis in GPS analysis operations, and presents the relationship between the Hadamard Variance and the MCS's Kalman Filter process noises ( $qs$ ).

## THE HADAMARD VARIANCE EQUATION

A mainstay of atomic clock characterization, the two-sample (Allan) Variance essentially examines the second difference of phase, equivalent to the first difference of the time-averaged frequencies over two successive adjacent time intervals ( $\tau$ ) [5]:

$$\sigma_y^2(\tau) = \frac{1}{2(M-1)} \sum_{i=1}^{M-1} (\bar{y}_{i+1} - \bar{y}_i)^2, \quad \bar{y}_i = \text{the time-averaged frequency over } \tau_i. \quad (1)$$

Similar in principle to the structure to the Allan Variance, the *three*-sample variance examines the *third* difference in phase, equivalent to the *second* difference of the time-averaged frequencies over *three* successive adjacent time intervals ( $\tau$ ). The timing community has commonly referred to this three-sample variance as the *Hadamard Variance*. Though the term *Hadamard Variance* has been used more generally in various applications of multi-sample time domain analysis, for the purposes of this paper, we shall define the Hadamard Variance as follows:

$${}_H\sigma_y^2(\tau) = \frac{1}{6(M-2)} \sum_{i=1}^{M-2} (\bar{y}_{i+2} - 2\bar{y}_{i+1} + \bar{y}_i)^2, \quad \bar{y}_i = \text{the time-averaged frequency over } \tau_i. \quad (2)$$

The Hadamard Deviation (the square root of the Hadamard Variance) identifies two noise types that the Allan Deviation does not *explicitly* identify [8]. For this paper, we shall name the following noise types: for  $\alpha = -3$ , "Flicker Walk FM"; for  $\alpha = -4$ , "Random Run FM" [5]. Figure 1 visually describes the noise types identified by the Hadamard Deviation [6].

In terms of phase, equation (2) converts to [8]:

$${}_H\sigma_y^2(\tau) = \frac{1}{6\tau^2(N-3)} \sum_{i=1}^{N-3} (x_{i+3} - 3x_{i+2} + 3x_{i+1} - x_i)^2, \quad x_i = \text{the phase measurement at } t_i. \quad (3)$$

or, equivalently:

$${}_H\sigma_y^2(\tau) = \frac{1}{6\tau^2} E[(x_{i+3} - x_{i+2}) - (x_{i+2} - x_{i+1}) - (x_{i+2} - x_{i+1}) + (x_{i+1} - x_i)]^2 \quad (4)$$

where  $E[.]$  is the expectation operator. Each phase measurement  $x_i = x(t_i)$  in equation (4) is separated from each neighboring successive phase measurement by a time interval value of  $\tau$ . Meaning,



$$x(t_{i+1}) = x(t_i + \tau), \quad (5)$$

$$x(t_{i+2}) = x(t_{i+1} + \tau) = x(t_i + 2\tau), \text{ and} \quad (6)$$

$$x(t_{i+3}) = x(t_{i+2} + \tau) = x(t_{i+1} + 2\tau) = x(t_i + 3\tau) \quad (7)$$

## MCS KALMAN FILTER TIME UPDATE PREDICTIONS

The propagation (time update), of Rubidium clock states in the MCS Kalman Filter, is modeled using the following polynomial expansion [7]:

$$\begin{bmatrix} x(t+\tau) \\ y(t+\tau) \\ z(t+\tau) \end{bmatrix} = \begin{bmatrix} 1 & \tau & (1/2)\tau^2 \\ 0 & 1 & \tau \\ 0 & 0 & 1 \end{bmatrix} \begin{bmatrix} x(t) \\ y(t) \\ z(t) \end{bmatrix} + \begin{bmatrix} \Delta x \\ \Delta y \\ \Delta z \end{bmatrix} \quad (8)$$

where  $\tau$  is the prediction span, and  $x(t)$ ,  $y(t)$ , and  $z(t)$  are the phase, frequency, and frequency drift values, respectively, of the clock in question. Note that  $y(t)$  is the time derivative of  $x(t)$ , and  $z(t)$  is the time derivative of  $y(t)$ .  $\Delta(x)$ ,  $\Delta(y)$ , and  $\Delta(z)$  are assumed to be random error increments, independent of  $x(t)$ ,  $y(t)$ , and  $z(t)$ , having a prediction covariance  $P$  represented by a function of the Kalman Filter process noises ( $qs$ ) [1,7]:

$$P = E \left[ \begin{bmatrix} \Delta x \\ \Delta y \\ \Delta z \end{bmatrix} \begin{bmatrix} \Delta x & \Delta y & \Delta z \end{bmatrix} \right] = \begin{bmatrix} q_1\tau + q_2\tau^3/3 + q_3\tau^5/20 & q_2\tau^2/2 + q_3\tau^4/8 & q_3\tau^3/6 \\ q_2\tau^2/2 + q_3\tau^4/8 & q_2\tau + q_3\tau^3/3 & q_3\tau^2/2 \\ q_3\tau^3/6 & q_3\tau^2/2 & q_3\tau \end{bmatrix} \quad (9)$$

An expansion of equation (8) produces the following equations:

$$\begin{bmatrix} x_{i+1} \\ y_{i+1} \\ z_{i+1} \end{bmatrix} = \begin{bmatrix} x_i + \tau y_i + (1/2)\tau^2 z_i \\ y_i + \tau z_i \\ z_i \end{bmatrix} + \begin{bmatrix} \Delta x_{i+1} \\ \Delta y_{i+1} \\ \Delta z_{i+1} \end{bmatrix} \quad (10)$$

$$\begin{bmatrix} x_{i+2} \\ y_{i+2} \\ z_{i+2} \end{bmatrix} = \begin{bmatrix} x_{i+1} + \tau y_{i+1} + (1/2)\tau^2 z_{i+1} \\ y_{i+1} + \tau z_{i+1} \\ z_{i+1} \end{bmatrix} + \begin{bmatrix} \Delta x_{i+2} \\ \Delta y_{i+2} \\ \Delta z_{i+2} \end{bmatrix} \quad (11)$$

$$\begin{bmatrix} x_{i+3} \\ y_{i+3} \\ z_{i+3} \end{bmatrix} = \begin{bmatrix} x_{i+2} + \tau y_{i+2} + (1/2)\tau^2 z_{i+2} \\ y_{i+2} + \tau z_{i+2} \\ z_{i+2} \end{bmatrix} + \begin{bmatrix} \Delta x_{i+3} \\ \Delta y_{i+3} \\ \Delta z_{i+3} \end{bmatrix} \quad (12)$$

Using equations (10), (11), and (12), and examining the differences between each successive  $x_i$ :

$$(x_{i+1} - x_i) = \tau y_i + (1/2)\tau^2 z_i + \Delta x_{i+1} \quad (13)$$

$$(x_{i+2} - x_{i+1}) = \tau y_{i+1} + (1/2)\tau^2 z_{i+1} + \Delta x_{i+2} \quad (14)$$

$$(x_{i+3} - x_{i+2}) = \tau y_{i+2} + (1/2)\tau^2 z_{i+2} + \Delta x_{i+3} \quad (15)$$

## AN EXPECTATION OPERATOR EXPANSION OF $H\sigma^2_y(\tau)$

Inserting equations (13), (14), and (15) into the following expression:

$$[ThirdDif] = [(x_{i+3} - x_{i+2}) - (x_{i+2} - x_{i+1}) - (x_{i+2} - x_{i+1}) + (x_{i+1} - x_i)] \quad (16)$$

obtains:

$$[ThirdDif] = \Delta x_{i+3} - 2\Delta x_{i+2} + \Delta x_{i+1} + \tau\{(y_i - y_{i+1}) - (y_{i+1} - y_{i+2})\} + (1/2)\tau^2\{(z_i - z_{i+1}) - (z_{i+1} - z_{i+2})\} \quad (17)$$

Examining the differences between each successive  $y_i$  and  $z_i$ , from equations (10), (11), and (12):

$$(y_{i+1} - y_i) = \tau z_i + \Delta y_{i+1} \quad (18)$$

$$(y_{i+2} - y_{i+1}) = \tau z_{i+1} + \Delta y_{i+2} \quad (19)$$

$$(z_{i+1} - z_i) = \Delta z_{i+1} \quad (20)$$

$$(z_{i+2} - z_{i+1}) = \Delta z_{i+2} \quad (21)$$

Equation (17) translates into:

$$[ThirdDif] = \Delta x_{i+3} - 2\Delta x_{i+2} + \Delta x_{i+1} + \tau\{(\tau z_{i+1} + \Delta y_{i+2}) - (\tau z_i + \Delta y_{i+1})\} + (1/2)\tau^2\{(\Delta z_{i+2}) - (\Delta z_{i+1})\} \quad (22)$$

With some more algebraic manipulation:

$$[ThirdDif] = \Delta x_{i+3} - 2\Delta x_{i+2} + \Delta x_{i+1} + \tau\{(\Delta y_{i+2} - \Delta y_{i+1}) + (\tau z_{i+1} - \tau z_i)\} + (1/2)\tau^2\{(\Delta z_{i+2}) - (\Delta z_{i+1})\} \quad (23)$$

$$[ThirdDif] = \Delta x_{i+3} - 2\Delta x_{i+2} + \Delta x_{i+1} + \tau\{(\Delta y_{i+2} - \Delta y_{i+1}) + (\tau \Delta z_{i+1})\} + (1/2)\tau^2\{(\Delta z_{i+2}) - (\Delta z_{i+1})\} \quad (24)$$

$$[ThirdDif] = \Delta x_{i+3} - 2\Delta x_{i+2} + \Delta x_{i+1} + \tau\{(\Delta y_{i+2} - \Delta y_{i+1})\} + (1/2)\tau^2\{(\Delta z_{i+2}) + (\Delta z_{i+1})\} \quad (25)$$

$$[ThirdDif] = \{\Delta x_{i+3}\} + \{-2\Delta x_{i+2} + \tau \Delta y_{i+2} + (1/2)\tau^2(\Delta z_{i+2})\} + \{\Delta x_{i+1} - \tau \Delta y_{i+1} + (1/2)\tau^2(\Delta z_{i+1})\} \quad (26)$$

Since we've now broken down this expansion into three independent polynomial terms:

$$E[ThirdDif]^2 = E[\{\Delta x_{i+3}\} + \{-2\Delta x_{i+2} + \tau \Delta y_{i+2} + (1/2)\tau^2(\Delta z_{i+2})\} + \{\Delta x_{i+1} - \tau \Delta y_{i+1} + (1/2)\tau^2(\Delta z_{i+1})\}]^2 \quad (27)$$

the independence of each term  $\{\}$  allows us to separate equation (27) into three individual expectation operators [4]:



$$E[ThirdDif]^2 = E[\Delta x_{i+3}]^2 + E[-2\Delta x_{i+2} + \tau \Delta y_{i+2} + (1/2)\tau^2(\Delta z_{i+2})]^2 + E[\Delta x_{i+1} - \tau \Delta y_{i+1} + (1/2)\tau^2(\Delta z_{i+1})]^2 \quad (28)$$

Expressing each term of  $E[ThirdDif]^2$  as a function of the Kalman Filter prediction covariance matrix [1]:

$$E[\Delta x_{i+3}]^2 = \begin{bmatrix} 1 & 0 & 0 \end{bmatrix} P \begin{bmatrix} 1 \\ 0 \\ 0 \end{bmatrix} = q_1\tau + (1/3)q_2\tau^3 + (1/20)q_3\tau^5 \quad (29)$$

$$\begin{aligned} E[-2\Delta x_{i+2} + \tau \Delta y_{i+2} + (1/2)\tau^2(\Delta z_{i+2})]^2 &= \begin{bmatrix} -2 & \tau & (1/2)\tau^2 \end{bmatrix} P \begin{bmatrix} -2 \\ \tau \\ (1/2)\tau^2 \end{bmatrix} \\ &= 4q_1\tau + (1/3)q_2\tau^3 + (9/20)q_3\tau^5 \end{aligned} \quad (30)$$

$$\begin{aligned} E[\Delta x_{i+1} - \tau \Delta y_{i+1} + (1/2)\tau^2(\Delta z_{i+1})]^2 &= \begin{bmatrix} 1 & -\tau & (1/2)\tau^2 \end{bmatrix} P \begin{bmatrix} 1 \\ -\tau \\ (1/2)\tau^2 \end{bmatrix} \\ &= q_1\tau + (1/3)q_2\tau^3 + (1/20)q_3\tau^5 \end{aligned} \quad (31)$$

By adding each term:

$$E[ThirdDif]^2 = 6q_1(\tau) + q_2(\tau^3) + (11/20)q_3(\tau^5) \quad (32)$$

Hence,

$${}_H\sigma_y^2(\tau) = \frac{1}{6\tau^2} E[ThirdDif]^2 = \frac{1}{6\tau^2} [6q_1(\tau) + q_2(\tau^3) + (11/20)q_3(\tau^5)] \quad (\text{for } \alpha = 0, -2, -4) \quad [6] \quad (33)$$

$${}_H\sigma_y^2(\tau) = q_1\tau^{-1} + (1/6)q_2\tau + (11/120)q_3\tau^3 \quad (\text{for } \alpha = 0, -2, -4) \quad (34)$$

## RELATING WHITE PM TO THE HADAMARD VARIANCE

Equation (34) does not, however, account for white PM noise ( $\alpha = 2$ ) [6], sometimes also referred to as *representation error* [1]. The Hadamard Variance can be expressed, in terms of phase measurements, as follows:

$${}_H\sigma_y^2(\tau) = \frac{1}{6\tau^2} E[x_{i+3} - 3x_{i+2} + 3x_{i+1} - x_i]^2 \quad (35)$$

When white PM is the *only* significant noise component, the individual phase values are uncorrelated with time, and may be separated [4]:

$${}_H\sigma_y^2(\tau) = \frac{1}{6\tau^2} \left\{ E[x_{i+3}]^2 + E[-3x_{i+2}]^2 + E[3x_{i+1}]^2 + E[-x_i]^2 \right\} \quad (\text{for } \alpha = 2) \quad (36)$$

When assuming that white PM is the primary noise source, the representation error, which we'll denote as  $q_0 = E[x_i]^2$ , is independent of  $t_i$ , and thus is a phase variance that is constant across time. Therefore,

$${}_H\sigma_y^2(\tau) = \frac{1}{6\tau^2} \left\{ (1+9+9+1)E[x_i]^2 \right\} = \frac{10}{3\tau^2} q_0 \quad (\text{for } \alpha = 2) \quad (37)$$

## THE HADAMARD-Q EQUATION

In the presence of both a) white PM, and b) the three noise types modeled by  $P$ , and assuming independence between the white PM and the other noise types, equations (34) and (37) can be combined into one that models four noise types, namely  $\alpha = 2, 0, -2$ , and  $-4$ :

$${}_H\sigma_y^2(\tau) = (10/3)q_0\tau^2 + q_1\tau^1 + (1/6)q_2\tau + (11/120)q_3\tau^3 \quad (38)$$

Note how this equation compares to the analogous equation relating the Allan Variance to the  $q_s$  [2,3]:

$$\sigma_y^2(\tau) = 3q_0\tau^2 + q_1\tau^1 + (1/3)q_2\tau + (1/20)q_3\tau^3 \quad (39)$$

For white FM, the Allan and Hadamard Variances are mathematically equivalent. For white PM, the two Variances are roughly the same, and, for random walk FM, the Variances differ by a factor of two. Though an analyst may use either the Hadamard Variance or the Allan Variance for deriving MCS  $q_s$ , each has its own set of advantages and disadvantages.

The primary advantage of the Hadamard Variance is the automatic removal of linear frequency drift [8]. Whereas the equation relating the Allan Variance to MCS  $q_s$  assumes that the analyst must apply a continuously dynamic correction for frequency drift, the Hadamard-Q equation doesn't require this assumption. The tradeoff, however, is that the Hadamard Variance incurs an extra computational burden, simply because it examines the *third* (vice the second) difference of phase. For analyzing GPS Cesium frequency standards, the increased computational load of the Hadamard Variance proves fruitless, only because the Allan Variance gets the job done more efficiently [3].

Many timing experts, over the years, have extensively used techniques for applying a continuously dynamic correction for frequency drift, prior to using the Allan Variance for deriving  $q_3$  values with high confidence. This paper does *not* address the issue of confidence in the  $q_3$  value produced by the Hadamard-Q equation. This paper does, however, present an easily understood relationship between a relatively lesser known equation (the Hadamard Variance), and a set of system parameters used by the MCS (the Kalman Filter  $q_s$ ). On initial appearance, given the computational capability, one can see the great potential utility of an algorithm that applies a relatively simple equation onto a large measurement data base, in order to derive Kalman Filter  $q_s$ , *without* the need to apply preparatory frequency drift corrections. In the future, the author hopes to further investigate a) the real-world utility of this relationship, b) the issue of estimate confidence, and c) the net gain from the increased utility balanced against the increased computational burden.



## CONCLUSION

The implication of the Hadamard Variance in GPS operations is as follows: Analysts at the MCS could simply gather a large data base of clock phase measurements, apply all known step corrections, perform a number of iterations of the Hadamard Variance equation, and plot the results to visually describe the noise characteristics of GPS Rubidium clocks (including  $\alpha = -4$ ). Consequently, the Hadamard Variance could offer GPS operators an alternate tool for characterizing GPS atomic frequency standard noise.

Perhaps more significantly, the implication of equation (38) is that GPS analysts now have an easily understood technique to relate raw clock phase measurements towards deriving important Kalman Filter clock estimation parameters ( $qs$ ), that are unique to the performance of each individual clock, and that will include  $q_3$  automatically, without any need for the preliminary removal of frequency drift.

The MCS hopes to make continued use of the Allan Variance, for both the characterization of Cesium clocks, and the derivation of their associated process noise values. This application of the Hadamard Variance widens the array of available tools for the characterization of *Rubidium* clocks, and the derivation of *their* associated process noise values. The GPS Block IIR satellite program will use a large percentage of Rubidium clocks. Certainly, the ever-important issue of refining Rubidium clock estimation may see its most important days in the years ahead.

## ACKNOWLEDGMENTS

The author wishes to thank the following people and agencies for their generous assistance with both our timing improvements and this paper:

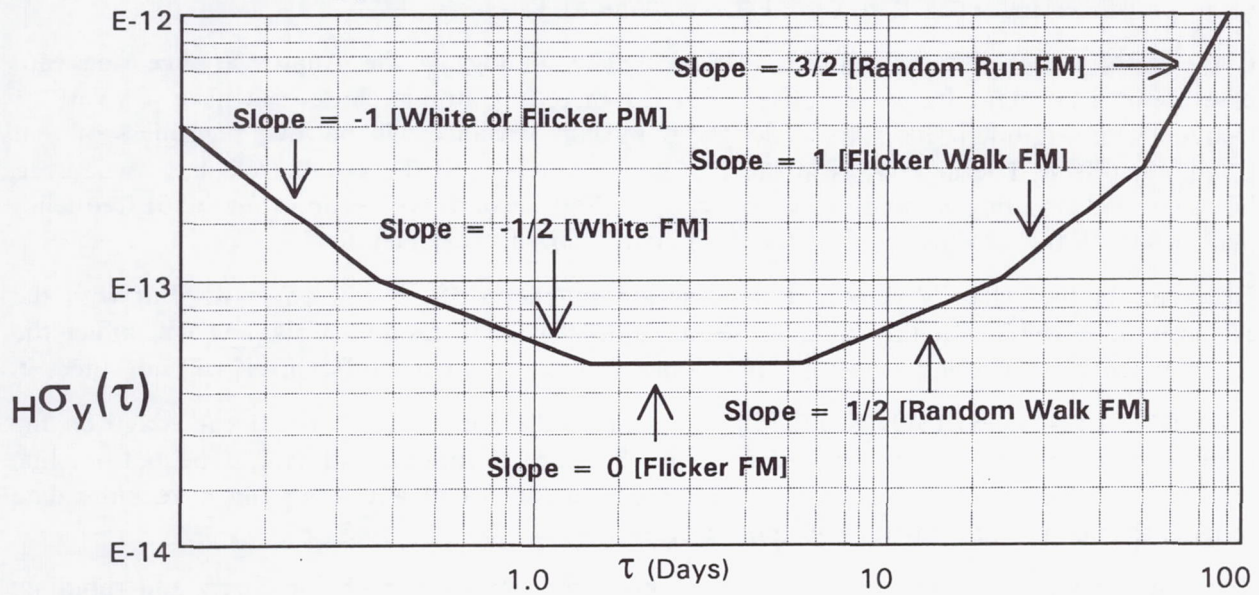
David W. Allan, Allan's TIME  
James A. Barnes, Senior Member, IEEE  
Kenneth R. Brown, Loral Federal Systems Division  
James W. Chaffee, Associate Member, IEEE  
Pamela C. Crum, B.A., Mathematics, Amherst College  
Sam R. Stein, Timing Solutions Corporation  
The people of the 2 SOPS  
Todd E. Walter, Stanford University  
Marc A. Weiss, NIST

## REFERENCES

- [1] Brown, Kenneth R., *The Theory of the GPS Composite Clock*, Proceedings of ION GPS-91, 11-13 Sep 91
- [2] Chaffee, James W., *Relating the Allan Variance to the Diffusion Coefficients of a Linear Stochastic Differential Equation Model for Precision Oscillators*, from the IEEE Transactions on Ultrasonics, Ferroelectrics, and Frequency Control, Vol. UFFC-34, No. 6, November 1987
- [3] Hutsell, Steven T., Capt, USAF, *Fine Tuning GPS Clock Estimation in the MCS*, Proceedings of PTTI-94, 5-8 Dec 94
- [4] Maybeck, Peter S., *Stochastic Models, Estimation and Control, Volume 1*, 1979
- [5] NIST Technical Note 1337, Mar 1990
- [6] Rutman, Jacques, Member, IEEE, *Characterization of Phase and Frequency Instabilities in Precision Frequency Sources, Fifteen Years of Progress*, Proceedings of the IEEE, Vol 66, No. 9, September, 1978
- [7] Taylor, John V., IV, Rockwell International, *Estimation of Clock Drift Rate States on GPS SVs Using Rb Frequency Standards* MFR, 31 Jan 94
- [8] Walter, Todd E., Stanford University, *A Multi-Variance Analysis in the Time Domain*, Proceedings of PTTI-92, 1-3 Dec 92



## Noise Types Identified by the Hadamard Deviation



Noise Type	Power-Law Spectral Density Exponent	$H\sigma_y(\tau)$ Log-Log Slope
White PM	$\alpha = 2$	-1
Flicker PM	$\alpha = 1$	-1
White FM	$\alpha = 0$	-1/2
Flicker FM	$\alpha = -1$	0
Random Walk FM	$\alpha = -2$	1/2
Flicker Walk FM	$\alpha = -3$	1
Random Run FM	$\alpha = -4$	3/2

Figure 1

## Questions and Answers

**SERGEY V. ERMOLIN (HEWLETT-PACKARD):** The Hadamard Variance does remove linear drift, that's true; and that saves you some time on preprocessing. But, it doesn't remove any drift beyond linear. As you showed on one of your first slides, that rubidium standards on board one of the space vehicles show not only linear drift, but possibly quadratic drift to some other power.

So still, if you wanted to go ahead with longer operational time, you would still have to do some preprocessing, even if you used the Hadamard Variance.

**CAPTAIN STEVEN HUTSELL (USAF):** The analogy is the Allan Variance does not care about a constant frequency offset. For instance, our atomic clocks can have a  $1 \times 10^{-11}$  frequency offset; but if it's stable enough, the Allan Variance will be low, regardless of that frequency offset. The analogy is in the Hadamard Variance, if the satellite clock, or whatever, has an already existing common offset of, say,  $3 \times 10^{-18}$  seconds per second squared of frequency drift, that will not adversely affect the Hadamard Variance calculations.

However, in the Allan Variance, if there is a frequency drift, it will affect it. But with the Hadamard, it won't. In the same sense, a random walk in random walk FM will affect the Allan Variance by causing a positive one slope. But the frequency offset itself will not affect it.

**DAVID ALLAN (ALLAN'S TIME):** Dr. Barnes did some work three decades ago on the confidence question, actually related to it, in the third difference estimate. The bottom line was that the confidence is worse by a significant amount, especially when you have finite data lengths that come into impact you quite adversely.

The other point is that it turns out a logarithmic drift estimator, both for quartz and rubidium is much better than linear. I think the graph that you showed outside of the turn-on transient probably would fit a logarithmic curve quite well.

So, one might be better doing logarithmic modeling if we deal with a lot of rubidiums in the future. Yes, one would expect that the logarithmic function could be fit to this quite well, outside of the first point.

The last one I would like to suggest that you think about — and I want to say that I think you've done a beautiful piece of work, but you can actually remove the effect of drift, kind of in real time, from the second difference operator, because you know the exact equation for the effect of drift on it until you can subtract that from and get an estimator variance without the drift effectively in real time. So, it doesn't need to impact the value of the variance if you don't want it to; and it gives you a tighter confidence of the estimate.

**CAPTAIN STEVEN HUTSELL (USAF):** Yes, and the intent of this is not really to present the best way to estimate frequency drift dynamically. Really, what I wanted to do was examine the way the MCS is currently set up. And right now, it does not have the capability to do what you just described. The MCS is only set up as a dynamic Kalman filter three-state vector that needs process noise values.

I completely agree that are far more sophisticated techniques to look at frequency drift than what's set up in the Kalman filter. Sorry, your first comment?



DAVID ALLAN (ALLAN'S TIME): [Inaudible].

CAPTAIN STEVEN HUTSELL (USAF): Yes, we see that too. We see it start to converge  
- - -

DAVID ALLAN (ALLAN'S TIME): [Inaudible].

CAPTAIN STEVEN HUTSELL (USAF): We agree. Over time, the frequency drift goes from a negative value, around  $3$  or  $4 \times 10^{-18}$ , and gradually starts logarithmically to approach zero.

At the beginning, however, sometimes we see it start hugely negative, like  $-1 \times 10^{-17}$ . Sometimes  $+1 \times 10^{-16}$ . We're talking about over the first 48 hours that we turn it on. We would need to address how we try to model that. It's also probably appropriate to ask what's causing that, what physical phenomenon is causing it to be positive at the beginning for some clocks, and negative for the others. But, I do agree.

# SIGNAL DELAY STABILITY OF A KU-BAND TWO-WAY SATELLITE TIME TRANSFER TERMINAL

D. Kirchner

Technical University Graz, Austria

H. Ressler and R. Robnik

Space Research Institute, Graz, Austria

## Abstract

*A fully automated two-way time and frequency transfer (TWSTFT) system including a satellite simulator, which allows to carry out signal delay measurements in conjunction with each time transfer measurement, is operated at the Technical University Graz (TUG). After a brief description of the system, results obtained during fifteen months of operation are presented and discussed. Finally envisaged experiments are mentioned.*

## INTRODUCTION

The signal delay stability of the receiving equipment (one-way methods) and of the receiving and transmit equipment (two-way methods) is a crucial parameter for the performance of time and frequency transfer systems. Apart from the use of transfer standards to assess the differential signal delay of stations, the use of local means to monitor signal delay variations — allowing frequent measurements — is of great interest. For satellite time transfer stations, this can be accomplished by using a satellite simulator attached to the antenna of the station. Such a system has been operated for longer than a year together with the two-way satellite time and frequency transfer (TWSTFT) station of the Technical University Graz (TUG), enabling the individual measurement of the difference of the transmit and receive delays for each time transfer session in a completely automated procedure<sup>[1]</sup>.

The correction which has to be applied to TWSTFT measurements is given by  $[(\tau_1^{TX} - \tau_1^{RX}) - (\tau_2^{TX} - \tau_2^{RX})]^{1/2}$ , i.e. the difference of the differential delays of the transmit and receive parts of earth stations 1 and 2 divided by two<sup>[2]</sup>. The transmit delay is the total delay from the transmitted one pulse per second (1 PPS) to the reference plane of the antenna and the receive delay is the total delay of the received 1 PPS. Both delays consist of the corresponding signal delays of the earth station, the modem, related equipment, and in the connecting cables. The employed satellite simulator (SATSIM) allows to measure most of these delays except some



remaining delays which have to be evaluated separately. The signal delays are measured by means of the spread-spectrum modem used for the time and frequency transfer measurements. The separate transmit and receive delays of a single modem can be measured by means of an oscilloscope, but only with low accuracy. With two modems the corresponding differential delays can be established with high accuracy.

## MEASUREMENT SETUP

A detailed description of the TWSTFT system used at TUG is given in [1]. The SATSIM used is of the de Jong type<sup>[3, 4]</sup> — this means one can measure the sum of the earth station transmit and receive delays as well as the receive delay only, thus allowing one to calculate the difference of the transmit and receive delay — but shows some modifications. The receive and transmit antennas are not simply waveguide-to-coax transitions, but are horn antennas and, in the receive part, there is a power splitter, making possible to measure power and frequency of the signal transmitted by the earth station. In the transmit part, a combination of attenuators is used to obtain the same signal power as received from the satellite. For shielding purposes all components are in a small metallic box with the horn antennas protruding from the box. The box is mounted on the feed boom of the parabolic antenna with the horns facing the feed. The side of the box with the horns is covered with microwave absorbing material and protection from rain is achieved by a small dome. The station is fully automated, providing remote control of transmit power, of transmit and receive frequencies, and of a spectrum analyzer for various measurement and monitoring purposes. Apart from the actual time transfer measurements, a time-transfer session consists of several accompanying measurements: collection of meteorological data, a counter check, the modem calibration, carrier-to-noise power density ratio ( $C/N_0$ ) measurements of the satellite beacon and of the carriers of the local and remote station, and the different loop measurements necessary for the calculation of the signal delays of the station.

A block diagram of the station from the point of view of the signal delays involved and the possible loop arrangements to measure the signal delays of interest is shown in Figure 1. The different loops and the corresponding counter readings ( $REF - PPSRX + b2$ ) are called: MOD for modem loop, ID for indoor loop (all indoor equipment is in a fully air-conditioned room), OD for outdoor loop, STR for SATSIM loop to measure the station transmit and receive delay, and SR for SATSIM loop to measure the station receive delay. Together with the wanted delays other delays are measured which can only partly be eliminated by combining different measurements. These remaining delays have to be evaluated separately. CAL is the modem calibration ( $REF - PPSTX + b1$ ) by which TWSTFT measurements have to be corrected to take into account the delay between the time reference REF and the transmitted 1 PPS PPSTX. Each delay indicated in a square gives the signal delay between the points marked by dots, e.g.  $u1$  is the signal delay from the modem output to the indoor switch input and so on. In order to distinguish between the transmit and receive delays mentioned above and indicated by  $\tau$ , the measured delays are indicated by  $t$ . The transmit delay  $t^{TX}$  (modem transmit output to satellite simulator input not including the cable connecting indoor and outdoor equipment) given by  $(u1 + i1 + o1 + u3 + u4)$  is obtained by calculating  $(STR - SR)$  and applying the correction  $[c1 + c2 + (s2 - s1) + (cc - uc)]$ . The receive delay  $t^{RX}$  (satellite simulator output



to modem receive input not including the cable connecting outdoor and indoor equipment) given by  $(d4 + d3 + o2 + i2 + d1)$  is obtained by calculating  $(SR - MOD - OD + ID)$  and applying the correction  $[-(c1 + c2) - s2 - (cc - uc) - (m1 + m2 - m3) - (i3 - o3 - i1 - i2)]$ . The differential delay  $(t^{TX} - t^{RX})/2$  is obtained by calculating  $(STR - 2*SR + MOD + OD - ID)/2$  and applying the correction  $[(c1 + c2) + (s2 - s1/2) + (cc - uc) + (m1 + m2 - m3)/2 + (i3 - o3 - i1 - i2)/2]$ . Apart from  $(c1 + c2)$  all other terms can either be assumed to be zero or smaller than 1 ns. The delay  $c1$  is 14.55 ns and  $c2$  is about 20 ns. The cables connecting the indoor and outdoor equipment (delays:  $cc$ ,  $uc$ ,  $dc$ ) are parts of equal lengths (approx. 30 m) of one cable and in the same duct. Therefore, signal delay variations are assumed to be equal for all of them. The sum of  $uc$  and  $dc$  and related delays  $(OD - ID)$  is measured for each session and the three individual delays ( $cc$ ,  $uc$ ,  $dc$ ) are measured occasionally like other delays which in the present setup cannot be measured in an automated mode. In the following the respective delays  $t$  are given without the above mentioned corrections and are designated by  $T$ .

## MEASUREMENTS AND RESULTS

TWSTFT measurements are carried out between two laboratories in the USA and six laboratories in Europe<sup>[5, 6]</sup>. Since summer 1994 in connection with each session all loop measurements necessary to calculate the differential delay are performed. Each single loop measurement is the mean of 100 measurements with one measurement per second. The completion of all loop measurements takes about fifteen minutes, but could be shortened to about 10 minutes. The measurement error estimated by an error budget taking into account the errors contributed by the single measurements is smaller than 50 ps.

In the following, measurements accompanying the European sessions are presented. The differential delay  $(T^{TX} - T^{RX})/2$  — computed from the delays as measured — and the outside temperature are given in Figures 2 and 3. There is an obvious correlation between the differential signal delay of the station and the outside temperature. Figure 4 shows the differential delay computed from the transmit and receive delays corrected for their modeled temperature and humidity behavior. For the modeling of the temperature and humidity dependence of the transmit and receive delays, polynomial fits were used. During the reported period of about fifteen months a total variation of the temperature of about 35°C and a total variation of the uncorrected differential delay of about 1.5 ns can be observed. The uncorrected data show a trend with a superimposed seasonal variation of about 600 ps. This trend still exists for the data with the modeled temperature and humidity dependence removed and seems to represent a kind of aging effect resulting in a delay increase of about 400 ps.

## DISCUSSION OF RESULTS

The stability<sup>[7]</sup> of the differential delay  $(T^{TX} - T^{RX})$  as measured and of the corrected one, together with stabilities typically obtained for TWSTFT measurements for averaging times up to 100 s and with stabilities of crucial system elements, is given in Figure 5. This is a composite time and frequency stability plot; thus, from only one graph the time and frequency transfer capability of a system can be estimated<sup>[1]</sup>. Stabilities were calculated from long-term sessions



performing one measurement per second or from measurements carried out three times per week (Monday, Wednesday, Friday) during the regular TWSTFT sessions also performing one measurement per second. The results obtained from the latter ones were interpolated to one-day intervals to obtain equally spaced data for the stability calculation, but no corrections to the obtained stabilities were applied<sup>[8]</sup>. The measurements of the differential delay show flicker noise PM with a level around 100 ps. This is in agreement with results obtained for TWSTFT common-clock experiments<sup>[9]</sup>. For averaging times up to some minutes TWSTFT usually shows white-noise PM behavior as indicated in Figure 5, with the noise level depending on the actual  $C/N_0$  of the signal supplied to the modem. The ultimate limit in the currently used TWSTFT measurement scheme is given by the stability of the electronic counter used for the time interval measurements. A more critical limit seems to result from phase variations between the reference frequency used by the modem for the signal generation and the time reference to which the measurements are referred. These phase variations are reflected in CAL, the modem calibration ( $REF - PPSTX + b1$ ). Stabilities of CAL for the initially used frequency distribution system and an upgraded system are also given in Figure 5. Because CAL is not measured every second during a TWSTFT session, but a mean value of 100 measurements performed before or after a session is used, the short-term stability of CAL is crucial for the short-term stability of TWSTFT measurements.

## CONCLUSION AND ENVISAGED ACTIVITIES

Performing TWSTFT measurements between stations both equipped with a SATSIM and correcting the TWSTFT data of each station by the measured signal delay variations could considerably improve the TWSTFT stability. In a measurement setup designed for fully automated measurements, a SATSIM can easily be included and operated. Because during the SATSIM operation the earth station is transmitting, about five minutes of extra satellite time is needed. The data obtained can immediately be used to correct the TWSTFT data for possible variations of the differential signal delay of the station. At the TUG a second earth station will soon be available, allowing common clock experiments between two stations both equipped with a SATSIM and, thus, the obtaining of some more information on the stability limits of TWSTFT systems. Furthermore, the second station will be used for detailed investigations concerning temperature and humidity dependence of the signal delays in order to optimize the station design.

## ACKNOWLEDGEMENTS

The contribution of INTELSAT providing free of charge satellite transponder time and the help of W. Schladowsky and H. Peintinger (OPTV) in administrative and technical matters is gratefully acknowledged. The loan of a MITREX modem initially by the U.S. Naval Observatory and later on by Prof. Hartl, University of Stuttgart, is deeply appreciated. The work was supported by the Austrian Academy of Sciences and the Jubilee Fund of the Austrian National Bank.



## REFERENCES

- [1] D. Kirchner, H. Ressler, and R. Robnik 1995, "An automated signal delay monitoring system for a two-way satellite time transfer terminal," Proceedings of the 9th European Frequency and Time Forum (EFTF), March 1995, Besançon, France, pp. 75-79.
- [2] D. Kirchner 1991, "Two-way satellite time transfer via communication satellites", *Proc. IEEE*, 79, 983-990.
- [3] G. de Jong 1990, "Accurate delay calibration of satellite ground stations for two-way time transfer", Proceedings of the 3rd European Frequency and Time Forum (EFTF), 1989, pp. 198-203; also Proceedings of the 21st Annual Precise Time and Time Interval (PTTI) Applications and Planning Meeting, 28-30 November 1989, Redondo Beach, California, pp. 107-116.
- [4] G. de Jong 1995, "Automated delay measurement system for an earth station for two-way satellite time and frequency transfer", *Proc. 26th Annual Precise Time and Time Interval (PTTI) Applications and Planning Meeting*, 6-8 December 1994, Reston, Virginia, pp. 305-318.
- [5] J.A. DeYoung, W.J. Klepczynski, A.D. McKinley, W. Powell, P. Mai, P. Hetzel, A. Bauch, J.A. Davis, P.R. Pearce, F. Baumont, P.C. Claudon, P. Grudler, G. de Jong, D. Kirchner, H. Ressler, A. Soering, C. Hackman, and L. Veenstra 1995, "The 1994 international transatlantic two-way satellite time and frequency transfer experiment: Preliminary results", Proceedings of the 26th Annual Precise Time and Time Interval (PTTI) Applications and Planning Meeting, 6-8 December, Reston, Virginia, pp. 39-49.
- [6] J.A. Davis, P.R. Pearce, D. Kirchner, H. Ressler, P. Hetzel, A. Soering, G. de Jong, P. Grudler, F. Baumont, and L. Veenstra 1994, "Two-Way satellite time transfer experiments between six European laboratories using the INTELSAT (VA-F13) satellite," Proceedings of the 8th European Frequency and Time Forum (EFTF), 1994, Germany, Vol.I, pp. 296-314.
- [7] D.W. Allan, and A. Lepek 1993, "Trends in international timing," Proceedings of the 7th European Frequency and Time Forum (EFTF), 1993, Switzerland, pp. 221-227.
- [8] C. Hackman, and T.E. Parker, "Noise analysis of unevenly spaced time series data," to be published in *Metrologia*.
- [9] C. Hackman, S.R. Jefferts, and T.E. Parker 1995, "Common-clock two-way satellite time transfer experiments," Proceedings of the 1995 IEEE International Frequency Control Symposium, 31 May-2 June 1995, San Francisco, California, pp. 275-281.



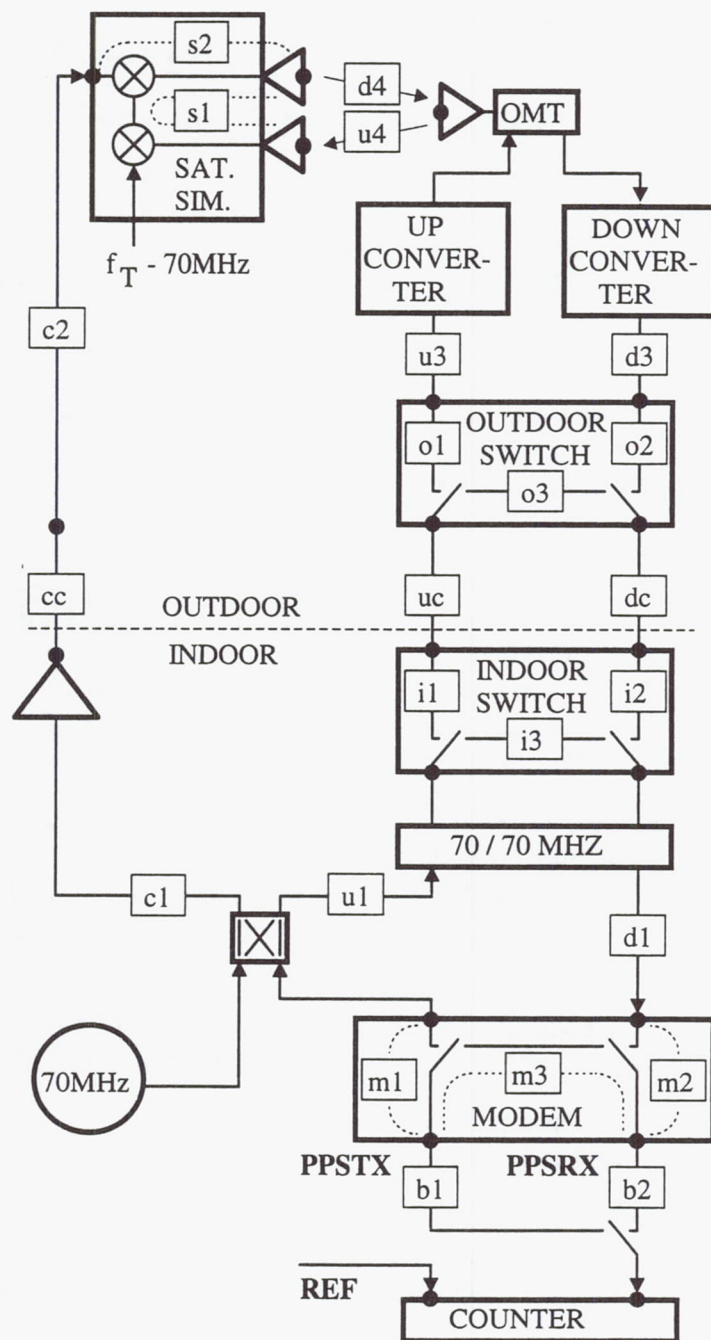


Figure 1 Station diagram showing the different signal delays and measurement loops.

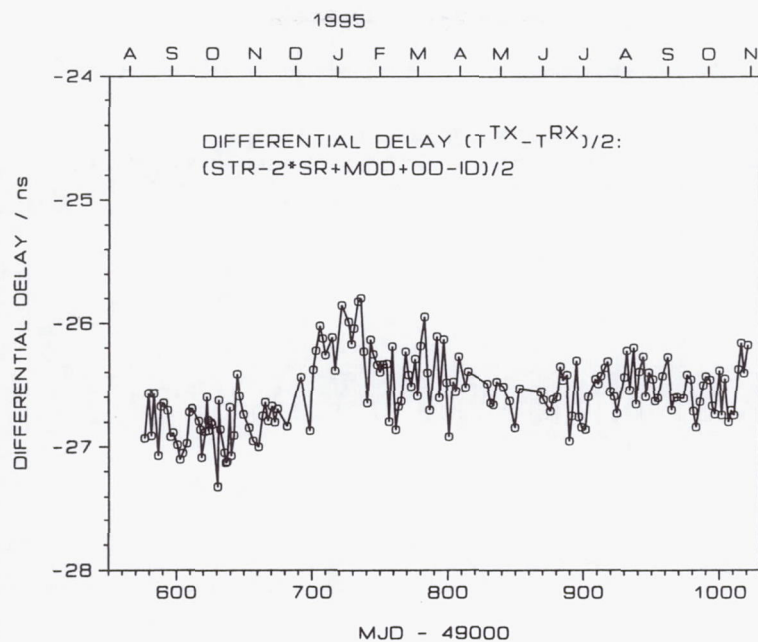


Figure 2 Differential delay  $(T^{TX} - T^{RX})/2$  computed from  $T^{TX}$  and  $T^{RX}$  as measured.

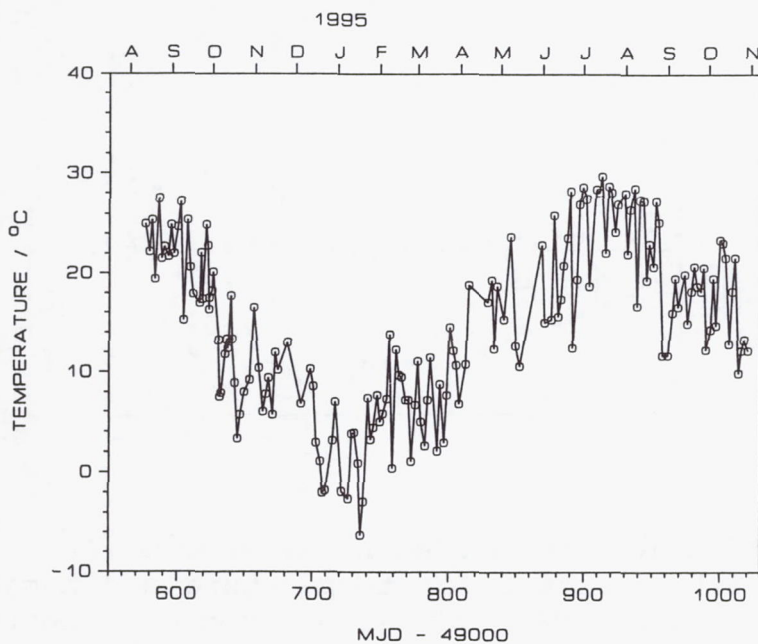


Figure 3 Outside temperature.



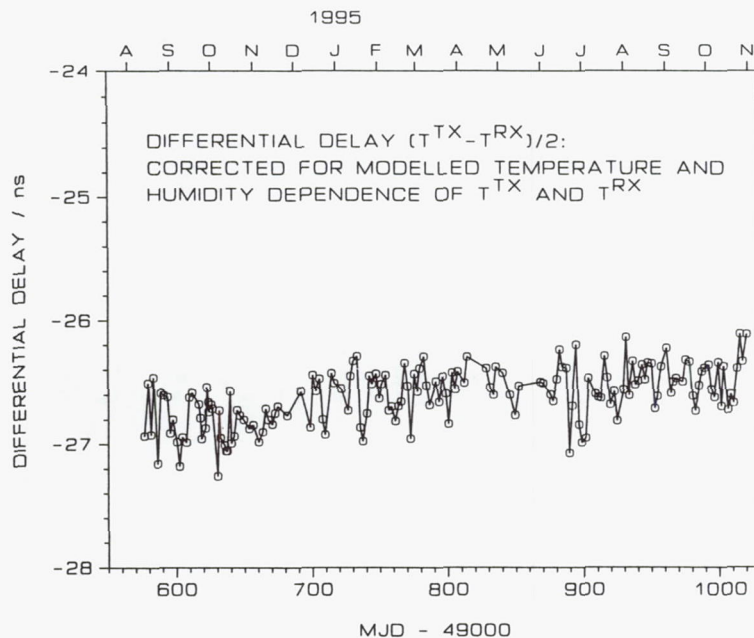


Figure 4 Differential delay  $(T^{TX} - T^{RX})/2$  computed from  $T^{TX}$  and  $T^{RX}$  corrected for modelled temperature and humidity dependence of  $T^{TX}$  and  $T^{RX}$

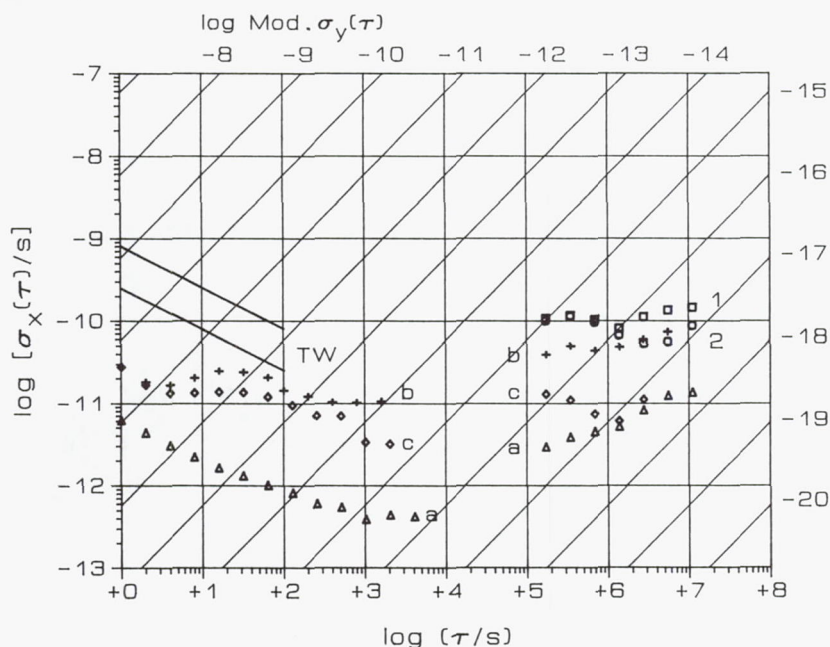


Figure 5 Stabilities of differential delays  $(T^{TX} - T^{RX})/2$  as measured (1) and corrected for temperature and humidity (2), of TWSTFT measurements (TW), of an electronic counter used for TWSTFT measurements (a), and of the modem calibration CAL for the initially used (b) and an upgraded (c) frequency and time distribution system.

## Questions and Answers

**DR. GERNOT WINKLER (USNO, RETIRED):** If you provide a correction, depending on temperature and humidity, you have to consider that humidity and temperature are strong correlators.

**DIETER KIRCHNER (TECHNICAL UNIVERSITY GRAZ):** Yes, I know.

**DR. GERNOT WINKLER (USNO, RETIRED):** It's better to use temperature and absolute water content, because that is the physical parameter which is independent of temperature — less correlated with temperature. So using absolute humidity, or grams per cubic meter water content, and temperature should give you a better result.

**DIETER KIRCHNER (TECHNICAL UNIVERSITY GRAZ):** Thank you for this comment, Dr. Winkler. But again, for the real operation, we will simply use the measured figures. Maybe I have to add an error budget is an error smaller than 50 picoseconds for one calibration measurement.



# DATA AND TIME TRANSFER USING SONET RADIO

Gary M. Graceffo  
HRB Systems  
Linthicum, Maryland 21090

## Abstract

*The need for precise knowledge of time and frequency has become ubiquitous throughout our society. The areas of astronomy, navigation and high-speed wide-area networks are among a few of the many consumers of this type of information. GPS has the potential to be the most comprehensive source of precise timing information developed to date; however, the introduction of Selective Availability has made it difficult for many users to recover this information from the GPS system with the precision required for today's systems.*

*The system described in this paper is a "SONET Radio Data and Time Transfer System." The objective of this system is to provide precise time and frequency information to a variety of end-users using a two-way data and time-transfer system. Although time and frequency transfers have been done for many years, this system is unique in that time and frequency information are embedded into existing communications traffic. This eliminates the need to make the transfer of time and frequency information a dedicated function of the communications system.*

*For this system, the Synchronous Optical Network (SONET) has been selected as the transport format from which precise time is derived. SONET has been selected because of its high data rates and its increasing acceptance throughout the industry. This paper details a proof-of-concept initiative to perform embedded time and frequency transfers using SONET Radio.*

## OVERVIEW

The SONET Radio Data and Two-Way Time-Transfer system (TTS) described in this paper is used to perform point-to-point data-and two-way time transfers between a master control site and a remote site. Each of these sites uses an ensemble of cesium clocks to maintain precise time and frequency. For the remote sites to perform as required, time-transfers must occur on a regular basis as a dedicated on-site maintenance function to maintain synchronization with the master control site. The use of embedded time-transfer technology will replace this dedicated function and allow continuous, dedicated, time transfers.

Synchronous Optical Network (SONET) is a Bellcore term for the Synchronous Digital Hierarchy (SDH) standardized by the International Telegraph and Telephone Consultative Committee (CCITT) in Europe and Asia. SONET is a high-speed fiber optic transport standard which will eliminate the different transmission schemes and rates used in Japan, Asia and the United States. SONET is a transport interface and method of transmission only; it is not a network in itself<sup>[1]</sup>. SONET is gaining wide acceptance in the telecommunications industry; therefore, it can be used to perform time transfers over many networks. The high data rates provided by SONET are very desirable for the application of time transfer. SONET



data rates range from OC-1 (51.84 Mbps) to OC-48 (2.488 Gbps) with a theoretical upper limit of OC-255 (13 Gbps). SONET is suitable for use in a broadcast medium (SONET Radio) as well.

This system is a proof of concept to demonstrate the use of an overhead byte in the SONET frame header to convey time information. The concept of using a header byte for time transfer has been detailed in a paper by M. Kihara entitled "SDH-Based Time and Frequency Transfer System"<sup>[2]</sup>. For this proof-of-concept demonstration, the synchronization will be performed during the exchange of routine message traffic between the master control site and a remote site. Due to the limited amount of transponder band width the initial proof-of-concept effort will be done at a sub-SONET rate. The modems that bridge the two networks will run at a data rate of 10 Mbps. The two networks on which the modems reside will run at an OC-3 data rate. It is anticipated that the time-transfer accuracy will be better than 3 nanoseconds and will have a frequency instability of  $7 \times 10^{-12}$  at 1 second.

In order to reduce the technical risk and to keep the development costs down, the system is designed to be modular and is comprised primarily of commercial-off-the-shelf (COTS) components. The hardware and software that comprise the communications encoder and decoder (COMDEC) unit are the only custom-designed components in the system. To maintain the philosophy of modularity, the same software and hardware are used at both the master and remote sites.

This system is the first phase of a multi-phase study. The overall goal is to embed time transfer information into the SONET overhead bytes in a variety of transmission mediums. The method has already had success over optical networks in Japan<sup>[2]</sup>.

## TIME CODE DEFINITION

The Timing Solutions Corporation (TSC), working with Judah Levine of NIST (National Institute of Standards and Technology), has detailed an approach using a single unused byte in the SONET frame header to convey the time-code<sup>[3]</sup>. TSC has attempted to maximize compatibility with a Japanese proposal to the ITU-R Working Party 7A regarding network time and frequency transfers. This system attempts to maximize compatibility with the approach set forth by TSC; however, some modifications to their approach are necessary due to bandwidth limitations in the radio link.

A SONET frame consists of two parts, a header and a synchronous payload envelope. The payload is unacceptable to convey time information because the data packets "float" within the envelope area<sup>[3]</sup>. The header, however, is not subjected to reallocation. For this reason, to achieve accurate time transfers, the header must be used to convey the timing information.

The time code is transmitted as a block of five words. Each word is represented by five bytes. The most significant bit in each time-code byte functions as an on-time marker to signal the start of a new time code sequence. The remaining seven bits in each byte are used to transmit the time-code sequence. A complete time-code sequence contains administrative information, modified Julian day (MJD) and time of day (TOD) to hundredths of a nanosecond. The time code length is flexible and can grow to meet future needs.

The first word of the time-code contains administrative information. This information includes: flags, sender's identifier and recipient's identifier. Flags include: message synchronization, primary/secondary identifier and master/slave identifier. The second word contains a message synchronization flag, message type field, a descriptive message code (ccc) field and the most



significant 28 bits of the time code. There are currently four types of messages defined. These message types are:

- Next frame contains a time mark (1111)
- NULL (1110)
- Frequency Information (0001)
- Time Information (0000)

The message type (1111) is used by the hardware and software to prepare to receive an on-time time marker to which the hardware must be synchronized. The message type NULL (1110) is used when time or frequency information is not being transmitted or to end the transmission of a time code. Message types (0001) and (0000) are used to identify the transmission of frequency or time information respectively. There are currently sixteen ccc codes identified. These codes are used to identify the type of frequency or time information being transmitted (i.e. absolute time, relative time, leap second notification, etc.)

The third word and subsequent words have the same format. Word three of the time code contains: a message synchronization flag, additional ccc information and 32 bits of time or frequency information. The third word is repeated until the entire time code is transmitted. Table 1 details the time-code sequence.

## SYSTEM DESCRIPTION

The SONET Radio Data and Two-Way Time-Transfer System is a node on a network. As shown in Figure 1, its function is to perform data and two-way time transfers between two networks. Figure 2 illustrates the architecture of the SONET Radio Data and Two-Way Time-Transfer System. The system has five component parts: Antenna unit, Transceiver unit, Modem, COMDEC unit, and the Ensemble. The communications decoder/encoder (COMDEC) unit illustrated in Figure 3 is the heart of the data and time-transfer system. The unit is designed to interface a modem to a SONET network while building or recovering a time code. The COMDEC unit is responsible for removing time information from the SONET header, passing the received time-code information to a personal computer (PC) and providing a 1 pulse per second (PPS) reference signal which is coherent with the received time-code information. Control of the COMDEC unit is through an external interface using a PC.

The procedure to initiate a time-transfer is as follows: the master control station (reference station) and the remote site each exchange time codes simultaneously. Each site sends a message type of (1111), which indicates that the next frame contains an on-time mark. The message type (1111) is used to reset the hardware and prepare to synchronize to the on-time mark. The next time byte that is transmitted has the most significant bit in the time-code byte set to 1, indicating the start of a time-code sequence. The following time-code bytes contain the message type, ccc code and the time information. The most significant bit of each subsequent frame is set to 0, indicating the on-time marker is not present. When a time-code transmission is completed a message type of "NULL" is transmitted, indicating the end of transmission.

When the COMDEC unit is in transmit mode the SONET frames to be transmitted are retrieved from the network by the SONET interface module and stored in the transmit buffer. The PC loads the transmit buffer with part of the time-transfer information and signals the digital signal processor (DSP)/controller microprocessor to begin transmission. The DSP obtains the fractional seconds part of the time code from the Transmit Time-Tag Unit and completes the time code with this information. The Transmit Frame Controller unit reads the Transmit Buffer a word at a time and sends it to the modem to be modulated, using binary phase shift keying



(BPSK), and converted from a baseband signal to an intermediate frequency (IF) of 70 MHz. The transceiver converts the IF signal to Ku-band for transmission.

When the COMDEC unit is in receive mode, it receives a bit stream that has been recovered by the modem. The COMDEC unit reconstructs the SONET frames from the recovered bit stream and records the embedded time code. The time code is placed in the receiver buffer for post processing by the PC. The time code is also loaded into a counter in the COMDEC unit. The counter is clocked using a submultiple of the recovered carrier. The counter generates a 1 PPS signal that is coherent with the transmitting site's ensemble. A Time Interval Counter (TIC) external to the COMDEC unit is used to measure the phase difference between the recovered 1 PPS signal and the station 1 PPS signal. A PC records the phase difference between the two 1 PPS signals. The recovered payload is placed in a SONET frame and the frames are sent to the appropriate devices on the network.

Once the measurement process has been completed, the two sites exchange measurements so that the relative phase offsets may be determined. Measurements are exchanged by placing the measurements in the SONET header and using the appropriate message type to identify the type of information being transmitted.

The ensemble is used to provide the data and time-transfer system with precise time and frequency information. All signals in the data and time-transfer system are coherently derived from the ensemble. The ensemble consists of a suite of three cesium clocks, two GPS receivers and a computer to continuously steer the master clock in frequency. The ensemble has a long-term instability of  $7 \times 10^{-14}$  at one second.

## RECIPROCITY

Two-way time transfer is used so that reciprocity in the path may be assumed. The measurements made at each site using the time interval counter reflect the phase difference of the two 1 PPS signals and the propagation delays. If these measurements are differenced, then the delay terms will cancel, leaving a residual of the phase difference between the two station clocks. This may be expressed as follows:

$$R(B) = B - A + TdAB \quad (\text{at site B}) \quad (1)$$

$$R(A) = A - B + TdBA \quad (\text{at site A}) \quad (2)$$

where

- $R(B)$  = time difference displayed on time interval counter at remote site (B)
- $R(A)$  = time difference displayed on time interval counter at the master site (A)
- $A$  = time displayed on clock A
- $B$  = time displayed on clock B
- $TdAB$  = aggregate of systematic delays between site A and site B
- $TdBA$  = aggregate of systematic delays between site B and site A
- $A - B$  = phase difference between clock A and clock B
- $B - A$  = phase difference between clock B and clock A

$$TdAB = TdT_A + TdAS + TdT_B + TdsB + TdrB \quad (3)$$



where

$T_{dT A}$	=	delay in the transmitter at site A
$T_{dAS}$	=	path delay from site A to satellite
$T_{dT B}$	=	transponder delay in the direction A to B
$T_{dsB}$	=	path delay from satellite to site B
$T_{drB}$	=	delay in the receiver at site B.

The delays in the receiver and the transmitter are removed through calibration. If reciprocity is assumed, then path delays and the transponder delays are equal in both directions and, therefore, cancel out. If we assume reciprocity and the sites exchange time interval measurements (i.e.  $R(A)$  and  $R(B)$ ), then each site can find its phase offset relative to the other site. If it is assumed the master station is the reference, then the remote site can determine its offset from the master clock.

The errors in the phase measurements made between the two stations are from three sources; they are: nonreciprocity in the path, noise in the measurement system and station calibration. The anticipated accumulated error as shown in Table 2 is expected to be a 2.5 nanoseconds. The primary contributor to the nonreciprocity in the system is the transponder path. This is because the upper part of the channel in the transponder will be used in one direction and the lower part of the channel will be used in the other direction. The phase ripple across the entire channel is a few nanoseconds. In order to null this effect, the transmission paths will flip-flop between the upper and lower channel in each direction. This will null the effects of transponder nonreciprocity and reduce the phase error to less than a nanosecond. Therefore, the goal of 3 nanoseconds accuracy is attainable.

## SUMMARY

Two Data and Embedded Time-Transfer Systems using a Radio SONET transport format will be built and tested. These systems are nodes on two networks and will function as a bridge between the two networks. These networks exchange data on a daily basis and perform continuous time transfers in an existing communications link. The time-transfer information needed by each site will be embedded in the SONET header during routine site-to-site communications. It is anticipated that time transfers on the order of 3 nanoseconds are very achievable with a frequency instability of  $7 \times 10^{-12}$  at one second. Testing of the system will occur, over an RF path, in the fall of 1996.

## REFERENCES

- [1] D. Spohn 1993, *Data Network Design* (McGraw Hill, New York).
- [2] M. Kihara, and A. Imaoka 1995, "SDH-based time and frequency transfer system," Proceedings of the 9th European Forum on Time and Frequency (EFTF), March 1995, Besançon, France.
- [3] S. Stein 1995, "Architecture of a two-way time transfer system using SONET OC-3 facility interface" (Timing Solutions Corporation, Boulder, Colorado).

### TIME TRANSFER FRAME FORMAT

WORD NUMBER	DEFINITION	RANGE
<b>Word 1</b>		
Byte 0		
bit 7	Message synchronization	1: on-time marker 0: all other times
bit 6	1 for primary, 0 for secondary	
bit 5	1 for master, 0 for slave	
bit 4-0	Master/Slave identifier	
Byte 1		
bit 7	Message synchronization	1: on-time marker 0: all other times
bit 6-0	Sender's ID	
Byte 2		
bit 7	Message synchronization	
bit 6-0	Recipient's ID	
Bytes 3-4		
bit 7	Message synchronization	1: on-time marker 0: all other times
bit 6-0	Reserved	
<b>Word 2</b>	Time and frequency information	
Byte 0		
bit 7	Message synchronization	1: on-time marker 0: all other times
bit 6-4	Reserved for additional information (ccc)	
bit 3-0	Message type	
Byte 1-4		
bit 7	Message synchronization	1: on-time marker 0: all other times
bit 6-0	Most significant 28 bits of time/frequency information	MJD 28 most significant bits.

Table 1



# TIME TRANSFER FRAME FORMAT(CON'T)

WORD NUMBER	DEFINITION	RANGE
<b>Word 3-0</b>		
Byte 0		
bit 7	Message synchronization	1: on-time marker 0: all other times
bit 6-4	Reserved for additional (ccc) information	
bit 3-0	Most significant 4 bits of 32 bit word	MJD 4 Least significant bits
Bytes 1-4		
bit 7	Message synchronization	
bit 6-0	7 bits of 32 bit word most significant to least significant order	1 msec $\leq T_m \leq$ 86400 sec 28 most significant bits of $T_m$
<b>Word 3-1</b>		
Byte 0		
bit 7	Message synchronization	1: on-time marker 0: all other times
bit 6-4	Reserved for additional (ccc) information	
bit 3-0	Most significant 4 bits of 32 bit word	4 least significant bits of $T_m$
Bytes 1-4		
bit 7	Message synchronization	1: on-time marker 0: all other times
bit 6-0	7 bits of 32 bit word most significant to least significant order	.25 psec $\leq T_p \leq$ 1 msec 28 most significant bits of $T_p$
<b>Word 3-2</b>		
Byte 0		
bit 7	Message synchronization	1: on-time marker 0: all other times
bit 6-4	Reserved for additional (ccc) information	
bit 3-0	Most significant 4 bits of 32 bit word	4 least significant bits of $T_p$

Table 1 (con't)

## ERROR ANALYSIS

Objective is a time-transfer with 40 nanoseconds (40,000 picoseconds) of error

$$\theta_E = \text{nonreciprocity} + \text{calibration\_errors} + \text{measurement\_noise}$$

Error sources	Magnitude (picoseconds)	
Station Calibration	200	For both stations
Nonreciprocity in path	-	
Ionospheric nonreciprocity	100	For Ku band
Tropospheric delays	<<100	For Ku band
transponders*	2000	
Measurement system	100	
	-----	
	2500	

\* - This can be eliminated with transponder multiplexing

**Table 2**



# INTERNETWORK COMMUNICATION USING SONET RADIO

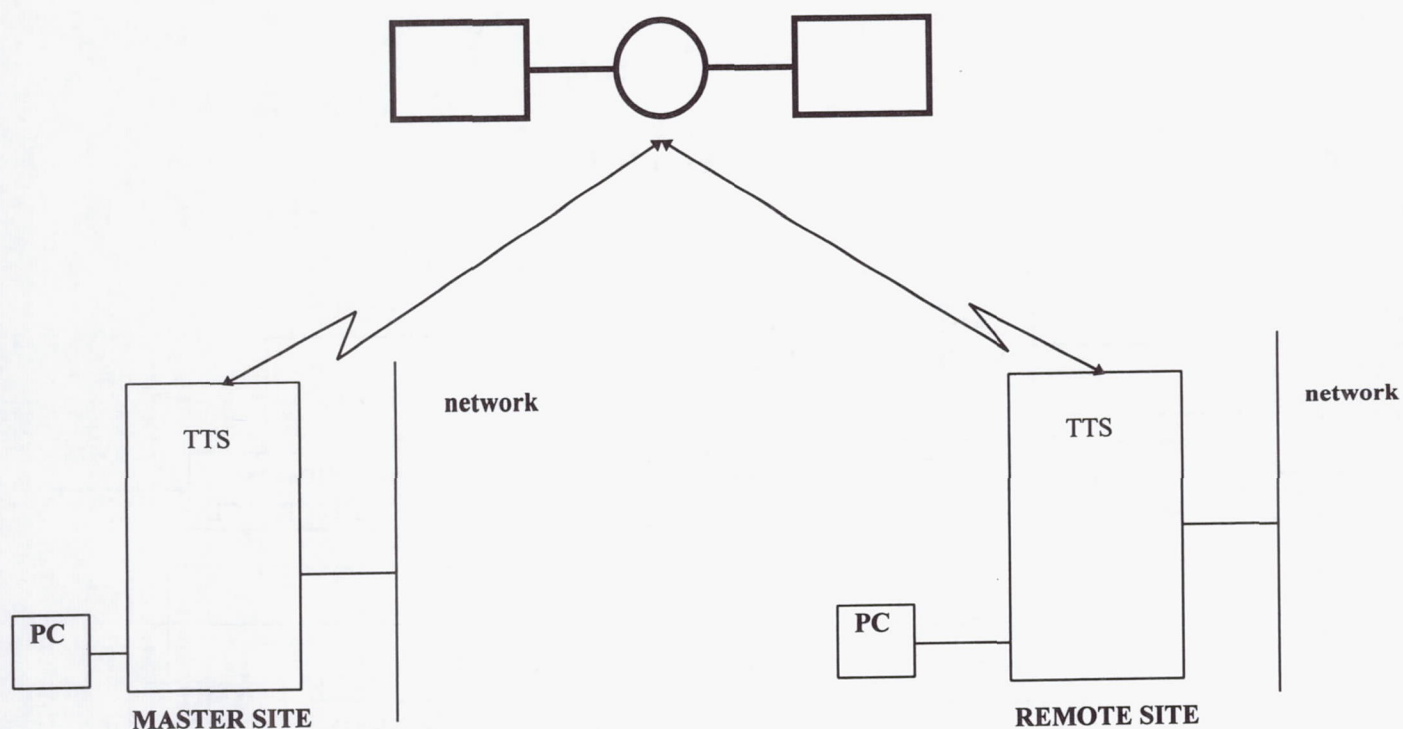


Figure 1

## SONET RADIO DATA AND TIME TRANSFER SYSTEM

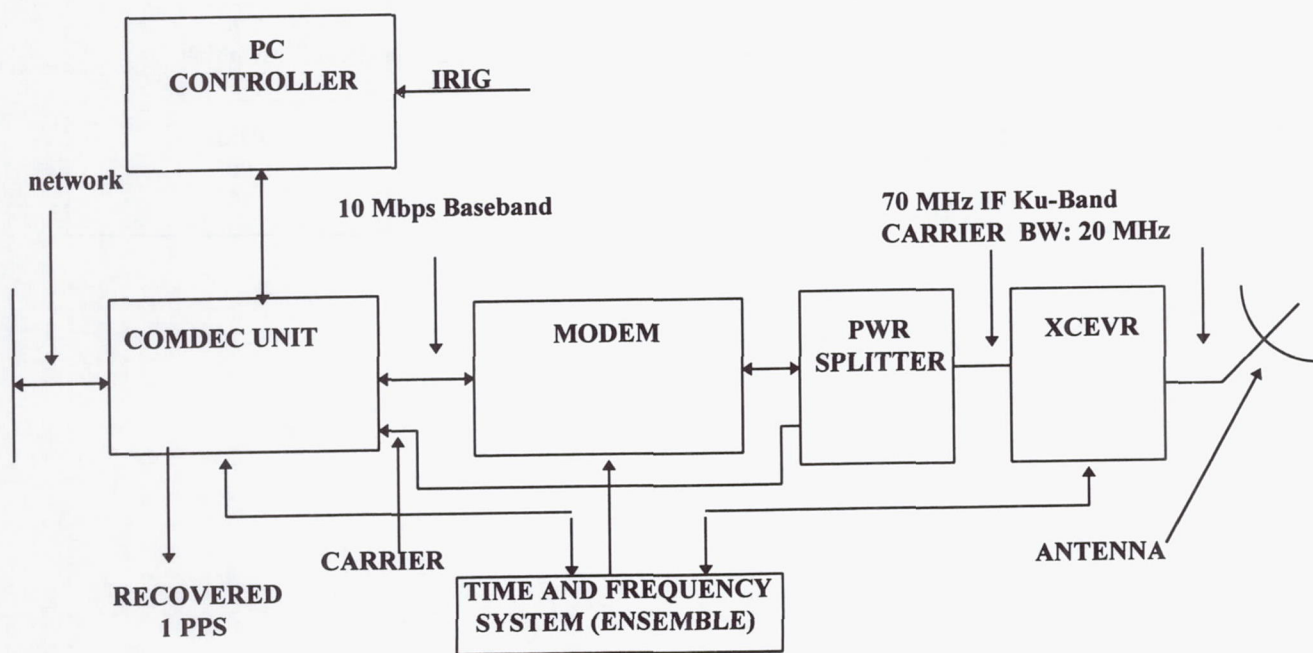


Figure 2

## COMDEC UNIT

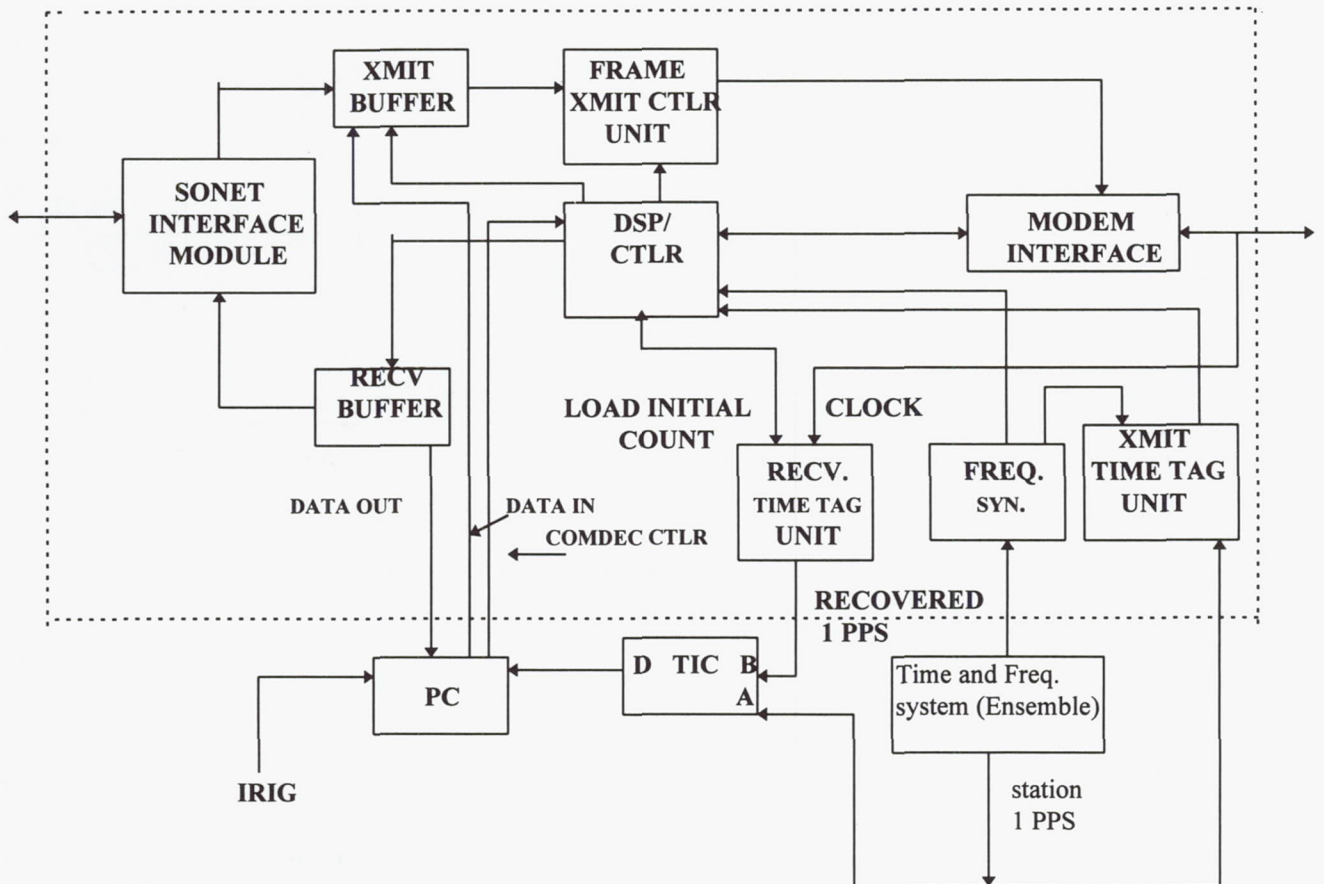


Figure 3



# VARIANCE ANALYSIS OF UNEVENLY SPACED TIME SERIES DATA

Christine Hackman and Thomas E. Parker  
National Institute of Standards and Technology  
Time and Frequency Division  
Boulder, Colorado 80303

## Abstract

We have investigated the effect of uneven data spacing on the computation of  $\sigma_x(\tau)$ . Evenly spaced simulated data sets were generated for noise processes ranging from white PM to random walk FM.  $\sigma_x(\tau)$  was then calculated for each noise type. Data were subsequently removed from each simulated data set using typical TWSTFT data patterns to create two unevenly spaced sets with average intervals of 2.8 and 3.6 days.  $\sigma_x(\tau)$  was then calculated for each sparse data set using two different approaches. First, the missing data points were replaced by linear interpolation and  $\sigma_x(\tau)$  calculated from this now full data set. The second approach ignored the fact that the data were unevenly spaced and calculated  $\sigma_x(\tau)$  as if the data were equally spaced with average spacing of 2.8 or 3.6 days. Both approaches have advantages and disadvantages, and techniques are presented for correcting errors caused by uneven data spacing in typical TWSTFT data sets.

## INTRODUCTION

Data points obtained from an experiment are often not evenly spaced. In this paper, we examine the application of  $\sigma_x(\tau) = 3^{-1/2}\tau(\text{mod}\sigma_y(\tau))^{[1]}$  to the unevenly spaced time-series data obtained from two-way satellite time and frequency transfer (TWSTFT). We do so by using  $\sigma_x(\tau)$  with both evenly and unevenly spaced simulated data of known power-law noise type and magnitude. The noise types examined are white phase modulation (WHPM), flicker phase modulation (FLPM), white frequency modulation (WHFM), flicker frequency modulation (FLFM), and random walk frequency modulation (RWFM)<sup>[2]</sup>.

Vernotte *et al.*<sup>[3]</sup> studied the analysis of noise and drift in unevenly spaced pulsar data. However, the data obtained from pulsar studies are much more sparse in time, with only about 2% of the possible data available. In TWSTFT, the task is less daunting: time transfers are typically measured on Monday, Wednesday, and Friday, so, in a perfect world, we would have a data density of 3 data points present out of a possible 7.

This paper is not intended to be a rigorous treatment of how to calculate  $\sigma_x(\tau)$  in all possible cases of unevenly spaced data. Rather, our purpose is to suggest methods and corrections which may be applied to data such as those produced by TWSTFT in order to obtain a more accurate assessment of the underlying time stability and noise type.



The National Institute of Standards and Technology (NIST) regularly performs time transfers with several laboratories in North America and Europe. Two of these laboratories are the United States Naval Observatory (USNO) in Washington, D.C. and the Van Swinden Laboratories (VSL) in Delft, the Netherlands. Typical data sets covering a 384-day period were chosen from the NIST-USNO and NIST-VSL time transfers to be used as templates.

## METHOD OF EVALUATION

We evaluated the use of  $\sigma_x(\tau)$  with unevenly spaced data having the five different power-law noise types: WHPM, FLPM, WHFM, FLFM, and RWFM. Ten independent data files were generated for each noise type. The WHPM, WHFM, and RWFM files were generated using a random-number generator and integration. The FLPM and FLFM files were generated according to the algorithm of Kasdin and Walter<sup>[4]</sup>. All 10 data files of each noise type had 384 evenly spaced data points spaced one day apart. In the next step, we removed data points from each file so that the remaining data points aligned with the data points obtained from NIST-USNO or NIST-VSL TWSTFT. This produced files containing 137 or 108 unevenly spaced data points, respectively. The missing data points were then filled in by linear interpolation between the remaining data points. After this last step, there are once again 384 evenly spaced data points. Therefore, for each simulated data file of each noise type, we finally had five data files:

- File Type 1: the originally generated 384 evenly spaced data points with known noise type and magnitude.
- File Type 2: a data file of 137 data points spaced as in the NIST-USNO time transfers. This file is obtained by removing the appropriate data points from File 1. The average spacing (see below) is 2.816 days.
- File Type 3: File 2 with the missing data points filled in via linear interpolation.
- File Type 4: a data file of 108 data points spaced as in the NIST-VSL time transfers. This file, like File 2, is obtained by removing points from File 1. The average spacing (see below) is 3.579 days.
- File Type 5: File 4 with the missing data points filled in by linear interpolation.

Having created all 50 files for a given noise type, we then performed a  $\sigma_x(\tau)$  analysis of each file. For the data files with even spacing (File Types 1, 3, and 5 above) we computed  $\sigma_x(m\tau_{0,even})$  in the usual fashion<sup>[1]</sup>, where  $m = 1, 2, 4, 8, 16, 32, 64, 128$  and  $\tau_{0,even} = 1$  day. For the files with unevenly spaced data (File Types 2 and 4) we computed  $\sigma_x(\tau)$  by treating the adjacent data points as if they were evenly spaced, with  $\tau_{0,avg}$  calculated as follows:

$$\tau_{0,avg} = (MJD_{last} - MJD_{first}) / (N - 1) \quad (1)$$

where  $MJD_{first}$  and  $MJD_{last}$  are the time tags for the first and last data points, and  $N$  is the number of data points. For File Type 2,  $\tau_{0,avg} = 2.816$  days, and for File Type 4,  $\tau_{0,avg} = 3.579$  days. In both of these latter cases, we computed  $\sigma_x(n\tau_{0,avg})$  for  $n = 1, 2, 4, 8, 16$ , and 32. Having obtained  $\sigma_x(\tau)$  vs  $\tau$  for all 50 files, we then computed the average values of  $\sigma_x(\tau)$  for each file type. Therefore, for each power-law noise type, we finally have five plots of  $\sigma_x(\tau)$  vs



$\tau$ :

1. Average  $\sigma_x(\tau) = 1, 2, 4, 8, 16, 32, 64,$  and  $128$  days) for File Type 1, that is, the files with known noise type. This plot shows the "correct" values for  $\sigma_x(\tau)$ .
2. Average  $\sigma_x(\tau) = 2.816, 5.632, 11.264, 22.528, 45.056,$  and  $90.112$  days) for File Type 2. This represents the results we obtain by using unevenly spaced data with the NIST-USNO distribution.
3. Average  $\sigma_x(\tau) = 1, 2, 4, 8, 16, 32, 64,$  and  $128$  days) for File Type 3. This represents the results we obtain by taking unevenly spaced data with the NIST-USNO distribution, performing linear interpolation to make an evenly spaced data file, and then performing the  $\sigma_x(\tau)$  analysis.
4. Average  $\sigma_x(\tau) = 3.579, 7.158, 14.316, 28.632, 57.264,$  and  $114.528$  days) for File Type 4. This represents the results we obtain by using unevenly spaced data with the NIST-VSL distribution.
5. Average  $\sigma_x(\tau) = 1, 2, 4, 8, 16, 32, 64,$  and  $128$  days) for File Type 5. This represents the results we obtain by taking unevenly spaced data with the NIST-VSL distribution, performing linear interpolation to make an evenly spaced data file, and then performing the  $\sigma_x(\tau)$  analysis.

Finally, for each average value of  $\sigma_x(\tau)$  for File Types 2–5, we computed a "correction factor." The correction factor is defined as

$$\text{correction factor}(\sigma_x(\tau)_{\text{File Type } j}) = \frac{\text{avg } \sigma_x(\tau)_{\text{File Type } 1}}{\text{avg } \sigma_x(\tau)_{\text{File Type } j}}. \quad (2)$$

In other words, multiplying the  $\sigma_x(\tau)$  values obtained using File Type  $j$  by the correction factors for File Type  $j$  produces the correct value for  $\sigma_x(\tau)$  as given by File Type 1. Because the  $\tau$  values for File Types 2 and 4 do not match the  $\tau$  values for File Type 1, various types of interpolation were used to obtain the correction factors for these two file types. The details of obtaining the correction factors for the different noise types and file types are discussed in the next section.

## RESULTS

Figures 1–5 show the results obtained for the noise types WHPM, FLPM, WHFM, FLFM, and RWFM. Each of the points shown corresponds to the mean of ten values. The standard deviation of each set of ten values was also computed, but, for visual clarity, error bars indicating 11 standard deviation are shown only on the File Type 1 (i.e., correct) values. Approximately the same size error bars should be applied to each of the file type curves.

Figure 1 shows the results obtained for white PM noise. There are several important points here. First of all, File Types 3 and 5 (interpolating unevenly spaced data to form evenly spaced

data) yield values of  $\sigma_x(\tau)$  which are much too small when  $\tau$  is less than the  $\tau_{0,avg}$  of the corresponding unevenly spaced data set. On the other hand, File Types 2 and 4 (the unevenly spaced data) yield  $\sigma_x(\tau)$  values which have the  $-1/2$  slope appropriate to white PM<sup>[1]</sup>, but which are consistently too high. In fact, for  $\tau \geq 8$  days, both of the methods used converge to yield approximately the same too-large values for  $\sigma_x(\tau)$ . For File Types 2 and 4, the white PM correction factor is in theory constant for all values of  $\tau$  and can be expressed as:

$$\text{correction factor (WHPM)} = \left( \frac{\tau_{0,even}}{\tau_{0,avg}} \right)^{1/2} \quad (3)$$

This occurs because with WHPM noise each data point in the time series is independent of all others.

Figure 2 shows the flicker PM results. Once again, File Types 3 and 5 yield values of  $\sigma_x(\tau)$  which are too small at short averaging times. Also, the lower- $\tau$  values of  $\sigma_x(\tau)$  for File Types 2 and 4 are again too high. However, the results obtained from all file types converge toward the correct value as  $\tau$  increases. Similar results are obtained for white FM (Figure 3) and flicker FM (Figure 4).

Figure 5 shows the RWFM results. Here, the use of interpolated data (File Types 3 and 5) provides virtually the same results as the originally generated data file (File Type 1) and the use of unevenly spaced data (File Types 2 and 4) provides values of  $\sigma_x(\tau)$  which are too large at small  $\tau$ . In fact, as we progress from the WHPM process to the low-frequency-dominated noise processes (e.g., RWFM)<sup>[2]</sup>, the use of linear interpolation to fill in missing data points becomes an increasingly better approximation of the truth. For lower values of  $\tau$ , using the unevenly spaced data becomes an increasingly worse approximation of the truth. As we progress from FLPM to RWFM, the results obtained using all methods converge on the correct value as  $\tau$  increases.

>From the results shown in Figures 1-5 we have computed correction factors. Table 1 shows the correction factors obtained from the file types (3 and 5) which have evenly spaced data. These correction factors were obtained by simply taking the ratio

$$\frac{\sigma_x(m\tau_{0,even})_{FileType1}}{\sigma_x(m\tau_{0,even})_{FileType3or5}}.$$

Tables 2-3 show the correction factors obtained for the file types (2 and 4) with unevenly spaced data. Because the averaging times for the unevenly spaced files (e.g. 2.816, 5.632, ..., etc. days for File Type 2) do not match the averaging times for File Type 1 (1, 2, 4, ..., etc. days), we cannot simply take a ratio of two values to get the correction factor. Generally, interpolation of some sort is required. Note that the correction factors for WHPM in Tables 2 and 3 all fall within 10% of the values calculated from Equation (3).



## DISCUSSION

There is, unfortunately, no way to apply these results blindly. The user will need to have an idea of what sort of noise types make sense in the context of his measurement. Initially, one should construct one  $\log \sigma_x(\tau)$  vs  $\log(\tau)$  plot using the original set of unevenly spaced data and one  $\log(\sigma_x(\tau))$  vs.  $\log(\tau)$  plot using a full data set formed by linear interpolation.

At medium-to-large averaging times (in our analysis,  $\tau \geq 8$  days), almost all methods, in their uncorrected state, provide the correct slope for the  $\log \sigma_x(\tau)$  vs  $\log(\tau)$  plot. For WHPM, the unevenly spaced data give the correct slope at all values of  $\tau$ . Thus, the user can determine which power-law noise process dominates at medium-to-long averaging times. (The exception to this rule occurs when RWFM predominates, and the unevenly spaced data are used to make the  $\log \sigma_x(\tau)$  vs.  $\log(\tau)$  plot. In this case, the slope of the plot is slow in converging to the correct  $+3/2$  value.) The more difficult part arises when the value of  $m$  in  $\tau = m\tau_0$  is small. It is here that we see the largest effects of not having an evenly spaced data set. In addition, in this regime the noise process which dominates a measurement often changes from one type to another.

If data are recorded on Monday, Wednesday, and Friday, it will be impossible to get a reliable estimate of  $\sigma_x(\tau = 1 \text{ day})$  — that information simply is not available. We can, however, make a fair estimate of  $\sigma_x(\tau = 2 \text{ days})$  in this case because Monday-Wednesday and Wednesday-Friday are each two-day intervals. To be completely safe, one could avoid stating values of  $\sigma_x(\tau)$  for  $\tau < \tau_{0,avg}$ . Finally, in this analysis, the ratio of the data length (384 days) to  $\tau_{0,avg}$  (2.816 and 3.579 days) was always greater than 100; therefore, it may not be appropriate to use these results with short, sparse data sets.

If there is only one, known, noise type present, then the correction factors shown in Tables 1-3 can be applied. Unless one has exactly the same average data spacing as we did, some interpolation may be needed in order to use the correction factors. Fortunately, the values of most of the correction factors are not strongly dependent on the average spacing for the range of spacing that was examined. If the noise type is not known, one could begin by deciding whether their results contain only measurement noise, or if there is a mixture of measurement noise and clock noise. Examples of the former are common-clock or closure TWSTFT experiments. An example of the latter is performing TWSTFT between two remotely located clocks. We examine each of these situations below.

## MEASUREMENT NOISE

If the results contain only measurement noise, then the noise type will most likely be white PM or flicker PM. Fortunately, as Figure 1 shows, if WHPM is the dominant noise type, the  $\log \sigma_x(\tau)$  vs  $\log(\tau)$  plot for the unevenly spaced data will have a clear  $-1/2$  slope and it will be obvious that the WHPM corrections should be applied. This method was used in Reference 5. Similarly, if the  $\log \sigma_x(\tau)$  vs  $\log(\tau)$  plot has zero slope at large  $\tau$  (Figure 2), then apply the FLPM corrections. In this case it is important to be certain that the noise type at large  $\tau$  has been correctly ascertained because, if the noise type is FLPM, the corrections which are applied at large  $\tau$  are fairly small. If the noise type is WHPM, the corrections which are



applied at large  $\tau$  are relatively large.

## COMBINATION OF CLOCK NOISE AND MEASUREMENT NOISE

If the experiment measures clock behavior (or some other quantity which is characterized by a low-frequency-dominated noise type), then the situation becomes more complicated because the results will contain a mixture of noise types — the noise type associated with the measurement and the noise type(s) associated with the behavior of the clocks under study. We have evaluated various analysis techniques and have arrived at the following recommendations which combine ease of use with acceptable accuracy.

First, examine the  $\sigma_x(\tau)$  plots for evidence of measurement noise (WHPM, FLPM). The simplest way to see if there is any measurement noise is to look at the  $\sigma_x(\tau)$  plot of the interpolated data set in the region where  $\tau$  is small to medium. As Figures 1-3 show, for WHPM, FLPM, and WHFM, the  $\sigma_x(\tau)$  plot of the interpolated data will curve down as  $\tau$  decreases to approach  $\tau = 1$  day. In the case of FLFM, the  $\sigma_x(\tau)$  plot of the interpolated data makes a straight line as  $\tau$  decreases. In the case of RWFM, the  $\sigma_x(\tau)$  plot curves up slightly as  $\tau$  decreases. Therefore, if the curve is downward at small  $\tau$  and if there is evidence of a flat transition area at medium  $\tau$ , there is probably significant measurement noise present.

If there indeed is measurement noise mixed in with the long-term noise, we suggest the following procedure (hereafter called the “hybrid method”): compute  $\tau_{0,avg}$  from the unevenly spaced data and then simply use the  $\sigma_x(\tau)$  values obtained from the interpolated data for  $\tau > \tau_{0,avg}$ . Then, estimate  $\sigma_x(m\tau_{0,even})$ , where  $m\tau_{0,even}$  is the largest integral multiple of  $\tau_{0,even}$  that is less than  $\tau_{0,avg}$ , as follows:

1. Using the values of  $\log \sigma_x(\tau = \tau_{0,avg})$  and  $\log \sigma_x(\tau = 2\tau_{0,avg})$  obtained from the unevenly spaced data, perform a linear extrapolation to smaller  $\tau$  to obtain an estimate for  $\log \sigma_x(\tau = m\tau_{0,even})$  for the unevenly spaced data set.
2. Compute the average of  $\log \sigma_x(\tau = m\tau_{0,even})$  obtained from Step 1 and  $\log \sigma_x(\tau = m\tau_{0,even})$  obtained from the interpolated data set.
3. Use this average value as an estimate of the correct value of  $\log \sigma_x(\tau = m\tau_{0,even})$ .

For example, the NIST-USNO data have  $\tau_{0,avg} = 2.816$  days. Therefore, to obtain values of  $\sigma_x(4 \text{ days} \leq \tau \leq 128 \text{ days})$  we would use the  $\sigma_x(\tau)$  values obtained from the interpolated data. To get an estimate of  $\sigma_x(\tau = 2 \text{ days})$  we would use the three steps outlined above. Further examples of this process are presented below.

This technique works because, for typical clock noise types (WHFM, FLFM, RWFM), the uncorrected values obtained from the interpolated data set are a pretty good estimate of the true values for medium to long averaging times. For measurement noise types WHPM, FLPM, and WHFM, at small values of  $\tau$ , taking the average of the logarithm of  $\sigma_x(\tau)$  associated with the interpolated and the unevenly spaced data sets yields an acceptable estimate of the true value of  $\sigma_x(\tau)$ . If inspection of the  $\sigma_x(\tau)$  plots reveals no hint of measurement noise (i.e., it appears that clock noise dominates even at small  $\tau$ , then determine the noise type from the



large- $\tau$  values of  $\sigma_x(\tau)$  and then apply the appropriate correction factors from Table 1 to the  $\sigma_x(\tau)$  values obtained from the interpolated data set.

We now show three examples of the analysis of mixed noise types, ranging from situations in which the measurement noise dominates out to medium  $\tau$  to situations in which the measurement noise is quickly overwhelmed by clock behavior. In Combination 1 (Figures 6a–6b), we see a case in which inspection of the initial  $\sigma_x(\tau)$  plots (Figure 6a) reveals obvious signs of the presence of both measurement and clock noise. The average data spacing is 2.816 days. As Figure 6b shows, using the hybrid method provides very good estimates of the correct values of  $\sigma_x(\tau)$ : the largest error is only 10% of the true  $\sigma_x(\tau)$ . In addition, we do not need to know precisely what types of noise are present (in this case, WHPM and WHFM) in order to arrive at the final estimates for  $\sigma_x(\tau)$ . Finally, we do not attempt to obtain a value for  $\tau = 1$  day.

In Combination 2, we again see signs of both measurement noise and clock noise in the initial  $\sigma_x(\tau)$  plots (Figure 7a). The average data spacing for Combinations 2 and 3 (see below) is 3.008 days. As Figure 7b shows, the hybrid method again provides a good estimate of the correct values for this combination of WHPM and FLFM.

In Combination 3, it is difficult to tell if there is any measurement noise present. The  $\sigma_x(\tau)$  plot of the interpolated data set exhibits a very faint downward curve as  $\tau$  decreases toward 1 day, but other than that, it looks like FLFM (Figure 8a). We have used both the hybrid technique and the simple application of the FLFM corrections (Table 1). As Figure 8b shows, the FLFM corrections work marginally better. As it turns out, the true  $\sigma_x(\tau)$  curve shows clear evidence of measurement noise (WHPM) only at  $\tau = 1$  day — a time interval about which we can gain no information from the sparse ( $\tau_{0,avg} = 3.008$  days) data set.

## CONCLUSIONS

We have used two typical TWSTFT time series data sets to investigate the impact of unevenly spaced data on the calculation of  $\sigma_x(\tau)$ . We have analyzed simulated data sets that have had points removed to match the TWSTFT data patterns.  $\sigma_x(\tau)$  was calculated from these sparse data sets using two techniques. One involves analyzing the sparse data as if they were evenly spaced with an average time interval, and the second uses interpolated data to recreate an evenly spaced data set. Correction factors for both approaches have been calculated for noise processes ranging from WHPM to RWFM. For all of the noise processes except WHPM, the values of  $\sigma_x(\tau)$  calculated with either of the two approaches converge on the correct values at large  $\tau$ . However, significant errors may be introduced for small  $\tau$ . Finally, we suggest techniques for estimating correct values of  $\sigma_x(\tau)$  in situations where the type of noise is unknown or where more than one noise type is present.

## ACKNOWLEDGEMENTS

The authors thank Judah Levine, Don Sullivan, Matt Young (all from the National Institute of Standards and Technology), and Jim DeYoung (United States Naval Observatory) for their useful comments concerning this manuscript.

## REFERENCES

- [1] D.W. Allan, M.A. Weiss, and J.L. Jespersen 1991, "*A frequency-domain view of time-domain characterization of clocks and time and frequency distribution systems*, Proceedings of the 45th Annual Symposium on Frequency Control, 29-31 May 1991, Los Angeles, California, pp. 667-678.
- [2] D.W. Allan 1987, "*Time and frequency (time-domain) characterization, estimation, and prediction of precision clocks and oscillators*," **IEEE Trans. Ultrasonics, Ferroelectrics, and Frequency Control**, 1987, UFFC-34, 647-654.
- [3] F. Vernotte, G. Zalamasky, and E. Lantz 1994, "*Noise and drift analysis of non-equally spaced timing data*," Proceedings of the 25th Annual Precise Time and Time Interval (PTTI) Applications and Planning Meeting, 29 November-2 December 1993, pp. 379-388.
- [4] N.J. Kasdin, and T. Walter 1992, "*Discrete simulation of power law noise*," Proceedings of the 1992 IEEE Frequency Control Symposium, 27-29 May 1992, Hershey, Pennsylvania, pp. 274-283.
- [5] C. Hackman, S.R. Jefferts, and T. Parker 1995, "*Common-clock two-way satellite time transfer experiments*," Proceedings of the 1995 IEEE Frequency Control Symposium, 31 May-2 June 1995, San Francisco, California, pp. 275-281.



Table 1: Correction Factors for File Types 3 and 5.

$\tau$ (days)	WHPM		FLPM		WIIFM		FLFM		RWFM	
(days)	USNO	VSL	USNO	VSL	USNO	VSL	USNO	VSL	USNO	VSL
1.0	4.02	4.74	3.28	4.02	2.71	3.24	1.94	2.15	1.22	1.23
2.0	1.56	1.83	1.51	1.85	1.51	1.80	1.38	1.53	1.16	1.18
4.0	0.88	0.93	1.07	1.33	1.16	1.32	1.13	1.24	1.07	1.11
8.0	0.67	0.64	0.98	1.01	1.05	1.13	1.04	1.08	1.02	1.06
16.0	0.60	0.53	0.98	0.96	1.01	1.02	1.01	1.02	1.01	1.02
32.0	0.61	0.57	0.95	0.94	1.00	1.00	1.00	1.01	1.00	1.00
64.0	0.58	0.53	0.91	0.93	1.00	1.00	1.00	1.00	1.00	1.00
128.0	0.50	0.49	1.02	1.08	1.00	1.00	1.00	1.00	1.00	1.00

Table 2. Correction Factors for File Type 2.

$\tau$ (days)	WHPM	FLPM	WHFM	FLFM	RWFM
2.816	0.60	0.67	0.80	0.64	0.16
4.0	0.59	0.71	0.87	0.76	0.27
5.632	0.59	0.81	0.92	0.86	0.41
8.0	0.58	0.85	0.95	0.94	0.57
11.264	0.58	0.90	0.97	0.99	0.71
16.0	0.57	0.94	0.99	1.01	0.84
22.528	0.57	0.97	1.00	1.01	0.92
32.0	0.56	0.94	1.00	1.01	0.97
45.056	0.56	0.89	1.02	1.01	1.00
64.0	0.55	0.88	1.04	1.02	1.00
90.1128	0.55	0.95	1.08	1.05	1.00

Table 3. Correction Factors for File Type 4.

$\tau$ (days)	WHPM	FLPM	WHFM	FLFM	RWFM
3.579	0.49	0.65	0.80	0.50	0.12
4.0	0.49	0.66	0.82	0.56	0.14
7.158	0.50	0.80	0.91	0.81	0.33
8.0	0.50	0.81	0.92	0.85	0.38
14.316	0.50	0.91	0.97	0.94	0.59
16.0	0.50	0.91	0.98	0.95	0.63
28.632	0.51	0.91	1.00	0.93	0.78
32.0	0.51	0.90	1.01	0.92	0.80
57.264	0.52	0.80	1.03	0.92	0.90
64.0	0.52	0.81	1.04	0.92	0.93
114.528	0.52	1.04	1.09	1.06	1.10

Average  $\sigma_x(\tau)$  vs.  $\tau$  for WHPM

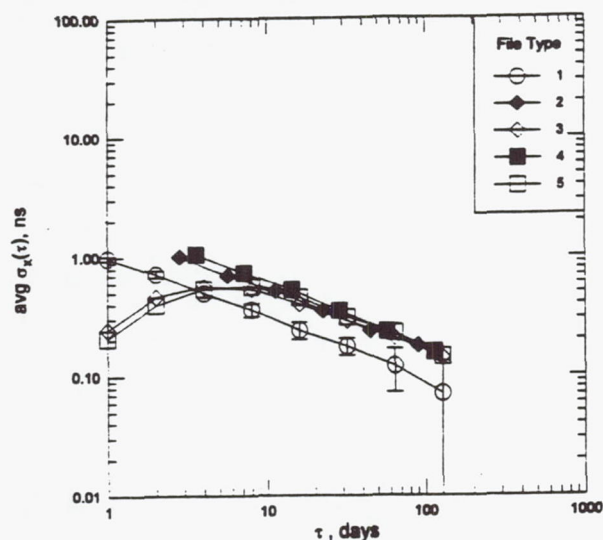


Figure 1.

The average values of  $\sigma_x(\tau)$  obtained from simulated WHPM data. "File Type 1" indicates the correct values obtained from the original evenly spaced simulated data. "File Type 2" and "File Type 3" show the results obtained when some of the original data points are deleted, thus forming an average data spacing of 2.816 days, and then the remaining points analyzed two different ways. "File Type 4" and "File Type 5" indicate results obtained when data are decimated to produce an average data spacing of 3.579 days. For visual clarity, the error bars are not shown for File Types 2-5. However, the sizes of the missing error bars are approximately the same as those shown for File Type 1.

Average  $\sigma_x(\tau)$  vs.  $\tau$  for FLPM

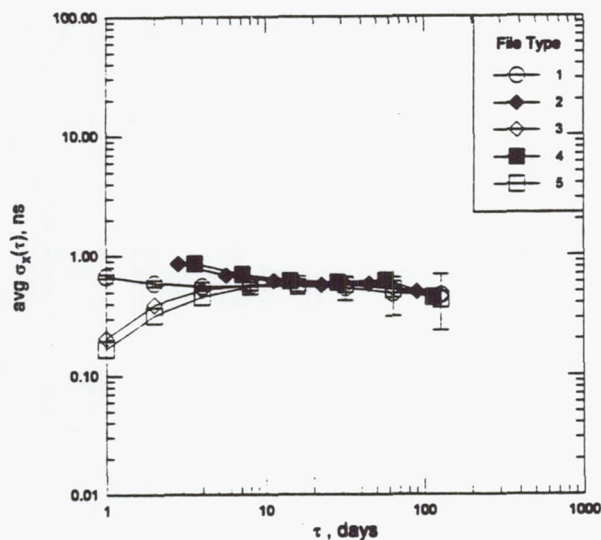


Figure 2.

The average values of  $\sigma_x(\tau)$  obtained from simulated FLPM data.

Average  $\sigma_x(\tau)$  vs.  $\tau$  for WHFM

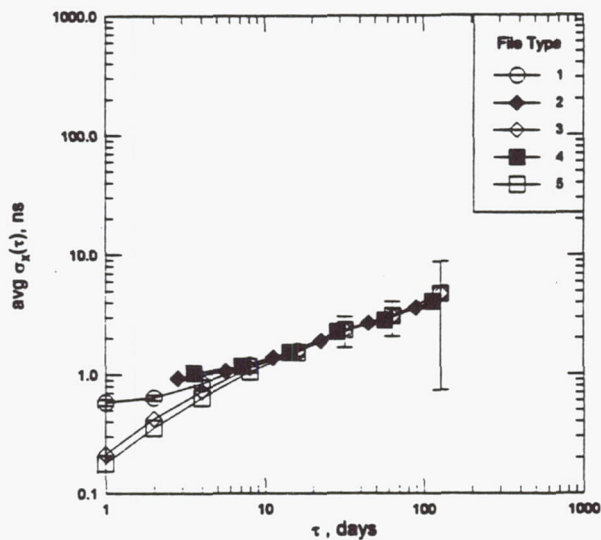


Figure 3.

The average values of  $\sigma_x(\tau)$  obtained from simulated WHFM data.



Average  $\sigma_x(\tau)$  vs.  $\tau$  for FLFM

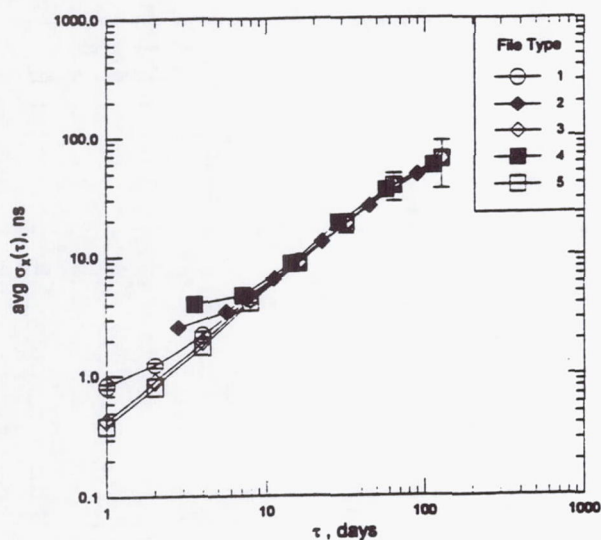


Figure 4.

The average values of  $\sigma_x(\tau)$  obtained from simulated FLFM data.

Average  $\sigma_x(\tau)$  vs.  $\tau$  for RWFM

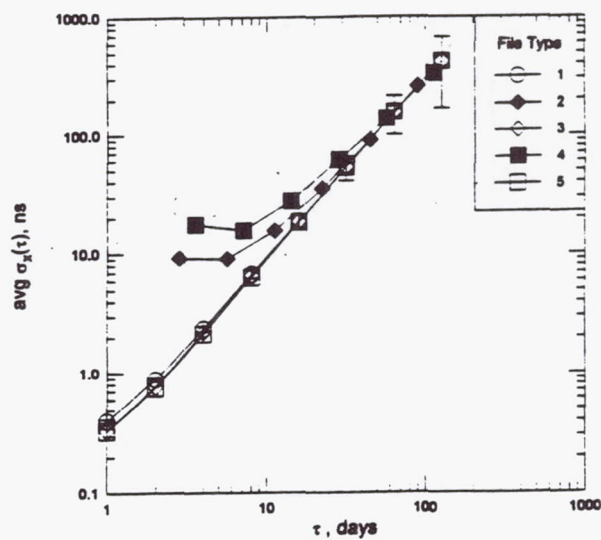


Figure 5.

The average values of  $\sigma_x(\tau)$  obtained from simulated RWFM data.

COMBINATION 1

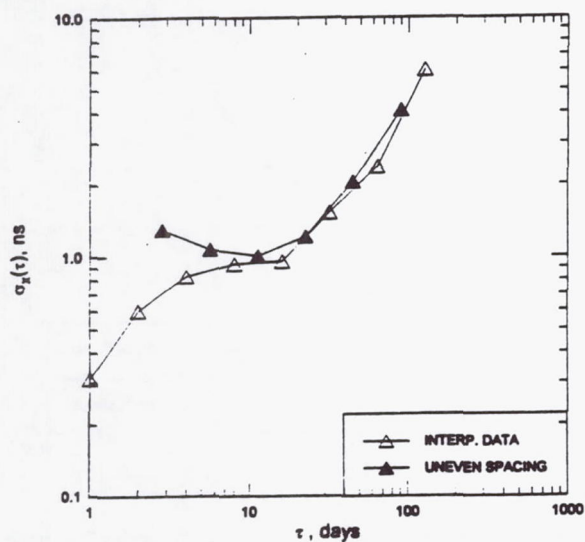


Figure 6a.

Uncorrected  $\sigma_x(\tau)$  values obtained from a sparse data set with a mixture of WHPM and WHFM noise types.

COMBINATION 1

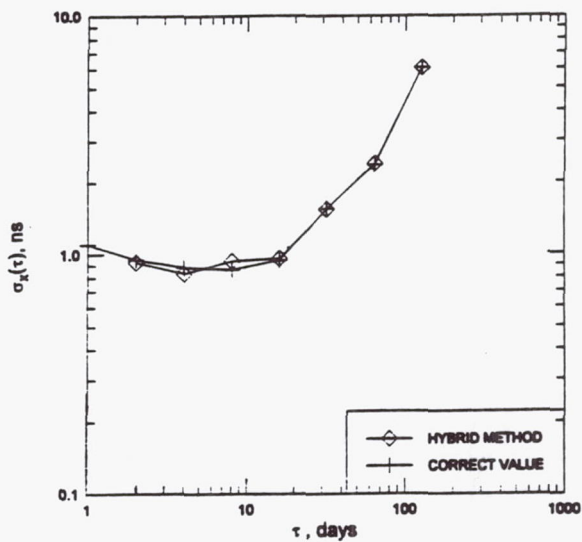


Figure 6b.

Corrected values of  $\sigma_x(\tau)$  obtained using the "hybrid" method and the values obtained from the original, evenly spaced data set.

## COMBINATION 2

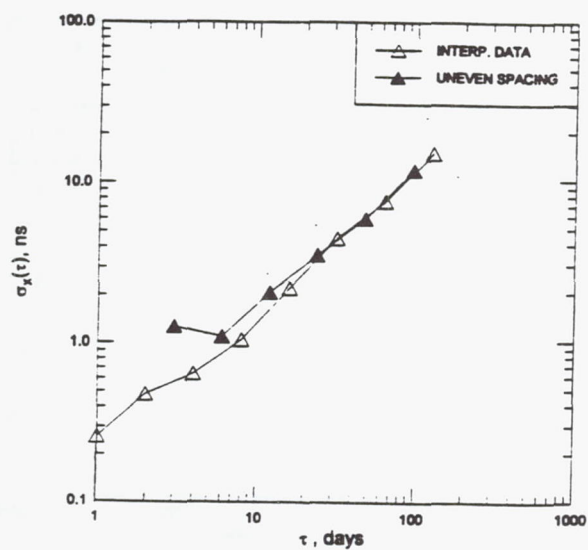


Figure 7a.

Uncorrected  $\sigma_X(\tau)$  values obtained from a sparse data set with a mixture of WHPM and FLFM noise types.

## COMBINATION 2

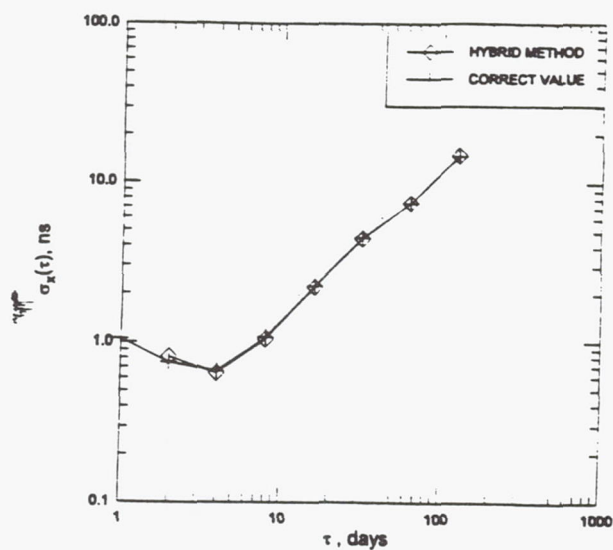


Figure 7b.

Corrected values of  $\sigma_X(\tau)$  obtained using the "hybrid" method and the values obtained from the original, evenly spaced data set.

## COMBINATION 3

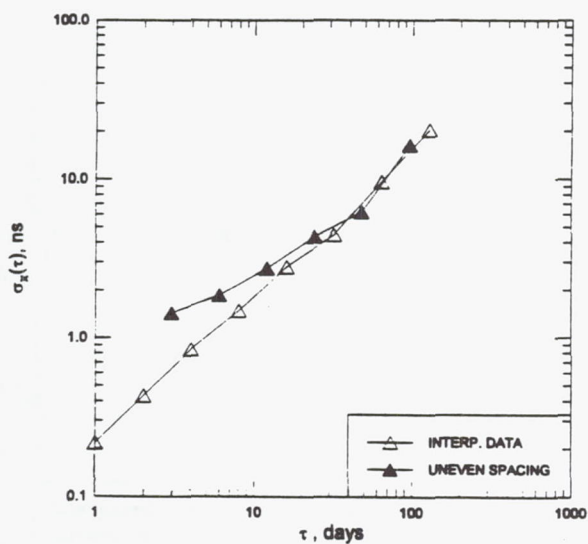


Figure 8a.

Uncorrected  $\sigma_X(\tau)$  values obtained from a sparse data set with a different mixture of WHPM and FLFM noise types.

## COMBINATION 3

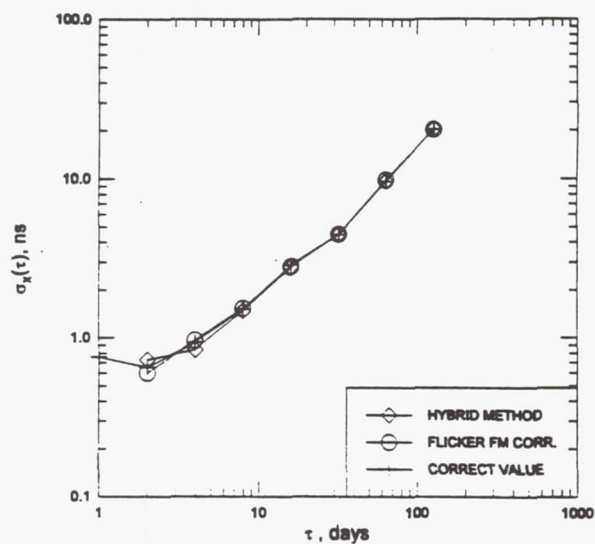


Figure 8b.

Corrected values of  $\sigma_X(\tau)$  obtained using the "hybrid" method, FLFM corrections only, and the values obtained from the original, evenly spaced data set.



# SOME OPERATIONAL ASPECTS OF THE INTERNATIONAL TWO-WAY SATELLITE TIME AND FREQUENCY TRANSFER (TWSTFT) EXPERIMENT USING INTELSAT SATELLITES AT 307 DEGREES EAST

J. A. DeYoung and A. McKinley  
U.S. Naval Observatory Time Service Department (USNO)  
Washington, D.C. 20392 USA

J. A. Davis  
National Physical Laboratory (NPL)  
Queens Road, Teddington, Middlesex, UK

P. Hetzel and A. Bauch  
Physikalisch-Technische Bundesanstalt (PTB)  
Braunschweig, Germany

## Abstract

*Eight laboratories are participating in an international TWSTFT experiment. Regular time and frequency transfers have been performed over a period of almost two years, including both European and transatlantic time transfers. The performance of the regular TWSTFT sessions over an extended period has demonstrated conclusively the usefulness of the TWSTFT method for routine international time and frequency comparisons.*

*Regular measurements are performed three times per week resulting in a regular but unevenly spaced data set. A method is presented that allows an estimate of the values of  $\sigma_y(\tau)$  to be formed from these data. In order to maximize efficient use of paid satellite time an investigation to determine the optimal length of a single TWSTFT session is presented. The optimal experiment length is determined by evaluating how long white PM instabilities are the dominant noise source during the typical 300-second sampling times currently used. A detailed investigation of the frequency transfers realized via the transatlantic TWSTFT links UTC(USNO)-UTC(NPL), UTC(USNO)-UTC(PTB), and UTC(PTB)-UTC(NPL) is presented. The investigation focuses on the frequency instabilities realized, a three-cornered-hat resolution of the  $\sigma_y(\tau)$  values, and a comparison of the transatlantic and inter-European determination of UTC(PTB)-UTC(NPL). Future directions of this TWSTFT experiment are outlined.*

## INTRODUCTION

TWSTFT has developed into a useful method for regular and routine time and frequency transfer. During the INTELSAT field trial, several important details related to TWSTFT



operations were identified as areas that needed further study or confirmation. This paper will discuss and give solutions to several of those. In the future satellite time will have to be paid for; therefore, a logical question to consider is what is an optimal single experiment length. In a routine operational TWSTFT system, one of the goals is to reduce satellite costs while optimizing the timing precision considering the typical noise sources encountered in the TWSTFT measurement systems over the range of 1 to 300 seconds. A paper was presented previously which studied the time-domain parts of the INTELSAT field trial<sup>[1]</sup>. This paper will concentrate on the frequency-domain results by presenting a detailed analysis of the realized long-distance transatlantic frequency comparisons. The specific frequency differences studied are UTC(USNO(MC2)) - UTC(NPL(H maser)), UTC(USNO(MC2)) - UTC(PTB(CS2)), and UTC(PTB(CS2)) - UTC(NPL(H maser)). UTC(USNO(MC2)) is a Sigma Tau Corporation hydrogen maser steered once a day by small changes in its synthesizer settings, hereafter UTC(USNO). UTC(PTB(CS2)) is generated by a laboratory cesium-beam primary frequency standard operated as a clock, hereafter UTC(PTB). UTC(NPL(H maser)) is generated by a steered Sigma Tau hydrogen maser where approximately every 100 days a rate change is manually applied, hereafter UTC(NPL).

## UNEQUALLY SPACED $\sigma_y(\tau)$ ESTIMATES

The following formulation has been developed to allow estimates of  $\sigma_y(\tau)$  to be obtained from unequally spaced time-domain data such as are encountered in TWSTFT. In the case of equally spaced data, it is equivalent to the classical two-sample deviation, which is the square root of the two-sample zero variance<sup>[2,3,4]</sup>. In the case of unequally spaced data, such as are encountered in TWSTFT, we apply a normalization to account for the unequal data spacing. The normalizing terms which have been added in the following equation are the multipliers  $\sqrt{(\tau_2)/\sqrt{(\tau_1)}}$  and  $\sqrt{(\tau_1)/\sqrt{(\tau_2)}}$ . The rest of the equation is standard.

$$\sigma_y(\tau) = \frac{\frac{1}{n} \sum_1^n \left[ \frac{\sqrt{(\tau_2)}}{\sqrt{(\tau_1)}} (x_{n-1} - x_n) - \frac{\sqrt{(\tau_1)}}{\sqrt{(\tau_2)}} (x_n - x_{n+1}) \right]}{\frac{\sqrt{2}}{n} \sum_1^n (\sqrt{\tau_1} \sqrt{\tau_2})}$$

## OPTIMUM EXPERIMENT LENGTH

Figure 1 shows TDEV,  $\sigma_x(\tau)$ , instability estimates formed from a large number of individual 300-second TWSTFT experiments obtained by USNO against nine other labs all using a mix of MITREX model 2500 and 2500A modems. Specifically, the TDEV instabilities were estimated from the differences of the time interval counter readings divided by two. The phase-instability floor for the average of these experiments is reached near an averaging time of 100 seconds. The 100-second optimal sampling was stated quite elegantly previously in [5]: "Averaging for about 100 seconds exceeds the performance specifications of the limiting components." The limiting components in this case are the measurement systems, which are dominated by thermally produced white PM noise out to 100-second averaging times.

Currently TWSTFT experiments are 300 seconds long (5 minutes). The 300 time interval counter readings from each laboratory or timing center are then differenced and divided by two to form a mean time difference for the experiment. Numerical experiments were performed to evaluate how an intermediate mean formed from 1 to (300-1) points deviated from the final mean formed from the full 300 points of a run. Figure 2 shows the results of the averaging of the



deviations from 1,492 experiments for UTC(USNO)-UTC(PTB) and UTC(USNO)-UTC(NPL). Generally, the subset means drop exponentially ( $1/\sqrt{N}$ ) for the first 100 seconds, which is the white PM instability region. After 100 seconds, the convergence is a linear monotonic slope ( $1/(1-N/300)$  behavior). TWSTFT is so good that on average a clock difference formed from a single 1-pulse-per-second (1pps) comparison is within approximately 500 picoseconds of the final value determined from the average of 300 1pps comparisons. A reasonable trade-off between length of the runs, cost of the satellite time, and measurement noise (averaging over the entire white PM regime of the measurement system being the ideal) seems to indicate that 120-second (2-minute) runs are optimal.

## FREQUENCY TRANSFER ANALYSIS

In an effort to determine the quality of the transatlantic frequency measurements, the following clock differences, which were directly measured or formed indirectly as indicated below, were used.

UTC(USNO)-UTC(NPL) directly measured via transatlantic,  
nominal experiment centers 14:12.5 U.T.,

UTC(USNO)-UTC(PTB) directly measured via transatlantic,  
nominal experiment centers 14:36.5 U.T.,

UTC(PTB)-UTC(NPL) = [UTC(PTB)-UTC(USNO)] + [UTC(USNO)-UTC(NPL)]  
indirectly formed via transatlantic, nominal experiment centers 14:24.5 U.T.,

and

UTC(PTB)-UTC(NPL) directly measured inter-European,  
nominal experiment centers 10:20.5 U.T.

## TRANSATLANTIC

The fractional frequency performance of the three transatlantic combinations as realized by TWSTFT is investigated first. These data were filtered so that only days where all three laboratories made TWSTFT sessions on the same day were used (MJD 49387 to 49952 with 141 days with common points). The resulting average  $\tau$  was 4.0 days. The clock difference UTC(PTB)-UTC(NPL) was formed indirectly via transatlantic TWSTFT sessions with UTC(USNO) in this section. It is important to note that there is a difference of measurement times of 24 minutes between the two directly measured experiments. In order to interpret these results correctly, we must remember that UTC(PTB) is a primary frequency standard used in the formation of UTC(BIPM) and is neither steered nor stepped either in frequency or in time. It is also important to stress again that both UTC(USNO) and UTC(NPL) are hydrogen masers and that both are steered towards an extrapolated UTC(BIPM). UTC(USNO) is steered once daily by very small changes in the masers' frequency synthesizer, while UTC(NPL) is steered by introduction of a rate change approximately once every 100 days.

Figure 3 shows UTC(USNO)-UTC(PTB) with an rms of  $1.7 \times 10^{-14}$  and a very slight drift of  $-2.2 \times 10^{-17}$  ( $7.8 \times 10^{-18}$ ) per day between UTC(PTB) and UTC(USNO). Figure 4 shows



UTC(USNO)-UTC(NPL) and has an rms of  $1.1 \times 10^{-14}$  and an estimated maximum frequency drift of  $6.6 \times 10^{-17}$  ( $\pm 1.1 \times 10^{-17}$ ) per day. Figure 5 shows UTC(PTB)-UTC(NPL), which was formed via transatlantic TWSTFT with UTC(USNO). The rms for UTC(PTB)-UTC(NPL) is  $1.9 \times 10^{-14}$  and an estimated maximum frequency drift of  $1.2 \times 10^{-16}$  ( $\pm 3.1 \times 10^{-17}$ ) per day. If one were to base decisions upon only the frequency-domain data presented in this paper, one might assume that a frequency drift is manifested in the UTC(USNO)-UTC(PTB) frequencies, for example. A drift interpretation would be an incorrect assumption. In reality, two very small discrete rate changes (frequency steps) are apparent in the time-domain UTC(USNO)-UTC(PTB) data and only appear unambiguously in the time-domain data.

Figure 6 gives a  $\sigma_y(\tau)$  plot showing the instabilities of the frequency comparisons. UTC(USNO)-UTC(PTB) TWSTFT frequencies show a constant lowering of the instabilities, with an approximate  $\tau^{-1/2}$  slope (white FM noise) from 4- to 250-day averaging times. This is astonishing even when considering the fact that UTC(PTB) is one of the primary inputs into the realization of frequency of UTC(BIPM) with respect to the SI second and towards which UTC(USNO) is steered. UTC(USNO)-UTC(NPL) exhibits a complex structure which is typical of the instability behavior of the UTC(USNO) and UTC(NPL), with the increased instabilities at the longer averaging times coming from the periodic component of the steering towards UTC(BIPM). The estimated minimum frequency instability for UTC(USNO)-UTC(NPL) is  $3.5 \times 10^{-15}$ , reached at an averaging time of 30 days.

Transatlantic TWSTFT-measured UTC(PTB)-UTC(NPL), using UTC(USNO) as an intermediary, exhibits a complex structure in the frequency instabilities which is typical of the instability behavior of the NPL hydrogen maser as steered towards UTC(BIPM). The estimated minimum frequency instability is  $6.3 \times 10^{-15}$ , reached at an averaging time of 60 days, and the rise at the longest averaging times comes from the periodic component of the steering.

These results indicate that the single 5-minute-long transatlantic TWSTFT instabilities are comparable to the short-baseline Vondrak smoothed GPS common-view experiments realized in Europe<sup>16,71</sup>

Using the  $\sigma_y(\tau)$  results for UTC(USNO)-UTC(PTB), UTC(PTB)-UTC(NPL), and UTC(NPL)-UTC(USNO), we may now resolve the instabilities for each clock system using a three-cornered-hat analysis at three selected averaging times and using the indicated number of points to form the instability estimate (see Table I).

## TRANSATLANTIC COMPARED TO INTER-EUROPEAN

We now difference the inter-European direct-measured values of UTC(PTB)-UTC(NPL) with the transatlantic (European-U.S.-European) formed determination of UTC(PTB)-UTC(NPL) to evaluate any degradation contributed by the transatlantic paths over the inter-European path. We should remember that there are 24 minutes between the transatlantic measurement of UTC(PTB) and UTC(NPL) against the intermediary UTC(USNO). There are also a total of 4 hours and 5 minutes between the inter-European and the transatlantic experiments. We have only compared TWSTFT data on days when both inter-European and transatlantic schedules have both had successful experiments. A total of 119 common points were matched over the interval MJD 49387 to 49943 and an average  $\tau$  of 4.63 days was determined. No further adjustments such as interpolation, filtering, etc. were made to the data.

In Figure 7 we present the frequency differences between UTC(PTB)-UTC(NPL), measured inter-European, and UTC(PTB)-UTC(NPL), measured by transatlantic determinations using UTC(USNO), which were determined approximately 4 hours apart. In an ideal case where



the clock comparisons were made simultaneously via TWSTFT, we would expect almost all of the noise sources to cancel out. However, this is not the case because of the approximately four hours between the comparisons of the transatlantic UTC(PTB)-UTC(NPL) and the inter-European UTC(PTB)-UTC(NPL) measurements. The standard deviation of the frequency differences is  $9.0 \times 10^{-15}$  and the scatter is presumably due to the non-simultaneous clock comparisons. In order to get a feeling for what was contributing to this frequency noise, we generated a frequency instability plot (see Figure 8).

A slope of  $\tau^{-1}$  is evident over the entire interval and must be either white or flicker PM noise. At averaging times greater than about 100 seconds, we are at the phase instability floor of the time-domain TWSTFT measurement systems (see Figure 1). This TWSTFT measurement system phase noise must be contributing to the frequency instabilities seen in Figure 7. It also appears that the phase-instability floor from the four hours between measurements is relatively constant over the entire interval from 100 seconds to 75 days. At the longest sampling time of approximately 75 days, the phase-instability floor from the four hours between measurements would introduce only an  $8 \times 10^{-16}$  uncertainty in the determinations of the UTC(PTB)-UTC(NPL) frequencies. The most important fact is that there is apparently no deterioration in the resulting time differences when measuring UTC(PTB)-UTC(NPL) via this transatlantic link using an intermediate timing center compared to the directly measured European time transfers when estimated for the ideal case of simultaneous measures.

## CONCLUSIONS AND FUTURE DIRECTIONS

It has been proven that, for the Mitrex modems currently being used for these TWSTFT experiments, averaging over 120 seconds (2 minutes) is optimal due to this being the region of white PM instabilities. Another important result presented shows that TWSTFT works very well even over very long distances and when using multi-hop experiments, with very little or no added noise.

TWSTFT has been proven to be very useful when applied to transfer of time and frequency between the best frequency standards and over long distances. TWSTFT will begin to be integrated as a routine time and frequency transfer method by the BIPM in the formation of International Atomic Time (TAI) beginning in 1996. Additional TWSTFT stations will be coming on-line in the future with the advent of new PN-code modems. A new TWSTFT-compatible modem, the AOA TWT-100 (USA), is available. A potentially new TWSTFT-compatible modem, TimeTECH<sub>gmbh</sub> SATRE (German) modem—currently used only for ranging—may soon be available. These new modems will allow more stations to come on-line for TWSTFT comparisons.

## REFERENCES

- [1] J.A. DeYoung, W.J. Klepczynski, A.D. McKinley, W. Powell, P. Mai, P. Hetzel, A. Bauch, J.A. Davis, P.R. Pearce, F. Baumont, P. Claudon, P. Grudler, G. de Jong, D. Kirchner, H. Ressler, A. Sdring, C. Hackman, and L. Veenstra 1995, "The 1994 International Transatlantic Two-Way Satellite Time and Frequency Transfer Experiment: Preliminary Results," Proceedings of the 26th Annual Precise Time and Time Interval (PTTI) Applications and Planning Meeting, 6-8 December 1994, Reston, Virginia, pp. 39-49.
- [2] D.W. Allan 1966, "Statistics of Atomic Frequency Standards," *Proc. IEEE*, **54**, 221-230.

- [3] J.A. Barnes, A.R. Chi, L.S. Cutler, D.J. Healey, D.B. Leeson, T.E. McGunigal, J.A. Mullen, W.L. Smith, R. Sydnor, R.F. Vessot, and G.M.R. Winkler 1971, "*Characterization of Frequency Stability*", IEEE Trans. Instr. Meas., IM-20, 105-120.
- [4] J. von Neumann, R.H. Kent, H.R. Bellinson, and B.I. Hart 1941, "*The Mean Square Successive Difference*," Ann. Math. Stat., 12, 153-162.
- [5] D.A. Howe 1987, "*Ku-Band Satellite Two-Way Timing Using a Very Small Aperture Terminal (VSAT)*," Proceedings of the 41st Annual Symposium of Frequency and Control, 27-29 May 1987, Philadelphia, Pennsylvania, pp. 149-159.
- [6] W. Lewandowski, G. Petit, and C. Thomas 1993, "*Precision and Accuracy of GPS Time Transfer*," IEEE Trans. Instr. Meas., IM-42, 474-479.
- [7] J.A. Davis, W. Lewandowski, D. Kirchner, P. Hetzel, G. de Jong, A. Sdring, F. Baumont, W. Klepczynski, T. Parker, J.A. DeYoung, W. Powell, A. McKinley, P.R. Pearce, K.A. Bartle, H. Ressler, R. Robnik, P. Claudon, P. Grudler, and L. Veenstra 1996, "*Preliminary Comparison of Two-Way Satellite Time and Frequency Transfer and GPS Common-View Time Transfer During the INTELSAT Field Trial*," Proceedings of the 27th Annual Precise Time and Time Interval (PTTI) Applications and Planning Meeting, 29 November-1 December 1995, San Diego, California, in press.



Table I. Three-cornered-hat resolution of  $\sigma_y(\tau)$ s at three averaging times (units in  $10^{-15}$ ).

COMBINATIONS			
$\tau = 4\text{d (log 0.6)}$ N=139	USNO-PTB 14.48	PTB-NPL 15.09	NPL-USNO 7.96
RESOLVED			
	USNO 4.76	PTB 13.68	NPL 6.38
COMBINATIONS			
$\tau = 33\text{d (log 1.5)}$ N=17	USNO-PTB 6.70	PTB-NPL 6.74	NPL-USNO 3.60
RESOLVED			
	USNO 2.49	PTB 6.22	NPL 2.60
COMBINATIONS			
$\tau = 64\text{d (log 1.8)}$ N=8	USNO-PTB 4.47	PTB-NPL 5.96	NPL-USNO 4.33
RESOLVED			
	USNO 1.27	PTB 4.29	NPL 4.14

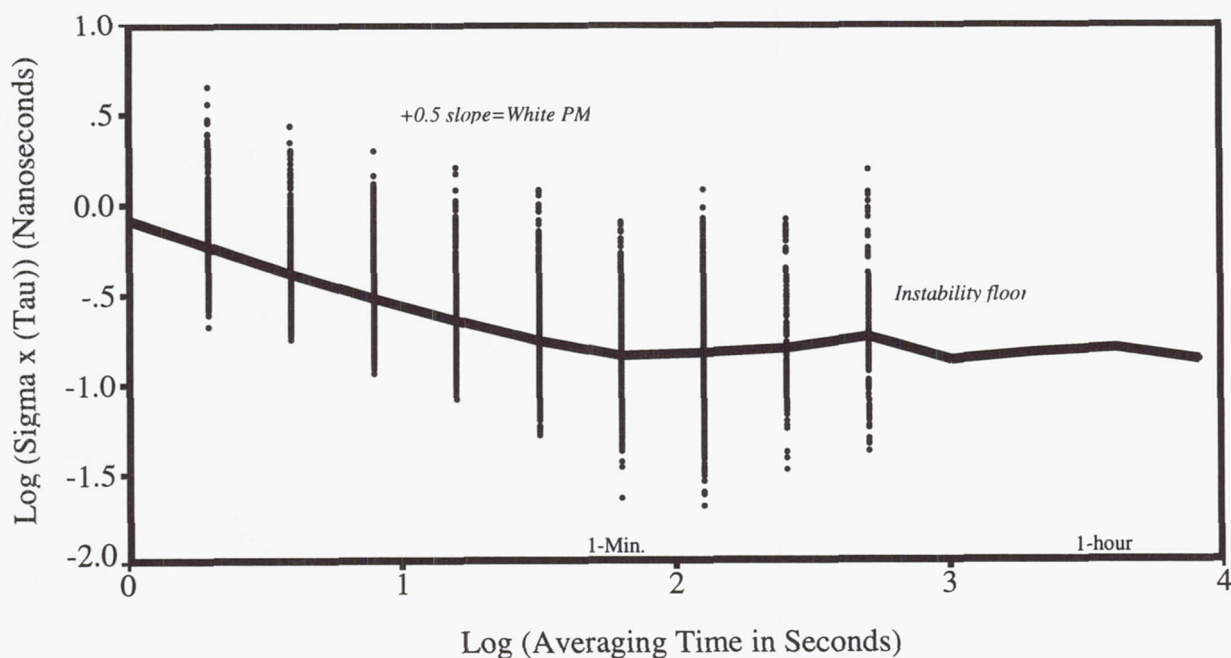


Figure 1. Time-domain instability estimates of 1,492 MITREX modem experiments.

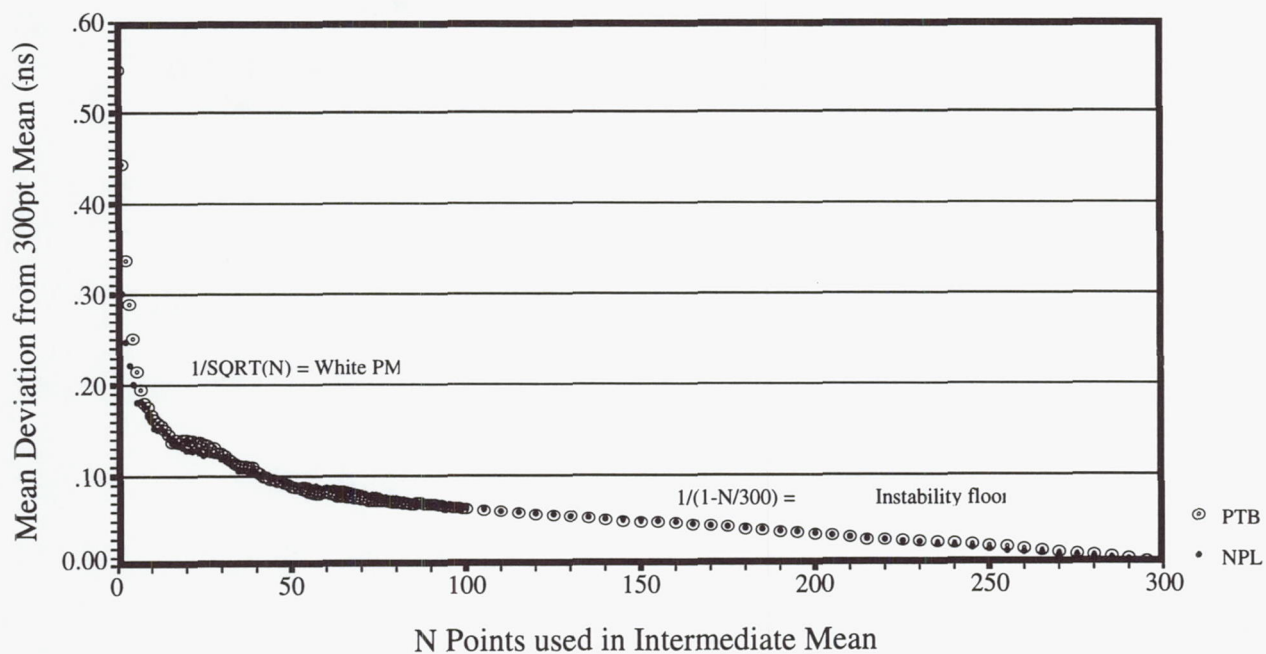


Figure 2. Convergence of intermediate means towards a 300-point mean.



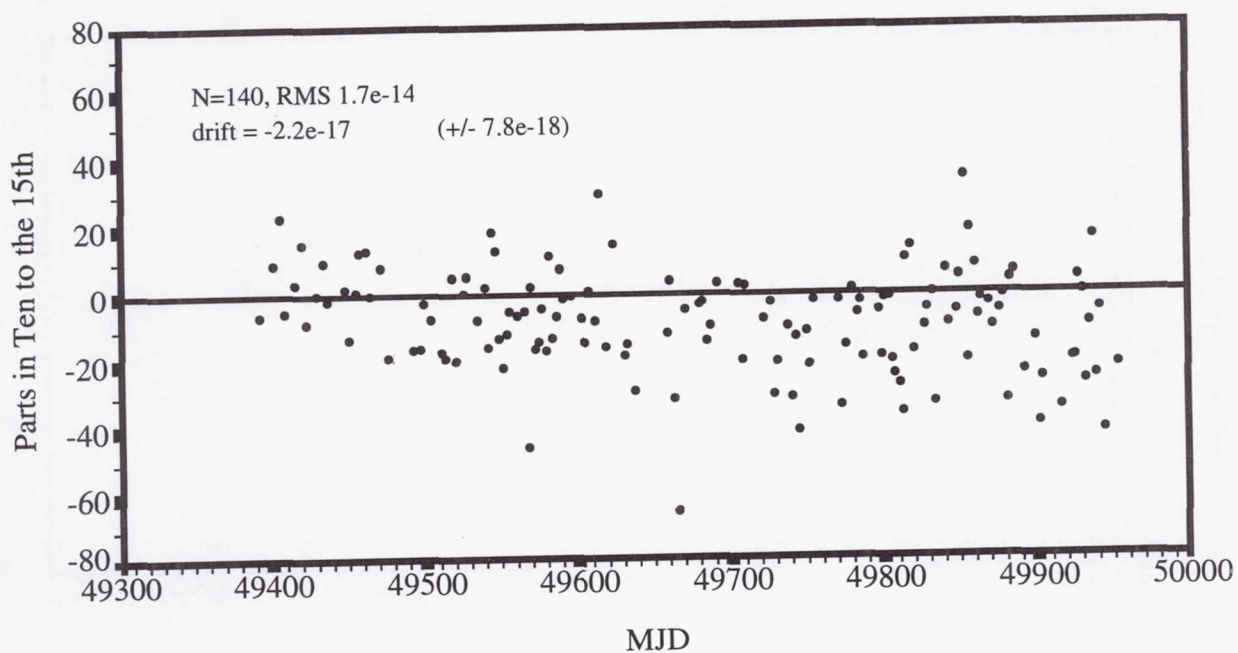


Figure 3. UTC(USNO)-UTC(PTB) via transatlantic TWSTFT.

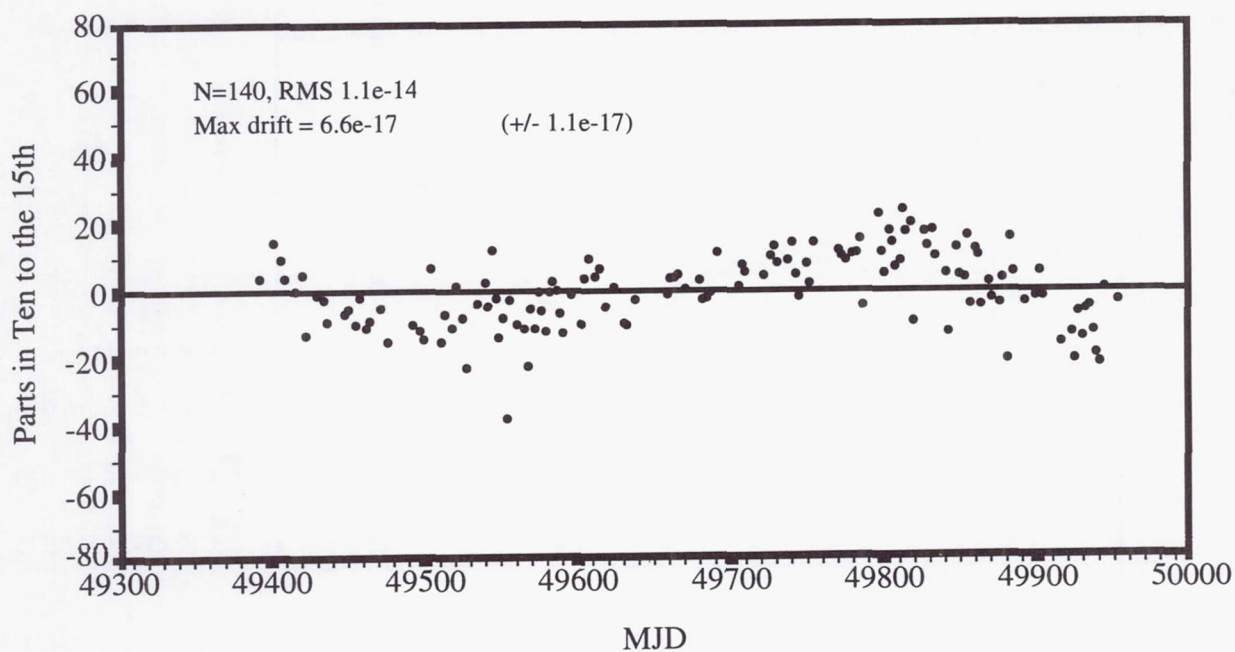


Figure 4. UTC(USNO)-UTC(NPL) via transatlantic TWSTFT.

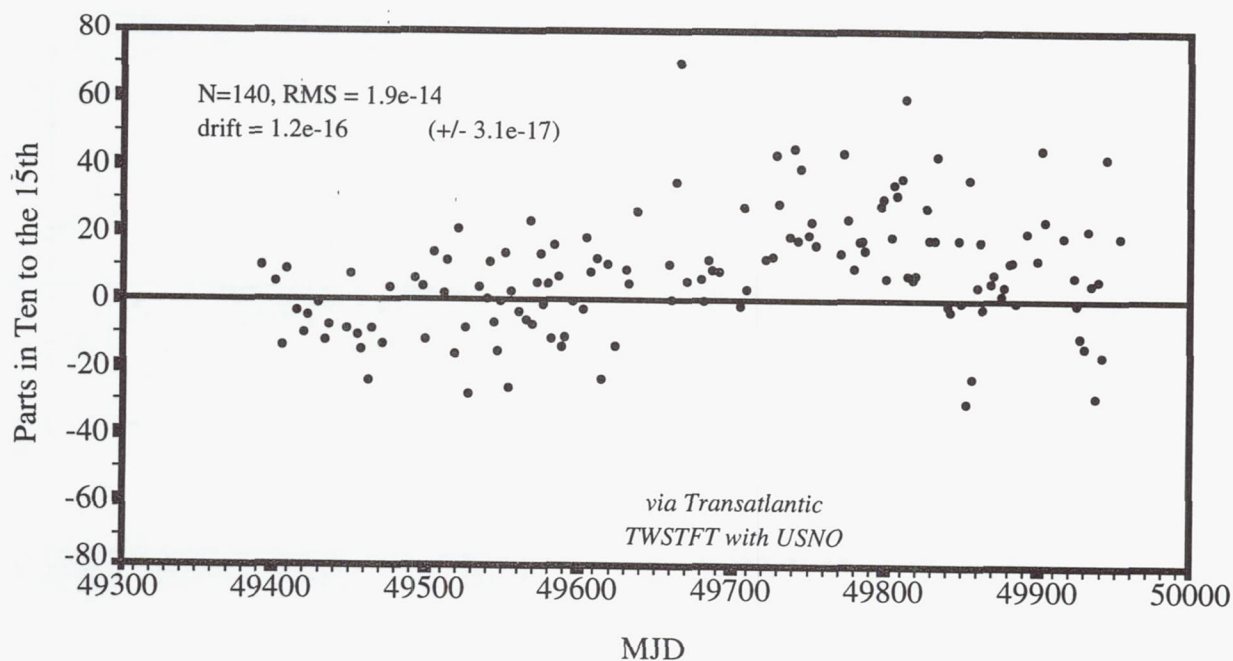


Figure 5. UTC(PTB)-UTC(NPL) via transatlantic TWSTFT with USNO.

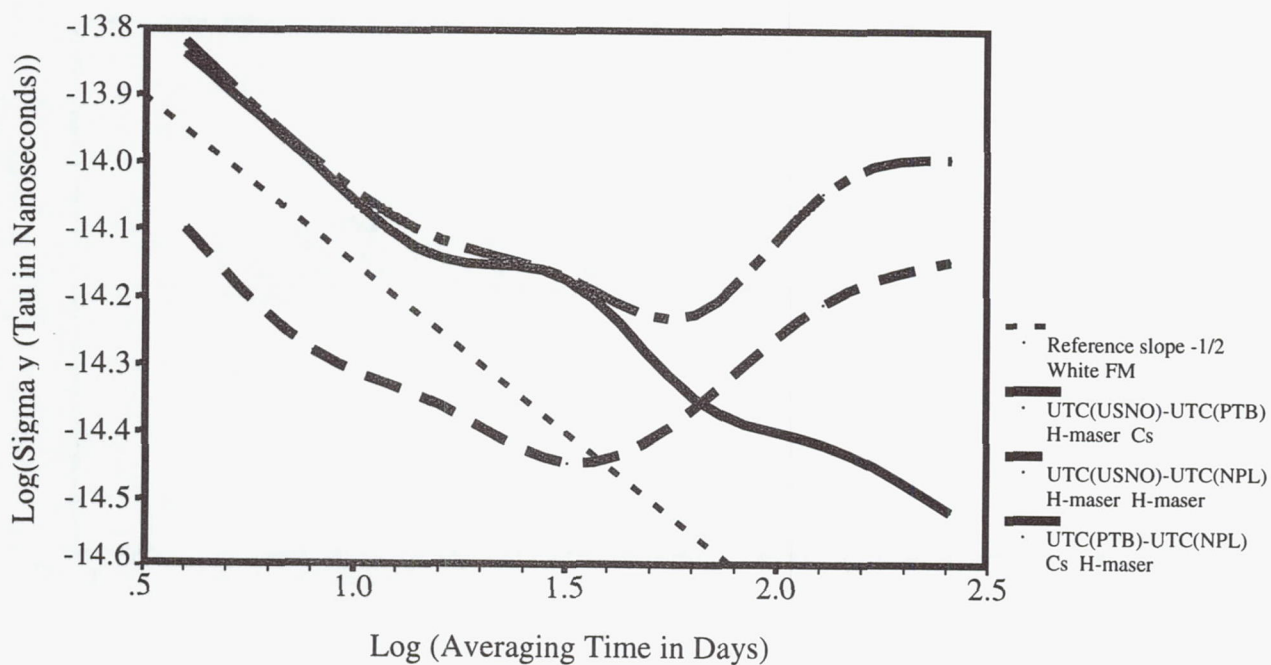


Figure 6. Frequency instabilities via transatlantic TWSTFT.



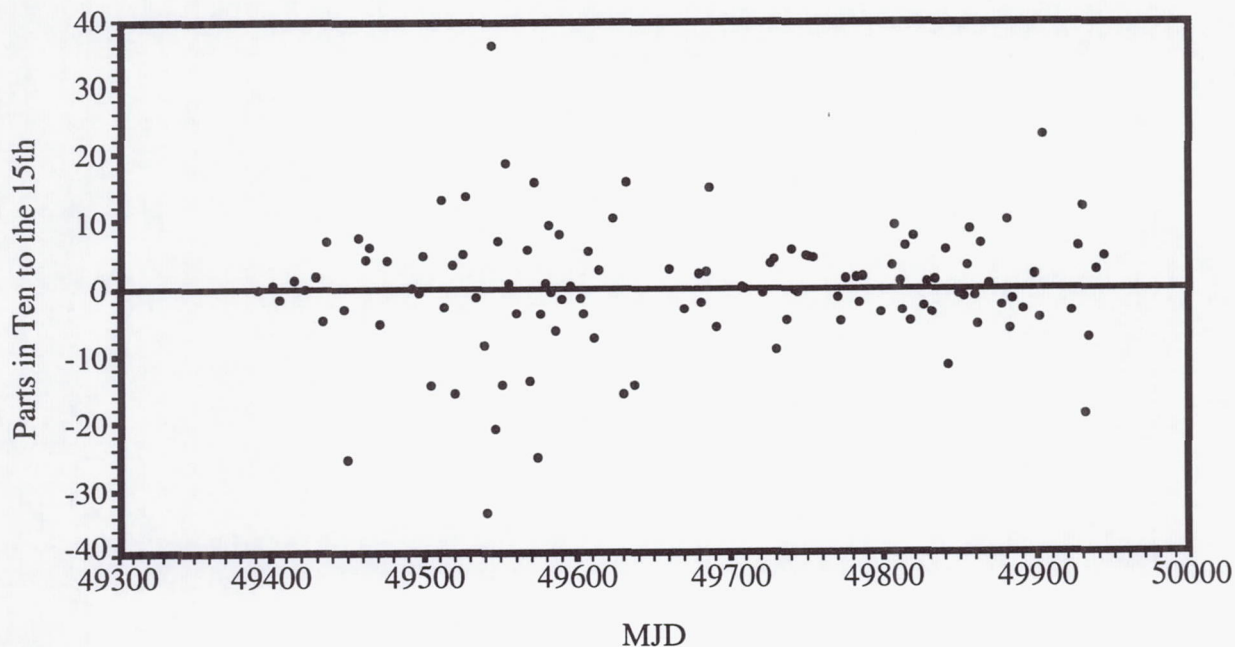


Figure 7. Frequency differences of UTC(PTB)-UTC(NPL) [inter-European] minus UTC(PTB)-UTC(NPL) [via transatlantic]. Four hours elapsed between the inter-European and transatlantic measurements.

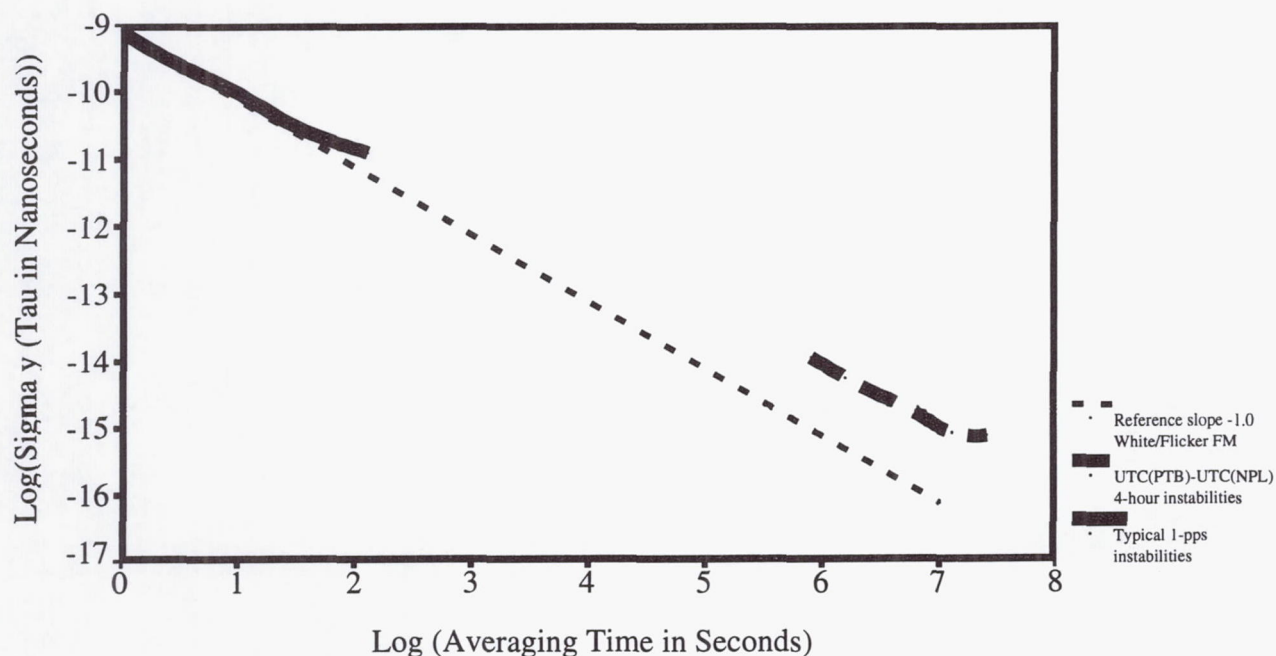


Figure 8. Frequency instabilities of UTC(PTB)-UTC(NPL) [inter-European] minus UTC(PTB)-UTC(NPL) [via transatlantic]. Four hours elapsed between the inter-European and transatlantic measurements. At the longest averaging times we are evaluating the  $\tau = 4$  hour instabilities of the time-domain measurement systems.

# PRELIMINARY COMPARISON OF TWO-WAY SATELLITE TIME AND FREQUENCY TRANSFER AND GPS COMMON-VIEW TIME TRANSFER DURING THE INTELSAT FIELD TRIAL

J. A. Davis<sup>1</sup>, W. Lewandowski<sup>2</sup>, J. A. DeYoung<sup>3</sup>,  
D. Kirchner<sup>4</sup>, P. Hetzel<sup>5</sup>, G. de Jong<sup>6</sup>,  
A. Söring<sup>7</sup>, F. Baumont<sup>8</sup>, W. Klepczynski<sup>3</sup>, A. McKinley<sup>3</sup>,  
T. Parker<sup>9</sup>, K. A. Bartle<sup>1</sup>, H. Ressler<sup>10</sup>,  
R. Robnik<sup>10</sup>, and L. Veenstra<sup>11</sup>

<sup>1</sup>National Physical Laboratory, Queens Road, Teddington, Middlesex, UK

<sup>2</sup>Bureau International des Poids et Mesures, Sèvres, France

<sup>3</sup>U.S. Naval Observatory, Washington, D.C. 20392, USA

<sup>4</sup>Technical University Graz, Graz, Austria

<sup>5</sup>Physikalisch-Technische Bundesanstalt, Braunschweig, Germany

<sup>6</sup>NMi, Van Swinden Laboratorium, Delft, the Netherlands

<sup>7</sup>Forschungs-und Technologiezentrum, Deutsche Telekom,  
Darmstadt, Germany

<sup>8</sup>Observatoire de la Côte d'Azur, Grasse, France

<sup>9</sup>National Institute of Standards and Technology, Boulder,  
Colorado 80303, USA

<sup>10</sup>Space Research Institute, Graz, Austria

<sup>11</sup>RSI, Comsat World Systems, Bethesda, Maryland 20817, USA

## Abstract

*For a decade and a half GPS Common-View time transfer has greatly served the needs of primary timing laboratories for regular intercomparisons of remote atomic clocks. However, GPS as a one-way technique has natural limits and may not meet all challenges of the comparison of the coming new generations of atomic clocks. Two-Way Satellite Time and Frequency Transfer (TWSTFT) is a promising technique which may successfully complement GPS. For two years, regular TWSTFT's have been performed between eight laboratories situated in both Europe and North America, using INTELSAT satellites. This has enabled an extensive direct comparison to be made between these two high performance time-transfer methods. The performance of the TWSTFT and GPS Common-View methods are compared over a number of time-transfer links. These links use a variety of time-transfer hardware and atomic clocks and have baselines of substantially different lengths. The relative merits of the two time-transfer systems are discussed.*



## INTRODUCTION

The performance of atomic clocks maintained at primary timing laboratories have improved considerably in recent years. There is now a challenge to develop suitable time and frequency transfer methods to exploit this improved performance. The standard method of intercomparing clocks contributing to International Atomic Time (TAI) is by common-view of Global Positioning System (GPS) satellites<sup>[1]</sup>. Two-Way Satellite Time and Frequency Transfer (TWSTFT) has in recent years been developed as an alternative time and frequency transfer method<sup>[2]</sup>. TWSTFT as a two-way time-transfer method, offers many potential advantages over the existing one-way methods. Due to the symmetrical nature of the TWSTFT method, several sources of systematic errors are either eliminated or greatly reduced. These include errors associated with Earth station and satellite positions along with ionospheric and tropospheric delay errors. The use of directional antennas and high frequency transmissions enables low power transmissions to be made with relatively high carrier-to-noise ratios, resulting in high precision measurements. The downside is that TWSTFT instrumentation is somewhat more expensive. Satellite time must also be purchased on a commercial geostationary satellite.

In this paper, a detailed study is presented of the comparison between regular TWSTFT and GPS common-view measurements. Measurements have been included from five European laboratories recorded over a period of two years. The (TWSTFT-GPS) differences obtained from each link were examined. Values of  $\sigma_y$  were calculated from the TWSTFT and GPS time transfers and also from the (TWSTFT-GPS) differences. Comparisons were made against  $\sigma_y$  values calculated from co-located atomic clock comparisons performed at NPL. Finally, discrepancies between the TWSTFT and GPS time transfers are explained in terms of changes in both instrumentation and environmental conditions at each laboratory.

## METHOD

The international TWSTFT field trial experiment has been performed during the last two years using an INTELSAT satellite at 307°E<sup>[3]</sup>. Six European and two North American laboratories have been participating in this experiment. The instrumentation used at each location has been described previously<sup>[4,5]</sup>. The results presented in this paper have been obtained from intercomparisons of data from five of the European Laboratories. These were the Technical University Graz, Graz, Austria (TUG), National Physical Laboratory, Teddington, UK (NPL), Van Swinden Laboratorium, Delft, the Netherlands (VSL), Forschungs- und Technologiezentrum, Deutsche Telekom, Darmstadt, Germany (FTZ), and Physikalisch-Technische Bundesanstalt, Braunschweig, Germany (PTB). The atomic clocks and TWSTFT Earth station instrumentation used at each location are summarized in Table 1. The provision of cost-free time by INTELSAT enabled the TWSTFT measurements to take place. Initially the INTELSAT (VA-F13) satellite at 307°E was used, but this was replaced by the INTELSAT (VII-F6) satellite. A schedule of TWSTFT measurements has been performed three times per week, with each individual time transfer lasting for five minutes. GPS measurements were made according to the BIPM International GPS common-view schedules 22, 23, 24, and 25. All GPS time receivers involved in this study are single-channel, C/A code, NBS-type.

## DATA ANALYSIS

The TWSTFT and GPS data sets are fundamentally different. The TWSTFT data consist of spot measurements of five minutes duration made every two or three days. In contrast, the GPS



readings are obtained from the mean of a series of up to 60 thirteen-minute measurements, spread throughout two days. The noise within a five-minute TWSTFT time transfer is substantially lower than the noise within a block of 13-minute GPS data. Underlying both sets of measurements are the variations of the atomic clocks. These short- and medium-term clock variations are small in the case of the hydrogen maser, but significantly larger in the case of commercial cesium clocks.

TWSTFT measurements were made on Mondays, Wednesdays, and Fridays. This measurement schedule resulted in a regular but unevenly spaced data set. A simple algorithm has been developed to calculate a good approximation to  $\sigma_y$ <sup>[6]</sup> under these conditions. This algorithm has been successfully implemented.

Time transfers were computed using the GPS common-view method for the period MJD (49354-49950). During this period the Block II satellites were permanently subjected to Selective Availability (SA), so strict common-views were required to remove the effect of the SA clock dither. All common views retained for this study fulfilled the following conditions: 15 s common-view tolerance, 765 s minimum duration of the track, 20° minimum elevation angle for satellites. The 15 s tolerance for common-views was necessitated by a fault in the NBS type receivers which begin observations 15 s later than scheduled. There were between 25 to 40 common-view tracks per day fulfilling these conditions. Values of the common-views were computed for the midpoints of the tracks. The coordinates of the GPS ground antenna were expressed in the ITRF88 reference frame with uncertainty ranging from 10 cm to 30 cm<sup>[7]</sup>. The coordinates for NPL, VSL, and FTZ were newly determined and the GPS data were corrected in post-processing. The distances between European time laboratories range from a few hundred kilometers to about one thousand kilometers. During the GPS common-view time transfer the errors due to broadcast satellite ephemerides, ionospheric, and tropospheric delays, are reduced to the level of 1 ns or lower<sup>[8,9]</sup>. Therefore, there is no need to use post-processed precise ephemerides and measurements of ionosphere and troposphere<sup>[10]</sup>. For each link, a Vondrak smoothing was performed on the values UTC(Lab1)-UTC(Lab2), which acts as a low-pass filter with a cut-off period ranging from 0.5 day to 2 days depending on the pair of laboratories<sup>[11]</sup>. Those cut-off periods have been chosen as being approximately the limit between the short time intervals, where the measurement noise is dominant, and the longer intervals where the clock noise prevails. Finally, the smoothed values were interpolated for the occurrence of the TWSTFT measurements. The Vondrak smoothing method is illustrated in Figure 1. The "cloud" of GPS data points are shown, along with the curve resulting from the smoothing. The GPS links were differentially calibrated with an uncertainty of about 2 ns<sup>[12]</sup>.

## RESULTS

Curves of the (PTB-NPL) time transfer made over a two-year period are shown in Figure 2. The offset between the two curves is due in part to the delay asymmetries of the TWSTFT instrumentation not being calibrated, and in part to an offset of 150 ns being added to clearly separate the two curves. Curves of the (TWSTFT-GPS) differences are shown in Figures 3, 4, and 5. Values of  $\sigma_y$  calculated for both the TWSTFT and GPS Common-View time transfers and (TWSTFT-GPS) differences are shown in Table 2.  $\sigma_y$  values were calculated with averaging times ( $\tau$ ) of 2.3, 4.7, and 7 days.

Several trends emerged. There is good agreement in the shape of the time-transfer curves obtained using the TWSTFT and GPS common-view methods. Values of the standard deviation calculated from the (TWSTFT-GPS) differences are shown in Table 3, both for the complete data set and for a sub-section. Outlying points that deviated substantially from the mean value



were removed before calculating the standard deviation using the points shown in Figures 3-5. The NPL-TUG differences exhibited the lowest standard deviation when calculated over the whole period. In order to compare (TWSTFT-GPS) differences over shorter periods, standard deviations have been calculated from subsets of the data which are free from rapid delay changes. The results obtained were encouraging. Standard deviations of between 1.4 ns and 2.7 ns were obtained over periods ranging from 70 to over 300 days. The most stable operation occurred on the (PTB-NPL) link, where a standard deviation of 1.4 ns was obtained for the (TWSTFT-GPS) differences over a period of 350 days.

Values of  $\sigma_y$  were calculated from TWSTFT, GPS, and (TWSTFT-GPS) data sets that contained only data collected on the same MJDs. When data were missing from one data set, the corresponding data were removed from the other data sets before processing. Any discrete delay steps occurring due to known instrumentation changes were removed before the  $\sigma_y$  values were calculated. Large discrete delay steps of amplitude 20 ns and 30 ns were removed from the FTZ data sets before calculating  $\sigma_y$ . These steps occurred only occasionally within a data set and were not typical of the data scatter. Values of  $\sigma_y$  varied considerably between the TWSTFT links. The (PTB-NPL) time transfer was the most stable link. These results were attributed to the use of an active Sigma Tau hydrogen maser at NPL and the Primary Cesium clock (CS2) at PTB compared with the use of commercial HP5071A cesium clocks at the other laboratories. With averaging times ( $\tau$ ) of 2.3 days or longer, the principal instability contributing to the  $\sigma_y$  values was clock noise. This is explained below.

For a given time transfer, values of  $\sigma_y$  were in almost all examples lower for the GPS common-view measurements when compared against the TWSTFT measurements. In most cases, the difference in  $\sigma_y$  values was quite small, but clearly significant. This difference was particularly noticeable on the most stable (PTB-NPL) link, with an averaging time ( $\tau$ ) of 2.3 days. In almost all examples, the values of  $\sigma_y$  obtained from the (TWSTFT-GPS) difference were significantly lower than the  $\sigma_y$  values obtained from the individual time transfers. This again indicated that the major contribution to the time transfer  $\sigma_y$  values is from clock noise. A significant proportion of this noise cancels in the (TWSTFT-GPS) differences, due to the partial elimination of noise from the clocks.

Despite the lower  $\sigma_y$  values obtained from the GPS time transfers, the conclusion should not be drawn that the GPS common-view method offers the best technique for clock comparison. The lower  $\sigma_y$  values may be due to the choice of TWSTFT and GPS measurement schedules, rather than to an intrinsically higher accuracy of the GPS method. The  $\sigma_y$  values obtained from a TWSTFT are calculated from "spot" five-minute readings, made either two or three days apart. In contrast, the  $\sigma_y$  values obtained from a GPS common-view time transfer are calculated from "weighted means" of up to two days' data, with approximately thirty satellite readings contributing to each day's data.  $\sigma_y$  values calculated from these mean values will be lower even in the case where two perfect time-transfer systems are used.

To illustrate the above point further, co-located clock comparisons have been made between two HP5071A commercial cesium clocks and an active hydrogen maser at NPL. One hundred days of measurements have been examined. Values of  $\sigma_y$  obtained from the comparisons are shown in Table 4, using averaging times ( $\tau$ ) of 2, 4, and 8 days. The  $\sigma_y$  values were calculated from single readings, from the mean of 48-readings taken over the two days, and from the (single reading - mean readings) differences. The results show the advantage of taking measurements throughout the 48-hour period. With a two-day averaging time, the  $\sigma_y$  values calculated from the mean readings were substantially lower than the  $\sigma_y$  values calculated from the single readings. The values of  $\sigma_y$  obtained from the co-located measurements were comparable with, and only slightly lower than, the  $\sigma_y$  values obtained from the TWSTFT and GPS time transfers. These



results suggest that a large fraction of each time transfer  $\sigma_y$  value is due to clock noise. These results also show that the differences between the  $\sigma_y$  values obtained from the TWSTFT and GPS common-view systems is most likely to be due to the choice of measurement schedule, rather than any intrinsically better delay stability of the GPS system.

Plots of (TWSTFT-GPS) differences show several trends. There are delay steps of several nanoseconds occurring within some of the instrumentation. Several, but not all, of these delay changes are associated with known delay changes of either the GPS or the TWSTFT instrumentation due to hardware replacement. Periodic delay changes with an annual period occur within the (VSL-NPL) differences. Temperature-dependent delay changes have been observed in previous studies of (TWSTFT-GPS) differences<sup>[13]</sup>.

## DISCUSSION

There are several possible improvements that may be made to both the TWSTFT and GPS common-view time-transfer systems used in this experiment. Neither the TWSTFT system nor the GPS system are presently operating using optimum hardware. The GPS system may benefit from the use of dual-frequency multichannel receivers, which make optimum use of the available GPS signals. Work has already been performed to improve the use of the GPS system for time transfer by, for example, better satellite ephemeris determination, improved Earth station coordinate determination, ionospheric measurement, and tropospheric modelling. The main limitation to the performance of the common-view GPS method is the delay stability of the receiver instrumentation. The TWSTFT system may benefit from the use of more recently designed modems. Further improvements may be obtained from the optimization of the Earth station instrumentation to minimize the delay instabilities. Satellite simulators may be used to measure the Earth station delay asymmetries during a TWSTFT measurement session.

The values of  $\sigma_y$  obtained using both the TWSTFT and GPS systems have been limited by the performance of the cesium atomic clocks at most locations. A parallel TWSTFT experiment has been taking place between Europe and North America. The combination of longer baseline time transfers and the possibility of operating with active hydrogen masers at both locations should make the study of these links of considerable interest. It will be of particular interest to examine the effects of ionospheric corrections, and precise ephemeris corrections applied to the GPS measurements, made over these relatively long links.

## CONCLUSIONS

TWSTFT and GPS common-view methods have been shown to be capable of providing high-precision time transfers. Values of  $\sigma_y(\tau = 2.3 \text{ days})$  as low as  $1.3 \times 10^{-14}$  and  $1.8 \times 10^{-14}$  have been reported for GPS common-view and TWSTFT respectively. This difference in  $\sigma_y$  values has been attributed to the behavior of the clocks when interrogated using the different measurement periods used by the two systems. Periodic delay changes of period one year were also observed. These changes correlated with outdoor temperature variations. Further work is required to obtain the optimum performance from both systems.



## ACKNOWLEDGEMENTS

This work has been supported under the UK National Measurement System Program for Time and Frequency. The work has also been funded by grants from the Austrian Academy of Science and the Jubilee fund of the Austrian National Bank.

## REFERENCES

- [1] W. Lewandowski, and C. Thomas 1991, "GPS Time Transfer," *Proc. IEEE*, Special Issue on Time and Frequency, **79**, 991-1000.
- [2] D. Kirchner 1991, "Two-Way Time Transfer Via Communication Satellites," *Proc. IEEE*, Special Issue on Time and Frequency, **79**, 983-990.
- [3] J.A. Davis, P.R. Pearce, D. Kirchner, H. Ressler, P. Hetzel, A.S. Söring, G de Jong, P. Grudler, F. Baumont, and L. Veenstra 1995, "European Two-Way Satellite Time Transfer Experiments Using the INTELSAT (VA-F13) Satellite at 30°E," *IEEE Trans. Instr. Meas.*, **44**, in press.
- [4] J.A. DeYoung, W.J. Klepczynski, A.D. McKinley, W. Powell, P. Mai, A. Bauch, J.A. Davis, P.R. Pearce, F. Baumont, P. Claudon, P. Grudler, G. de Jong, D. Kirchner, H. Ressler, A. Söring, C. Hackman, and L. Veenstra 1995, "The 1994 International Transatlantic Two-Way Satellite Time and Frequency Transfer Experiment: Preliminary Results," Proceedings of the 26th Annual Precise Time and Time Interval (PTTI) Applications and Planning Meeting, 6-8 December 1994, Reston, Virginia, pp. 39-49.
- [5] J.A. Davis, P.R. Pearce, D. Kirchner, H. Ressler, P. Hetzel, A. Söring, G. de Jong, P. Grudler, F. Baumont, H. Ressler, and L. Veenstra 1994, "Two-Way Satellite Time Transfer Experiments Between Six European Laboratories Using the INTELSAT(VA-F13) Satellite," Proceedings of the 8th European Frequency and Time Forum (EFTF), March 1994, Germany, pp. 296-316.
- [6] J.A. DeYoung, J.A. Davis, D. Kirchner P. Hetzel, A. Bauch, and A. McKinley 1995, "Some Operational Aspects of the International Two-Way Satellite Time Transfer Experiment, Using the Intelsat Satellite at 30°E," Proceedings of the 27th Annual Precise Time and Time Interval (PTTI) Applications and Planning Meeting, 29 November-1 December 1995, San Diego, California, in press.
- [7] W. Lewandowski 1992, "World-Wide Unification of Ground-Antenna Coordinates for Ultra-Accurate GPS Time Transfer," *Proc. Journées Spatiales Temporaires*, Observatoire de Paris, pp. 142-147.
- [8] D. Kirchner, and C. Lentz 1994, "Tropospheric Corrections to GPS Measurements Using Locally Measured Meteorological Parameters Compared With General Tropospheric Corrections," Proceedings of the 25th Annual Precise Time and Time Interval (PTTI) Applications and Planning Meeting, 29 November-2 December 1993, Marina del Rey, California, pp. 231-248.
- [9] W. Lewandowski, G. Petit, and C. Thomas 1990, "Precision and Accuracy of GPS Time Transfer," *IEEE Trans. Instr. Meas.*, **42**, 474-479.

- [10] W. Lewandowski, and M.A. Weiss 1990, "*The Use of Precise Ephemerides for GPS Time Transfer*," Proceedings of the 21st Annual Precise Time and Time Interval (PTTI) Applications and Planning Meeting, 28-30 November 1989, Redondo Beach, California, pp. 95-106.
- [11] J. Vondrak 1969, "*A Contribution to the Problem of Smoothing Observational Data*," *Bull. Astron. Inst. Czech.*, 20, pp. 349-355.
- [12] W. Lewandowski, and F. Baumont 1995, "*Determination of the Differential Time Corrections Between GPS Time Equipment Located at the Observatoire de Paris, Paris, France, the Observatoire de la Côte d'Azur, Grasse, France, the National Physical Laboratory, Teddington, United Kingdom, the Van Swinden Laboratorium, Delft, the Netherlands, the Physikalisch-Technische Bundesanstalt, Braunschweig, Germany, the Forschungs- und Technologiezentrum, Darmstadt, Germany, and the Technical University, Graz, Austria*," Report BIPM-94/12.
- [13] D. Kirchner, H. Ressler, P. Grudler, F. Baumont, C. Veillet, W. Lewandowski, W. Hanson, W. Klepczynski, and P. Uhrich 1993, "*Comparison of GPS Common-View and Two-Way Satellite Time Transfer Over a Baseline of 800 km*," *Metrologia*, 30, 183-192.



Table 1 Atomic clocks and TWSTFT instrumentation.

Laboratory	TUG	NPL	VSL	FTZ	PTB
Clock	HP5071A	Hydrogen Maser	HP5071A	HP5071A	CS2 Primary Caesium
TWSTFT Antenna	1.8m	2.4m	3.0m	1.8m	1.8m
TWSTFT Modem	MITREX 2500	MITREX 2500	MITREX 2500	MITREX 2500A	MITREX 2500A

Table 2 Values of  $\sigma_y$  calculated from TWSTFT and GPS time transfer and (TWSTFT-GPS) differences.

LINK	TWSTFT Time Transfer $\sigma_y \times 10^{14}$			GPS Time Transfer $\sigma_y \times 10^{14}$			(TWSTFT - GPS) Difference $\sigma_y \times 10^{14}$		
	$\tau=2.3$ days	$\tau=4.7$ days	$\tau=7.0$ days	$\tau=2.3$ days	$\tau=4.7$ days	$\tau=7.0$ days	$\tau=2.3$ days	$\tau=4.7$ days	$\tau=7.0$ days
NPL-TUG	2.4	1.5	1.2	2.3	1.4	1.2	1.3	0.6	0.5
VSL-NPL	5.1	5.5	4.5	4.8	5.3	4.4	2.8	1.7	0.9
VSL-TUG	5.8	4.5	4.8	5.6	4.0	4.4	2.0	1.3	1.0
FTZ-VSL	5.1	5.3	4.7	4.4	4.9	4.6	4.6	4.7	1.7
FTZ-NPL	3.6	2.7	2.5	3.0	2.5	2.4	2.0	1.3	1.1
FTZ-TUG	4.3	2.7	2.6	4.0	2.7	2.5	2.3	1.4	1.1
PTB-FTZ	3.8	2.7	2.4	3.6	2.4	2.3	0.9	0.7	1.2
PTB-VSL	4.3	3.6	3.4	4.2	3.1	3.2	2.6	1.6	1.0
PTB-NPL	1.8	1.0	1.0	1.3	0.8	0.9	1.7	0.8	0.6
PTB-TUG	2.9	1.6	1.3	2.6	1.6	1.4	1.5	0.9	0.8

Table 3 Standard deviations calculated from the (TWSTFT-GPS Common-View) differences.

LINK	Standard Deviation (Complete Period)	Duration of subset (MJDs)	Standard Deviation (subset)
NPL-TUG	2.4 ns	49471-49840	1.5 ns
VSL-NPL	4.1 ns	49707-49805	1.4 ns
VSL-TUG	4.6 ns	49590-49709	2.7 ns
FTZ-VSL	14.5 ns	49670-49754	2.9 ns
FTZ-NPL	7.4 ns	49670-49805	1.6 ns
FTZ-TUG	9.1 ns	49635-49805	1.5 ns
PTB-FTZ	11.7 ns	49657-49805	1.6 ns
PTB-VSL	4.3 ns	49670-49840	2.4 ns
PTB-NPL	2.5 ns	49600-49950	1.4 ns
PTB-TUG	3.4 ns	49567-49950	2.3 ns

Table 4  $\sigma_y$  values calculated from co-located measurements made at NPL

	Single Readings $\sigma_y \times 10^{14}$			Mean Readings $\sigma_y \times 10^{14}$			Difference $\sigma_y \times 10^{14}$		
	$\tau=2.0$ days	$\tau=4.0$ days	$\tau=8.0$ days	$\tau=2.0$ days	$\tau=4.0$ days	$\tau=8.0$ days	$\tau=2.0$ days	$\tau=4.0$ days	$\tau=8.0$ days
Maser-123	1.8	1.4	0.7	1.3	1.3	0.6	1.7	0.4	0.3
Maser-404	3.2	1.8	0.9	2.2	1.4	1.0	1.6	0.8	0.3
123-404	3.6	2.3	1.0	2.6	1.9	1.0	1.8	0.9	0.3

Maser = Sigma Tau Hydrogen Maser  
 123 = HP5071A High performance clock  
 404 = HP5071A Standard clock.



Figure 1

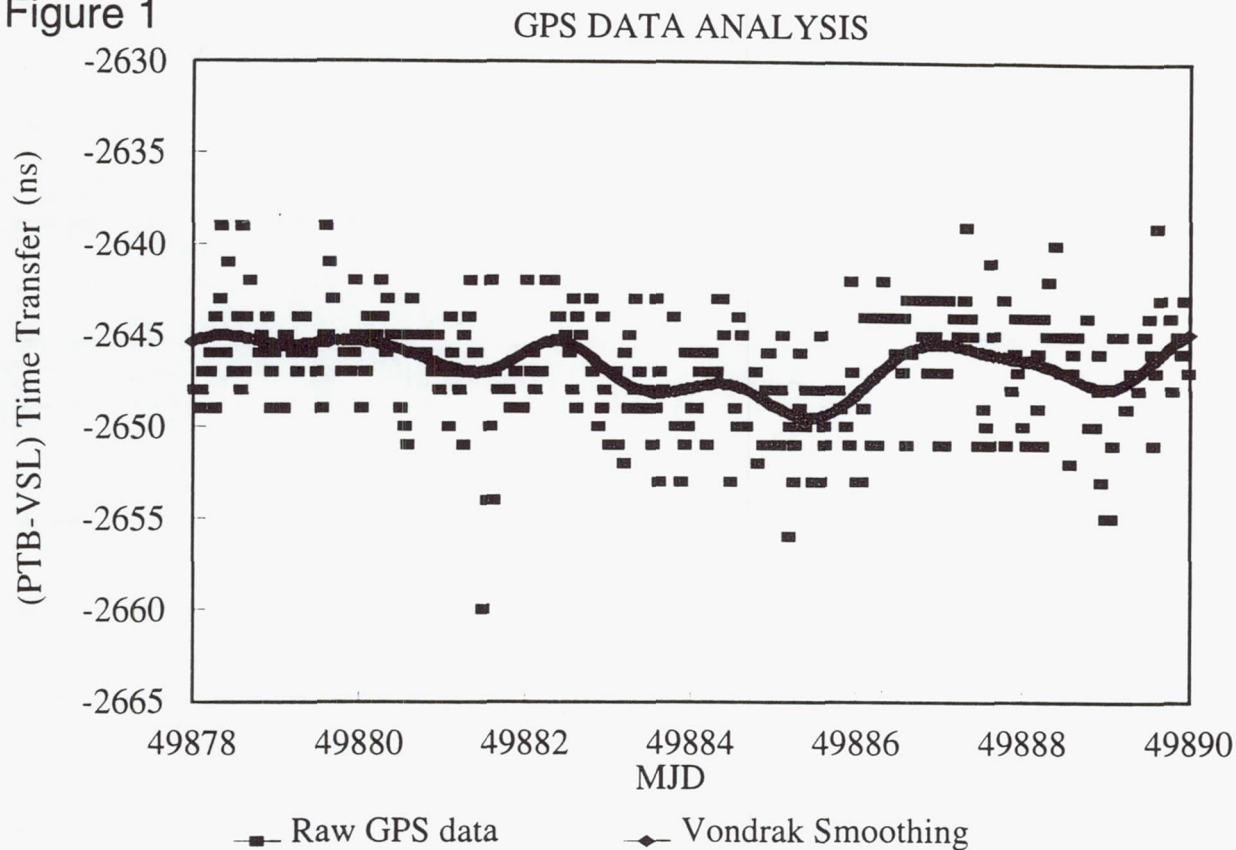


Figure 2

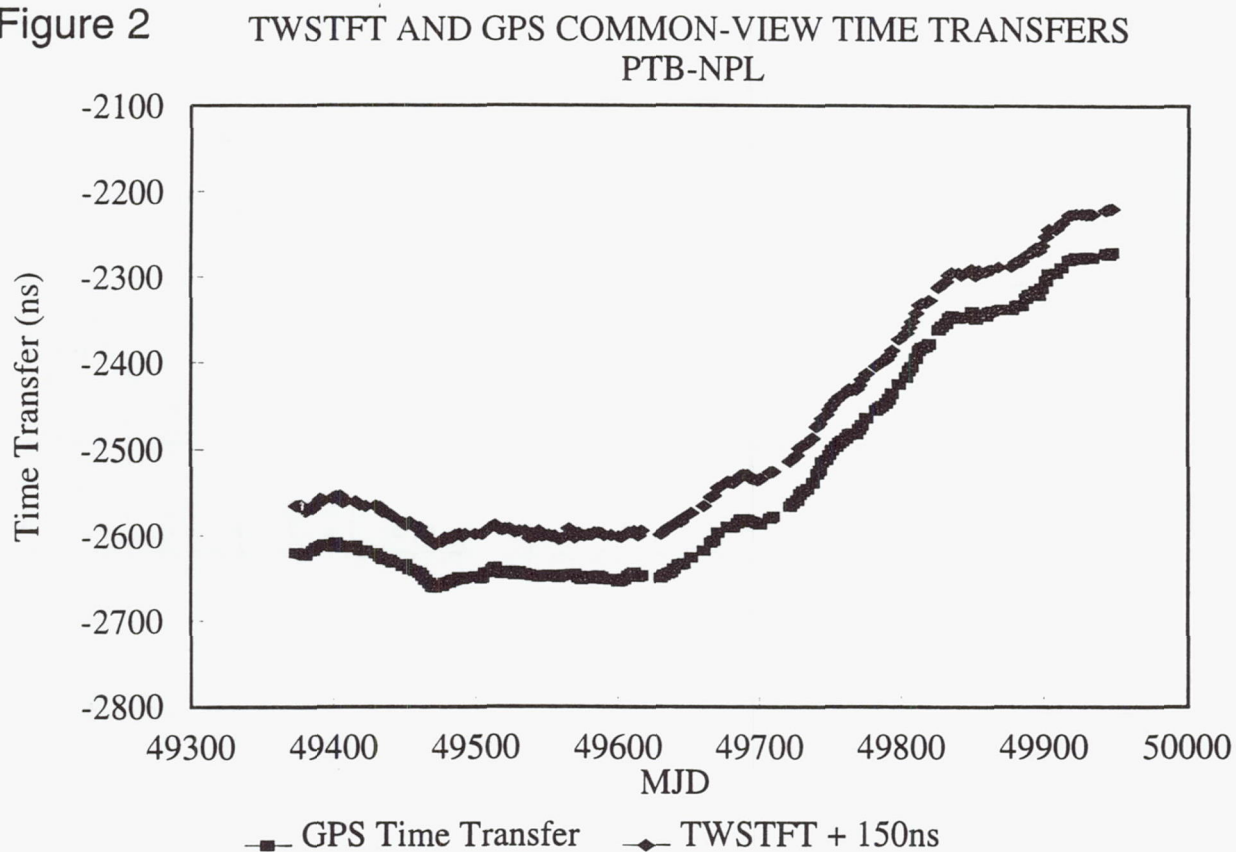


Figure 3

(TWSTFT - GPS COMMON-VIEW) DIFFERENCES  
PTB-NPL

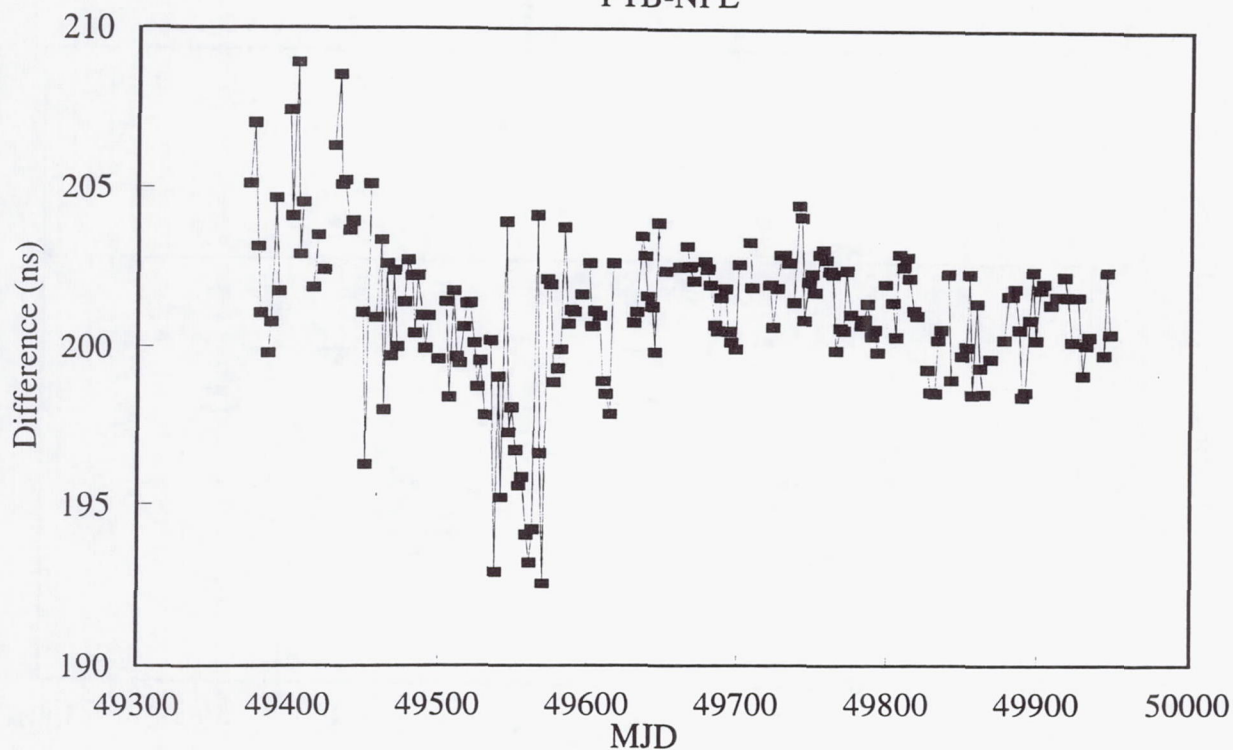


Figure 4

(TWSTFT - GPS COMMON-VIEW) DIFFERENCES  
PTB-TUG

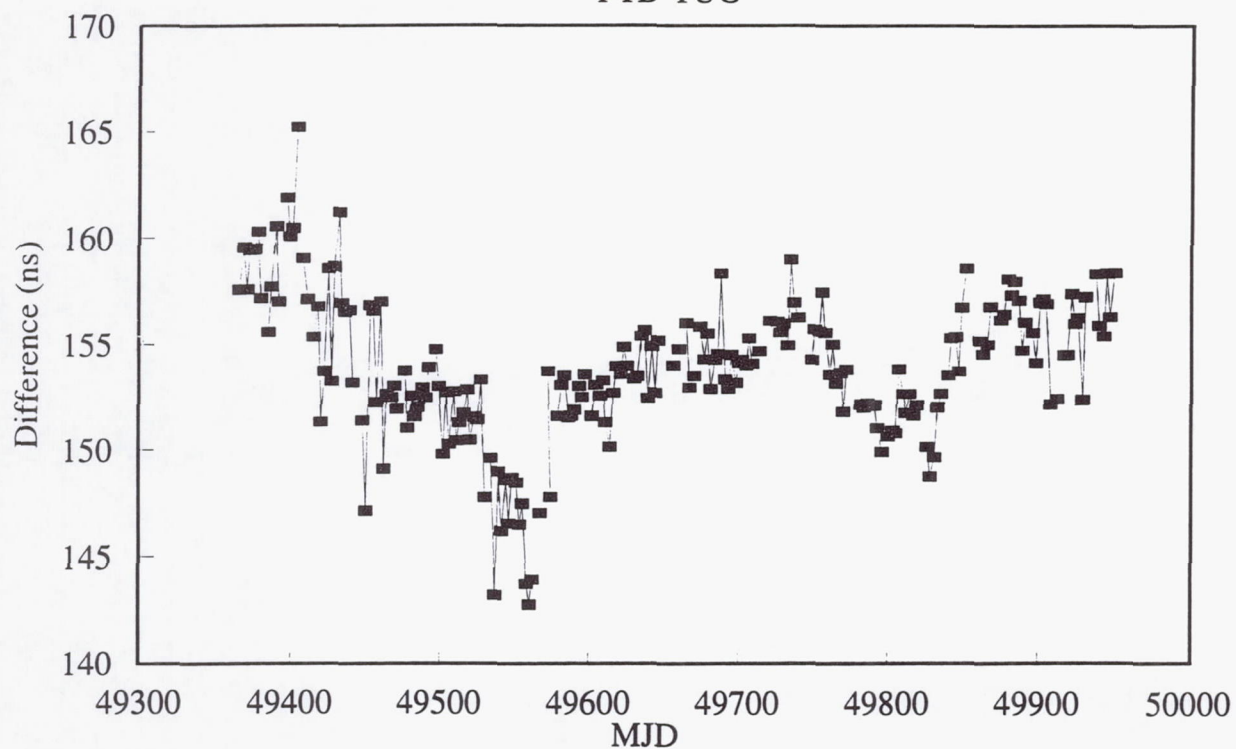
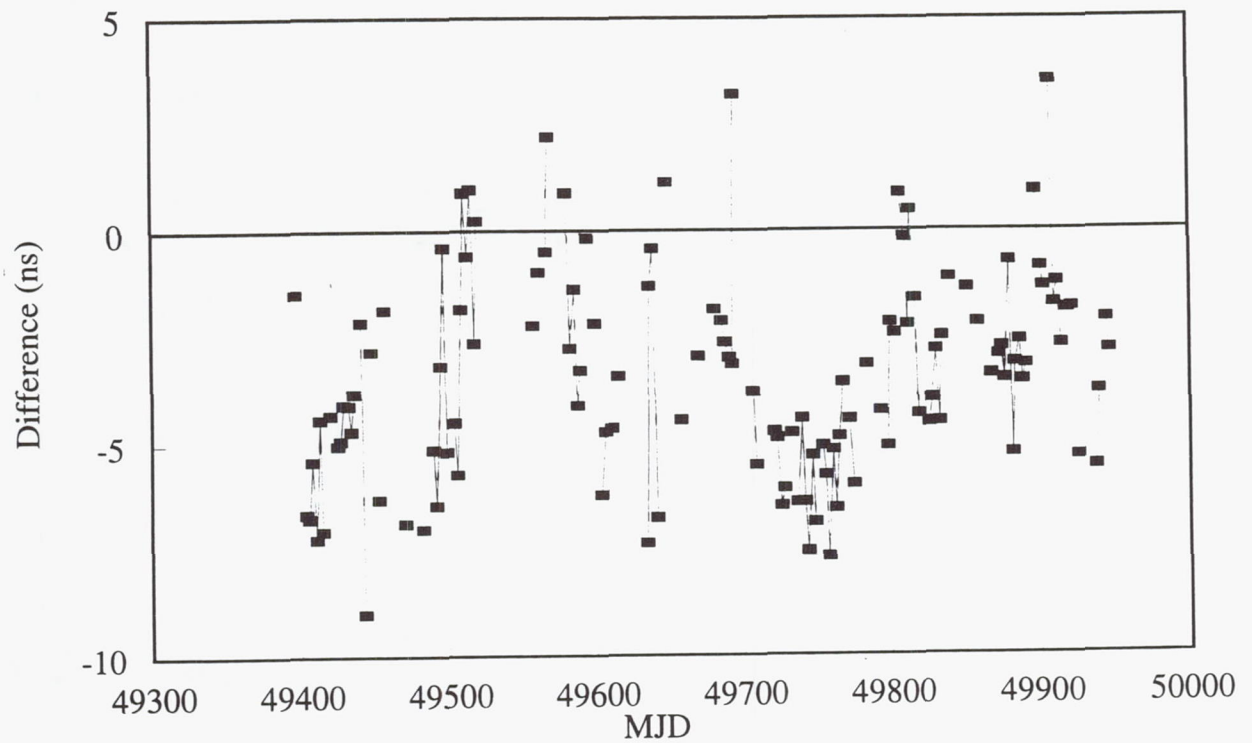




Figure 5

(TWSTFT - GPS COMMON-VIEW) DIFFERENCES  
VSL-NPL



# **RESULTS OF THE CALIBRATION OF THE DELAYS OF EARTH STATIONS FOR TWSTFT USING THE VSL SATELLITE SIMULATOR METHOD**

**Gerrit de Jong**  
NMI Van Swinden Laboratorium, P.O. Box 654,  
2600 AR Delft, the Netherlands

**Dieter Kirchner**  
Technical University Graz, Graz, Austria

**H. Ressler**  
Space Research Institute, Graz, Austria

**Peter Hetzel**  
Physikalisch Technische Bundesanstalt, Braunschweig, Germany

**John Davis, Peter Pears**  
National Physical Laboratory, Teddington, UK

**Bill Powell, Angela Davis McKinley, Bill Klepczynski, James DeYoung**  
U.S. Naval Observatory, Washington, D.C. 20392, USA

**Christine Hackman, Steve R. Jefferts, and Thomas E. Parker**  
National Institute of Science and Technology,  
Boulder, Colorado 80303, USA

## **INTRODUCTION**

Two-Way Satellite Time and Frequency Transfer (TWSTFT) is the most accurate and precise method of comparing two remote clocks or time scales. The accuracy obtained is dependent on the accuracy of the determination of the non-reciprocal delays of the transmit and the receive paths. When the same transponders in the satellite at the same frequencies are used, then the non-reciprocity in the Earth stations is the limiting factor for absolute time transfer.

In each Earth station, the clock signal (1 pulse per second = 1PPS) is modulated on an IF



carrier frequency, then up-converted to the transmit up-link frequency, amplified by a high-power amplifier (HPA), and radiated to the satellite by the antenna. The signal from the companion station clock is received at the satellite down-link frequency by the same antenna, amplified by a low-noise amplifier (LNA), and then down-converted to the IF frequency and demodulated to the received clock signal.

The cables used in the station in the transmit path may differ from the cables in the receive part; the filter and tuned circuit delays may differ as well. The stability of these delays may also be affected by difference in temperature coefficients, temperature gradients, and thermal time constants; these limit the frequency transfer capability of TWSTFT.

During September, October, and December 1994, six Earth stations participating in a TWSTFT experiment on the INTELSAT satellite at 307°East were calibrated in an absolute way using the NMi-VSL Satellite Simulator method. They were also calibrated in a relative way by a visiting small USNO Earth station called Fly Away Satellite Terminal (FAST). Calibration results and the difference with preliminary FAST co-location results are presented.

## METHOD

The results at several Earth stations are obtained with the method and instrumentation developed at the NMi Van Swinden Laboratory using a special satellite simulator (Figs. 1 and 2) to determine the differences of the transmit and receive delays from absolute measurements. The principle of this method has been described earlier<sup>[4,1]</sup>. We have separated the determination of the delay inside the modem from the delays external to the modem (Fig. 3). Firstly, the sum of the receive (RX) delay and a calibrated cable was measured using the satellite simulator (Fig. 4). Then by subtracting the known delay of the calibrated cable, the RX-delay was found. Next, the sum of transmit (TX) and RX delay external to the modem IF TX-output and IF RX-input was measured using the satellite simulator (Fig. 3). The TX-delay was then found by subtraction of the calculated RX-delay. The difference between TX and RX delay was calculated. The transmit delay inside the modem was determined by using an oscilloscope to measure the delay between the transmitted 1PPS pulse and the resulting phase modulation change in the IF TX-output signal (Figs. 5 and 6). By subtraction of this delay from the sum of the internal transmit and receive delay in the modem, the receive delay was calculated. The overall difference between transmit and receive delays was then calculated. This difference was also determined at the travelling FAST Earth station, so the comparison of the results of co-location and the VSL satellite method was possible. Further details of the used procedures can be found in Annexes 1 and 2.

## EQUIPMENT

The equipment that was transported to the various sites fitted in a metal suitcase sized about 1 x 0.4 x 0.4 meter; its total weight was about 18 kg. It consisted of the satellite simulator, a source for the 1425 MHz translation frequency, and a 70 MHz CW unmodulated IF signal source and a set of coaxial cables. Both sources were phase-locked to the local 5 or 10 MHz clock frequency. A set of cables was also supplied. A wide band amplifier for 70 MHz was necessary to drive the satellite simulator 70 MHz port. The delay of this amplifier was also measured because it was part of the "calibrated cable" delay.



## VISITED LABS

The equipment was first used at NPL. The FAST team had a very tight schedule and had a very heavy task apart from setting up the FAST TWSTFT station. VSL introduced the equipment and assisted in the determination of the delays there; the internal modem delays at NPL were determined later. Then at VSL, the FAST station and modem delays were determined, as well as the VSL station and modem delays. The same was done by the station operators at PTB and TUG, but at FTZ and OCA there was not enough time. Later on also, the USNO and the NIST station and modem delays were measured by VSL. It was found that the applied power for the translation frequency, the 70 MHz IF frequency, and their power ratio had to be optimized to obtain the strongest mixer down-frequency signal from the Satellite Simulator.

## RESULTS

The results are given in Table 1. Two types of modems were in use. The first generation MITREX 2500 and the second generation MITREX 2500A (modified digital) modems made by Prof. Hartl at the University of Stuttgart, Germany. The 2500 internal TX and RX delays are grouped together, while the 2500A show a greater spread. The transmit and the filters inside the 2500A are small SAW filters, which have a larger group delay compared to lumped element filters for the same frequency and bandwidth. It appeared also that these two modems differed slightly in the 1PPS modulation method and associated timing. Details of the 2500 modem and the 2500A modem at PTB are shown in Fig. 7. It is not clear if, apart from the 200 ns offset, this difference gives other effects, such as different cross-correlation properties.

## CONCLUSION

Some systematic differences in modems have been discovered and consideration should be given to recommending only one modulation and timing method for MITREX modems and its compatibles because of the strong dependency of the TWSTFT accuracy on reciprocity.

From the comparison (Table 2) of the FAST co-location relative method and the satellite simulator absolute method to determine the non-reciprocal delays, we conclude an excellent agreement of the two methods to the 10 ns level.

The significant deviations of multiples of 100 ns between the two methods with the MITREX 2500A modems at USNO and PTB should be further investigated.

The overall conclusion is that if any station has measured its TX and RX delay difference using the satellite simulator calibration method, it can start accurate absolute time comparisons with any other station that has calibrated its delay similarly, provided the same satellite transponder is used.

## REFERENCES

- [1] G. de Jong, and M.C. Polderman, M.C. 1995, "Automated Delay Measurement System for an Earth Station for Two-Way Satellite Time and Frequency Transfer," Proceedings of the 26th Annual Precise Time and Time Interval (PTTI) Planning and Applications Meeting, 7-9 December 1994, Reston, Virginia, pp. 305-318.



- [2] J. DeYoung, A. McKinley, J.A. Davis, P. Hetzel, and A. Bauch 1996, "*Some Operational Aspects of the International Two-Way Satellite Time and Frequency Transfer (TWSTFT) Experiment Using INTELSAT Satellites at 307°E*," Proceedings of the 27th Annual Precise Time and Time Interval (PTTI) Applications and Planning Meeting, San Diego, California, 29 November-1 December 1995, in press.
- [3] G. de Jong, G. 1990, "*Accurate Delay Calibration for Two-Way Time Transfer Earth Stations*," Proceedings of the 21th Annual Precise Time and Time Interval (PTTI) Applications and Planning Meeting, 28-30 November 1989, Redondo Beach, California, pp. 107-115.
- [4] D. Kirchner, et al. 1995, "*An Automated Signal Delay Monitoring System for a Two-Way Satellite Time Transfer Terminal*," Proceedings of the European Frequency and Time Forum (EFTF), March 1995, Besançon, France, pp. 75-79.
- [5] J.A. DeYoung et al. 1995, "*The 1994 International Transatlantic Two-Way Satellite Time and Frequency Transfer Experiment: Preliminary Results*," Proceedings of the 26th Annual Precise Time and Time Interval (PTTI) Applications and Planning Meeting, 7-9 December 1994, Reston, Virginia, pp. 39-50.
- [6] G. de Jong 1994, "*Two-Way Satellite Time Transfer: Overview and Recent Developments*," Proceedings of the 25th Annual Precise Time and Time Interval (PTTI) Applications and Planning Meeting, 29 November-2 December 1993, Marina del Rey, California, pp. 101-117.
- [7] L.B. Veenstra 1991, "*International Two-Way Satellite Time Transfer Using INTELSAT Space Segment and Small Earth Stations*," Proceedings of the 22nd Annual Precise Time and Time Interval (PTTI) Applications and Planning Meeting, 4-6 December 1990, Vienna, Virginia, pp. 393-400.
- [8] D. Kirchner 1991, "*Two-Way Time Transfer Via Communication Satellites*," **Proc. IEEE**, 79, 983-990.

## ANNEX 1

Details of the Earth station delay calibration procedure using the NMi-VSL Satellite Simulator:

1. Make the set-up as described; refer to the Fig. 3. Be sure the down-converter is tuned to the Transmit frequency minus 1495 MHz for Europe and minus 2225 MHz for USA. To test the setup, connect a spectrum analyzer to the 70 MHz RX IF signal at point A. Set the Center Frequency of the spectrum analyzer to 70.000 MHz. The Transmit Gain at the Mitrex should be at +20 dB.

2. Switch the MITREX modem to Clean Carrier. You should now observe a clean carrier at the center. The signal strength should be at least equal to the normal RX clean carrier signal from the satellite. Adjust for maximum signal by rotating the SatSimulator, so the correct polarization is found. If the signal is too strong, place the SatSimulator closer to the rim of the reflector, or further away and insert extra attenuation at the 70 MHz input of the amplifier in the DF/5 harmonic generator box.

3. Switch the MITREX back from Clean Carrier, reconnect the RX IF cable to the MITREX, and try to lock on the signal by setting the RX code equal to the TX code. If locked, observe the P-signal meter; signal strength should be similar to the signal strength from the satellite. Fine-tune the receive frequency of the down-converter so that the delta-f meter shows near zero. If successful, proceed to the following step.

4. When locked to the signal of the SatSimulator, take readings from the Time Interval Counter (TIC). This value is the sum of all the TX and RX equipment delays: in the MITREX, the cables, the up- and down-convertors, the RF Power Amplifier, the feeds, the distance to the SatSimulator, the SatSimulator RF delay, and the Low Noise Amplifier. Note the averaged value as [1].

5. Now connect Calibration Cable end E to the 70 MHz TX output C and TX IF cable end C to 70 MHz output E of the 70 MHz CW generator, so they are interchanged (Fig. 4). The MITREX should again lock. Now the delay is measured of Calibration Cable + amplifier (E-F), SatSimulator IF port F to RF port, distance to the reflector, and the complete RX delays. Note the averaged TIC reading as [2].

6. Connect MITREX 70 MHz TX IF output C with a short known cable to 70 MHz RX IF input A. After lock, note the sum of the internal TX and RX delay of the MITREX modem corrected by the delay of the short cable as [3].

7. If not known previously, the delay [7] of the Calibration Cable E-F should be determined. For this we need two other cables that in turn can be connected to Calibration Cable end F. We can use the already present cables TX IF Cable C-D and RX IF Cable A-B.

7.1 Interconnect TX IF Cable end D and RX IF Cable end B. Cable ends C and D remain connected to MITREX output C and input A. We now measure the sum of the two cables (C-D) + (A-B). Note the value as [4].

7.2 Connect Calibration Cable end E to Mitrex TX IF output C, Calibration Cable end F to RX IF cable end B, and RX IF cable end A to Mitrex RX IF input A. Note this new delay as [5].

7.3 Leave Calibration Cable end E connected to TX IF output C, connect Calibration Cable end F to TX IF Cable end D, and TX IF Cable end C to RX IF input A. Note this delay as [6].



7.4 The delay of the Calibration Cable, including the amplifier (E-F), can now be calculated as:  $[7] = 1/2([5]-[3]) + ([6]-[3]) - ([4]-[3])$ . The delay of the used amplifier in Europe was:  $(3.1 \pm 0.3)$  ns. Twice the delay in the calibration cable branch inside the satellite simulator is added to this delay. This delay was  $(1.1 \pm 0.1)$  ns, so the value 2.2 ns was added to the final result.

8. The equipment RX RF delay from SatSimulator to MITREX RX IF input A is now calculated:  $[8] = [2] - [3] - [7]$ .

9. The equipment TX RF delay from MITREX TX IF output C to the SatSimulator is now calculated:  $[9] = [1] - [3] - [8]$ .

10. The RF TX-RX difference external to the modem  $[10] = [9] - [8]$ .

11. The TX delay inside the MITREX modem from 1PPS TX to 70 MHz TX IF output C is measured using i.e. a digitizing oscilloscope. Trigger on the 1PPS TX output and then determine the delay to the first 70 MHz phase reversal while using TX code 3 or 7. Note the value as  $[11]$ .

12. The RX delay inside the modem can be calculated:  $[12] = [3] - [11]$ .

13. The TX-RX difference inside the modem  $[13] = [11] - [12]$ .

14. The total TX-RX difference of the station is  $[14] = [10] + [13]$ .

15. This value  $[14]$  can be compared to results of this asymmetry correction by other relative methods, such as co-location. In that case, the TX-RX difference of this station also has to be measured by the Satellite Simulator method and half of the combined TX-RX difference is taken into account, as was done in Tables 1 and 2.

## ANNEX 2

### Details of the internal MITREX modem delay calibration:

In the MITREX modems 2500 and 2500A the 1 pulse per second (1PPS TX) is modulated on the pseudo-noise (PN) bit sequences (each sequence consists of 10000 chips of 400 ns, giving a total duration of 4 ms) by first delaying one sequence by a half-chip (= 200 ns) and then advancing the next sequence by a half-chip with respect to the normal timing.

MITREX codes no. 3 and no. 7 both appear to have the 2 last bits of their sequence equal to 1, and both have the first bit of its sequence equal 0, followed by a number of 1-bits. So the bit sequence near the beginning of a 4 ms period consists normally 800 ns of 1 (two last bits), 400 ns of 0 (first bit), and then the all 1's. When the 1PPS TX is modulated, the timing of the bits in MITREX 2500 is: 800 ns of 1, 600 ns of 0 (the first bit is extended from 400 ns to 600 ns), and then 1's. In the MITREX 2500A this is: 1000 ns of 1, 400 ns of 0, then all the 1's. So in the MITREX 2500, the beginning of the first bit coincides with the beginning of the 1PPS TX pulse used for the measurements, but in the MITREX 2500A this was true for USNO and FTZ, but not for PTB: the 1PPS TX is 200 ns extra ahead (see Fig. 7).

However, to accommodate the bandwidth restrictions required by the satellite operator, the MITREX modems have band filters in the transmit path. These filters exhibit a response time after applying a frequency signal for the first time and also after reversing the phase of the applied signal. It is this response time constant which gives a delay to the phase-modulated signal: after a filter the phase reversal is retarded with respect to the input signal. With an oscilloscope this displacement delay with respect to 1PPS TX can be measured.

Also amplitude changes (amplitude going to zero between phase reversals) are introduced: a resonant circuit can only reverse its phase at zero amplitude. We make use of this property to find on an oscilloscope the start of the first bit of the 4 ms sequence that contains the 1PPS TX information. This first bit in the MITREX 2500 has a pattern with a unique 600 ns width (and 1000 for 2500A), as already mentioned. The internal transmit delay is the time between the first edge of the 1PPS TX pulse and the zero-crossing and associated phase reversal at the beginning of the unique 600 or 1000 ns pattern at the 70 MHz TX output.

### Differences between MITREX 2500 and 2500A modems:

In the MITREX 2500 modem, the negative going slope of the 1PPS TX is "on time," while this in the MITREX 2500A is the positive slope. The output pattern of the MITREX 2500A differs slightly from that of the MITREX 2500 (Fig. 5). In the case of PTB, the 1PPS TX pulse is coming out too early by 200 ns, so the pattern was shifted by 200 ns. This correction has been applied in the reported data. In the Modem(TX+RX) delay values of the MITREX 2500A modems at FTZ and USNO, this 200 ns shift does not appear.

### Procedure:

1. Determine for the 1PPS TX signal the parameters used at the station for the Time Interval Counter input:
  - a. the slope of the first edge (negative for MITREX 2500 or positive for 2500A)
  - b. the trigger level for this edge (mostly +0.5 V)
  - c. the termination (50 ohm preferred)
2. Set the MITREX TX code to 3 (or 7).
3. Connect the 1PPS TX signal to channel 1 of the (digital) oscilloscope. Set the slope, trigger



level, and termination according to step 1. Set trigger source to channel 1 only. The first slope of the 1PPS TX pulse should now be visible.

4. Connect the 70 MHz TX signal to channel 2 (choose AC coupling, 50 ohm termination). Leave trigger source to channel 1. Set time base to 1 microsecond per div. If possible, use envelope averaging mode. Now find the unique 600 or 1000 ns wide pattern; the picture should be comparable to Fig. 5. When identified, change the time base and/or offset for the best resolution, so that the 1PPS TX slope is located near the beginning of the picture and the desired zero-crossing and the associated phase reversal is near the end (Fig. 6). Measure now the time difference between the trigger point on the 1PPS TX and the zero-crossing at the beginning of the unique 600 or 1000 ns pattern. The cursor readouts might be used for this. After correcting for the difference in cable delay of the used cables for channels 1 and 2 (and for the 200 ns 1PPS modulation shift in the case of a 2500A modem), this is the internal MITREX transmit delay between the 70 MHz TX output and the 1PPS TX output.

Table 1. TWSTFT station SATSIM calibration results in ns

STATIONS	FAST	VSL	TUG	NPL	NIST	PTB	USNO	FTZ
Date	94-10-03	94-10-01	94-10-17	94-09-27	94-12-14	94-10-08	94-12-09	92-12-03
Time	14:30		13:00		23:58	15:30	16:30	
MITREX Modem								
Type	2500	2500	2500	2500	2500	2500A	2500A	2500A
Internal Modem Delays								
TX+RX	1159.9	1194.7	1160.7	1158.7	1168.9	2054.8	1856.3	1867.0
TX	310.0	319.6	299.8	313.0	275.0	798.0	591.5	592.0
RX	849.9	875.1	860.9	845.7	893.9	1256.8	1264.8	1275.0
TX-RX	-539.9	-555.5	-561.1	-532.7	-618.9	-458.8	-673.3	-683.0
IF Delays								
TX+RX	2343.8			2371.2				
TX+CAL	2476.6			2433.5				
CAL+RX	2459.5			1772.3				
CAL+ampl.	740.2	698.8	558.7	139.6	332.9	1225.2	332.9	
RF+Mod. Delays								
CAL+RX	2475.1	2540.0		1435.8	1871.0	4542.0	2496.2	
TX+RX	2982.9	2532.6		1417.2	2581.5	4516.7	3162.8	
RF Delays								
CAL+RX	1315.2	1345.3	991.1	277.1	702.1	2487.2	639.8	
RX	575.0	646.5	432.4	137.5	369.2	1262.0	306.9	
TX+RX	1823.0	1337.9	854.5	258.5	1412.6	2461.9	1306.4	
TX	1248.0	691.4	422.1	121.0	1043.4	1199.9	999.5	
SATSIM								
CORR	2.1	2.1	2.1	2.1	2.1	2.1	2.1	
TX-RX	675.2	47.0	-8.3	-14.4	676.3	-60.0	694.7	
Total STATION								
TX-RX	135.3	-508.5	-569.4	-547.1	57.4	-518.8	21.4	



Table 2. Comparison of the SATSIM results to FAST co-location

STATIONS	VSL	TUG	NPL	NIST	PTB	USNO
Date	94-10-01	94-10-17	94-09-27	94-12-14	94-10-08	94-12-09
Time		13:00		23:58	15:30	16:30
Modem type MITREX	2500	2500	2500	2500	2500A	2500A
Total STATION TX-RX	-508.5	-569.4	-547.1	57.4	-518.8	21.4
Total FAST TX-RX	135.3	135.3	135.3	135.3	135.3	135.3
FAST-STATION (TX-RX)	643.8	704.7	682.4	77.8	654.1	113.9
0.5(FAST-STATION)	321.9	352.3	341.2	38.9	327.0	56.9
FAST CO-LOCATION	325.4	360.5	327.0		426.0	446.1
Correction N×100ns	0.0	0.0	0.0	0.0	100.0	400.0
DIFF FAST-SATSIM	3.5	8.2	-14.2		-1.0	-10.8

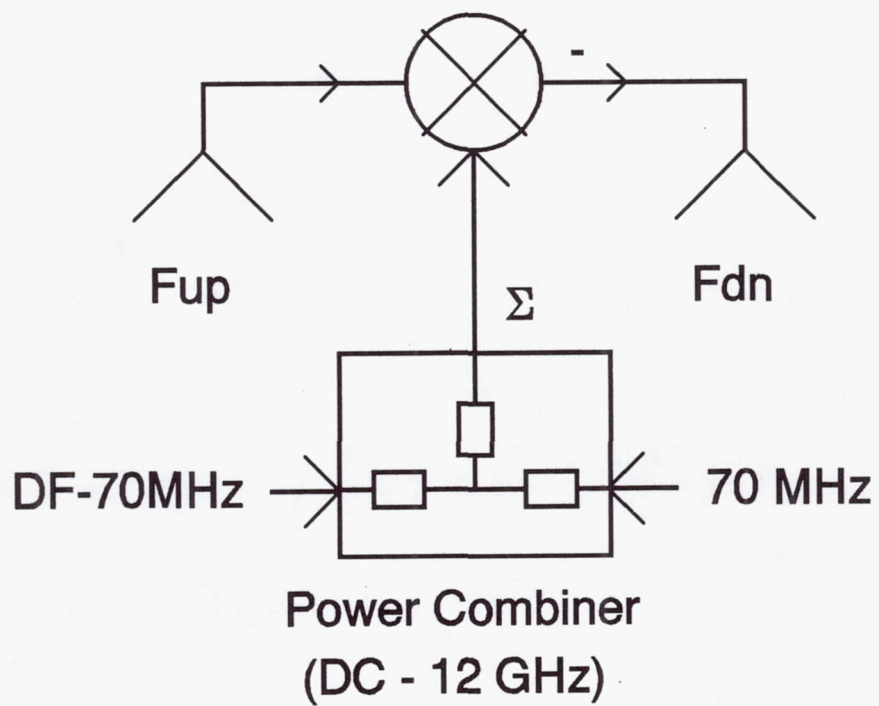


Fig. 1 Principle of the NMi-VSL Satellite Simulator

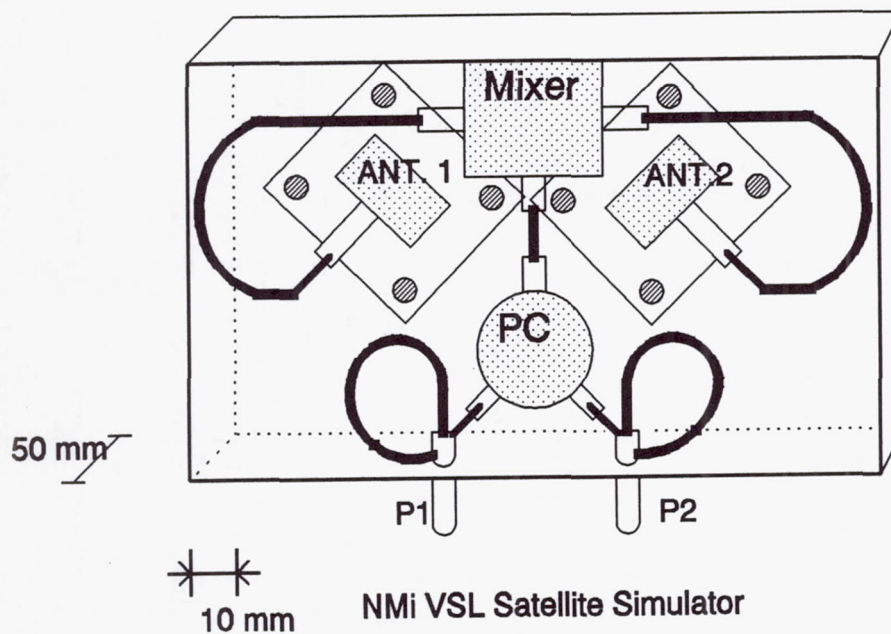


Fig. 2 Lay-out of the NMi-VSL Satellite Simulator



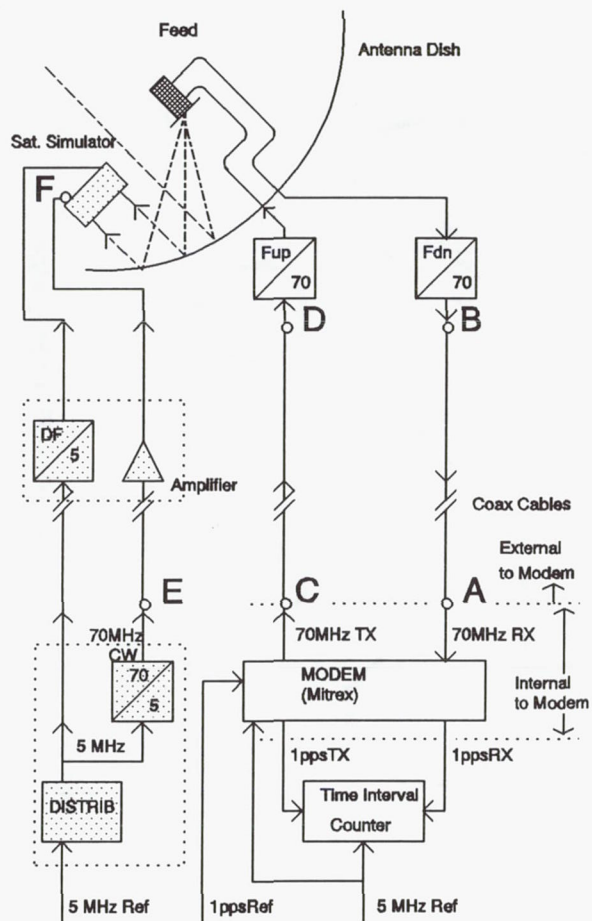


Fig. 3 Measurement of (TX+RX) delay with the NMI-VSL Satellite Simulator

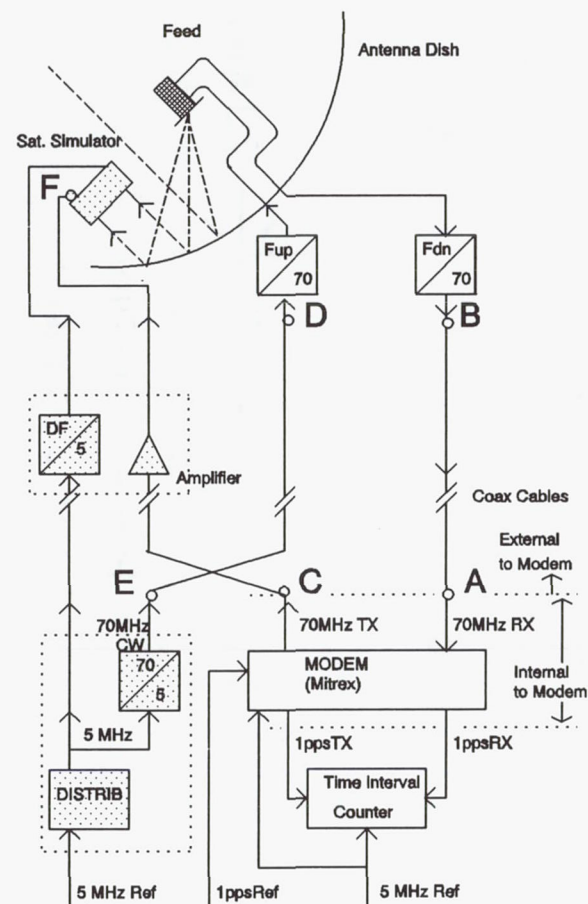


Fig. 4 Measurement of RF (CAL + RX) delay using SATSIM

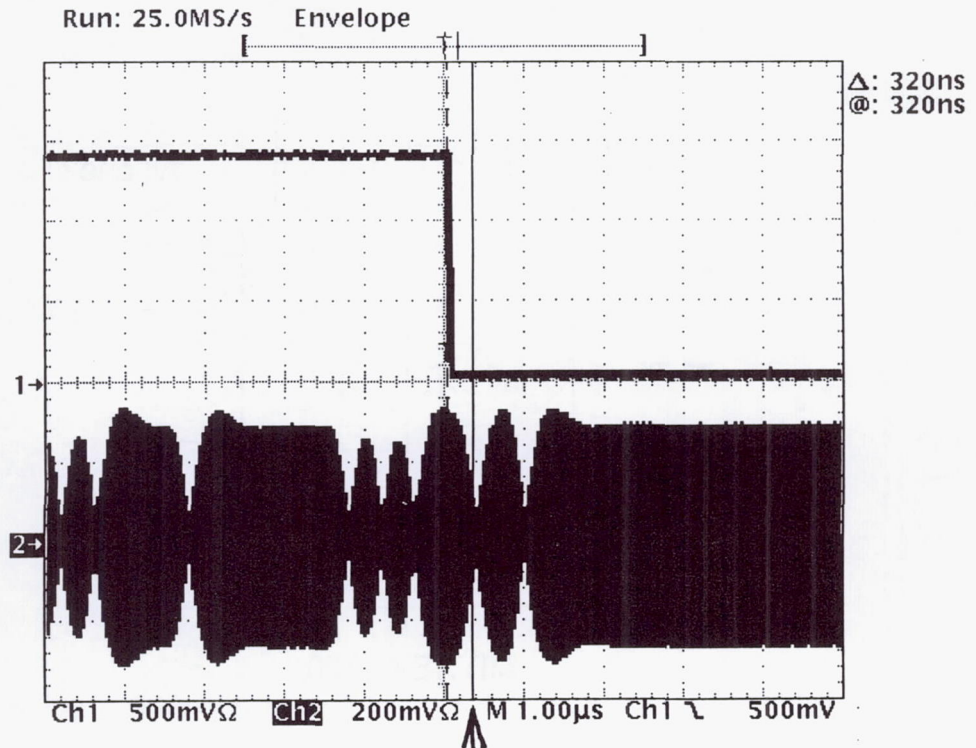


Fig. 5 The 70 MHz TX signal near the 1 PPS TX Ref. transition 1  $\mu$ s/div.

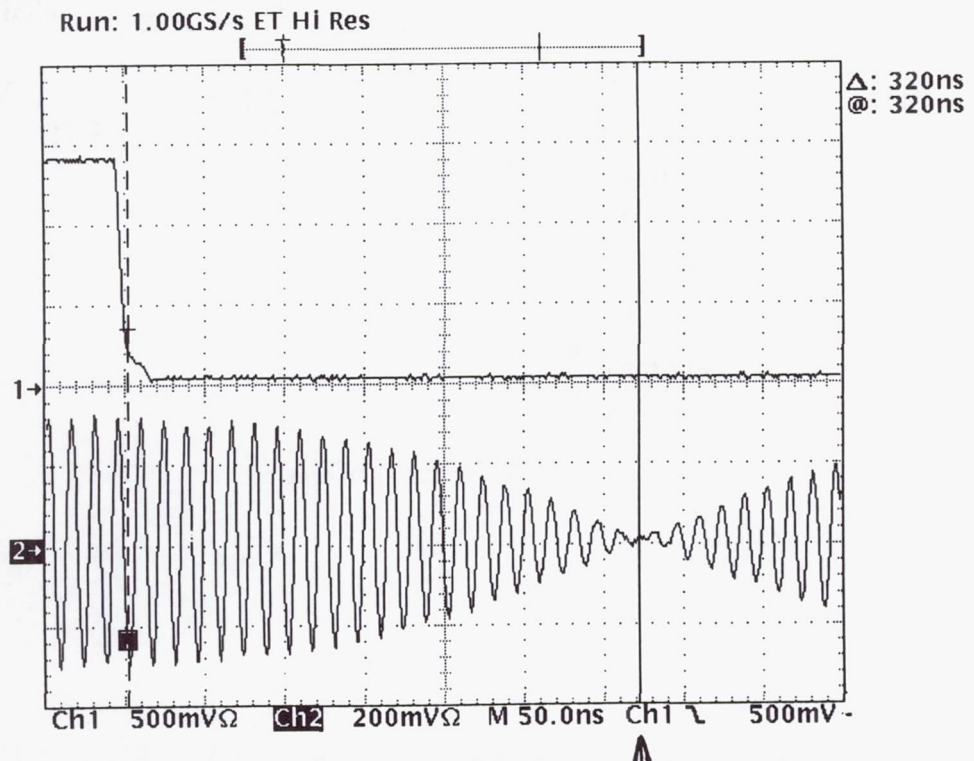


Fig. 6 The 70 MHz TX signal near the 1 PPS TX Ref. transition 50 ns/div.



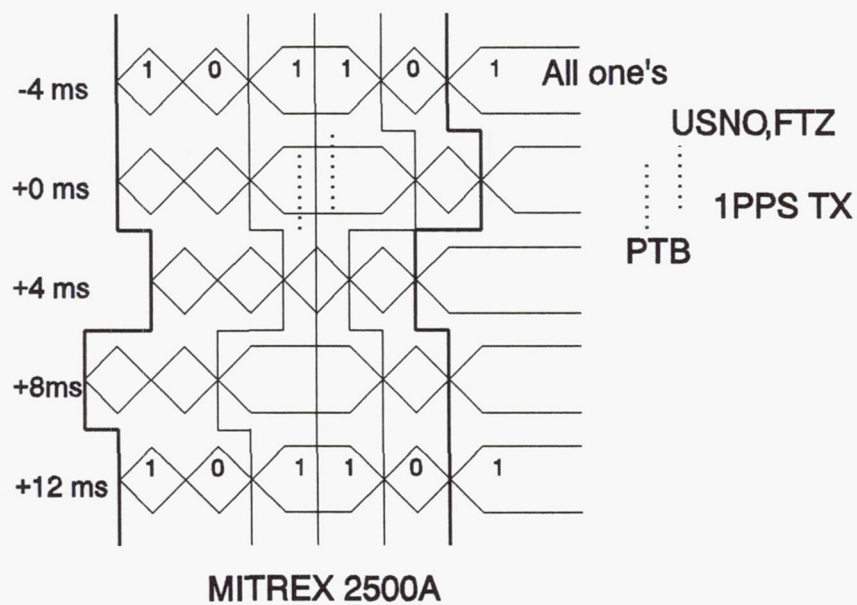
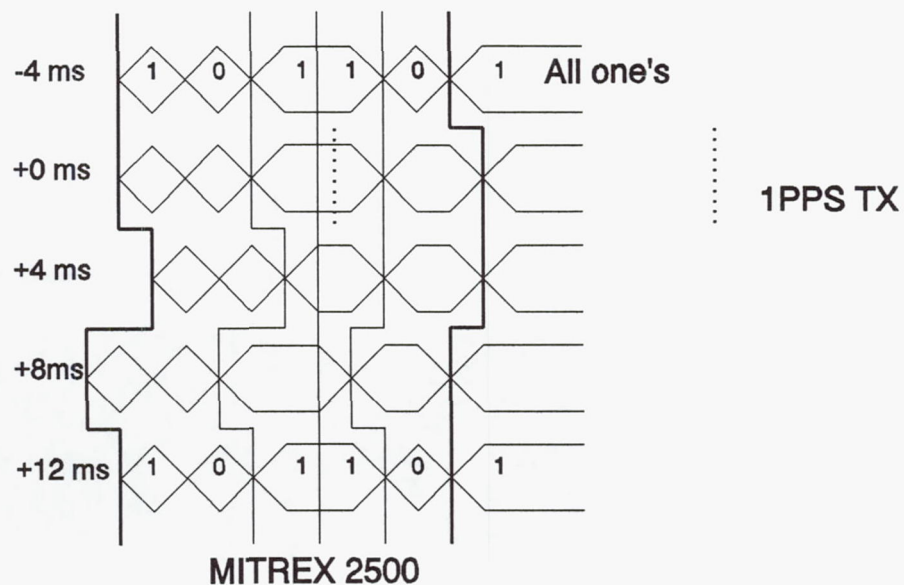


Fig. 7 Timing differences between MTREX 2500 and 2500A

# ACCURATE TIME/FREQUENCY TRANSFER METHOD USING BI-DIRECTIONAL WDM TRANSMISSION

Atsushi Imaoka and Masami Kihara  
NTT Optical Network Systems Laboratories  
1-2356 Take, Yokosuka, Kanagawa, 238-03, Japan

## Abstract

*An accurate time transfer method is proposed using bi-directional wavelength division multiplexing (WDM) signal transmission along a single optical fiber. This method will be used in digital telecommunication networks and yield a time synchronization accuracy of better than 1 ns for long transmission lines over several tens of kilometers. The method can accurately measure the difference in delay between two wavelength signals caused by the chromatic dispersion of the fiber in conventional simple bi-directional dual-wavelength frequency transfer methods. We describe the characteristics of this difference in delay and then show that the accuracy of the delay measurement can be obtained below 0.1 ns by transmitting 156 Mb/s time reference signals of 1.31  $\mu\text{m}$  and 1.55  $\mu\text{m}$  along a 50 km fiber using the proposed method. The sub-nanosecond delay measurement using the simple bi-directional dual-wavelength transmission along a 100 km fiber with a wavelength spacing of 1 nm in the 1.55  $\mu\text{m}$  range is also shown.*

## INTRODUCTION

In digital telecommunication networks, a reference frequency is already being distributed to network nodes in order to synchronize digital switching and multiplexing equipment. If the transmission delay is compensated for by measuring the round-trip path delay using the outgoing and incoming paths, accurate time transfer over long distances will be achieved. The proposed method will yield a time synchronization accuracy of better than 1 ns for long transmission lines over several tens of kilometers. This is useful for operating a distribution network, for locating faults, and in several network time services.

Accuracy in time transfer is determined by the accuracy to which the propagation delay is measured. Since the round-trip path is comprised of paired physically-independent fibers in conventional communication systems<sup>[1]</sup>, the delay measurement accuracy is limited by the asymmetry of the fiber length. A delay-measuring system using simple bi-directional dual-wavelength transmission along a single fiber<sup>[2]</sup> eliminates fiber-length asymmetry, but it incurs error due to the chromatic dispersion of the fiber.

This paper proposes a novel delay-measuring system using bi-directional WDM transmission along a single optical fiber, which can eliminate the error caused by fiber dispersion. The effects



from the difference in delay between the two wavelength signals and the variations are described. The 1.31  $\mu\text{m}$  and 1.55  $\mu\text{m}$  signal transmissions along a 50 km fiber are tested and the feasibility of sub-nanosecond time transfer using the proposed method is confirmed. The bi-directional dual-wavelength transmission along a 100 km fiber is also shown, with a wavelength spacing of 1 nm in the 1.55  $\mu\text{m}$  range. In such a close wavelength transmission system, measuring the sub-nanosecond delay is possible using a simple bi-directional dual-wavelength transmission method (i.e., not using the proposed method).

## DELAY MEASURING METHOD

Simple bi-directional dual-wavelength optical transmission for transferring time signals is shown in Figure 1. The master and slave nodes are connected with a single optical fiber and wavelength division multiplexers/demultiplexers. The reference time signals are generated by the reference clock installed in the master node and transmitted from the master to the slave node using  $\lambda_1$  wavelength light. This  $\lambda_1$  light is modulated using a digital data stream which includes time signals. The feedback time signals are transferred from the slave to the master node using  $\lambda_2$  wavelength light. The time interval counter continuously measures the round-trip delay,  $\tau_{sum}$ , which is the sum of  $\lambda_1$  propagation delay,  $\tau_1$ , and  $\lambda_2$  delay,  $\tau_2$ . The  $\lambda_1$  propagation delay is estimated as half of  $\tau_{sum}$  in this scheme. The delay information is sent to the slave node. In this node, the reference time signal derived from the  $\lambda_1$  light is advanced by electrical phase compensation techniques according to the received delay information.

In this method, the delay measurement error is due to the difference in delay between two wavelength signals, which is caused by the chromatic dispersion of the optical fiber. The proposed delay measurement scheme, presented in Figure 2, compensates for the error due to this fiber dispersion. The reference time signals are always transmitted from the master to the slave using the  $\lambda_1$  wavelength light. The two 1x2 optical switches change the transfer direction of the  $\lambda_2$  wavelength light which transfers the probe time signals. When  $\lambda_2$  signals are transferred from the slave to the master, the time interval counter (TI<sub>1</sub>) measures the round-trip signal delay,  $\tau_{sum}$ . The difference in delay,  $\tau_{diff}$ , equals  $\tau_2 - \tau_1$ , which can be measured by transferring the  $\lambda_2$  signals from the master to the slave in the same direction as the  $\lambda_1$  signals. The  $\lambda_1$  propagation delay can be accurately determined from the following relationship by measuring both the sum and difference terms.

$$\tau_1 = (\tau_{sum} - \tau_{diff})/2 \quad (1)$$

The optical fiber delays,  $\tau_1$  and  $\tau_2$ , vary with changes in the environment, especially temperature. Hence, both  $\tau_{sum}$  and  $\tau_{diff}$  must be measured repeatedly. The measurement interval required to accurately transfer time depends on the characteristics of the variations in  $\tau_1$  and  $\tau_2$ . They are discussed in the following section.



## EFFECT OF DISPERSION

The difference in delay between two wavelength signals is caused by the difference in the group refractive index between the two wavelengths. The chromatic dispersion,  $D$ , is the wavelength variation coefficient of the group refractive index and is illustrated in Figure 3. The characteristic parameters of the dispersion are zero-dispersion wavelength,  $\lambda_0$ , and the dispersion slope at zero-dispersion wavelength,  $S_0$ . The hatched area shown in Figure 3 expresses the difference in delay between two wavelengths,  $\lambda_1$  and  $\lambda_2$ .

We consider here the difference in delay,  $\tau_{diff}$ , and its variation,  $\Delta\tau_{diff}$ . This variation,  $\Delta\tau_{diff}$ , is caused by the difference in the change of the fiber dispersion characteristics with temperature between two wavelength signals. Assuming that  $S_0$  is constant against temperature change in the range from  $\lambda_1$  to  $\lambda_2$  and that the zero-dispersion wavelength is only shifted by temperature change,  $\tau_{diff}$  and  $\Delta\tau_{diff}$  with temperature are

$$\tau_{diff} = \frac{1}{2}S_0 \cdot ((\lambda_2 - \lambda_0)^2 - (\lambda_1 - \lambda_0)^2) \cdot L, \quad (2)$$

$$\Delta\tau_{diff} = S_0 \cdot (\lambda_1 - \lambda_2) \cdot \frac{d\lambda_0}{dT} \cdot L. \quad (3)$$

where  $L$ ,  $\Delta T$ , and  $d\lambda_0/dT$  denote the fiber length, temperature change, and the temperature dependence of zero-dispersion wavelength, respectively.

The normal single mode fiber (SMF) has a zero-dispersion wavelength around 1310 nm. The dispersion shifted fiber (DSF) has a  $\lambda_0$  around 1550 nm and is optimized for transmission in the 1550 nm wavelength region. A typical value of the dispersion slope is about +0.07 ps/nm<sup>2</sup>/km. It is reported that the temperature dependence of the zero-dispersion wavelength,  $d\lambda_0/dT$ , is about +0.03 nm/°C[3]. Figure 4 shows the difference in delay per unit fiber length,  $\tau_{diff}/L$ , as a function of the wavelength difference  $\Delta\lambda_0 (= \lambda_1 - \lambda_2)$  for three different zero-dispersion wavelength fibers. In this calculation, the above parameters and  $\lambda_1 = 1550$  nm were used. The zero-dispersion wavelength of 1310 nm denotes the system using the SMF. The  $\lambda_0 = 1550$  nm and  $\lambda_0 = 1600$  nm are the best and worst cases using the 1.55  $\mu$ m DSF, respectively, because the zero-dispersion wavelength of the DSF is specified in the region from 1500 to 1600 nm[4].

As shown in Figure 4,  $\tau_{diff}/L$  becomes 2.0 ns/km in the system using 1550 nm and 1310 nm as dual-wavelength signals, where  $\lambda_0 = 1550$  nm. For example, the  $\tau_{diff}$  becomes 100 ns where  $L = 50$  km and it must be compensated for by using our proposed scheme described in the above section for ensuring sub-nanosecond time transfer. Where  $\Delta T = 40^\circ\text{C}$ , the  $\Delta\tau_{diff}$  becomes 1.0 ns, thus,  $\tau_{diff}$  must be measured frequently according to the temperature change by changing the direction of the  $\lambda_2$  signals in the proposed method.

If two close wavelength signals around 1550 nm are used, the difference in delay and its variation become small. For example, where  $\lambda_0 = 1600$  nm,  $\Delta\lambda = 1$  nm,  $L = 100$  km, and  $\Delta T = 40^\circ\text{C}$ ,  $\tau_{diff}$  and  $\Delta\tau_{diff}$  are 350 ps and 8.4 ps, respectively. If these values can be ignored, an accurate time transfer will be achieved using a simple bi-directional dual-wavelength time transfer scheme in which two wavelength signals are close. The system using close wavelength



signals within the 1.55  $\mu\text{m}$  band has several advantages compared to the 1.31 and 1.55  $\mu\text{m}$  WDM systems: the fiber span can be wider, higher bit-rate signals can be transmitted, and the amount of short-term jitter is expected to be smaller. Recently, many wavelength multiplexing devices such as the arrayed waveguide grating<sup>[5]</sup> and the fiber grating filter<sup>[6]</sup> have been developed for the 1.55  $\mu\text{m}$  multi-wavelength division multiplexing system. Therefore, such close wavelength multiplexing and demultiplexing can be easily performed.

## EXPERIMENTAL RESULTS

### 1.31 $\mu\text{m}$ + 1.55 $\mu\text{m}$ WDM Transmission

Two 155.52 Mb/s timing reference signals were transmitted bi-directionally along a 50 km 1.55  $\mu\text{m}$  dispersion shifted fiber (DSF). The DSF had a loss of 0.2 dB/km and a zero dispersion at the 1556 nm wavelength. Fabry-Perot multi-mode laser diodes (FP-LDs) operating at 1548 nm and 1315 nm were used as the  $\lambda_1$  and  $\lambda_2$  light sources with the respective output power of -0.4 dBm and +1.8 dBm. Both FP-LDs were directly modulated by 155.52 Mb/s digital signals that included time signals of one pulse per second. The details of the digital signals including time signals were presented in our previous report<sup>[7]</sup>. Nominal sensitivity of the optical receivers was -36 dBm at 1550 nm and -37 dBm at 1310 nm. Wavelength-selective couplers and low/high wavelength pass filters were used as wavelength division multiplexers/demultiplexers, and total isolation exceeded 60 dB. To change the direction of the  $\lambda_2$  signals, we manually changed the fiber connections instead of using optical switches.

Error-free transmission was confirmed in both bi-directional and uni-directional transmission of the  $\lambda_1$  and  $\lambda_2$  signals. The bare fiber, wound on bobbins, was set in a temperature-controlled chamber and its temperature was varied. The  $\tau_{sum}$  and  $\tau_{diff}$  were measured using time interval counters (Stanford Research Systems; model SR620). Due to the fact that both master and slave were set in the same laboratory, true values of  $\tau_1$  and  $\tau_2$  could be directly measured. Under uni-directional transmission conditions, the  $\tau_1$ ,  $\tau_2$ , their difference,  $\tau_{diff}$ , and the chamber temperature are plotted in Figure 5. The short-term jitter appearing in the  $\tau_{diff}$  data is estimated to be mainly due to the electrical circuit used to derive the time signals from the 156 Mb/s signals and the resolution of the time interval counters. The variation of  $\tau_1$  or  $\tau_2$  was about 74 ns for a temperature change of 40°C. The thermal coefficient of the bare-fiber delay, 37 ps/°C/km, obtained from the above results, agrees with the previous reported results<sup>[8]</sup>. The difference in delay,  $\tau_{diff}$ , was 113.6 ns at 25°C and the variation of  $\tau_{diff}$  was about 1.2 ns in this experiment. Under the our experimental conditions in which  $\lambda_1 = 1548$  nm,  $\lambda_2 = 1315$  nm,  $\lambda_0 = 1556$  nm,  $\Delta T = 40^\circ\text{C}$ , and  $L = 50$  km,  $\tau_{diff}$  is 102 ns and  $\Delta\tau_{diff}$  is 0.98 ns from equations (2) and (3). These calculated values agree with the experimental results. The difference in delay and its variation under these conditions cannot be ignored for sub-nanosecond time transfer and must be measured and compensated for by using the proposed method.

The measured values of  $\tau_1$ ,  $\tau_{sum}/2$  in the bi-directional transmission and the  $\tau_{diff}/2$  measured in the uni-directional transmission are plotted against temperature in Figure 6. The error in determining  $\tau_1$ , which equals the difference between  $\tau_1$  and the value obtained from equation



(1), is also plotted. The measured value of  $\tau_1$  agrees with the delay determined from  $\tau_{sum}$  and  $\tau_{diff}$  within about 0.1 ns over the entire temperature range. This result shows that sub-nanosecond time transfer is possible using the proposed method in the 1.31  $\mu\text{m}$  and 1.55  $\mu\text{m}$  WDM system.

## WDM Within 1.55 $\mu\text{m}$ Band Transmission

Distributed feedback (DFB) lasers emitting +3 dBm of optical power at 1547 and 1546 nm were used as  $\lambda_1$  and  $\lambda_2$  light sources. Two bit-rate signals of 155.52 Mb/s and 2.48832 Gb/s, including reference time signals, were tested and were used to directly modulate both DFB-LDs. The sensitivity of the optical receivers was -36 dBm for 156 Mb/s signals and -32 dBm for the 2.488 Gb/s signals. The arrayed waveguide gratings, which have 16 channels with a wavelength spacing of 1 nm in the 1.55  $\mu\text{m}$  band, were used as wavelength division multiplexers/demultiplexers<sup>[9]</sup>. The insertion loss was about 7 dB and the crosstalk with other wavelengths was below -30 dB. We demonstrated both 156 Mb/s bi-directional transmission through a 100 km DSF and 2.488 Gb/s bi-directional transmission through a 75 km DSF while altering the temperature range of the bare DSF wound on bobbins. The DSF had a zero dispersion at the 1561 nm wavelength. The variation of independently measured delay  $\tau_1$ ,  $\tau_2$ , and their difference,  $\tau_{diff}$ , for the 156 Mb/s and 2.488 Gb/s transmissions are plotted with fiber temperature in Figure 7 and Figure 8, respectively.

From equation (2),  $\tau_{diff}$  of 100 km and 75 km transmissions are +100 ps and +76 ps under the experimental conditions. The experimentally measured  $\tau_{diff}$  in Figure 7 and Figure 8 were about +0.2 ns and 0.0 ns, respectively. These values agree with the theoretical values within about 0.1 ns. The difference between the experimental and theoretical values is estimated to be caused by the resolution of the time interval counter. Figures 7(b) and 8(b) show the filtered difference in delay,  $\tau_{diff}$ , with a time constant of 100 s. The filtered  $\tau_{diff}$  in Figure 7(b) and Figure 8(b) varied within 100 ps and 50 ps, respectively. The theoretical value of  $\Delta\tau_{diff}$  due to the temperature change is below 10 ps and it does not appear in Figure 7(b) and Figure 8(b). These results show that the sub-nanosecond delay can be measured using a simple bi-directional transmission in such a close wavelength transmission within the 1.55  $\mu\text{m}$  range.

The square root of the Time Variance<sup>[10, 11]</sup>,  $\sigma_x(\tau)$ , of the  $\tau_{diff}$ , is plotted in Figure 9. The error of the time interval counter (model SR620) is also plotted. The error was measured using the following scheme: the time signal used in the above experiment was split; one was input into the start channel of the counter, and the other was input into the stop channel through a several-meter-long coaxial cable as the proper delay. The  $\sigma_x(\tau)$  in the averaging time region,  $t < 100$  s, was proportional to  $\tau^{-1/2}$ , which presented white noise phase modulation (PM). In this short term region, the variation of the  $\tau_{diff}$  is estimated to include both the jitter due to the electrical circuit used to derive the time signals and the error of the counter. In particular, the result of the 2.488 Gb/s transmission experiment almost coincided with  $\sqrt{2}$  times the value of the counter error. This agreement shows the accuracy of the delay measurement in the 2.488 Gb/s transmission in the region,  $t < 100$  s, was almost solely restricted by the error of the counter, because the noise was characterized by white noise PM and the  $\tau_{diff}$  was the



difference between two values,  $\tau_1$  and  $\tau_2$ , which were obtained by two independent counters. In the region of  $t > 100$  s,  $\sigma_x(\tau)$  was proportional to  $\tau^0$  and the variations were characterized by flicker PM. The flicker noises of both the 156 Mb/s and 2.488 Gb/s transmissions were larger than the counter error in the region where  $t > 1000$  s. The causes of these noises are not clear.

## CONCLUSION

An accurate time transfer method using bi-directional WDM signal transmission was proposed. The 1.31  $\mu\text{m}$  and 1.55  $\mu\text{m}$  signal transmission along a 50 km fiber was tested and the feasibility of sub-nanosecond time transfer using the proposed method was shown. We also demonstrated the bi-directional dual-wavelength transmission along a 100 km fiber with a wavelength spacing of 1 nm in the 1.55  $\mu\text{m}$  range. In such a close wavelength transmission system, the sub-nanosecond delay can be measured using a simple bi-directional dual-wavelength transmission method. These results show that the optical transmission fibers over several tens of kilometers have the capability of time synchronization accuracy of better than 1 ns.

## ACKNOWLEDGEMENTS

The authors wish to thank Dr. Masafumi Koga, Yoshiyuki Hamazumi, Hitoshi Obara, and Dr. Takeshi Kawai of NTT Optical Network Systems Laboratories for their help with the experiments.

## REFERENCES

- [1] A. Imaoka, and M. Kihara 1993, "Time signal distribution in communication networks based on synchronous digital hierarchy," Proceedings of the 24th Annual Precise Time and Time Interval (PTTI) Applications and Planning Meeting, 1-3 December 1992, McLean, Virginia, pp. 303-310.
- [2] D. Johnson, M. Calhoun, R. Sydnor, and G. Lutes, "A wide-band fiber optic frequency distribution system employing thermally controlled phase compensation," Proceedings of the 24th Annual Precise Time and Time Interval (PTTI) Applications and Planning Meeting, 1-3 December 1992, McLean, Virginia, pp. 365-374.
- [3] H. Onaka, K. Otsuka, H. Miyata, and T. Chikama 1994, "Measuring the longitudinal distribution of four-wave mixing efficiency in dispersion-shifted fibers," *IEEE Photon. Technol. Lett.*, **6**, 1454-1456.
- [4] ITU-T Recommendation G. 653, 1993, "Characteristics of a dispersion-shifted single-mode optical fiber cable."
- [5] H. Takahashi, K. Oda, H. Toba, and Y. Inoue 1995, "Transmission characteristics of arrayed waveguide  $N \times N$  wavelength multiplexer," *IEEE J. Lightwave Technol.*, **13**, 447-455.

- [6] E. Fertein, S. Legoubin, M. Douay, S. Canon, P. Bernage, and P. Niay 1991, "*Shifts in resonance wavelength of Bragg gratings during writing or bleaching experiments by UV illumination within germanosilicate optical fibre*," *Electron. Lett.*, **27**, 1838-1839.
- [7] M. Kihara and A. Imaoka 1995, "*SDH-based time and frequency transfer system*," Proceedings of the 9th European Frequency and Time Forum (EFTF), Besançon, France, March 1995.
- [8] N. Shibata, Y. Katsuyama, Y. Mitsunaga, M. Tateda, and S. Seikai 1983, "*Thermal characteristics of optical pulse transit time delay and fiber strain in a single-mode optical fiber cable*," *Applied Optics*, **22**, pp. 979-984.
- [9] M. Koga, Y. Hamazumi, A. Watanabe, and K. Sato 1995, "*Optical path cross-connect systems transport experiment with simulated five-node network*," *Electron. Lett.*, **31**, 1470-1472.
- [10] D.W. Allan, D.D. Davis, J. Levine, M.A. Weiss, N. Hironaka, and D. Okayama 1990, "*New inexpensive frequency calibration service from NIST*," Proceedings of the 44th Annual Symposium on Frequency Control, 23-25 May 1990, Baltimore, Maryland, pp. 107-116.
- [11] D.W. Allan, M.A. Weiss, and J.L. Jespersen 1991, "*A frequency-domain view of time-domain characterization of clocks and time and frequency distribution systems*," Proceedings of the 45th Annual Symposium on Frequency Control, 29-31 May 1991, Los Angeles, California, pp. 667-678.



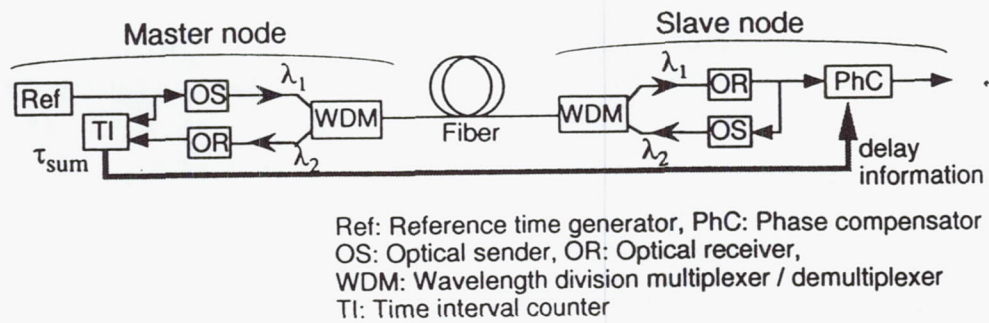


Fig. 1 Time transfer method using simple bi-directional dual-wavelength transmission. The delay information is actually transmitted with reference time signals including the  $\lambda_1$  light.

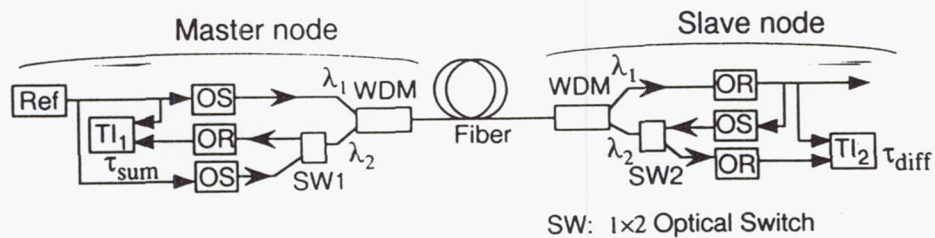


Fig. 2 Proposed delay measurement scheme.

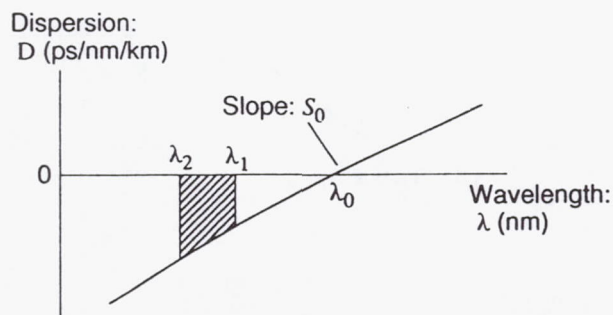


Fig. 3 Chromatic dispersion of optical fiber and its characteristic parameters. The hatched area shows the difference in delay between two wavelengths,  $\lambda_1$  and  $\lambda_2$ .

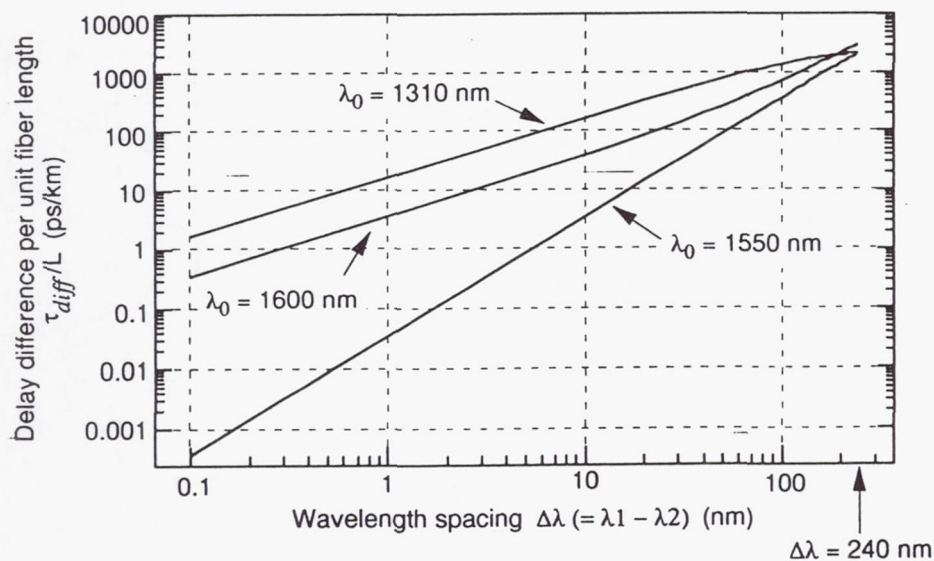


Fig. 4 Delay difference per unit fiber length between two wavelength signals, where the zero dispersion wavelength  $\lambda_0 = 1550$  nm and the dispersion slope  $S_0 = +0.07$  ps/nm<sup>2</sup>/km.



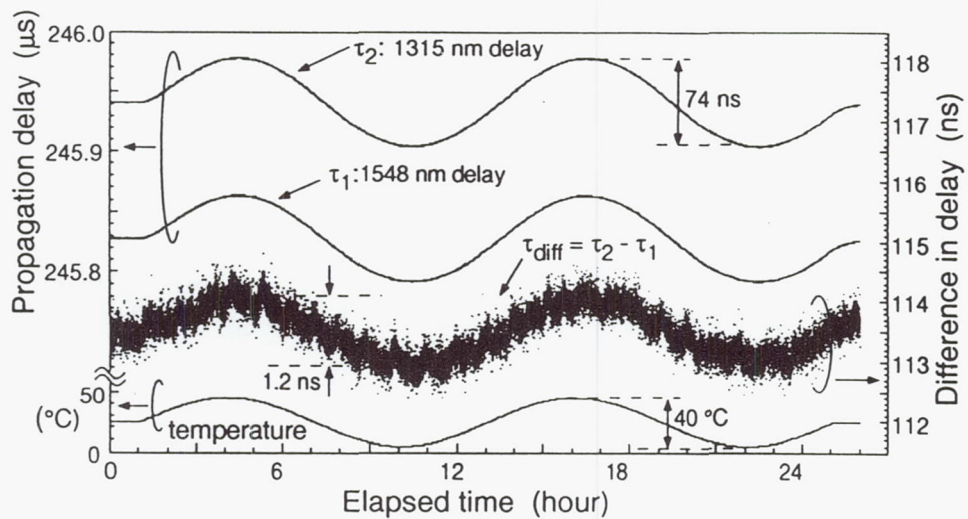


Fig. 5 Measured variations of propagation delay and the difference in delay with temperature change.

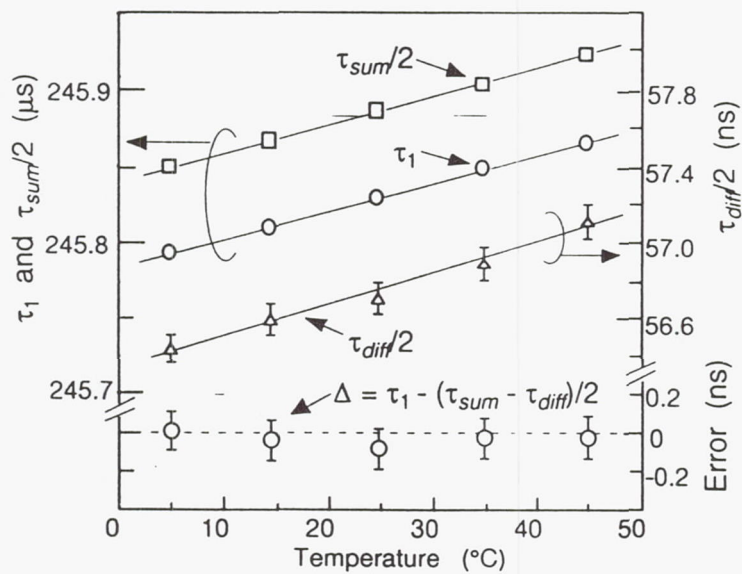


Fig. 6 Measured  $\tau_1$ ,  $\tau_{sum}/2$ ,  $\tau_{diff}/2$ , and the error in determining delay,  $\Delta$ , with temperature.

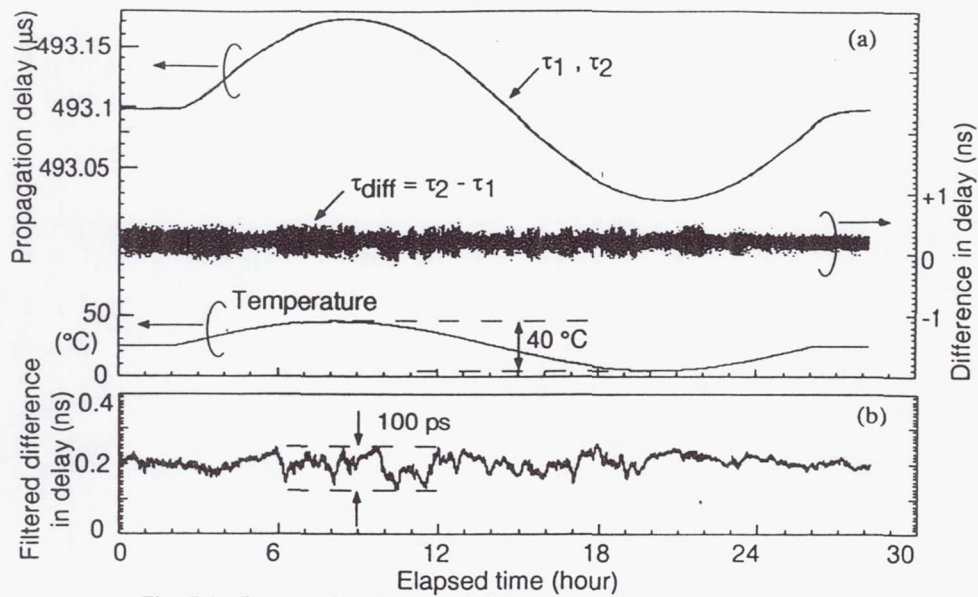


Fig. 7 (a) Propagation delay and difference in delay with temperature.  
 (b) Filtered difference in delay with time constant of 100 s.  
 $\Delta\lambda = 1 \text{ nm}$ , bit rate = 156 Mb/s,  $L = 100 \text{ km}$

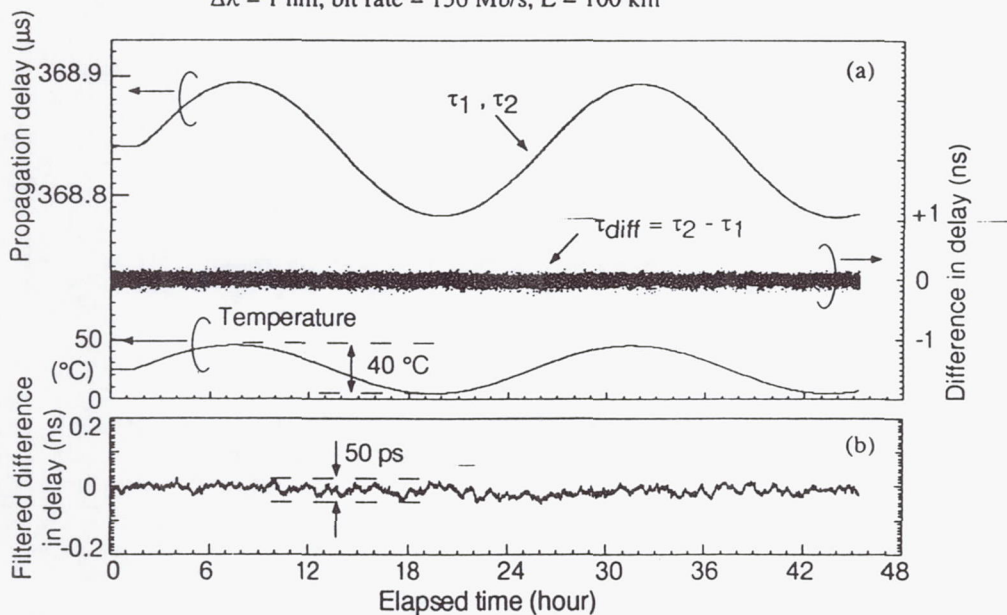


Fig. 8 (a), (b) same as above in conditions of:  
 $\Delta\lambda = 1 \text{ nm}$ , bit rate = 2.488 Gb/s,  $L = 75 \text{ km}$



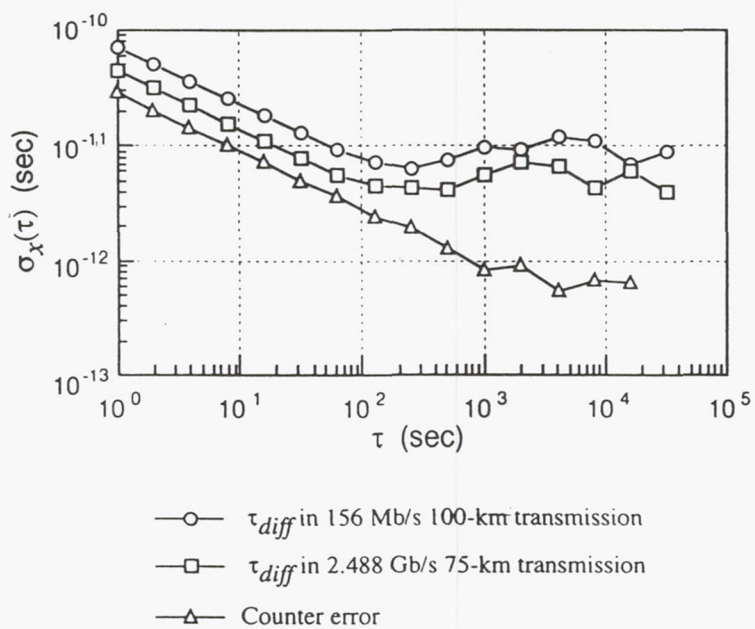


Fig. 9 The square root of Time Variance [11],[12] of  $\tau_{diff}$  compared with the measurement error of the counter.

## Questions and Answers

**DAVID ALLAN (ALLAN'S TIME):** If this were extended to longer paths, 1000 kilometers, what would you expect the accuracy to be? Is this extendable to, say, 1000 kilometers?

**ATSUSHI IMAOKA (NTT):** It depends on the range.

**DAVID ALLAN (ALLAN'S TIME):** Okay, so 1000 kilometers, what would you expect the error to be for it?

**ATSUSHI IMAOKA (NTT):** About 10 nanoseconds.



# LIMITS TO THE STABILITY OF PULSAR TIME

Gérard Petit

Bureau International des Poids et Mesures  
92312 Sèvres Cedex, France

## Abstract

*The regularity of the rotation rate of millisecond pulsars is the underlying hypothesis for using these neutron stars as "celestial clocks." Given their remote location in our galaxy and to our lack of precise knowledge on the galactic environment, a number of phenomena affect the apparent rotation rate observed on earth. This paper reviews these phenomena and estimates the order of magnitude of their effect. It concludes that an ensemble pulsar time based on a number of selected millisecond pulsars should have a fractional frequency stability close to  $2 \times 10^{-15}$  for an averaging time of a few years.*

## INTRODUCTION

Millisecond pulsars have a very regular period of rotation, which suggests that they may be considered as flywheels, generating a pulsar time scale (PT) to which atomic time (AT) can be compared over time intervals of several years. Presently the relative frequency instability of (AT-PT) is at the level of one to two parts in  $10^{14}$  for averaging times of several years. From the observation of many pulsars, an ensemble pulsar time can be derived which is more stable than each individual scale<sup>[1]</sup>.

The apparent period of rotation observed on earth differs from the proper period by terms originating, on the one hand, in the relativistic transformation between the reference frame of the pulsar and the geocentric one and, on the other, in variations in the time of flight of the signal caused by the interstellar medium or gravitation. For this reason, the observed instability of pulsar time may be intrinsic or may arise in the effects just mentioned.

In this paper the phenomena that can affect the apparent period of rotation of a pulsar are reviewed and their magnitudes are estimated with a view to computing the relative frequency stability that can be expected from pulsar time. This stability is evaluated by means of the Allan deviation  $\sigma_y(\tau)$  for an averaging duration  $\tau$ . In this study we are mainly interested in the frequency stability over several years, which implies that pulsar observations must cover ten years or more. A synthesis of the known limits to the stability of pulsar time is presented in the Allan deviation curves of Figure 1.



## BASIC CONSIDERATIONS

A first component limiting the stability of PT is the measurement noise: this is considered to be white phase noise with a measurement uncertainty of order one microsecond. This type of noise averages to zero as the number of measurements increases so that it is always possible to consider that its effect can be made arbitrarily small by increasing the number of the observations and the duration over which they take place. In practice, a reasonable supposition is that one observation, with an uncertainty of one microsecond, is taken every ten days, yielding a stability of  $1 \times 10^{-15}$  for an averaging time of three years (Figure 1).

A second component arises from the need to adjust the timing data to estimate the astrometric parameters of the pulsar: its position and proper motion are determined by a fit of periodic terms with a period of one year; its period  $P$  and period derivative  $\dot{P}$  are determined by a parabolic fit. This procedure sets limits to the stability of PT that are linked to the stability of the reference atomic time scale for integration durations of six months, due to the periodic terms, and of order the total duration of the observations, due to the parabolic fit<sup>[1]</sup>. At very long averaging times, the frequency stability of atomic time is believed to be essentially constant, to within the uncertainty of the primary frequency standards ( $1 \rightarrow 2 \times 10^{-14}$  over the period 1980–1995). For this reason all phenomena that have power law spectra  $S(f) \sim f^{-\alpha}$ , where  $\alpha$  is 4 (random walk in frequency) or 5 and 6 (“red noise”), are affected by the parabolic fit<sup>[2]</sup>. These types of noise would have Allan deviations varying as  $\sigma_y(\tau) \sim \tau^{(\alpha-3)}$ , which would mean that the frequency instability they introduce increases indefinitely with the averaging time: the effect of the adjustment is to prevent this from happening (Figure 2). This situation occurs for many of the physical phenomena described in the following section.

## PHYSICAL PHENOMENA AFFECTING THE APPARENT PERIOD OF ROTATION

### Intrinsic Variations

Regular lengthening of the period of rotation of a pulsar (represented by a constant  $\dot{P}$ ) results from the loss of energy by emission of electromagnetic waves and relativistic particles. This is not discussed further as it is considered an (as yet) inescapable fact that the period changes with a rate  $\dot{P}$  that must be measured, since it cannot be predicted by theory. This phenomenon is a “secular” one modelled by a single parameter. The second-order period derivative  $\ddot{P}$  is not expected to contribute significantly<sup>[3]</sup> for reasonable durations of observation (centuries).

Another phenomenon which may affect the period of rotation is precession of the spin axis. Several theories have been proposed that involve different modes of precession that would cause changes in the rotation rate or in the direction of the emission<sup>[4, 5]</sup>. Some of these phenomena would be periodic, and could eventually be modelled by a small number of parameters, but as no firmly established theory is available it would be necessary to determine the parameters by adjustment of the timing data. The effect of such periodic signatures is treated below, in the section dealing with orbiting companions.

Geodetic precession of the spin axis has been observed for a pulsar in a binary system<sup>[6]</sup>. It



causes long-term variations in the timing data because the part of the emission zone which happens to be directed towards the earth changes. If the geodetic precession is small (weakly relativistic binary system), the quadratic fit ( $P$  and  $\dot{P}$ ) should absorb most of the effect. For a strongly relativistic system that might not be the case, but in such a system the pulsar might become unobservable, its emission not being any more in the direction of the earth. So the geodetic precession is not expected to significantly affect the observed rotation rate of most binary millisecond pulsars ( $\sigma_y(\tau) \sim 1 \times 10^{-15}$ ).

Other phenomena linked to the internal structure of pulsars are abrupt changes in the rotation rate, followed by a relaxation period, that have been observed in many pulsars, mainly young ones<sup>[7]</sup>. Such glitches have not been observed in millisecond pulsars, but it is conceivable that they occur with an amplitude so small that they cannot readily be identified. In any case, the rotation rate must experience intrinsic noise caused by events affecting the structure of the pulsar itself or the emission mechanism. For obvious reasons, these phenomena are not well known.

Intrinsic noise is more easily studied on "long period" pulsars because the population is more numerous, because it has been observed for a longer time, and because the changes in the period of rotation are relatively larger than for millisecond pulsars so that they stand out clearly in the stability analysis. Some authors have tried to relate these instabilities with the period and period derivative using ad-hoc formulas. For example, Cordes and Helfand<sup>[8]</sup>, followed by Dewey and Cordes<sup>[9]</sup>, defined an "activity parameter"  $A$  by comparing the RMS of the timing residuals of a pulsar with that of the Crab pulsar. They showed experimentally that  $A$  could be related to  $P$  and  $\dot{P}$  by the ad-hoc formula:

$$A = a \log P + b \log \dot{P} + c$$

where  $a$ ,  $b$  and  $c$  are constants. Similarly Arzoumanian *et al.*<sup>[10]</sup> defined an absolute parameter  $\Delta(T)$  as the logarithm of the magnitude of the cubic term that can be adjusted to the timing residuals over an interval of duration  $T$ . They showed that, provided that the timing residuals are reasonably cubic, the parameters  $A$  and  $\Delta$  are related. They also determined experimentally an ad-hoc formula:

$$\Delta(T = 10^8 \text{ s}) = 6.6. \times 0.6 \log \dot{P},$$

where all quantities with dimension of time are expressed in seconds. From this, it is possible to estimate the frequency variations due to the cubic-like residuals. One finds, for  $\tau$  significantly lower than the total observation duration  $T$ ,

$$\sigma_y(\tau) \approx \dot{P}^{0.6} (4 \times 10^6 / T) (\tau / T). \quad (1)$$

This formula has been determined by analysis of standard pulsars, not millisecond pulsars. When applying it, by extrapolation, to millisecond pulsars for which the smallest values of the period derivative are of order  $10^{-20} \text{ ss}^{-1}$ , it suggests that these pulsars have an intrinsic stability of a few parts in  $10^{15}$  for averaging durations of a few years (Figure 1). Formula (1) may provide only a very crude estimate, but it is consistent with the fact that, of the two pulsars



observed over the longest duration, 1855+09 ( $\dot{P} = 1.78 \times 10^{-20} \text{ss}^{-1}$ ) has a better apparent stability than 1937+21 ( $\dot{P} = 1.05 \times 10^{-19} \text{ss}^{-1}$ ).

### Gravitational Interactions at the Position of the Pulsar

The ideal pulsar is an isolated object in uniform motion, having no gravitational interaction with other bodies. Its apparent period of rotation then differs from the proper period by a constant factor (Doppler effect). In the real world, we consider three classes of gravitational interaction that affect the pulsar, and therefore the long-term stability of its apparent rotation rate.

The first is gravitational interaction with other masses not in a bound orbit with the pulsar. If a pulsar is submitted to a constant acceleration, its period derivative is biased, but the timing residuals (after the quadratic fit) are not affected. If, however, the pulsar moves in a gravitational field its period derivative, to first order, varies linearly with time:  $\ddot{P}$  is then proportional to the first derivative of the gravitational acceleration, usually called the jerk. Orders of magnitude of the acceleration  $a$ , and therefore of the jerk  $\dot{a}$ , have been estimated for various cases: pulsar in a cluster<sup>[11, 12]</sup>, encounter with a star<sup>[12]</sup>, average effect of galactic stars, white dwarfs, and giant molecular clouds<sup>[13]</sup>. As expected, the largest effect is for the pulsar in a cluster, where the jerk can reach  $10^{-19} \text{ms}^{-3}$ , which would cause cubic-like timing residuals of amplitude tens of microseconds. This is a maximum value, so it is not possible to unambiguously identify this effect in the actual observations of pulsars in clusters (such as 1821-24 and 1620-26). Gravitational acceleration is identified, however, as the cause for a negative value of  $\dot{P}$  for some pulsars in clusters. The gravitational jerk could cause a frequency instability in the  $10^{-14}$  range for  $\tau$  of a few years (Figure 1). For pulsars not in clusters, this effect is several orders of magnitude lower, except in the case of an improbable close encounter with a star.

The second gravitational interaction is with one or several companions in a bounded system. In this case the position of the pulsar moves with respect to the barycenter of the system, so causing a periodic signature in the timing data. The interaction is described by a small number of parameters (Keplerian parameters) that have to be determined from the timing data. If the duration of observation does not span several orbital periods, it is not possible to determine the orbital parameters reliably, so possible companions with orbital periods comparable with the duration of the observations have to be considered as a source of long-term instability. The order of magnitude of the effect is proportional to the mass of the companion: For a Jupiter-like planet orbiting the pulsar in a few tens of years, the amplitude of the periodic effect would be several seconds and, after quadratic fit, the effect on the timing residuals would still be to cause variations in the observed rotation rate of order  $10^{-10}$ . Even a Pluto-like planet in a similar orbit would cause variations close to  $10^{-14}$  (Figure 1). It is, therefore, to be hoped that millisecond pulsars do not have sizeable planets, with long periods, around them.

The third interaction is with gravitational waves. Gravity waves sweeping over an area change the space-time metric and, therefore, affect the proper time of clocks in this area relative to clocks elsewhere. Pulsar Time and Atomic Time are affected differently and this shows up in the timing residuals. Due to the short-term noise of pulsar timing and to the adjustment



of yearly terms, measurements are sensitive only to waves with periods of several years for which the only source is probably stochastic background from the early universe (primordial gravitational waves or waves originating in vibrations of cosmic strings). Their power spectrum is expected to vary as  $f^{-5}$ , but their expected amplitude is uncertain by at least fifteen orders of magnitude<sup>[14]</sup>. It is not possible, therefore, to specify an order of magnitude for this effect in Figure 1. Rather, millisecond pulsar timing results make it possible to constrain the energy density of the gravitational wave background<sup>[15]</sup>, and so to discriminate among cosmological models of the universe.

## Signal Propagation

Two effects can be held responsible for variations in the time of propagation from the pulsar to the earth which can cause long-term variations in the apparent rotation rate: one is the dispersion by the interstellar medium, and the other is the gravitational effect of intervening masses.

The interstellar medium is dispersive, like the earth's ionosphere, and this causes a propagation delay along with variations in the angle of arrival. These variations cause scintillation phenomena in which can be distinguished the diffractive regime (short-term variations,  $\sim 100$ s) and the refractive regime (at longer averaging times). These phenomena change continuously due to the relative motion of the pulsar, the solar system, and the medium itself. Their effect on pulsar timing has been studied by many authors<sup>[16, 17, 18]</sup>. As the effect is essentially proportional to the inverse square of the frequency, it can be determined by dual-frequency observations. Uncertainties in this determination originate in non-dispersive effects (that can be approximated by higher order terms of the frequency) and possible changes in the pulse shape with frequency. It is expected that, after taking into account the dispersive effect by dual-frequency observations, the remaining effect has the power spectrum of white or flicker phase noise and induces a frequency instability of not more than  $2 \times 10^{-14}/\tau$  with  $\tau$  in years (Figure 1) if the signal from the pulsar crosses a large part of the galaxy<sup>[18]</sup>. For a pulsar closer to us, this value can be one order of magnitude smaller.

Masses close to the path from the pulsar to Earth cause a gravitational delay and a "bending" of the path. The bending causes a change in the angle of arrival (similar to refraction by the interstellar medium), but this is lower than  $10^{-8}$  rad for an average star crossing the line of sight so has limited impact on the long-term stability. On the other hand, the gravitational delay can be significant<sup>[19]</sup>: A star of one solar mass with a closest approach of  $10^{-8}$  rad to the pulsar-earth path could perturb the frequency stability by a few parts in  $10^{14}$  ( $\tau$  = a few years, see Figure 1). This is very unlikely: typically, the star closest to the path might have an angular separation of order  $10^{-5}$  rad (a few seconds of arc), but it is unlikely that this star and the pulsar would also have a relative proper motion large enough for this angle to change by several times its value during the period of observation. The average value of the gravitational delay effect can be estimated to be no larger than about  $2 \times 10^{-15}$  (Figure 1).



## Gravitational Interactions at the Position of Earth

All effects noted that can modify the position of the pulsar can also affect the position of the barycenter of the solar system (SSB) and the position of the earth relative to the SSB. Gravitational effects on the SSB are of similar magnitude to those on the pulsar itself, or are smaller. The solar system is not inside a cluster of stars and the surrounding star population is quite well known, so direct gravitational effects on the position of the SSB are expected to have a negligible influence on the long-term stability of pulsar time. The effect of gravitational waves is similar to that on the pulsar.

Presently it seems that the most important source of uncertainty in the SSB position is that due to uncertainty in the masses of outer planets, or to the omission of some masses. As an example, an error in the mass of one of the large asteroids by the amount of its present uncertainty would correspond to a periodic change in the SSB position of about 300m (i.e. one microsecond in timing residuals) with a period of a few years. Uncertainties in the masses of the outer planets<sup>[20]</sup> may be the cause of a larger shift of the SSB, but with periods from tens of years to a few hundred years so that the effect on the timing residuals, after quadratic fit, is not larger. Overall it is thought that the uncertainty in the SSB position and in the relativistic transformation from the topocentric frame of observation to the barycentric reference frame does not cause frequency variations greater than a few parts in  $10^{15}$  ( $\tau$  = a few years, see Figure1). In addition, any error originating in the orbit of the earth would, to first order, be absorbed by the parameters representing the position and proper motion of the pulsar, as these are determined from the timing data. Such errors would not directly affect the long-term stability of pulsar time.

## CONCLUSIONS

From the above presentation, it seems that the long-term ( $\tau$  = a few years) stability of pulsar time should be a few parts in  $10^{15}$  for a number of millisecond pulsars. In selecting pulsars for computing an ensemble average, one should avoid, or give a low weight to, the following:

- Pulsars inside clusters because of the direct gravitational effect: the inclusion of a second period derivative might be sufficient to account for this effect, but it would require a longer observation period to decorrelate this term from other effects.
- Pulsars for which the dispersion measure is very large, which are more likely to show residual effects of the interstellar medium (after removal of the dispersive effect with dual-frequency observations).
- Pulsars with high values of the period derivative, which might be intrinsically more noisy.

Periodic terms with periods of years to tens of years (e.g. due to pulsar companion, precession, motion of the SSB) and other systematic effects (gravitational delay) may be detectable only after a very long period of observation. In the mean time, their effect should be treated as noise. In general, all the effects noted above are uncorrelated among pulsars and can be reduced by averaging. Gravitational effects on the SSB would show a definite signature, which



could ultimately make it possible to discriminate among them. Provided the distribution of pulsars is isotropic, however, the magnitude of these effects would also be reduced by averaging. In conclusion, an ensemble pulsar time should be stable to a few parts in  $10^{15}$  for averaging durations of several years. This value is comparable to the stability of current atomic time scales for averaging durations of 10 days to a few months<sup>[21]</sup>. It is also close to the uncertainty of recent atomic frequency standards<sup>[22]</sup> which will provide the accuracy and, therefore, the long-term stability, of atomic time scales in the future. Comparisons of atomic time and pulsar time are, therefore, useful, although their main function is to examine the physical phenomena affecting pulsars themselves, the propagation of signals, or the ephemerides of the solar system.

## REFERENCES

- [1] G. Petit, and P. Tavella 1995, "*Pulsars and time scales*, *Astron. Astrophys.*, in press.
- [2] R. Blandford, R. Narayan, R.W. Romani, 1984, *J. Astrophys. Astr.*, 5, 369.
- [3] J.H. Taylor, 1991, *Proc. IEEE*, 79, 1054.
- [4] N.K. Glendenning 1990, *Astrophys. J.*, 359, 186.
- [5] J.A. Gil, A. Jessner, and M. Kramer, 1993, *Astron. Astrophys.*, 271, L17.
- [6] J.M. Weisberg, R.W. Romani, and J.H. Taylor 1989, *Astrophys. J.*, 347, 1030.
- [7] J. McKenna, and A.G. Lyne 1990, *Nature*, 343, 349.
- [8] J.M. Cordes, and D.J. Helfand 1980, *Astrophys. J.*, 239, 640.
- [9] R.J. Dewey, and J.M. Cordes 1989, in *Timing Neutron Stars*, eds. H. Vögelman and E.P.J. van den Heuvel, p. 119.
- [10] Z. Arzoumanian, D.J. Nice, J.H. Taylor, S.E. Thorsett 1994, *Astrophys. J.*, 422, 671.
- [11] D.C. Backer, R.S. Foster, S. Sallmen 1993, *Nature*, 365, 817.
- [12] E.S. Phinney 1992, *Phil. Trans. R. Soc. London, A* 341, 39.
- [13] T. Damour, J.H. Taylor 1991, *Astrophys. J.*, 366, 501.
- [14] K.S. Thorne 1987, in *300 Years of Gravitation*, eds S.W. Hawking and W. Israel, p. 330.
- [15] D.R. Stinebring, M.F. Ryba, J.H. Taylor, R.W. Romani 1990, *Phys. Rev. Lett.*, 65, 285.
- [16] B.J. Rickett 1977, *Ann. Rev. Astron. Astrophys.*, 134, 390.
- [17] J.W. Armstrong 1984, *Nature*, 307, 527.
- [18] R.S. Foster, and J.M. Cordes 1990, *Astrophys. J.*, 364, 123.
- [19] K. Ohnishi, M. Hosokawa, T. Fukushima, and M. Takeuti 1995, *Astrophys. J.*, 448, 271.

- [20] J.G. Williams, and E.M. Standish 1989, in **Reference Frames in Astronomy and Geophysics**, eds. J. Kovalevsky, I.I. Mueller, and B. Kolaczek, p. 67.
- [21] C. Thomas, and J. Azoubib 1995, "*TAI computation: study of an alternative choice for implementing an upper limit of clock weights*," *Metrologia*, in press.
- [22] A. Clairon, P. Laurent, G. Santarelli, S. Ghezali, S.N. Lea, and M. Bahoura 1995, **IEEE Trans. Instrum. Meas.**, IM-44, 128.



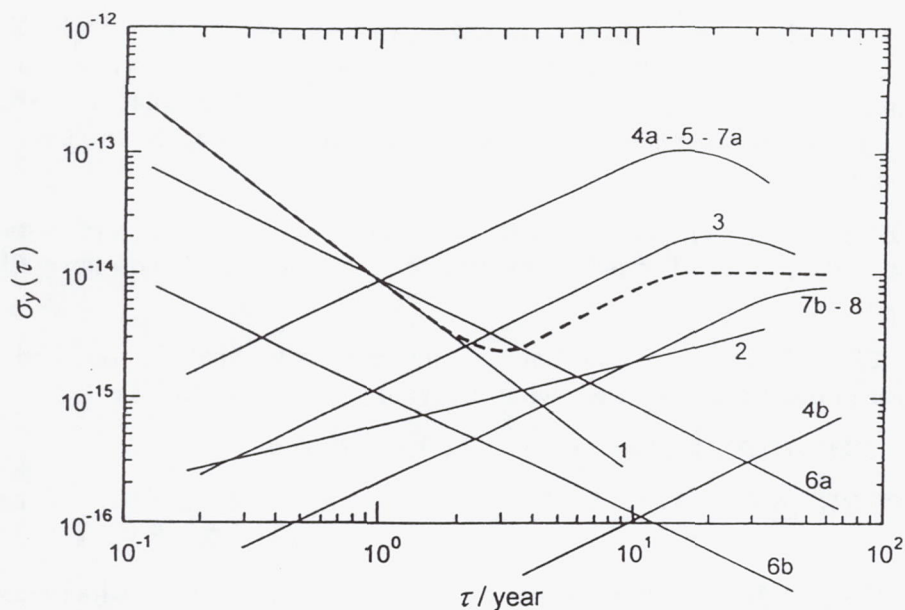


Figure 1. Fractional frequency stability of the effect on pulsar timing of several phenomena: 1 = measurement noise; 2 = geodetic precession; 3 = intrinsic noise; 4 = gravitational jerk (a = maximum, b = typical); 5 = gravitational pull of long period companion; 6 = interstellar medium (a = maximum, b = typical); 7 = gravitational delay of intervening mass (a = maximum, b = typical); 8 = error in solar system barycentre. The dashed curve represents the stability of pulsar time, assuming average conditions for the effects above.

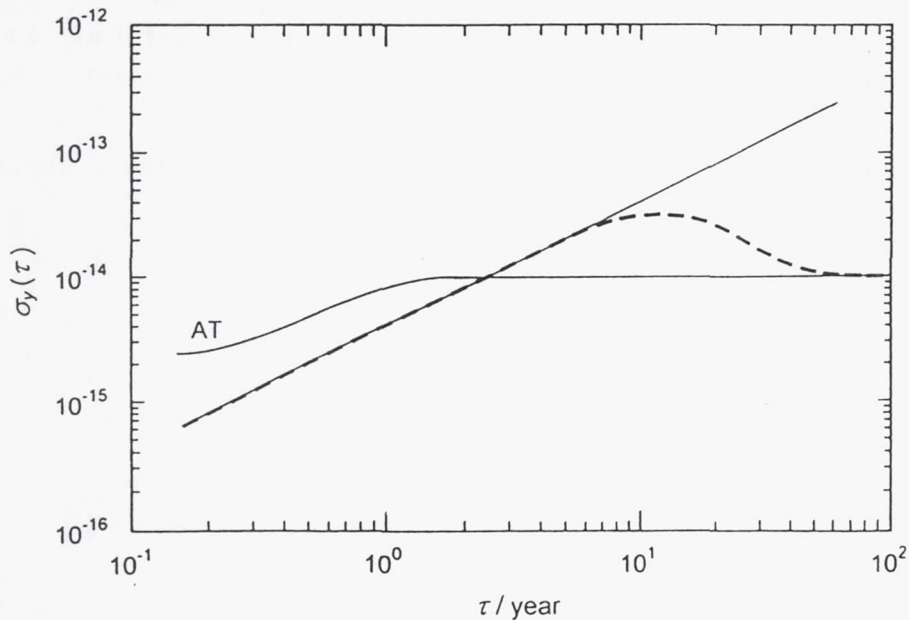


Figure 2. Fractional frequency stability of the current atomic time (AT) and of the effect on pulsar timing of a phenomenon with "red noise" spectrum before (solid line) and after (dashed line) the quadratic fit that determines the period  $P$  and its derivative  $\dot{P}$ .

## Questions and Answers

**DAVID ALLAN (ALLAN'S TIME):** According to Professor Backer at UC Berkeley, and I think Professor Taylor also confirms this, that they have intrinsically within the model, that there is a P double dot as well as a P dot. And they don't know what it is and how big it is. And so, this gives you other low frequency problems which probably don't impact things at  $2 \times 10^{-15}$ .

**GERARD PETIT (BIPM):** Yes, the intrinsic P double dot is at a level which is several magnitudes lower at the time of infusion. Of course, if you have 1000, you have a better length to stop the range.

**ROGER FOSTER (NRL):** Can you make a comment about what do you think it's going to take to establish pulsar time? At least, what are your thoughts at BIPM?

**GERARD PETIT (BIPM):** Do you mean the time it takes?

**ROGER FOSTER (NRL):** What kind of effort does it take on the part of the community to establish that?

**GERARD PETIT (BIPM):** Well, more than 50 millisecond pulsars which are known, the first thing is to observe them regularly. That's not really the case because it would require a continuous report from the observatory.

The second thing is that those who observe the pulsar data are available, which is not always the case.

The third thing is to discover new pulsars so as to be able to choose among a larger set to try to find the right pulsar, which has very good stability. I would say that if we had, say, a half a dozen pulsars in the  $10^{-15}$  class observed for 10, 15 years, we can learn something about atomic time.

**ROGER FOSTER (NRL):** I agree. I'll speak a little bit about this this afternoon.



# GPS MOVING VEHICLE EXPERIMENT

O. J. Oaks  
Wilson Reid  
Naval Research Laboratory  
Washington, D.C. 20375-5000

James Wright  
Christopher Duffey  
Charles Williams  
Computer Sciences Raytheon

Hugh Warren  
SFA, Inc.

Tom Zeh  
Naval Undersea Warfare Center  
Detachment AUTECH

James Buisson  
Antoine Enterprises

## Abstract

*The Naval Research Laboratory (NRL), in the development of timing systems for remote locations, had a technical requirement for a Y code (SA/AS) GPS precise time transfer receiver (TTR) which could be used both in a stationary mode or mobile mode. A contract was awarded to the Stanford Telecommunication Corporation (STEL) to build such a device. The Eastern Range (ER) also had a requirement for such a receiver and entered into the contract with NRL for the procurement of additional receivers. The Moving Vehicle Experiment (MVE) described in this paper is the first in situ test of the STEL Model 5401C Time Transfer System in both stationary and mobile operation.*

*The primary objective of the MVE was to test the timing accuracy of the newly developed GPS TTR aboard a moving vessel. To accomplish this objective, a joint experiment was performed with personnel from NRL and the ER at the Atlantic Undersea Test and Evaluation Center (AUTECH) Test Range at Andros Island. This range is under the direction of the Naval Undersea Warfare Center (NUWC), Newport, Rhode Island. The test was conducted through the West Palm Beach (WPB) Detachment of the NUWC.*

*Results and discussion of the test are presented in this paper.*

## BACKGROUND

The U.S. Naval Research Laboratory (NRL), in the development of timing systems for remote locations, had a technical requirement for a Y code (SA/AS) GPS precise time transfer receiver (TTR) which could be used both in a stationary mode or mobile mode. A contract was awarded to the Stanford Telecommunication Corporation (STEL) to build such a device. The Eastern Range (ER) also had a requirement for such a receiver and entered into the contract with NRL for the procurement of additional receivers. The Moving Vehicle Experiment (MVE) described in this paper is the first *in situ* test of the STEL Model 5401C Time Transfer System in both stationary and mobile operation.

## OBJECTIVE

The primary objective of the MVE was to test the timing accuracy of the newly developed GPS TTR aboard a moving vessel. To accomplish this objective, a joint experiment was performed with personnel from NRL and the ER at the Atlantic Undersea Test and Evaluation Center (AUTEC) Test Range at Andros Island. This range is under the direction of the Naval Undersea Warfare Center (NUWC), Newport, Rhode Island. The test was conducted through the West Palm Beach (WPB) Detachment of the NUWC.

## PARTICIPANTS

The following personnel and their organizations participated in this experiment:

Name	Organization	Title
O. J. Oaks	Naval Research Laboratory	Code 8153 , Head
James Wright	Computer Sciences Raytheon	Timing Systems, Leader
Christopher Duffey	Computer Sciences Raytheon	Timing Systems Engineer
Chauncey Dunn	Computer Sciences Raytheon	Timing Systems O&M, Mgr.
Charles Williams	Computer Sciences Raytheon	Timing Systems O&M , Tech.
Hugh Warren	SFA, Inc.	Engineer
Wilson Reid	Naval Research Laboratory	Code 8153
Ernie Moody	NUWC, Newport	Code 3891, Head
Jack Cecil	AUTEC WPB	Code 3814, Head
Tom Zeh	AUTEC WPB	Program Manager
Dave Cooney	AUTEC Andros Island	Program Test Conductor
Jeff Byrne	AUTEC WPB	Engineer
Linda Tough	AUTEC Andros Island	Range User Coordinator
Laurie Robinson	AUTEC Andros Island	Data Analysis Group
Ed Cote	AUTEC Andros Island	Launch Recovery Sys. Eng.
Gerald Phifer	AUTEC Andros Island	Security Engineer
Rick Beasley	AUTEC Andros Island	R/V Ranger, Captain
Chris Holly	AUTEC Andros Island	R/V Ranger, 1st Mate
Mike Boyle	AUTEC Andros Island	R/V Ranger, 2nd Mate
James Buisson	Antoine Enterprises	Consultant to SFA, Inc.

## METHODOLOGY AND IMPLEMENTATION

To begin the MVE, tests were first conducted in a stationary mode at a known location at the AUTEC pier to assure calibration and initial data validation. The GPS TTR antenna was located directly above a Defense Mapping Agency (DMA) benchmark survey point (Photo 1). Two receivers were used and configured as shown in Figure 1 and Photo 2. The GPS TTR (S/N15) was later removed from the shed on the pier (Photo 3) and used aboard the AUTEC vessel, R/V Ranger. The ship is shown in Photos 4 and 5. While the test was performed on the vessel, the GPS TTR antenna was mounted on the rail adjacent to the bridge of the ship, as shown in Photo 6.

The atomic frequency standards used in the experiment were supplied by Computer Sciences Raytheon (CSR), who is the ER contractor, from their Cape Canaveral Range Operation Control Center (ROCC). The HP 5061A cesium frequency standard (S/N 2383) was maintained



in the ROCC laboratory prior to the MVE. Timing data relative to UTC(USNO) were recorded for ten days prior to its being transported. The 5061A was equipped with an external battery supply, and continuous operation of the clock was maintained throughout the test. The test included a 2-hour drive from Cape Canaveral to West Palm Beach, a 45-minute plane ride from WPB to the AUTECH Andros Island Site, and movement from the pier shed to the ship (Photos 7 and 8).

As shown in Figure 1, both STEL GPS TTRs were driven by the 5 MHz signal from the HP5061A (S/N 2383) frequency standard, to assure calibration of the complete system before removing TTR (S/N 15) to the ship. Figures 2 and 3 depict the equipment configuration next employed. Each of the TTRs was driven by independent frequency standards. The HP5061A frequency standard supplied 5 MHz to TTR (S/N 15), and the FTS 4050 (S/N A167) cesium frequency standard supplied the required 5 MHz to TTR (S/N 20).

The FTS 4050 cesium frequency standard was shipped to AUTECH Andros, with no battery supply, in a powered-down condition. Before being connected to the GPS TTR, its phase was adjusted to within 1 nanosecond of that of the HP5061A. This was done so that at the end of the MVE onboard test, the HP frequency standard could again be compared to the FTS 4050 to assure continuous operation of the HP 5061A clock during the test. The two clocks were operated during a 24-hour period to determine the frequency offset between the two clocks prior to the transport of the HP clock onboard the R/V Ranger.

Figure 4 shows the equipment configuration for the STEL TTR S/N 15 driven by the HP5061A as it was used during the MVE sea trial portion of the test. Photos 9, 10, and 11 show the equipment as it was configured on the bridge of the Ranger.

The AUTECH Andros Test Range was chosen because the Navy routinely performs tests using ships such as the Ranger, and NRL could easily procure space and time as a secondary experimenter at a minimum cost to conduct the MVE. The AUTECH Range performs both a surface radar tracking and in-water precise tracking of the Navy vessels. The precise in-water system uses hydrophone pingers. All tracking data of the ship during the MVE were supplied to the experimenters at the conclusion of the test.

## RESULTS

Data obtained on 14 May 1995, with the equipment configured as shown in Figure 1, are presented in Figures 5 and 6. The plots show the phase difference between the HP5061A clock and UTC(USNO), as measured through GPS using the two TTRs. The 9-nanosecond quantization of the receiver output can easily be seen in the graph. Essentially no phase offset exists between the two receivers, and each receiver realized a peak-to-peak variance of approximately 40 nanoseconds, with an rms deviation of 11.8 nanoseconds and 12.3 nanoseconds respectively. This is considered excellent performance for receivers on a stationary platform.

The tests were repeated on 15 May 1995 in the same configuration, and the essentially identical results are presented in Figures 7 and 8. The rms deviation was 11.9 nanoseconds for TTR (S/N 20) and 10.2 nanoseconds for TTR (S/N 15).

The receivers were then configured as shown in Figures 2 and 3, that is, with each receiver on its own frequency standard. TTR (S/N15) was driven by the HP clock, while TTR (S/N 20) was now driven by the FTS clock.

Results obtained during the period of 15 to 16 May are presented in Figures 9 and 10.

Immediately evident is a frequency offset of the FTS clock from the HP clock, as shown in Figure 10. The larger phase offset in Figure 10 can then be attributable to the accumulated phase due to the frequency offset of the FTS clock, since the two clocks were synchronized on 12 May. Figure 11 presents residuals to a linear fit using the data from Figure 10. The rms deviation of each receiver during this period was 15.3 nanoseconds for TTR (S/N 15) and 15.3 nanoseconds for TTR (S/N 20).

The final results were obtained during the sea trials after TTR (S/N 15) and the HP clock had been placed aboard the R/V Ranger. Figure 12 is the data obtained with Receiver 20 at the shed on the pier. The rms deviation of this data set was 10.7 nanoseconds. Figure 13 presents results obtained from the sea trials. During this period, the speed of the ship changed from stationary to about 10 knots, with the heading varying 360 degrees. Because of the nature of the primary experiments, sudden shocks and vibrations were received by the test equipment. As can be seen in Figure 13, the results were excellent during the entire trial. The rms deviation during the sea trial was calculated to be 14.8 nanoseconds.

## CONCLUSIONS

Figures 14 and 15 are a succinct summary to the MVE. Depicted on Figure 14 is the measured offset of the HP 5061A clock from UTC(USNO) for the entire period of the experiment. Figure 15 presents the residuals to a linear fit of the data and the accompanying statistics. Data for the first ten days were taken at the ROCC lab prior to deployment to AUTECH. Data for the next six days were obtained at the pier in the AUTECH Andros Range. Data for the 17th day were obtained during the sea trials. The final data points were obtained after the clock had been transported back to its original location at the ROCC. The overall closure has an rms deviation of 13 nanoseconds using all the data collected. This is excellent performance and is well within the system specification.





Photo 1 - Initial Set Up on Pier  
(2 antennas)

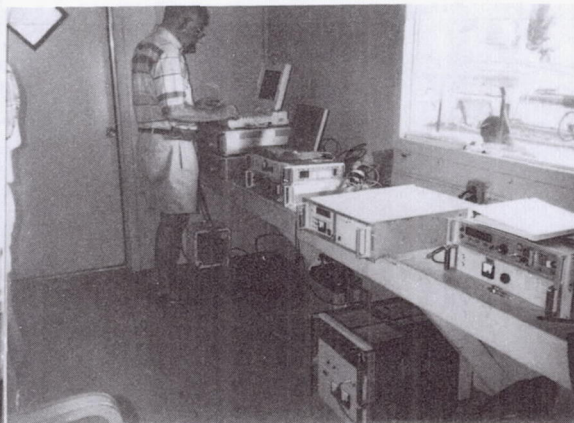


Photo 2 - Equipment in Pier Facility

**MOVING VEHICLE EXPERIMENT  
EQUIPMENT CONFIGURATION #1  
LOCATION: PIER SITE  
5/13/95 - 5/16/95**

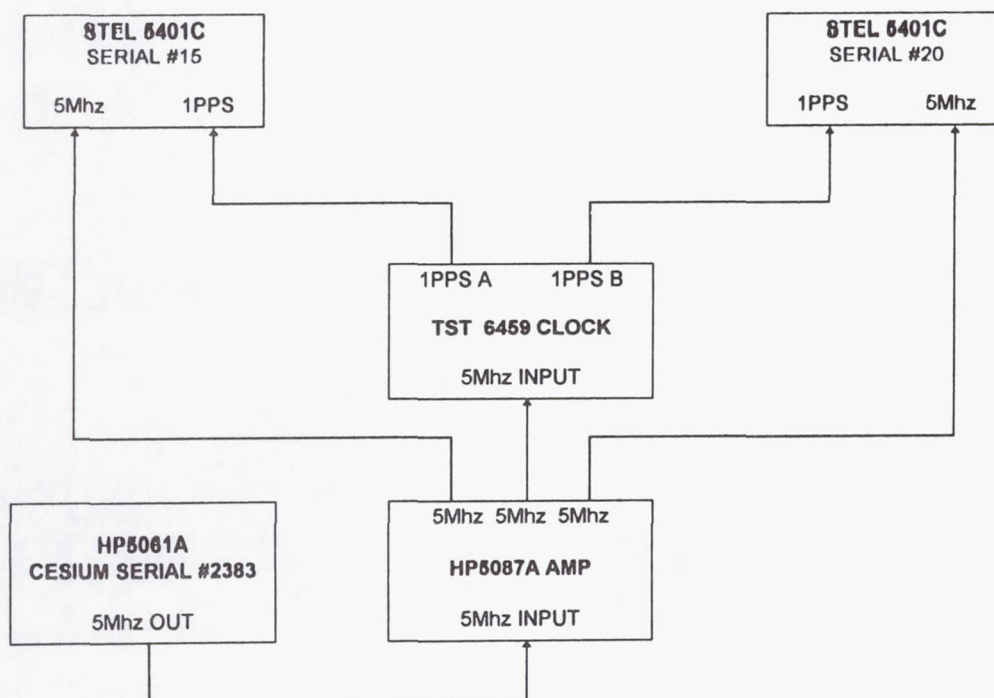


Figure 1 - Initial Equipment Configuration Pier Site



Photo 3 - Pier Site From RV Ranger Bridge



Photo 4 - RV Ranger Vehicle



Photo 5 - RV Ranger View of Outside Bridge

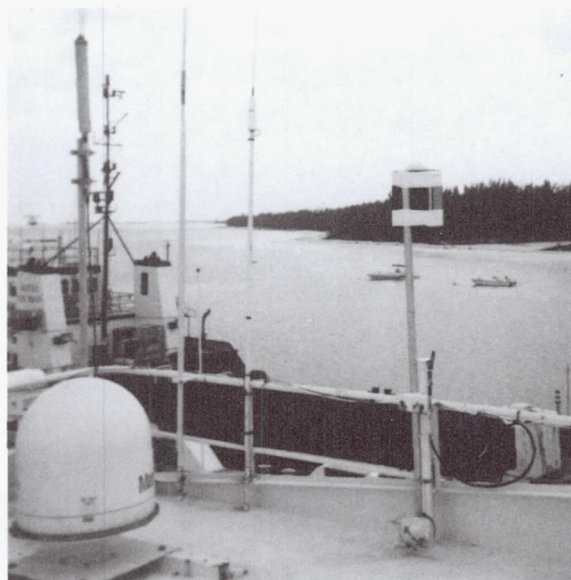


Photo 6 - GPS Antenna on RV Ranger Bridge Area



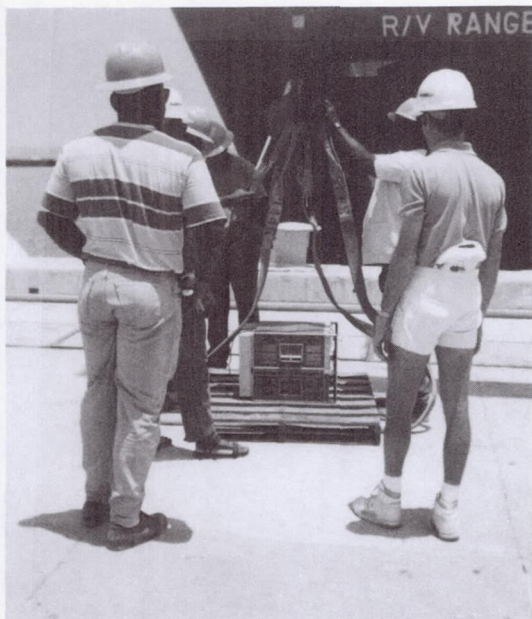


Photo 7 - Cesium Clock on Pier



Photo 8 - Cesium Clock in Flight

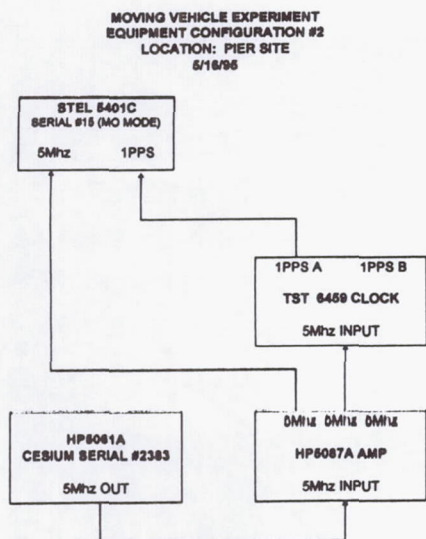


Figure 2 - Equipment Configuration at Pier Site Prior to Shipboard

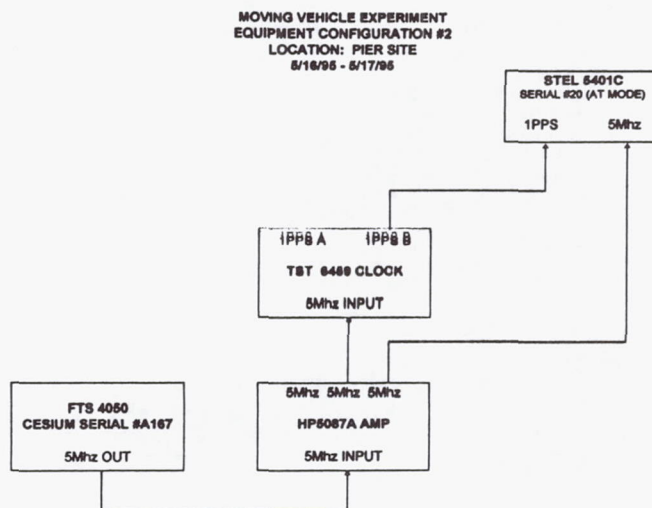


Figure 3 - Final Equipment Configuration at Pier Site

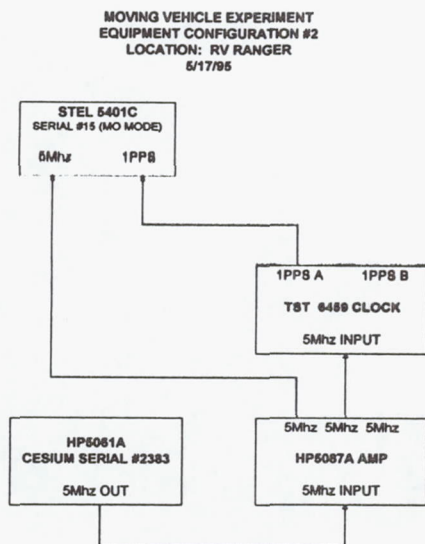


Figure 4 - Equipment Configuration on RV Ranger

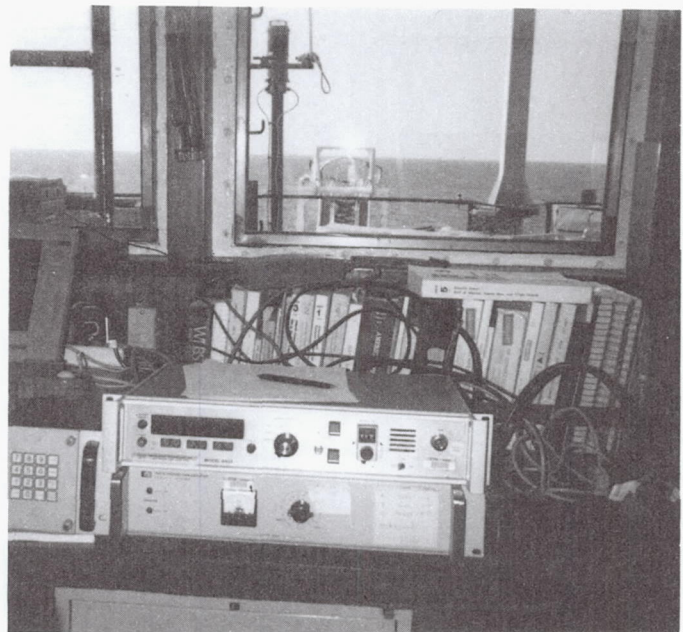


Photo 9 - Equipment in Bridge on RV Ranger

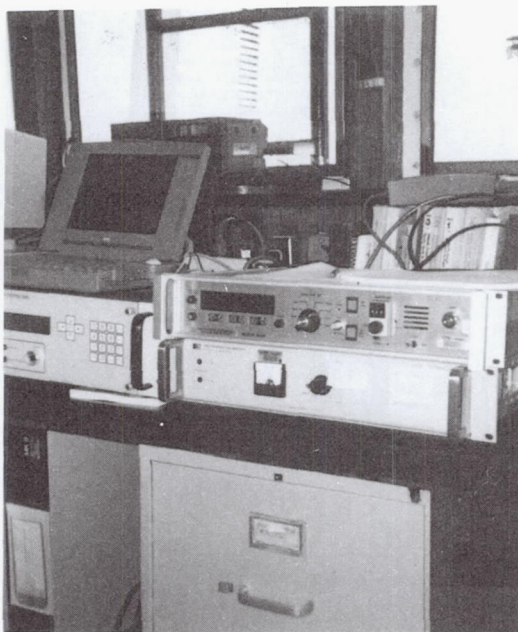


Photo 10 - Equipment on RV Ranger

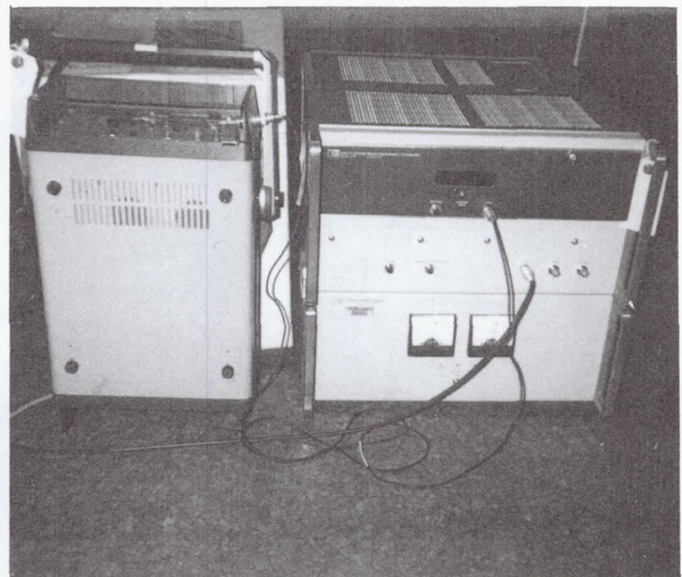


Photo 11 - Clock Onboard RV Ranger



PHASE OFFSET OF HP5061A (S/N 2383) FROM UTC (USNO)  
MEASURED BY TTR (S/N 20) IN MOBILE MODE  
LOCATED AT PIER SITE

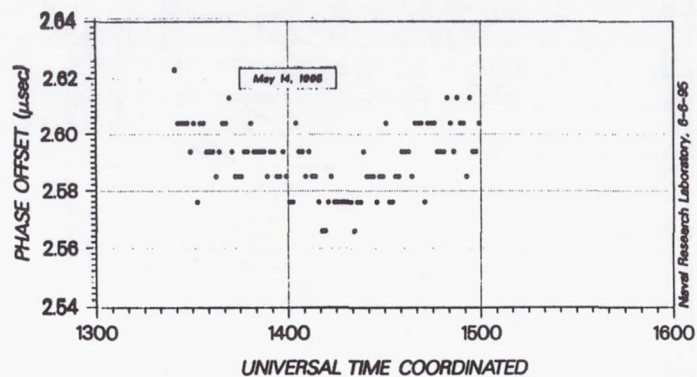


Figure 5

PHASE OFFSET OF HP5061A (S/N 2383) FROM UTC (USNO)  
MEASURED BY TTR (S/N 15) IN MOBILE MODE  
LOCATED AT PIER SITE

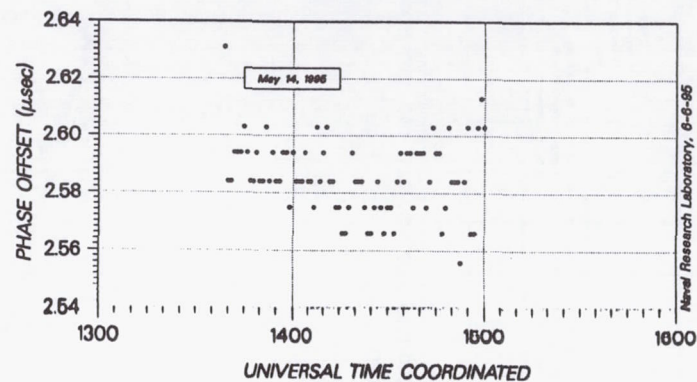


Figure 6

PHASE OFFSET OF HP5061A (S/N 2383) FROM UTC (USNO)  
MEASURED BY TTR (S/N 20) IN MOBILE MODE  
LOCATED AT PIER SITE

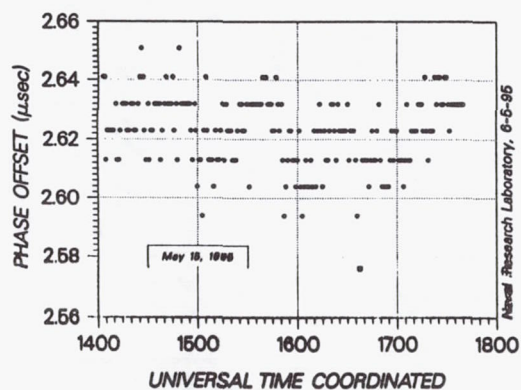


Figure 7

PHASE OFFSET OF HP5061A (S/N 2383) FROM UTC (USNO)  
MEASURED BY TTR (S/N 15) IN MOBILE MODE  
LOCATED AT PIER SITE

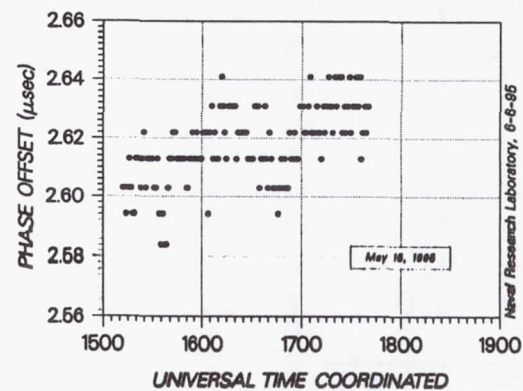


Figure 8

PHASE OFFSET OF HP5061A (S/N 2383) FROM UTC (USNO)  
MEASURED BY TTR (S/N 15) IN MOBILE MODE  
LOCATED AT PIER SITE

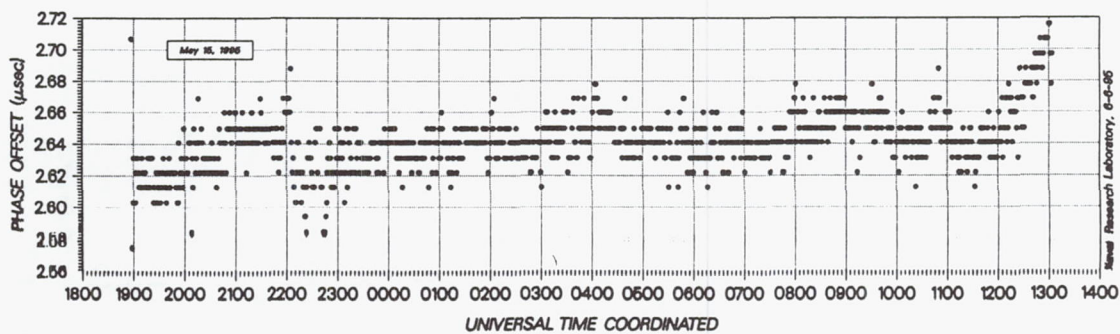


Figure 9

PHASE OFFSET OF FTS 4050 (S/N A167) FROM UTC (USNO)  
MEASURED BY TTR (S/N 20) IN AUTOMATIC TRACK MODE  
LOCATED AT PIER SITE

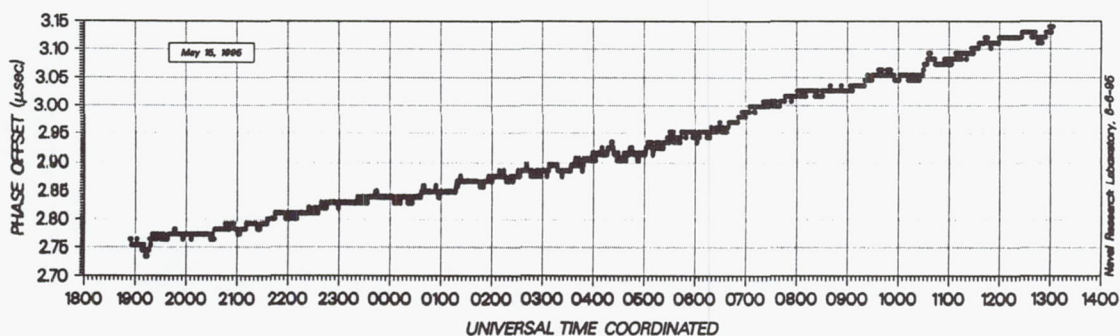


Figure 10

PHASE OFFSET OF FTS 4050 (S/N A167) FROM UTC (USNO)  
MEASURED BY TTR (S/N 20) IN AUTOMATIC TRACK MODE  
LOCATED AT PIER SITE

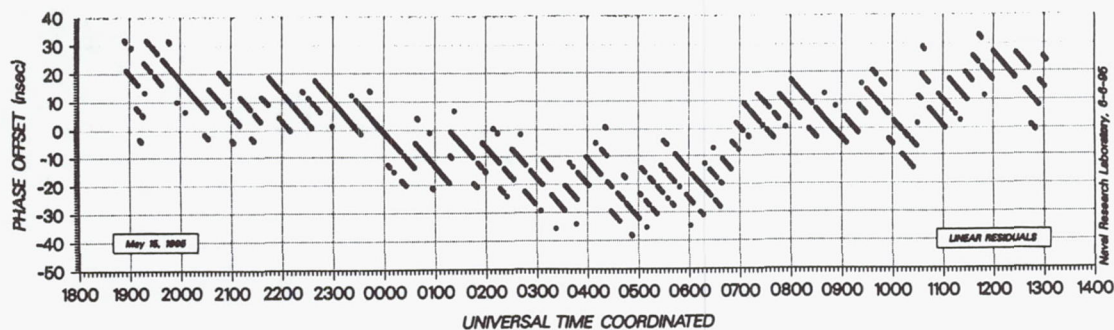


Figure 11



PHASE OFFSET OF FTS 4050 (S/N A167) FROM UTC (USNO)  
MEASURED BY TTR (S/N 20) IN AUTOMATIC TRACK MODE  
LOCATED AT PIER SITE

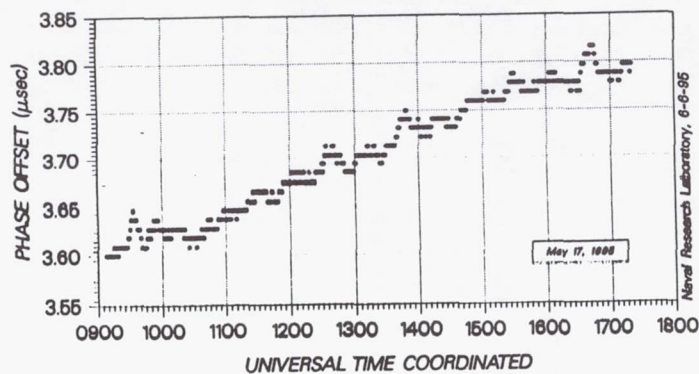


Figure 12

PHASE OFFSET OF HP5061A (S/N 2383) FROM UTC (USNO)  
MEASURED BY TTR (S/N 15) IN MOBILE MODE  
LOCATED ABOARD R/V RANGER

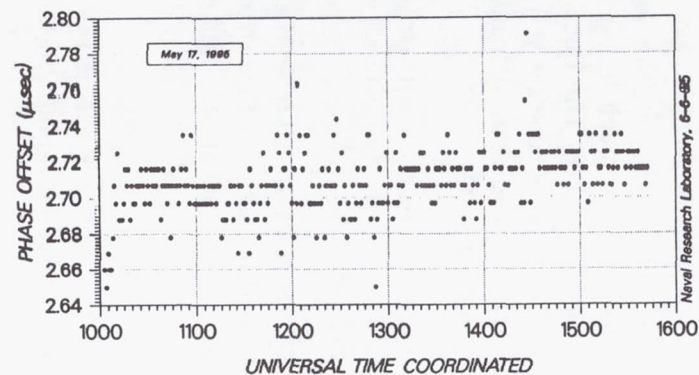


Figure 13

PHASE OFFSET OF HP5061A (S/N 2383) FROM UTC (USNO)  
BEFORE, DURING, AND AFTER MVE EXPERIMENT

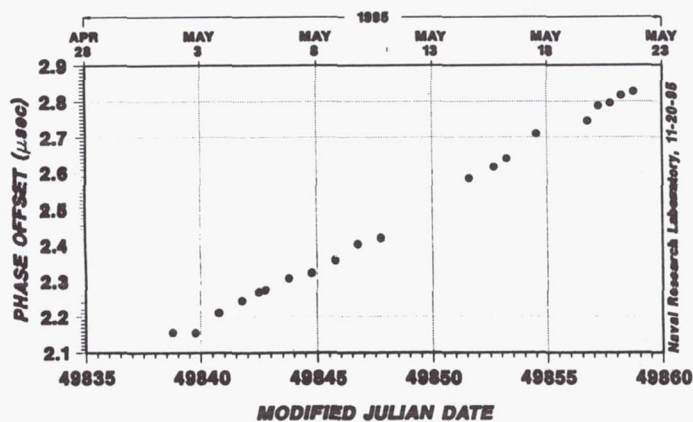


Figure 14

PHASE OFFSET OF HP5061A (S/N 2383) FROM UTC (USNO)  
BEFORE, DURING, AND AFTER MVE EXPERIMENT  
LINEAR RESIDUALS

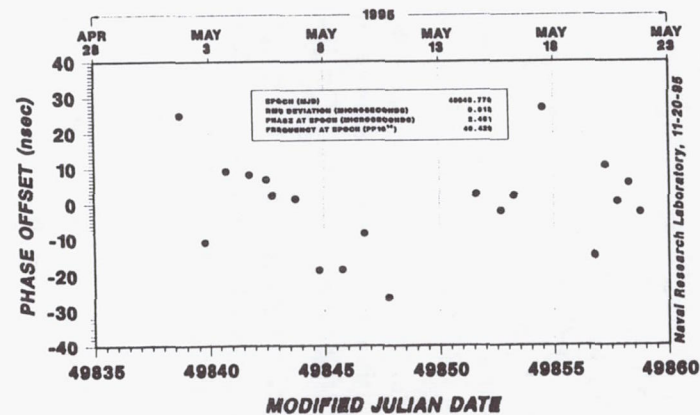


Figure 15

## Questions and Answers

**HAROLD CHADSEY (USNO):** Chris and I had talked earlier about this, this is a loaded question for him. When I gave my presentation, I said it was part of a much larger report. It turns out that Chris's report is the final section that I was unable to do. The question is for you: What type of processing did you do to get such smooth results; because, if you do it out on six-second data points, the six-second data points will vary by more than 50 nanoseconds? When you do your moving position, what was your offset standing still?

The receivers that I was using had offsets in latitude and longitude by approximately a meter; and the altitude was approximately two to three meters, on average, but would exceed 20 meters on the six-second level. I'm just wondering, what did you see?

**CHRISTOPHER S. DUFFEY (COMPUTER SCIENCES RAYTHEON):** We didn't — there's no processing done on this data to smooth it out or correct any — other than removal of the frequency drift in that one cesium. In fact, we were quite surprised that the initial results came up on the prediction for cesium because it's so close. Maybe we've got a couple good receivers.

I haven't shown — we ditched the difference data of the lat, long and altitude of the AUTEK-provided coordinates, they had finger data on our vessels during the whole time. And we haven't quite finished crunching it all. But you do see some small offsets, less than 10 meters, for sure, and probably rms-positioning errors of around six meters difference.

**HAROLD CHADSEY (USNO):** Your results are obviously not six-second data points. How did you get the data points?

**CHRISTOPHER S. DUFFEY (COMPUTER SCIENCES RAYTHEON):** All of those data points were out of RS-232 port of the receiver. And, I look back on it and they were one-minute points.

**HAROLD CHADSEY (USNO):** One-minute averages?

**CHRISTOPHER S. DUFFEY (COMPUTER SCIENCES RAYTHEON):** Yes. The receiver has a Kalman filter in it. So unless you disable that, you are going to get some smoothing in the operation.

**HAROLD CHADSEY (USNO):** Okay, that would be the difference between ours; because, I wasn't using the internal Kalman filtering; we avoided that and wired around it.



# **BONNEVILLE POWER ADMINISTRATION TIMING SYSTEM**

**Kenneth E. Martin  
Bonneville Power Administration  
Vancouver, Washington 98666**

## **INTRODUCTION**

The Bonneville Power Administration (BPA) is a power marketing agency for the U.S. Federal government. It was established to market power from the federal dams being constructed on the Columbia River and has evolved into the major bulk power supplier in the Pacific Northwest. BPA sells power produced at Federal generating facilities, coordinates the Columbia river hydro system, and transmits power for other utilities.

Time is an integral part of BPA's operational systems. Generation and power transfers are planned in advance. Utilities coordinate with each other by making these adjustments on a timed schedule. Price varies with demand, so billing is based on time. Outages for maintenance are scheduled to assure they do not interrupt reliable power delivery. Disturbance records are aligned with recorded timetags for analysis and comparison with related information. Advanced applications like traveling wave fault location and real-time phase measurement require continuous timing with high precision.

Most of BPA is served by a Central Time System (CTS) at the Dittmer Control Center near Portland, OR. This system keeps time locally and supplies time to both the control center systems and field locations via a microwave system. It is kept synchronized to national standard time and coordinated with interconnected utilities. It is the official BPA time.

There are a few BPA applications which are not served by the CTS. BPA's traveling wave fault locator requires microsecond accuracy which is higher precision than IRIG-B can provide. This system, called FLAR for "Fault Location Acquisition Reporter," only has to be synchronized within the system and primarily uses a high frequency pulse over microwave. Some substations remote from the control center do not receive reliable time from the CTS. In some cases they used a free-running source manually reset on an occasional basis. In other cases a WWV or GOES timing receiver was used.

Power system control and operation is described in the next section of this paper. After that BPA timing systems including CTS, FLAR, time dissemination, and phasor measurements are described. References are provided for further reading.

## POWER SYSTEM PRINCIPLES

Electric power is transmitted from generator to load primarily by alternating current (AC) systems. For reliability and economy, transmission systems are connected into grids that have many generators and load areas. Power systems in North America are interconnected into four grids.<sup>[1]</sup> The Western Systems Coordinating Council (WSCC) grid covers the largest area, including the western US and Canada from the Rocky Mountains to the Pacific Ocean. By being part of a grid, each utility gains access to more generators and more transmission paths, which reduces the risk of outage due to failure. Also, sharing generating resources can result in significant savings in meeting peak loads, staggering maintenance, and using the most economical sources. However, interconnection also requires synchronization and controls to prevent a problem in one part of the system from causing problems in another.

There are two distinct synchronizing issues found in power systems. First, electric energy must be used as it is generated. No one has created a successful electricity reservoir or battery suitable for power system use. Load must be constantly in balance with generation. Second, power is produced and transmitted primarily as a 60 Hz (in North America) alternating current (AC). Synchronous devices such as generators and motors must be kept in phase with each other, tracking through frequency changes and disturbances. A primary utility task is keeping load balanced with generation and keeping synchronized with its neighbors.

Every utility is a member of a control area. An area controller, usually a large utility, is responsible for maintaining generation-load balance within that area. If there is insufficient generation for the load, an import from another area will be scheduled, and vice versa. However, power transfer won't just occur just because it is scheduled. It is a result of the phase relationship between areas. Power transfer between two points in an AC system is defined by

$$\frac{P = V_1 V_2 \sin \phi}{Z}$$

where  $V_1$  and  $V_2$  are the voltages at each point,  $Z$  is the line impedance between them, and  $\phi$  is the included voltage phase angle. Since substation voltages are controlled at a constant level and line impedances are fixed, the power transfer is determined primarily by the phase angle between stations<sup>[2]</sup>.

So how is the phase angle set? Phase angle is the integral of frequency. Deviation of frequency from the nominal 60 Hz will either advance or retard the phase angle relative to other areas. Frequency in turn follows the generation-load balance. Despite advances in alternative energy sources, electric power is produced primarily by turning an alternator with a turbine. Power  $P$  produced in the turbine is expressed by  $P = T\omega$  where  $T$  is the torque and  $\omega$  is the angular velocity. A decrease of electric load on the alternator reduces the resisting torque, so the speed of rotation increases to absorb the power applied to the turbine. Conversely, an increase in electric load will cause the machine to slow down. The alternator speed determines the AC frequency. Consequently, the area phase angle is controlled by adjusting the generator-load balance within the area.

Interconnected utilities cooperate to keep the system operating on schedule. Individual genera-



tors and even small areas tend to be self-regulating. If a generator gets a little ahead, the power transfer increases which loads the generator and pulls it back into synchronism. Stabilizers are used to prevent local oscillation within the system. Beyond that, the area controller monitors area frequency and inter-area power transfer, minimizing error through generation control. A system timekeeper records accumulated system time error that results from sustained frequency errors. Coordinated system frequency adjustments continually drive the system time error to zero. Measurements for these controls are made by a CTS at the area control center. Each CTS maintains reference to a national standard so that measurements throughout the grid agree.[3]

#### CTS SYSTEM DIAGRAM

Bonneville Power Administration

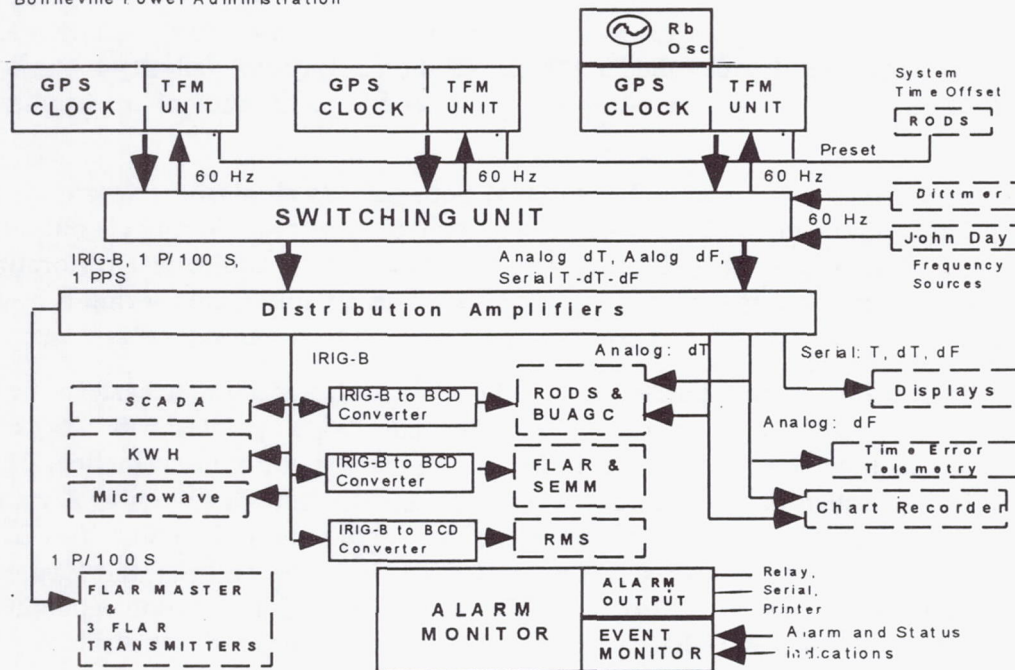


Figure 1. BPA Central Time System

## CTS

In 1994 BPA installed a new CTS based on GPS. It replaced the original single redundant unit installed in 1974 based on WWVB. This new system has triply redundant primary sources, a voting switchover unit, and extensive monitoring. It provides all the time functions previously supplied by the CTS, including time and frequency error and IRIG-B. It also provides the synchronizing reference for the FLAR system (Figure 1). A framed T1 signal output will be added for the new fiber optic communication link.

The primary sources are fully equipped GPS receivers. Each has its own antenna and separate AC power circuit. The two primary units have a battery back up as well. The third, the reference

unit, has a rubidium oscillator with either manual or automatic GPS tuning, selectable by the user. Each receiver generates an IRIG-B, a 1 PPS, and a 1P/100S signal. Each is also equipped with a frequency and time monitor unit which computes power system frequency and accumulated time error. These quantities are output in both analog and a serial format.

Outputs from all three receivers are fed into a switching unit. In normal operation the switching unit compares the three outputs of each quantity against a user set tolerance. If any one of the three exceeds the tolerance, the unit is selected out. If the primary unit is selected out, all outputs are switched to the secondary unit. Once a unit is selected out, the switch drops into a primary-standby mode with the remaining two units. If any of the outputs from the now primary unit fails, the switch will select the last unit. Manual restoration is required to restore the voting mode to prevent multiple switching that could disrupt outputs. Manual mode selection includes three unit voting, two input normal/standby, or any single unit.

The outputs from the switch pass to distribution amplifiers. These are also fully alarmed for output failure. They are also designed for high isolation to prevent failure of one load from affecting other equipment. Separate outputs are provided for different systems to minimize the effects of a failure.

The whole system is fully alarmed with a PC that both records all alarms and groups them for output to other equipment. Selected alarms are sent to a printer. Grouped outputs can be sent out a serial link or routed to a relay. The PC records both failure and restoration times, whether they result in a change in the output or not. This complete monitoring is a great help in analyzing the "mystery event" that so often plagues high-tech automated systems.

A second identical system was purchased for the new control center in eastern Washington. Both systems have been in service about a year. They have been operated with a 1  $\mu$ s tolerance on time, 20 ms in time deviation, and 5 mHz in frequency error measurements. There have been only a few disturbances which caused the three receivers in each system to deviate enough to exceed these limits. Two of these we investigated at length seem to be due to the GPS system itself. Those cases seemed to affect all three receivers at both the Dittmer and Eastern control centers, which are 300 miles apart. Ironically, without the extensive alarming capabilities of the new CTS, those disturbances would have not been noticed, as they did not result in observable system output changes. If GPS is going to play a central role in power system operation, we need better access to timely information for resolving anomalies.

## FLAR

A short circuit on a high-voltage transmission line will create an ionized path that will sustain the short, even if the original cause is removed. Usually momentarily disconnecting the line will allow the ionized path to dissipate enough that the line can be returned to service. Occasionally, equipment is damaged and repair is required before restoration. In this latter case, locating the fault quickly is important and sometimes difficult. A tree in a line is easy to spot if you know where to look; an shorted insulator may be quite difficult to pinpoint.

When a fault occurs on a transmission line, the current increases, voltage decreases, phase angle increases, and a high-frequency wave propagates in both directions from the fault at nearly



the speed of light. The distance from a terminal to the fault can be computed by comparing the line impedance per unit distance with the apparent impedance produced by the fault. This technique does not work well with series compensation (capacitors) and can be thrown off by load current and magnetic coupling with adjacent power lines. Other methods involve measuring characteristics of the high-frequency traveling wave. In the FLAR system, BPA has pioneered a technique that compares the arrival times of the traveling wave at substations on either side of the fault (Figure 2)<sup>[4, 5]</sup>. The traveling waves cover about 1 ft/ns, so 1  $\mu$ s timing accuracy allows fault location within 1000 ft. This is about the spacing between high voltage transmission line towers, where faults are most likely to occur.

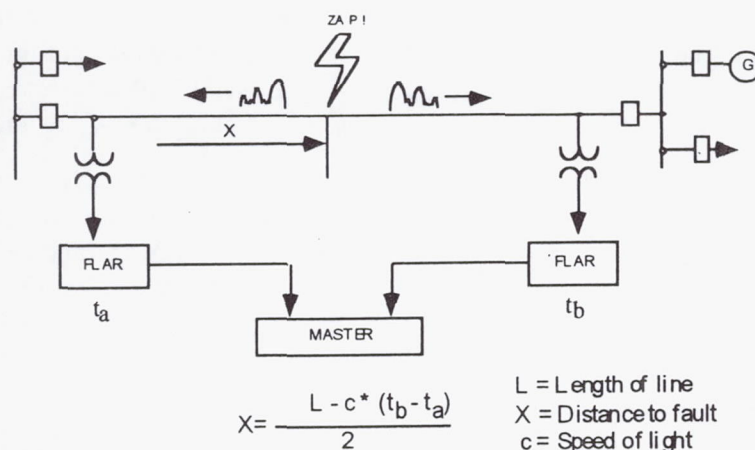


Figure 2. FLAR traveling wave fault locator diagram.

The FLAR system has microcomputer-based remote units installed at 24 key substations. Each has a clock synchronized by a high-frequency pulse sent every 100 seconds over the microwave system. The traveling waves are timetagged and reported to a master computer at the control center. The master correlates the timetags, computes the fault location, and reports it to system dispatching.

The system has proven to be accurate and reliable. The drawback is the synchronization pulse, which uses 60 kHz of high frequency bandwidth on an analog microwave system. It is only available to major stations within BPA's service area. In 1989 we began extending it by synchronizing the microwave pulse to UTC time using a GPS receiver. Then we could use another GPS receiver to supply the same pulse to a FLAR remote unit that was off the microwave system<sup>[6]</sup>. Finally, in 1992 we defined a data protocol and hardware configuration that allowed using a GPS receiver for a FLAR remote unit. Since then we used these GPS-FLAR receivers to extend our FLAR system to include tie lines with other utilities and several stations without microwave. We are making most new additions with this technology. Eventually, the analog microwave will be replaced with digital systems and the system will all be replaced with GPS.

## STANDARD TIME DISSEMINATION

CTS still distributes standard time over microwave voice channels in IRIG-B format. In some locations this works well; in others it has always been a problem. It looks like a modulated 1 kHz signal should transmit easily over a 300-3000 Hz voice channel, but it isn't that simple. IRIG-B modulation produces signal energy at 10 Hz, 100 Hz, and harmonics of 1 kHz which are outside of the passband. Phase slips on a frequency division multiplex misalign the IRIG-B harmonics. These effects distort the decoded signal, making it difficult to read, especially for automatic recording equipment. Local time generation can overcome that problem.

In addition to problems with centralized time distribution itself, there are still locations without access to central distribution. In the past there was little in these smaller substations that needed a precise time source. Now almost all protection and monitoring equipment is microprocessor-based and records information with a time stamp. These systems also have capability for remote access, which makes having an accurate time reference even more important.

In response to both of these problems, we are now using GPS receivers more commonly for time dissemination. We have found they are easy to install and operate reliably. They are cost-competitive with any other time system with the same level of reliability and accuracy. The GPS-FLAR receivers also output IRIG-B, giving us two functions for the price of one box. However, the issue of centralized time and verification remain. How do we know if a GPS receiver is operating and is providing the same time as the CTS?

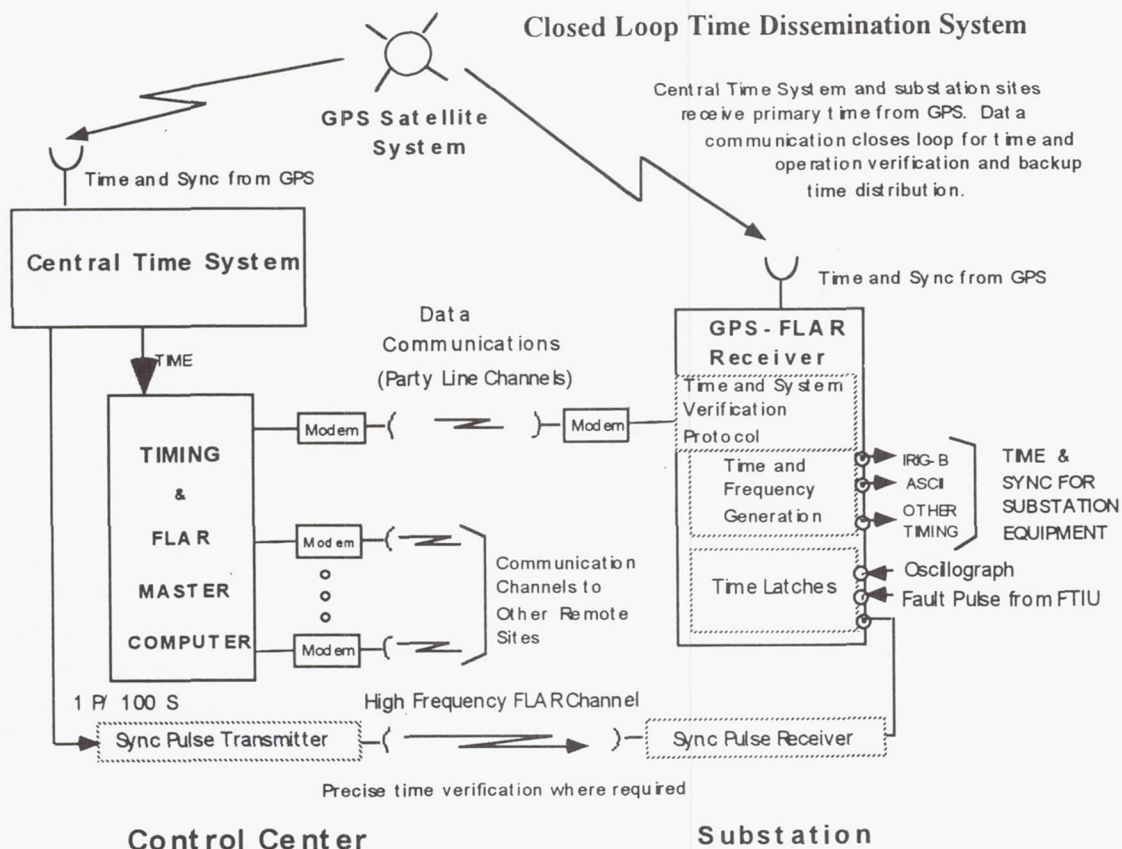


Figure 3. GPS based closed loop timing system.



In designing the new GPS-FLAR receiver, we included commands for time verification and error flags. All the FLAR remote units are polled by a master. The query for GPS-FLAR receivers includes asking the remote time, which is compared with the master time. If they differ by more than a fixed delay, the receiver is reported as having a failure. Flags for things like oscillator error and loss of lock are also checked and flagged. While this technique cannot verify GPS time with precision, it closes the time dissemination loop with the CTS and assures time coordination system-wide (Figure 3).

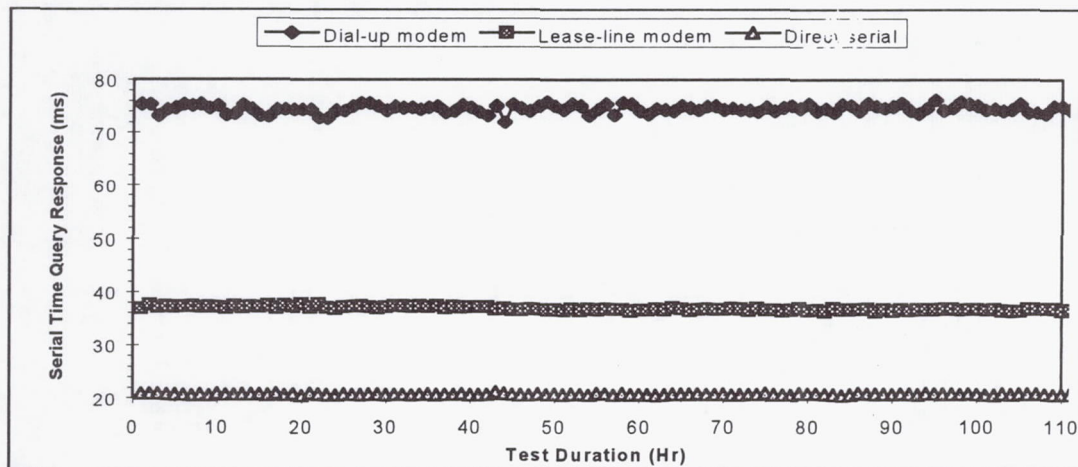


Figure 4. Time delay through serial communications--includes computer latency and delays in data switches.

We tested this technique of time verification through serial communications to be sure it was reliable. The GPS receivers we used time-stamped the time query message to the nearest millisecond (Figure 4). We used a PC to do the polling and timed the query using an internal timing board. We found the delay using a directly connected, 4800 BPS 4-wire modem was 37 ms, with a time variation of  $\pm 1$  ms. Using a dial-up, 4800 BPS 2-wire modem, the overall delay increased to 75 ms, with a range of  $\pm 5$  ms. A local, directly connected receiver provided a reference for the computer timing latency and delays through the local data switch.

## PHASOR MEASUREMENT

A phasor is a vector representation of a sinusoidal quantity which includes both magnitude and phase angle. A power signal is a 60 Hz (or 50 Hz) sinusoid and is commonly analyzed in phasor format. Measurement of power signals in phasor format in real time presents unique opportunities for power system controls. A Phasor Measurement Unit (PMU) is a microcomputer-based system that digitizes the three phase waveforms and derives phasors in real time using FFT techniques<sup>[7]</sup> (Figure 5). These devices are still in the research and testing stages, though there is already a standard for their implementation (IEEE 1344).

BPA has been involved in test systems with two different PMUs. The first one, a prototype unit, samples waveforms at 720 samples/second and derives phasors at the same rate. The second one takes 2880 samples/second, but decimates to 720/second for deriving phasors. Both use 12 samples for the Fourier transform, which is one cycle at 60 Hz. The three phasors combine into a single positive sequence phasor representing the magnitude and phase of a balanced three-phase system. It is a good representation of the state of a real power system in all but extreme fault conditions. By precisely timing the sampling clock with a GPS receiver, phase angle can be accurately computed between any two measurement points<sup>[8]</sup>. As noted in [1], power transfer is directly related to the phase angle between stations. At 60 Hz, one electrical degree is equivalent to 46  $\mu$ s. A desirable accuracy of 0.1 electrical degree requires 5  $\mu$ s synchronization between PMUs.

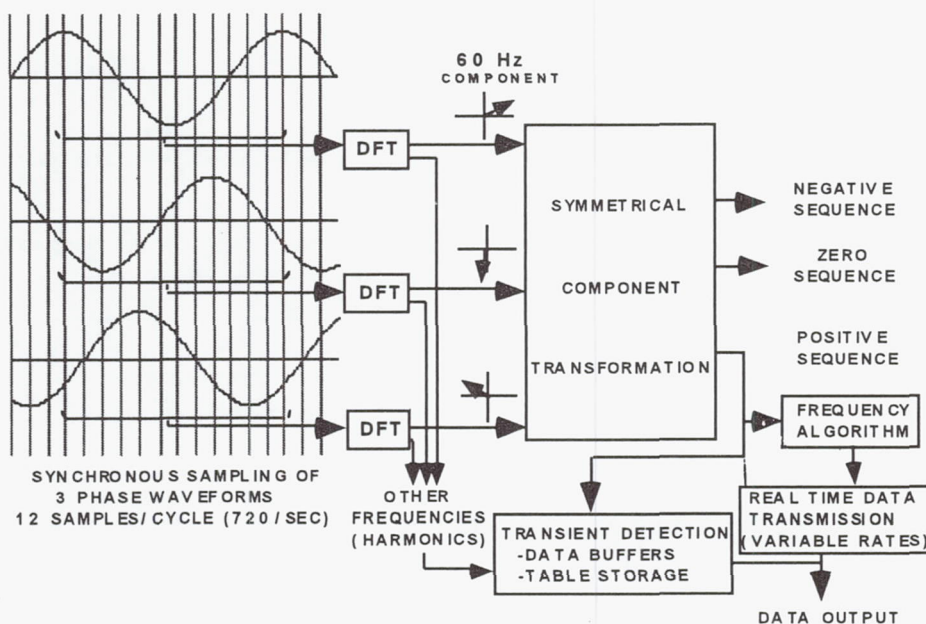


Figure 5. Phasor Measurement Unit signal processing diagram.

BPA tested two prototype PMU's on the main transmission link between the Pacific Northwest and Southwest (Washington to southern California). The two PMU's were synchronized with GPS receivers. A master terminal at the BPA Laboratories in Vancouver, Washington, recorded the data. The purpose of the test program was both to evaluate the phasor measurement system and to provide operational information on the GPS receivers used for the precise time source. The overall results were excellent. In 4 years of field deployment, the only hardware failure was a chip in a GPS receiver<sup>[8]</sup>. Phasor data responded with greater accuracy and less noise than comparable analog telemetered data.

The newer PMUs are production units currently being deployed in a wide area system control



test. BPA is installing four units in Montana, Washington, and Oregon. Other utilities in the western system are installing units in their service areas in Arizona, Utah, and California. The data from the total of 20 units will be transmitted in real time to a major substation near Los Angeles for control of a DC transmission link to Oregon.

## CONCLUSIONS

We are continually trying to coordinate timing systems. Most events impact more than one system, so relating data from several systems is crucial. The problem is new applications occasionally have timing requirements that cannot be met with existing systems. It is usually cheaper and more expedient to build a separate timing system, even though it does not coordinate with the others. We are continually trying to update old systems to newer technology and to provide reference for newer applications.

Through GPS we have a common time base that is accurate enough for all current power system applications. BPA is working toward a comprehensive time system using GPS for the universal source, but with enough internal system transfer to assure internal coordination. It is somewhat risky building an infrastructure around an external system over which we have no control. We like many others, will be lending our influence to assure GPS remains an open and reliable system into the foreseeable future.

## REFERENCES

- [1] R.E. Wilson 1991, "Uses of precise time and frequency in power systems," *Proc. IEEE*, 79, 1009-1018.
- [2] C.L. Wadhwa 1983, *Electrical Power Systems* (Wiley Eastern Limited), Chap. 17, p. 514.
- [3] N. Cohn 1967, "Considerations in the regulation of interconnected areas," *IEEE Trans. Power Appar. Sys.*, PAS-86, 1527-1538.
- [4] D.C. Erickson, and J. Andres 1982, "Automatic Fault Location Using MICROTIME," BPA Document No. AFL-100-01.
- [5] J. Esztergalyos, D.C. Erickson, and J. Andres 1984, "The application of synchronous clocks for power system fault location, control, and protection," Western Protective Relay Conference, 23 October 1984.
- [6] M.A. Street 1991, "Delivery and application of precise timing for a traveling wave fault detector system," Proceedings of 22nd Annual Precise Time and Time Interval (PTTI) Applications and Planning Meeting, 4-6 December 1990, Vienna, Virginia, NASA Publication 3116, pp. 355-360.
- [7] A.G. Phadke, J.S. Thorpe, and M.G. Adamiak 1983, "A new measurement technique of tracking voltage phasors, local system frequency and rate of change of frequency," *IEEE Trans. Power Appar. Sys.*, PAS-102, No. 5.
- [8] K.E. Martin 1992, "Phasors measurement system test," 1992 BPA Engineering Symposium, April 1992, Portland, OR, 2, pp. 689-704.

## Questions and Aswers

**ED URR (WORLD CLASS):** In the flare test that you've been utilizing for the last year, what is the accuracy with respect to fault location you've been able to obtain?

**KENNETH E. MARTIN (BONNEVILLE POWER ADMINISTRATION):** You mean what percentage of them we actually locate?

**ED URR (WORLD CLASS):** How close can you get?

**KENNETH E. MARTIN (BONNEVILLE POWER ADMINISTRATION):** This technique allows locating within about 300 meters. Typically, the failures happen at transmission towers, because it's the shortest distance to short-to-ground or short to phase-to-phase, although not always; and so, we try to maintain a one-microsecond resolution which allows us to pinpoint it to a tower.

Generally, I would say that if we get plus and minus a tower, we're doing quite well; and it's quite accepted by most people.

**ED ERR (WORLD CLASS):** Secondly, are you involved in the phase or test measurements that are being done in conjunction with EPRI, BPA, PG&E, LADWP, APS in Salt River? If so, can you comment on them?

**KENNETH E. MARTIN (BONNEVILLE POWER ADMINISTRATION):** Yeah, we are involved in that. That particular system is a very large-scale system; as you just mentioned, they're all over the place. I'll refer you to this slide right here: Each one of the utilities that you mentioned has several phase or measurement units in its service area; we have one in Eastern Montana, one at Grand Coulee, one near John Day, one at Molin; there are some over here in Northern Arizona, Northern New Mexico; there's actually one — I think it's going to go in in Western Colorado. And then the rest of them are all in Southern California, Central California and Arizona.

All the signals from these are supposed to be fed in in real time, to the controllers on the south end of the DC transmission line from here up to Salilo, which is on the Columbia River. The idea is to, by controlling the power that's transferred over the DC transmission line, we should be able to stabilize the swing between the Northwest and the Southwest, which regularly occurs.



# DIRECT-Y: FAST ACQUISITION OF THE GPS PPS SIGNAL

1Lt. O. M. Namoos  
Space and Missile Center  
Los Angeles Air Force Base, California 90009-5500

Dr. R. S. DiEsposti  
The Aerospace Corporation  
Los Angeles, California 90009

## Abstract

*The NAVSTAR Global Positioning System (GPS) provides positioning and time information to military users via the Precise Positioning Service (PPS), which typically allows users a significant margin of precision over the commercially available Standard Positioning Service (SPS). Military sets that rely on first acquiring the SPS Coarse Acquisition (C/A) code, read from the data message the handover word (HOW) that provides the time-of-signal transmission needed to acquire and lock onto the PPS Y-code. Under extreme battlefield conditions, the use of GPS would be denied to the warfighter who cannot pick up the un-encrypted C/A code. Studies are underway at the GPS Joint Program Office (JPO) at the Space and Missile Center, Los Angeles Air Force Base that are aimed at developing the capability to directly acquire Y-Code without first acquiring C/A code. This paper briefly outlines current efforts to develop "direct-Y" acquisition, and various approaches to solving this problem. The potential ramifications of direct-Y to military users are also discussed.*

## INTRODUCTION

At the most basic level, GPS is a system that allows users to calculate their position and time by triangulating from multiple reference points (GPS satellites that are in view), whose positions are known at any given time. Twenty-four satellites form the current full constellation. These space vehicles (SVs) are distributed into six orbital planes, with four SVs per plane in circular orbits about 20,000 km above the earth's surface.

The GPS signals and codes were designed very carefully to enable user sets to operate autonomously, to acquire and track GPS satellite signals, and to compute accurate navigation and time solution even when the user equipment (UE) does not have valid almanac and ephemeris prior to start. In addition, the signals were designed to provide two levels of service, the Standard Positioning Service (SPS) or civilian service, which is available to all users, and the Precise Positioning Service (PPS), available only to military users. To prevent unauthorized users from utilizing or spoofing PPS, the military ranging signals were encoded. This encoding and spoof prevention mechanism is termed Anti-Spoofing (AS). To limit accuracy to SPS users,



artificial ranging errors are introduced into the ranging signals. The existence of these errors in the GPS signal is referred to as Selective Availability (SA). Military UE are equipped with cryptokeys which allow the removal of SA errors and allow the tracking of the encrypted precise ranging signals.

The ranging signals take the form of Pseudorandom (PRN) codes. Each satellite transmits a unique Coarse Acquisition (C/A) code for SPS and Precise (P) Code for PPS. The precise code is normally replaced by its encrypted equivalent Y-code. GPS user sets obtain ranging measurements by acquiring and tracking a SV PRN code. Some military UE first acquire the C/A code and then acquire a time mark to allow transition to Y-code track. In the event that those UE are denied access to the C/A code, they would not be able to utilize PPS either. A solution to this problem is to upgrade those UE to allow the direct acquisition of the Y-code without first acquiring C/A code. In the following sections, we discuss the PRN codes and UE acquisition and track functions to explain why direct-Y acquisition is not as simple as it sounds. Details about technology enhancements required to support direct-Y and tradeoffs between technology and Concept of Operations (CONOPS) are also discussed.

## SIGNAL IN SPACE AND CODE STRUCTURE<sup>[1]</sup>

Each satellite transmits unique C/A and P(Y) PRN codes. These codes appear to be random but actually are exactly reproducible in much the same way as a sequence of outputs from a random number generator when supplied with an initial seed. Each C/A code is a Gold code with bit rate (or chipping rate) of 1.023 MHz and repetition period of 1023 bits. The C/A code thus repeats every 1 ms.

The GPS UE forms a pseudo-range (PR) measurement by locking on to the code corresponding to one of the SVs. This is done by correlating a replica of the code generated within the UE with the received, down-converted satellite signal. All satellites broadcast C/A code using the L1 carrier frequency of 1.57542 GHz. The UE's antenna receives signals from all satellites in view. However, the orthogonality property of the codes allows a channel of the UE to track an individual satellite signal. This method of communication is termed code-multiplexing. PR measurements made by receiver channels tracking four or more satellites can then be used to calculate a navigation solution and GPS time.

When generating the signal, the SV adds to each code, in modulo two fashion, a 50 Hz navigation message (referred to as the NAV message). The resulting bit sequence is used to phase shift the L1 carrier (phase-shift keying), which is then broadcast. The PRN code itself provides no information. Its function is to provide a mechanism for the UE to lock on to the phase of the satellite signals so that signal times of transit can be measured. The times of transit, relative to the UE clock, when multiplied by the speed of light, are the PR measurements. GPS UE typically have two tracking loops, one that tracks the code and provides the PR measurements, and one that tracks the carrier, which provides delta range (DR) or Doppler-like measurements. A typical measurement frequency is 1 Hz.

The 50 Hz NAV message is demodulated once the loops begin track. Included in the NAV message is the entire satellite constellation almanac, ephemeris for that particular satellite, and



satellite clock offset relative to the GPS time standard. This data are needed, along with four or more PR measurements, in order for the user set to compute position and time. The C/A code signal component nominal power specification is -160 dBW.

Another property of the C/A PRN codes is that the signal frequency spectrum is spread out over a 2 MHz bandwidth (about twice the chipping rate) centered at the carrier frequency. This enables the signal to be more robust to interference and jamming.

The PPS P(Y) codes have a chipping rate of 10.23 MHz. Because of the higher rate compared to C/A code, they tend to provide more accurate PR. Similar to the C/A codes, there is a unique P(Y) code for each SV. Normally, each SV can broadcast either the un-encrypted P-code or the encrypted Y-code, but not both. The Y-code is normally broadcast, and thus the P-code is usually not available. The P-code has a repetition period of one week. The Y-code, which is the encrypted version of the P code, does not repeat.

In a way similar to C/A signal generation, the NAV message is added to the P(Y)-code prior to phase shifting the carrier. In this case, however, the signal is applied to two transmitted carriers, the L1 carrier, in quadrature with C/A, and the L2 carrier at 1.22760 GHz. The P-code signal component power specification is -163 dBW on L1 and -166 dBW on L2. The spread spectrum of the signal is about twice the chipping rate, or 20 MHz. This offers better resistance to wideband interference than the C/A code, which is only spread over 2 MHz.

## SIGNAL ACQUISITION, TRACKING, AND PVT COMPUTATION

To acquire a SV, the received RF signal is first down-converted and then correlated with the PRN code of a particular SV generated within the UE. If a current constellation almanac is available in UE memory and if the UE roughly knows its location, then the acquisition mode logic can select a SV which is within view. For example, a satellite most nearly overhead would have the highest power level and slowest change in geometry, thus being better suited for the first SV to acquire.

Current UE, including some military UE, first acquire C/A code. Following acquisition, SPS or civilian UE track C/A code while PPS, or military UE, hand over to Y-code.

The C/A code repeats every 1 ms. UE performs acquisition by a search over time (in intervals of half chips or smaller fractions of a chip) until a peak shows up in the correlation function. The time offset giving the peak is the amount of time that the code has to be slewed, relative to the UE clock, to track the SV signal. Figure 1 illustrates how the receiver correlates the received signal to a known algorithm that is stored in memory. In some cases, an additional search over frequency may be needed to limit signal processing losses due to loss of coherency. During integration, loss of signal coherency is caused by phase-shifting (Doppler) of the signal relative to the generated PRN code. Doppler is due to such effects as user velocity along the line of sight (LOS) and oscillator frequency offset.



## SPS USER EQUIPMENT

To solve for user position and time, unaided GPS sets use PR measurements from four satellites. First, the set generates a duplicate of the C/A code for the satellite it wants to track. It then slews the code forward or backward in time to maintain correlation with the incoming signal. The amount of time shift between the user clock and the incoming signal is the PR measurement. This can be seen from Figure 1, as discussed above. PR is simply the time shift multiplied by the speed of light.

PR measurements are corrected for ionospheric and tropospheric delays (which affect the speed of transmission through the atmosphere), the SV clock error (which is included in the navigation message), relativity effects, and interchannel bias. The corrected PR measurements and satellite location (via ephemeris data) are used to estimate user Position, Velocity, and Time (PVT).

A batch least-squares algorithm can be applied to four or more PR measurements to estimate user location and UE clock time offset. The precise instantaneous GPS time can then be obtained by adding the estimated time offset to the UE clock time. Rather than a batch filter, the navigation solution is usually obtained through the use of an iterative Kalman-Bucy navigation filter, which optimally weighs the PR measurements (and DR measurements if available) based on measurement and user motion statistical models.

## PPS USER EQUIPMENT

The military UE that first acquire C/A code then begin tracking and demodulation of the NAV message, and read the HOW in the NAV message. The HOW of a particular epoch corresponds to an epoch in the P(Y)-code sequence. The UE uses this information to determine where in the internally generated P(Y)-code sequence to initiate correlation for tracking. If the user has a rough knowledge of location, a current almanac, and SV clock corrections, the Y-code acquisition of subsequent channels should proceed fairly quickly. To initiate tracking, subsequent channels need only slew their code phase, relative to the first channel, by an amount corresponding to the difference in user to satellite path length between the first SV and the subsequent SV.

## C/A CODE ACQUISITION VS. DIRECT-Y ACQUISITION

Since the C/A code repeats every 1 ms and chips at 1.023 MHz, then at most, 1023 chips (or 1 ms) of time uncertainty would have to be searched in order to acquire. The military UE that acquire C/A code demodulate the NAV message and use the HOW to transition to Y-code. Now consider direct P(Y) acquisition without the HOW. P-code repeats once per week and chips at 10.23 MHz. The starting phase for the P(Y)-code correlation search would be based on the time as given by the UE clock (or an externally provided GPS time fix). If the UE clock were just one second in error, 10.23 million chips would have to be searched to acquire Y-code directly. Assuming 20 ms of integration dwell on each half-chip searched, a single dwell sequential searching scheme would take about 5 days to complete.



## WHY DIRECT-Y?

As the role of GPS as a force-enhancer matures, an increasing number of military users are finding applications for it. Among them are Precision Guided Munitions (PGMs), Combat Search and Rescue (CSAR) forces, tanks, transporter vehicles, and many others. The increasing reliance on GPS may make it a target for enemy jamming and spoofing in the field. Since C/A code can be rendered unreliable by such tactics, military users should reduce their reliance on it to the extent possible.

## HOW TO ACHIEVE DIRECT-Y — TECHNOLOGIES AND CONOPS

So what is needed to support direct-Y acquisition? Obviously, as the above example illustrates, accurate time is very helpful. Thus, clock and oscillator technology and stability are very important. However, another approach is to apply fast acquisition Application Specific Integrated Circuits (ASICs) that perform many correlation searches in parallel. ASICs having the ability to perform 1023 parallel correlations have already been developed, and a 2046 direct-Y chip development is currently being sponsored by the GPS Joint Program Office (JPO) and the Avionics Lab at Wright-Patterson AFB. Other approaches are related to constraints or modifications made to the Concept of Operations (CONOPS). For example, an external time fix may be provided prior to a direct-Y acquisition attempt.

So the three ways to attack the problem are: (1) use of enhanced oscillator technology, (2) use of parallel correlation ASICs, (3) CONOPS to initialize time and GPS parameters. However, each platform and user set, along with its standard operational concept, will impose certain constraints on power, battery life, size, weight, cost, and ability to initialize. For example, an atomic clock may be entirely appropriate for an avionics unit, but not so for a handheld unit due to size, battery life, and cost constraints.

These issues are described below in more detail along with other supporting technologies.

## CONOPS

The Concept of Operations refers to how the GPS UE is initialized, used, and maintained. Initialization for direct-Y consists of accurate time, current almanac or ephemerides, and other SV parameters. For very fast Time to First Fix (TTFF), the satellite ephemeris needs to be provided via data initialization. The reason for this is that 30 seconds or more is required to read the ephemeris subframe data after track and data demodulation begins. Ephemeris data for four or more SVs in track are needed before an accurate PVT solution can be computed. Also, for the case of direct-Y acquisition, the cryptokey needs to be provided so that Y-code may be generated in the UE correlation block.

Some UE, like handheld units, are able to get initialization parameters via data transfer from another handheld which is currently tracking or has recently tracked GPS. Other UE, like avionics units, may be initialized via other means prior to launch. For example, an atomic



clock, which is free-running between missions and GPS fixes, may allow accurate enough time to support fast direct-Y. The various initialization alternatives are being investigated in a CONOPS trade study by the GPS JPO.

## **PARALLEL CORRELATORS**

Consider the previous example of direct-Y acquisition in the presence of a one-second time uncertainty. The single-dwell sequential search requires about 5 days. If a 1000 parallel correlator ASIC is used, then the acquisition time reduces from 5 days to 5 days/1000, or about 7 minutes.

## **CLOCK ACCURACY AND STABILITY**

For large time uncertainties (uncertainties larger than the number of chips that can be searched in parallel), the acquisition time is approximately proportional to the uncertainty. A free-running clock has error that depends on the initialization accuracy plus the error that develops over time due to oscillator frequency error. The frequency-dependent error generally depends on the elapsed time since the last fix. These errors are also sensitive to temperature variations for uncompensated oscillators. A GPS UE clock may be synched by reacquiring GPS and resetting the receiver clock to match GPS time. This is one way of limiting time error growth.

## **BATTERY AND SOLAR CELL TECHNOLOGY**

A handheld UE will most probably operate on battery power. In the battlefield, an external time fix prior to direct-Y acquisition may not be practical. Thus, the UE clock will need to be left free-running between GPS fixes. Depending on oscillator power requirements (more accurate oscillators generally require more power), this may cause significant power consumption which will reduce battery life. Also, periodic GPS fixes may be performed for the sole purpose of limiting build-up in clock error, but each fix would further drain the battery. GPS tracking cannot be left running continuously due to large power demands and battery life constraints. Thus improved battery technology or the use of solar cell technology are of value.

## **TECHNOLOGY/CONOPS TRADES**

Direct-Y acquisition time is directly related to the number of chips which need to be searched, which depends on the time uncertainty. The acquisition time is approximately inversely proportional to the number of chips which can be searched in parallel, or the number of parallel correlators. Thus, there is an obvious trade-off of correlator technology and clock technology.

If time can be maintained accurately with a free-running UE clock, then an accurate time fix for direct-Y is not needed. If an accurate external time fix can be provided at commencement of a direct-Y acquisition attempt, then an accurate free-running clock is not needed.



Trade-off parameters include technology, such as the number of parallel correlators in an ASIC, clock stability, and battery capability. All these factors affect cost, weight, size, logistics, and technology development and integration risk. Additional operations to initialize prior to mission start may also be traded with ASIC and clock technology. However, there is always an advantage in making a system as autonomous as possible in order to minimize operational burden.

## SEARCH OVER TIME AND DOPPLER

Several contractors have been funded to perform analysis to characterize direct-Y requirements and to develop technology directly applicable to direct-Y. These studies have determined that a two-dimensional search may be required in order to detect the SV signal in high jamming environments — a search both over time and frequency. The search in frequency is called Doppler search. Doppler causes the received signal to gradually move out of phase relative to the generated SV code. This out-of-phase effect causes losses in correlation. Losses are more pronounced in high J/S environments since longer integration intervals are required to increase the SNR to a sufficient level to allow detection. The Doppler search partially compensates for these losses. Doppler is due to several effects: (1) errors in the SV velocity (this is the reason for the requirement of current almanac or ephemeris), (2) errors in the user velocity (these may be compensated for by providing inertial aiding data from an INS), (3) oscillator frequency offset and frequency drifts during the correlation interval. Considering item 3 and previous discussion, both clock accuracy (absolute time accuracy) and short-term stability (constancy of oscillator frequency over the correlation interval) are important when performing direct-Y.

## DIRECT-Y PERFORMANCE MEASURES

Some criteria to measure direct-Y acquisition performance are acquisition time, probability of detection, and probability of false detection. Acquisition time is defined as the time required to detect a satellite or to obtain a positive correlation after a search over time and frequency. Probability of detection is the probability, given some correlation search procedure, of detecting an SV signal, given that it is actually present in the received signal. Probability of false detection is the probability that a SV is declared present, and is actually not present in the received signal. Also, for this application, probability of false detection includes the case of a SV being detected at an incorrect time offset and/or frequency offset. Once detection occurs, the time and frequency offsets are used to initiate code and carrier phase tracking loops. If the initial time and frequency parameters are incorrect or are not accurate enough, the tracking loops will not be able to maintain track. Considering this, a parameter more important than the probability of false detection is the probability of correctly initiating a successful track. Other performance measures are the time to recover from a failed tracking attempt and achieve a successful acquisition, by either: trying other peaks in the time/frequency region, expanding the search over a larger region of time and/or frequency, extending the integration interval to provide a higher probability of detection and a lower probability of false detection, switching the acquisition attempt to other SVs, etc.



Other performance parameters include: (1) TTFFM (Time to First Measurement) - time to positively acquire and begin track of an SV and obtain a PR measurement, (2) TTFF (Time to First Fix) - time to first obtain a valid PVT navigation solution at mission start, (3) TTSF (Time to Subsequent Fix) - following a GPS track interruption, the time to reacquire and obtain a valid PVT solution. Often a TTFF measure needs to include probability of success, e.g., TTFF=10, 95%.

In order to obtain an unaided PVT solution, the following steps are required, assuming a valid almanac. First, a SV signal has to be acquired, as described above, using either C/A code or P(Y) code. Then code and carrier track has to be established on the first SV and three or more subsequent SVs. The navigation message of each SV has to be demodulated to provide SV ephemeris and other parameters which are used in the solution of PVT. About 30 seconds are required to read the navigation subframe data to give the ephemeris data pertaining to a satellite (unless the ephemeris data are downloaded into UE prior to mission or direct-Y start). PR (and DR if available) measurements can be extracted for each channel while in track lock. The measurements are fed to a navigation filter to estimate PVT. In addition, to obtain PPS accuracy, a military UE needs the cryptokey to allow generation and track of Y-code and the removal of the SA errors.

Parameters which affect acquisition performance include:

- J/S - Jammer-to-signal power ratio, usually expressed in dB or dB per unit BW
- Time uncertainty - The error between GPS time and the UE clock time.
- Oscillator error - The frequency offset and drift in frequency. Since time is obtained by integrating frequency, these effects cause a buildup in time offset. Also, the variation of the oscillator frequency from a standard constant value. An oscillator frequency offset causes a Doppler offset. The oscillator stability over the correlation period is important, since drift causes loss of signal coherency and subsequent signal processing losses.
- User position and motion uncertainty - User position error contributes to the size of the time search window, but is usually small relative to the time uncertainty effect. User velocity and acceleration, unless compensated for, contributes to the Doppler offset. To compensate for user velocity and acceleration during correlation, an inertial aiding signal from an INS can be provided to appropriately slew the code and carrier signals. Even with inertial aiding, INS errors will contribute to a Doppler offset.
- SV motion uncertainty - Primarily due to SV velocity errors. For current almanac or ephemeris, they will probably be much smaller than the user position and velocity errors.

Figures 2 and 3 illustrate the effects of J/S and time uncertainty on acquisition time.

## ENHANCED GPS FOR COMBAT SYSTEMS (EGCS)

Due to the importance of GPS in the battlefield, the GPS JPO at Los Angeles AFB and the Avionics Lab at Wright-Patterson AFB have been funding studies aimed at developing



technologies to enable direct-Y acquisition. The Enhanced GPS for Combat Systems (EGCS) Program consists of four primary projects that, if completed, would result in significant advances towards achieving this capability. There are two main approaches to this problem. The first is to have very accurate time information input to the correlator that is searching the Y-code. The second approach uses multiple correlators (or similar signal processing techniques), which operate in parallel to simultaneously search over different correlation time offsets.

## CLOCK ACCURACY

Many current GPS UE use relatively low-power, low-cost quartz oscillator technology that provides a free-running accuracy on the order of a millisecond for elapsed times approaching an hour. As discussed above, these oscillators are not well-suited for direct-Y acquisition. Two issues are important. First, in order to avoid searching over a large interval of time, the unit must know the GPS time extremely accurately. Microsecond level accuracy would make direct-Y acquisition attainable without the need for parallel correlation circuits. The second issue is the stability of the oscillator. User sets that are employed in the field, in most cases, are not able to calibrate their clocks frequently, at least not without a GPS fix. Initialization of the units can be performed periodically, but not regularly enough to keep the oscillator frequency from drifting significantly from the calibrated value. Most GPS UE will not observe a stability problem. Every time the unit acquires the GPS signal, it resets its clock and recalibrates the oscillator frequency using the time available in the PVT solution. If the unit is used a few times a day, its accuracy may stay within acceptable limits. However, some UE, like handheld units, can be left inoperable for longer periods to conserve battery power. Still others, like the Combat Survivor Evader Locator (CSEL) survival radio currently under development, may go months without use. The operator may not be able to plan on its use ahead of time to have it calibrated beforehand.

For these reasons, EGCS is monitoring an effort to miniaturize atomic (cesium) clocks. The miniature atomic clock under development is projected to provide time accurate to 10 microseconds after one day. If successful, this approach could enable direct-Y acquisition without the need for many parallel correlators. While the atomic clock may be suitable for avionics UE, it may not be applicable to handheld UE due to the power requirement of about 300 mW. Key issues for the miniature atomic clock are the power requirement, size, and cost. So far, great strides have been made in all three areas, but it may be a few more years before this technology will be available for operational use.

Another clock technology has been developed by the Army Research Lab<sup>[2]</sup>. This is the Microcomputer Compensated Crystal Oscillator (MCXO), which has the property of providing time accuracies on the order of 1 ms per day with very low power requirement (25-75 mW).

The JPO is actively seeking other methods of getting an accurate time signal into the hardware on demand without relying on reading the navigation message. Potential solutions include developing the necessary interfaces to transfer time and other parameters between two GPS user sets, or directly from an off-board atomic clock. Additionally, a time mark can be broadcast in the UE.



## PARALLEL CORRELATION SIGNAL PROCESSING

The other three projects within EGCS are analyzing and/or developing various multiple correlator designs. Two approaches consist of correlation ASICs having between 1000 to 8000 taps, effectively allowing 1000 to 8000 parallel correlations. Preliminary analysis shows that the designs are promising. Using an 1023 tap ASIC developed by another project, the acquisition of the Y-code was demonstrated in a laboratory environment using GPS signal generators<sup>[3]</sup>. The significant challenges that remain are miniaturizing the technology enough to fit the size constraints of the smaller UE, and reducing the power consumption of the chips to be compatible with power budgets and battery life.

The third approach is also a parallel processing scheme. The design performs a Fast Fourier Transform (FFT) on the incoming signal and the known Y-code, and multiplies the two in the spectral domain. The correlation function is then given by the inverse FFT. This procedure takes less steps than the correlation approach, and is expected to yield better results. However, the implementation of this approach in a brassboard for demonstration has proven to be more challenging.

## RELEVANCE TO THE PTTI COMMUNITY

Clearly, direct-Y causes the user to be much more dependent on having as accurate time as possible. As indicated by Figure 3, acquisition time is highly dependent on time uncertainty. Therefore, one of the key avenues for improving direct-Y performance is to provide more accurate time information to the UE so that parallel correlation can be done over a narrower search window. We have examined various notional schemes for providing periodic time updates to an airborne receiver to keep its clock accurate and calibrated within acceptable limits. Various data busses have been suggested, such as the 1553 digital data bus, as well as the RS422 data interface, and the PTTI port<sup>[4]</sup>. However, there is very little concurrence on what type of time accuracy is attainable from each of the above-mentioned approaches.

One interesting approach leverages technology that is already being incorporated into the GPS Receiver Applications Module (GRAM)<sup>[5]</sup>. The GRAM will eventually be an open architecture interface board that enables GPS receivers to interface with a variety of commercially available applications cards via a standard interface protocol. Included in the GRAM design is an interface to a PTTI time source that may be provided by the vehicle hosting the receiver. Today, this PTTI "hook" may have little use. Re-integrating existing receivers in aircraft platforms in order to provide the PTTI signal to the receiver would be cost-prohibitive. But the ramifications of this approach to future generations of receivers are unmistakable. The battlefield of the future is becoming more communications-intensive. Already, major programs are underway to link a multitude of weapons platforms into single battle management functions. It is envisioned that a single theater commander can have total control over all assets in the theater. The commander will be able to get status on each unit in the field, sea, or air and optimize an offensive or defensive strategy based on location and condition of all assets. Finally, the commander would be able to automatically task each unit, even in an electronically saturated environment. As this vision becomes reality, there may be a growing interest in



accurate time sources for all military weapons platforms. Accurate time may be necessary to enable the use of Time Division Multiple Access (TDMA) communications concepts that allow a multitude of users to share the same bandwidth by assigning each user a precise time window in which to transmit.

Other applications, like weapons guidance systems and many others have been proposed that require highly accurate time. As these applications mature, the value of delivering precise time to the platforms increases. Ultimately, it is conceivable that the value of time would be high enough to justify major investments into methods of providing precise time.

## ACKNOWLEDGEMENTS

The authors would like to thank Lt. Col. Donald Latterman, GPS Chief Engineer, Dr. Joseph Clifford of the Aerospace Corporation, and Maj. Al Mason from the GPS Joint Program Office for editing this paper to ensure the technical accuracy of its content and its suitability for public release. Their feedback was invaluable in sorting out some of the finer details of the code acquisition process.

## REFERENCES

- [1] GPS Interface Control Document ICD-GPS-200, Revision C, Initial Release, 10 October 1993.
- [2] R. Filler, and J. Vig 1995, "*Low-power oscillator/clock for direct P-Code acquisition*," US Army Research Lab, Proceedings of ION Conference, June 1995.
- [3] "*Enhanced GPS for Combat Systems (EGCS)*," Interstate Electronics Corp., August 1995.
- [4] GPS User Equipment - Precise Time and Time Interval (PTTI) Interface, Revision A, ICD-GPS-060, 2 June 1986.
- [5] "Guidelines for the Global Positioning System (GPS) Receiver Application Module (GRAM)", GPS-GRAM-001, 8 August 1995.

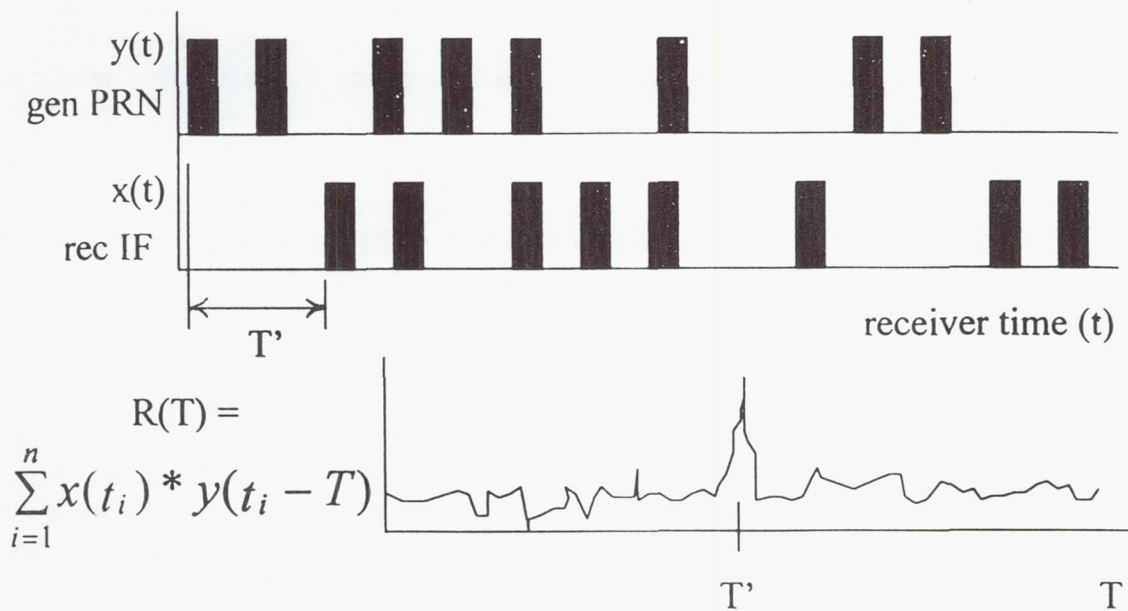


Figure 1 Acquisition by Correlation

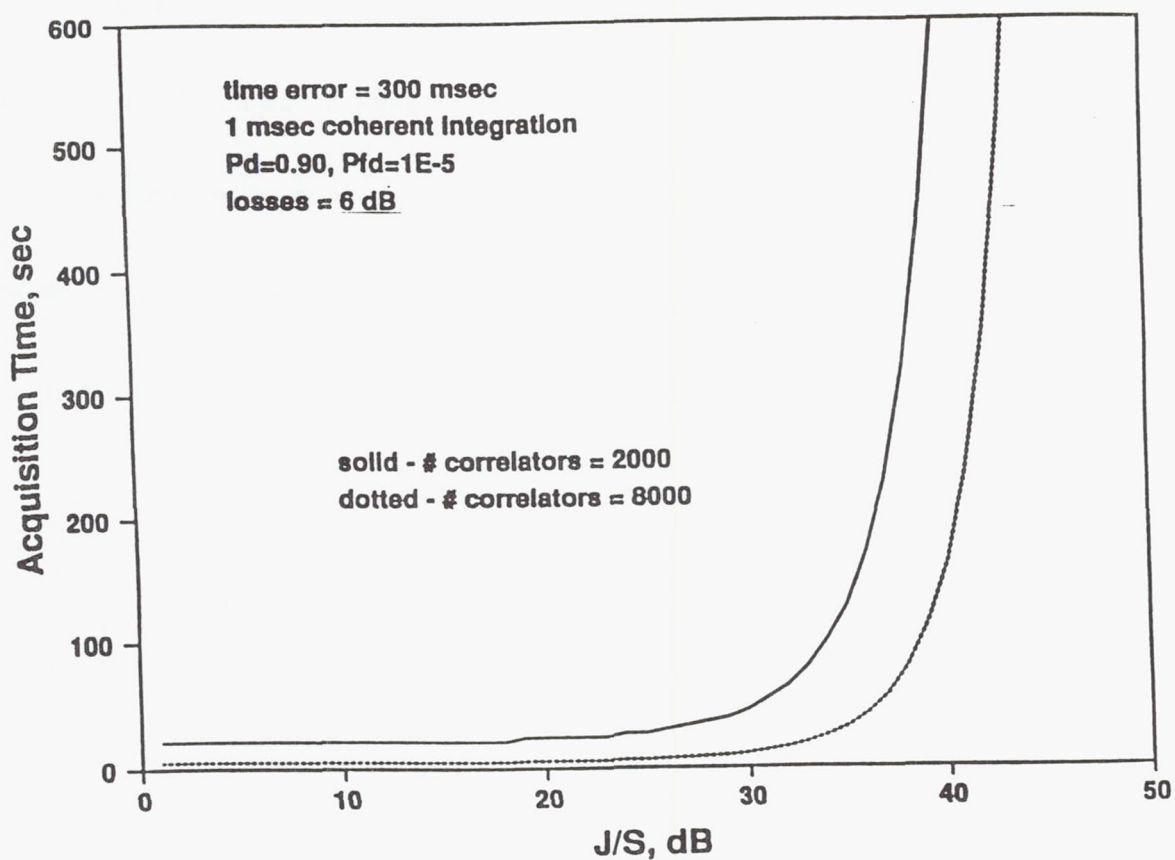


Figure 2 Acquisition Time Vs JS



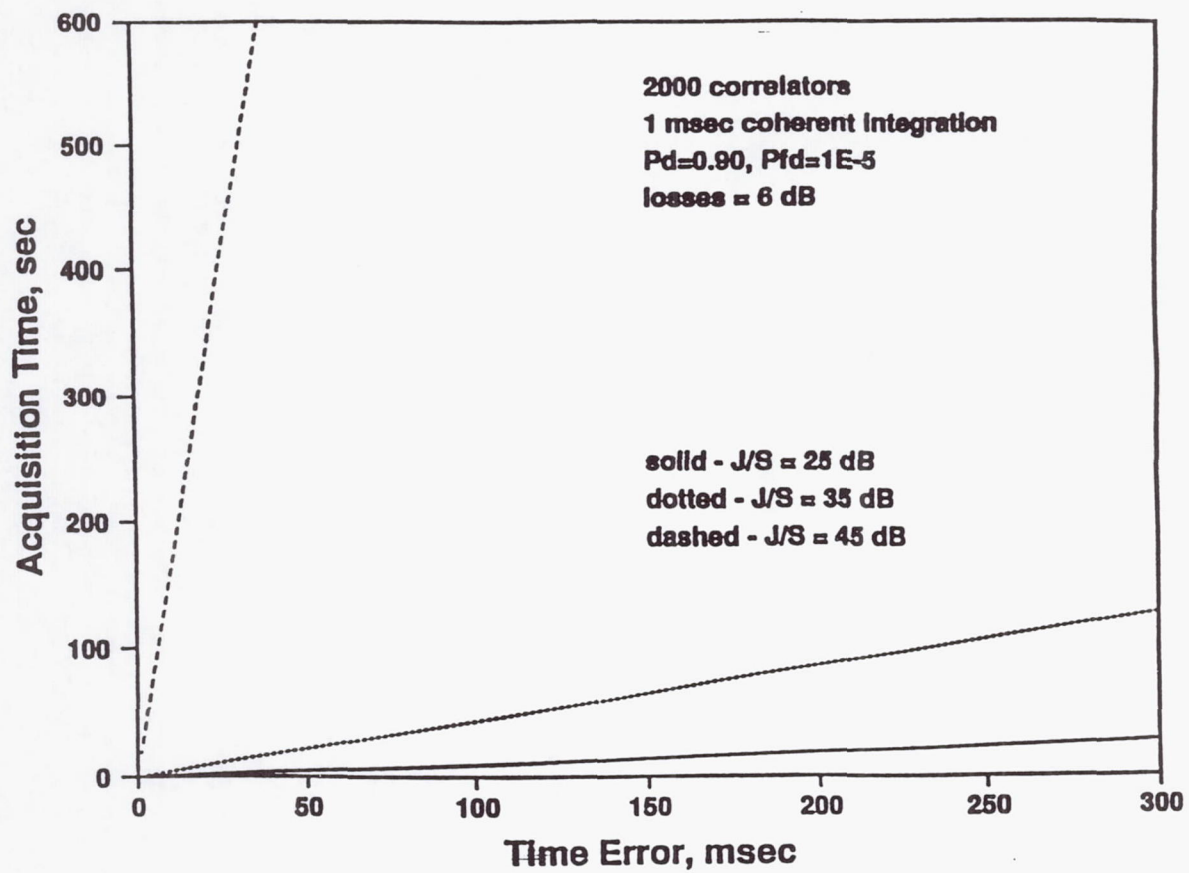


Figure 3 Acquisition Time Vs Time Error

# THE WSMR TIMING SYSTEM: TOWARD NEW HORIZONS

William A. Gilbert  
Bob Stimets

White Sands Missile Range, New Mexico 88002

## Abstract

*In 1991, White Sands Missile Range (WSMR) initiated a modernization program for its Range Timing System. The main focus of this modernization program was to develop a system that was highly accurate, easy to maintain, and portable. The logical decision at the time was to develop a system based solely on Global Positioning System (GPS) technology. Since that time, WSMR has changed its philosophy on how GPS would be utilized for the Timing System. This paper will describe WSMR's initial modernization plans for its Range Timing System and how certain events have led to a modification of these plans.*

## INTRODUCTION

The primary function of the WSMR Timing System is to provide time and time interval information to Range instruments and facilities. At present, the instruments requiring this information receive it in one of three ways: by VHF broadcast, wire line distribution, and (recently) by Global Positioning System (GPS) time and frequency receivers. Much of the equipment used to provide the Timing information in the first two methods is over twenty years old. While this equipment continues to function remarkably well, many of the components required to maintain it are no longer available. Additionally, new requirements placed on the Timing System for site-to-site time correlation have exceeded the technical capabilities of much of this equipment.

To meet these new requirements for time correlation and to replace a significant portion of the aging equipment, WSMR has embarked on a modernization program. This paper will describe the current Range configuration for Timing, the approach WSMR is using for its modernization, and how unexpected events have affected the approach. It should be noted that the modernization program is in its infancy and the approaches explained in this paper may change slightly. Furthermore, two potential enhancements to the chosen approach will be discussed.



## **CURRENT RANGE CONFIGURATION**

### **RANGE AREA**

The majority of the WSMR Timing System is divided into three Range areas (See Figure 1). The Timing System supplies time and time interval information to over 100 instrumentation vans and about 150 fixed locations. Customers include project facilities and Range instrumentation consisting of Telemetry, Radar, Optics, and Computer systems.

To accommodate the variety of customer requirements and yet maintain time correlation among all customer sites, the Timing System produces a standard time signal from its Master Clock. This signal is then distributed to most customer sites using VHF and fixed distribution stations where it is translated into the time format required by the customer.

### **WSMR MASTER TIME GENERATION SYSTEM**

The WSMR Master Time Generation System (at Uncle 2 in the South Range) uses a cesium-beam time standard as its Master Clock. The output of this Clock feeds time code generators that produce the IRIG time codes used for distribution. This System stays within one microsecond of Coordinated Universal Time (UTC) by utilizing Loran C and GPS.

### **VHF BROADCAST STATIONS**

The WSMR Timing System has two VHF broadcast stations that transmit IRIG-B timing. These stations are Uncle 5 in the South Range and Uncle 52 in the North Range. The combination of these two stations provide coverage to 95 percent of the Range area.

### **FIXED DISTRIBUTION STATIONS**

Fixed distribution stations located throughout the Range receive Timing signals from either Uncle 5 or Uncle 52. These stations synchronize their time code generators to this Timing signal and distribute time codes using wire line or cable. Figure 1 illustrates their site locations and their relationship to the Master Station.

### **MOBILE DISTRIBUTION STATIONS**

For areas of WSMR that do not have wire line services available from a fixed distribution station, WSMR Timing provides a mobile distribution service. Currently WSMR Timing has three mobile distribution stations available for on Range support. Each system is capable of generating IRIG time code formats and receiving a synchronizing signal from radio Timing or GPS.

### **WSMR MOBILE CLOCKS**

Timing operates two transportable clock facilities for calibration of the Timing System and validation of GPS receivers. These clocks provide precision on-time pulses for comparison with a pulse generated by the Timing equipment at the customer location. Either the equipment's



time is corrected or the time offset is recorded. Once these calibrations are made, these clocks complete a loop closure by comparing their precision pulses with their synchronization source.

## THE INITIAL APPROACH

The initial approach was to develop a Timing System using GPS as the only method of time transfer. GPS time and frequency receivers would be installed in all individual fixed and mobile customer facilities. These GPS receivers would provide the basic time and frequency outputs required for approximately seventy percent of the customers. For customers requiring additional time and time interval information or formats, time code generators synchronized to the GPS signal would be installed and would provide the additional formats. A similar approach would be used at all fixed facilities. Each fixed facility would use a single GPS receiver that had a IRIG-A and IRIG-B serial modulated time code output. These output signals would synchronize all time generation equipment located within the facility. To ensure the GPS receivers were working properly, status information about the GPS receivers would be sent to one of the three service centers (Uncle 2, Uncle 6, or Uncle 25) using the RS-232 port. Once all facilities were supplied with GPS receivers, the VHF broadcast stations would be shut down. The Master Station would remain but its function would change. It would primarily be used to test and validate Timing equipment, distribute Timing signals to local users, and to provide an additional syntonization source for the telecommunications system. The Station would be modernized using GPS capabilities to discipline rubidium standards, and would have time generation equipment synchronized to the GPS signal.

This was the initial approach taken for modernizing the WSMR Timing System. This approach seemed to satisfy most users and the promoters of GPS technology. The general consensus was: if GPS receivers were installed everywhere, the Timing signal would be more accurate, calibrations of Timing equipment would be eliminated, and modernizing the Timing system would be relatively easy to implement. Then personnel within the Timing System started asking the following questions: "Could GPS be disrupted and what mechanisms could be put in place if a disruption occurred?" And "Does the hardware that is going to be purchased have external synchronization capability?" Well, at first these question were for most part ignored. Or the standard answer was "GPS will always be available and, if for some reason it wasn't, the internal clocks will have the ability to flywheel with very low drift rates." Then it happened! GPS receivers in the North Range would not lock up during several hours in the day. "How could this be? This is GPS equipment, GPS is always available; it must be faulty equipment." However, when the equipment was tested in Central or South range, the GPS equipment worked perfectly. Finally, after some investigation, it was discovered that methods for jamming GPS equipment were being tested in the northern part of the Range. Concurrently, other incidents of loss of lock were traced to interference from legally operating instruments on the Range. It now was time to listen to the questions asked above, come up with solutions, and to implement a modified approach.



## THE MODIFIED APPROACH

The GPS jamming tests and interference incidents provided the incentive necessary to take a second look at how the Timing System would be modernized. The first area reviewed was the mobile instrumentation systems. WSMR's mobile instrumentation systems support a large number of missions at many locations. Often one mobile may be required to support at more than one location in a day. Moving from one location to another requires removing power; GPS interference in the new site area could prevent attaining lock and, hence, knowing what time it is. A secondary source for time information would, therefore, be beneficial to these systems. In some fixed facilities, time and time information requirements are less critical and the equipment can be left on. In these, a secondary means of providing Timing information is not necessary because the internal oscillators have very low drift rates and can flywheel during periods of GPS interference. However, a benefit of a secondary source would be the ability to compare the time information received from the secondary with that generated from a GPS input signal. This would provide some additional assurance of the validity of the site's time information.

It was decided to include a secondary source for time information in the modernization of the WSMR Timing System. It was further decided to use the existing VHF broadcast system as a secondary source for synchronization. To accommodate the concept of dual sources at any site, it was decided to have a time generation device that could receive GPS, receive VHF, or accept a wire line IRIG signal. This would provide flexibility to users and would enhance Timing availability. The design for the new Master Station was modified as well. The new design would use GPS to initialize the time generation components and then to function as an independent reference (for comparison with cesium standards). By using GPS as a reference instead of the synchronizing source, the System would still maintain UTC traceability and yet be able to operate independently of the GPS source (since the VHF system uses the Master Station's serial modulated IRIG-B output for its broadcasts).

At this point it is necessary to explain some of the reasons for choosing the VHF system as the secondary time transfer method. The most obvious of reasons was the availability of existing equipment that could be used. The existence of this hardware provided a quick solution to a concern that required immediate attention (interference with GPS). The VHF broadcast system provides coverage to 95 percent of the Range. It transmits a serial modulated IRIG-B format that can be used to achieve Timing accuracies of 10 microseconds or less if the general location of the receiver site be known. Also there are currently available modular VHF receivers that could easily be used in the time generation device described above. Although the VHF system does not have as good site to site time correlation capability as GPS, it could be used as the only source for time transfer for the majority of the missions at WSMR. Finally, the VHF system at WSMR has been a reliable source for time transfer for years.

## POSSIBLE FUTURE ENHANCEMENTS

Significant upgrades of the WSMR Timing System have only occurred at widely spaced, irregular intervals. Since there is no reason to expect this situation to change, the current modernization

has to carry the System quite some time into the future. The modernization must be able to accommodate advances in technology and unexpected changes in political (and budgetary) priorities.

**GLONASS** One area considered was the use of the GLONASS network. The existence of another, independent, source of reference time is attractive. Since low-cost commercial GLONASS receivers did not appear to be imminent in the U.S. market, this feature was not incorporated into the initial implementation. However, the Master Clock configuration is flexible enough to allow for incorporating this additional reference in the future. Also, since many of the GPS receivers in the new System will be plug-in modules, there is the potential for supplementing these with new combined GPS/GLONASS receiver modules, should that capability emerge in the U.S. market.

**Precise Positioning System (PPS)** Use of the PPS portion of GPS offers the potential for increasing the accuracy of received Timing. There is a significant cost difference, however, between an approved PPS receiver and a commercial GPS Timing receiver. Evaluation of current and potential requirements (or even desires) for Timing accuracy to WSMR customer facilities reveals very few in the accuracy range that PPS serves; so the investment required to provide PPS capability to the whole Timing System would not be prudent. The Master Clock will be provided with PPS capability, however; also, several PPS receivers will probably be obtained to accommodate the rare customer who might have a requirement. WSMR would not be able to meet a requirement for a large number of sites to be within 100 or fewer nanoseconds (with S/A enabled) under the current approach.

## CONCLUSION

GPS offers the Timing System the capability of providing customers Timing accuracy of 300 nanoseconds, or better, referenced to UTC. WSMR will use this capability whenever and wherever it can be used to enhance the Timing System. In those cases where GPS cannot be used, the VHF system will continue to be a reliable second source.



# AUTHENTICATION, TIME-STAMPING AND DIGITAL SIGNATURES

Judah Levine  
Time and Frequency Division  
National Institute of Standards and Technology  
Boulder, Colorado 80303

## Abstract

*Time and frequency data are often transmitted over public packet-switched networks, and the use of this mode of distribution is likely to increase in the near future as high-speed logical circuits transmitted via networks replace point-to-point physical circuits. Although these networks have many technical advantages, they are susceptible to eavesdropping, spoofing, and the alteration of messages enroute using techniques that are relatively simply to implement and quite difficult to detect.*

*I will discuss a number of solutions to these problems, including the authentication mechanism used in the Network Time Protocol (NTP) and the more general technique of signing time-stamps using public-key cryptography. This public-key method can also be used to implement the digital analog of a Notary Public, and I will discuss how such a system could be realized on a public network such as the Internet.*

## INTRODUCTION

Time and frequency transmissions — both the signals themselves and the interchanges of data that form the basis for national and international coordination — are generally transmitted with only moderate security and only cursory authentication. Although this openness has served us well up until now, the increasing importance of time and frequency information in many areas ranging from synchronous communications to the coordination of access to distributed databases means that the disruption of a time service may be very serious and costly. In addition, the continuing problems posed by computer viruses and worm programs should teach us that attacks on networks and computer systems are not necessarily motivated solely (or even primarily) by financial gain, and that attacking an important and visible system might be considered a challenge, and “just because it’s there” could be enough of a motivation. It is important to begin now to consider how the security of our transmissions can be improved before any of our systems comes under a determined attack.

Jamming transmissions or cutting cables may have serious consequences by denying service to a particular group of users, but the effects tend to be localized and relatively easy to detect — even if correcting the problem can be both arduous and expensive. Data modifications that



do not produce obvious disruptions or degradations are potentially much more serious. These changes are not readily detected; in the worst case the corrupted transmissions may be accepted as genuine for some time.

The various methods for protecting and authenticating data that I will discuss fall into two broad categories — methods that are intended to insure the integrity of existing time signals or data transmissions and methods that are potentially useful as ends in themselves in protecting or authenticating other kinds of time-sensitive messages and transactions.

## SINGLE-KEY ENCRYPTION

The simplest way of protecting data is to add some form of check-sum to it and then encrypt either the complete message or just the checksum. Only someone who knows the key can alter the data without invalidating the original checksum. There are any number of methods that can be used for this purpose, including those that effectively “chain” messages together to prevent adding spurious messages or replaying older valid ones<sup>[1]</sup>.

There are a number of technical difficulties with this system, including devising robust methods for dealing with noisy channels and lost messages, but the most serious practical difficulty is probably the distribution of the encryption and decryption keys. Whether these keys are implemented in software (using passwords or phrases) or in hardware (using an artifact such as a magnetic card), distributing keys requires a substantial investment of people and money and is probably never as secure as the advocates of such systems would claim.

In spite of these practical difficulties, the Internet-based Network Time Protocol (NTP) supports optional authentication and validation using single-key encryption<sup>[2]</sup>. When this mode is enabled, the transmitter of an NTP message computes an authenticator derived from the message itself and a secret key using the Data Encryption Standard (DES) in a mode similar to the “block-chaining” method specified by NIST<sup>[3]</sup>. The resulting checksum is then appended to the end of the message together with an integer specifying which of several possible keys has been used to compute it. The relationship between this integer and the actual key value must be sent to each receiver via an external, unspecified, secure channel. The receiver validates the message by repeating the same procedure and comparing the checksum it has computed with the value received in the message<sup>[4]</sup>. Although the DES standard defines both an encryption and a decryption algorithm, the decryption algorithm is not used by NTP so that the same software can be used at both ends. Furthermore, while both transmitter and receiver must use the same algorithm to authenticate the time packets, there is no reason why it must be the Data Encryption Standard, and the later versions of NTP support authentication using either DES or a variant of an algorithm called MD5<sup>[5]</sup>.

In addition to the usual problems associated with distributing and maintaining the key database, authentication may degrade the accuracy of time-stamps transmitted using the NTP protocol. The checksum must be computed after the entire message has been constructed, and it therefore inevitably delays the transmission of the packet by an amount that depends on the speed of the processor and on its load. This delay appears as an increase in the out-bound network transit-time; depending on the mode of the association, there may be no corresponding in-



bound delay to preserve the symmetry. It is possible to make an approximate correction for the time needed to compute the checksum by inserting an estimate for this time into the NTP configuration file, so that the problem introduced by the authentication is due not so much to the delay it introduces, but to the unmodeled fluctuations in this delay caused by changes in load and similar factors.

Although this authentication method can be used by a private network of machines exchanging time messages only among themselves, it cannot be used to authenticate packets from a machine that is publicly available, such as the NIST primary time server. (The authentication in this case is only for the benefit of the client machines — the server itself has no need for authentication since it is synchronized to UTC via external means and does not accept network-based synchronization information.) The key used by the receiver to verify the authenticity of a packet is the same as the key used by the transmitter to produce it, so that the key used by a primary server must be widely known if the authenticity of its time packets is to be verified by its clients. But once the key is widely known, numerous other machine can use it to generate “authentic” packets as well, so that its use provides little or no security. In practice, therefore, the authentication scheme incorporated into NTP is only useful in validating transmissions among a group of peers which are under the control of a single management entity.

The NTP protocol also supports an authentication mechanism based on the Internet address of the time source — a machine can be configured to accept information only if the network address of the source matches one of the entries in an internal table<sup>[4]</sup>. Although the time needed for this check can be made outside of the primary packet-exchange loop so that it does not degrade the transit-time estimate, the procedure can be quite lengthy if many addresses must be examined. As a consequence, this procedure is useful to safeguard a relatively small group of machines. It does not provide fool-proof protection even in this case because of the increasingly common practice of “ip-address spoofing.”

## DUAL-KEY ENCRYPTION

Dual-key encryption (often called public-key encryption) is designed to overcome some of the problems with conventional single-key methods that I discussed in the previous section. A dual-key system uses two different keys (and usually two complementary procedures as well) to perform encryption and decryption. These ideas can be realized in a number of different ways, but all of them share the same basic properties<sup>[6]</sup>. A message,  $M$ , is encrypted using an encryption key  $e$  and an encryption procedure  $E$  to produce a cipher text  $C$ . Thus

$$C = E(e, M). \quad (1)$$

There exists a decryption procedure  $D$  and a key  $d$  so that applying them to the cipher text recovers the original message:

$$M' = D(d, C), \quad (2)$$



where  $M'$  is identical to  $M$  if and only if the key  $d$  is the cryptographic inverse of the key  $e$ . As with most cryptographic systems, the procedures  $E$  and  $D$  are well known; the security lies in the choice of the keys  $e$  and  $d$ . Although the two keys must be related mathematically, it is computationally infeasible to compute one from the other in any finite time. Different algorithms realize this secret linkage differently: in some cases the keys are the prime factors of a very large number, and the security rests on the difficulty of computing such factors. In other systems, the linkage is realized through discrete logarithms modulo a large integer, and the security comes from the difficulty of inverting such procedures.

The dual-key system may be used in two different ways. If the encryption key is made public and the decryption key kept secret, then anyone can encrypt a message, but only the holder of the secret key can read the resulting cipher text. This configuration could be used to encrypt electronic mail messages or data transmissions, for example, so that only the intended recipient could read them<sup>[7]</sup>. If, on the other hand, the encryption key is kept secret and the decryption key is made public, then only the holder of the key can encrypt a message but anyone can read it. The existence of the encrypted text authenticates the authorship of the corresponding plain-text message, because only the holder of the secret key could have computed the encryption. There is no need to archive the message or the cipher text — the authentication can be verified by anybody, since both the decryption algorithm and the key are publicly known. Displaying the two versions is then a form of “digital signature” — the holder of the secret key can use the display as proof of authorship, and a third party can use the display to prevent the message from being repudiated. (Preventing a valid message from being repudiated by its author often has important legal and commercial applications<sup>[6]</sup>.) Although I would focus on the authentication aspects of a digital signature in the current discussion, both the encryption and authentication functions would be useful in the time and frequency business.

The dual-key system changes the problems associated with distributing the keys, but it does not eliminate them. The secret key must remain secret, of course, but the more difficult issue is insuring that the public key, which must be widely available by definition, is not altered surreptitiously. A random alteration is the digital equivalent of jamming a radio signal — it may break the system locally, but is relatively easy to detect. Altering the public key so that it is the inverse of another private key is a more serious problem. If a third party with malicious intentions can manage to replace the legitimate public key with one that is the complement of his own private key, then a variety of more sophisticated attacks becomes possible, at least some of which have been discussed in the literature<sup>[8]</sup>. One way to address this problem is to have a central trusted repository for the public keys, but this simply pushes many of the problems we have been discussing into the design of this repository — it must be very secure and robust because it will become both an attractive target to attack and a single point of failure. The methods it uses to authenticate its responses to legitimate requests for public keys must be carefully studied as well to minimize the probability of undetected spoofing.

Dual-key systems operating in the “digital signature” mode can provide a mechanism for authenticating time signals in principle, but there are a number of practical difficulties that have prevented their widespread use. The key distribution problems discussed above are a significant difficulty. In addition, the time needed to compute the digital signature may significantly affect



the accuracy of the transmissions. The computations are much more intensive than those required for single-key methods, and computing a signature may take an appreciable fraction of a second — even on a fast processor with optimized code. As with single-key methods, the average delay introduced by the computation could be estimated and a correction for it could be incorporated into the software, but the load fluctuations are likely to be more important because the correction itself is significantly larger. Furthermore, the complexity of the calculations can place a heavy load on a primary time server, which may have to respond to more than 10 requests/second during peak load.

## A DIGITAL TIME-STAMP SERVICE

There are many situations where it is important to be able to prove that a document in digital format existed on a certain date and time in its current form. Examples include the disclosure of inventions, and many business transactions where time is a factor. The digital-signature algorithms can be combined with time signals in digital format to provide a publicly available time-stamp service for such documents that has many of the features of a Notary Public. In addition, the digital time-stamp service has a number of features that are not available with a traditional Notary including authenticating “documents” that are not text at all (such as a digitized photograph, a musical composition, or a compiled computer program) and providing authentication for a document without the need for revealing its contents to the authenticating authority.

The general principles of this system are derived from the dual-key cryptography discussed above: The document to be signed is submitted to a timing laboratory such as NIST; the NIST server adds a time-stamp and then signs the result using its private key; the resulting compound document can be verified by anyone who has the corresponding public key without involving NIST at all — only the public key and the appropriate algorithm are required. The mathematics underlying the signature algorithm guarantees that the document, the time-stamp, and the signature originated from NIST and that neither the document nor the time-stamp could have been altered without invalidating the signature. Since the signature is an explicit function of the compound document, neither it nor the time-stamp can be reused on another document. Finally, the authentication of a signature can be performed independently of the original signatory and there is no need for a central repository of signed documents.

The basic design would not necessarily detect a “replay” attack in which a valid document is re-transmitted a second time. If such attacks are a concern (as they might be with the message, “Deposit \$100 to my account ...”) then simply adding sequence numbers to each message will detect the second message as a duplicate.

This general procedure can be strengthened and generalized in a number of important ways:

1. Using a technique known as “hashing” it is possible to eliminate the need to submit the document itself to the signature authority. A “hash” function is a one-way function that accepts a digital string of characters and computes a fixed-length output value based on the entire string. The check-sum characters often used in digital transmissions and the last character of the numbers used to identify products to a supermarket scanner are



simple examples. The hash computation is a unique function of its input in the sense that changing any character of the input changes the hash, but it possesses no inverse — the input cannot be constructed knowing the hash output except by trial and error. Since the hash function is a unique function of its input, signing it is equivalent to signing the original, with the advantage that the original is not limited to printable text but can be a digitized photograph, a digital recording or any string of digital numbers. The exact contents need not be revealed to the signature authority. As a result, the hash values can be transmitted over insecure public channels so that the digital signature system can be implemented using ordinary electronic mail.

2. If the system that receives the messages and adds the time-stamp is also a time-server for the network, then the accuracy of its time can be verified at any time (using NTP, for example) independently of the signature algorithm. The NIST time-servers, for example, receive 50000+ requests for time every day, so that any attempt to alter the time used for the stamping process would be widely detected almost immediately.
3. The security of the system ultimately depends on the security of the private key used to sign the documents. If this private key is stored on the machine that is visible on the public network, then a successful network-based attack on this machine might reveal the secret key and compromise the entire system. This problem can be addressed by storing the key on a second "back" machine that is connected to the time-stamp machine via a private link that is not visible from the network. The two functions of signing and time-stamping are divided in this configuration, with the front machine adding the time-stamp and the back machine computing the signature. While the time-stamp machine must operate in "real time" signing documents as soon as they arrive, the back machine that computes the signature does not have this requirement. It can operate in a batch mode at discrete intervals, taking messages from an input queue on the front machine and returning them to an output queue there. The signed messages on the output queue can be returned to the sender or can be forwarded to a third party as required.
4. The concept of using two machines can be generalized to improve the reliability of the system by constructing several "front" and several "back" machines. The various "front" machines might accept messages in a number of different formats including electronic mail, scanned images, and binary digital files of unspecified format.

As in the previous discussion, the overall structure can be realized using a number of different algorithms, both in the computation of the hash function and in the actual signature process itself. The modular nature of the procedure makes it relatively simple to change to a new algorithm without breaking the overall system.

## CONCLUSIONS

The increasing use of public packet-switched channels to transmit time and frequency signals and data raises concerns that these transmissions may be intercepted or modified by third parties with malicious intent. We have discussed a number of ways of safeguarding and authenticating



messages sent over public networks; none of them is widely used at this time and all have some practical drawbacks. In addition to the issues we have already discussed, some of the algorithms are proprietary and can only be used with a rather expensive license and others are considered sensitive and cannot be exported outside of the US without a special export license<sup>[9]</sup>.

The experiences of the PC and Internet communities is that financial gain is not necessarily the only motive for attacking network-based services. Given these experiences, it is probably only a matter of time before a serious assault is attempted. It is probably useful to begin to think about these issues now while we can do so without the threat of an imminent network-based attack hanging over our deliberations.

As more and more documents are transmitted and stored in digital format, there will be an increasing need for the digital equivalent of a Notary Public. The public-key algorithms that we have discussed can be combined with precise digital time signals to realize such a system at only modest cost.

## REFERENCES

- [1] B. Cipra 1993, "*Electronic time-stamping: the notary public goes digital*," *Science*, 261, 162-163.
- [2] D.L. Mills 1991, "*Internet time synchronization: The Network Time Protocol*," *IEEE Trans. Comm.*, 39, 1482-1493.
- [3] Federal Information Processing Standard 46: The Data Encryption Standard, 1977, National Bureau of Standards.
- [4] D.L. Mills 1992, "*Network Time Protocol (Version 3), specification, implementation and analysis*," Network Working Group Report RFC-1305.
- [5] R. Rivest 1992, "*The MD5 message digest algorithm*," Network Working Group Report RFC-1321.
- [6] J. Nechvatal 1991, "*Public-Key Cryptography*," NIST Special Publication 800-2.
- [7] S. Garfinkel 1995, "*PGP - Pretty Good Privacy*," Sebastopol, California, O'Reilly & Associates, chap. 3.
- [8] B. Schneier 1994, *Applied Cryptography* (John Wiley & Sons, New York), chap. 3.
- [9] Reference [8], chap. 18, pp. 448-454.

## Questions and Answers

**GERARD PETIT (BIPM):** Just a remark: I'm glad to let you know that you have already taken steps to prevent scrambling of our missages. We send that to USNO by fax.

**JUDAH LEVINE (NIST):** Yes, I know. And we get it by regular mail as well. I understand that you are not totally susceptible to E-mail transport. But that's an example, it's not the only example, there are problems. For example, we put our data on STP side, and anybody can get it. And many other laboratories go through the same thing.

**KENNETH E. MARTIN (BONNEVILLE POWER ADMINISTRATION):** I wonder, it seems like people that are be going to be doing mischief, that you might have, you know, kind of the basic idiot level who couldn't do anything on the network anyway because they don't understand it, that kind of technology; but then you've got more and more sophisticated people that might want to do you damage clear up to the point of, let's say, a disgruntled insider; it seems like you might be creating a very elaborate system for a nonexistent segment there to protect yourself. In other words, you still have the possibility of some insider that could be changing your things because they're unhappy about something; and there's nothing you can do about that.

**JUDAH LEVINE (NIST):** I agree with the premise that insiders are very difficult to deal with. I don't necessarily agree that there's nothing you can do. There are strategies, which I obviously haven't talked about; there are strategies which can begin to address the concept of insiders in which, while an insider can do something, they leave a trail which points back to them, in which there is a unique key which you'll have to have to enter before you can do anything, and that key is associated with you, and so on and so on.

The answer is 'yes, that's a serious problem.' The question of what the probability of outsiders is is hard to know; I can't tell you what the probability is; I can only point to history in saying that a lot of people have gone to a lot of trouble to destroy PC's of the people that they don't know. That's my only comment.

**1ST LT. OMAR M. NAMOOS (USAF):** Are there reasons that NSA — I don't know much about encryption, but I know that NSA doesn't recognize the DES standard as good for secure communications or securing information. And, are there reasons that that's the case? Is it maybe a vulnerability of the DES system that makes it more susceptible than you say?

**JUDAH LEVINE (NIST):** The answer to those kinds of questions is those who know, don't say and those who say, don't know. So with that as a prefix, there are rumors that the DES algorithm can be broken and that the NSA knows how to break it. Whether that's true or not is — perhaps it is, perhaps it isn't.

In the open literature, there are proposed attacks on the DES algorithm. None of them works in the finite time against a full-blown algorithm, the full 16-round algorithm. Whether there are secret attacks that people don't know about, I don't know. I'm an unclassified kind of guy. And the classified guys won't tell you. So, there it is.



# APPLICATION OF MILLISECOND PULSAR TIMING TO THE LONG-TERM STABILITY OF CLOCK ENSEMBLES

Roger S. Foster  
Remote Sensing Division, Code 7210  
Naval Research Laboratory  
Washington, D.C. 20375-5351

Demetrios N. Matsakis  
U.S. Naval Observatory  
Washington, D.C. 20392-5420

## Abstract

*We review the application of millisecond pulsars to define a precise long-term time standard and positional reference system in a nearly inertial reference frame. We quantify the current timing precision of the best millisecond pulsars and define the required precise time and time interval (PTTI) accuracy and stability to enable time transfer via pulsars. Pulsars may prove useful as independent standards to examine decade-long timing stability and provide an independent natural system within which to calibrate any new, perhaps vastly improved atomic time scale. Since pulsar stability appears to be related to the lifetime of the pulsar, the new millisecond pulsar J1713+0747 is projected to have a 100-day accuracy equivalent to a single HP5071 cesium standard. Over the last five years, dozens of new millisecond pulsars have been discovered. A few of the new millisecond pulsars may have even better timing properties.*

## INTRODUCTION

Regular timing measurements of millisecond pulsars provide a unique metrology data set produced by natural sources in a nearly inertial reference frame. Since the discovery of the first millisecond pulsar in 1982, the utility of these sources as precise time standards has been clearly recognized<sup>[1,2]</sup>. Decade-long observations of the first two millisecond pulsars now show irregularities in the timing residuals that are most likely due to intrinsic rotational instability in the star itself<sup>[3]</sup>. With terrestrial time standards generally improving an order of magnitude every seven years or so, questions have been raised about the utility of radio pulsars for timekeeping applications. This paper will attempt to address some of the fundamental limitations of pulsar data.

Despite a clear indication on the limit to the precision of millisecond pulsars, they may have great utility in anchoring an inertial space-time reference frame free from the gravitational effects of our solar system. Cesium time scales show irregularities due to physical limitations of the atomic clocks beyond about six months. Specifically, International Atomic Time (TAI) now



has a measured stability of about  $2.5 \times 10^{-15}$  on a time scale of 1 month. The use of different clock ensemble time scales results in measurable changes in millisecond pulsar timing data (e.g. [4]). To date, only two millisecond pulsars have been timed reliably for over five years[3]. Table 1 gives the current best estimates of the timing precision and astrometric accuracy of the two longest timed millisecond pulsars (PSR B1855+09 & B1937+21) plus four additional millisecond pulsars that have been timed for shorter time spans.

Table 1: Pulsar Precision

Pulsar Name	Observation Duration (years)	Timing Precision (us)	RA Precision (mas)	DEC Precision (mas)	Reference
B1937+21	8.2	0.2	0.03	0.06	[3]
B1855+09	6.9	1.0	0.07	0.12	[3]
J1713+0747	1.8	0.4	0.2	0.3	[5]
B1257+12	2.6	2.3	0.4	1.0	[6]
J2322+2057	2.3	2.9	1.0	2.0	[7]
J2019+2425	2.7	3.0	0.6	0.9	[7]

## TIME SCALE IMPROVEMENTS

It is not practical to derive exact numerical values for the stability of pulsars because the pulsar timing data are actually residuals to a multi-parameter fit to pulsar parameters (such as the period, spin-down rate, position, and proper motion), whose covariance depends upon the length of the data set. In the case of the original millisecond pulsar B1937+21, we chose to estimate the instability by generating a series of random numbers characterized by white and random walk frequency noise, removing a solution to pulsar parameters, and observing the differences between the true and simulated residuals. A similar technique was applied to cesium and maser data, except that only an overall frequency offset and drift were removed; the terrestrial clock characteristics derived this way proved consistent with those of Breakiron<sup>[8]</sup>, which extend only out to time scales of a few months. Using this comparison, the pulsar B1937+21 proved to be about 6 times noisier than an individual HP5071 cesium time standard. The comparison becomes even less exact for time scales longer than several months, as higher-order terms would be masked in the data sets.

Another consideration is that the available millisecond pulsar data for B1937+21 extend back to 1984. Through the parameter-fitting process, all the pulsar timing data are influenced by instabilities in TAI (or TT) since then (see [9] for an explanation of the current definition of various time scales). This has the effect of masking the recent dramatic improvements in TAI (see Figure 1). Future pulsar data will benefit from the improved TAI since about 1990. With long enough data sets it may be possible to take this into account, so as to improve our determination of apparent pulsar irregularities and increase the utility of a pulsar time scale.

## A NEW BEST PULSAR CLOCK

An example of one of the new generation of millisecond pulsars found as part of the recent large scale sky surveys is PSR J1713+0747. The pulsar was discovered in a systematic survey



of the radio sky using the Arecibo radio telescope<sup>[10,11]</sup>. After 22 months of timing, the binary millisecond pulsar J1713+0747 appears to be the most stable millisecond pulsar yet observed<sup>[12]</sup>. Current timing precision from this pulsar now rivals the best results obtained from pulsars B1937+21 and B1855+09. Figure 2 shows the fractional frequency stability of PSR 1713+0747 compared to PSR B1855+09 and B1937+21. The stability parameter is defined as  $\sigma_z(t) = [(m/T)^3 S_m]^{1/2}$ , where  $T$  is the data span,  $S_m$  is the spectral density, and  $m = 1, 2, 4, \dots$  is a sub-interval<sup>[12]</sup>. The timing solution for this pulsar includes the measurement of the pulsar's annual parallax, proper motion, and its relativistic "Shapiro delay" due to the light travel delay through the gravitational potential of the companion star<sup>[5]</sup>.

These observations are used to place limits on the mass of the neutron star and its companion. With a post-fit weighted root-mean-square timing residual of approximately 0.4  $\mu$ s, and a characteristic age of roughly 9 billion years, this pulsar may prove to be an important celestial clock in the construction of a pulsar timing array. The source has a large enough radio flux density that it can be used in the future as a target source for observations with the Very Long Baseline Array (VLBA).

The above-mentioned millisecond pulsar was found with the Arecibo radio telescope prior to the current major upgrade. The construction has resulted in a complete loss of observing potential above 430 MHz since late 1994 and at all frequencies since early 1995. The current construction schedule does not call for resumed operations until the end of 1996 or possibly early 1997. Irregular observations of PSR 1713+0747 and other Arecibo pulsars are going on at other major radio telescopes around the world, but their low sensitivity and sporadic schedules will greatly diminish the quality of pulsar data until the Arecibo upgrade is completed.

## LIMITATIONS TO PULSAR CLOCK AND PULSAR TIME

The limitations of millisecond pulsars to establishing a stable spatial-temporal reference frame can come from the following sources: (1) instabilities in the pulsar itself, (2) uncertainties in the Earth-based atomic time scale, (3) source position errors due to planetary ephemeris errors or errors in the pulsar position, (4) additional noise sources including propagation effects from the interstellar medium and the gravitational wave background, (5) detector hardware noise sources, (6) errors in the time-transfer system, and (7) unmodeled binary orbit effects. Many of the effects are discussed in recent reviews of pulsar timing, including Backer<sup>[13,14]</sup>, Taylor<sup>[15]</sup>, and Backer and Hellings<sup>[16]</sup>.

Primary interest in millisecond pulsar stability comes from limitations set by intrinsic rotational instabilities driven by physics in the neutron star interior. Recent stability analysis of a large population of pulsars, including millisecond pulsars by Arzoumanian *et al.* <sup>[17]</sup>, indicate a strong correlation between pulsar timing noise and pulsar period derivative (this could equivalently be correlated with pulsar age assuming spin-down due to magnetic braking). A best linear fit through the timing stability-period derivative plane for 139 pulsars, including a number of millisecond pulsars, indicates a stability trend that can be parameterized as

$$\Delta_8 = 6.6 + 0.6 \log \dot{P}, \quad (1)$$

where  $\Delta_8$  is a fixed time interval stability parameter over a reference time interval of  $10^8$  seconds. The stability equation is defined from:



$$\Delta(t) = \log\left(\frac{1}{6\nu} \|\ddot{\nu}\| t^3\right), \quad (2)$$

where  $\nu$  is the rotational frequency, and  $\ddot{\nu}$  is the second derivative of the rotational frequency of the Taylor expansion of the pulsar's rotational phase:

$$\phi = \phi_0 + \nu t + \frac{1}{2} \dot{\nu} t^2 + \frac{1}{6} \ddot{\nu} t^3 + \dots \quad (3)$$

Assuming that millisecond pulsars spin-down due to magnetic dipole braking, then the pulsar age correlates with the period derivative, implying that older pulsars with smaller period derivatives are more stable.

## A GREAT SUCCESS

The successful discovery of numerous field millisecond pulsars by various all sky pulsar surveys (e.g. [10,11,18-27]). Since 1989 a number of major pulsar search efforts have increased the total number of known millisecond pulsars in the Galactic field to 29 (see Figures 3 and 4).

More than 75 percent of these new sources are in binary systems with white-dwarf companions. Deep optical observations with ground- (Keck 10-m telescope) and space-based (Hubble Space Telescope) instruments along with ground-based astrometric observations, will allow determination of the pulsar optical position to better than 30 milliarcseconds (mas). With the new Very Long Baseline Array (VLBA), several of these pulsars will have a large enough flux densities to establish radio positions with respect to the extragalactic reference frame<sup>[28]</sup>. Using pulsar timing data, radio interferometric data and optical astrometry, we can use these new millisecond pulsars to tie together the radio, dynamical, and optical reference frames to better than 30 mas. Over the next five years, data from the dozens of new millisecond pulsars should provide a large ensemble of pulsars for use in establishing an inertial spatial-temporal reference frame.

## THE FUTURE OF PULSAR TIMING

The initial goal of establishing a pulsar timing array to define an inertial space-time reference frame will require timing about 10 millisecond pulsars with 100 ns timing precision for at least 10 years. The PTTI requirements to reach this goal are an absolute timing accuracy of 10-20 ns, and a stability of 10 ns over 1 year, or a fractional frequency stability of  $3 \times 10^{-16}$  (this will give the atomic clock time scale an order of magnitude improvement over the best pulsar clock). If these requirements can be met and maintained, then TT will not be the limiting source of precision in the long-term timing of millisecond pulsars. With a sufficient number of radio pulsars being timed, the use of UTC as an absolute reference time scale could be eliminated. UTC would only be needed as the carrier time to transfer pulsar arrival time measurements between successive observations. The pulsars themselves could be used as the ultimate reference time scale.

On an even longer-term basis, a pulsar ensemble could be used to time a hundred millisecond pulsars over a hundred years at better than 100 ns timing precision, given improvements in radio telescope receiver hardware, and the development of better pulsar timing systems. Millisecond pulsars will in the future have an important role to play in tying together three distinct reference frames: the radio, the dynamical, and the optical. These natural clocks will



also offer an independent means for verification of terrestrial time scales, testing for relativistic effects in the solar system, and of models of planetary ephemerides. The proper maintenance of pulsar timing data will be critical to enable pulsar time to be applied over a hundred-year astronomical program by a future generation of astronomers. Because of the precision of millisecond pulsars, we note that they could in fact be used to recover the absolute phase of the atomic time scale, if it were ever lost due to some unforeseen global mishap. A pulsar space-time reference frame defined with significant precision could be used to establish a space-time coordinate system useful for passive interplanetary spacecraft navigation, without need for two-way communication.

The next generation of pulsar timing programs will have to wait until sometime in 1997 to begin full scale operation. Two of the major northern hemisphere radio telescope facilities, the Arecibo Observatory (AO) radio telescope and the Green Bank Telescope (GBT), are undergoing a major upgrade or are under construction. Both instruments are currently scheduled to start regular operations in 1997. Until that time, smaller telescopes like the NRAO 42-m, Jodrell Bank, the Bonn 100-m, the Very Large Array, and the Nançay radio telescope will have to carry on with limited pulsar observations.

## ACKNOWLEDGEMENTS

We would like to provide special thanks to Scott Lundgren and Paul Ray, both National Research Council postdoctoral fellows who have contributed to the development of the ideas discussed in this paper. Frederick Josties also contributed to the data analysis upon which some of the conclusions in this paper are based. Basic research in precision pulsar astrophysics at the Naval Research Laboratory is supported by the Office of Naval Research.

## REFERENCES

- [1] D.C. Backer, S.R. Kulkarni, C. Heiles, M.M. Davis, and W.M. Goss 1982, *Nature*, **300**, 615.
- [2] J.H. Taylor 1991, *Proc. IEEE*, **79**, 1054.
- [3] V.M. Kaspi, J.H. Taylor, and M.F. Ryba 1994, *Astrophys. J.*, **428**, 713.
- [4] D.N. Matsakis, and R.S. Foster 1995, in *Amazing Light* (Springer-Verlag, Berlin).
- [5] F. Camilo, R.S. Foster, and A. Wolszczan 1994, *Astrophys. J.*, **437**, L39.
- [6] A. Wolszczan 1994, *Science*, **264**, 538.
- [7] D.J. Nice, and J.H. Taylor 1995, *Astrophys. J.*, **441**, 429.
- [8] L.A. Breakiron 1995, Proceedings of the 26th Annual Precise Time and Time Interval (PTTI) Applications and Planning Meeting, 6-8 December 1994, Reston, Virginia, pp. 369-380.
- [9] P.K. Seidelmann, and T. Fukushima 1992, *Astron. Astrophys.*, **265**, 833.
- [10] R.S. Foster, A. Wolszczan, and F. Camilo 1993, *Astrophys. J.*, **410**, L91.
- [11] R.S. Foster, B.J. Cadwell, A. Wolszczan, A., and S.B. Anderson 1995, *Astrophys. J.*, **454**, 826.

- [12] R.S. Foster, F. Camilo, and A. Wolszczan 1995, in Proceedings of the Seventh Marcel Grossmann Meeting on General Relativity (World Scientific).
- [13] D.C. Backer 1993, Springer-Verlag Lecture Notes in Physics, 418, 193.
- [14] D.C. Backer 1995, in Proceedings of the Seventh Marcel Grossmann Meeting on General Relativity (World Scientific).
- [15] J.H. Taylor 1992, *Phil. Trans. Roy. Soc. Lond. A*, 341, 117.
- [16] D.C. Backer, and R.W. Hellings 1986, *Ann. Rev. Astron. Astrophys.*, 24, 537.
- [17] Z. Arzoumanian, D.J. Nice, and J.H. Taylor 1994, *Astrophys. J.*, 422, 671.
- [18] F. Camilo, D.J. Nice, and J.H. Taylor 1993, *Astrophys. J.*, 412, L37.
- [19] D.J. Nice, J.H. Taylor, and A.S. Fruchter, A. S. 1993, *Astrophys. J.*, 402, L49.
- [20] S.E. Thorsett, W.T.S. Deich, S.R. Kulkarni, J. Navarro, and G. Vasisht 1993, *Astrophys. J.*, 416, 182.
- [21] M. Bailes, *et al.* 1994, *Astrophys. J.*, 425, L41.
- [22] F. Camilo 1994, in *The Lives of Neutron Stars*, NATO ASI Ser., ed. A. Alpar, U. Kiziloglu, and J. can Paradis (Kluwer, Dordrecht), p. 243.
- [23] F. Camilo 1995, Ph.D. thesis, Princeton University.
- [24] D.R. Lorimer, L. Nicastrol, L., A.G. Lyne, R.N. Manchester, S. Johnston, J.F. Bell, N. D'Amico, and P.A. Harrison 1995, *Astrophys. J.*, 439, 933.
- [25] S.C. Lundgren, A.F. Zepka, and J.M. Cordes 1995, *Astrophys. J.*, 453, 419.
- [26] P.S. Ray, *et al.* 1995, *Astrophys. J.*, 443, 265.
- [27] P.S. Ray 1995, Ph.D. thesis, California Institute of Technology.
- [28] R.J. Dewey, M.J. Ojeda, C.R. Gwinn, D.L. Jones, and M.M. Davis 1996, *Astron. J.*, in press.



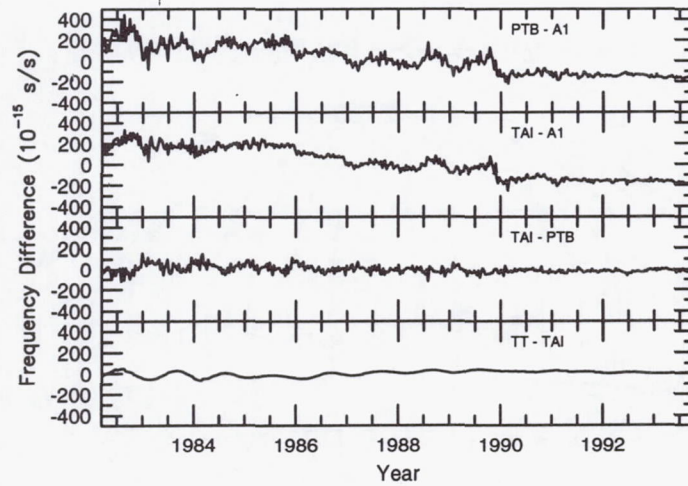


Fig. 1.— Frequency difference between free-running timescales of TAI, PTB, and USNO (A.1) in fs/s. The USNO and PTB timescales are independent, but TAI is gently steered towards the PTB, whereas the USNO clocks' contribution to TAI has increased to 40%. Nevertheless, improvement since 1990 is obvious. The lowest panel shows the difference between TT and TAI, where TT represents TAI recomputed using hindsight corrections to clock weights, offsets, and drifts. A constant frequency offset has been removed from all plots. Data were obtained from the BIPM by anonymous ftp to address 145.238.2.2. The time range shown is from January 1982 to December, 1993. The figure is from Matsakis and Foster (1995) [4]

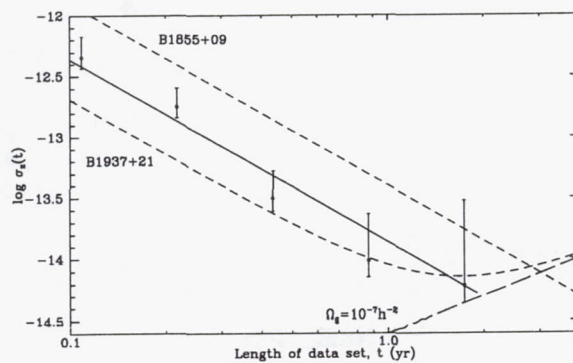


Fig. 2.— Twenty-two months of pulsar timing data from PSR J1713+0747 show that it has better long-term timing accuracy than either PSR B1855+09 or PSR B1937+21. (This figure is from Foster, Camilo, & Wolszczan (1995) [12])

### Field Millisecond Pulsars (1989)

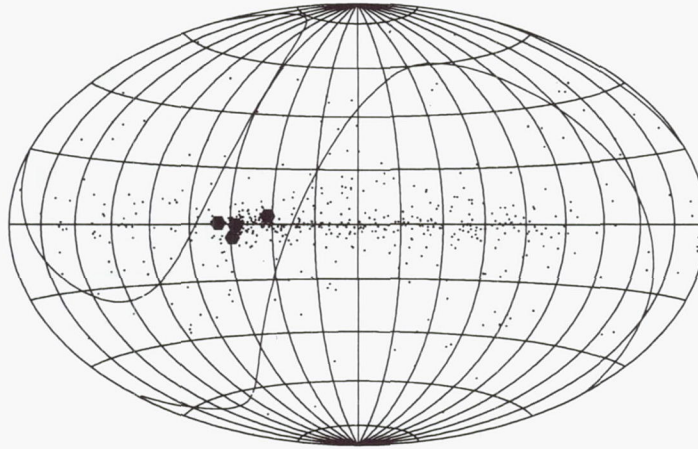
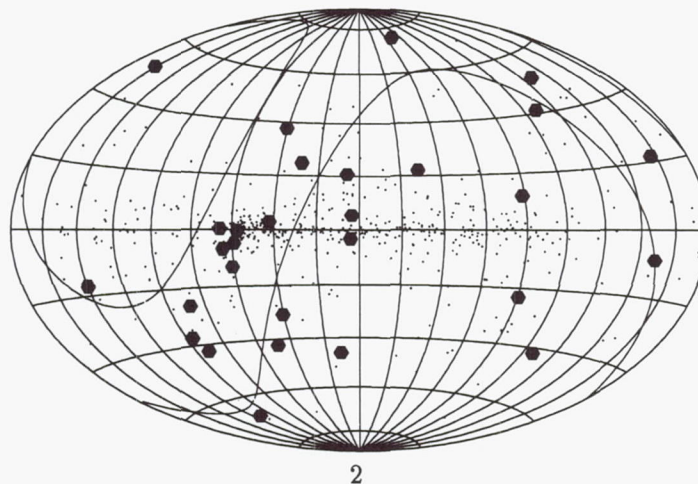


Fig. 3.— A plot in galactic coordinates of the known millisecond pulsars in 1989 (large hexagons). All the known non-millisecond pulsars in the galactic field are plotted as dots. Note the location of the millisecond pulsars in the region of the galactic plane visible using the Arecibo telescope from -1 to +38 degrees declination (solid lines).

### Field Millisecond Pulsars (1995)



2

Fig. 4.— The same plot as in Figure 3 except now the 29 known millisecond pulsars (as of November 1995) in the galactic field are plotted. Note the wide distribution around the sky indicative of a large galactic scale height.



## Questions and Answers

**JUDAH LEVINE (NIST):** You talked about stabilities of something in the  $10^{-15}$  for a year; but most of the commercial time scales that you could get at are much worse than that, USNO or NIST, or something, are probably above a part in  $10^{14}$  in a year. Could you talk about how you know where you are when you think you are?

**ROGER FOSTER (NRL):** Well, I think we don't. And I think that the way that we're going to perhaps improve this is that we're going to independently couple in some of the astrometry aspects of this — at least, on the times scales less than a decade where the astrometry issue becomes important, we can get independent astrometry measurements, independent reference frame times, that we'll be able to at least remove those variables from the equation and improve it. We also have the opportunity with multiple pulsars of timing the pulsars against themselves.

**JUDAH LEVINE (NIST):** I don't know the exact analysis that you made, but I thought it was necessary to remove the electron content along the path; that within an independent parameter, it's kind of an adjust for.

**ROGER FOSTER (NRL):** That's correct. The electron column is fitted out, and that does come into one of the issues of stability. One of the interesting aspects of the population of galactic field pulsars is that because they're high latitudes, they're basically outside of the galactic plane; and the electron columns tend to be rather low where these effects are minimal.

**GERARD PETIT (BIPM):** Could you comment on the number of pulsars that could be found and probably galactic?

**ROGER FOSTER (NRL):** I think the number over the next decade or so will probably approach several hundred of these millisecond pulsars. And that has to do with just extrapolation of the surface density in which they have been detected in general surveys. Roughly, about one per 200 or 300 square degrees; and there are about 42,000 square degrees.

**DAVID ALLAN (ALLAN'S TIME):** I'm excited about the possibilities that millisecond pulsar timing can bring from the physics point of view. I think we have to be careful how we utilize the data or how we think about the data. For example, we have a report from the LPTF on the cesium fountain of  $3 \times 10^{-15}$  accuracy. Accuracy has intrinsically no tau value. And so, it can carry frequency in the absolute sense for any integration time you wish. We expect that these accuracies will improve in other standards. As we do the same extrapolation that you've done for pulsars for the terrestrial clock community, we expect within a couple of decades to be in parts in  $10^{18}$ . If you now look at the fundamental limits of pulsars, millisecond pulsar timing, due to interstellar medium, et cetera, this requires integration times from fundamental limits of about 200 years, just for the first tau value. In order to have a confidence on that, a millennium of data would be needed.

So I think we have to be careful as we make big plans, and this is a planning meeting. I think we can never expect millisecond pulsar timing to contribute in a significant way to an understanding of the uniform time scale and accuracy, in terms of stability, setting time scales (as you've alluded to), studying physics. Looking for gravitational waves, there is much excitement and a good reason to proceed with these studies. But I think we have to be a little careful in how we couch it.



# A NOVEL PHOTONIC CLOCK AND CARRIER RECOVERY DEVICE

X. Steve Yao, George Lutes, and Lute Maleki  
Jet Propulsion Laboratory  
California Institute of Technology  
Pasadena, CA

## Abstract

*As data communication rates climb toward ten Gb/s, clock recovery and synchronization become more difficult, if not impossible, using conventional electronic circuits. We present in this article experimental results of a high speed clock and carrier recovery using a novel device called the photonic oscillator that we recently developed in our laboratory. This device is capable of recovering clock signals up to 70 GHz. To recover the clock, the incoming data is injected into the photonic oscillator either through the optical injection port or the electrical injection port. The free running photonic oscillator is tuned to oscillate at a nominal frequency equal to the clock frequency of the incoming data. With the injection of the data, the photonic oscillator will be quickly locked to the clock frequency of the data stream while rejecting other frequency components associated with the data. Consequently, the output of the locked photonic oscillator is a continuous periodical wave synchronized with the incoming data or simply the recovered clock. We have demonstrated a clock to spur ratio of more than 60 dB of the recovered clock using this technique. Similar to the clock recovery, the photonic oscillator can be used to recover a high frequency carrier degraded by noise and an improvement of about 50 dB in signal-to-noise-ratio was demonstrated.*

*The photonic oscillator has both electrical and optical inputs and outputs and can be directly interfaced with a photonic system without signal conversion. In addition to clock and carrier recovery, the photonic oscillator can also be used for 1) stable high frequency clock signal generation, 2) frequency multiplication, 3) square wave and comb frequency generation, and 4) photonic phase locked loop.*

## INTRODUCTION

Clock recovery by optically injection-locking a microwave oscillator<sup>[1]</sup> or a pulsed laser with an incoming data stream have been demonstrated by many authors<sup>[2-6]</sup> with varied degrees of success. In this paper, we report a different clock/carrier recovery scheme based on injection locking a novel photonic oscillator<sup>[7]</sup> we will refer to as a Light Induced Microwave Oscillator (LIMO).<sup>[8, 9]</sup> This oscillator converts continuous light energy into a spectrally pure microwave signal and can operate up to 75 GHz with phase noise below -140 dBc/Hz at 10 kHz frequency offset. This scheme can recover a clock or carrier from both optical and electrical data signals. Equally important, the recovered clock/carrier is also in both the optical and electrical domains.



This hybrid nature of the LIMO based device makes interfacing with a photonic transmission system simple.

The superior performance of the LIMO results from the use of electrooptic and photonic components which are generally characterized with high efficiency, high speed, low dispersion, and low loss at RF and microwave frequencies.

The LIMO takes advantage of the high equivalent Q of a long optical delay line to achieve highly stable narrow linewidth oscillation. Its spectral purity surpasses that of the best crystal oscillators particularly at high frequencies.

## DESCRIPTION

Referring to Figure 1, light from a laser is applied to an E/O modulator, the output of which is launched into a long optical fiber and detected with a photodetector. The output of the photodetector is amplified and filtered then fed back to the electrical port of the modulator. This configuration supports self sustained oscillations, at a frequency determined by the delay in the optical fiber, modulator bias setting, and the bandpass characteristics of the filter. It also provides for both electrical and optical inputs and outputs. An analysis of the LIMO, which is beyond the scope of this paper, was given previously<sup>[8]</sup>.

There are two important characteristics of the LIMO for frequency and timing applications. The phase noise is reduced by increasing the length of the delay line and the phase noise is independent of frequency. Figures 2(a and b) show the theoretical and measured phase noise of the LIMO as a function of the delay in the delay line and Figures 3(a and b) show the phase noise of the LIMO at different frequencies.

## EXPERIMENT

The LIMO can recover a clock or carrier from both optical and electrical signals. Equally important, the recovered clock or carrier is also in both the optical and electrical domains. This hybrid nature of the LIMO based device makes interfacing with a photonic communication system simple.

In the case of clock recovery incoming data is injected into the LIMO either optically or electrically. The free running LIMO is tuned to oscillate at a nominal frequency close to the clock or carrier frequency of the incoming signal. With the injection of the incoming signal, the LIMO will quickly lock to its clock or carrier frequency while rejecting other frequency components (harmonics and subharmonics) associated with the signal.

Figure 4 shows the experimental setup used to demonstrate 100 MHz and 4.95 GHz clock recovery. Switches SW-1 and SW-2 are in the 'A' position for the 100 MHz clock recovery experiment and in position 'B' for the 4.95 GHz clock recovery experiment. In either experiment, using switch SW-3, we could choose to look at the LIMO output in the time domain with a Tektronix 2465B oscilloscope or in the frequency domain with an HP 8562 spectrum analyzer.



In the 100 MHz clock recovery experiment we used an HP 8080 Word Generator System to generate a stream of repetitive 64-bit words at 100 Mb/s and we tuned the LIMO to oscillate near 100 MHz. We injected the data into the bias port of the E/O modulator through a filter and a bias T. The 100 MHz filter with a 3 dB bandwidth of 10 MHz was used to reduce unwanted frequency components of the input data. We used the first bit of each word to trigger the oscilloscope's sweep so the whole word could be displayed. The HP 8080 system's data pattern can be selected to be either return-to-zero (RZ) or non-return-to-zero (NRZ) so both types of data were used in our experiments. Clock recovery is independent of the word chosen, as long as it is balanced. However, for an infinitely long NRZ random data stream, the clock frequency component is zero. In order to recover the clock from such a data stream a procedure to convert NRZ data format to RZ format is required.<sup>[10]</sup>

Figure 5 is the oscilloscope display of the experimental results in the time domain that demonstrated successful clock recovery from an NRZ data stream. Figure 5a shows the input data, while Figure 5b and Figure 5c show the recovered clock. In Figure 5c the time span was reduced 10 times to show the recovered clock in more detail. In all three figures, the upper trace is the first bit of the input data used to trigger the oscilloscope. The fact that the recovered clock can be clearly displayed on the oscilloscope when the first bit of data is used as the trigger indicates that the recovered clock is synchronized with the data.

When viewed in the frequency domain on the spectrum analyzer, the input data stream has some frequency components stronger than the clock frequency. After clock recovery the power of the recovered clock is more than 62 dB above the strongest frequency component of the data.

Note that the recovered clock level is almost independent of the input signal level, a feature that is desirable for clock recovery and is inherent in injection locked oscillators. Other proposed high speed clock recovery circuits use automatic gain control and limiting amplifiers to achieve constant amplitude.<sup>[11]</sup>

To extend our clock recovery experiment to higher data rates we simulated a stream of 4.95 Gb/s data by up converting a stream of 100 Mb/s RZ data using an RF mixer as shown in Fig. 4 with switches SW-1 and SW-2 in the 'B' position. The LIMO used in these experiments was constructed using an electrooptic modulator made by E-Tek Dynamics. We used a common reference signal from a hydrogen maser to synchronize the word generator and an HP 8672A synthesized signal generator. The frequency of the signal generator's output was chosen to be 4.85 GHz and was used to up convert the 100 Mb/s RZ data from the word generator to 4.95 GHz. The signal out of the mixer has a center band, an upper sideband and a lower sideband, which all contain the data information. We used a filter centered at 5 GHz with a bandwidth of 255 MHz to select only the upper sideband, which effectively simulated a stream of 4.95 Gb/s RZ data.

Figures 6a and 6b show the frequency spectrum of the data before and after clock recovery respectively. As expected, the clock frequency was strongly amplified by the LIMO while other frequency components remained unchanged, resulting in a recovered clock with a signal-to-spur ratio of about 60 dB.



Although in the demonstrations the data were injected into the electrical injection port, similar results are expected if the data are in the optical domain and are injected into the LIMO through the optical injection port, since the data in the optical domain will be automatically converted by the internal photodetector into the electrical domain before affecting the LIMO. We estimate that only a few microwatts of optical signal power is required to ensure a satisfactory clock recovery for many applications. Clock recovery via optical injection is important because it enables the clock of a high-speed data stream in a fiber-optic system to be directly recovered without first converting the data to electrical pulses.

Similar to clock recovery, a carrier buried in noise can also be recovered by the LIMO. In the experiment, we added noise to a clean 100 MHz test signal and adjusted the Signal-to-Noise-Ratio (SNR) until it was approximately 3 dB in a 100 kHz bandwidth. After carrier recovery, the SNR of the test signal was improved more than 50 dB. Figure 7 is the spectrum analyzer display of the signal before and after recovery. The frequency span of the spectrum analyzer was set to 10 MHz and its resolution bandwidth was set to 100 kHz.

## CONCLUSION

We have demonstrated a novel photonic oscillator with an operation frequency up to 75 GHz, limited only by the speed of the E/O modulator used in the LIMO. It can be controlled and accessed both optically and electronically, making it attractive for easily interfacing with a complex fiber optic systems. We have demonstrated its use for clock or carrier recovery with very low phase noise. We have also shown that the LIMO has a number of other attractive properties including output power which is virtually independent of the input power of the signal to be recovered, fast acquisition time for phase locking, wide tracking range, and wide frequency tunability.

We thank M. Calhoun of JPL and S. Cao of E-Tek Dynamics for lending us E/O modulators used in the experiments. This research is carried out by the Jet Propulsion Laboratory under a contract with the National Aeronautics and Space Administration.

## REFERENCES

- [1] R. D. Esman, K. J. Williams, M. H. White, and V. Uzunoglu, "Microwave subcarrier and clock recovery by an optically injected CPSO," *IEEE Photon. Techn. Lett.* 3 (2), pp 179–181 (1991).
- [2] K. Smith and J. K. Lucek, "All-optical clock recovery using a mode-locked laser," *Electron. Lett.*, 28(19), pp 1814–1816, 1992.
- [3] A. D. Ellis, K. Smith, and D. M. Patrick, "All optical clock recovery at bit rates up to 40 Gb/s," *Electron. Lett.*, 29(15), pp 1323–1324 (1993)
- [4] D. M. Patrick and R. J. Manning, "20 Gb/s all-optical clock recovery using semiconductor nonlinearity," *Electron. Lett.*, 30(2), pp 151–152 (1994)

- [5] P. E. Barnsley, H. J. Wicks, G. E. Wickens, and D. M. Spivit, "All-optical clock recovery from 5 Gb/s RZ data using a self-pulsating 1.56  $\mu$ m laser diode," *IEEE Photon. Techn. Lett.* 3(10), pp 942–945 (1991)
- [6] M. Jinno and T. Matsumoto, "All-optical timing extraction using a 1.5  $\mu$ m self-pulsating multielectrode DFB LD," *Electronic Letters* 24(23), pp 1426–1427 (1988)
- [7] X. S. Yao and L. Maleki, "High frequency optical subcarrier generator," *Electron. Lett.*, 30(18), pp. 1525–1526 (1994).
- [8] X. S. Yao and L. Maleki, "Light Induced Microwave Oscillator," Submitted to *Journal of Optical Society of America B*. Also in *The TDA Progress Report 42–123*, Jet Propulsion Laboratory, [http://tda.jpl.nasa.gov/progress\\_report](http://tda.jpl.nasa.gov/progress_report), pp. 32–42 (1995).
- [9] X. Steve Yao and Lute Maleki, "A novel photonic oscillator," *The TDA Progress Report 42–121*, Jet Propulsion Laboratory, pp. 32–42 (1995), [http://tda.jpl.nasa.gov/progress\\_report](http://tda.jpl.nasa.gov/progress_report).
- [10] D. Wolever, *Phase-locked circuit design*, Prentice Hall, Englewood Cliffs, 1991.
- [11] H. Ichino, M. Tugashhi, M. Ohhata, Y. Imai, N. Ishihata, G. Sano, "Over-10-Gb/s ICs for future light wave communications," *J. Lightwave Techn.*, 12(2) pp 308–319 (1994).



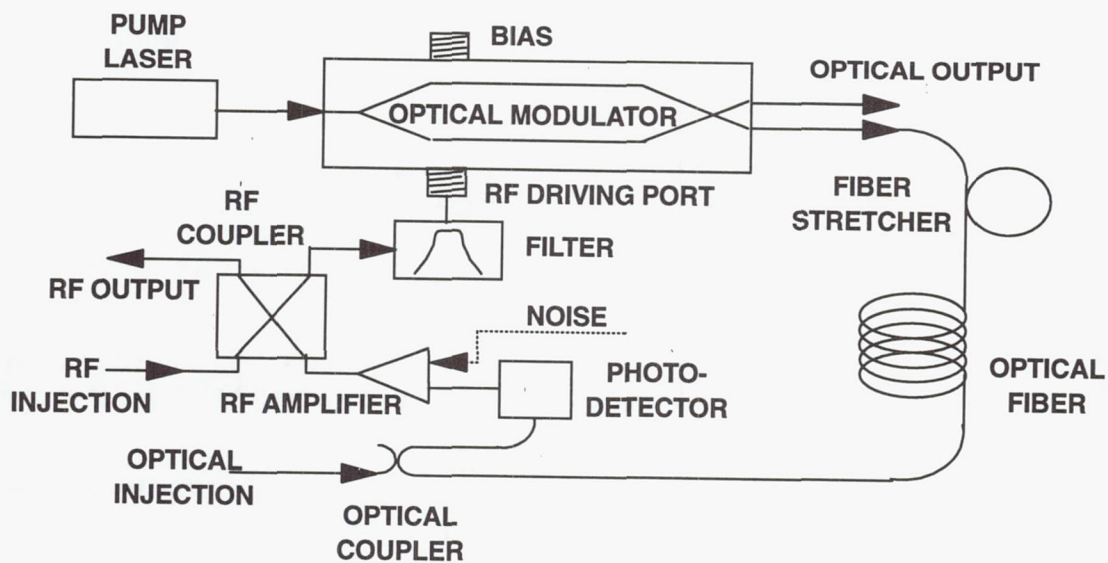


Fig. 1 Schematic of the LIMO.

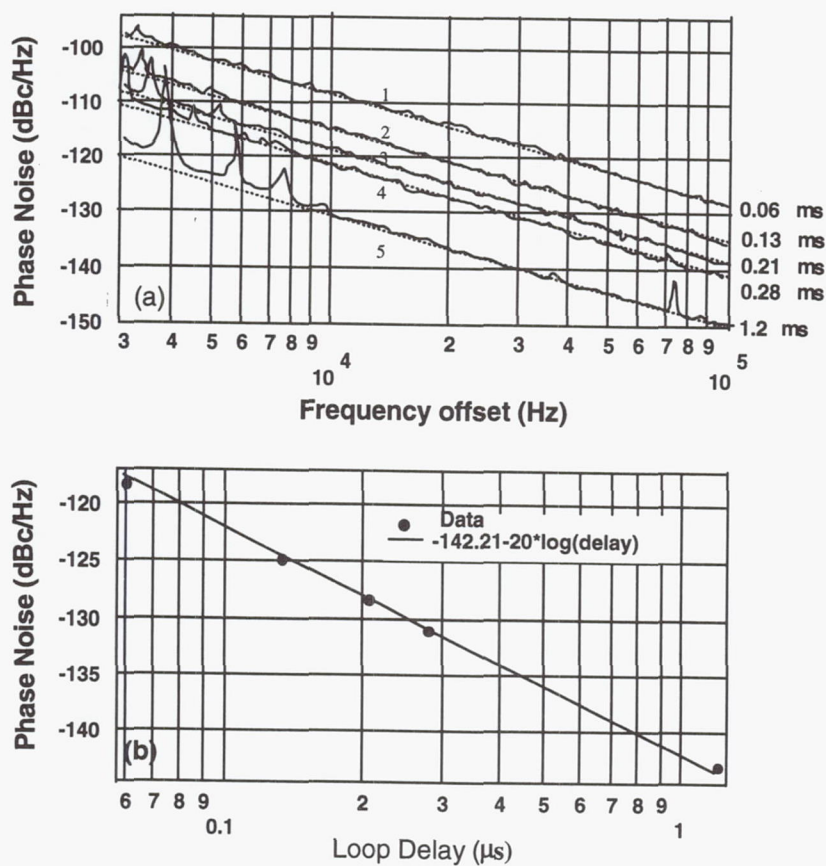


Fig. 2 The theoretical and measured phase noise of the LIMO as a function of the delay in the delay line.

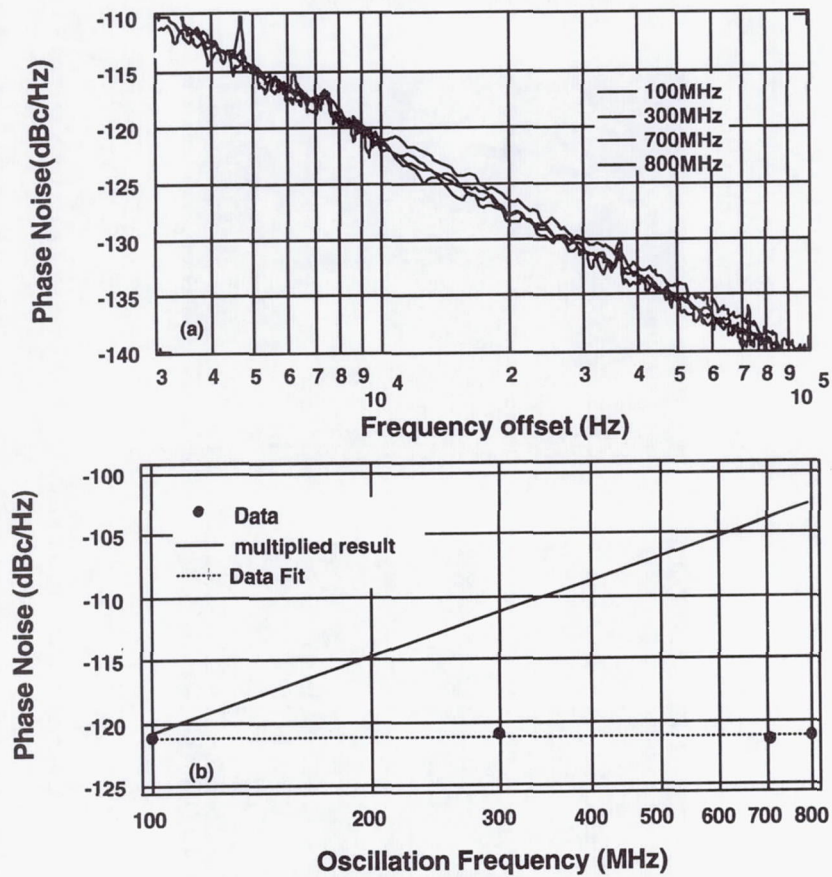


Fig. 3. The phase noise of the LIMO at different frequencies.

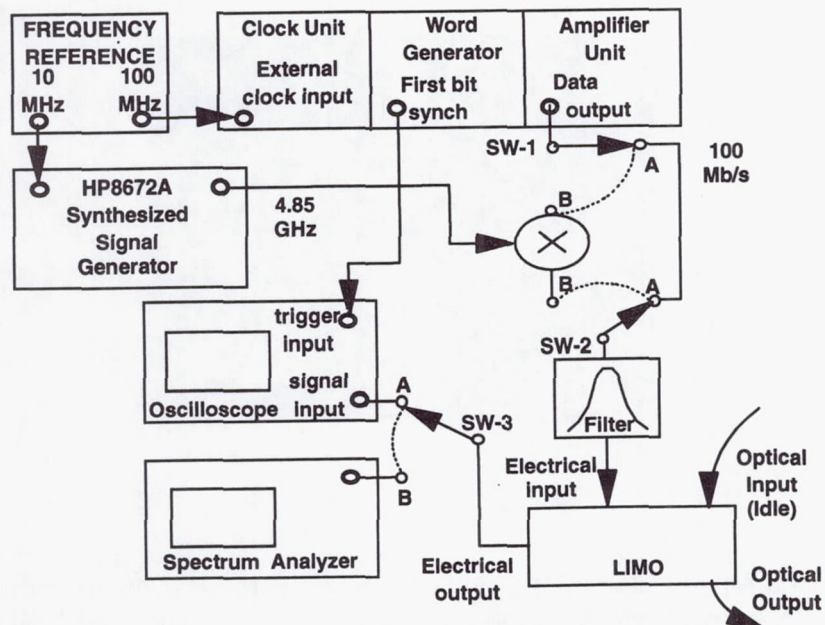


Fig. 4 The experimental setup used to demonstrate 100 MHz and 4.95 GHz clock.



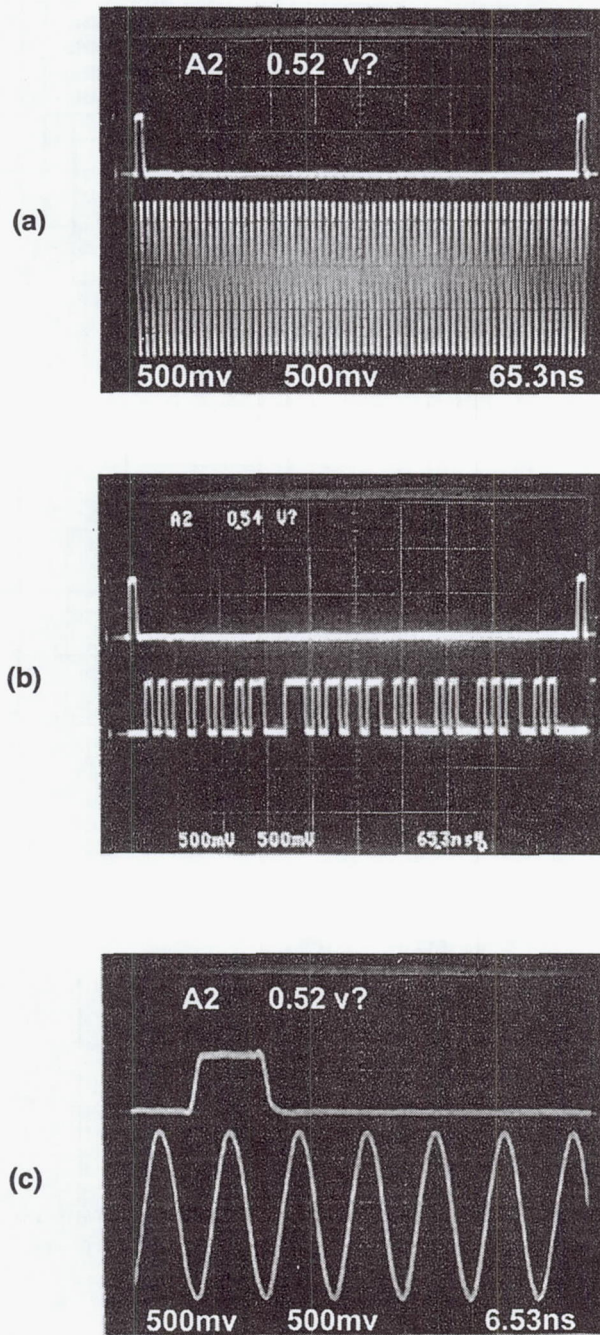
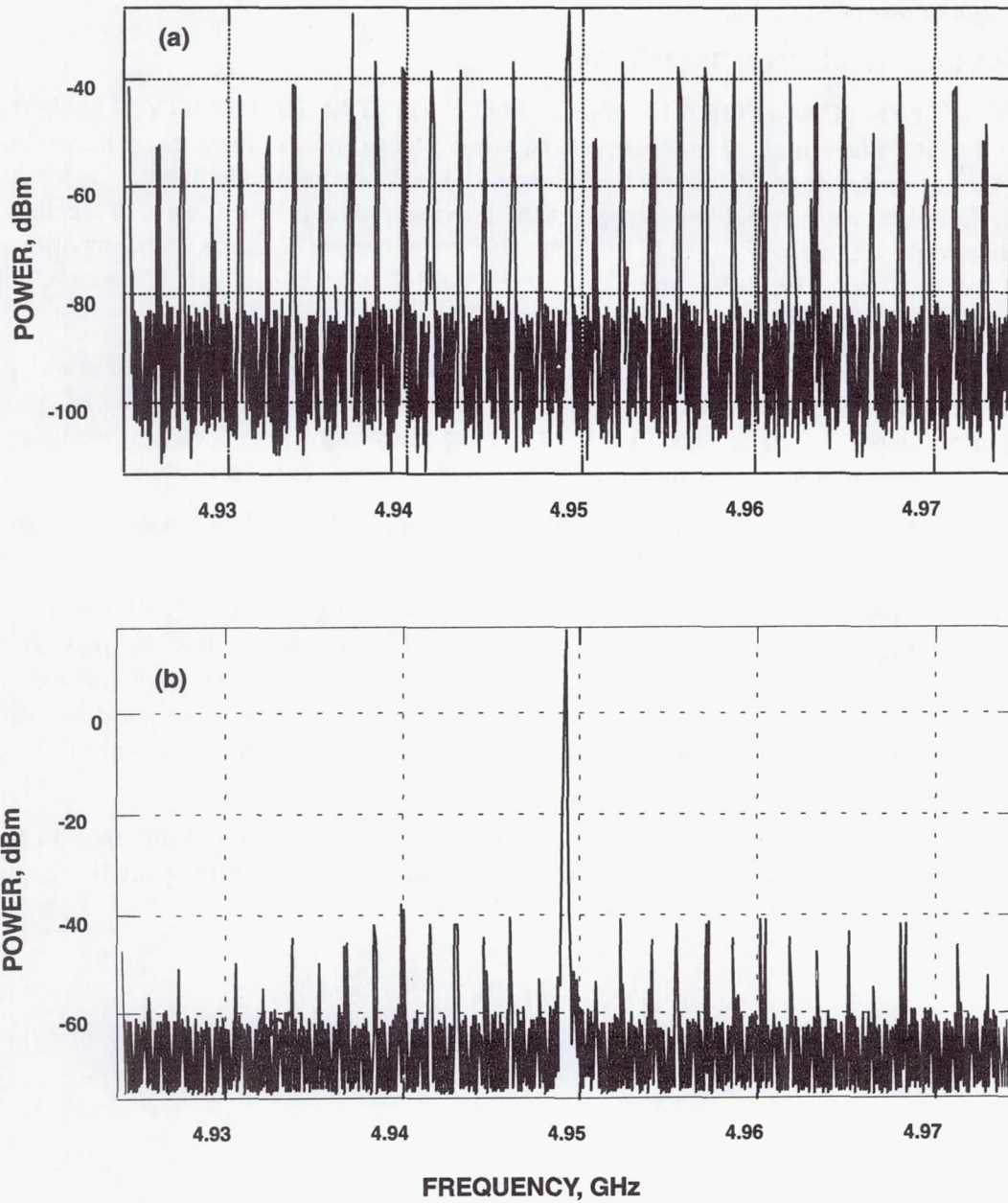


Fig. 5 The oscilloscope display of the experimental results in the time domain. (a) shows the input data, while (b) and (c) show the recovered clock. In (c) the time span was reduced 10 times to show the recovered clock in more detail. In all three figures, the upper trace is the first bit of the input data used to trigger the oscilloscope.



Figs. 6(a) and 6(b) show the frequency spectrum of the data before and after clock recovery.



## Questions and Answers

**DAVID ALLAN (ALLAN'S TIME):** What kind of powers have you been able to appreciate at this point? I know you have to have the amplifier in a loop.

**GEORGE LUTES (CALIFORNIA INSTITUTE OF TECHNOLOGY):** You mean the total DC input powers?

**DAVID ALLAN (ALLAN'S TIME):** Yes.

**GEORGE LUTES (CALIFORNIA INSTITUTE OF TECHNOLOGY):** Well, the way we're running, it's fairly high. However, lasers, sonic electro-lasers, have been becoming very efficient. Lasers better than 50 percent efficiency and are becoming available. So it's hard to tell exactly how low we can get the power. But, I suspect that in the future, if we find some good applications for this device, that we'll be able to put it on a single chip, an optical chip – except for the fiber, the delay line, of course. I think that power can be gotten down to certainly less than a watt.

Then there's another aspect to this oscillator, too, that might be interesting to some people. We believe that it will not be nearly as susceptible to vibration as other types of oscillators that use tuning devices, such as crystals and saw-delay lines and things like that which are very susceptible to microphonics. This one should be much less susceptible to that.

**DAVID ALLAN (ALLAN'S TIME):** Is the temperature delay of the delay line, the temperature fix on the delay line any problem at all?

**GEORGE LUTES (CALIFORNIA INSTITUTE OF TECHNOLOGY):** Well, it is. If you want really high stability, we have done some calculations using a low thermal coefficient of delay fiber for the delay line. And it has a very broad curve that goes through a zero coefficient of delay at a certain temperature. So, we have looked at how good we think we could do if we control the temperature of the delay line to that temperature within reasonable limits.

The numbers we get are pretty amazing, but we've been in this business long enough to know that it's easier said than done! So, I'm not going to say anything about what those numbers turned out to be, but certainly better than crystal oscillators.

# SPACECRAFT DOPPLER TRACKING AS A XYLOPHONE DETECTOR

Massimo Tinto  
Jet Propulsion Laboratory  
California Institute of Technology  
Pasadena, California 91109

## Abstract

*We discuss spacecraft Doppler tracking in which Doppler data recorded on the ground are linearly combined with Doppler measurements made on board a spacecraft. By using the four-link radio system first proposed by Vessot and Levine<sup>[1]</sup>, we derive a new method for removing from the combined data the frequency fluctuations due to the Earth troposphere, ionosphere, and mechanical vibrations of the antenna on the ground. Our method provides also a way for reducing by several orders of magnitude, at selected Fourier components, the frequency fluctuations due to other noise sources, such as the clock on board the spacecraft or the antenna and buffeting of the probe by non gravitational forces<sup>[2]</sup>. In this respect spacecraft Doppler tracking can be regarded as a xylophone detector.*

*Estimates of the sensitivities achievable by this xylophone are presented for two tests of Einstein's theory of relativity: searches for gravitational waves and measurements of the gravitational red shift.*

*This experimental technique could be extended to other tests of the theory of relativity, and to radio science experiments that rely on high-precision Doppler measurements.*

## INTRODUCTION

Spacecraft Doppler tracking is the most sensitive technique to date for measuring distances and velocities of objects in the solar system, leading to information on masses and higher order moments of gravity fields of planets, their satellites, and asteroids<sup>[3, 4]</sup>. Doppler measurements have also been utilized to search for gravitational waves in the millihertz frequency region<sup>[5, 6]</sup>, and for placing upper limits on amplitudes of signals characterizing relativistic effects<sup>[7, 8]</sup>. These Doppler observations, however, suffer from noise sources that can be, at best, partially reduced or calibrated by implementing specialized and expensive hardware. The fundamental limitation is imposed by the frequency fluctuations inherent in the clocks referencing the microwave system. Current generation hydrogen masers achieve their best performance at about 1000 seconds integration time with a fractional frequency stability of a few parts in  $10^{-16}$ . This integration time is also comparable to the propagation time to spacecraft in the outer solar system.



The frequency fluctuations induced by the intervening media have severely limited the sensitivities of these experiments. Among all the propagation noise sources, the troposphere is the largest and the hardest to calibrate to a reasonably low level. Its frequency fluctuations have been estimated to be as large as  $10^{-13}$  at 1000 seconds integration time<sup>[9]</sup>.

In order to systematically remove the frequency fluctuations due to the troposphere in the Doppler data, it was pointed out by Vessot and Levine<sup>[1]</sup> and Smarr *et al.*<sup>[10]</sup> that by adding to the spacecraft payload a highly stable frequency standard, a Doppler readout system, and by utilizing a transponder at the ground antenna, one could make Doppler one-way (earth-to-spacecraft, spacecraft-to-earth) as well as two-way (spacecraft-earth-spacecraft, earth-spacecraft-Earth) measurements. This way of operation makes the Doppler link totally symmetric and allows the complete removal of the frequency fluctuations due to the earth troposphere, ionosphere, and mechanical vibrations of the ground antenna by properly combining the Doppler data recorded on the ground with the data measured on the spacecraft. Their proposed scheme relied on the possibility of flying a hydrogen maser on a dedicated mission. Although current designs of hydrogen masers have demanding requirements in mass and power consumption, it seems very likely that by the beginning of the next century new space-qualified atomic clocks, with frequency stability of a few parts in  $10^{-16}$  at 1000 seconds integration time, will be available. They would provide a sensitivity gain of almost a factor of one thousand with respect to the best performance crystal-driven oscillators. Although this clearly would imply a great improvement in the technology of spaceborne clocks, it would not allow us to reach a Doppler sensitivity better than a few parts  $10^{-16}$ . This would be only a factor of five or ten better than the Doppler sensitivity expected to be achieved on the future Cassini project, a NASA mission to Saturn, which will take advantage of a high radio frequency link (32 GHz) in order to minimize the plasma noise, and will use a specially built water vapor radiometer for calibrating up to 95% of the frequency fluctuations due to the troposphere<sup>[11]</sup>.

In this paper we adopt the radio link configuration first envisioned by Vessot and Levine<sup>[1]</sup>, but we combine the Doppler responses measured on board the spacecraft and on the ground in a different way, as it will be shown in the following sections. Furthermore our technique allows us to reduce by several orders of magnitude, at selected Fourier components, the noise due to the clock on board the spacecraft, or to the antenna and buffeting of the probe by non gravitational forces<sup>[2]</sup>. This experimental approach could also be extended to other tests of the relativistic theory of gravity and to radio science experiments that rely on high-precision Doppler measurements.

## DOPPLER TRACKING AS A XYLOPHONE DETECTOR

In Doppler tracking experiments a distant interplanetary spacecraft is monitored from earth through a radio link, and the earth and the spacecraft act as test particles. In a *one-way* operation a radio signal of nominal frequency  $\bar{\nu}_0$  referenced to an on board clock is transmitted to earth, where it is compared to a signal referenced to a highly stable clock. In a *two-way* operation instead a radio signal of frequency  $\nu_0$  is transmitted to the spacecraft, and coherently transponded back to earth. In both configurations relative frequency changes  $\Delta\nu/\nu_0$  as functions of time are measured, and the physical effects the experimenter is trying to observe appear in



the Doppler observable as small frequency changes of well-defined time signature<sup>[3, 4, 5]</sup>.

If a Doppler readout system is added to the spacecraft radio instrumentation, and a transponder is installed at the ground station (Figure 1), one-way as well as two-way Doppler data can also be recorded on board the spacecraft<sup>[1]</sup>. If we assume the earth clock and the on board clock to be synchronized, then the one-way and two-way Doppler data measured at time  $t$  on the earth ( $E_1(t)$ ,  $E_2(t)$  respectively), and the one-way and two-way Doppler measured at the same time  $t$  on the spacecraft ( $S_1(t)$ ,  $S_2(t)$ ), have the following analytic expressions

$$E_1(t) = E_1^0(t) + C_{sc}(t-L) - C_E(t) + T(t) + B(t-L) + A_{sc}(t-L) + EL_{E_1}(t) + P_{E_1}(t) \quad (1)$$

$$E_2(t) = E_2^0(t) + C_E(t-2L) - C_E(t) + 2B(t-L) + T(t-2L) + T(t) + A_E(t-2L) + A_{sc}(t-L) + TR_{sc}(t-L) + EL_{E_2}(t) + P_{E_2}(t) \quad (2)$$

$$S_1(t) = S_1^0(t) + C_E(t-L) - C_{sc}(t) + T(t-L) + B(t) + A_E(t-L) + EL_{S_1}(t) + P_{S_1}(t) \quad (3)$$

$$S_2(t) = S_2^0(t) + C_{sc}(t-2L) - C_{sc}(t) + 2T(t-L) + B(t-2L) + B(t) + A_{sc}(t-2L) + A_E(t-L) + TR_E(t-L) + EL_{S_2}(t) + P_{S_2}(t) \quad (4)$$

where  $E_1^0(t)$ ,  $E_2^0(t)$ ,  $S_1^0(t)$ ,  $S_2^0(t)$  are the contributions of a signal (a gravitational wave pulse or a red shift for instance) to the four Doppler data, and  $L$  is the distance to the spacecraft measured in seconds.

In Equations (1, 2, 3, 4) we have denoted with  $C_E(t)$  the random process associated with the frequency fluctuations of the clock on the earth,  $C_{sc}(t)$  the relative frequency fluctuations of the clock on board,  $B(t)$  the joint effect of the noise from the antenna and buffeting of the spacecraft by non gravitational forces,  $T(t)$  the joint frequency fluctuations due to the troposphere, ionosphere, and ground antenna,  $A_E(t)$  the noise of the radio transmitter on the ground,  $A_{sc}(t)$  the noise of the radio transmitter on board,  $TR_{sc}(t)$  and  $TR_E(t)$  the noise due to the transponder on board and on the ground respectively,  $EL_{E_1}(t)$ ,  $EL_{E_2}(t)$ ,  $EL_{S_1}(t)$ , and  $EL_{S_2}(t)$  the noises from the electronics at the ground station and on the spacecraft in the one-way and two-way data, and  $P_{E_1}(t)$ ,  $P_{E_2}(t)$ ,  $P_{S_1}(t)$ , and  $P_{S_2}(t)$  the frequency fluctuations due to the interplanetary plasma. Note that the noise due to the transmitters on the ground and on board have been denoted with the same random processes ( $A_E(t)$  and  $A_{sc}(t)$  respectively) in the four Doppler responses. This is correct as long as the two radio signals of frequencies  $\nu_0$  and  $\bar{\nu}_0$  transmitted from the earth and the spacecraft are amplified within the operational bandwidth (typically forty to fifty megahertz) of the same transmitters<sup>[13, 14]</sup>. The Doppler data  $S_1(t)$  and  $S_2(t)$  are then time-tagged, and telemetered back to earth in real time or at a later time during the mission.

In Equations (1, 2, 3, 4) it is important to note the characteristic time signatures of the noises  $C_E(t)$ ,  $C_{sc}(t)$ ,  $B(t)$ ,  $T(t)$ ,  $A_E(t)$ , and  $A_{sc}(t)$ <sup>[9, 10, 12]</sup>. It was first pointed out by Vessot



and Levine<sup>[1]</sup> that, by properly combining some of the four Doppler data, it was possible to calibrate the frequency fluctuations of the troposphere, ionosphere, and ground antenna noise,  $T(t)$ . Their pioneering work, however, left open the question on whether there existed some other, perhaps more complicated, linear combinations of the data that would further improve the sensitivity of Doppler tracking. In what follows we answer this question, and derive a method that allows us to uniquely identify an optimal way of combining the data.

Let  $\widetilde{E}_1(f)$  be the Fourier transform of the time series  $E_1(t)$

$$\widetilde{E}_1(f) \equiv \int_{-\infty}^{+\infty} E_1(t) e^{2\pi i f t} dt, \quad (5)$$

and similarly let us denote by  $\widetilde{E}_2(f)$ ,  $\widetilde{S}_1(f)$ ,  $\widetilde{S}_2(f)$  the Fourier transforms of  $E_2(t)$ ,  $S_1(t)$ , and  $S_2(t)$  respectively. The most general linear combination of the four Doppler data given in Eqs. (1, 2, 3, 4), can be written in the Fourier domain as follows:

$$\widetilde{y}(f) \equiv a(f, L) \widetilde{E}_1(f) + b(f, L) \widetilde{E}_2(f) + c(f, L) \widetilde{S}_1(f) + d(f, L) \widetilde{S}_2(f) \quad (6)$$

where the coefficients  $a$ ,  $b$ ,  $c$ ,  $d$  are for the moment arbitrary functions of  $f$  and  $L$ . If we substitute in Equation (6) the Fourier transforms of Eqs. (1, 2, 3, 4) we deduce the following expression

$$\begin{aligned} \widetilde{y}(f) = & \left[ a \widetilde{E}_1^0(f) + b \widetilde{E}_2^0(f) + c \widetilde{S}_1^0(f) + d \widetilde{S}_2^0(f) \right] + \\ & + \widetilde{C}_E(f) \left[ -a + b (e^{4\pi i f L} - 1) + c e^{2\pi i f L} \right] + \\ & + \widetilde{C}_{sc}(f) \left[ a e^{2\pi i f L} - c + d (e^{4\pi i f L} - 1) \right] + \\ & + \widetilde{T}(f) \left[ a + b (e^{4\pi i f L} + 1) + c e^{2\pi i f L} + 2d e^{2\pi i f L} \right] + \\ & + \widetilde{B}(f) \left[ a e^{2\pi i f L} + 2b e^{2\pi i f L} + c + d (e^{4\pi i f L} + 1) \right] + \\ & + \widetilde{A}_E(f) \left[ b e^{4\pi i f L} + c e^{2\pi i f L} + d e^{2\pi i f L} \right] + \\ & + \widetilde{A}_{sc}(f) \left[ a e^{2\pi i f L} + b e^{2\pi i f L} + d e^{4\pi i f L} \right] + \\ & + a \left[ \widetilde{E} \widetilde{L}_{E_1}(f) + \widetilde{P}_{E_1}(f) \right] + b \left[ \widetilde{T} \widetilde{R}_{sc}(f) e^{2\pi i f L} + \widetilde{E} \widetilde{L}_{E_2}(f) + \widetilde{P}_{E_2}(f) \right] + \\ & + c \left[ \widetilde{E} \widetilde{L}_{S_1}(f) + \widetilde{P}_{S_1}(f) \right] + d \left[ \widetilde{T} \widetilde{R}_E(f) e^{2\pi i f L} + \widetilde{E} \widetilde{L}_{S_2}(f) + \widetilde{P}_{S_2}(f) \right]. \quad (7) \end{aligned}$$

The four coefficients  $a$ ,  $b$ ,  $c$ ,  $d$ , can be determined by requiring the transfer functions of the random processes  $\widetilde{C}_E(f)$ ,  $\widetilde{C}_{sc}(f)$ ,  $\widetilde{T}(f)$ ,  $\widetilde{B}(f)$ ,  $\widetilde{A}_E(f)$ ,  $\widetilde{A}_{sc}(f)$  in Equation (7) to be simultaneously equal to zero, and by further checking that this solution gives a non-zero signal in the corresponding combined data. This condition implies that  $a$ ,  $b$ ,  $c$ ,  $d$  must satisfy a homogeneous linear system of six equations in four unknowns. We calculated the rank of the  $(6 \times 4)$  matrix associated with this linear system by using the algebraic computer language *Mathematica*, and

we found it to be equal to two. The corresponding solution can be written in the following way

$$\begin{aligned} a(f, L) &= c(f, L) e^{-2\pi i f L} - d(f, L) [e^{2\pi i f L} - e^{-2\pi i f L}] \\ b(f, L) &= -c(f, L) e^{-2\pi i f L} - d(f, L) e^{-2\pi i f L}, \end{aligned} \quad (8)$$

where  $c$  and  $d$  can be any arbitrary complex functions not simultaneously equal to zero. After substituting Equation (8) into Equation (7), we have derived the expressions for the signal in the case of a gravitational wave pulse or in the variation of the gravitational potential as experienced by a spacecraft orbiting a celestial body (redshift measurements). We found that for both these signals their combined Doppler responses (Equation (7)) also vanish. These results imply that, at any Fourier frequency  $f$  and for these two specific Doppler experiments, we can remove only one of the considered noise sources. Among all the noise sources affecting spacecraft Doppler tracking, the frequency fluctuations due to the troposphere, ionosphere, and mechanical vibrations of the ground antenna,  $\tilde{T}(f)$ , are the largest. We can choose  $a$ ,  $b$ ,  $c$ ,  $d$  in such a way that the transfer function of  $\tilde{T}(f)$  in the combined data is equal to zero. From Equation (7) we find that  $a$ ,  $b$ ,  $c$ ,  $d$ , must satisfy the following equation

$$a(f, L) = -b(f, L) [e^{4\pi i f L} + 1] - c(f, L) e^{2\pi i f L} - 2d(f, L) e^{2\pi i f L}. \quad (9)$$

Since  $b$ ,  $c$ ,  $d$  can not be equal to zero simultaneously, we will choose  $c$  to be equal to  $1/2$ , and  $b$ ,  $d$  to be equal to zero. In other words we will consider only linear combinations of one-way Doppler data. Note that with this choice we eliminate from  $y(t)$  the frequency fluctuations due to the transponders and the interplanetary plasma affecting the two-way Doppler data. These considerations imply the following expression for  $\tilde{y}(f)$

$$\begin{aligned} \tilde{y}(f) &= \frac{1}{2} [\tilde{S}_1^0(f) - \tilde{E}_1^0(f) e^{2\pi i f L}] + \tilde{C}_E(f) e^{2\pi i f L} - \frac{1}{2} \tilde{C}_{sc}(f) [e^{4\pi i f L} + 1] + \\ &+ \frac{1}{2} \tilde{B}(f) [1 - e^{4\pi i f L}] + \frac{e^{2\pi i f L}}{2} [\tilde{A}_E(f) - \tilde{A}_{sc}(f) e^{2\pi i f L}] + \\ &+ \frac{1}{2} [\tilde{P}_{S_1}(f) - \tilde{P}_{E_1}(f) e^{2\pi i f L}] + \frac{1}{2} [\tilde{E} \tilde{L}_{S_1}(f) - \tilde{E} \tilde{L}_{E_1}(f) e^{2\pi i f L}]. \end{aligned} \quad (10)$$

Equation (10) shows that the transfer functions of the noise of the on board clock,  $\tilde{C}_{sc}(f)$ , and of buffeting  $\tilde{B}(f)$ , can in principle be set to zero (not simultaneously) at specific Fourier frequencies. In searches for gravitational wave pulses it has been shown<sup>[2]</sup> that one can reduce by several orders of magnitudes the noise of the on-board clock at the nulls of its transfer function without removing the gravitational wave signal. For redshift experiments instead, a cancellation of the noise of the on-board clock at those frequencies removes also the signal. If, however, measurements of  $y(t)$  are made at the Fourier frequencies for which the transfer function of  $\tilde{B}(f)$  is equal to zero, some further improvement in sensitivity can be achieved<sup>[15]</sup>.



## EXPECTED XYLOPHONE SENSITIVITIES

In what follows we provide the expression for the noise in  $y(t)$  at the xylophone frequencies in the case of gravitational wave searches. The analogous expression for redshift experiments can easily be derived in similar fashion.

Let  $\delta$  be the time interval over which a Doppler tracking search for gravitational waves is performed. The corresponding frequency resolution  $\Delta f$  of the data is equal to  $1/\delta$ . This implies that the fluctuations of the clock on board can be minimized at the following frequencies

$$f_k = \frac{(2k-1)}{4L} \pm \frac{\Delta f}{2} ; \quad k = 1, 2, 3, \dots \quad (11)$$

At these frequencies, and to first order in  $\Delta f L$ , the Doppler response  $\tilde{y}(f_k)$  is equal to

$$\begin{aligned} \tilde{y}(f_k) \approx & \frac{1}{2} \left[ \widetilde{S}_1^0(f_k) + i(-1)^k \widetilde{E}_1^0(f_k) \right] + i(-1)^{k+1} \widetilde{C}_E(f_k) \pm (\pi i \Delta f L) \widetilde{C}_{sc}(f_k) + \\ & + \widetilde{B}(f_k) + \frac{1}{2} \left[ \widetilde{E} \widetilde{L}_{S_1}(f_k) - i \widetilde{E} \widetilde{L}_{E_1}(f_k) (-1)^{k+1} \right] + \\ & + \frac{1}{2} \left[ \widetilde{P}_{S_1}(f_k) - i \widetilde{P}_{E_1}(f_k) (-1)^{k+1} \right] + \\ & + \frac{1}{2} \left[ \widetilde{A}_{sc}(f_k) + i \widetilde{A}_E(f_k) (-1)^{k+1} \right] . \end{aligned} \quad (12)$$

For a typical gravitational wave experiment,  $\delta = 40$  days, and  $\Delta f = 3.0 \times 10^{-7}$ . Therefore, the frequency fluctuations of a clock on board a spacecraft that is out to 1 AU are reduced at the xylophone frequencies by the following amount:

$$\frac{\pi \Delta f L}{c} = 4.7 \times 10^{-4} .$$

We should point out, however, that these resonant frequencies in general will not be constant, since the distance to the spacecraft will change over a time interval of forty days. As an example, however, let us assume again  $L = 1$  AU,  $\delta = 40$  days, and  $f = 5 \times 10^{-4}$  Hz. The variation in spacecraft distance corresponding to a frequency change equal to the resolution bin width ( $3 \times 10^{-7}$  Hz) is equal to  $1.0 \times 10^5$  Km. Trajectory configurations fulfilling a requirement compatible to the one just derived have been observed during past spacecraft missions<sup>[9]</sup>, and therefore we do not expect this to be a limiting factor.

From Equation (12) we can estimate the expected root-mean-squared (r.m.s.) noise level  $\sigma(f_k)$  of the frequency fluctuations in the bins of width  $\Delta f$ , around the frequencies  $f_k$  ( $k = 1, 2, 3, \dots$ ). This is given by the following expression

$$\sigma(f_k) = [S_y(f_k) \Delta f]^{1/2} , \quad k = 1, 2, 3, \dots , \quad (13)$$



where  $S_y(f_k)$  is the one-sided power spectral density of the noise sources in the Doppler response  $y(t)$  at the frequency  $f_k$ . In what follows we will assume that the random processes representing these noises are uncorrelated with each other, and their one-sided power spectral densities are as given in Table I. In this table we have assumed a frequency stability of  $1.0 \times 10^{-16}$  at 1000 seconds integration time for the clock at the ground station. Although this is a factor of four better than what has been measured so far<sup>[11]</sup>, it seems very likely that by the beginning of next century such a sensitivity can be achieved. As far as the other sensitivity figures provided in Table I are concerned, they are as given in the Riley *et al.* report<sup>[11]</sup>. This document is a summary of a detailed study, performed jointly by scientists and engineers of NASA's Jet Propulsion Laboratory and the Italian Space Agency (ASI) Alenia Spazio, for assessing the magnitude and spectral characteristics of the noise sources that will determine the Doppler sensitivity of the future gravitational wave experiment on the Cassini mission. Included in Table I is also the spectral density of the noise of a crystal-driven ultra-stable oscillator (USO).

If dual radio frequencies in the uplink and downlink are used, then the frequency fluctuations due to the interplanetary plasma can be entirely removed<sup>[11]</sup>. We will refer to this configuration as MODE I. If only one frequency is adopted instead, which we will assume to be Ka-Band (32 GHz), we will refer to this configuration as MODE II. Ka-Band is planned to be used on most of the forthcoming NASA missions, and will be implemented on the ground antennas of the Deep Space Network (DSN) by the year 1999 for the Cassini mission.

In Figure 2 we plot the r.m.s.  $\sigma(f_k)$  of the noise as a function of the frequencies  $f_k$  ( $k = 1, 2, 3, \dots$ ), assuming that an interplanetary spacecraft is out to a distance  $L = 1.0$  AU. For this configuration the fundamental frequency of the xylophone (Equation (11)) is equal to  $5.0 \times 10^{-4}$  Hz. A complete analysis covering configurations with spacecraft at several other distances is given in<sup>[2]</sup>.

The MODE I configuration is represented by two curves, depending on whether an atomic clock (circles) or a USO (squares) is operated on board the spacecraft. Sensitivity curves for the MODE II configuration are also provided, again with an atomic clock on board (up-triangles) or a USO (down-triangles). The best sensitivity is achieved in the MODE I configuration, regardless of whether an atomic clock or a USO is operated on board the spacecraft (circles and squares are over imposed). This is because the amplitude of the noise of the clock on board is reduced by a factor  $\pi \Delta f L / c = 4.7 \times 10^{-4}$  at the xylophone frequencies. At  $f = 10^{-3}$  Hz the corresponding r.m.s. noise level is equal to  $4.7 \times 10^{-18}$ , and it increases to a value of  $5.7 \times 10^{-18}$  at  $f = 10^{-2}$  Hz. As far as the MODE II configuration is concerned, the r.m.s. noise level is equal to  $7.9 \times 10^{-18}$  at  $f = 10^{-3}$  Hz, while it decreases to  $6.3 \times 10^{-18}$  at  $f = 10^{-2}$  Hz. This is due to the fact that the one-sided power spectral density of the fractional frequency fluctuations due to the interplanetary plasma decays as  $f^{-2/3}$ .

In Figure 3 we turn to redshift experiments with a spacecraft out to 5 AU, and we assume an observing time of 40 hours. This example can be considered as representative of a spacecraft orbiting the planet Jupiter. The reduction factor of the buffeting noise  $B(t)$  (see Equation (10)) is now equal to

$$\frac{\pi \Delta f L}{c} = 5.5 \times 10^{-2} , \quad (14)$$



and the xylophone frequencies are given by the following relation

$$f_k = \frac{k}{2L} \pm \frac{\Delta f}{2} ; \quad k = 1, 2, 3, \dots \quad (15)$$

We also have assumed that when plasma calibration is not implemented, the frequency fluctuations due to interplanetary scintillation are estimated at opposition. This of course does not represent a general situation but only an example.

The best sensitivity is achieved in the MODE I configuration and by using an atomic clock on board. At the Fourier frequency  $f = 2.0 \times 10^{-4}$  Hz the sensitivity is equal to  $3.0 \times 10^{-17}$ , and it increases slowly at higher frequencies. In the MODE II configuration and with an atomic clock on board the sensitivity degrades by about a factor of three with respect to the previous configuration. If a USO is used instead, then MODE I and II are totally equivalent, since the USO is the dominant noise source. In this case at  $f = 2.0 \times 10^{-4}$  the sensitivity of the xylophone is equal to  $1.4 \times 10^{-14}$ , and improves as  $f^{-1/2}$  as the frequency increases.

## CONCLUSIONS

We have discussed a method for significantly increasing the sensitivity of two Doppler tracking experiments, namely searches for gravitational waves and measurements of the redshift effect. Our method relies on a properly chosen linear combination of the one-way Doppler data recorded on board with those measured on the ground. It allows us to remove entirely the frequency fluctuations due to the troposphere, ionosphere, and antenna mechanical, and for a spacecraft that is tracked for forty days out to 1 AU in search for gravitational waves, it reduces by almost four orders of magnitude the noise due to the on-board clock. For a redshift experiment instead, with a spacecraft out to 5 AU, our technique allows us to reduce by about two orders of magnitude the noise of the antenna and buffeting of the spacecraft.

The experimental technique presented in this paper can be extended to a configuration with two spacecraft tracking each other through a microwave or a laser link. Future space-based laser interferometric detectors of gravitational waves<sup>[16]</sup>, for instance, could implement this technique as a backup option, if failure of some of their components would make the normal interferometric operation impossible.

As a final note, a method similar to the one presented can be used in all those radio science experiments in which one-way and two-way spacecraft Doppler measurements are used as primary data set. We will analyze the implications of the sensitivity improvements that this technique will provide for direct measurements of the following quantities such as searches for possible anisotropy in the velocity of light, measurements of the Parameterized Post-Newtonian parameters, measurements of the deflection and time delay by the sun in radio signals, and occultation experiments. This research is in phase of development, and will be the subject of a forthcoming paper.

## REFERENCES

- [1] R.F.C. Vessot, and M.W. Levine 1979, *Gen. Relativ. Gravit.*, 10, 181.
- [2] M. Tinto, *Phys. Rev. D*, in press.
- [3] J.D. Anderson, *et al.* 1980, *Science*, 207, 449-453.
- [4] J.D. Anderson, *et al.* 1986, *Icarus*, 71, 337-349.
- [5] F.B. Estabrook, and H.D. Wahlquist 1975, *Gen. Rel. Grav.*, 6, 439.
- [6] J.W. Armstrong, R. Woo, and F.B. Estabrook 1979, *Astrophys. J.*, 30, 574.
- [7] I.I. Shapiro, *et al* 1977, *J. Geophys. Res.*, 82, 4329-4334.
- [8] J.D. Anderson, *et al.* 1978, *Astronautica*, 5, 43-61.
- [9] J.W. Armstrong 1989, in *Gravitational Wave Data Analysis*, ed. B.F. Schutz (Kluwer, Dordrecht), p. 153.
- [10] L.L. Smarr, R.F.C. Vessot, C.A. Lundquist, R. Decher, and T. Piran 1983, *Gen. Relativ. Gravit.*, 15, 2.
- [11] A.L. Riley, D. Antsos, J.W. Armstrong, P. Kinman, H.D. Wahlquist, B. Bertotti, G. Comoretto, B. Pernice, G. Carnicella, and R. Giordani 1990, Jet Propulsion Laboratory Report, Pasadena, California, 22 January 1990.
- [12] T. Piran, E. Reiter, W.G. Unruh, and R.F.C. Vessot 1986, *Phys. Rev. D*, 34, 984.
- [13] R. Perez 1989, Jet Propulsion Laboratory, InterOffice Memorandum 3337-89-098, 3 October 1989.
- [14] B.L. Conroy, and D. and Lee 1990, *Rev. Sci. Instrum.*, 61, 1720.
- [15] M. Tinto, unpublished.
- [16] *LISA: (Laser Interferometer Space Antenna), Proposal for a Laser-Interferometric Gravitational Wave Detector in Space*, 1993, MPQ 177 (Max-Planck-Institute für Quantenoptik, Garching bei München).



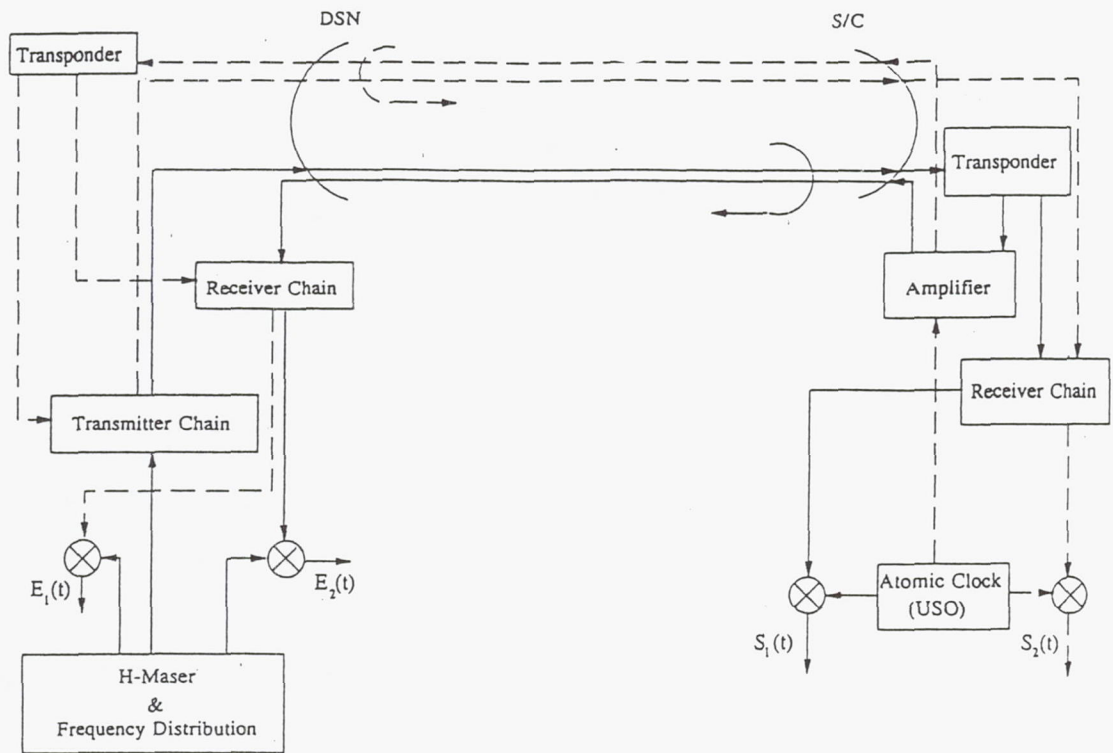


Figure 1.

Block diagram of the radio hardware at the ground antenna of the NASA Deep Space Network (DSN) and on board the spacecraft (S/C), that allows the acquisition and recording of the four Doppler data  $E_1(t)$ ,  $E_2(t)$ ,  $S_1(t)$ , and  $S_2(t)$ .

Error Source	Allan Deviation @ 1,000 sec.	Fractional Frequency One-Sided Power Spectral Density
One-Way Plasma (@ Ka-Band)	$4.9 \times 10^{-16}$	$2.7 \times 10^{-30} f^{-2.5}$
H-Maser	$1.0 \times 10^{-16}$	$6.2 \times (10^{-28} f + 10^{-33} f^{-1} + 10^{-30})$
Frequency Distribution	$1.0 \times 10^{-17}$	$1.3 \times 10^{-26} f^2$
Receiver chain	$3.1 \times 10^{-17}$	$1.3 \times 10^{-25} f^2$
Transmitter chain	$3.4 \times 10^{-16}$	$2.3 \times 10^{-28}$
Thermal Noise	$3.8 \times 10^{-17}$	$1.9 \times 10^{-25} f^2$
Spacecraft Antenna & Buffeting	$5.8 \times 10^{-17}$	$5.0 \times 10^{-42} f^{-3} + 10^{-31} + 5.0 \times 10^{-30}$
Spacecraft Amplifier	$5.0 \times 10^{-17}$	$4.0 \times 10^{-27} f$
USO	$9.5 \times 10^{-14}$	$6.5 \times 10^{-27} f^{-1}$

Table I

List of the noise sources entering into the combined Doppler response  $y(t)$ . The Allan deviation at a given integration time  $\tau$  is a statistical parameter for describing frequency stability. It represents the root-mean-squared expectation value of the random process associated with the fractional frequency changes, between time-contiguous frequency measurements, each made over time intervals of duration  $\tau$ . The numbers provided in this table are taken from the Riley *et al.* report [11].

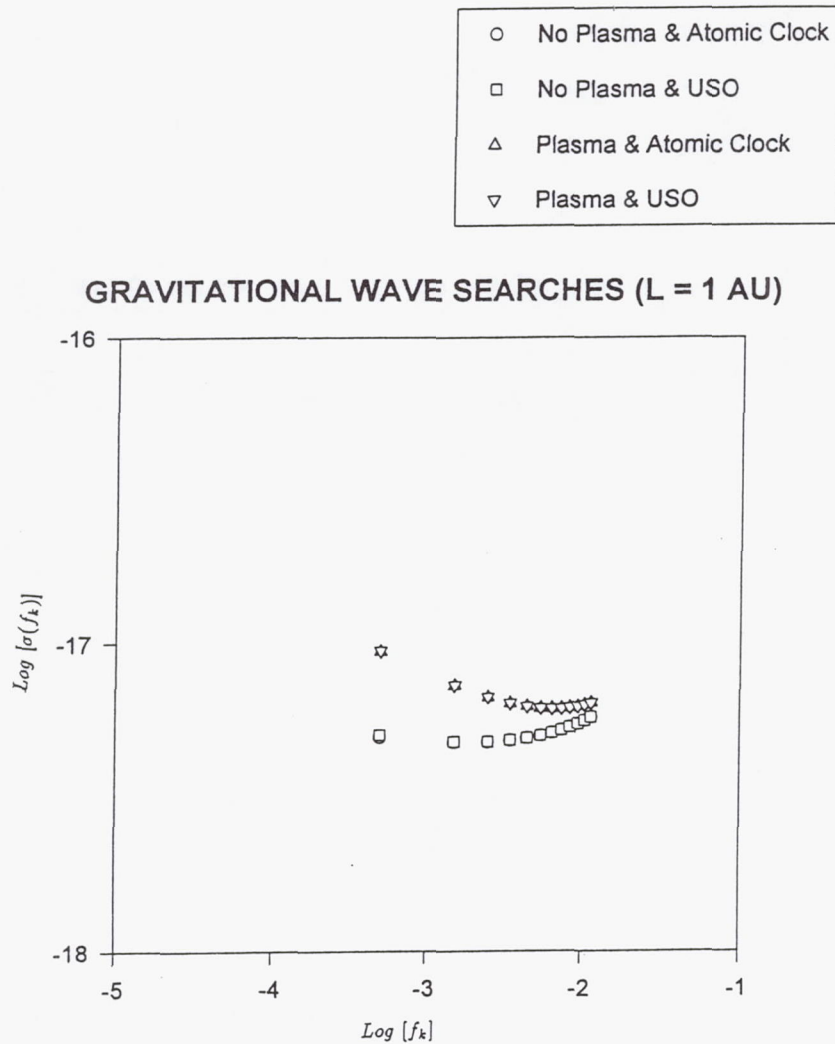


**Figure 2.**

The r.m.s. noise level as a function of the frequencies  $f_k$  ( $k = 1, 2, 3, \dots$ ), estimated for a spacecraft that is out to a distance  $L = 1.0$  AU searching for gravitational waves. Sensitivity figures for the four distinct configurations are represented with four different symbols. Circles represent r.m.s. values as functions of the xylophone frequency when plasma frequency fluctuations are totally removed and an atomic standard is on board. Squares are sensitivity values again with plasma calibration, but now with a USO on the spacecraft. Up-triangles are used for representing sensitivity figures affected by plasma noise at Ka-Band, and an atomic clock is used on board. Down-triangles assume a plasma noise at Ka-Band, but now with a USO on board.



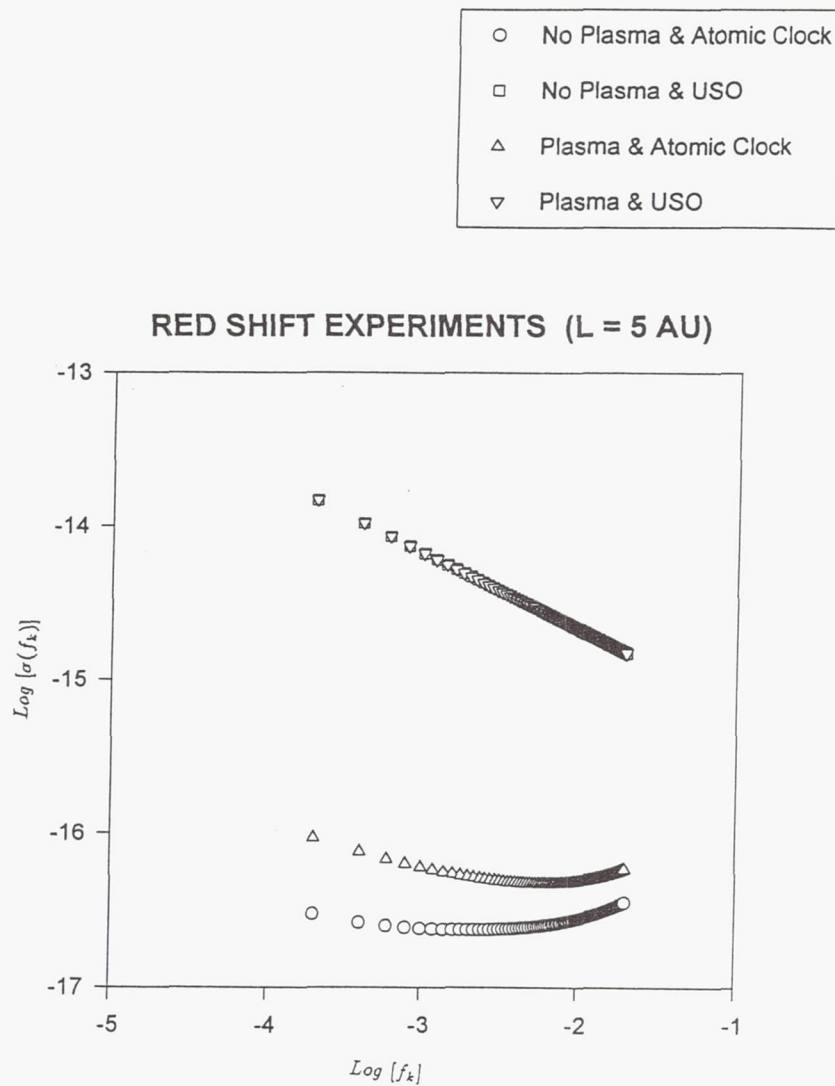


Figure 3.

The r.m.s. noise level as a function of the frequencies  $f_k$  ( $k = 1, 2, 3, \dots$ ), estimated for a spacecraft that is out to a distance  $L = 5.0$  AU and tracked during a red shift experiment.

# PTTI '95 ATTENDEES' LIST

**David W. Allan**

Allan's Time  
PO Box 66  
Fountain Green, VT 84632  
Tel: 801-445-3216  
Fax: 801-445-3215

**Patricia L. Artis**

DNA/SRF  
5400 Port Royal Road  
Springfield, VA 22151  
Tel: 703-321-0008  
Fax: 703-321-7521

**CDR Mark Atkisson**

U.S. Naval Observatory  
3450 Massachusetts Ave., NW  
Washington, DC 20392-5420  
Tel: 202-653-1097  
Fax: 202-653-1497

**Heinz Badura**

Efratom  
3 Parker  
Irvine, CA 92718  
Tel: 714-770-5000

**Thomas B. Bahder**

Army Research Laboratory  
2800 Powder Mill Road  
Adelphi, MD 20783  
Tel: 301-394-2042  
Fax: 301-394-2103  
bahder@arl.mil

**Richard G. Bailey**

Datum, Inc.  
1363 S. State College Blvd.  
Anaheim, CA 92806  
rbailey@datum.com

**James A. Barnes**

2946 Kalmia Ave.  
Apt. 47  
Boulder, CO 80301  
Tel: 303-546-6238

**Thomas R. Bartholomew**

TASC  
1190 Winterson Road  
Linthicum, MD 21090  
Tel: 410-805-4927  
Fax: 410-850-0404  
trbartholomew@tasc.com

**John M. Battle**

Telecom Solutions  
85 Tasman Drive  
San Jose, CA 95134  
Tel: 408-428-7921

**Leland G. Baum**

Allen Osborne Assoc.  
756 Lakefield Road  
Westlake Village, CA 91361  
Tel: 805-495-8420  
Fax: 805-373-6067

**Francoise S. Baumont**

Observatoire de la Cote d'Azur  
Avenue Copernic  
Grasse 06130  
France  
Tel: 33 93 40 5338  
Fax: 33 93 40 5333  
baumont@ocar01.obs-azur.fr

**Ronald L. Beard**

Naval Research Laboratory  
4555 Overlook Avenue SW  
Washington, DC 20375  
USA  
Tel: 202-767-2595  
Fax: 202-767-2845  
beard@juno.nrl.navy.mil

**Nat D. Bhaskar**

Aerospace Corp.  
2350 E. El Segundo St.  
El Segundo, CA  
Tel: 310-336-3396  
Fax: 310-336-3396

**Robert E. Blair**

USAF  
AGMC/MLE  
813 Irving Wicke Drive  
Heath, OH 43057  
Tel: 614-522-7377

**Martin B. Bloch**

FEI  
55 Charles Linburgh Blvd.  
Uniondale, NY 11553  
Tel: 516-794-4500

**Lee A. Breakiron**

U.S. Naval Observatory  
3450 Massachusetts Avenue, NW  
Washington, DC 20932-5420  
Tel: 202-653-1888  
Fax: 202-653-0909  
lab@tycho.usno.navy.mil

**David S. Briggs**

Datum Inc.  
FTS  
34 Tozer Road  
Beverly, MA 01915-5510  
Tel: 508-927-8220  
Fax: 508-927-4099

**Ronald R. Brown**

Bellcore  
445 South St.  
Morristown, NJ 07960  
sync2@cc.bellcore.com

**Dennis D. Brunnenmeyer**

Cedar Ridge Systems  
PO Box 820  
Cedar Ridge, CA 95924-0820  
Tel: 916-477-9015  
Fax: 916-477-9085

**Stan Bustia**

Computech - Odetics  
24694 Ashland Dr.  
Laguna Hills, CA 92653  
Tel: 714-837-8421  
Fax: 714-837-7388



**Edgar W. Butterline**  
AT&T  
900 Rtes 202 & 206 N  
Rm 3C130E  
Bedminster, NJ 07921  
Tel: 908-234-4545

**Malcolm D. Calhoun**  
Jet Propulsion Laboratory  
4800 Oak Grove Dr.  
Pasadena, CA 91109  
Tel: 818-354-9763  
Fax: 818-393-6773

**Carlo Carnebianca**  
Nuova Telespazio  
965 Via Tiburtina  
Roma 00156  
Italy  
Tel: 39 64 079 3422  
Fax: 39 64 079 3217

**William L. Carpar**  
NRAD  
Code 771  
San Diego, CA 92152-5000  
Tel: 619-553-7144

**Ralph W. Carpenter**  
EG&G  
35 Congress Street  
Salem, MA 01970  
Tel: 508-745-3200  
Fax: 508-741-4923

**William F. Cashin**  
Efratom Time and Frequency  
Products  
3 Parker  
Irvine, CA 92718  
Tel: 714-770-5000  
Fax: 714-770-9289

**Tom P. Celano**  
TASC  
12100 Sunset Hills Road  
Reston, VA 22090  
Tel: 703-834-5000  
celano@aol.com

**Harold A. Chadsey**  
U.S. Naval Observatory  
3450 Massachusetts Avenue, NW  
Washington, DC 20392-5420  
Tel: 202-653-1888  
Fax: 202-653-0909  
hc@planck.usno.navy.mil

**Laura G. Charron**  
U.S. Naval Observatory  
3450 Massachusetts Avenue, NW  
Washington, DC 20392-5420  
Tel: 202-653-1529  
Fax: 202-653-8776  
lgc@spica.usno.navy.mil

**Dan Chislon**  
Telecom Solutions  
85 W. Tasman Dr.  
San Jose, CA 95134  
Tel: 408-428-7948  
Fax: 408-428-7895  
dchislon@telecom.com

**Clayton Coker**  
Applied Research Lab  
University of Texas  
10000 Burnet Road  
Austin, TX 78713-8092  
Tel: 512-835-3514  
Fax: 512-835 3259  
ccoker@arlut.utexas.edu

**Franco Cordara**  
Istituto Elettrotecnico Nazionale  
91 Strada Delle Cacce  
Turin 10135  
Italy  
Tel: 39 11 391 9239  
Fax: 39 11 346 384  
metf@tf.ien.it

**Michael Costa**  
Lockheed Martin  
1111 Lockheed Way  
Bldg. 195A, Org. 48-70  
Sunnyvale, CA 94089  
Tel: 408-742-8928

**Dwin Craig**  
Naval Research Laboratory  
Code 8152  
Washington, DC 20375-5000  
Tel: 202-404-7067  
Fax: 202-767-2845  
craig@blennie.nrl.navy.mil

**Jeff D. Crockett**  
Efratom Time and Frequency  
Products  
3 Parker  
Irvine, CA 92718  
Tel: 714-770-5000  
Fax: 714-770-9289

**Carlos Cuevas**  
Hughes Space and Comm. Co.  
PO Box 92919  
Los Angeles, CA 90009  
Tel: 310-364-7217  
Fax: 310-364-7186

**Len Cutler**  
Hewlett-Packard  
5301 Stevens Creek Blvd.  
Santa Clara, CA 95052  
Tel: 408-553-2506  
Fax: 408-553-2058

**Peter Daly**  
University of Leeds  
Dept. Electronic & Elec. Eng.  
Leeds LS2 9JT  
United Kingdom  
Tel: 44 113 233  
Fax: 44 113 2032

**Jim Danaher**  
3S Navigation  
23141 Plaza Pointe Dr.  
Laguna Hills, CA 92653  
Tel: 714-830-3777  
Fax: 714-830-8411  
glonassman@aol.com

**Sam Dang**  
NWAD  
PO Box 5000  
Corona, CA 91718-5000  
Tel: 909-273-4749

**Gerrit de Jong**  
NMi Van Swinden Lab  
PO Box 654  
Delft 2600 AR  
Netherlands  
Tel: 31 15 269 1500  
Fax: 31 15 261 2971  
gdejong@nmi.nl

**Edoardo Detoma**  
SEPA  
Corso Giulio Cesare 300  
Torino 10154  
Italy  
Tel: 39 22 6878523  
Fax: 39 22 2420372

**James A. DeYoung**  
U.S. Naval Observatory  
3450 Massachusetts Avenue, NW  
Washington, DC 20392-5420  
Tel: 202-653-1034  
Fax: 202-653-0909  
dey@herschel.usno.navy.mil

**Janise Dickerson**  
Arbiter Systems, Inc.  
PO Box 2279  
Paso Robles, CA 93446  
Tel: 805-237-3831  
Fax: 805-238-5717

**Bill Dickerson**  
Arbiter Systems, Inc.  
PO Box 2279  
Paso Robles, CA 93446  
Tel: 805-237-3831  
Fax: 805-238-5717

**William A. Diener**  
Jet Propulsion Laboratory  
4800 Oak Grove Dr.  
Pasadena, CA 91109  
Tel: 818-354-6670  
Fax: 818-393-6773

**Raymond S. DiEsposti**  
The Aerospace Corp.  
PO Box 92957  
MS/681  
Los Angeles, CA 90009  
Tel: 310-336-8404  
Fax: 310-336-5076

**Gary L. Dieter**  
U.S. Air Force  
2SOPS  
300 O'Malley Ave  
Suite 41  
Falcon AFB, CO 80912  
Tel: 719-567-6393  
dietergl@fafb.af.mil

**Gerard L. Dietrich**  
Lockheed Martin  
PO Box 9048  
Philadelphia, PA 19101  
Tel: 610-354-5794  
Fax: 610-354-2668

**Thomas P. Donaher**  
Spectracom Corporation  
101 Despatch Drive  
East Rochester, NY 14445  
Tel: 716-381-4827  
Fax: 716-381-4998

**Barbara A. Donaldson**  
EG&G  
35 Congress St.  
Salem, MA 01970  
Tel: 508-745-3209, ext. 583  
Fax: 508-741-4923

**Robert C. Dreyer**  
B&J Marketing  
17074 Dearborn Street  
Northridge, CA 91325  
Tel: 818-993-0048  
Fax: 818-993-5758  
Bdreyer@aol.com

**Christopher S. Duffey**  
Computer Sciences Raytheon  
4270 Grovewood Ln.  
Titusville, FL 32780  
Tel: 407-494-2014  
Fax: 407-494-7604  
duffeyc@pafb.af.mil

**Peter L. England**  
TrueTime  
2835 Duke St.  
Santa Rosa, CA 95407  
Tel: 707-528-1230

**Thomas English**  
Efratom Time and Frequency  
Products  
3 Parker  
Irvine, CA 92718  
Tel: 714-770-5000  
Fax: 714-770-9289

**Sergey V. Ermolin**  
Hewlett-Packard Co.  
5301 Stevens Creek Blvd.  
SIV-23  
Santa Clara, CA 95051  
Tel: 408-553-2869  
sermolin@se.hp.com

**Sheila Faulkner**  
U.S. Naval Observatory  
3450 Massachusetts Ave., NW  
Washington, DC 20392-5420  
Tel: 202-653-1460  
Fax: 202-653-0909  
scf@spica.usno.navy.mil

**Ray Filler**  
U.S. Army  
AMSRL-PS-ED  
Fort Monmouth, NJ 07703  
Tel: 908-427-2467  
Fax: 908-427-4805  
rfiller@arl.mil

**Richard H. Flamm**  
Lockheed  
1100 Lockheed Way  
Titusville, FL 32780  
Tel: 407-867-3145  
Fax: 407-867-7968

**Henry F. Fliegel**  
The Aerospace Corporation  
2350 E. El Segundo Boulevard  
El Segundo, CA 09245  
Tel: 310-336-1710  
Fax: 310-336-5076  
fliegel@courier1.aero.org

**CAPT Kent W. Foster**  
U.S. Naval Observatory  
3450 Massachusetts Ave., NW  
Washington, DC 20392-5420  
Tel: 202-653-1538  
Fax: 202-653-1497

**Roger S. Foster**  
Naval Research Laboratory  
Code 7210  
Washington, DC 20375  
Tel: 202-767-0669  
Fax: 202-404-8894  
foster@risa.nrl.navy.mil



**R. Michael Garvey**  
Frequency and Time Systems  
34 Tozer Road  
Beverly, MA 01915  
Tel: 508-927-8220  
Fax: 508-927-4099  
garvey@world.std.com

**Garth Gelster**  
Hewlett-Packard Company  
MS 52U/16  
5301 Stevens Creek Boulevard  
Santa Clara, CA 85052-8059  
Tel: 408-246-4300  
Fax: 408-553-2058

**Glen G. Gibbons**  
GPS World  
859 Willamette Street  
Eugene, OR 97401  
Tel: 541-984-5286  
Fax: 541-344-3514  
mggpsworld@aol.com

**Al Gifford**  
U.S. Naval Observatory  
3450 Massachusetts Ave., NW  
Washington, DC 20392-5420  
Tel: 202-653-1097  
Fax: 202-653-1497

**William A. Gilbert**  
White Sands Missile Range  
White Sands, NM 88002  
Tel: 505-678-3396

**Chad Gillease**  
TrueTime, Inc.  
2835 Duke Ct.  
Santa Rosa, CA 95407  
Fax: 707-527-6640

**Gary M. Graceffo**  
HRB Systems  
800 International Dr.  
Linthicum, MD 21090  
Tel: 301-567-8619

**Joe C. M. Green**  
Allied Signal Technical Services  
129 N. Hill Ave.  
Pasadena, CA 91106  
Tel: 818-584-4472  
Fax: 818-584-4480  
joseph.c.green@jpl.nasa.gov

**Charles A. Greenhall**  
Jet Propulsion Laboratory  
MS 298-100  
4800 Oak Grove Drive  
Pasadena, CA 91109  
Tel: 818-393-6944  
Fax: 818-393-6773  
cgreen@fridge.jpl.nasa.gov

**Fran Groat**  
Hewlett-Packard  
5301 Stevens Creek Blvd.  
Santa Clara, CA 95052  
Tel: 408-553-2506  
Fax: 408-553-2058

**Robert L. Hamell**  
Jet Propulsion Laboratory  
4800 Oak Grove Dr.  
Pasadena, CA 91109  
Tel: 818-354-4944

**Michael M. Hamilton**  
Telecom Solutions  
85 W. Tasman Dr.  
San Jose, CA 95117  
Tel: 408-433-0910

**Walter C. Harding**  
NISE East Det Norfolk  
NAVELEX  
PO Box 1376  
Norfolk, VA 23501  
Tel: 804-396-0516  
Fax: 804-396-0518

**Edward J. Harrison, Jr.**  
Computer Sciences Corp.  
3470 Constellation Dr.  
Davidsonville, VA 21035  
Tel: 410-956-6031

**Gregory E. Hatten**  
2SOPS/Falcon AFB  
300 O'Malley Ave.  
Suite 341  
Falcon AFB, CO 80912  
Tel: 719-598-8119  
Fax: 719-567-6307  
hattenge@fafb.af.mil

**Gildas H. Herman**  
Tekelec Telecom  
29 Avenue de la Baltique  
Les Ulis 91953  
France  
Tel: 33 1 69 82 2007

**James W. Hodson**  
NRAD Warminster Detachment  
Street and Jacksonville Road  
Warminster, PA 18974  
Tel: 215-441-2698  
jhodson@bluefish.nosc.mil

**Douglas W. Hogarth**  
20241 194th Place, NE  
Woodinville, WA 98072-8889  
Tel: 206-788-1507  
dougho@microsoft.com

**Dave A. Howe**  
NIST  
325 Broadway  
Boulder, CO 80303  
Fax: 303-497-6461  
dhowe@boulder.doc.gov

**Capt. Steven T. Hutsell**  
USAF  
2d Space Operations Squadron  
300 O'Malley Avenue  
Suite 41  
Falcon AFB, CO 80912-3041  
Tel: 719-567-6394  
Fax: 719-567-6307  
hutsellst@fafb.af.mil

**Atsushi Imaoka**  
NTT Optical Network  
Systems Laboratories  
1-2356 Take  
Yokosuka Kanagawa 238-03  
Japan  
Tel: 81 468 59 2025  
Fax: 81 468 55 1282  
imaoka@exa.onlab.ntt.jp

**Jeffrey S. Ingold**  
Allied Signal Technical Services  
1 Bendix Road  
Columbia, MD 21045  
Tel: 410-964-7188  
Fax: 410-964-7187  
jsingold@atsc

**Marilynn Ison**  
Defense Mapping Agency  
SMC/CZD  
2435 Vela Way  
Suite 1613  
Los Angeles AFB, CA 90245-5500  
Tel: 310-363-2284  
Fax: 310-363-0643  
isonms@gps1.laafb.af.mil

**Bernardo Jaduszliwer**  
The Aerospace Corp.  
PO Box 92957  
MS/253  
Los Angeles, CA 90009  
Tel: 310-336-9217  
Fax: 310-336-1636  
jaduszliwer@aero.org

**Calvin James**  
AlliedSignal Technical Services  
One Bendix Road  
Columbia, MD 21045  
Tel: 410-964-7726  
Fax: 410-997-5278  
jamesc@clmmpoos.atssc.allied.com

**Nicolette M. Jardine**  
U.S. Naval Observatory  
3450 Massachusetts Ave., NW  
Washington, DC 20392-5420  
Tel: 202-653-1662  
Fax: 202-653-0909  
nj@tycho.usno.navy.mil

**Maj. Calvin J. Johnson**  
U.S. Air Force  
Space Warfare Center  
8626 Alpino Valley Dr.  
Colorado Springs, CO 80902  
Tel: 719-567-9102  
Fax: 719-567-9315  
goffd@fafb.af.mil

**Ken Johnston**  
U.S. Naval Observatory  
3450 Massachusetts Ave., NW  
Washington, DC 20392-5420  
Tel: 202-653-1513  
Fax: 202-653-1497

**Sarunas K. Karuza**  
The Aerospace Corp.  
Po Box 92957  
Los Angeles, CA 90009-2957  
Tel: 310-336-6837  
Fax: 310-336-6225

**Shalom Kattan**  
Guide Technology, Inc.  
1630 Zanker Road  
San Jose, CA 95129  
Tel: 408-453-8511  
Fax: 408-453-8515  
skattan@aol.com

**Ralph E. Kaufman**  
Qualcomm Inc.  
6455 Lusk Blvd.  
San Diego, CA 92121  
Tel: 619-658-4004  
rfaufman@qualcomm.com

**Bahman Kiazand**  
Allied Signal Technical Services  
129 N. Hill Ave.  
Pasadena, CA 91106  
Tel: 818-584-4460  
Fax: 818-584-4480

**Sonia U. Kim**  
3S Navigation  
23141 Plaza Point Drive  
Laguna Hills, CA 92653  
Tel: 714-830-3777  
Fax: 714-830-8411  
nav3s@aol.com

**Dieter Kirchner**  
Technical University Graz  
Inffeldgasse 12  
Graz A-8010  
Austria  
Tel: 316 463697

**Albert Kirk**  
Jet Propulsion Laboratory  
4800 Oak Grove Dr.  
Pasadena, CA 91109  
Tel: 818-354-3038  
Fax: 818-393-6773

**William J. Klepczynski**  
U.S. Naval Observatory  
3450 Massachusetts Ave., NW  
Washington, DC 20392-5420  
Tel: 202-653-1521  
Fax: 202-653-0909  
kz@bode.usno.navy.mil

**Paul A. Koppang**  
U.S. Naval Observatory  
3450 Massachusetts Avenue, NW  
Washington, DC 20392-5420  
Tel: 202-653-0350  
Fax: 202-653-0909  
pak@tycho.usno.navy.mil

**Nicholas Koshelyaevsky**  
IMVP GP VNIIFTRI  
Mendeleevo  
Moscow 141570  
Russia  
Tel: 7 095 534 8222  
Fax: 7 095 534 0609  
atime@adonis.iasnet.com

**Paul F. Kuhnle**  
Jet Propulsion Laboratory  
4800 Oak Grove Dr.  
Pasadena, CA 91109  
Tel: 818-354-2715  
Fax: 818-393-6773  
paul.f.kuhnle@jpl.nasa.gov

**Marty D. Lavoie**  
Telecom Solutions  
85 W. Tasman Ave.  
San Jose, CA 95134-1703  
Tel: 408-428-7940  
Fax: 408-428-7897  
mlavoie@telecom.com

**Julius C. Law**  
Jet Propulsion Laboratory  
4800 Oak Grove Dr.  
MS 298-100  
Pasadena, CA 91109  
Fax: 818-393-6773  
julius.c.law@jpl.nasa.gov

**David Lee**  
Hewlett-Packard  
5301 Stevens Creek Blvd.  
Santa Clara, CA 95052  
Tel: 408-553-3338  
Fax: 408-553-2029  
david@sc.hp.com



**Albert Leong**

The Aerospace Corporation  
2350 El. Segundo Blvd.  
El Segundo, CA 90245-4691  
Tel: 310-336-2328  
Fax: 310--336-6225

**Sigfrido M. Leschiutta**

Politecnico di Torino  
24 Corso Suca Abruzzi  
Torino 10125  
Italy  
Tel: 39 11 5644035  
Fax: 39 11 5644093

**Judah Levine**

NIST  
325 Broadway  
Boulder, CO 80303  
Tel: 303-492-7785  
Fax: 303-492-5235  
jlevine@boulder.nist.gov

**Wlodzimierz Lewandowski**

BIPM  
Pavillon de Breteuil  
Sevres 92310  
France  
Tel: 33 1 4507 7063  
wlewandowski@bipm.fr

**Funming Li**

Efratom Time and Frequency  
Products  
3 Parker  
Irvine, CA 92718  
Tel: 714-770-5000  
Fax: 714-770-9289

**Heng-Dao Lin**

Telecommunications Laboratoires  
No. 12. Lane 551, Sec. 3  
Min-Tsu Road, Yang-Mei  
Tao-Yuan 326  
Taiwan  
Tel: 886 3 424-4440  
Fax: 886 3 484-5474

**Chuck Little**

Hewlett-Packard  
5301 Stevens Creek Blvd.  
Santa Clara, CA 95052  
Tel: 408-553-2506  
Fax: 408-553-2058  
chuck\_little@hp0200.desk.hop.com

**Pete Lopez**

TRAK Systems  
4726 Eisenhower Blvd.  
Tampa, FL 33634  
Tel: 813-884-1411 ext. 291  
Fax: 818-884-0981

**Douglas R. Lowrie**

EG&G  
35 Congress Street  
Salem, MA 01970  
Tel: 508-745-3200  
Fax: 508-741-4923

**John McK. Luck**

Orroral Geodetic Observatory  
Scrivener Building  
Dunlop Court  
Bruce ACT  
Australia  
Tel: 61 6 235 7111  
Fax: 61 6 235 7103  
orroral@auslig.gov.au

**Edward M. Lukacs**

U.S. Naval Observatory  
11820 SW 166th Street  
Miami, FL 33177  
Tel: 305-235-0515  
eml@gate.net

**Landa N. Luong**

Hewlett-Packard Co.  
MS 53L-49  
5301 Stevens Creek Blvd.  
Santa Clara, CA 95052-8059  
Tel: 408-553-2911  
Fax: 408-553-2029  
landa@sc.hp.com

**George F. Lutes**

Jet Propulsion Laboratory  
4800 Oak Grove Dr.  
Pasadena, CA 91109  
Tel: 818-354-6210  
Fax: 818-393-6773  
glutes@fridge.jpl.nasa.gov

**Dave Madden**

Newark AFB  
AGMC/MLEE  
813 Irving Wick Dr. W  
Newark, OH 43057  
Tel: 614-522-7344  
Fax: 614-522-7002  
madden@ml-mail.newark.af.mil

**Leo A. Mallette**

Hughes Space & Communications  
2309 S. Santa Anita Ave  
Arcadia, CA 91006  
Tel: 310-364-9243

**Ken E. Martin**

Bonneville Power Admin.  
PO Box 491  
Vancouver, WA 98666  
Tel: 360-418-2694  
Fax: 360-418-2602  
kemartin@bpa.gov

**Edward Mattison**

SAO  
60 Garden St.  
Cambridge, MA 02138  
Tel: 617-495-7265  
Fax: 617-496-7690  
emattison@cfa.harvard.edu

**Gary B. McIntire**

RDA  
6714 Doane Ave  
Springfield, VA 22152  
Tel: 703-321-0008

**Angela D. McKinley**

U.S. Naval Observatory  
3450 Massachusetts Avenue, NW  
Washington, DC 20392-5420  
Tel: 202-653-1528  
Fax: 202-653-0909  
amd@tycho.usno.navy.mil

**Jack McNabb**

TRAK Microwave  
Systems Div.  
4726 Eisenhower Blvd.  
Tampa, FL 33634  
Tel: 813-884-1411 ext. 253  
Fax: 813-884-0981

**Marvin Meirs**

FEI  
55 Charles Linburgh Blvd.  
Uniondale, NY 11553  
Tel: 516-794-4500

**Mihran Miranian**

U.S. Naval Observatory  
3450 Massachusetts Ave., NW  
Washington, DC 20392-5420  
Tel: 202-653-1522  
Fax: 202-653-0909

**Hossein Joe Mobaraki**

Allied Signal Technical Services  
129 N. Hill Ave.  
Pasadena, CA 91106  
Tel: 818-584-4520  
Fax: 818-584-4480  
hossein.j.mobaraki@jpl.nasa.gov

**Sung H. Moon**

U.S. Air Force  
HQ AFC4A/TNSC  
203 W. Losey Street,  
Room 2000  
Scott AFB, IL 62225  
Tel: 618-256-5027  
Fax: 618-256-8944  
moon@afc4a.safb.af.mil

**David C. Munton**

Applied Research Lab  
University of Texas  
10000 Burnet Road  
Austin, TX 78713-8092  
Tel: 512-835-3831  
Fax: 512-835-3259  
dmunton@arlut.utexas.edu

**Leonardo Mureddu**

Cagliari Astronomical Observatory  
Str 54 Localita Poggio dei Pini  
Capoterra (CA) 09012  
Italy  
Tel: 39 70 725246  
Fax: 39 70 725425  
mureddu@ca.astro.it

**1st Lt. Omar M. Namooos**

U.S. Air Force  
GPS-JPO  
2435 Vela Way  
#1613  
Los Angeles AFB, CA 90009-5500  
Tel: 310-363-6922  
Fax: 310-363-6922 ext. 36  
namoosom@gps1.laafb.af.mil

**Lisa M. Nelson**

NIST  
MS 847.4  
325 Broadway  
Boulder, CO 80303-3328  
Tel: 303-497-3378  
Fax: 303-497-3228  
lnelson@central.bldrdoc.gov

**Jerry R. Norton**

Johns Hopkins University  
Applied Physics Laboratory  
Johns Hopkins Road  
Laurel, MD 20723  
Fax: 301-953-1093  
jerry.norton@jhu.apl.edu

**Dean T. Okayama**

USDOC - NIST Radio Station  
WWVH  
PO Box 417  
Kekaha, HI 96752-0417  
Tel: 808-335-4361  
Fax: 808-335-4747  
dokayama@pmrf.navy.mil

**A. W. "Skip" Osborne**

Allen Osborne Associates, Inc.  
756 Lakefield Road  
Westlake Village, CA 91361-2624  
Tel: 805-495-8420  
Fax: 805-373-6067  
aoa@netcom.com

**Terry N. Osterdock**

Absolute Time Corp.  
800 Charcot Ave  
Suite 110  
San Jose, CA 95131  
Tel: 408-383-1520  
Fax: 408-383-0706

**Thomas E. Parker**

NIST  
325 Broadway  
Boulder, CO 80303  
Tel: 303-497-7881  
Fax: 303-497-6461  
tparker@bldrdoc.gov

**Ralph E. Partridge**

Los Alamos National Laboratory  
PO Box 1663  
MS-P942  
Los Alamos, NM 87545  
Tel: 505-665-1617  
Fax: 505-665-2450  
7231.440@compuserve.com

**Peter Z. Paulovich**

NISE East Det Norfolk  
NAVELEX  
PO Box 1376  
Norfolk, VA 23501  
Tel: 804-396-0287  
Fax: 804-396-0518

**Eric B. Paulsen**

Jet Propulsion Laboratory  
4800 Oak Grove Dr.  
Pasadena, CA 91109  
Tel: 818-354-3345  
Fax: 818-393-3013  
epaul@kilroy.jpl.nasa.gov

**Bruce Penrod**

TrueTime, Inc.  
2835 Duke Ct.  
Santa Rosa, CA 95407  
Fax: 707-527-6640

**Harry E. Peters**

Sigma Tau Standards Corp.  
PO Box 1877  
Tuscaloosa, AL 35403  
Tel: 205-553-0038  
Fax: 205-553-2768

**Ted O. Pollard**

Absolute Time Corp.  
800 Charcot, #110  
San Jose, CA 95131  
Tel: 408-383-1518  
Fax: 408-383-0706

**Terry A. Powell**

412 TW/TSRE  
306 E. Popson  
Edwards AFB, CA 93524  
Tel: 805-277-6120  
Fax: 805-277-5377

**Monojit Raha**

ESE  
142 Sierra Street  
El Segundo, CA 90245  
Tel: 310-335-1525

**David W. Rea**

Spectrum Geophysical Instruments  
1952 Roanoke Ave.  
Tustin, CA 92680  
Tel: 714-544-3000  
Fax: 714-544-8307



**Donald E. Rea**

Spectrum Geophysical Instruments  
1952 Roanoke Ave.  
Tustin, CA 92680  
Tel: 714-544-3000  
Fax: 714-544-8307

**Victor S. Reinhardt**

Hughes Space and Communications  
PO Box 97919  
MS SCS12W327  
Los Angeles, CA 90009  
Tel: 310-416-4980  
Fax: 310-416-5050  
vsreinhardt@ccgate.hac.com

**William J. Riley**

EG&G  
35 Congress St.  
Salem, MA 01970  
Tel: 508-745-3200  
Fax: 508-741-4923

**Ronald C. Roloff**

Datum  
Frequency & Time Systems  
8005 McKenstry Drive  
Laurel, MD 20723  
Tel: 301-725-3636  
Fax: 301-953-0246  
rroloff@clark.net

**Ken Sandfeld**

Odetics  
1585 S. Manchester Ave.  
Anaheim, CA 92802  
Tel: 714-780-7684  
sandfeld@odetics.com

**Wolfgang Schaefer**

TimeTech GmbH  
Nobelstrohe 15  
70569 Stuttgart  
Germany

**Timothy F. Sheridan**

Space and Naval Warfare Systems  
Command  
2451 Crystal Dr.  
Arlington, VA 22245-5200  
Tel: 703-602-3893  
Fax: 703-602-1535  
sheridat@smtp-gw.spawar.navy.mil

**Joel F. Small**

NRAD  
53150 Systems Street  
Code 771  
San Diego, CA 92075  
Tel: 619-553-6704  
jsmall@nosc.mil

**Robert W. Snow**

Allen Osborne Associates, Inc.  
756 Lakefield Road  
Westlake Village, CA 91361-2624  
Tel: 805-495-8420  
Fax: 805-373-6067  
aoa@netcom.com

**Edward M. Spivak**

Absolute Time Corp.  
800 Charcot Avenue  
Suite 110  
San Jose, CA 95131  
Tel: 408-383-1522  
Fax: 408-383-0706

**Samuel R. Stein**

Timing Solutions Corp.  
1025 Rosewood  
Suite #200  
Boulder, CO 80304  
Tel: 303-939-8481  
Fax: 303-443-5152  
srsten@ibm.net

**Hagop M. Stephanian**

Hewlett-Packard  
5301 Stevens Creek Blvd.  
Santa Clara, CA 95052  
Tel: 408-553-2500

**Dave Stowers**

Jet Propulsion Laboratory  
4800 Oak Grove Dr.  
MS 298-100  
Pasadena, CA 91109  
Tel: 818-354-7055  
Fax: 818-393-6773  
dstowers@fridge.jpl.nasa.gov

**Richard A. Strand**

U.S. Air Force  
203 W. Losey Street  
Scott AFB, IL 62225  
Tel: 618-256-3979  
Fax: 618-256-8944  
strand@afc4a.safb.af.mil

**Richard L. Sydnor**

Jet Propulsion Laboratory  
4800 Oak Grove Dr.  
Pasadena, CA 91109  
Tel: 818-354-2763  
Fax: 818-393-6773  
sydnor@fridge.jpl.nasa.gov

**Ed Tabibian**

Wave Technologies  
1500 Wyatt Dr.  
#9  
Santa Clara, CA 95054  
Tel: 408-986-8150  
Fax: 408-986-0530

**Philip E. Talley**

1022 Eagle Crest  
Macon, GA 31211  
Tel: 912-745-3415

**Claudine Thomas**

BIPM  
Pavillon de Breteuil  
92312 Sevres Cedex  
France  
Tel: 33 1 45 07 7073  
cthomas@bipm.fr

**Massimo Tinto**

Jet Propulsion Laboratory  
4800 Oak Grove Dr.  
Pasadena, CA 91109-8099  
Tel: 818-354-0798  
Fax: 818-393-4643

**Pierre J-M Uhrich**

BNM-LPTF  
Observatoire de Paris  
61 Avenue de L'Observatoire  
Paris 75014  
France  
Tel: 33 1 4051 2216  
Fax: 33 1 4325 5567  
pierre.uhrich@obspm.fr

**M. J. Van Melle**  
Rockwell - Space Operation Center  
5505 Flintridge Dr.  
Colorado Springs, CO 80918  
Tel: 719-567-2705  
Fax: 719-567-2664

**Francine Vannicola**  
U.S. Naval Observatory  
3450 Massachusetts Ave., NW  
Washington, DC 20392-5420  
Tel: 202-653-1525  
Fax: 202-653-0909  
fmv@cassini.usno.navy.mil

**Christian Veillet**  
OCA  
Av Copernic  
Grasse 06130  
France

**Roger Viet**  
Hewlett-Packard  
5301 Stevens Creek Blvd.  
Santa Clara, CA 95052

**John Vig**  
U.S. Army Research Laboratory  
AMSRL-PS-ED  
Ft. Monmouth, NJ 07703-5601  
Tel: 908-427-4270  
Fax: 908-427-4805  
jvig@arl.mil

**Frank J. Voit**  
The Aerospace Corp.  
PO Box 92957  
M1-110  
Los Angeles, CA 90009  
Tel: 310-336-6764  
Fax: 310-336-6225

**Samuel C. Ward**  
1127 E. Delmar Blvd.  
#237  
Pasadena, CA 91106  
Tel: 818-683-3269

**S. Clark Wardrip**  
ATSC  
726 Foxenwood Drive  
Santa Maria, CA 93455-4221  
Tel: 805-937-6448  
Fax: 805-734-4790

**Toney C. Warren**  
Telecom Solutions  
85 Tasman Drive  
San Jose, CA 95134  
Tel: 408-428-7830  
Fax: 408-428-7895  
micropak@ix.netcom.com

**Brian Way**  
ESE  
142 Sierra Street  
El Segundo, CA 90245  
Tel: 310-322-2136

**Werner Weidemann**  
Datum Efratom Division  
3 Parker  
Irvine, CA 92718  
Tel: 714-770-5000  
Fax: 714-770-9289

**Paul J. Wheeler**  
U.S. Naval Observatory  
3450 Massachusetts Ave., NW  
Washington, DC 20392-5420  
Tel: 202-653-0516  
Fax: 202-653-0909  
paul@tsee2.usno.navy.mil

**Joe White**  
NRL  
4555 Overlook Ave  
MS 8151  
Washington, DC 20375  
Tel: 202-767-5111  
Fax: 202-767-4050  
white@juno.nrl.navy.mil

**Jay D. Wiedwald**  
Lawrence Livermore  
National Lab  
PO Box 5508  
L-493

Livermore, CA 94550  
Tel: 510-422-1338  
Fax: 510-422-1930  
wigwam@llnl.gov

**Gernot. M. R. Winkler**  
U.S. Naval Observatory  
3450 Massachusetts Ave., NW  
Washington, DC 20392-5420  
Tel: 202-653-1520  
Fax: 202-653-0909  
gw@fermi.usno.navy.mil

**William H. Wooden, II**  
Defense Mapping Agency  
8613 Lee Highway  
Stop A-1  
Fairfax, VA 22031-2137  
Tel: 703-275-8449  
Fax: 703-275-8659  
woodenb@dma.gov

**C. Andy Wu**  
The Aerospace Corp.  
4452 Canoga Drive  
Woodland Hills, CA 91364  
Tel: 310-336-0437  
wu@courier3.aero.org

**Tom R. Wuerschmidt**  
White Sands Missile Range  
IDD-RR  
White Sands, NM 88002  
Tel: 505-678-2411  
Fax: 505-678-0310

**Edward N. Yrisarri, Jr.**  
1445 Melody Lane  
Roanoke, TX 76262  
Tel: 817-431-6195  
Fax: 817-431-0153

**Victor S. Zhang**  
NIST  
325 Broadway  
Boulder, CO 80303  
Tel: 303-497-3977  
Fax: 303-497-6461  
zhang@boulder.nist.gov



**REPORT DOCUMENTATION PAGE**Form Approved  
OMB No. 0704-0188

Public reporting burden for this collection of information is estimated to average 1 hour per response, including the time for reviewing instructions, searching existing data sources, gathering and maintaining the data needed, and completing and reviewing the collection of information. Send comments regarding this burden estimate or any other aspect of this collection of information, including suggestions for reducing this burden, to Washington Headquarters Services, Directorate for Information Operations and Reports, 1215 Jefferson Davis Highway, Suite 1204, Arlington, VA 22202-4302, and to the Office of Management and Budget, Paperwork Reduction Project (0704-0188), Washington, DC 20503.

<b>1. AGENCY USE ONLY (Leave blank)</b>		<b>2. REPORT DATE</b> May 1996	<b>3. REPORT TYPE AND DATES COVERED</b> Conference Publication	
<b>4. TITLE AND SUBTITLE</b> 27th Annual Precise Time and Time Interval (PTTI) Applications and Planning Meeting			<b>5. FUNDING NUMBERS</b>  Code 502 C-NAS5-31000	
<b>6. AUTHOR(S)</b>  Dr. Richard Sydnor, Technical Editor				
<b>7. PERFORMING ORGANIZATION NAME(S) AND ADDRESS(ES)</b>  Goddard Space Flight Center Greenbelt, Maryland 20771			<b>8. PERFORMING ORGANIZATION REPORT NUMBER</b>  96B00076	
<b>9. SPONSORING/MONITORING AGENCY NAME(S) AND ADDRESS(ES)</b>  NASA Aeronautics and Space Administration Washington, D.C. 20546-0001			<b>10. SPONSORING/MONITORING AGENCY REPORT NUMBER</b>  NASA CP-3334	
<b>11. SUPPLEMENTARY NOTES</b>  Richard Sydnor: Jet Propulsion Laboratory, Pasadena, CA. Other sponsors: U. S. Naval Observatory; Jet Propulsion Laboratory; Space and Naval Warfare Systems Command; Naval Research Laboratory; Army Electronics Technology and Devices Laboratory; Rome Laboratory; and Air Force Office of Scientific Research.				
<b>12a. DISTRIBUTION/AVAILABILITY STATEMENT</b>  Unclassified-Unlimited Subject Category: 70 Report available from the NASA Center for AeroSpace Information, 800 Elkridge Landing Road, Linthicum Heights, MD 21090; (301) 621-0390.			<b>12b. DISTRIBUTION CODE</b>	
<b>13. ABSTRACT (Maximum 200 words)</b>  This document is a compilation of technical papers presented at the 27th Annual PTTI Applications and Planning Meeting, held November 29 - December 1, 1995, at The Doubletree Hotel at Horton Plaza, San Diego, California. Papers are in the following categories: <ul style="list-style-type: none"><li>• Recent developments in rubidium, cesium, and hydrogen-based frequency standards, and in cryogenic and trapped-ion technology.</li><li>• International and transnational applications of Precise Time and Time Interval technology with emphasis on satellite laser tracking, GLONASS timing, intercomparison of national time scales and international telecommunications.</li><li>• Applications of Precise Time and Time Interval technology to the telecommunications, power distribution, platform positioning, and geophysical survey industries.</li><li>• Applications of PTTI technology to evolving military communications and navigation systems.</li><li>• Dissemination of precise time and frequency by means of GPS, GLONASS, MILSTAR, LORAN, and synchronous communications satellites.</li></ul>				
<b>14. SUBJECT TERMS</b>  Frequency Standards, Hydrogen Masers, Cesium, Rubidium, Trapped Ion, Crystals, Time Synchronization, Precise Time, Time Transfer, GPS, GLONASS, Satellite Clocks, Jitter, Phase Noise			<b>15. NUMBER OF PAGES</b>  502	
<b>16. PRICE CODE</b>				
<b>17. SECURITY CLASSIFICATION OF REPORT</b>  Unclassified	<b>18. SECURITY CLASSIFICATION OF THIS PAGE</b>  Unclassified	<b>19. SECURITY CLASSIFICATION OF ABSTRACT</b>  Unclassified	<b>20. LIMITATION OF ABSTRACT</b>  Unlimited	